13 June 2008 | $10

Science

FORESTS IN FLUX

AAAS

cell sciences®

www.CytokineCenter.com

www.cellsciences.com

Cytokine Center

Browse our web site with over 1300 proteins, including recombinant cytokines, growth factors, chemokines and neurotrophins. Daily shipping and competitive pricing are offered. Bulk quantities of many proteins available.

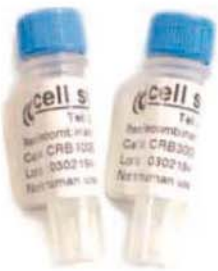

PROTEINS

4-1BBL
4-1BB Receptor
6 Ckine
ACAD8
ACAT2
gAcrp30/Adipolean
Activin A
Activin B
ACY1
ADAT1
Adiponectin
ADRP
AITRL
Akt1
Alpha-Feto Protein (AFP)
Alpha-Galactosidase A
Angiopoietin-1 (Ang-1)
Angiopoietin-2 (Ang-2)
Angiostatin K1-3
Annexin-V
apo-SAA
Apoliprotein A-1
Apoliprotein E2
Apoliprotein E3
Apoliprotein E4
APRIL
Artemin
ATF2
Aurora A
Aurora B
BAFF
BAFF Receptor
BCA-1 / BLC / CXCL13
BCMA
BD-1
BD-2
BD-3
BDNF
Betacellulin
Bivalirudin
BMP-2
BMP-4
BMP-6
BMP-7
BMP-13
sBMPR-1A
Brain Natriuretic Protein
BRAK
Breast Tumor Antigen
C5a
C5L2 Peptide
C-10
C-Reactive Protein
C-Src
Calbindin D-9K
Calbindin D-28K
Calbindin D-29K
Calmodulin
Calcitonin Acetate
Carbonic Anhydrase III
Carcino-embryonic Antigen
Cardiotrophin-1
Caspase-3
Caspase-6
CD4
CD14
CD22
CD40 Ligand / TRAP
CD95 / sFas Ligand
CD105 / Endoglin
CHIPS
CNTF
Collagen
CREB
CTACK / CCL27
CTGF
CTGFL / WISP-2
CTLA-4 / Fc
CXCL16
CYR61
Cytokeratin 8
DEP-1
Desmopressin
Disulfide Oxidoreductase
E-selectin
ECGF
EGF
Elafin / SKALP
EMAP-II
ENA-78 / CXCL5
Endostatin
Enteropeptidase
Eotaxin / CCL11
Eotaxin-2
Eotaxin-3 (TSC)
EPHB2
EPHB4
Epigen
Epiregulin
Eptifbatide
Erk-2
Erythropoietin (EPO)
Exodus-2
Fas Ligand
Fas Receptor
FGF-1 (acidic)
FGF-2 (basic)
FGF-4
FGF-5
FGF-6
FGF-7 / KGF
FGF-8
FGF-9
FGF-10
FGF-16
FGF-17
FGF-18
FGF-19
FGF-20
sFGFR-1 (IIIc) / Fc Chimera
sFGFR-2 (IIIc) / Fc Chimera
sFGFR-3 / Fc Chimera
sFGFR-4 / Fc Chimera
sFlt-1 (native)
sFlt-1 (D3)
sFlt-1 (D4)
sFlt-1 (D5)
sFlt-1 (D7)
Flt3-Ligand
sFlt-4
sFlt-4 / Fc Chimera
Follistatin
FSH
Fractalkine / CX3C
G-CSF
α-Galactosidase A
Galectin-1
Galectin-3
Gastrointestinal CA
GCP-2
GDF-3
GDF-9
GDF-11
GDNF
GLP-1
Glucagon
GM-CSF
Goserelin
GPBB
Granzyme B
GROα
GROβ
GROγ
GRO/MGSA
Growth Hormone
Growth Hormone BP
GST-p21/WAF-1
HB-EGF
HCC-1
HGF
Histdyl-tRNA synthetase
Histrelin
HRG1-β1
I-309
I-TAC
IFN-α
IFN-α A
IFN-α 2a
IFN-α 2b
IFN-β
IFN-γ
IFN-Omega
IGF-I
IGF-II
proIGF-II
IGFBP-1
IGFBP-2
IGFBP-3
IGFBP-4
IGFBP-5
IGFBP-6
IGFBP-7
IL-1α
IL-1β
IL-2
IL-3
IL-4
sIL-4 Receptor
IL-5
IL-6
sIL-6 Receptor
IL-7
IL-8 (72 a.a.)
IL-8 (77 a.a.)
IL-9
IL-10
IL-11
IL-12
IL-13
IL-13 analog
IL-15
IL-16 (121 a.a.)
IL-16 (130 a.a.)
IL-17
IL-17B
IL-17D
IL-17E
IL-17F
IL-19
IL-20
IL-21
IL-22
IL-31
Insulin
IP-10
JE
JNK2a1
JNK2a2
KC / CXCL1
KGF
L-asparaginase
LAG-1
LALF Peptide
LAR-PTP
LBP
LC-1
LD-78β
LDH
LEC / NCC-4
Leptin
LIGHT
LIX
LKM
LL-37
Lungkine / CXCL15
Lymphotactin
sLYVE-1
M-CSF
MCP-1 (MCAF)
MCP-2
MCP-3
MCP-4
MCP-5
MDC (67 a.a.)
MDC (69 a.a.)
MDH
MEC
Mek-1
MIA
Midkine
MIG / CXCL9
MIP-1α / CCL3
MIP-1β / CCL4
MIP-3 / CCL23
MIP-3α / CCL20
MIP-3β / CCL19
MIP-4 (PARC) / CCL18
MIP-5 / CCL15
MMP-3
MMP-7
MMP-13
Myostatin
Nanog
NAP-2
Neurturin
NFAT-1
β-NGF
NOGGIN
NOV
NP-1
NT-1/BCSF-3
NT-3
NT-4
Ocreotide
Oncostatin M
Osteoprotegerin (OPG)
OTOR
Oxytocin
p38-α
PAI-1
Parathyroid Hormone
PDGF-AA
PDGF-AB
PDGF-BB
PDGF-CC
Persephin
PF-4
PIGF-1
PIGF-2
PKA α-subunit
PKC-α
PKC-γ
Pleiotrophin
PLGF-1
Polymyxin B (PMB)
PRAS40
PRL-1
PRL-2
PRL-3
Prokineticin-2
Prolactin
Protirelin
PTHrP
PTP1B
PTP-IA2
PTP-MEG2
PTP-PEST
sRANK
sRANKL
RANTES
RELM-α
RELM-β
Resistin
RPTPβ
RPTPγ
RPTPμ
SCF
SCGF-α
SCGF-β
SDF-1α
SDF-1β
Secretin
SF20
SHP-2
STAT1
c-Src
TACI
TARC
TC-PTP
TECK
TFF2
TGF-α
TGF-β1
TGF-β2
TGF-β3
Thymosin α1
sTIE-1/Fc Chimera
sTIE-2/Fc Chimera
TL-1A
TNF-α
TNF-β
sTNF-receptor Type I
sTNF-receptor Type II
TPO
sTRAIL R-1 (DR4)
sTRAIL R-2 (DR5)
TRAIL/Apo2L
TSG
TSH
TSLP
TWEAK
TWEAK Receptor
Urokinase
EG-VEGF
VEGF121
VEGF145
VEGF165
VEGF-C
VEGF-C I125
VEGF-E
HB-VEGF-E
sVEGFR-1
sVEGFR-2
sVEGFR-3
Visfatin
WISP-1
WISP-2
WISP-3
WNT-1

480 Neponset Street, Building 12A, Canton, MA 02021 • TEL (781) 828-0610 • EMAIL info@cellsciences.com

CALL TOLL FREE (888) 769-1246 • FAX (781) 828-0542 • VISIT www.cellsciences.com

GE Healthcare

Whatman®

Whatman is now part of GE Healthcare.

Creating a centre of excellence in separation technology.

The considerable expertise of Whatman in the fields of sample preparation and filtration technologies has earned them an outstanding reputation world wide. Whatman has key enabling technologies used in the understanding of gene and protein functions. Combining the skills of the two companies will enable GE Healthcare to create strong added value for customers giving unparalleled support to a wide range of research and lab applications.

For more information visit www.gelifesciences.com/whatman

imagination at work

Volume 320, Issue 5882

COVER

The influence of human society on the future of the world's forests and the role of forests in the global carbon cycle are discussed in the special section beginning on page 1435.

Image: Micha Pawlitzki/Zefa/Corbis

DEPARTMENTS

1391 *Science* Online
1392 This Week in *Science*
1396 Editors' Choice
1398 Contact *Science*
1401 Random Samples
1403 Newsmakers
1513 New Products
1518 *Science* Careers

EDITORIAL

1395 Forest Research for the 21st Century
by Raman Sukumar
>> Forests in Flux section p. 1435

SPECIAL SECTION

Forests in Flux

INTRODUCTION

The Future of Forests 1435

NEWS

A Second Chance for Rainforest Biodiversity 1436
Critical Time for African Rainforests 1439
Letting 1000 Forests Bloom 1442

REVIEW

Forests and Climate Change: Forcings, Feedbacks, and the Climate Benefits of Forests 1444
G. B. Bonan

PERSPECTIVES

Forests of the Past: A Window to Future Changes 1450
R. J. Petit, F. S. Hu, C. W. Dick

Predictive Models of Forest Dynamics 1452
D. Purves and S. Pacala

Reducing Greenhouse Gas Emissions from Deforestation and Forest Degradation: Global Land-Use Implications 1454
L. Miles and V. Kapos

Managing Forests for Climate Change Mitigation 1456
J. G. Canadell and M. R. Raupach

Beyond Deforestation: Restoring Forests and Ecosystem Services on Degraded Lands 1458
R. L. Chazdon

Changing Governance of the World's Forests 1460
A. Agrawal, A. Chhatre, R. Hardin

>> Editorial p. 1395; Science *Careers articles p. 1514; for related online content, see p. 1391 or go to www.sciencemag.org/forests/*

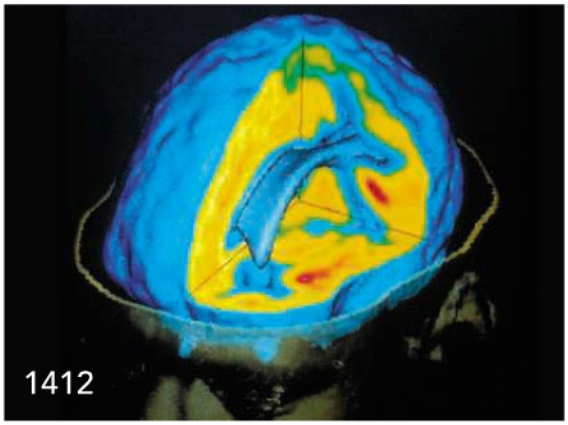

NEWS OF THE WEEK

Changes in Peer Review Target Young Scientists, Heavyweights 1404
Design Changes Will Increase ITER Reactor's Cost 1405
Two Years On, a Mud Volcano Still Rages—and Bewilders 1406
Unstoppable
SCIENCESCOPE 1407
Scientists Race Against the Clock to Gauge Landslide Risk 1408
Have Desert Researchers Discovered a Hidden Loop in the Carbon Cycle? 1409
U.S. Climate Change Bill Dies, But the Energy Remains 1410
Nepal Counts on Science to Turn Struggling Country Around 1411

NEWS FOCUS

Growing Pains for fMRI 1412
Don't Be Seduced by the Brain
India's Education Bonanza Instills Hope—and Concern 1415
New Efforts to Detect Explosives Require Advances on Many Fronts 1416

CONTENTS continued **>>**

BioProcess™ INTERNATIONAL CONFERENCE & EXHIBITION

THE Meeting Place for the Bioprocessing Industry

OVER 1500 ATTENDEES
4 Comprehensive Tracks
110 Presentations featuring 40 Case Studies
New FDA and Industry Plenary Session
Site Tours to Genentech and Irvine Scientific
3 Pre-Conference Workshops

September 23-26, 2008
***Disneyland*® Hotel • Anaheim, California**

From Climbing to the Top of the Earth to Launching into Orbit...

BioProcess International™ 2008 brings you inspiration for the future of a streamlined industry with keynote presentations by visionaries who have climbed the highest mountains, surmounted physical challenges to achieve world endurance records, and supported the launch of NASA shuttles and spacecraft. In addition to the keynotes, the program remains fully grounded in nuts and bolts case studies from biopharmaceutical industry speakers that will help you bring back new tips that can improve your processes tomorrow, while you plan for the coming decade's changes.

Keynote Presentations

Biosimilars – Follow-on Biologics Subsequent Entry Biologics – Biogenerics?

Robert L. Garnick, Ph.D.
Senior Vice President
Regulatory, Quality and Compliance
Genentech, Inc.

The Challenges and Successes of Creating a Biologics Organization within Pfizer

Rick Rutter, Ph.D.
Vice President
Pharmaceutical Sciences Biologics
Pfizer Inc

Using Knowledge Management for Technical Collaboration across Generations

Jeanne Holm, Ph.D.
Chief Knowledge Architect
NASA Jet Propulsion Laboratory

Paths to Flexible Regulatory Notification of Large Molecule Life-Cycle Changes

John K. Towns, Ph.D.
Director
Global CMC Regulatory Affairs
Eli Lilly and Co.

Manufacturing Support – Lessons Learned and Trends for the Future

Konstantin Konstantinov, Ph.D.
Vice President
Technology Development
Genzyme Corp.

How to Motivate Staff to Implement Lean Manufacturing to Raise the Bottom Line

Rob Bryant, MBA
Vice President, Quality, Lean/Six Sigma
Program Lead Master Blackbelt
Computer Sciences Corporation

Special Exhibit Hall Keynote Presentation

The Treacherous Path to Success in the Biotech Industry

Prof. Charles L. Cooney
Robert T. Haslam (1911) Professor, Department of Chemical Engineering, and Faculty Director, Deshpande Center of Technological Innovation, **MIT**

Biopharmaceutical Production Series

Maximize Your Savings by Registering Early
www.IBCLifeSciences.com/BPI/US

Organized by ibc Life Sciences

Priority Code B8171AD22

SCIENCE EXPRESS

www.sciencexpress.org

NEUROSCIENCE

The Spread of Ras Activity Triggered by Activation of a Single Dendritic Spine

C. D. Harvey, R. Yasuda, H. Zhong, K. Svoboda

When strengthened, individual synapses on dendritic spines contain an activated small regulatory protein that spreads to nearby spines, possibly altering their sensitivity.

10.1126/science.1159675

PHYSICS

Entangled Images from Four-Wave Mixing

V. Boyer, A. M. Marino, R. C. Pooser, P. D. Lett

Passing light through a warm cloud of rubidium atoms creates quantum mechanically entangled twin images.

10.1126/science.1158275

BIOCHEMISTRY

Micelles Protect Membrane Complexes from Solution to Vacuum

N. P. Barrera, N. Di Bartolo, P. J. Booth, C. V. Robinson

Gas-phase lipid micelles protect a large complex of membrane proteins, allowing its subunit composition and ligand binding to be assessed by mass spectrometry.

10.1126/science.1159292

ASTRONOMY

Supernova Shock Breakout from a Red Supergiant

K. Schawinski et al.

A burst of ultraviolet light reveals the initial expansion of a star leading to a supernova and identifies the star as a red supergiant.

10.1126/science.1160456

LETTERS

Biofuels: Waste Not Want Not 1419
L. P. Koh, H. T. W. Tan, N. S. Sodhi
Biofuels: Too Soon to Give Up *D. Arvizu*
Biofuels: Think Outside the Cornfield *R. A. Sedjo*
Biofuels: Putting Current Practices in Perspective
J. R. Porter, N. Chirinda, C. Felby, J. E. Olesen
Response *J. Fargione* et al.

CORRECTIONS AND CLARIFICATIONS 1422

BOOKS *ET AL.*

Retaking Rationality How Cost-Benefit Analysis Can Better Protect the Environment and Our Health 1423
R. L. Revesz and M. A. Livermore, reviewed by O. H. Pilkey

When We Left Earth The NASA Missions 1424
R. Dale and B. Howard, Executive Producers, reviewed by J. M. Pasachoff

BROWSINGS On Trees 1424

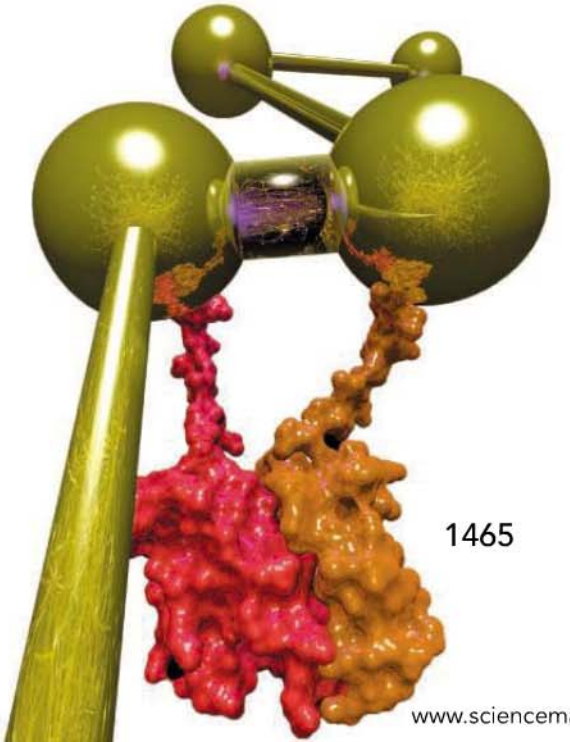

1465

POLICY FORUM

Yucca Mountain Revisited 1426
I. J. Winograd and E. H. Roseboom Jr.

PERSPECTIVES

How Enzymes Work 1428
D. Ringe and G. A. Petsko

How Do Proteins Interact? 1429
D. D. Boehr and P. E. Wright
>> *Research Article p. 1471*

Sex and Poison in the Dark 1430
R. Fischer >> *Report p. 1504*

Enceladus—Oasis or Ice Ball? 1432
S. W. Kieffer and B. M. Jakosky

Unfolding Lipid Metabolism 1433
J. D. Horton >> *Report p. 1492*

1424

BREVIA

PLANT SCIENCE

Germination, Genetics, and Growth of an Ancient Date Seed 1464
S. Sallon et al.
A 2000-year-old date seed—recovered from archaeological excavations near the Dead Sea in Israel—successfully germinated and grew. >> *Science Podcast*

RESEARCH ARTICLES

CELL BIOLOGY

An in Vivo Map of the Yeast Protein Interactome 1465
K. Tarassov et al.
A method that identifies pairs of proteins that are 8 nanometers apart produces a map of interacting proteins in living yeast, finding known and previously unknown networks.

BIOCHEMISTRY

Recognition Dynamics Up to Microseconds Revealed from an RDC-Derived Ubiquitin Ensemble in Solution 1471
O. F. Lange et al.
In solution, ubiquitin assumes all conformations seen in crystal structures of its complexes, indicating that it binds by conformational selection rather than induced fit. >> *Perspective p. 1429*

CONTENTS continued >>

Bio-Plex® Multiplex Suspension Array System

ELISAs Weighing You Down? Try Bio-Plex.

The new automated Bio-Plex Pro™ wash stations make Bio-Plex assays a more productive alternative.

In a single well, evaluate up to 50 cytokines, chemokines, or growth factors, and use focused disease-related assay panels to better understand:

- Acute phase response
- Cancer
- Diabetes
- Inflammation
- Signal transduction

Run fewer experiments, use less sample, and increase productivity with Bio-Plex multiplex assays.

For more information, go to **www.bio-rad.com/bio-plex/**

Bio-Plex Pro Assays

Bio-Plex Pro Wash Station

The Bio-Plex suspension array system includes fluorescently labeled microspheres and instrumentation licensed to Bio-Rad Laboratories, Inc. by the Luminex Corporation.

To find your local sales office, visit **www.bio-rad.com/contact/**
In the U.S., call toll free at 1-800-4BIORAD (1-800-424-6723)

Visit us on the Web at **discover.bio-rad.com**

BIO-RAD

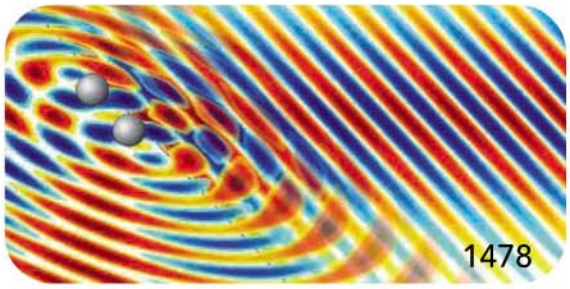

REPORTS

PHYSICS

Probing Cold Dense Nuclear Matter 1476
R. Subedi et al.
Electron-beam experiments reveal that some neutrons within ^{12}C nuclei tend to form close, dynamical pairs with protons but that pairs of the same particle type are rare.

CHEMISTRY

Laser-Induced Electron Tunneling and Diffraction 1478
M. Meckel et al.
Extracting electrons from O_2 and N_2 with a laser and redirecting some to diffract off the atoms reveals the geometry of electronic orbitals and maps the nuclei.

CHEMISTRY

Electrical Resistance of Long Conjugated Molecular Wires 1482
S. H. Choi, B. Kim, C. D. Frisbie
The stepwise synthesis of molecules of increasing length on a gold substrate reveals a change in electron transport from tunneling to hopping as molecule length increases.

ATMOSPHERIC SCIENCE

The Impact of Stratospheric Ozone Recovery on the Southern Hemisphere Westerly Jet 1486
S.-W. Son et al.
Models show that as stratospheric ozone recovers, westerly tropospheric winds at high southern latitudes should weaken, not strengthen as was thought, affecting Antarctic climate.

CLIMATE CHANGE

Evidence for Upwelling of Corrosive "Acidified" Water onto the Continental Shelf 1490
R. A. Feely et al.
As a result of anthropogenic CO_2 uptake, corrosive seawater undersaturated with calcium carbonate shoaled on the continental shelf of western North America in 2007.

MOLECULAR BIOLOGY

Regulation of Hepatic Lipogenesis by the Transcription Factor XBP1 1492
A.-H. Lee, E. F. Scapa, D. E. Cohen, L. H. Glimcher
In mice, a transcription factor known to participate in secretion is also necessary for induction of lipid synthesis by carbohydrates in the liver. *>> Perspective p. 1433*

CELL SIGNALING

The Rag GTPases Bind Raptor and Mediate Amino Acid Signaling to mTORC1 1496
Y. Sancak et al.
Nutrients, specifically amino acids, are sensed by small guanosine triphosphatases, which bind to a signaling complex, moving it close to the nucleus where it initiates cell growth.

ECOLOGY

Animal Versus Wind Dispersal and the Robustness of Tree Species to Deforestation 1502
D. Montoya, M. A. Zavala, M. A. Rodríguez, D. W. Purves
In Spanish forests, tree species with seeds that are dispersed by animals are more resilient in a fragmented forest than those with wind-dispersed seeds.
>> Science Podcast

DEVELOPMENTAL BIOLOGY

VelB/VeA/LaeA Complex Coordinates Light Signal with Fungal Development and Secondary Metabolism 1504
Ö. Bayram et al.
The multiprotein velvet complex in the fungus *Aspergillus nidulans* coordinates light-responsive development and the generation of secondary metabolites such as antibiotics and toxins.
>> Perspective p. 1430

MOLECULAR BIOLOGY

Activation of the Cellular DNA Damage Response in the Absence of DNA Lesions 1507
E. Soutoglou and T. Misteli
Protein complexes that usually assemble on and repair damaged DNA can form at undamaged sites to halt the cell cycle if several of the proteins are first tethered there.

NEUROSCIENCE

Transfer of Learning After Updating Training Mediated by the Striatum 1510
E. Dahlin, A. S. Neely, A. Larsson, L. Bäckman, L. Nyberg
Individuals who become better at a letter recognition test through practice also improve at a different task, even without practice, when both tasks utilize the same brain region.

SPECIAL FEATURE

Careers in Forest Ecology

www.sciencecareers.org

Sustaining Forests in a Changing World 1514
A Self-Made Climber
Measuring the Impact of Invasive Plants
An Adventurous Physicist

>> Forests in Flux section p. 1435; for related online content, see p. 1391 or go to www.sciencemag.org/forests/

AAAS
ADVANCING SCIENCE, SERVING SOCIETY

SCIENCE (ISSN 0036-8075) is published weekly on Friday, except the last week in December, by the American Association for the Advancement of Science, 1200 New York Avenue, NW, Washington, DC 20005. Periodicals Mail postage (publication No. 484460) paid at Washington, DC, and additional mailing offices. Domestic individual membership and subscription (51 issues): $144 ($74 allocated to subscription). Domestic institutional subscription (51 issues): $770; Foreign postage extra: Mexico, Caribbean (surface mail) $55; other countries (air assist delivery) $85. First class, airmail, student, and emeritus rates on request. Canadian rates with GST available upon request, GST #1254 88122. Publications Mail Agreement Number 1069624. **Printed in the U.S.A.**

Change of address: Allow 4 weeks, giving old and new addresses and 8-digit account number. **Postmaster:** Send change of address to AAAS, P.O. Box 96178, Washington, DC 20090–6178. **Single-copy sales:** $10.00 current issue, $15.00 back issue prepaid includes surface postage; bulk rates on request. The identification code for *Science* is 0036-8075. *Science* is indexed in the *Reader's Guide to Periodical Literature* and in several specialized indexes.

CONTENTS continued >>

APPLIED® IMAGING
A Genetix Company

Ariol®
Rock solid data

Genetix

Are you 100% certain you can see all of the positives on your tissue sections? Human perception changes from one individual to another but what you see is crucial for target identification from drug discovery through to clinical diagnostics. Accurate, objective interpretation of microscope slides, along with extraction of numerical data and permanent, retrievable records is key to advancing and standardizing your research.

Ariol is the automated image analysis system for the quantification of protein biomarkers on slides. Delivering quantified, objective and reproducible data from the identification of disease biomarkers to studying gene copy number at cellular level and for research into predicting disease prognosis.

Manual imaging and analysis is a bottleneck. Ariol removes bottlenecks by providing high speed, automated scanning and image analysis of batches of slides. The end result is high resolution, high quality, automatically captured and analyzed data ready for review.

Capable of both brightfield and fluorescent imaging, Ariol rapidly scans and quantifies IHC, FISH, immunofluorescence, micrometastases, angiogenesis, DNA Ploidy, and tissue microarray slides. FDA cleared for *in vitro* diagnostic use of HER-2/neu, ER, and PR IHC, PathVysion® and the detection of micrometastases in bone marrow.

For rock solid research data; mine for more information at www.genetix.com/ariolscience

Take the lead in tissue analysis

Europe
BioScience Centre,
Times Square,
Newcastle Upon Tyne,
NE1 4EP, UK
+44 (0) 191 202 3100

Humboldtstr. 12,
D-85609,
Dornach near Munich,
Germany
+49 (0) 89 944 90 105

USA
120 Baytech Drive,
San José,
CA95134-2302,
USA
+1 (408) 719 6400

Coral dissolve in acidic waters.

SCIENCE**NOW**

www.sciencenow.org

HIGHLIGHTS FROM OUR DAILY NEWS COVERAGE

A Volcanic Preview of Acidic Oceans
Natural experiment predicts which species will win and which will lose from rising carbon dioxide levels.

Say Goodbye to Wimpy Paper
New nanopaper tougher than cast iron.

To Stop a Seizure
An acidic brain blocks convulsions in mice—but only if they have the right ion channel.

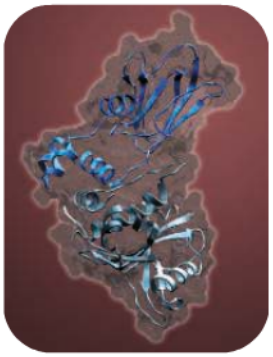

A VHL and elongin B and C complex.

SCIENCE **SIGNALING**

www.sciencesignaling.org

THE SIGNAL TRANSDUCTION KNOWLEDGE ENVIRONMENT

PERSPECTIVE: Intracellular Signaling by Akt—Bound to Be Specific
T. F. Franke
Multiple interacting proteins modulate the activity of the serine/threonine kinase Akt.

PERSPECTIVE: pVHL—A Multipurpose Adaptor Protein
I. J. Frew and W. Krek
The von Hippel-Lindau tumor suppressor controls transcription-dependent and -independent cellular processes.

PODCAST
E. M. Adler and A. M. VanHook
Microvesicles carrying an oncogenic form of the epidermal growth factor receptor provide a mechanism for lateral spread of the malignant phenotype.

GLOSSARY
Find out what ASC, ChIP, and SNS mean in the world of cell signaling.

SPECIAL CONTENT

Forests in Flux

SCIENCE **CAREERS**

www.sciencecareers.org/career_development

FREE CAREER RESOURCES FOR SCIENTISTS

***Science* Careers Podcast: An Interview With Catherine Cardelús**
K. Travis
The young rainforest ecologist talks about what it's like to work in the forest canopy.

SCIENCE **ONLINE FEATURE**

VIDEO: Forests in Flux
An accompaniment to this week's special section on the future of forests in light of climate change and human activity.

SCIENCE**PODCAST**

www.sciencemag.org/about/podcast.dtl

FREE WEEKLY SHOW

Download the 13 June special *Science* Podcast on forests to hear about seed dispersal and tree resilience, growth of an ancient date seed, preserving rainforest biodiversity, and more.

CREDITS: (SCIENCE NOW) RICCARDO RODOLFO-METALPA; (SCIENCE CAREERS) JAMES E. WATKINS JR; (SCIENCE SIGNALING) C. BICKEL

Separate individual or institutional subscriptions to these products may be required for full-text access.

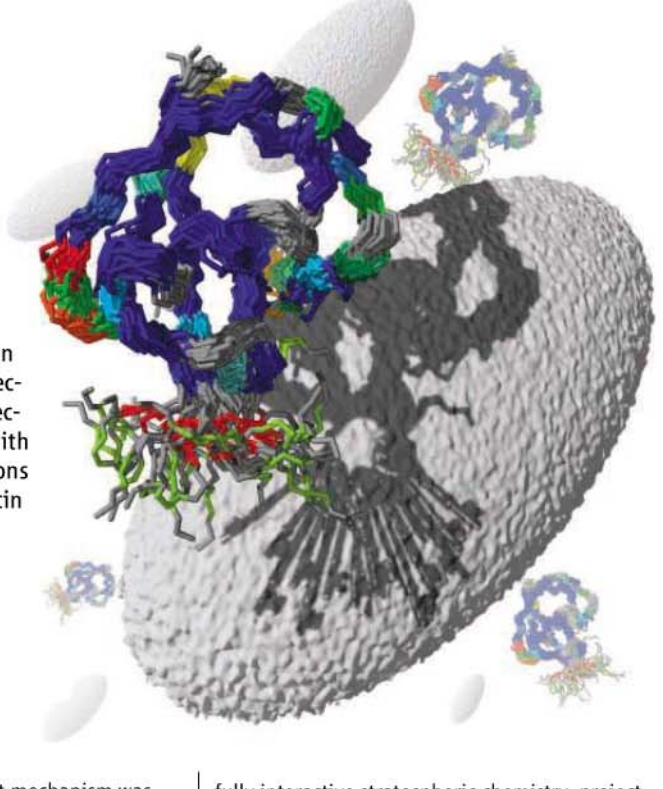

Conformational Selection in Ubiquitin >>

Protein dynamics are important to function, but it has been difficult to study dynamics over the relevant time scale—nanoseconds to microseconds. Now **Lange *et al.*** (p. 1471; see the Perspective by **Boehr and Wright**) combine extensive NMR data with molecular dynamics approaches to study molecular fluctuations of the protein ubiquitin in this time frame. Unbound ubiquitin displays collective motions that allow it to sample all configurations found in bound ubiquitin in 46 known crystal structures, in which, for the most part, the bound ubiquitin is in complexes with other proteins. Molecular recognition by ubiquitin can thus be explained by conformational selection rather than by induced fit.

An Internal Probe

Molecular structures are largely determined from the patterns that result when x-ray or electron beams scatter off the molecules placed in their path. **Meckel *et al.*** (p. 1478) show that structural information can also be obtained by tracking the momentum of an electron ejected from the molecule itself by a strong laser field. Specifically, electron and ion trajectories were mapped after multiphoton ionization of prealigned gas-phase N_2 and O_2 by ultrashort laser pulses. The low momentum electrons reveal the geometry of the highest occupied molecular orbital from which they emerged, whereas the high momentum electrons ricochet back to the parent ion and diffract, providing information on the nuclear positions.

Considering Molecular Wires at Length

The resistance of ordinary metallic wires increases linearly as they get longer, but when small molecules are used as wires, the mechanisms that govern electron transport can change as the molecule gets longer and lead to more dramatic changes in conductivity. Experimental studies of this effect can be challenging because the formation of the molecular junction (how it attaches to its metal electrode and how the molecular layer orders) could change as the wires get longer. **Choi *et al.*** (p. 1482) avoided this complication by synthesizing conjugated molecules on a gold substrate through reactions that increased the length in a stepwise fashion from 1 to 7 nanometers. A metal-coated atomic force microscope tip was used to measure conductivity, and the expected change from a tunneling to a hopping transport mechanism was observed, as well as a drop of conductivity when nonconjugated units were introduced into the molecule's backbone.

Different Partners Are Stronger

The nuclei of atoms contain protons and neutrons, which do not behave independently within the nucleus: Some of the particles tend to pair up, in essence creating locally within the nucleus a higher effective density. **Subedi *et al.*** (p. 1476, published online 29 May) explored the nature of these nucleon pairs by beaming high-energy electrons into a carbon-12 foil to displace protons and neutrons. By examining the type and momentum of the displaced nucleons, the authors determined that most of the pairs were mixed neutron-proton pairs. This finding may have implications for understanding neutron stars, where the particle density is particularly high.

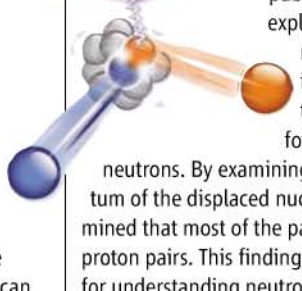

Ozone's Influence

In recent decades, the westerly winds of the southern hemispheric jet stream have accelerated on the poleward side of the jet; this acceleration has been attributed to a combination of effects from increasing greenhouse gas concentrations and decreasing amounts of stratospheric ozone, and this strengthening has been predicted to continue. **Son *et al.*** (p. 1486) find differently. A recent set of models, which include fully interactive stratospheric chemistry, project that the summer tropospheric westerly winds in the Southern Hemisphere will decrease on the poleward side of the jet, owing to the gradual diminution of the ozone hole through the year 2050. This would have important consequences for climate in the Southern Hemisphere, and highlights the importance of stratospheric ozone recovery as an agent of climate change.

Acid Tests

A somewhat neglected but extremely important consequence of the ongoing anthropogenic rise in the concentration of atmospheric carbon dioxide is that the ocean is becoming more acidic as it absorbs more of the gas. This acidification is making seawater more corrosive toward calcium carbonate, the material used by many marine organisms to make their exoskeletons. **Feely *et al.*** (p. 1490, published online 22 May) report results from 13 hydrographic transects from southern Canada to northern Mexico. Potentially corrosive seawater upwelled onto large portions of the continental shelf in 2007. Such seasonal upwelling of such waters onto the shelf is a natural phenomenon, but the ocean uptake of anthropogenic CO_2 has exposed increasing portions of the shelf to potentially damaging effects.

Fat Controller

The synthesis of lipids in the liver depends on transcriptional pathways under the influence of carbohydrate intake. **Lee *et al.*** (p. 1492; see the Perspective by **Horton**) provide evidence for a rather unexpected addition to the list of transcription factors involved in lipid metabolism,

CREDITS (TOP TO BOTTOM): GUNNAR SHROEDER; SUBEDI ET AL.

XBP1. XBP1 is already known to regulate the unfolded protein response (UPR) in the endoplasmic reticulum, influencing the secretory capacity of a variety of cell types. Mice lacking XBP1 expression in the liver after birth showed reduced levels of cholesterol and triglycerides as a result of attenuated lipid synthesis in the liver. In wild-type mice, XBP1 was induced by the feeding of carbohydrates and corresponded with the expression of several other genes associated with fatty-acid synthesis. It remains unclear exactly how XBP1 helps regulate the complex lipogenic transcriptional network in response to carbohydrate intake.

Location Matters

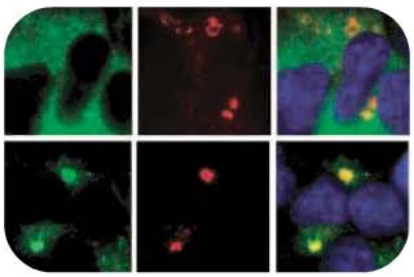

The signaling pathway through which cells modulate protein synthesis and cell growth in response to amino acids has been tricky to unravel. **Sancak *et al.*** (p. 1496, published online 22 May) add a key piece to the puzzle with experiments that reveal a role for a group of small guanosine triphosphatases known as Rag proteins (RagA, -B, -C, and -D). RagC associates with the mTORC1 protein kinase complex, a key regulator of cell growth. This interaction of Rag proteins with mTORC1 appears to be necessary and sufficient to convey nutrient availability signals when cells are exposed to amino acids. The physical interaction of Rag proteins with mTORC1 appears not to regulate activity of mTOR, but to influence its localization within the endomembrane system of the cell.

The Wood and the Trees

Predicting the effects of habitat destruction on individual species in real ecosystems is key to conservation planning. The Spanish Forest Inventory, which consists of >98,000 plots across the forested parts of mainland Spain, represents the largest tree data set available for which the presence and absence of different tree species have been quantified. Using this data set, **Montoya *et al.*** (p. 1502) analyzed the relationship between habitat loss and species persistence for 34 Iberian tree species at large spatial scales. Differences in responses to deforestation (in terms of species persistence at inventoried sites) were driven strongly by the dispersal mechanism: tree species with animal-dispersed seeds were more resistant to deforestation than those with wind-dispersed seeds and, in six cases, individual tree species actually responded positively to locally reduced tree cover. This relationship might not persist, however, if populations of dispersal vectors in turn begin to suffer from the effects of deforestation themselves.

Damage Detection

A break in both strands of the DNA double helix is potentially very dangerous for organisms because the free ends can recombine inappropriately with other parts of the genome and cause substantial damage. Eukaryotic cells sense and attempt to repair such breaks very rapidly, through the recruitment of DNA repair proteins to the sites of damage, forming nuclear repair foci. **Soutoglou and Misteli** (p. 1507, published online 15 May) have tethered various repair factors individually to unbroken DNA in human tissue culture cells and find that, surprisingly, even in the absence of DNA damage, repair foci form at the tether site. The DNA damage response may thus involve amplification of the damage-signaling cascade, and the damage-sensing proteins may detect alterations in the higher-order structure of chromatin around the break.

Training, Transfer, and the Striatum

Training causes task-specific performance enhancement and altered patterns of brain activity. Training can also improve performance of untrained related or transfer tasks. **Dahlin *et al.*** (p. 1510) trained human subjects on a letter memory task for several weeks. Compared to controls, these subjects showed significant improvements over time, and this training also improved an untrained, but related task. No transferred improvement was observed in an unrelated task. Simultaneous brain-imaging scans revealed that transfer after updating training was mediated by the striatum, in line with predictions from computational modeling that the striatum plays a key role in updating working memory.

CREDIT: SANCAK *ET AL.*

CONTACT US

Author Submissions
www.submit2science.org

Editorial
202-326-6550
E-mail: science_editors@aaas.org
(for general editorial queries)

E-mail: science_letters@aaas.org
(for letters to the editor)

E-mail: science_reviews@aaas.org
(for returning manuscript reviews)

E-mail: science_bookrevs@aaas.org
(for general book review queries and transmission of book review manuscripts)

News
202-326-6500
E-mail: science_news@aaas.org

International Office
+ 44 (0) 1223 326 500
http://intl.sciencemag.org
E-mail: subs@science-int.co.uk

Permissions
202-326-7074
E-mail:
science-permissions@aaas.org

Advertising
Recruitment 202-326-6543
E-mail:
advertise@sciencecareers.org
Product 202-326-6537
E-mail:
science_advertising@aaas.org

Institutional Subscriptions
202-326-6417
E-mail: membership3@aaas.org

Site-licensing
202-326-6730
E-mail: scienceonline@aaas.org

Science Signaling
www.sciencesignaling.org
E-mail: sciencesignaling@aaas.org

***Science* Careers**
www.sciencecareers.org

***Science* Classic**
www.sciencemag.org/classic
E-mail: scienceclassic@aaas.org

Science
AAAS

www.sciencemag.org
American Association for
the Advancement of Science
1200 New York Avenue, NW
Washington, DC 20005 USA

Call for Papers

Science Signaling

Now accepting original research submissions

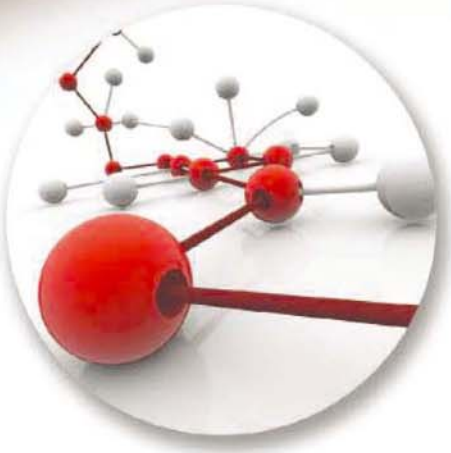

ISSN: 1937-9145

From the publishers of ***Science, Science Signaling***, formerly known as ***Science*'s** STKE, will add original research starting September 2008. Each week the journal will publish leading-edge findings in addition to the current features, including Perspectives, Reviews, Protocols, Meeting Reports, Book Reviews, Teaching Resources, and the Database of Cell Signaling.

Science Signaling showcases high-impact research in cellular regulation in such fields as molecular biology, development, immunology, neuroscience, microbiology, physiology and medicine, pharmacology, biochemistry, cell biology, bioinformatics, and systems biology. Submit your research that provides new concepts and new understanding of biological signal transduction for consideration.

Subscribing to ***Science Signaling*** ensures that you and your lab have the latest cell signaling resources. From basic science to design of therapeutics, from molecules to networks and systems design, read the best source – ***Science Signaling***.

Announcing Chief Scientific Editor for *Science Signaling* –

Michael B. Yaffe, M.D., Ph.D.
Associate Professor, Department of Biology
Massachusetts Institute of Technology

Submit your paper to:
stke.sciencemag.org/about/help/research.dtl

Science Signaling
AAAS

Raman Sukumar is professor of ecology at the Indian Institute of Science, Bangalore, India, working in the areas of wildlife ecology, tropical forest ecology, and climate change. E-mail: rsuku@ces.iisc.ernet.in

Forest Research for the 21st Century

LAST MONTH THE UNITED NATIONS (UN) CONCLUDED A BIODIVERSITY CONFERENCE IN Bonn, Germany, where delegates from 191 countries negotiated "access to and sharing of the benefits of the rich genetic resources of the world." Many of these resources reside in forests, which cover 4 billion hectares or 30% of Earth's land. Forests are decreasing at a rate of 7 million hectares annually, mostly in the tropics. How can research encompassing the ecological, social, economic, and political dimensions of forest conservation contribute to reducing forest destruction and maintaining biodiversity, climatic stability, and the livelihoods of the poor, 40 to 50% of whose resources come from forests?

We continue to learn about how rainforests support so many species in so little space. We also better understand how the social drivers of change, including subsistence needs, global market forces, and political governance, result in the degradation and fragmentation of forests. But much less has been achieved in addressing how to attain forest sustainability in all its dimensions.

Monitoring the global status of forests and changes in their attributes, as is being done by the Food and Agriculture Organization of the UN (with government data), must continue, in combination with satellite-based remote sensing, to know where the most rapid changes are taking place, as shown for Amazonia, Africa, and southeast Asia. Also, computer modeling of vegetation has used climatic data from general circulation models to simulate shifts in global biome boundaries under changing climate, and empirical-statistical "bioclimate envelope" models have done likewise for plant species distributions. These analyses provide a broad understanding of the spatial direction of potential shifts in biomes and species but need refinement for use in regional adaptation strategies for forest conservation.

We need to know more about forest structure and function: plant physiological ecology (photosynthesis, respiration, and nutrient and water use); phenology (leaf flush and senescence, flowering and pollination, fruiting and dispersal, and seed germination and regeneration); community competitive interactions; and population dynamics. This knowledge may help in predicting how trees will respond to changes in temperature, precipitation, and other climatic variables projected for this century—information needed to take measures to minimize species extinction.

Forests have been promoted for their role in carbon sequestration and climate mitigation, but the strength and duration of the terrestrial carbon sink are unclear, especially for tropical forests. Vulnerability to invasive species, pests, diseases, and fires has to be factored into these studies as well as the complex carbon and nutrient dynamics of forest soils.

As for the sustainable management of forests, there are two major components: the harvest of roundwood valued at U.S. $64 billion annually and of non-wood products with a reported value of U.S. $4.7 billion annually. Sustainable harvest of industrial roundwood from temperate forests has considerable scientific backing (such as in Sweden), but this is not the case with tropical forests. Although hundreds of millions of people across the tropics depend directly on fuelwood and non-wood products, we still need to develop sustainable harvest practices. This complex task requires research on all aspects of plant species' biology, and the ability to separate the influences of natural factors versus human use in their dynamics. Socioeconomic changes have to be factored into research on future demand and supply of non-wood forest products. In Malaysia, there are now attempts to sustainably manage rainforest logging, although large-scale conversion of forests to oil palms for biofuel production has already occurred.

China is increasing its forest area of 200 million hectares by planting 4 million hectares annually. Brazil is aiming at carbon credits for reducing deforestation, presently 3 million hectares per year. India has made similar demands for forest conservation and afforestation. Research should help integrate such efforts with the broader goals of carbon sequestration, biodiversity conservation, and reversing forest fragmentation.

Given environmental variability and the long-lived nature of trees, long-term studies with comprehensive mandates extending from basic to applied research are likely to be the most useful in providing the scientific basis for sustainable forest management. **– Raman Sukumar**

10.1126/science.1160329

CREDITS: (LEFT) INDIAN INSTITUTE OF SCIENCE; (RIGHT) AP

EDITED BY GILBERT CHIN AND JAKE YESTON

CLIMATE SCIENCE

Clearing up Cloudy Data

Aerosols have a huge influence on climate, largely through how they affect clouds by what is termed their indirect effect. The indirect aerosol effect is the sum of two distinct phenomena: first, the response of cloud drop density and size to changes in aerosol properties; and second, the response of cloud albedo to changes in cloud drop density and size. Both components must be known to determine the whole effect, but most of the experimental and field studies conducted to date have addressed only the first process, leaving large uncertainties. Roberts *et al.* describe a method to quantify both phenomena at once, thereby enabling direct observation of aerosol-cloud-albedo interactions. They use a stack of three autonomous unmanned aerial vehicles below, at, and above cloud level, to simultaneously measure the radiometric and microphysical properties of individual clouds. Their results therefore pave the way for resolving the largest current source of uncertainty in the quantification of the radiative forcing of climate. — HJS

Proc. Natl. Acad. Sci. U.S.A. **105**, 7370 (2008).

MATERIALS SCIENCE

Caged Protection

Aerogels are mesoporous materials whose very low densities lead to unusual thermal and acoustic properties. However, their high porosity makes them brittle and has limited their use to a few specialized applications. Leventis *et al.* show that by crosslinking vanadia aerogels with isocyanates to form a conformal coating, they achieve a composite material with an idealized morphology. Unlike more common silica aerogels, mesoporous vanadia consists of entangled wormlike fragments, which fused together at contact points in the polymer-coated composite. In compressive tests, the silica and vanadia aerogels showed similar trends, with the polymer crosslinked materials exhibiting greater strength and toughness. However, one important difference was that the silica aerogels cracked and fractured when highly compressed, whereas the vanadia counterparts could carry a high load even at 91% strain and showed excellent properties under cryogenic conditions. Although vanadia is too expensive to use on a large scale, the authors envision that with the right combination of aerogel morphology and polymer-aerogel interactions, strong aerogels could be prepared from silicon, iron, or aluminum oxides. — MSL

J. Mater. Chem. **18**, 2475 (2008).

CHEMISTRY

Small-Cluster Coexistence

When metal clusters are adsorbed on metal oxide surfaces, their properties can change, especially if they interact with defect sites and undergo charge transfer. Simic-Milosevic *et al.* explored the extent of such charge transfer in a model system, in which magnesium oxide films [three monolayers (MLs) of MgO(001)] were grown on a Ag(001) surface; Au was then deposited at low coverages (0.03 ML) at very low temperatures (5 K), and its structure was studied with a scanning tunneling microscope (STM). Although most of the Au was present as isolated atoms, two types of dimer could be observed that either lay flat on the surface (shown at left) or stood upright. Manipulations with the STM tip could form the flat dimers from the atoms and then convert them to the upright form. Density functional theory calculations indicated that the upright form is more stable and adsorbs as a neutral species onto surface oxygen sites, whereas the flat form is negatively charged and places the Au atoms over Mg. These results show that the spread in energy between different electronic states may be low enough to allow substantial coexistence on a surface. — PDS

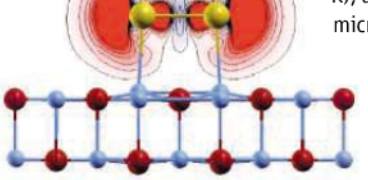

J. Am. Chem. Soc. **130**, 10.1021/ja8024388 (2008).

EVOLUTION

Monarch Menace

Parasites are known to harm their hosts, although from an evolutionary perspective it is not intuitively obvious why an organism that depends on another for its survival and transmission would risk killing its partner. Virulence may be an unavoidable outcome of a parasite using host resources to replicate, which causes damage and provokes costly immune responses; parasites would thus be expected to limit their replication to a submaximal level. To test this hypothesis, de Roode *et al.* collected data on the migratory North American monarch butterfly and a spore-forming protozoan parasite. As expected, greater parasite replication and greater spore loads reduced the probability of a butterfly emerging successfully from a chrysalis and also reduced the subsequent mating success and life span of female butterflies. The tradeoff was that female monarchs with the lowest parasite loads transferred spores to only 20% of their eggs, even though the fecundity of the parasitized butterflies was unaltered by spore load. Significant differences in virulence were observed between eastern (less tolerant of virulence) and western monarchs. Because eastern migration is 10 times longer, butterflies carrying highly virulent genotypes of parasite could die of the effects of parasitism en route. — CA

Proc. Natl. Acad. Sci. U.S.A. **105**, 7489 (2008).

MOLECULAR BIOLOGY

Fragile DNA

The iconic image of DNA is a double helix, yet it can also adopt more exotic conformations such as the guanine (G) quadruplex, where four strands of G-rich DNA align (intra- or intermolecularly) in a stacked rectangular arrangement via Hoogsteen bonds between the Gs. Although the in vitro evidence for such structures is plentiful, the extent (or, indeed, the consequence) of their existence in vivo is less clear. It is known that runs of Gs are vulnerable to deletion and that a protein linked to Fanconi anemia, FancJ, can help to protect such fragile sites.

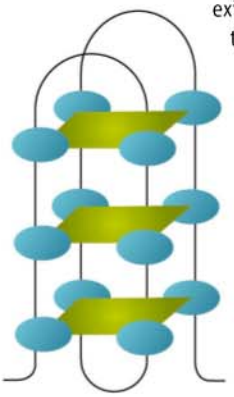

Guanine quadruplex.

In *Caenorhabditis* in which the FancJ homolog *dog-1* is deleted, Kruisselbrink *et al.* show that the G4 DNA tracts most prone to deletion have the characteristics of a canonical G quadruplex and that G3 sites—those missing one of the four legs—are not fragile. Furthermore, within the G-rich sequences, those with the greatest ability to fold into a quadruplex are most likely to suffer deletion, occasionally at a very high frequency. The small size of the deletions, less than 300 base pairs, suggests that G4 DNA preferentially stalls the replication machinery on the lagging strand, the tangled mess being extricated only by removal of the offending region up to the nearest upstream Okazaki fragment. The loss of FancJ in Fanconi anemia patients may sensitize over 300,000 predicted G4 sites in the genome to deletion, and thence produce a predisposition to cancer. — GR

Curr. Biol. **18**, 10.1016/j.cub.2008.05.013 (2008).

PLANT SCIENCE

Coping with Heavy Metal

Cadmium seems to be useless to plants but manages to hitchhike its way into plant cells through transporters used to import iron, calcium, and zinc. Various processes serve to sequester and thus detoxify cadmium; plants contaminated by cadmium are an unfortunate source of heavy metal in human and animal diets. Dutilleul *et al.* find that the expression of selenium-binding proteins was increased in *Arabidopsis* seedlings after exposure to cadmium, and the overexpression of the selenium-binding proteins served to protect *Arabidopsis* from the toxic effects of high levels of cadmium. Binding studies indicate direct interactions between cadmium and selenium-binding protein, the function of which in the normal unstressed plant remains unclear. Better insight into how plants deal with toxic metals could contribute to developing plants that are able to detoxify soils or to reducing trace toxicity in the food chain. — PJH

Plant Physiol. **147**, 239 (2008).

Science Signaling AAAS

<< Making Sense of EPO Receptors

Erythropoetin (EPO) signaling contributes to organ development, as well as to the differentiation of erythrocytes. The abundance of the EPO receptor (EPO-R) increases after removal of one lung (pneumonectomy) in dogs. In the same system, Zhang *et al.* report that the abundance of EPO-R appears to be regulated by the sense EPO-R transcript (sEPO-R), as well as by either the antisense transcript (asEPO-R) or by proteins encoded by two open reading frames (ORFs) within the antisense transcript. Both transcripts were detected in the normal canine lung; the abundance of sEPO-R increased modestly after pneumonectomy, whereas that of asEPO-R and EPO-R more than doubled. Coexpression of sEPO-R and asEPO-R increased the abundance of EPO-R in transfected human cells as compared to sEPO-R alone. The putative ORF1 protein was not needed to elevate EPO-R in transfected cells. In contrast, EPO-R production increased when a construct that included ORF2 and 300 base pairs 5′ of the ORF2 start site was cotransfected with sEPO-R; however, when the upstream region was not included, EPO-R abundance did not increase. The enhancing effect was restored by mutating the start codon of ORF2. The authors propose that asEPO-R has several regulatory elements, with the RNA having stimulatory effects and the ORF2 protein negative effects on EPO-R synthesis. — NRG

Proc. Natl. Acad. Sci. U.S.A. **105**, 7612 (2008).

CREDIT: KRUISSELBRINK *ET AL.*, *CURR. BIOL.* **18**, 10.1016/J.CUB.2008.05.013 (2008)

www.sciencemag.org

Science

1200 New York Avenue, NW
Washington, DC 20005
Editorial: 202-326-6550, FAX 202-289-7562
News: 202-326-6581, FAX 202-371-9227
Bateman House, 82-88 Hills Road
Cambridge, UK CB2 1LQ
+44 (0) 1223 326500, FAX +44 (0) 1223 326501

Subscription Services For change of address, missing issues, new orders and renewals, and payment questions: 866-434-AAAS (2227) or 202-326-6417, FAX 202-842-1065. Mailing addresses: AAAS, P.O. Box 96178, Washington, DC 20090-6178 or AAAS Member Services, 1200 New York Avenue, NW, Washington, DC 20005

Institutional Site Licenses please call 202-326-6755 for any questions or information

Reprints: Author Inquiries 800-635-7181
Commercial Inquiries 803-359-4578

Permissions 202-326-7074, FAX 202-682-0816

Member Benefits AAAS/Barnes&Noble.com bookstore www.aaas.org/bn; AAAS Online Store http://www.apisource.com/aaas/ code MKB6; AAAS Travels: Betchart Expeditions 800-252-4910; Apple Store www.apple/eppstore/aaas; Bank of America MasterCard 1-800-833-6262 priority code FAA3YU; Cold Spring Harbor Laboratory Press Publications www.cshlpress.com/affiliates/aaas.htm; GEICO Auto Insurance www.geico.com/landingpage/go51.htm?logo=17624; Hertz 800-654-2200 CDP#343457; Office Depot https://bsd.officedepot.com/portalLogin.do; Seabury & Smith Life Insurance 800-424-9883; Subaru VIP Program 202-326-6417; VIP Moving Services http://www.vipmayflower.com/domestic/index.html; Other Benefits: AAAS Member Services 202-326-6417 or www.aaasmember.org.

science_editors@aaas.org	(for general editorial queries)
science_letters@aaas.org	(for queries about letters)
science_reviews@aaas.org	(for returning manuscript reviews)
science_bookrevs@aaas.org	(for book review queries)

Published by the American Association for the Advancement of Science (AAAS), *Science* serves its readers as a forum for the presentation and discussion of important issues related to the advancement of science, including the presentation of minority or conflicting points of view, rather than by publishing only material on which a consensus has been reached. Accordingly, all articles published in *Science*—including editorials, news and comment, and book reviews—are signed and reflect the individual views of the authors and not official points of view adopted by AAAS or the institutions with which the authors are affiliated.

AAAS was founded in 1848 and incorporated in 1874. Its mission is to advance science, engineering, and innovation throughout the world for the benefit of all people. The goals of the association are to: enhance communication among scientists, engineers, and the public; promote and defend the integrity of science and its use; strengthen support for the science and technology enterprise; provide a voice for science on societal issues; promote the responsible use of science in public policy; strengthen and diversify the science and technology workforce; foster education in science and technology for everyone; increase public engagement with science and technology; and advance international cooperation in science.

Information for Authors
See pages 634 and 635 of the 1 February 2008 issue or access www.sciencemag.org/about/authors

EDITOR-IN-CHIEF **Bruce Alberts**
EXECUTIVE EDITOR **Monica M. Bradford**
DEPUTY EDITORS **R. Brooks Hanson, Barbara R. Jasny, Katrina L. Kelner**
NEWS EDITOR **Colin Norman**

Editorial supervisory senior editor Phillip D. Szuromi; **senior editor/perspectives** Lisa D. Chong; **senior editors** Gilbert J. Chin, Pamela J. Hines, Paula A. Kiberstis (Boston), Marc S. Lavine (Toronto), Beverly A. Purnell, L. Bryan Ray, Guy Riddihough, H. Jesse Smith, Valda Vinson; **associate editors** Jake S. Yeston, Laura M. Zahn; **online editor** Stewart Wills; **associate online editors** Robert Frederick, Tara S. Marathe; **web content developer** Martyn Green; **book review editor** Sherman J. Suter; **associate letters editor** Jennifer Sills; **editorial manager** Cara Tate; **senior copy editors** Jeffrey E. Cook, Cynthia Howe, Harry Jach, Barbara P. Ordway, Trista Wagoner; **copy editors** Chris Filiatreau, Lauren Kmec, Peter Mooreside; **editorial coordinators** Carolyn Kyle, Beverly Shields; **publications assistants** Ramatoulaye Diop, Joi S. Granger, Jeffrey Hearn, Lisa Johnson, Scott Miller, Jerry Richardson, Jennifer A. Seibert, Brian White, Anita Wynn; **editorial assistants** Carlos L. Durham, Emily Guise, Patricia M. Moore; **executive assistant** Sylvia S. Kihara; **administrative support** Maryrose Madrid

News deputy news editors Robert Coontz, Eliot Marshall, Jeffrey Mervis, Leslie Roberts; **contributing editors** Elizabeth Culotta, Polly Shulman; **news writers** Yudhijit Bhattacharjee, Adrian Cho, Jennifer Couzin, David Grimm, Constance Holden, Jocelyn Kaiser, Richard A. Kerr, Eli Kintisch, Andrew Lawler (New England), Greg Miller, Elizabeth Pennisi, Robert F. Service (Pacific NW), Erik Stokstad; **intern** Elsa Youngsteadt; **contributing correspondents** Jon Cohen (San Diego, CA), Daniel Ferber, Ann Gibbons, Mitch Leslie, Charles C. Mann, Virginia Morell, Evelyn Strauss, Gary Taubes; **copy editors** Linda B. Felaco, Melvin Gatling; **administrative support** Scherraine Mack, Fannie Groom; **bureaus** New England: 207-549-7755, San Diego, CA: 760-942-3252, FAX 760-942-4979, Pacific Northwest: 503-963-1940

Production director James Landry; **senior manager** Wendy K. Shank; **assistant manager** Rebecca Doshi; **senior specialist** Chris Redwood; **specialist** Steve Forrester; **Preflight director** David M. Tompkins; **manager** Marcus Spiegler; **specialist** Jessie Mudjitaba

Art director Kelly Buckheit Krause; **associate art director** Aaron Morales; **illustrators** Chris Bickel, Katharine Sutliff; **senior art associates** Holly Bishop, Laura Creveling, Preston Huey, Nayomi Kevitiyagala; **associate** Jessica Newfield; **photo editor** Leslie Blizard

***Science* International**

Europe (science@science-int.co.uk) **editorial: international managing editor** Andrew M. Sugden; **senior editor/perspectives** Julia Fahrenkamp-Uppenbrink; **senior editors** Caroline Ash, Stella M. Hurtley, Ian S. Osborne, Stephen J. Simpson, Peter Stern; **editorial support** Deborah Dennison, Rachel Roberts, Alice Whaley; **administrative support** John Cannell, Janet Clements, Louise Smith; **news: europe news editor** John Travis; **deputy news editor** Daniel Clery; **contributing correspondents** Michael Balter (Paris), John Bohannon (Vienna), Martin Enserink (Amsterdam and Paris), Gretchen Vogel (Berlin); **intern** Lauren Cahoon

Asia Japan Office: Asca Corporation, Eiko Ishioka, Fusako Tamura, 1-8-13, Hirano-cho, Chuo-ku, Osaka-shi, Osaka, 541-0046 Japan; +81 (0) 6 6202 6272, FAX +81 (0) 6 6202 6271; asca@os.gulf.or.jp; **asia news editor** Richard Stone (Beijing: rstone@aaas.org); **contributing correspondents** Dennis Normile (Japan: +81 (0) 3 3391 0630, FAX 81 (0) 3 5936 3531; dnormile@gol.com); Hao Xin (China: + 86 (0) 10 6307 4439 or 6307 3676, FAX +86 (0) 10 6307 4358; cindyhao@gmail.com); Pallava Bagla (South Asia: +91 (0) 11 2271 2896; pbagla@vsnl.com)

Africa Robert Koenig (contributing correspondent, rob.koenig@gmail.com)

EXECUTIVE PUBLISHER **Alan I. Leshner**
PUBLISHER **Beth Rosner**

Fulfillment Systems and Operations (membership@aaas.org); **director** Waylon Butler; **customer service supervisor** Pat Butler; **specialists** Laurie Baker, Latoya Casteel, LaVonda Crawford, Vicki Linton; **data entry supervisor** Cynthia Johnson; **specialist** Tarrika Hill

Business Operations and Administration director Deborah Rivera-Wienhold; **assistant director, business operations** Randy Yi; **senior financial analysts** Michael LoBue, Jessica Tierney; **financial analysts** Benjamin Aronin, Priti Pamnani; **rights and permissions: administrator** Emilie David; **associate** Elizabeth Sandler; **marketing director** John Meyers; **marketing managers** Allison Pritchard, Darryl Walter; **marketing associates** Aimee Aponte, Alison Chandler, Mary Ellen Crowley, Marcia Leach, Julianne Wielga, Wendy Wise; **international marketing manager** Wendy Sturley; **marketing executive** Jennifer Reeves; **marketing/member services executive** Linda Rusk; **site license sales director** Tom Ryan; **sales manager** Russ Edra; **sales and customer service** Mehan Dossani, Iquo Edim, Kiki Forsythe, Catherine Holland, Phillip Smith, Philip Tsolakidis; **electronic media: manager** Lizabeth Harman; **project manager** Trista Snyder; **assistant manager** Lisa Stanford; **senior production specialists** Christopher Coleman, Walter Jones; **production specialists** Nichele Johnston, Kimberly Oster

Advertising director worldwide ad sales Bill Moran

Product (science_advertising@aaas.org); **midwest** Rick Bongiovanni: 330-405-7080, FAX 330-405-7081; **west coast/w. canada** Teola Young: 650-964-2266; **east coast/e. canada** Christopher Breslin: 443-512-0330, FAX 443-512-0331; **uk/europe/asia** Michelle Field: +44 (0) 1223 326524, FAX +44 (0) 1223 326532; **japan** Mashy Yoshikawa: +81 (0) 33235 5961, FAX +81 (0) 33235 5852; **senior traffic associate** Deiandra Simms

Commercial Editor Sean Sanders: 202-326-6430

Classified (advertise@sciencecareers.org); **us: recruitment sales manager** Ian King: 202-326-6528, FAX 202-289-6742; **inside sales manager: midwest/canada** Daryl Anderson: 202-326-6543; **inside sales representative** Karen Foote: 202-326-6740; **key account manager** Joribah Able; **northeast** Alexis Fleming: 202-326-6578; **southeast** Tina Burks: 202-326-6577; **west** Nicholas Hintibidze: 202-326-6533; **sales coordinators** Erika Foard, Rohan Edmonson, Shirley Young; **international: sales manager** Tracy Holmes: +44 (0) 1223 326525, FAX +44 (0) 1223 326532; **sales** Marium Hudda, Alex Palmer, Alessandra Sorgente; **sales assistant** Louise Moore; **japan** Mashy Yoshikawa: +81 (0)3 3235 5961, FAX +81 (0)3 3235 5852; **advertising production operations manager** Deborah Tompkins; **senior production specialists** Robert Buck, Amy Hardcastle; **senior traffic associate** Christine Hall; **publications assistant** Mary Lagnaoui

AAAS Board of Directors retiring president, chair David Baltimore; **president** James J. McCarthy; **president-elect** Peter C. Agre; **treasurer** David E. Shaw; **chief executive officer** Alan I. Leshner; **board** Lynn W. Enquist, Susan M. Fitzpatrick, Alice Gast, Linda P. B. Katehi, Nancy Knowlton, Cherry A. Murray, Thomas D. Pollard, Thomas A. Woolsey

AAAS
ADVANCING SCIENCE, SERVING SOCIETY

17

~~9~~ gigs and beyond.

Only the SOLiD™ System delivers you the promise of next generation genomics — today. With its unique two-flow cell configuration and unmatched scalability, nine gigabases was just the beginning. Brought to you by the company that automated sequencing and backed by the service and support you have come to depend upon — the SOLID generation delivers.

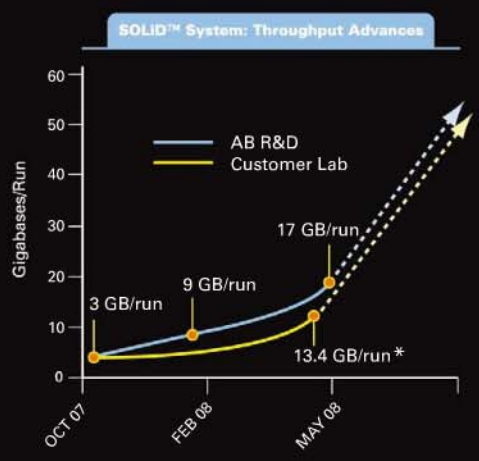

17 GB demonstrated — R&D
13.4 GB demonstrated — Customer

* Biology of Genomes Meeting CSH, May 2008

For SOLID PROOF, visit solid.appliedbiosystems.com

Applied Biosystems

Give Knowledge

Advance the Science of Gift Giving. Give *Science* Each Week.

Special Gift Subscription Rate*
Professional $99 Postdoc/Student $50

Give 51 issues of *Science* along with the same yearlong benefits of AAAS membership that you enjoy.

You'll give colleagues a career boost and students an academic leg-up. You'll intrigue and enlighten friends; educate and entertain family members. And you'll add new supporters for the AAAS international, public policy, education, and career programs that advance science and serve society.

Order online—Go to:

promo.aaas.org/giftmay2
or call 1-866-434-AAAS (2227)

When you give *Science*, you receive our popular AAAS shirt.

Science
AAAS

*New members only. International orders will receive *Science* Digital edition — to place an order outside the U.S., go to promo.aaas.org/giftmay2

Quantifying Journal Costs

The real cost of communicating scientific research worldwide—including publishing, distributing, and reading journals—is about $115 billion, according to a report from the U.K.-based Research Information Network (RIN). Of that, $3.7 billion is spent in the form of time donated by peer reviewers.

The figures are based on cost and salary information from publishers and libraries. The group concluded that the United Kingdom is more than doing its bit. It has 3.3% of the world's researchers, but they're shouldering 8.7% of the worldwide cost of peer review. And U.K. publishers put out more than 20% of the world's scientific literature.

The average cost of producing a scientific article is roughly $8000, RIN estimates, and there are limited ways of shaving costs. If 90% of their material appeared only online, publishers would save $2.1 billion on printing and distribution. And getting authors to pay for publication would save publishers and libraries $1 billion. The bulk of the overall price tag represents consumption: Academics devote an estimated $66 billion worth of their time to reading articles.

She Grinds, He Knaps

The earliest permanent dwellings, dated to about 12,000 years ago, are often divided into rooms or spaces for working, eating, or sleeping. But a site nearly twice that old along the Sea of Galilee in northern Israel suggests that humans living in temporary dwellings also divided their spaces into activity areas that may have corresponded to a division of labor between the sexes.

In 1989, a drought revealed the remains of six brush huts. The site, called Ohalo II, yielded thousands of plant remains and has been extensively studied for clues to the transition from hunting and gathering to farming (*Science*, 29 June 2007, p. 1830).

A team led by archaeobotanist Ehud Weiss of the Weizmann Institute of Science in Rehovot, Israel, divided the 12-square-meter floor area of one of the huts into a 50-square grid and plotted the distribution of nearly 60,000 seeds and other plant remains. A very high concentration, including food staples such as wild barley and millet grass, was found in the north end of the hut, centered around a grinding stone, the team reports in the August issue of the *Journal of Archaeological Science*. The hut's south end, which contained evidence that flint was knapped to make stone tools, yielded far fewer plant remains.

Dolores Piperno, an archaeobotanist at the Smithsonian Institution in Washington, D.C., says that the authors make an "excellent case for the conscious and differential use of space." Drawing upon the anthropological and ethnographic literature, the team suggests that women may have done the grinding and men the knapping.

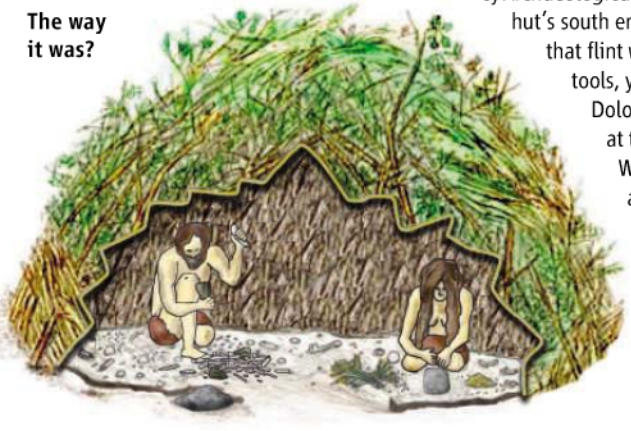

The way it was?

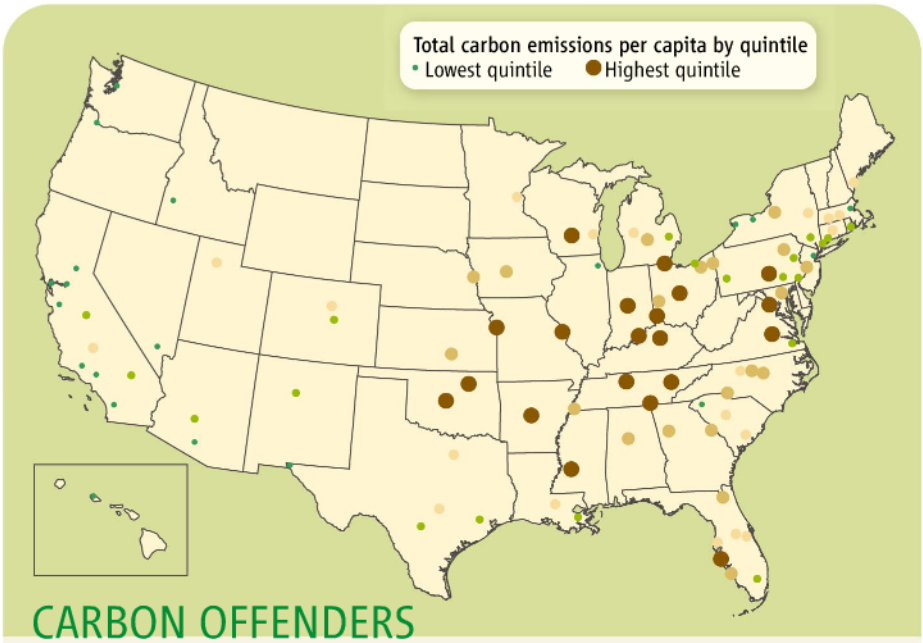

CARBON OFFENDERS

Residents of the eastern half of the United States are the worst carbon offenders, according to a new report from the Brookings Institution in Washington, D.C., which has quantified the per capita carbon footprint of the nation's 100 largest urban areas. The Lexington, Kentucky, area, with high sprawl, little rail transit, lots of air conditioning, and heavy reliance on coal power, has the highest yearly per capita emission in the country—3.46 metric tons—whereas residents of Honolulu, Hawaii, have the lowest, at 1.36 tons, according to the report, *Shrinking the Carbon Footprint of Metropolitan America*.

Gore's Götterdämmerung

"Hotter! It's getting hotter!" chants the chorus in falsetto as a heavyset man in flowing robes rises on a mechanical platform, pointing his sword at a hockey stick–shaped graph of climate trends. Such a scene might appear in the opera version of *An Inconvenient Truth*, which will be staged at La Scala in Milan, Italy, in 2011. Italian composer Giorgio Battistelli, 53, is currently at work on the opera, the latest in a series of accolades for Al Gore.

"As a researcher on global warming and as an aficionado of opera, I am delighted," says Michael Schlesinger, a physicist at the University of Illinois, Urbana-Champaign, who says he plans to attend the premiere. But there are climate-opera skeptics among Italy's music scholars. "I think that such a thing cannot work, from an artistic point of view," says Nicola Giosmin, a composer and musicologist at the Cherubini Conservatory of Music in Florence. It will be difficult not to "oversimplify" the science, he points out, adding that Al Gore's political life may not have enough core dramatic elements—"sex, betrayal, murder"—to sustain the plot.

CREDITS (TOP TO BOTTOM): BROOKINGS INSTITUTION; PHIL MCCARTEN/CORBIS; RACHEL BROWN-GOODMAN

New Products, Services, and Solutions

EDITED BY YUDHIJIT BHATTACHARJEE

Three Q's >>

Going off to college at 19 is not unusual. But **Alia Sabur** is a materials scientist who starts this week as a professor at Konkuk University in Seoul, South Korea. *Guinness World Records* lists her as the world's youngest university professor, based on her accepting the position a few days shy of her 19th birthday. A New York City native, Sabur graduated at 14 from Stony Brook University in New York and then earned master's and Ph.D. degrees in materials science from Drexel University in Philadelphia, Pennsylvania.

Q: You're at a point in your career that most people are still chasing in their 30s and 40s. What are your goals?
I'm interested in the research aspect as well as the teaching aspect [of academia]. One of the advantages of having a Ph.D. is that I can go and learn different subjects without taking classes and worrying about grades. Of all the experiences in my life, doing a Ph.D. is not one I want to repeat. Also, I'm branching out into public speaking to help motivate others, especially young girls, to go into science and technology.

Q: How will you relate to students who are older than you?
I'm used to everybody being older than me. Once I start talking, people can tell I know what I'm talking about.

Q: Why Korea?
I have never visited Asia. I thought it would be an interesting experience. [Konkuk] has closely related research to what I'm doing, and I thought there would be some potential collaborations with Stony Brook. Their president got his Ph.D. from Stony Brook.

CREDITS (TOP TO BOTTOM): TOBY ARMSTRONG; DPA

IN THE COURTS

IN GRATITUDE. A federal court's decision to award Cornell University and an affiliate organization $184 million in a patent infringement lawsuit against Hewlett-Packard (HP) could bring Hwa Torng a windfall of $46 million. The 75-year-old electrical engineer, a former professor at Cornell, plans to give most of it away to help students at community colleges.

In the early 1980s, Torng invented a technology to enable computer processors to execute multiple instructions at once. Cornell's suit against HP, filed in 2001, claimed that HP used the technology from 1996 to 2006, when the patent expired, without obtaining a license. HP argued that the technology it used was its own, different invention. On 30 May, after less than 7 hours of deliberations, a federal jury in Syracuse, New York, agreed with Cornell.

HP may still appeal. But whatever the eventual settlement, Torng's share would be 25%. He intends to use most of the money to fund scholarships for students at community colleges. "I have a strong feeling about those kids; many of them come from not-so-well-to-do families," says Torng, who grew up in Taiwan and immigrated to the United States 52 years ago. Torng's wife also emigrated from Taiwan. "We're just grateful for the opportunities that we've had," he says.

MOVERS

NEW FRONTIERS. Ernst-Ludwig Winnacker learned a thing or two about grantmaking when he ran Germany's premier research agency, the DFG, from 1998 to 2006, and more recently the European Research Council. Now the 67-year-old biologist will bring that experience to bear as the new secretary general of the Human Frontier Science Program Organization (HFSPO).

Funded by 36 countries, HFSPO supports work on the complexity of living organisms, a topic that Winnacker says is "close to my heart" and coming into its prime. "Biology is really only now becoming quantitative, and the HFSP is prepared for that," with its focus on tackling complexity, he says. The program awards grants to international collaborations and provides fellowships for researchers to travel abroad for postdoctoral research or to branch out into new disciplines. Winnacker will take over from Nobelist Torsten Wiesel on 1 January 2009 as the organization marks its 20th year.

THEY SAID IT

"In response to an inquiry, Mr. Maxim acknowledged that the following people listed as co-authors on several of his publications are 'fabricated' names and that he is the 'single real author': C. Turinici, M. Gheorge, D. Smith, R. Johns, S. Dupue, and D. Antrik. In other cases, Mr. Maxim has not consulted his co-authors and submitted publications without their knowledge."
—The IEEE *Journal of Solid-State Circuits* in a 6 June note retracting a number of papers by Adrian Maxim, an Austin, Texas–based semiconductor engineer.

Slice of Life >>

LOST AND FOUND. Primatologists and hunters are often at odds, but a young German researcher may owe her life to a group of Congolese hunters.

Esther Carlitz, 23, went missing on 22 May after she and a colleague left their research camp to track a group of bonobos. Carlitz got hungry and decided to make her way back alone to Lui Kotal, a camp inside the Salonga National Park in the Democratic Republic of the Congo that belongs to the Max Planck Institute for Evolutionary Anthropology in Leipzig.

Carlitz wandered for 6 days in the forest without food before coming across a hunters' camp. A search party that had combed the area for nearly 2 weeks finally found her on the morning of 3 June in the company of three of the hunters, tired but otherwise in surprisingly good shape, said Max Planck spokesperson Christina Beck. The hunters "took extremely good care of her," says Beck.

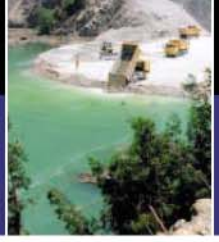

Sichuan's threatening lakes
1408

A desert CO_2 sink?
1409

NATIONAL INSTITUTES OF HEALTH

Changes in Peer Review Target Young Scientists, Heavyweights

After a year of gathering advice on how to improve its overloaded peer-review system, the U.S. National Institutes of Health (NIH) last week unveiled a plan to ease the workload on both applicants and reviewers and to help young investigators. The changes incorporate many recommendations from two advisory committees. But NIH rejected a suggestion aimed at eliminating an apparent bias favoring researchers who resubmit their grant applications after being turned down.

NIH Director Elias Zerhouni asked internal and external advisory working groups last June to suggest ways to cope with a record number of applications, a continued flat budget, and a shortage of quality reviewers. NIH's response to their report (*Science*, 29 February, p. 1169) was presented last week to the director's advisory committee by the co-chair of both panels, Lawrence Tabak, director of the National Institute of Dental and Craniofacial Research. Cell biologist Keith Yamamoto of the University of California, San Francisco, who co-chaired the external group, says he's "disappointed" that NIH rejected the advice on resubmitted proposals but that he's "basically happy with" the overall response.

NIH plans to shorten the allowed length of applications from 25 pages to 12, to focus more on the anticipated impact of the research and less on methods and other details. Proposals will be given scores on five criteria, not just an overall score, to provide clearer feedback. In addition, reviewers will score all applications, even those in the bottom of the pile that are now "triaged," or set aside. At the end of a study section meeting, reviewers will rank applications to reduce ambiguity.

NIH also followed suggestions for making reviewing more attractive to busy researchers. For example, reviewers can participate in 12 sessions over 6 years instead of 4 years and potentially share the duty with a colleague. Those receiving high-prestige awards from NIH or holding at least three basic research grants will be obliged to serve if asked. NIH will also offer a grant extension of up to $250,000—about 9 months' funding—to some 500 reviewers who have participated in at least 18 study section meetings. Tabak says this is intended to compensate them for time away from the bench spent preparing for and attending each meeting. NIH has not yet estimated the costs, but Tabak says "it is a zero-sum game" assuming most would have their grants renewed anyway.

However, NIH officials nixed a key recommendation to jettison a system that allows researchers who don't win funding the first time around to resubmit the proposal up to two more times. Reviewers tend to favor these amended applications over first-time submissions, the working groups found, perhaps because the applicants responded to reviewers' comments or because reviewers know it's the investigator's last shot. Since the doubling of NIH's budget ended in 2003, the share of the total pot claimed by first-time submissions has shrunk from about 60% to 30% (see lower graph). To level the playing field, the two panels recommended that all proposals be considered "new" so that resubmitted ones get no particular advantage. NIH also rejected the proposal that fatally flawed applications be labeled "not recommended for resubmission," instead leaving it up to reviewers to offer this advice in comments.

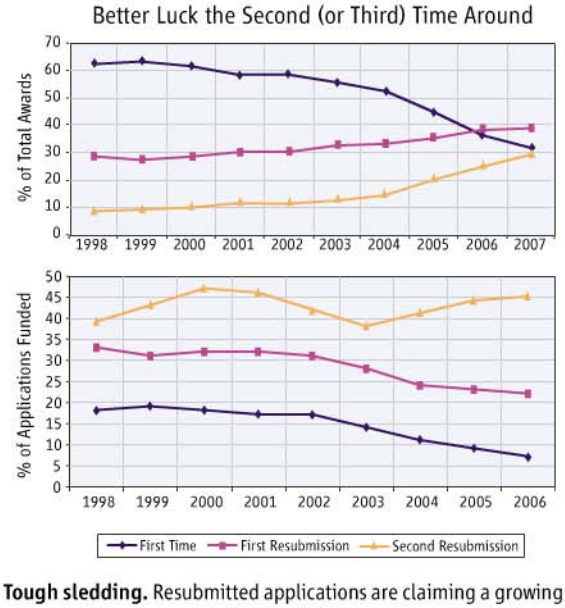

Tough sledding. Resubmitted applications are claiming a growing share of the overall pool of funded R01 research grants (*top*), and the success rate for first-time proposals, which make up about two-thirds of all applications, has plummeted to single digits (*above*).

These two proposals didn't go over well with the community. "There was a huge outcry about this. People feel like they need a second chance, a third chance," Zerhouni says. "We're not comfortable with changing the system radically to reduce the number of resubmissions," says Howard Garrison, public affairs director of the Federation of American Societies for Experimental Biology in Rockville, Maryland, which urged NIH to abandon these ideas.

Instead, NIH plans to "carefully rebalance success rates among" the three types of submissions so as to fund a larger portion on the first round, according to Tabak. The burden will fall on each institute's advisory council.

To help out young, first-time investigators, NIH will review their proposals separately within a study section. Officials plan to pilot setting a funding cutoff point for all early-stage proposals across all study sections. Since 2007, Zerhouni has set a goal of funding at least 1500 new investigators a year, about 150 more than in 2006. NIH also plans to double its funding for high-risk awards to about 1% of the agency's R01 budget.

NIH also tempered a suggestion aimed at distributing scarce resources. The advisory panel had recommended that NIH require principal investigators to spend at least 20% of their time on each grant, creating a de facto cap of four grants. But Zerhouni says it is "not practical to have a hard-and-fast rule" because the amount of time scientists spend on nonresearch activities, such as teaching, varies by institution. Instead, applicants who already have $1 million in NIH funding will have to explain why they need more.

NIH plans to implement the changes over the next 18 months.

–JOCELYN KAISER

SOURCE: NIH

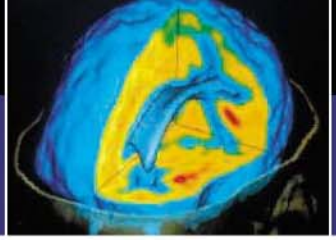

More than just a pretty picture?
1412

India's university expansion
1415

FUSION RESEARCH

Design Changes Will Increase ITER Reactor's Cost

The €10 billion ITER fusion project hopes to demonstrate that a burning plasma can be controlled to produce useful energy. This month, ITER's funders face their own daunting task of keeping the project's budget under control, as scientists present a wish list of design changes.

The changes are needed, say the researchers, because of advances in fusion science since the baseline reactor design was published in 2001. Although the wish list won't be publicly revealed until ITER's governing council meets in Japan on 17–18 June, insiders say the design tweaks are going to require more money, a fact that will not go down well with governments funding the project. "Where the pain level is for each [ITER] member is impossible to say," says David Campbell, assistant head of ITER's department of fusion science and technology.

The design review is not the council's only headache. The prices for steel and copper have skyrocketed this decade, and at the end of last year, the U.S. Congress zeroed out the country's ITER contribution from the 2008 budget. "The June council will be a key meeting," says Campbell.

ITER, or International Thermonuclear Experimental Reactor, has been on the drawing board since the mid-1980s. In 2001, the "final" design was ready, and, after much wrangling over the site, the governments of China, the European Union, Japan, Russia, South Korea, and the United States agreed to build it at Cadarache in southern France (*Science*, 1 July 2005, p. 28). (India joined the effort in 2006.) But before construction starts this year, ITER managers decided to ask researchers to review whether the design could be improved to give the project the best chance of meeting its goals (*Science*, 13 October 2006, p. 238).

Led by Günter Janeschitz of Germany's Karlsruhe research center and completed late last year, the redesign report is said to recommend 80 modifications, including changes to the plasma's microwave heating system, the complex arrangements of magnets to hold the plasma in place, and the diverter, a device around the bottom of the doughnut-shaped vessel that extracts spent fuel. ITER staff and the Science and Technology Advisory Committee—a panel of fusion experts appointed by ITER members—have been poring over the report, trying to separate out the essential from the merely desirable, and estimating how much the changes will cost and their impact on the construction schedule. "All of these things cost money, … [so] we must be careful not to make a list so long that the bill shocks everyone," says a senior European fusion researcher who asked not to be named.

One of the most contentious recommendations concerns a system to control explosive releases of energy at the edges of the plasma called edge-localized modes (ELMs). If they are too large, ELMs can erode the wall of the reactor vessel and damage the diverter. The current ITER design already contains a system to control ELMs: rapidly firing a stream of frozen deuterium pellets into the plasma, each of which causes a mini-ELM that does no damage. But researchers using the DIII-D fusion reactor in San Diego, California, discovered another way: A weak magnetic field can make the edge of the plasma slightly leaky and take the sting out of ELMs.

Such a system would be simpler and more efficient than pellet injection, but to create the magnetic field requires adding electromagnetic coils inside the reactor vessel—a major and expensive design change. Some think it's too soon to decide on such a major modification. "It's clear the field has an effect. But we don't yet understand the physics. It'll take 3 to 4 years to nail it down," says Hartmut Zohm of the Max Planck Institute for Plasma Physics in Garching, Germany. Zohm and others suggest that a redesign could make space for the coils with the decision to install them taken later.

ITER council members will also be eager to hear about the U.S. budget situation. The decision by Congress last December to remove the $149 million ITER funding from the fiscal year 2008 budget was considered unfortunate but not catastrophic by ITER insiders. "In 2009, we'll be ready to get running," says Ned Sauthoff, head of the U.S. ITER effort, adding: "We're a family. We'll figure out how to get through this." Last month, the U.S. Senate approved spending $55 million on ITER this year as part of a bill now before Congress to fund the military in Iraq and Afghanistan. The bill's fate is uncertain, however, as the Bush Administration opposes any additional domestic spending.

The talk in Washington is that, with a presidential election looming, Congress will simply extend the current budget for another 6 months, leaving ITER out in the cold until April 2009. This could prompt some ITER members to query the United States's commitment to the project. Says ITER project construction leader Norbert Holtkamp: "If the U.S. doesn't restore funding in 2009, then we have a very tricky problem. We have to ensure that 2009 is okay."

–DANIEL CLERY

CREDIT: AGENCE ITER FRANCE

Making space. Construction workers clear the ground for ITER at Cadarache.

Still going strong. Gases waft from the crater of the mud volcano on Indonesia's Java Island.

CREDIT: REUTERS/SIGIT PAMUNGKAS/LANDOV

GEOLOGY

Two Years On, a Mud Volcano Still Rages—and Bewilders

As a disastrous mud eruption on Indonesia's Java Island marks its second anniversary, the unprecedented event continues to stir debate about whether it resulted from an exploratory gas well drilling accident or a distant earthquake and how long it will last. The mud volcano, nicknamed Lusi, has been disgorging mud at a rate of up to 150,000 cubic meters per day. Officials are struggling to contain the effluent within dikes that are regularly breached and built anew farther out.

In November 2006, ground deformation near the volcano ruptured a natural gas pipeline, killing 13 people. Lusi's mud has engulfed 750 hectares, destroying the homes of more than 30,000 people as well as factories and farms. "Sadly, it's not about simple technical problems anymore. It's more [about] economic and social and political problems," says Satria Bijaksana, a geophysicist at Institut Teknologi Bandung.

Lapindo Brantas, the oil and gas exploration company that operated the ill-starred gas well, and the government have promised compensation to landowners, but it has been slow in coming. Hundreds of families are still living in temporary shelters. In two separate cases, Indonesian courts have ruled the eruption a natural disaster, absolving Lapindo Brantas of liability. Ivan Valentina Agaung, a lawyer for Walhi, an Indonesian environmental group that filed one of the suits, says the group is appealing to a higher court in hopes of getting Lapindo Brantas to take responsibility for environmental rehabilitation.

For scientists, Lusi is an intriguing specimen. A flurry of papers refines previous work on the eruption's dynamics and offers insights into the evolution of mud volcanoes. "This is a great opportunity. Nobody knows how other mud volcanoes looked when they were first appearing," says Adriano Mazzini, a geologist at the University of Oslo.

There is general agreement on the sequence of events. On 27 May 2006 at 5:54 a.m. local time, a magnitude-6.3 earthquake struck near Yogyakarta, in central Java. Between 5 and 8 a.m. the following day, Lapindo Brantas's gas well, which was being drilled 250 kilometers to the east near the town of Sidoarjo, began to flood. Workers shut the well's blowout preventer to keep the fluid from gushing out the top. They noted that pressure inside the well rose rapidly before gradually subsiding. Early in the morning of 29 May, mud began burbling out of the ground about 150 meters away.

In a February 2007 article in *GSA Today*, Richard Davies, a geologist at the University of Durham, U.K., and colleagues claimed that the drillers penetrated a porous limestone formation about 2800 meters below the surface, inadvertently tapping into a highly pressurized aquifer. The borehole's casing didn't extend deep enough to protect rock from cracking under the pressure when the blowout preventer was shut, he concluded. Water then channeled its way to the surface, bringing mud with it (*Science*, 2 February 2007, p. 586).

That's not how Mazzini and his colleagues see it. In the 30 September 2007 issue of *Earth and Planetary Science Letters*, they argued that the region's geological structures, pressurized hydrocarbon deposits, common in the region, and a seismic fault created conditions "perfect for a mud volcano." The only thing missing was a trigger, Mazzini says. The drilling might have contributed, he says, but he believes a more important factor was that the Yogyakarta earthquake reactivated the fault. At roughly the same time Lusi broke, mud also erupted from eight fissures along a 100-kilometer stretch of the fault line. "I don't think this is a coincidence," he says.

Global Positioning System (GPS) data and an obvious kink in a rail line show that ground along the fault has shifted up to half a meter since the Yogyakarta earthquake. But Michael Manga, a geologist at the University of California, Berkeley, who has studied how earthquakes trigger distant volcanic eruptions, contends that the quake was too small and too far away from the fault to influence it. In recent decades, he says, "there were many earthquakes that were both closer and bigger and by any measure more likely to have triggered an eruption."

In a paper published online on 5 June in *Earth and Planetary Science Letters*, Manga, Davies, and colleagues suggest that the fault is likely to be shifting in response to the movement of vast amounts of material to the surface. The mechanism is not clear. Co-author Rudi Rubiandini, a petroleum engineer at the Institut Teknologi Bandung, says the analysis "makes every other reason [for the eruption] impossible." Most earth scientists agree that the well must have had some effect, says James Mori, a seismologist at Kyoto University in Japan. But he says researchers can't determine whether the volcano would have formed without the drilling.

While sympathizing with Lusi's victims, geologists say they relish the rare opportunity to study a mud volcano's birth and evolution. GPS and satellite-based interferometric synthetic aperture radar data indicate that the surface near the volcano's vent is collapsing into a funnel shape, characteristic of sand draining from the top bulb of an hourglass. Davies and colleagues concluded in a paper published

UNSTOPPABLE

The mud volcano Lusi is unique in its longevity and the volume of material ejected. It may also be setting records for the number of failed attempts to plug it.

Immediately after the 29 May 2006 eruption, Lapindo Brantas—the company whose exploratory drilling, some claim, triggered the eruption—pumped concrete into the well to try to stop the gush of hot, salty water from a subsurface aquifer. When that failed, the company brought in a consultant from Houston, Texas, who directed the drilling of two relief wells intended to intercept the original borehole and pump in high-density drilling mud to plug the leak. This effort was abandoned when the wells were short of their target—also, reportedly, because Lapindo Brantas ran out of money.

In February 2007, following a proposal from geophysicist Satria Bijaksana and two colleagues from Institut Teknologi Bandung, Lapindo Brantas started dropping into the vent clusters of concrete balls, 20 centimeters and 40 centimeters in diameter, roped together with steel cables. The objective, Bijaksana says, was "to reduce the sheer volume of mud coming out of the vent to a manageable level." This effort was abandoned after 398 of a planned 1000 clusters had been dropped; a government agency that took over management of the disaster concluded that the balls were having little effect.

The only hope of plugging Lusi is to drill another relief well to plug the original well at a point below where it was breached, says Rudi Rubiandini, a petroleum engineer at Institut Teknologi Bandung. He estimates that the well would cost $70 million to $100 million. But that is unlikely to happen, he says: "Our government now thinks this is a natural disaster and impossible to kill." **–D.N.**

online on 21 May in *Environmental Geology* that between June 2006 and September 2007, the funnel's center sank at about 4 centimeters per day, which in 3 years would produce a sag of 44 meters. They also report that areas outside the funnel are rising, probably due to movement of the fault.

Scientists are puzzling over other phenomena as well. Since March 2007, the flow has periodically stopped for hours or days only to resume with its previous vigor. The likely explanation, Davies says, is that the weight of mud at the surface is collapsing the vent deep underground. Pressure backs up until it breaks through the blockage. In addition, there have been 88 minieruptions of water and methane where the ground is subsiding. Rubiandini believes the subsidence is cracking open pressurized gas pockets. And along the fault, geysers of water have suddenly shot up in the middle of yards, rice paddies, and even within factories, probably due to the rearrangement of subsurface plumbing. "The volcano is taking on a life of its own," Davies says.

How long this will go on, he says, is anybody's guess. **–DENNIS NORMILE**

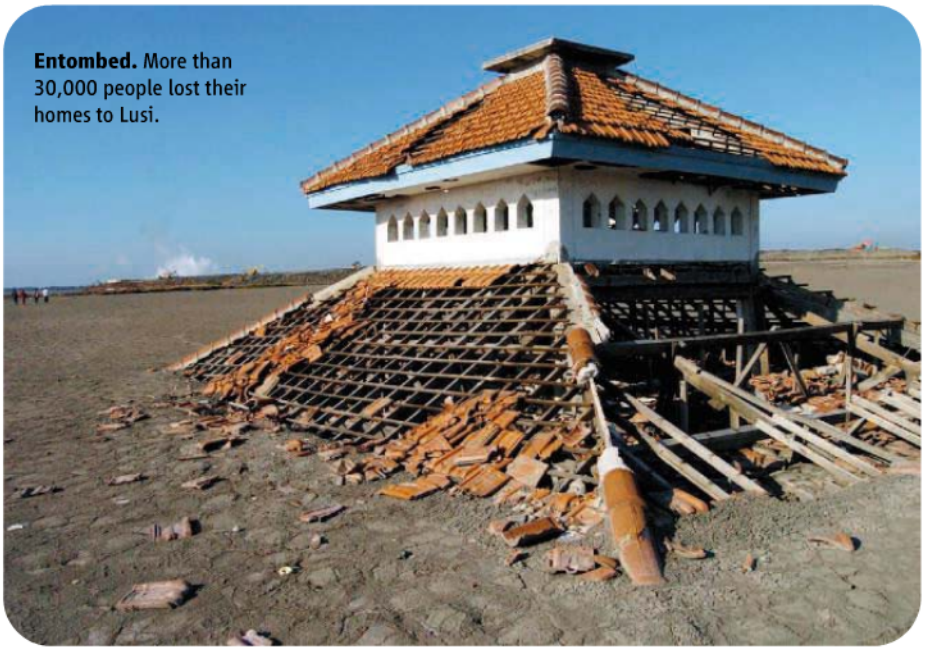

Entombed. More than 30,000 people lost their homes to Lusi.

CREDIT: MAMAT/AFP/GETTY IMAGES

More Political Heat on NIH

The U.S. Congress is ramping up its investigations into how the National Institutes of Health (NIH) monitors financial conflicts of interest among grantees.

One high-profile case involves Harvard University and Massachusetts General Hospital child psychiatrist Joseph Biederman. Last week, as first reported in *The New York Times*, Senator Chuck Grassley (R–IA) alleged that Biederman and two colleagues had failed to report to their institutions hundreds of thousands of dollars in income from consulting for a half-dozen or so drug companies. Grassley has asked Harvard whether the researchers broke university rules that prohibit faculty members from conducting clinical trials of products made by companies from whom they have received payments exceeding $20,000. Grassley, who has accused NIH Director Elias Zerhouni of "lax" oversight of extramural research, wants to require drug companies to report all payments to physicians in a public database.

Also last week, two Republicans on the House Energy and Commerce Committee asked Zerhouni to look into whether two Cornell University researchers studying a new screening test for lung cancer had to disclose a financial stake in the study's outcome. Democrats on the committee have leveled similar accusations at rival researchers leading an NIH-funded clinical trial (*Science*, 2 May, p. 602).

Harvard and NIH say investigations are under way, including a "systemwide review of policies" at NIH. In the past, NIH has said it lacks the authority to directly monitor conflicts of interest involving its grantees and instead relies on universities to police themselves. Grassley's letter to NIH says he is looking at cases involving more than 20 other universities. **–JOCELYN KAISER**

A Smart Investment

BERLIN—Berlin officials like to joke that the city is "poor but sexy." Now they can add "and smart." Despite chronic budget shortfalls, Berlin's city government has pledged €160 million ($250 million) over the next 4 years to attract top researchers to the city's universities and institutes. The "Berlin International Forum for Excellence" has the chance to make Berlin "one of the most important locations for research in the world," said Jürgen Zöllner, the city's senator for science and education. Augmented by private donations, the funding will be used to top up salaries of world-class researchers, set up graduate schools in "areas of excellence," and attract visiting scholars. **–GRETCHEN VOGEL**

WENCHUAN EARTHQUAKE

Scientists Race Against the Clock to Gauge Landslide Risk

XIAO JIA QIAO, CHINA—In a vale ringed by mountains bearing the tan scars of numerous landslides, bulldozers are carving a diversion channel to relieve pressure from the rising waters of a blocked river. On 12 May, the Wenchuan earthquake sent about 2 million cubic meters of limestone rubble hurtling down a mountainside here, obliterating houses in Xiao Jia Qiao village and creating a 70-meter-high dam on the Chaping River. Near the dam, the Chaping's jade-green waters are choked with flotsam, including a few bloated pillows and a pair of red doors. In the last few weeks, the river, now a lake, has risen 50 meters, submerging houses along its banks. "I'm surprised how fast the water is coming up," says Wei Fangqiang, a physical geographer at the Institute of Mountain Hazards and Environment (IMHE) in Chengdu, who first glimpsed the 300-meter-wide dam on 16 May.

The gravest threat to survivors of the magnitude-7.9 Wenchuan earthquake, history shows, may be new lakes like this one. In 1933, a landslide dam formed by a magnitude-7.5 earthquake in Sichuan Province burst 45 days after the quake; the flood killed about 8000 people, some 2000 more than the number who died in the earthquake itself, says Wei.

A 150-person engineering brigade from Hubei Province has been working round the clock for 8 days digging a channel to bypass the dam. With heavy rain in the forecast, Wei says, the Chaping River should rise faster and reconnect with its downstream segment in a few days. If all goes according to plan, the channel should draw down the Chaping gradually, reducing the risk of the dam giving way and unleashing a torrent on people living in tents downstream.

As perilous as the situation is at Xiao Jia Qiao, the landslide dam here is considered "medium risk," one of five in this category; IMHE has classified seven others as high-risk. The most dangerous of all, says IMHE geomorphologist Cui Peng, was at Tangjiashan, where some 242 million cubic meters of the Jianjiang River had piled up behind a fragile earth barrier.

The government had evacuated more than 100,000 people downstream in the Mianyang area and had a contingency plan to quickly evacuate a million more. The main objective has been to keep the flow rate through a diversion channel fast enough to compensate for the rain-fed Jianjiang River's rise. Army troops earlier this week fired rockets at boulders near the channel to try to boost the flow rate, according to the Xinhua News Agency. Water began moving through the channel, and officials declared a "decisive victory" this week in lowering the level of the lake.

As *Science* went to press, 69,142 people were known to have perished and 17,551 were missing after the Wenchuan earthquake. Now that the search for survivors has ended, the overriding task is to provide adequate housing and food for more than 1.5 million people who lost homes in the quake and to guard against the spread of disease in the vulnerable displaced population.

A few days after the initial shock, Cui's team struck out into the disaster zone to examine some of the debris dams (*Science*, 23 May, p. 996). In the meantime, crewless planes from the Institute of Remote Sensing Applications in Beijing imaged the area to help chart major landslides among the estimated several thousand triggered by the earthquake. A team led by Tang Huiming, an expert on geological hazards at China University of Geosciences in Wuhan, has found evidence of old landslides where fresh ones occurred. Still, the extent of the devastation is mind-boggling, says Tang: "I've never seen anything like this before."

In all, Cui and his colleagues have identified more than 100 landslide dams. Researchers with IMHE and the Chengdu Hydropower Survey and Design Institute zeroed in on 33 for detailed analysis. The Chinese government is attempting to divert water at the 12 dams deemed medium or high risk and four others. "It's quite difficult to say" how well the diversion channels will work, says Cui. "Nobody has very good experience for dealing with megalandslide dams."

Meanwhile, another threat is looming. Scores of landslides—nobody knows how many—have blocked gullies that are dry now but can fill with water during the rainy season. Many smaller dams are known from remote sensing, says Cui, but "only from a field survey can we say which are dangerous." IMHE researchers plan to fan out around Sichuan to identify which of the clogged gullies have villages or temporary shelters for displaced people near their outlets. Wei was planning to deliver a report on this threat to Sichuan authorities earlier this week. "I'm worried that the blocked gullies could create a serious disaster," he says.

In the months to come, Cui and his IMHE colleagues will help determine where it is safe to rebuild homes in this shattered corner of Sichuan Province. Studying how the mountain slopes have changed is a critical piece of the government's reconstruction effort. "We have to figure out which places are suitable for people to live and which are too dangerous," says Cui. With the huge number of survivors roughing it in tents and other temporary shelters, the scientists will have to work fast.

–RICHARD STONE

Rough-hewn floodgate. Workers sculpt a channel through debris blocking the Chaping River.

CREDIT: R. STONE/SCIENCE

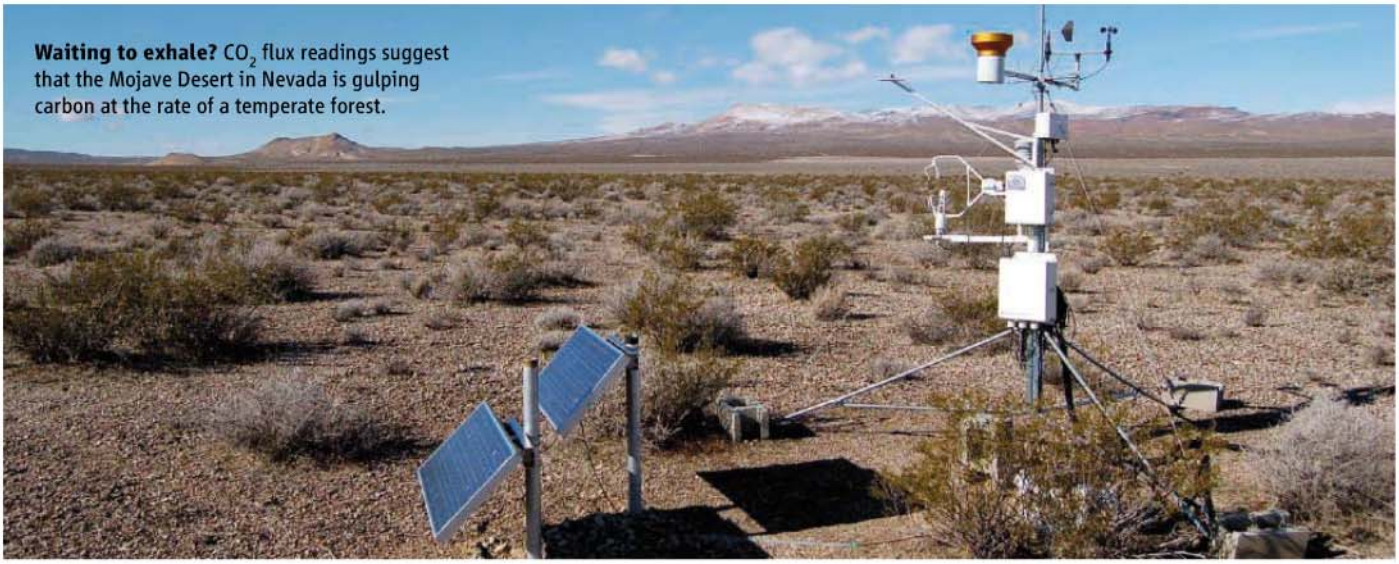

Waiting to exhale? CO_2 flux readings suggest that the Mojave Desert in Nevada is gulping carbon at the rate of a temperate forest.

CREDIT: DESERT RESEARCH INSTITUTE, NEVADA

ECOSYSTEMS

Have Desert Researchers Discovered A Hidden Loop in the Carbon Cycle?

URUMQI, CHINA—When Li Yan began measuring carbon dioxide (CO_2) in western China's Gubantonggut Desert in 2005, he thought his equipment had malfunctioned. Li, a plant ecophysiologist with the Chinese Academy of Sciences' Xinjiang Institute of Ecology and Geography in Urumqi, discovered that his plot was soaking up CO_2 at night. His team ruled out the sparse vegetation as the CO_2 sink. Li came to a surprising conclusion: The alkaline soil of Gubantonggut is socking away large quantities of CO_2 in an inorganic form.

A CO_2-gulping desert in a remote corner of China may not be an isolated phenomenon. Halfway around the world, researchers have found that Nevada's Mojave Desert, square meter for square meter, absorbs about the same amount of CO_2 as some temperate forests. The two sets of findings suggest that deserts are unsung players in the global carbon cycle. "Deserts are a larger sink for carbon dioxide than had previously been assumed," says Lynn Fenstermaker, a remote sensing ecologist at the Desert Research Institute (DRI) in Las Vegas, Nevada, and a co-author of a paper on the Mojave findings published online last April in *Global Change Biology*.

The effect could be huge: About 35% of Earth's land surface, or 5.2 billion hectares, is desert and semiarid ecosystems. If the Mojave readings represent an average CO_2 uptake, then deserts and semiarid regions may be absorbing up to 5.2 billion tons of carbon a year—roughly half the amount emitted globally by burning fossil fuels, says John "Jay" Arnone, an ecologist in DRI's Reno lab and a co-author of the Mojave paper. But others point out that CO_2 fluxes are notoriously difficult to measure and that it is necessary to take readings in other arid and semiarid regions to determine whether the Mojave and Gubantonggut findings are representative or anomalous.

For now, some experts doubt that the world's most barren ecosystems are the long-sought missing carbon sink. "I'd be hugely surprised if this were the missing sink. If deserts are taking up a lot of carbon, it ought to be obvious," says William Schlesinger, a biogeochemist at the Cary Institute of Ecosystem Studies in Millbrook, New York, who in the 1980s was among the first to examine carbon flux in deserts. Nevertheless, he says, both sets of findings are intriguing and "must be followed up."

Scientists have long struggled to balance Earth's carbon books. While atmospheric CO_2 levels are rising rapidly, our planet absorbs more CO_2 than can be accounted for. Researchers have searched high and low for this missing sink. It doesn't appear to be the oceans or forests—although the capacity of boreal forests to absorb CO_2 was long underestimated. Deserts might be the least likely candidate. "You would think that seemingly lifeless places must be carbon neutral, or carbon sources," says Mojave co-author Georg Wohlfahrt, an ecologist at the University of Innsbruck in Austria.

About 20 kilometers north of Urumqi, clusters of shanties are huddled next to fields of hops, cotton, and grapes. Soon after the Communist victory over the Nationalists in 1949, soldiers released from active duty were dispatched across rural China, including vast Xinjiang Province, to farm the land. At the edge of the sprawling "222" soldier farm, which is home to hundreds of families, oasis fields end where the Gubantonggut begins. The Fukang Station of Desert Ecology, which Li directs, is situated at this transition between ecosystems.

In recent years, average precipitation has increased in the Gubantonggut, and the dominant *Tamarix* shrubs are thriving. Li set out to measure the difference in CO_2 absorption between oasis and desert soil. An automated flux chamber measured CO_2 depletion a few centimeters above the soil in 24-hour intervals on select days in the growing season (from May to October) in 2005 and in 2006. The desert readings ranged from 62 to 622 grams of carbon per square meter per year. Li assumed that *Tamarix* and a biotic crust of lichen, moss, and cyanobacteria up to 5 centimeters thick are responsible for part of the uptake. To rule out an organic process in the soil, Li's team put several kilograms in a pressure steam chamber to kill off any life forms and enzymes. CO_2 absorption held steady, according to their report, posted online earlier this year in *Environmental Geology*.

"The sterilization treatment was impressive," says biogeochemist Pieter Tans, a climate change expert with the U.S. National Oceanic and Atmospheric Administration in Boulder, Colorado. "They may have found a significant effect, previously neglected, but I would like to see more evidence." Indeed, the high end of the Urumqi CO_2 flux estimates are off the charts. "That's more carbon uptake than our fastest growing southern forests. It's a ▶

huge number. I find it extremely hard to believe," says Schlesinger, who nonetheless says the Chinese team's methodology looks sound.

At first, Li was flummoxed. Then, he says, he realized that deserts are "like a dry ocean." The pH of oceans is falling gradually as they absorb CO_2, forming carbonic acid. "I thought, 'Why wouldn't this also happen in the soil?' " Whereas the ocean has a single surface for gas exchange, Li says, soil is a porous medium with a huge reactive surface area. One question, Tans notes, is why the desert soils would remain alkaline as they absorb CO_2. Li suggests that ongoing salinization drives pH in the opposite direction, allowing for continual CO_2 absorption. But where the carbon goes—whether it is stowed largely as calcium carbonate or other salts—is unknown, Li says. Schlesinger too is stumped: "It takes a long time for carbonate to build up in the soil," he says. At the apparent rate of absorption in China, he says, "we'd be up to our ankles in carbon."

Missing sink? *Tamarix* shrubs are thriving in China's Gubantonggut Desert, but the soil itself may be socking away far more CO_2 at night.

One possibility, DRI soil chemist Giles Marion speculates, is that at night, CO_2 reacts with moisture in the soil and perhaps with dew to form carbonic acid, which dissolves calcium carbonate—a reaction that warmer temperatures would drive in reverse, releasing the CO_2 again during the day. (Unlike most minerals, carbonates become more soluble at lower temperatures.) In that case, Marion says, Li's nighttime absorption would tell only half the story: "I would expect that over a year, there would be no significant increase in soil storage due to this process," he says, as the dynamic of carbon sequestration in the soil would vary from season to season. Li agrees that this scenario is plausible but notes that his daytime measurements of CO_2 flux did not negate the nighttime uptake.

In any case, other researchers say, absorption alone cannot explain the substantial uptake in the Mojave. Wohlfahrt and his colleagues measured CO_2 flux above the loamy sands of the Nevada Test Site, where the United States once tested its nuclear arsenal. From March 2005 to February 2007, the desert biome absorbed on average roughly 100 grams of carbon per square meter per year—comparable to temperate forests and grassland ecosystems—the team reported in its *Global Change Biology* paper.

Three processes are probably involved in CO_2 absorption, Wohlfahrt says: biotic crusts, alkaline soils, and expanded shrub cover due to increased average precipitation. "We currently do not have the data to say where exactly the carbon is going," he says. Like the Urumqi team, Wohlfahrt and his colleagues observed CO_2 absorption at night that cannot be attributed to photosynthesis. "I hope we can corroborate the Chinese findings in the Mojave," he says. Arnone and others, however, believe that carbon storage in soil is minimal.

Wohlfahrt suspects biotic crusts play a key role. "People have almost completely neglected what's going on with the crusts," he says. Others are not so sure. "I'm mystified by the Mojave work. There is no way that all the CO_2 absorption observed in these studies is due to biological crusts, as there are not enough of them active long enough to account for such a large sink," says Jayne Belnap of the U.S. Geological Survey's Canyonlands Research Station in Moab, Utah. She and her colleagues have studied carbon uptake in the southern Utah desert, which has similar crust species. "We do not see any such results," she says.

Provided the surprising CO_2 sink in the deserts is not a mirage, it may yet prove ephemeral. "We don't want to say that these ecosystems will continue to gain carbon at this rate forever," Wohlfahrt says. The unexpected CO_2 absorption may be due to a recent uptick in precipitation in many deserts that has fueled a visible surge in vegetation. If average annual rainfall levels in those deserts were to abate, that could release the stored carbon and lead to a more rapid buildup of atmospheric CO_2—and possibly accelerate global warming.

–RICHARD STONE

ENVIRONMENT

U.S. Climate Change Bill Dies, But the Energy Remains

After weeks of preparation, the U.S. Senate failed to engage in a historic debate last week on how to reduce greenhouse gas emissions. But that hasn't stopped both sides from declaring victory in what amounts to a dry run for next year, under a new president and a new Congress.

Scientific and environmental groups that see such legislation as a national priority say a Democratic proposal to put a price on carbon and create a trillion-dollar market in carbon credits—which would shift money from polluters to "green" companies, governments, and the public—has at least helped frame a debate they hope to win next year. In rebuttal, Republican opponents and the Bush Administration, which promised to veto it, believe they stood up against a badly flawed bill that would have crippled economic growth and cost families thousands of dollars.

The actual cause of death for the Climate Security Act of 2008 (S.3036), ironically, was a failure by proponents to limit debate. Their inability to invoke cloture—which requires 60 votes in the 100-member body—meant that opponents would be able to postpone a vote indefinitely. That led Democratic leaders to pull the plug on 6 June. But supporters claim that the 54 senators who expressed support for moving ahead with the legislation is itself remarkable and provides a solid foundation upon which to build.

"Clearly, we knew we weren't going to get a bill this year," admits Brendan Bell, Washington representative for the Union of Concerned Scientists (UCS), which helped organize a petition signed last month by 1700 scientists and economists calling for "swift and sharp cuts" in emissions. "But in 2 years, we've gone from people denying we have a problem and saying we need to study the issue to people saying, 'Let's look

CREDIT: M. STONE

ASIA

Nepal Counts on Science to Turn Struggling Country Around

KATHMANDU—Nepal's new leaders have a surprising strategy for making the poor Himalayan nation's transition from monarchy to republic a success: They plan to shower money on science. High on the agenda of Nepal's new legislative body, the Constituent Assembly, is to approve next month a $125 million budget for the Ministry of Environment, Science, and Technology (MEST)—a whopping 12-fold increase over 2007. "This is so much money that scientists may not [be able to] spend it all," says science ministry senior adviser Devi Paudyal.

Perhaps most remarkable is the source of the promised windfall: the Maoists, a group once labeled as terrorists that won the largest share of assembly seats in elections in April. In a manifesto published shortly before the election, the Maoists declared that "Without science, a country cannot develop." Before launching a bloody, decade-long insurgency, the group's leader, Prachanda, had earned a degree in agricultural science from the Institute of Agriculture and Animal Science in Rampur and taught science in a prep school.

Some in Nepal's tiny scientific community are cautiously optimistic. "Past governments were not aware about the value of science," says botanist Dayananda Bajracharya, a science adviser to Girija Koirala, the current prime minister. "The new government has promised they will give more attention to science. Hopefully, they will keep their word." Others say they will believe it when they see it. "Most of the political parties talk about these things, but when it comes to reality, the budget is always full," says Pramod Jha, a botanist at Tribhuvan University in Kathmandu.

Based on World Bank figures on research and development spending as a percentage of gross domestic product (GDP), Nepal ranks behind the island nation of Mauritius as well as Burundi, the country with the world's lowest per capita GDP. Nepal's first university, Tribhuvan, opened its doors only in 1959, and the Nepal Academy of Science and Technology (NAST) was established in 1982. One restraint on scientific development is an unchecked brain drain by Nepal's few rising science stars, says Bajracharya.

Science for the masses. Maoist leader Prachanda has promised a big boost for R&D in Nepal.

The Maoists plan to bet heavily on biotechnology, an area the previous government tried to nurture. Last year, NAST broke ground on a three-story biotech lab in Kathmandu that it hopes to complete by summer 2009; MEST plans to begin construction of a national Biotechnology Research and Development Center later this year. This fall, Tribhuvan, Nepal's top university, will open a graduate program in biotechnology.

These efforts are primarily intended to exploit Nepal's biological riches. Scientists here in recent years have launched programs to find medicinal plants and pinpoint active compounds. But with scant tools for molecular analyses, "we haven't been able to do much," says NAST Vice Chancellor Hom Bhattarai. "We want to get modern equipment."

With Nepal recently beset by gasoline and electricity shortages, a large portion of the supersized science budget will be devoted to research on clean energy, says Paudyal. One project the new government intends to fund is development of *Jatropha curcas*, a variety of a shrub used for biofuel, which is better acclimated to high altitude.

In the long term, raising Nepal's science game will require reducing the country's appalling 51% illiteracy rate—the 15th highest in the world, according to the United Nations. "The public at large thinks science is too sophisticated for a country like Nepal," says Bajracharya. It may take another (science) revolution to change that. **–JERRY GUO**

Jerry Guo is a writer in New Haven, Connecticut.

at the details of how to address it.' "

Of course, the details are supremely important. Within 24 hours of the vote, for example, 10 Democratic senators who supported ending debate said that the bill contained provisions that would have to be revised before they could vote for it. That's on top of dozens of amendments introduced by both sides of the aisle but never taken up by the Senate. "To be honest, we have a lot of work to do next year," says an aide to one prominent Democrat. "We probably have only 40-some votes, and we need 60 if we're ever going to pass something."

Getting to a cloture-proof majority may mean a lot of tinkering with the bill, agrees Daniel Lashof, director of the climate center at the Natural Resources Defense Council in Washington, D.C.: "Last week was the first time that the Senate had really focused on climate legislation, and the amendments that people introduced showed their concerns about topics that we'll need to address." He cited provisions to protect energy-intensive manufacturing processes such as steel that would face competition from companies not constrained by any carbon-trading system and low-income families hit hard by higher energy prices.

Although a climate change bill is unlikely to return to the Senate agenda this year, Congress could still set the tone of next year's debate, for example, by responding to the public outcry over $4-a-gallon gasoline. "They could go in the right or wrong direction," says Lashof, "by either adopting a throwback response to drill our way out of high prices or by accelerating efforts to develop alternative fuels."

In fact, some advocates of sharp reductions in greenhouse gas emissions say that they are happy the Senate failed to act. "Certainly, we are much better off," says James Hansen, director of NASA's Goddard Institute for Space Studies in New York City, who regards the UCS petition as too mild and who favors a carbon tax that would be returned to the public. "Giving most of the money away to special interests … is a terrible path to go down," he says. Such policies risk triggering a taxpayer revolt, he says, which would derail any lasting solution to global warming. **–JEFFREY MERVIS**

CREDIT: PRADEEP SHRESTHA/AFP/GETTY IMAGES

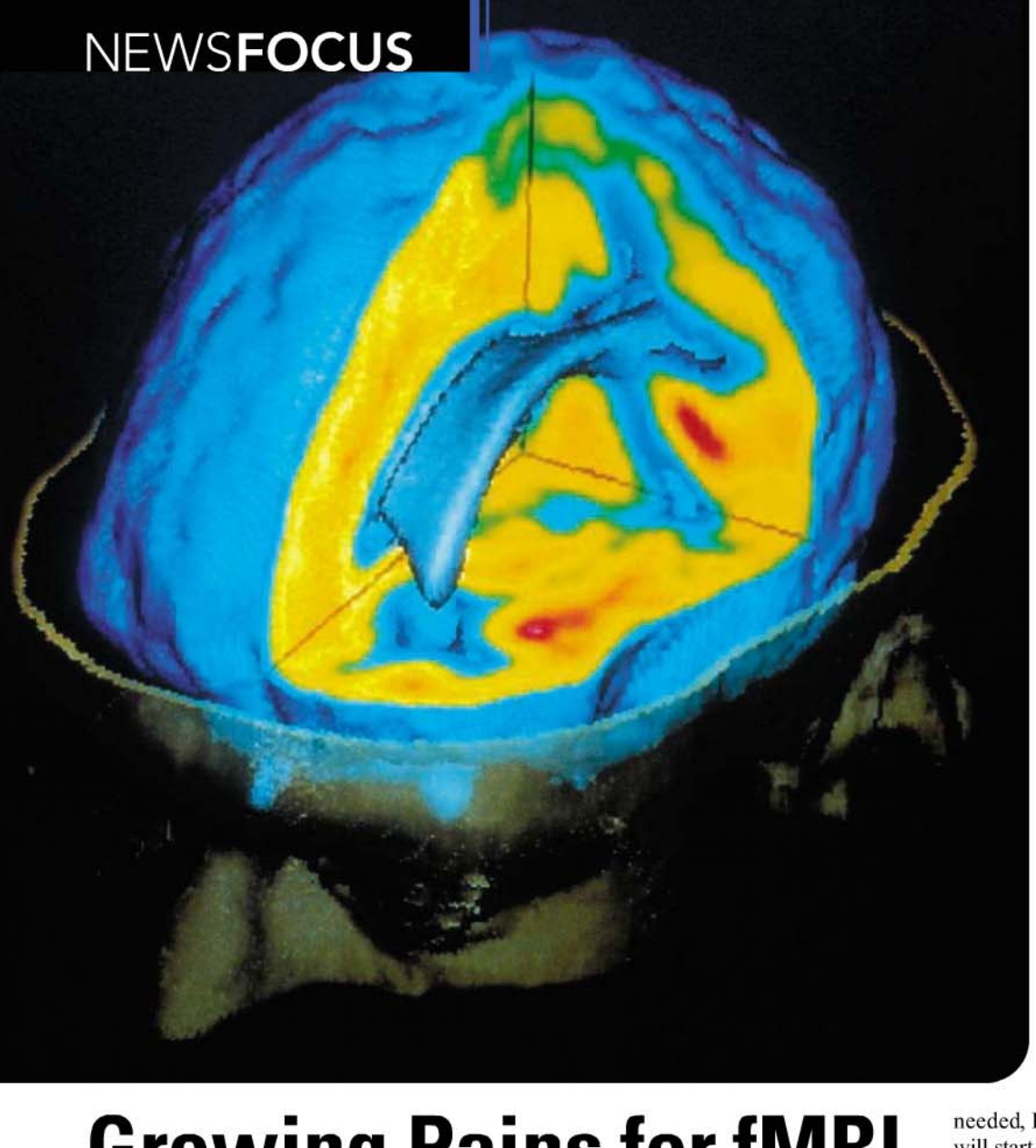

Growing Pains for fMRI

As the use of functional magnetic resonance imaging has exploded, some researchers say the field could use a dose of rigor. Will new experimental approaches come to the rescue?

Last November, the op-ed page of the *New York Times*, which typically airs political controversies, managed to create one of its own. It published a column describing a study in which 20 undecided voters had their brain activity scanned by functional magnetic resonance imaging (fMRI) while viewing photographs and videos of the major candidates in the upcoming U.S. presidential election. The findings revealed "some voter impressions on which this election may well turn," according to the authors, who included a political scientist, a neuroscientist, and several people affiliated with FKF Applied Research, a company based in Washington, D.C., that sells fMRI-based marketing studies.

The column infuriated some neuroscientists and ignited an animated discussion in the imaging field. "It was really closer to astrology than it was to real science," says Russell Poldrack of the University of California, Los Angeles (UCLA), who drafted a letter to the newspaper that was signed by 16 other cognitive neuroscientists and published 3 days later. "It epitomized everything that a lot of us feel is wrong about where certain parts of the field are going, which is throw someone in a scanner and tell a story about it."

Since its introduction in the early 1990s, fMRI has transformed neuroscience. Now in its teenage years, the fMRI field is still experiencing growing pains. Some cognitive neuroscientists say they're frustrated that many studies—including some of those that garner the most attention in the popular press—reveal little about the neural mechanisms of human cognition. "The problem right now with imaging is that doing experiments right is really, really hard, but getting pictures out is really, really easy," says Steven Petersen, a veteran brain-imaging researcher at Washington University in St. Louis, Missouri.

At the same time, there are signs that the field is maturing, as researchers confront the limitations of fMRI. Such efforts include painstaking experiments that match human fMRI data with analogous fMRI data and electrophysiological recordings of neural activity in monkeys, as well as new analytical methods capable of revealing information processing in the brain that would be impossible to detect with standard methods. "I think [these methods] are really going to revolutionize how we think about our data," says Poldrack. They also have the potential to introduce more rigor into fMRI research—something that's badly needed, Poldrack says, otherwise, "people will start to see fMRI as neophrenology, just telling stories and not giving explanations."

Neuroimagers gone wild

What irked Poldrack and others most about the *Times*'s op-ed was the way the authors inferred particular mental states from the activation of particular brain regions: Activity in the anterior cingulate cortex indicated mixed feelings about Hillary Clinton, for example, whereas amygdala activation indicated "voter anxiety" about Republican candidate Mitt Romney.

The basic problem, the objectors wrote in their letter, is that it's not possible to infer a particular mental state (such as anxiety) from the activation of a particular brain region (such as the amygdala). Although it's true that anxiety engages the amygdala, says co-signer Elizabeth Phelps, a cognitive neuroscientist at New York University, so do intense smells, sexually arousing images, and many other things. To conclude that Romney makes voters

anxious based on amygdala activation alone is unjustified, Phelps says.

The neuroscientist co-author on the op-ed piece, Marco Iacoboni of UCLA, stands by the column's conclusions as reasonable and says he's been surprised and stung by what he views as an overly harsh and hypocritical rebuke. After all, he points out, most of his critics use similar "reverse inferences" themselves.

That's true, says Poldrack, and it's a problem the field needs to confront. He and others argue that reverse inferences are particularly common in newer fields such as social cognitive neuroscience and neuroeconomics (not to mention neuropolitics), fields in which researchers are still trying to identify the cognitive processes underlying the behaviors they study. As an example, Poldrack points to a widely cited paper that used fMRI to investigate brain activity in subjects pondering moral dilemmas (*Science*, 14 September 2001, p. 2105); some of the brain regions that lit up had been linked in previous studies to emotional and "rational" cognitive processes, and the authors concluded that these two types of processes are active, to different degrees, in different types of moral judgments. But the strength of such arguments hinges on how specifically a given brain area is linked to a given mental process. Poldrack points out, for example, that some of the "emotional" brain regions in the morality study have also been connected to memory and language—a caveat that is rarely mentioned in media coverage of the work (*Science*, 9 May, p. 734).

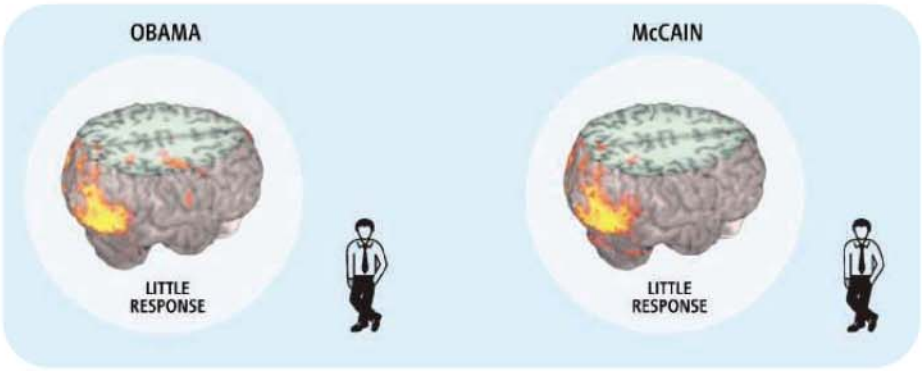

Political blunder? The *New York Times* used this graphic, showing that U.S. presidential candidates Barack Obama and John McCain stimulated relatively little activity in the brains of undecided voters, to illustrate online a brain-imaging study published as an op-ed column last November.

Monkeying around

The general public may be easily seduced by pretty images generated by fMRI (see sidebar, below), but even neuroscientists sometimes seem to fall under the spell and overlook the method's limitations. One constraint is the narrow sliver of the human experience that can be captured when a person has to keep his or her head still for long periods inside an fMRI scanner. Another is the resolution. Using fMRI to spy on neurons is something like using Cold War–era satellites to spy on people: Only large-scale activity is visible. With standard fMRI equipment, the smallest cube of brain tissue that can be imaged is generally a few millimeters on a side. Each such "voxel" (a mashup of volume and pixel) contains millions of neurons. And although neurons can fire hundreds of impulses per second, the fMRI signal—which indicates an increase in oxygenated blood bringing energy to active neurons—develops sluggishly, over several seconds. This makes fMRI a crude tool for investigating how circuits of intricately connected neurons do the computational work of cognition and behavior, says Roger Tootell, a neuroscientist at Harvard University. "fMRI is really good for telling you where to look," he says, "but I don't think you can ever really come up with mechanisms."

Tootell is one of a handful of researchers trying to circumvent such obstacles by combining human fMRI with monkey experiments. The general idea, he explains, is to follow up on the human findings by using fMRI to identify analogous regions of the monkey brain and then record the activity of individual neurons there with microelectrodes.

In some cases, single neuron recordings have confirmed fMRI findings. In 2006, Tootell and colleagues reported microelectrode data showing that 97% of neurons in the monkey equivalent of the fusiform face area—a region of the temporal cortex that appears in human fMRI studies to respond selectively to images of faces—do indeed respond preferentially to faces (*Science*, 3 February 2006, p. 670). But Tootell says that more recent human fMRI experiments his group has done suggest that neurons in an adjacent "place" region in the temporal cortex respond preferentially to edges, not places per se. The researchers are planning monkey experiments to investigate the preferences of neurons in this region in greater detail.

Such studies, he says, can also begin to reveal mechanisms of visual object processing in the brain, such as how "face" or "place" neu-

DON'T BE SEDUCED BY THE BRAIN

Few advances in neuroscience have generated as much public interest as the ability to see the human brain in action. The enthusiasm isn't hard to understand. Methods such as functional magnetic resonance imaging (fMRI) have enabled researchers to bring distinctly human attributes—love, faith, morality—under scientific scrutiny.

But the images generated by such methods may have a power to captivate that reaches beyond their power to explain. Psychologists David McCabe of Colorado State University in Fort Collins and Alan Castel of the University of California, Los Angeles, recently asked 156 undergraduate students to evaluate several mock news articles describing brain-imaging studies. But the research each described was bogus. One study, for instance, reached the dubious conclusion that because watching television and doing arithmetic problems both activate the temporal lobes of the brain, watching television improves arithmetic abilities.

Students saw one of three versions of each article: the text alone, the text plus an fMRI image depicting activity in part of the brain, or the text plus a bar chart summarizing the fMRI result. Those who saw the brain image rated the scientific reasoning in the article as more compelling than did the others even though the images themselves added no relevant information, McCabe and Castel reported in the April issue of *Cognition*.

People seem to believe that images of brain activity make a behavioral observation more real, says bioethicist Éric Racine of the Institut de Recherches Cliniques de Montréal in Canada. Racine calls this effect "neurorealism" and says it's often amplified by media coverage that oversimplifies research findings and glosses over caveats. In other words, don't let the pretty colors fool you. You don't need an fMRI scan to know that candy tastes good, pain feels bad, and television won't turn you into a genius at math. **–G.M.**

CREDITS (TOP TO BOTTOM): JENNIFER DANIEL; DAN LOPEZ-PANIAGUA

rons acquire their selectivity by combining inputs from low-level neurons that respond to simpler features such as texture, curvature, and the orientation of lines. "It's a beautiful paradigm when you can bring it to bear," Petersen says of the parallel human-monkey work. The drawback, he says, aside from the incredibly time-consuming experiments, is that it can't be applied to study many types of cognition—language, for example.

There's a pattern here

A very different approach to overcoming some of fMRI's constraints comes from new analysis tools borrowed from machine-learning research. In a standard fMRI study, neuroscientists average together the fMRI activation for neighboring voxels. This averaging makes it easier to detect differences between experimental conditions—viewing photos of faces versus places, for example—but it assumes that neurons from different voxels in the region of interest all behave the same way. That's almost certainly not the case, says Nikolaus Kriegeskorte, a neuroscientist at the National Institute of Mental Health in Bethesda, Maryland.

To sidestep this issue, Kriegeskorte and others have been working with statistical tools called multivariate pattern classifiers to take a finer grained look at brain activity that considers patterns of activation across many individual voxels without averaging. These methods shift the focus from trying to identify specific brain regions that are activated during a particular task to trying to identify how the relevant information is processed in the brain.

The first demonstration of this approach was a study by cognitive neuroscientist James Haxby, now at Dartmouth College (*Science*, 28 September 2001, p. 2425). He and colleagues monitored brain activity elicited by hundreds of images of various types of objects, including faces, cats, houses, and scissors, and identified statistically distinct activity patterns elicited by each type of object.

In 2005, two research teams published papers in *Nature Neuroscience* showing that similar methods made it possible to determine the orientation of lines a subject was viewing based on fMRI activation in the primary visual cortex, a feat previously thought impossible because neurons that share a preference for lines of a particular orientation pack into columns narrower than a voxel. That got even more people interested, says Rajeev Raizada of Dartmouth, who organized a session on these methods at an April meeting of the Cognitive Neuroscience Society in San Francisco, California.

Raizada and others at the session presented a variety of new findings illustrating how this new analysis of fMRI data can reveal information processing in the brain that would be overlooked by conventional analyses. Raizada, for example, presented a study in which he and colleagues investigated fMRI responses to the sounds /ra/ and /la/ in the brains of 10 native English and 10 native Japanese speakers. The Japanese language does not distinguish between these sounds, and most native speakers can't hear the difference.

Inside the scanner, each subject listened to six variations of each /ra/ and /la/ while the researchers collected fMRI data for each variation. Using a pattern classifier, Raizada determined that English—but not Japanese—speakers exhibited distinct activity patterns in the right primary auditory cortex for /ra/ and /la/. In fact, subjects who were best able to distinguish the sounds had the most distinct activity patterns. Each sound is apparently represented by different patterns—but similar overall levels—of neural firing in the auditory cortex of English speakers, Raizada says, which explains why the conventional fMRI analysis can't pick up this distinction.

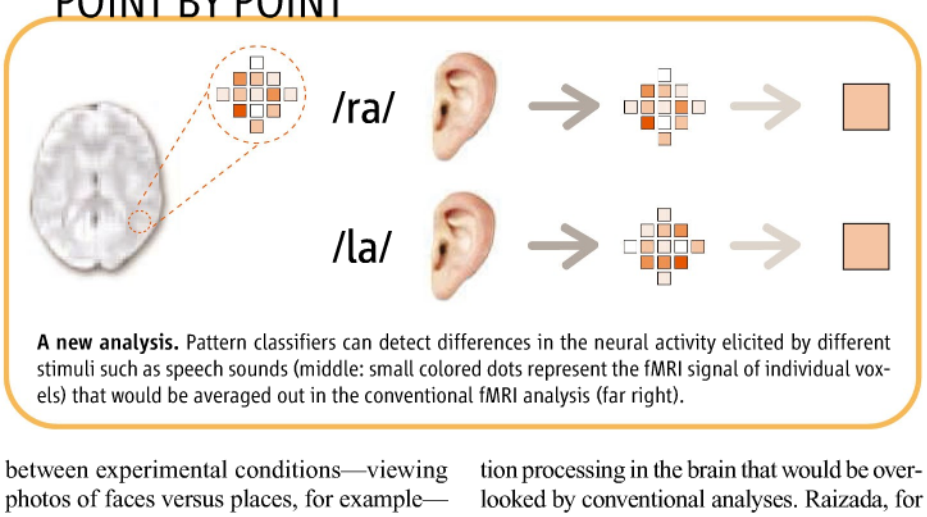

A new analysis. Pattern classifiers can detect differences in the neural activity elicited by different stimuli such as speech sounds (middle: small colored dots represent the fMRI signal of individual voxels) that would be averaged out in the conventional fMRI analysis (far right).

Other researchers are taking note of such findings. "This is an exciting new direction," says Adam Aron, a cognitive neuroscientist at the University of California, San Diego. "Instead of looking at whether this or that brain region is activated, now you're talking about whether the activity in many different voxels can predict what people are seeing or hearing." Poldrack predicts that classifiers will help rescue researchers from the logical perils of reverse inference. Instead of inferring that a photo of Mitt Romney induces anxiety, for example, researchers could collect patterns of brain activity evoked by known anxiety inducers (photos of spiders, snakes, and hypodermic needles, perhaps) and see whether the pattern Romney elicits is a statistical match.

An expanding toolbox

Yet even with the promise of these new tools, fMRI remains limited to revealing correlations between cognitive processes and activity in the brain. "The way to use it well is as one tool in a toolbox, as a way of testing hypotheses where you have converging techniques and evidence," says Aron.

To that end, growing numbers of neuroscientists are using fMRI and related methods to investigate the connectivity between different brain regions involved in cognitive functions such as language and memory. One fMRI approach is to identify brain regions whose activity is synchronized when subjects perform a given task. In some cases, researchers are probing further to determine if those areas that fire together are physically wired together, using a relatively new MRI method called diffusion tensor imaging that can visualize the axon tracts that connect regions in the living human brain.

Others are trying to establish causal links between brain and behavior. Having linked a brain region to a particular behavior using fMRI, for example, some researchers are following up with transcranial magnetic stimulation experiments in which focused magnetic fields noninvasively and temporarily disrupt neural activity in that region. If the behavior is then altered, the region must play a role in controlling it.

With such a convergence of methods and other advances, perhaps one day it will even be possible to divine the intentions of undecided voters. But that day does not seem near at hand. In the *Times* op-ed piece, the authors reported that their scans indicated that voters were "unengaged" with two candidates in particular, Barack Obama and John McCain, ironically, the two men now battling for the U.S. presidency. **–GREG MILLER**

CREDIT: RAJEEV RAIZADA

UNIVERSITIES

India's Education Bonanza Instills Hope—and Concern

The government of India is embarking on a major expansion of its higher education system. But is quantity being substituted for quality?

NEW DELHI—Indian higher education is in a funk. Too few institutions serve too few students, and there are too few professors to teach them. To remedy this, the government has unveiled an ambitious plan that would vastly expand access to higher education. Later this month, as a first step, three new Indian Institutes of Technology (IIT) will join the country's vaunted network of science universities; three more will follow in the coming weeks.

Over the next 5 years, India plans to invest $21 billion on higher education, a whopping ninefold increase over the previous 5 years. "Our government is committed to investing more, much more, in education, especially science education," Prime Minister Manmohan Singh said last January when he announced the initiative. Bricks and mortar are a high priority: The government intends to open eight IITs—six this year and two later on—as well as 82 other institutions (see box). "All this marks a quantum leap in the infrastructure available for good-quality teaching and research," Singh said. Other elements include an expansion of scholarship programs and higher pay. Graduate students will receive a 50% hike in their living stipends to $300 a month, and research associates are getting a 33% salary boost to $400 a month. "A long-felt legitimate need has been met," says science minister Kapil Sibal.

But some observers worry that India is moving too fast and that as a result quality will inevitably suffer. This year's crop of six IITs will increase the number of these elite institutions to 13. As a sign of how quickly the government is moving, the new IITs, based in Patna, Medak, and in the states of Gujarat, Orissa, Punjab, and Rajasthan, will work out of makeshift campuses at existing universities until permanent facilities open in coming years.

India has 378 universities and 18,064 colleges, and among men and women ages 17 to 22, the enrollment rate has increased from less than 1% in 1950 to about 10%, or 11.2 million young people, in 2007, according to the University Grants Commission (UGC) in New Delhi. Despite the gains, experts agree that India is underserved. "No country has been able to become an economically advanced country if its enrollment ratio in higher education has been less than 20%," says UGC Chair Sukhadeo Thorat. (The gross enrollment rate in the United States and Canada is about 60%.) "Higher education is not serving the cause of young people of India," says Arjun Singh, minister for human resource development.

Part of the cure is to steer more young people into science. Under a new program called Innovation in Science Pursuit for Inspired Research, 1 million students bound for university over the next 5 years will receive $125 scholarships simply as a reward for considering a future career in science. Another initiative, Scholarships for Higher Education, plans to hand out 10,000 scholarships each year, worth $2200 apiece, to talented students to enroll in bachelor's and master's science courses. "We must make science a preferred discipline of study for our students," Singh said.

A key question is who will teach the throngs of new students. The 16 centrally funded Indian universities are already facing a shortfall of nearly 2000 teachers, and IIT has about 900 vacant faculty posts. According to the All India Council for Technical Education, almost a third of faculty positions in academia are unfilled. "Teaching is no longer a glamorous profession," laments chemist Man Mohan Sharma of the University Institute of Chemical Technology in Mumbai. Entry-level industry jobs command salaries that are three times higher than those of tenured faculty. "Scholarly habits are dying," says Sharma. That poses a conundrum as India's higher education system grows. "I don't know from where quality faculty would come to teach in these new institutions," says J. S. Rajput, former director of the National Council of Education Research and Training in New Delhi.

For that reason, some eminent outsiders are urging India to proceed with caution. "Don't do it too fast. Institutes are limited by the few good people who need to be nurtured," says David Baltimore, a Nobel laureate at the California Institute of Technology in Pasadena, who earlier this year toured Indian labs. He suggests that India "build a couple of really fine institutions" over a few decades. P. V. Indiresan, former director of IIT in Chennai, shares that view: "Over-expansion of university education cheapens it." It seems, Indiresan says, that India "prefers large quantity with bad quality rather than a small quantity of high quality."

Going slow was never an option, says Sam Pitroda, chair of the National Knowledge Commission in New Delhi, which advises India's prime minister. "There is still resistance at various levels in the government to new ideas, experimentation," he says. That means, for now, that it is full steam ahead for India's education expansion.

–PALLAVA BAGLA

CREDIT: PALLAVA BAGLA

Science for the masses. India's plan to boost education should make scenes like this biotechnology class at Guru Gobind Singh Indraprastha University in New Delhi more common.

By the Numbers: Education for All?

India plans to open 90 higher education institutions in the next 5 years:

- Indian Institutes of Technology (8)
- Indian Institutes of Management (7)
- Central universities (30)
- Indian Institutes of Science Education and Research (5)
- Indian Institutes of Information Technology (20)
- National Institutes of Technology (20)

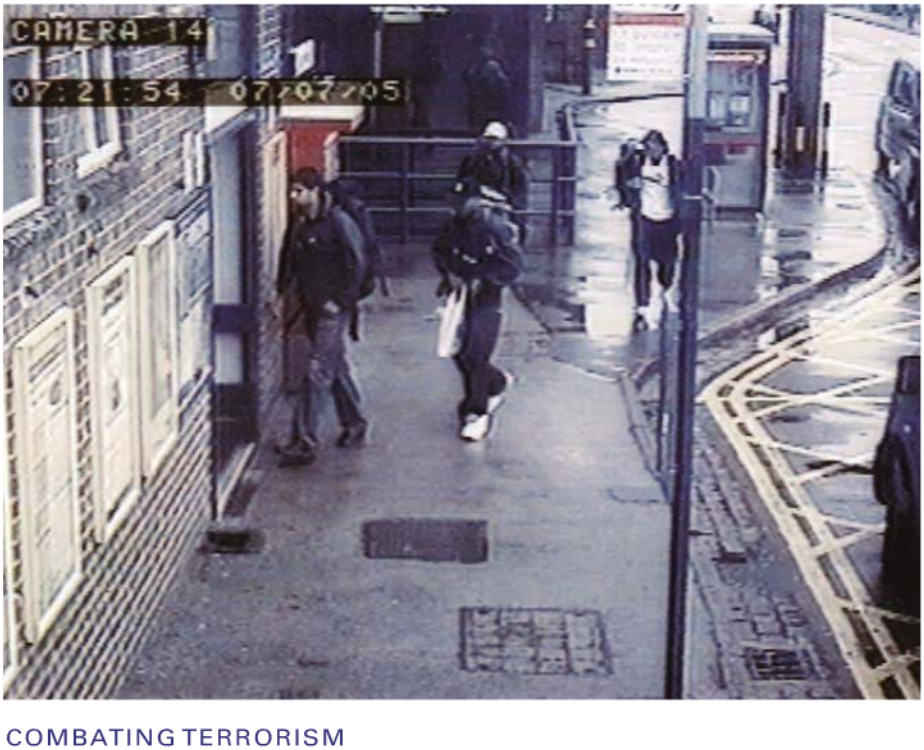

Under the radar. The four London bombers were caught on a surveillance camera as they entered a train station in July 2005.

COMBATING TERRORISM

New Efforts to Detect Explosives Require Advances on Many Fronts

A boost in government funding is stimulating research on new ways to stop terrorists before they strike in public places

The four young men who walked into the Luton railway station outside London with backpacks on their shoulders on the morning of 7 July 2005 looked like students on their way to college. They turned out to be suicide bombers. Between 8:50 and 9:47 a.m., they triggered explosions inside subway trains in London and on a double-decker bus that killed 52 commuters. Their weapon of choice was an organic explosive concocted from easily available chemicals.

The previous year, in Madrid, terrorists had used cell phones to detonate bombs that killed 191 people on four trains. The two incidents are a grim reminder that it is virtually impossible to detect explosives or would-be bombers from a distance. In addition, detection methods now in use at airports and checkpoints, including metal detectors, x-ray screening of baggage, and mass spectrometry of swabs taken from suspicious bags and individuals, are woefully inadequate.

Faced with the ongoing threat from such improvised explosive devices (IEDs)—the notorious weapons of choice in Iraq and Afghanistan—governments around the world have stepped up efforts to detect them before they wreak havoc in crowded subways, stadiums, shopping malls, and other public settings. Last year, the U.S. National Science Foundation (NSF) awarded $20 million for basic research on sensors, imaging tools, surveillance systems, and other techniques to detect explosives. And in February, the University of Rhode Island (URI) in Kingston and Northeastern University in Boston, each received the first $2 million of what could be $12 million grants from the Department of Homeland Security (DHS) to create centers on explosives detection. "We need to engage the academic community more fully to tackle the IED problem," says Douglas Bauer, program manager for explosives research at DHS's science and technology directorate.

The new approaches include sensors to pick up the faintest whiff of explosives in the air; imaging tools to detect, from afar, a bomb strapped to a person's body; and software to sift through video surveillance for suspicious behavior. The diversity is intentional. "There's not going to be a silver bullet," warns Michael Silevitch, an electrical engineer at Northeastern who co-directs the new DHS center.

Better sensors

When security personnel at airports want to check a bag for explosives, they perform a quick chemical analysis by wiping the bag with a swab and running the swab through a spectrometer. A team led by chemist Vinayak Dravid at Northwestern University in Evanston, Illinois, hopes to make such chemical sensing of explosives ubiquitous and automatic. In a 2006 *Science* paper (17 March 2006, p. 1592), Dravid and his colleagues showed that a device made by attaching a microcantilever beam to a transistor base can work as a biological sensor. The targeted biological molecules bind to receptor molecules coated on the cantilever's surface and cause it to bend. The stress from the bending is transmitted to the cantilever's base, where it dampens the mobility of electrons in the transistor and reduces the flow of current. The change in current signals that the biological entity has been sensed. Dravid and his colleagues want to use the same principle to detect vapors of explosive compounds in the air by coating the cantilever beam with a film that selectively absorbs molecules of explosives such as TNT.

Researchers have already developed such films from molecules such as thiosalicylic acid, which shows partial selectivity for TNT. One idea is to shoot a current through the beam to ignite a miniexplosion of a TNT molecule on the surface, which would deflect it and reduce the transistor current momentarily. Another idea is to shine different frequencies of infrared radiation on the cantilever; it would bend only at the frequency absorbed by the explosive. The resulting drop in current would alert authorities to a potential threat.

Dravid envisions a sensor system with arrays of cantilevers that sense the same explosive molecule through these different mechanisms. "If all of them got triggered, you could be reasonably certain that the explosive was in the environment," says Dravid. Such a system could be installed in the ceiling of a subway station or an auditorium and connected wirelessly to the nearest police station.

Researchers at Johns Hopkins University (JHU) in Baltimore, Maryland, are trying another chemistry-based approach, using semiconducting polymer films that have

pores shaped to allow explosive molecules to embed in them in the same way a key fits into a lock. As the explosive molecules get lodged in the polymer, its conductivity goes up. "The big advantage is that this could be deployed on a wide scale at a low cost," says JHU chemical engineer Howard Katz, co–principal investigator of the project. Katz imagines lining the walls of airports and subways with the polymer, which would transmit alarm signals to a computer monitored by security officials.

Neither approach has been tested, and Katz and Dravid are still far from building a prototype. Because the vapor pressure of many explosive compounds is very low, any device must ensure that air samples delivered to the sensor contain a sufficiently high concentration of whatever explosive molecules have been detected.

Another approach to finding explosions is to pick out their molecular signatures from afar. Xi-Cheng Zhang, an electrical engineer at Rensselaer Polytechnic Institute in Troy, New York, thinks that terahertz (THz) beams might be the answer.

THz radiation lies between the infrared and microwave parts of the electromagnetic spectrum and can pass through barriers such as clothing and plastic without being a health hazard. In recent years, some airports have begun testing THz imaging systems to look for concealed weapons on airline passengers. Researchers have also found that most explosive molecules absorb THz radiation at frequencies between 0.5 to 1.0 THz, so explosives stand out in reflected THz beams. Zhang and his colleagues, including Northeastern's Silevitch, are hoping to exploit this property to detect explosives from distances of 100 meters or more.

Silevitch's goal is to "find a suicide bomber standing a football field away from us," a distance that would give security forces time to act. One fundamental problem is that water vapor in the air degrades THz signals at the frequency useful for detecting explosives. So far, Zhang says, he and his colleagues have demonstrated the concept at distances ranging from 3 to 30 meters, the latter on a cold, dry winter day that offered ideal conditions for the technology. In experiments under more humid conditions, the detectable range dropped to less than 10 meters.

Long-range detection of explosives would make security at airports and other venues much less intrusive, says URI chemist Jimmie Oxley, co-director of the DHS center. "Our vision for airports is to go back to the past, when there were no checkpoints," she says. "You would be scanned, but you would not know it."

CREDIT: NEVILLE ELDER/CORBIS

Outsmarting the terrorists

Researchers must also cope with the ever-changing nature of the threat. In recent years, security officials have been alarmed by the increasing use of homemade explosives such as triacetone triperoxide (TATP) and hexamethylene triperoxide diamine, which were used in the London bombings. Richard Reid, the man who tried unsuccessfully to set off an explosive in his shoe onboard a 2001 American Airlines flight from Paris to Miami, intended to use TATP as his detonating charge to set off another, more conventional, explosive.

Derived from ingredients such as acetone and hydrogen peroxide, TATP is easy to concoct. "With $17 worth of chemicals from the department store, you can make enough TATP to bring down a Boeing 747," says Ehud Keinan, a chemist at Technion-Israel Institute of Technology in Haifa who has studied TATP for 2 decades. Conventional explosives such as TNT, by contrast, are harder to manufacture and, thus, are typically stolen from military arsenals or purchased on the black market.

Peroxide-based explosives present a novel challenge for security agencies. Unlike conventional explosives made from nitrates, TATP has a low molecular weight, which makes it difficult to detect with standard mass spectrometry. Police and airport authorities have begun training dogs to sniff out TATP. Some airports are now equipped with ion mobility spectrometers, which can detect peroxide-based explosives from swabs. And some companies, including one owned by Keinan, are selling devices specifically to detect these materials. But officials say better and cheaper detection tools are needed.

Oxley and others have been working with DHS to update the list of organic compounds that terrorists could form into explosives. "Anticipating the next material is one of our goals," she says. "The hard part is to determine when an innocuous but energetic material can become detonable. It's usually a matter of scale." Oxley hopes to determine that threshold for a number of compounds.

At the Naval Postgraduate School in Monterey, California, computer scientist Neil Rowe and his colleagues are hoping to work on another approach: detecting terrorists before they strike by developing software to identify suspicious behaviors in video feeds. In one experiment, the researchers instructed volunteers to act suspiciously in a parking lot, for example, by leaving a box outside a car. A software program tried to spot these anomalous activities by analyzing factors such as a sudden acceleration in a person's movement, indicating flight from a crime scene. The software correctly flagged two-thirds of the target behaviors observed by surveillance cameras.

Rowe acknowledges that deploying such a system could yield an unacceptably high number of false positives and that knowing how a suicide bomber might behave in anticipation of an attack is still a distant goal. "You have to look for a number of subtle clues," he says. But a high failure rate doesn't ruffle Bruce Hamilton, program director for NSF's explosives and related threats program. Blue-sky research, he says, is key to "tackling this horrible problem."

–YUDHIJIT BHATTACHARJEE

Sniffing a hazard. Security officials say using dogs to search for explosives is not good enough.

Counting costs and benefits 1423

Proceeding with uncertainty 1426

Enzyme catalysis 1428

LETTERS | BOOKS | POLICY FORUM | EDUCATION FORUM | PERSPECTIVES

LETTERS

edited by Jennifer Sills

Biofuels: Waste Not Want Not

THE REPORTS "LAND CLEARING AND THE BIOFUEL CARBON DEBT" (J. FARGIONE *ET AL.*, 29 February, p. 1235) and "Use of U.S. croplands for biofuels increases greenhouse gases through emissions from land-use change" (T. Searchinger *et al.*, 29 February, p. 1238) underscore the sobering reality that producing biofuels from edible crops will drive agricultural expansion, which could negate greenhouse gas (GHG) savings brought about by substituting biofuels for gasoline or result in net GHG emissions.

Other recent studies also highlight potential environmental impacts of producing food crop–based biofuels (*1*–*4*). Nevertheless, many scientists remain optimistic that with technological advancements (such as lignocellulose-to-ethanol conversion), there are real opportunities in generating biofuel energy from waste biomass (*3*).

Urban trees. Horticultural waste biomass from Singapore's planted trees could help offset the nation's fossil fuel consumption.

Singapore is a small (~700 km^2) tropical island in Southeast Asia with few natural resources. It relies heavily on imports of fossil fuels to meet its energy demands. This island nation ranks 20th in the world in terms of per capita carbon dioxide emissions (*5*), and it serves as an ideal case study to demonstrate the potential of using cellulosic wastes to supply a city's energy demands and reduce its GHG emissions. Singapore's urban areas are home to about 1 million planted trees, which produce 50,000 to 156,000 tons of horticultural waste biomass (tree trunks, twigs, and leaves) each year (*6*). A recent study estimates that each ton of woody biomass feedstock can produce 288 to 371 liters of cellulosic ethanol (*7*). This translates to between 14 and 58 million liters of ethanol fuel that can potentially be produced annually from Singapore's horticultural wastes, which can displace 1.6 to 6.5% of the city's transport gasoline demand (888 million liters) (*8*). Furthermore, recent studies estimate that use of cellulosic ethanol can reduce GHG emissions by 70 to 90% compared with conventional gasoline (*9*).

Our analysis suggests that biofuel produced from horticultural wastes can offset part of a city's energy needs. To realize the potential of biofuels as a petroleum alternative, we need to both expedite the development of new biofuel technologies and diversify the portfolio of biofuel feedstocks.

LIAN PIN KOH,[1]* HUGH T. W. TAN,[2] NAVJOT S. SODHI[2]

[1]Institute of Terrestrial Ecosystems, ETH Zürich, Universitätstrasse 16, 8092 Zürich, Switzerland. [2]Department of Biological Sciences, National University of Singapore, 14 Science Drive 4, Singapore 117543.

*To whom correspondence should be addressed. E-mail: lian.koh@env.ethz.ch

CREDIT: LIAN PIN KOH

References

1. P. J. Crutzen, A. R. Mosier, K. A. Smith, W. Winiwarter, *Atmos. Chem. Phys. Discuss.* **7**, 11191 (2007).
2. L. P. Koh, *Conserv. Biol.* **21**, 1373 (2007).
3. C. B. Field, J. E. Campbell, D. B. Lobell, *Trends Ecol. Evol.* **23**, 65 (2008).
4. J. P. W. Scharlemann, W. F. Laurance, *Science* **319**, 43 (2008).
5. World Resources Institute, Climate Analysis Indicators Tool (CAIT) version 5.0 (http://cait.wri.org).
6. National Parks Board Singapore, *National Parks Board Annual Report 2005–2006 Facts and Figures* (www.nparks.gov.sg/imgs/pdfs/05/005-Facts&Figures.pdf).
7. General Motors *et al.*, *Well-to-Wheel Analysis of Energy Use and Greenhouse Gas Emissions of Advanced Fuel/Vehicle Systems—A European Study* (www.lbst.de/gm-wtw).
8. International Energy Agency, "Energy balances of OECD countries" and "Energy balances of non-OECD countries" (http://data.iea.org/ieastore/statslisting.asp).
9. International Energy Agency, "Biofuels for transport: An international perspective" (www.iea.org/Textbase/publications/free_new_Desc.asp?PUBS_ID=1262).

Biofuels: Too Soon to Give Up

BIOFUELS ARE ESSENTIAL TO REDUCING OUR reliance on foreign oil and reducing greenhouse gas emissions. The recent Report by J. Fargione *et al.* ("Land clearing and the biofuel carbon debt," 29 February, p. 1235) claims that we need to be careful to avoid unintended consequences of biofuels. The accompanying Report by T. Searchinger *et al.* ("Use of U.S. croplands for biofuels increases greenhouse gases through emissions from land-use change," 29 February, p. 1238) adds that increased use of biofuels will actually increase carbon dioxide emissions because of deforestation and a sudden and major shift in land use.

Although there has been substantial rebuttal to the assumptions in the two Reports (*1*, *2*), these studies do highlight the need for a comprehensive analysis of the effects of biofuel production. Fortunately, new efforts are under way to address this issue. The Intergovernmental Panel on Climate Change will produce a comprehensive Special Report on the GHG Mitigation Potential of Renewable Energy. Also, the U.S. Department of Energy's Office of Energy Efficiency and Renewable Energy and its national labs are committed to sustainability and have been addressing these issues, including a comprehensive life-cycle analysis of large-volume production of biofuel by the National Renewable Energy Laboratory, which will be vetted by leading scientists in the United States and around the world.

There is significant potential for second-generation biofuels to reduce carbon emissions when compared to first-generation biofuels

technologies. However, the challenge to our nation in reducing our dependence on foreign oil is too great to abandon first-generation technology for fear of unintended consequences; instead, we must learn from comprehensive life-cycle analyses how to avoid those consequences as the biofuels market evolves.

DAN ARVIZU

National Renewable Energy Laboratory, U.S. Department of Energy, Washington, DC 20585, USA, and Task Force on Sustainable Energy, National Science Board, Arlington, VA 22230, USA.

References

1. Department of Energy, "New studies portray unbalanced perspectives on biofuels: DOE committed to environmentally sound biofuels development" (http://www1.eere.energy.gov/biomass/news_ detail.html?news_id=11794).
2. T. D. Searchinger, "Response to new fuels alliance and DOE analysts' criticisms of *Science* studies of greenhouse gases and biofuels" (www.princeton.edu/~tsearchi/writings.html).

Biofuels: Think Outside the Cornfield

THE REPORT BY T. SEARCHINGER *ET AL.* ("Use of U.S. croplands for biofuels increases greenhouse gases through emissions from land-use change," 29 February, p. 1238) adds to the growing concerns regarding the inadequacies and risks associated with corn biofuels [e.g., (*1*)]. The study correctly points out, as does the Report by J. Fargione *et al.* ("Land clearing and the biofuel carbon debt," 29 February, p. 1235), that the conversion of many types of natural landscapes to grow corn for feedstock is likely to create substantial carbon emissions that will exacerbate global warming. Because of the potential problems with corn-based biofuels, it is useful to consider other alternatives.

One example is switchgrass, which grows well on marginal lands that are not well suited to corn or many other grains (*2*). Switchgrass would have another advantage: It is a self-seeding crop, which means farmers would not have to plant and reseed after harvesting.

Another alternative biofuel feedstock is wood from sustainably managed forests, which are common in much of the world today. These forests, managed for growth and renewability, are an increasing source of traditional industrial wood (*3*). As with grasses, trees can grow readily on land unsuitable for corn and grains. Furthermore, the wood is drawn from the incremental growth of a forest, thereby leaving the basic forest system and its carbon intact. Wood feedstock could be drawn from existing sources or from additional forests planted on marginal agricultural land without compromising the basic sustainable forest system, releasing substantial volumes of carbon, or utilizing high-quality crop lands (*4*). Moreover, infrastructure systems are currently in place, allowing wood to be harvested and transported.

Unlike corn and most grains, studies show that biofuels from grasses and wood have large net GHG gas savings. Indeed, grasses and trees enhance the ability of land to capture carbon through biomass and soils (*5*).

ROGER A. SEDJO

Resources for the Future, Washington, DC 20036, USA. E-mail: Sedjo@rff.org

References

1. F. Runge, B. Senauer, "How biofuels could starve the poor," *Foreign Affairs* (6 April 2007).
2. D. Tillman, J. Hill, C. Lehman, *Science* **314**, 1598 (2006).
3. J. Carle, P. Vuorinen, A. Del Lungo, *For. Prod. J.* **52**, 1 (2002).
4. B. Sohngen, R. Mendelsohn, R. Sedjo, *Am. J. Agr. Econ.* **81**, 1 (1999).
5. K. Sorensen, "Colorado State and USDA scientists find significant greenhouse gas reductions associated with biofuel crop systems" (Colorado State University, Natural

Resource Ecology Laboratory, and the U.S. Department of Agriculture, Agricultural Research Service, 2007); http://newsinfo.colostate.edu/index.asp?url=news_item_display&news_item_id=11182593.

Biofuels: Putting Current Practices in Perspective

WE HAVE THREE COMMENTS REGARDING THE Report on the carbon debt of biofuels by J. Fargione *et al.* ("Land clearing and the biofuel carbon debt," 29 February, p. 1235).

First, the argument that converting land from permanent vegetation to biomass has detrimental environmental effects has to be tempered by the fact that, globally, relatively little land is used for biofuels. Biofuels currently cover about 10 million hectares (*1*) out of a total cropping land area of 1.5 billion hectares and a total pasture area of 4.5 billion hectares. In addition, the total greenhouse gas debt—composed of CO_2, CH_4, and N_2O emissions—caused by biofuel primary production is small compared with the debt associated with the 26% of the ice-free global terrestrial surface given over to animal grazing and the 33% of arable land used to produce animal feed. More than 60% of global wheat, barley, and maize and more than 90% of soybean production is used as animal feed (*2*).

Second, land clearance combined with existing agricultural practice and fuel conversion technologies is the worst possible scenario for biomass. Growing crops for energy requires new thinking about crops and agricultural systems. The food crop "ideotype" (*3*)—developed to have a short stem, small erect leaves, and high C and N harvest indices—was the model plant of the green food revolution of the 1960s. Biomass for energy, harvested for its carbon and not for its nitrogen (protein) content, requires a different ideotype. A long growing season is necessary, as is large leaf size to compete against weeds. Fungal disease resistance should be multigenic, and mixed cultivar plantings should be encouraged. Perenniality rather than an annual habit would also confer advantages in reducing crop establishment energy costs and emissions of CH_3 and NO_2. Biomass crops intended for fermentation require high concentrations of low molecular weight carbohydrates, in order to reduce energy inputs. Low N fertilizer inputs and high N use efficiency are desirable biomass properties for low emissions of N_2O (*4*), the major greenhouse gas of cereal food crops.

Third, biomass energy production requires plantings, rotations, and management that generate ecosystem services such as carbon sequestration, pollination, and biodiversity conservation as well as primary food production (*5*).

JOHN R. PORTER,[1] NGONIDZASHE CHIRINDA,[2] CLAUS FELBY,[1] JØRGEN E. OLESEN[2]

[1]Faculty of Life Sciences, University of Copenhagen, 1870 Frederiksberg, Denmark. [2]Det Jordbrugsvidenskabelige Fakultet, Århus Universitet, 8830 Tjele, Denmark.

References

1. OECD, *Biofuels: Is the Cure Worse Than the Disease?* R. Doornbosch, R. Steenblik, Eds. (OECD, Paris, 2007).
2. H. Steinfeld *et al.*, *Livestock's Long Shadow* (FAO, Rome, 2006).
3. C. M. Donald, *Euphytica* **17**, 385 (1968).
4. P. J. Crutzen, *Atmos. Chem. Phys. Discuss.* **7**, 11191 (2007).
5. B. Kuemmel *et al.*, *Biomass Bioenergy* **15**, 407 (1998).

Response

PORTER *ET AL.* CONTEND THAT THE TOTAL LAND area currently devoted to biofuel production is insufficient for the CO_2 released by land use change to be meaningful on a global scale. The focus of our paper was not on the current

magnitude of global greenhouse gas emissions from land clearing for biofuels, but on what would happen to CO_2 release if biofuel production were to expand greatly by using newly cleared lands. The amount of land dedicated to biofuel production is increasing rapidly (*1*, *2*). Current biofuel land clearing emissions may not yet be a major contributor to global agricultural GHG emissions, but that is poor justification for letting them become so. Similarly, we agree that crop production for animal feed already contributes substantially to GHG emissions, but we do not see this as grounds to develop biofuels that do the same.

Porter *et al*. then suggest that biofuel crops should be improved to increase yield and therefore the fossil fuel offset per hectare. We agree that perennial crops will be essential for the future of sustainable biofuels. Indeed, this has been a central focus of the emerging biofuel industry for decades (*3*–*6*) and was a main point of our Report. However, opportunities for biofuel and bioenergy production extend beyond dedicated biofuel crops to include waste biomass and algae. The agronomic approaches suggested by Porter *et al*. must still account for possible impact on land clearing and should be compared against alternative methods of production that do not cause land clearing.

Finally, Porter *et al*. advocate consideration of ecosystem services as a part of the biomass cropping system. We concur. This echoes similar calls we have made for optimizing the value of ecosystem services that can be provided by well-designed food and biomass cropping systems (*4*, *7*–*9*).

JOSEPH FARGIONE,[1] JASON HILL,[2,3] DAVID TILMAN,[2]* STEPHEN POLASKY,[2,3] PETER HAWTHORNE[2]

[1]The Nature Conservancy, 1101 West River Parkway, Suite 200, Minneapolis, MN 55415, USA. [2]Department of Ecology, Evolution, and Behavior, University of Minnesota, St. Paul, MN 55108, USA. [3]Department of Applied Economics, University of Minnesota, St. Paul, MN 55108, USA.

*To whom correspondence should be addressed. E-mail: tilman@umn.edu

References

1. National Corn Growers Association, "2005 World of Corn" (Chesterfield, MO, 2005).
2. National Corn Growers Association, "2008 World of Corn" (Chesterfield, MO, 2008).
3. S. B. McLaughlin, L. A. Kszos, *Biomass Bioenergy* **28**, 515 (2005).
4. D. Tilman, J. Hill, C. Lehman, *Science* **314**, 1598 (2006).
5. E. Heaton, T. Voigt, S. P. Long, *Biomass Bioenergy* **27**, 21 (2004).
6. R. D. Perlack, J. W. Ranney, W. F. Barron, J. H. Cushman, J. L. Trimble, *Biomass* **9**, 145 (1986).
7. D. Tilman *et al.*, *Science* **292**, 281 (2001).
8. D. Tilman, K. G. Cassman, P. A. Matson, R. Naylor, S. Polasky, *Nature* **418**, 671 (2002).
9. V. H. Dale, S. Polasky, *Ecol. Econ.* **64**, 286 (2007).

CORRECTIONS AND CLARIFICATIONS

Editors' Choice: "Leave it to Mimi" (16 May, p. 850). The first author of the *PLoS Biology* study was Zauberman, not Zuberman.

News Focus: "The roots of morality" by G. Miller (9 May, p. 734). Jordan Grafman's affiliation was reported incorrectly. He is at the National Institute of Neurological Disorders and Stroke.

Letters to the Editor

Letters (~300 words) discuss material published in *Science* in the previous 3 months or issues of general interest. They can be submitted through the Web (www.submit2science.org) or by regular mail (1200 New York Ave., NW, Washington, DC 20005, USA). Letters are not acknowledged upon receipt, nor are authors generally consulted before publication. Whether published in full or in part, letters are subject to editing for clarity and space.

REGULATORY POLICY

Reforming Cost-Benefit Calculations

Orrin H. Pilkey

In *Retaking Rationality*, Richard Revesz and Michael Livermore take a long, hard, and skeptical look at the issue of cost-benefit ratio analysis as it is used to shape the United States' regulatory policies. They argue that the present approach to cost-benefit ratios is biased against regulation. As a result, worthwhile regulations, especially those concerned with environmental and health issues, often don't pass muster or are diluted beyond recognition.

The cost-benefit ratios taken to task by Revesz (a professor at the New York University School of Law) and Livermore (a law clerk at the U.S. Court of Appeals for the D.C. Circuit) are not the more widely familiar ones pursued by government agencies before approving a project. I am a veteran of decades of evaluating cost-benefit ratios prepared by the U.S. Army Corps of Engineers for coastal projects, and I would argue that these too should be reproved. For example, one common analysis requires predicting the lifespan of artificial beaches, a hopeless exercise that requires knowledge of when the next big storm will occur.

Cost-benefit ratios became a fixture of American government during the Reagan Administration, as part of its vilification of government inefficiency and in response to perceived runaway government overregulation. In the eyes of pro-regulators, the Office of Information and Regulatory Affairs (the cost-benefit gatekeeper) became a black hole. Regulations went in but never came out—or so it was perceived—and cost-benefit ratios were in large part responsible. As a result, environmental, consumer, and labor interests became very skeptical of cost-benefit analysis. In a process that can be likened to throwing the baby out with the bath, they abandoned the field of battle and chose other paths to argue for needed regulations.

Revesz and Livermore contend that cost-benefit ratios, properly and fairly done, can be very useful tools and that the environmental community should rejoin the battle. They also note the great need for looking back to see how accurate the assumptions behind past cost-benefit analyses have been.

The authors summarize their concerns by recognizing eight fallacies that are often assumed in cost-benefit analysis of proposed regulations. Here, I touch on sound bites from five of them.

Fallacy: All unintended consequences are bad. There is a strong tendency for anti-regulators to look only at negative collateral consequences, which systematically biases cost-benefit analysis against regulation. In 1992, a judge threw out the National Highway Traffic Safety Administration's attempt to require increased fuel efficiencies on new cars because it would encourage manufacture of smaller cars, which in turn would increase highway deaths.

CREDIT: JOE SUTLIFF

Ironically, in cost-benefit analyses by the Corps and other agencies, the opposite is the problem; negative consequences are downplayed. The Mississippi River–Gulf Outlet channel leading from New Orleans to the sea contributed substantially to the flooding of the 9th Ward in Hurricane Katrina. The storm surge effect was predicted before construction but ignored in the cost-benefit analysis.

Fallacy: Older people are less valuable. How should we measure lives saved by regulations? One method now coming to the fore (and replacing deaths-avoided calculations) is the life-years approach. The method is based on the fact that the death of a young person represents the loss of a greater amount of lifetime than the death of an old person. If we were to apply the life-years approach to smog control, one could disregard the more smog-susceptible older population and look only at the benefits to 40-year-olds. Doing so, one calculates a large life-years benefit, which favors a regulation that allows a relatively high level of air pollution (to the detriment of the elderly).

Fallacy: People cannot adapt. Quality-Adjusted Life Years (QALY) is a method for determining the benefits of medical procedures on the assumption that procedures that result in a higher quality of life should receive the highest priority for public funding. QALYs are determined by asking healthy people how they view a given disability; for example, what is the quality of life of a person in a wheelchair? But this is neither fair nor accurate. How would a healthy person know? Most people adjust to their health problems, and many people in wheelchairs lead happy and productive lives. The dollar value of a QALY is of course unfathomable.

Fallacy: Industry cannot adapt. In 1970, as vice-president of Ford Motors, Lee Iacocca proclaimed "the Clean Air Act could prevent continued production of automobiles … [and] is a threat to the entire American economy and to every person in America." But industry adapted.

Fallacy: People value only what they use. The principle that people may value something even if they don't use it is endangered. Exxon was forced to pay a lot of money for the oil spill in Prince William Sound, Alaska, even though most of us will never see the sound. However, in 2002 the Office of Management and Budget downgraded a forest preservation regulation by ignoring the existence value of ancient forests.

Rather than offer concrete suggestions on what to do about the problems of cost-benefit analysis, Revesz and Livermore take a justice-should-prevail attitude. But education about the problems is a good first step. In that sense, *Retaking Rationality* is an important book: well written and providing abundant examples of the shortcomings of evaluating regulations with slanted cost-benefit analyses.

10.1126/science.1159664

Retaking Rationality
How Cost-Benefit Analysis Can Better Protect the Environment and Our Health

by Richard L. Revesz and Michael A. Livermore

Oxford University Press, New York, 2008.
262 pp. $34.95, £18.99.
ISBN 9780195368574.

The reviewer is at the Nicholas School of the Environment, 103 Old Chemistry Building, Box 90227, Duke University, Durham, NC 27708, USA. E-mail: opilkey@duke.edu

TELEVISION: SPACE

Celebrating NASA's Voyages

Jay M. Pasachoff

A celebration of NASA's success is surely due in this, its 50th anniversary year, and in *When We Left Earth* the Discovery Channel provides a good one. NASA worked with the interestingly named Dangerous Films, a London studio, on the project. No quick survey, the series, through its six-part structure, provides space and time to show both the thrill of exploration and the history of progress.

Although the series is advertised as high definition, in truth only the interviews with former astronauts and the flight director Chris Kraft were recorded in that format. Viewers who have made the switch to high-definition television will find these sequences contrast with the historical NASA footage, which has, however, been carefully and digitally remastered. On the old films, one can see the grain and the blurriness. But even on a big screen, those aspects didn't matter, given the obvious care spent finding and cleaning the old footage.

A preview that I attended at New York's American Museum of Natural History presented episode 2, "Friends and Rivals," about the Gemini missions. It was engrossing, especially as one who remembers eagerly waiting for the space program's progress, to follow the series of steps. Narrator Gary Sinise explained how new and challenging tasks were added to each mission—such as a space walk that was moved forward two missions from when it was originally planned, in order to keep up with the Soviets.

The remastered clips from NASA's film vaults are interspersed with interviews with former astronauts and others who played major roles in the American space program. These participants are all identified at one time or another, but unfortunately not necessarily at their first appearances. And then the identifications do not usually appear again, a minor annoyance.

Notably one of the interviewees in the film is Neil Armstrong, whose absence from last year's excellent theatrical release *In the Shadow of the Moon* (*1*) was obvious. After the screening, I asked Bill Howard, one of the executive producers, how he managed to get the notoriously reclusive Armstrong to participate. Howard replied that it was simply persistence. He did admit that word presumably got around from other astronauts that the series was serious and worthy of his time. In addition to the inter-

When We Left Earth
The NASA Missions

Richard Dale and Bill Howard, Executive Producers

Dangerous Films, London, for the Discovery Channel. Six 1-hour episodes, 8, 15, and 22 June 2008. DVD, 6 episodes plus 5 additional hours of NASA film highlights, mission clips, and astronaut interviews. $69.95. http://dsc.discovery.com/tv/nasa/nasa.html

The reviewer, co-author of *The Cosmos: Astronomy in the New Millennium*, is at Hopkins Observatory, Williams College, Williamstown, MA 01267, USA. E-mail: jay.m.pasachoff@williams.edu

BROWSINGS

Trees. A Visual Guide. Tony Rodd and Jennifer Stackhouse. University of California Press, Berkeley, 2008. 304 pp. $29.95. ISBN 9780520256507.
Trees. The Macmillan Visual Guide. Pan Macmillan, Sydney, Australia. 306 pp. A$45. ISBN 9781405038478.
Despite difficulties in defining "tree," there is general agreement about the features of the plants to which the word is applied. They are perennial, grow from the top, are typically tall (over 3 m for single-stemmed forms; over 6 m for multi-stemmed ones), and are usually woody. In this pictorial survey of the world of trees, horticulturalists Rodd and Stackhouse take an inclusive view. Besides those members of the dicotyledons, conifers, and ginkos that possess trunks having tissue laid down by cambium cells, the authors admit tall and long-lived cycads, palms, yuccas, cacti, and tree ferns. After discussing tree anatomy, growth, and adaptations to predators and climate, they summarize the taxonomic diversity of trees and highlight 99 notable examples drawn from the more than 75,000 extant species. They also introduce important forest communities (such as the *Nothofagus* forest of southern South America, below), the many human uses of trees, and the invaluable roles trees play in shaping environments, atmosphere, and climate.

The Tree. A Natural History of What Trees Are, How They Live, and Why They Matter. Colin Tudge. Crown, New York, 2007. 479 pp. $27.95, C$36.95. ISBN 9781400050369.
The Secret Life of Trees. How They Live and Why They Matter. Allen Lane, London, 2006. 454 pp. £20. ISBN 9780713996982.
Aiming to promote a connoissseurship that combines knowledge and appreciation, Tudge weaves from his own encounters with trees around the world a thorough introduction to their biology, variety, and impor-

CREDIT: GETTY IMAGES

view, Armstrong appears in very interesting footage from his Gemini VIII mission—in which he was in real danger when the spacecraft started twirling faster than a revolution per second.

After the premiere's showing, Scott Carpenter, the fourth American in space (after Alan Shepard, Gus Grissom, and John Glenn) and second to orbit Earth, answered questions from the stage. Now in his eighties, he is sanguine about the future of the space program even given NASA's current financial problems. But for him, apparently, the key point is that the space exploration now being discussed will be accomplished eventually rather than on some specific time scale. Responding to my mentioning the 1960s space race with the Soviet Union, he suggested that the NASA budget might benefit if there was competition from China.

Outward bound. Saturn V rockets carried the Apollo missions into orbit.

The series is being broadcast as three sets of paired episodes. "Ordinary Supermen," covering the start of the American manned-space program and Project Mercury, aired along with "Friends and Rivals" on 8 June. "Landing the Eagle" (on developments through Apollo 11's lunar landing) and "A Home in Space" (presenting the subsequent moon missions through Apollo 17 and Skylab) will appear this coming Sunday. The series concludes 22 June with "The Shuttle" (from the early successes of the reusable, large-capacity vehicle to the tragic loss of Challenger) and "A New Space Age" (about the Hubble Space Telescope, its repair, and the International Space Station).

If I were making movies to celebrate NASA's 50th birthday, I would divide the material more evenly between crewed and uncrewed space exploration. We astronomers tend to think more of NASA's triumphs in its robotic missions: the Chandra x-ray, Spitzer infrared, and Compton gamma-ray observatories; Swift, which this year provided the first x-ray observations of a supernova at the moment of its eruption; planetary probes, including the current Cassini at Saturn, Huygens's landing on Titan, Spirit and Opportunity still roving the surface of Mars, and now Phoenix (with its successful landing in a martian polar region); smaller, solar spacecraft such as the Transition Region and Coronal Explorer; and international collaborations on other projects.

Nonetheless, the six episodes provide enough fireworks for a delightful birthday celebration for NASA. The series and its accompanying online materials will reward viewers—including those too young to have watched robotic spacecraft and crew members take humanity's first steps off the surface of Earth.

References and Notes

1. Reviewed by J. M. Pasachoff, *Science* **318**, 752 (2007).

10.1126/science.1160937

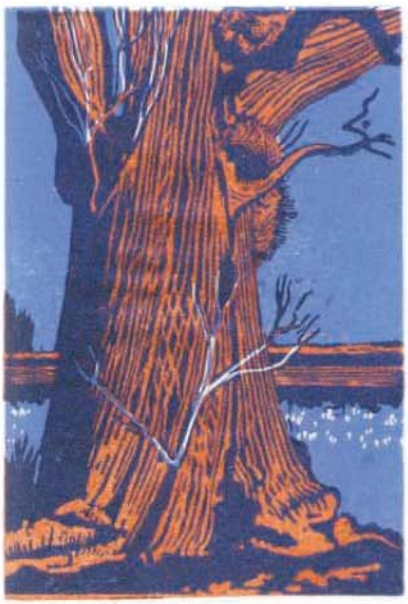

tance. He begins by defining his subject as "a big plant with a stick up the middle." After examining the problems of identification, naming, and classification, he sketches key events in the evolution of trees and provides a short paean to wood. Tudge devotes the book's central third to a family-by-family accounting of extant trees. The author then turns to their lives: how they grow, reproduce, and age; why they live where they do; and how they interact with predators, pollinators, symbionts, and one another. In the concluding "Trees and Us," he promotes sustainable agroforestry as a necessary response to the threats of deforestation and climate change.

Out of the Woods. The Armchair Guide to Trees. Will Cohu, illustrations by Mungo McCosh. Short Books, London, 2007. 272 pp. £14.99, $29.95. ISBN 9781904977834.

In this far-from-typical guide to Britain's trees, Cohu studiously avoids botanical terminology and takes "literary licence with names throughout." Instead, he offers readers a ramble through woodlands of oak and ash, past alders and birches lurking in lay-bys, and down city streets lined with cherries. Paying particular attention to leafless forms of winter trees and stressing characters (including smells) that make sense to the casual observer, he hopes to impart the "jizz" by which trees, like birds, may be rapidly identified. To help people love what they look at, he includes "biography and gossip." The colloquial, sometimes poetic, text is accompanied by McCosh's evocative woodcuts (such as "an old sweet chestnut" [*Castanea sativa*], left).

The Great Cacti. Ethnobotany and Biogeography. David Yetman. University of Arizona Press, Tucson, 2008. 311 pp. $59.95. ISBN 9780816524310. Southwest Center Series.

Although not considered trees by some, columnar cacti reach heights over 20 m. The circa 130 species are found in desert, arid scrubland, and tropical deciduous habitats from Arizona and Florida south to southern Argentina (right, *Pachycereus weberi* from Oaxaca, Mexico). Some occur as scattered individuals, others can form impressive forests. They often flourish at inhospitable sites: steep slopes; dry, hot, or cold climates; rocky, barren, or salty soils. Many have been important to human cultures, providing food, shelter, medicines, and hallucinogens. Yetman gives especially detailed accounts for taxa from northwestern Mexico, where he has long worked among the Seris, Mayos, and Guarijíos.

NUCLEAR WASTE

Yucca Mountain Revisited

Despite hundreds of studies and dozens of workshops and panels, Yucca Mountain remains controversial as a repository for radioactive wastes.

Isaac J. Winograd* and Eugene H. Roseboom Jr.

In papers published over a quarter of a century ago (*1*–*3*), we discussed the assets and liabilities of isolating high-level radioactive wastes (HLWs) (chiefly spent fuel from nuclear reactors) from the environment by burying them in areas with deep water tables, specifically within the several-hundred-meter-thick unsaturated zones common to the arid and semiarid Southwest U.S.A. This idea—endorsed for further study by our colleagues at the U.S. Geological Survey and by scientists at Lawrence Berkeley Laboratory (*4*) and the U.S. Nuclear Regulatory Commission (*5*)—eventually led to identification of Yucca Mountain (YM) (see photograph) as a potential repository for HLWs. In the ensuing decades, a voluminous body of knowledge of the geology, hydrology, geochemistry, and paleoclimatology of YM and the surrounding southern Great Basin was acquired and documented in hundreds of studies by federal, state, university, and industry scientists. As a result of these efforts, this region is the best-characterized portion of the Great Basin. Despite this unprecedented body of earth science information (*6*, *7*), YM remains controversial for storage (*8*) and possible ultimate disposal (*8*) of HLWs. With the benefit of hindsight, we examine several reasons for this outcome, two of which would apply to any site being considered for the geologic isolation of HLWs, and suggest a potential way to move beyond the controversy.

Sites in the United States at which spent nuclear fuel, other high-level radioactive waste, and/or surplus plutonium are stored at the surface. Yucca Mountain, NV, also shown.

The idea of storing radioactive waste at YM was born into political controversy. In 1987, Congress, via an amendment to the Nuclear Waste Policy Act of 1982, selected YM from a group of three previously identified potential repository sites. The 1982 Act had mandated detailed study of all three sites before selection of a finalist, a requirement dispensed with by the amendment. Not surprisingly, the Nuclear Waste Policy Amendments Act of 1987 became known among Nevadans as the "screw Nevada bill." That YM had been identified several years earlier as a potential repository solely on the strength of its technical attributes was thus irrevocably lost on the public who rightly resented the change in site-selection rules.

A second factor contributing to the controversy is the nature of scientific and first-of-a-kind engineering endeavors. The more we learn about a given subject—especially one involving the interface of multiple disciplines over geologic time frames—the more complex it becomes. Another decade of study of YM will likely provide the data needed to address some of the current questions about this site, but probably will also introduce new questions, as well as unearth surprises. Thus, there is unlikely to be complete closure. Nor will honest disagreements among scientists and engineers regarding some YM issues likely ever cease. This reality enables critics of this use of YM to ignore major attributes of the site while highlighting the unknowns and technical disputes for the press. Not surprisingly, the press, the public, and our elected officials are left with the impression of a flawed site.

A related matter is the quest for quantitative estimation of the environmental effects over geologic time frames. The U.S. Court of Appeals for the District of Columbia Circuit was aware that some of the radionuclides in HLWs have half-lives of thousands to millions of years and followed a recommendation of the National Research Council (*9*) regarding time frames. On 9 July 2004, they ruled that the U.S. Environmental Protection Agency (USEPA) should revise its YM standard for permissible releases of radioactivity to the environment to encompass a time frame of hundreds of thousands to a million years. Before the court's ruling, the USEPA considered a 10,000-year time frame as an achievable requirement. Before the U.S. Department of Energy (USDOE) can obtain a license from the U.S. Nuclear Regulatory Commission (USNRC) to operate YM, it will have to demonstrate to the USNRC that this site complies with USEPA's revised standard.

To demonstrate compliance, computer models have been constructed to simulate the interaction of all the geochemical, hydrogeo-

Emeritus, U.S. Geological Survey, Reston, VA 20192, USA.

*Author for correspondence. E-mail: ijwinogr@usgs.gov

logic, and other geologic processes that are currently believed to control the release of radionuclides to the environment over the next several hundred thousand years. These "performance assessments" are invaluable tools for identifying poor to marginal sites, for pinpointing key unknowns in a site deemed worthy of study, and for periodic evaluations of a site during repository construction and operation. However, given the inherent impediments to prediction in the earth and biological sciences (*10*–*15*), such estimates of repository performance over the time frames mandated by the court's ruling are likely to be challenged. This ruling, in our opinion, introduces a legal obstacle to geologic isolation of HLWs first proposed a half-century ago by the National Research Council (*16*) of the U.S. National Academy of Sciences and repeatedly endorsed by international panels in subsequent decades (*17*).

A third factor influencing the public's adverse perceptions about YM is the belief that emplacement of HLWs underground precludes their retrieval in the event of discovery of a major flaw with geologic isolation, a future decision to reprocess the spent fuel, or the future availability of a superior isolation scheme. However, this belief ignores one of the major attributes of YM for HLW isolation. The repository is to be constructed 300 meters above the water table within consolidated volcanic strata, a physical setting that lends itself to retrieval and monitoring of the HLWs (*3*).

Last, and hardly least, is the decades-old public opposition to a geologic repository, not only in Nevada and across the United States, but in Europe as well (*17, 18*). This opposition stems from various concerns and/or agendas, including: fear of nuclear radiation; distrust of governmental and technical community assurances regarding safety; opposition to nuclear power; and various NIMBY ("not in my backyard")–related issues (*17, 18*). We suspect that even in the absence of technical questions regarding YM, it would still be opposed by segments of the public.

In view of the above matters, it has been argued that HLWs should be stored at the surface, perhaps even for a century or two during which time better solutions may develop (*17*). However, extended surface storage of the HLWs (presently about 60,000 metric tons) at 72 commercial reactor sites—many adjacent to metropolitan areas and all next to rivers, lakes, or the ocean—introduces its own set of uncertainties. For example, what is the likelihood that more pressing future national problems could cause final isolation of the HLWs to be postponed indefinitely? What is the probability that the funds for HLW disposal, now being generated by a surcharge on nuclear-generated electricity, will still be available a century in the future? In the event of accidents, sabotage, or a loss of institutional control, a variety of scenarios can be envisioned that would create environmental hazards greater than any that could result from emplacement of HLWs in an underground repository. In their analysis of the likelihood of future human intrusion into a HLW repository, the National Research Council concluded [(*9*), p. 106], "there is no technical basis for predicting either the nature or the frequency of occurrence of intrusions." This conclusion applies even more compellingly to HLWs presently stored at the surface not only at nuclear power plants but also at dozens of other locations (see map, page 1426).

Given that both geologic isolation of HLWs and their storage at the surface are fraught with uncertainty, how might we proceed with the disposition of HLWs in a manner that restores public confidence? First, it behooves the earth science community, the involved federal agencies, and the mainstream environmental groups to inform the courts, the public, and legislators that, in view of the unending questions, potential surprises, and limitations on prediction that are inherent to the scientific endeavor, the fate of HLWs over time frames of hundreds of millennia is not knowable. There need be no embarrassment to admit to the limitations of our explanatory and predictive capabilities. After all, questions regarding the cause of the ice ages still abound after more than a century and a half of study (*19*), and earthquake prediction remains elusive after decades of work (*20*). Decisions on the isolation of HLWs, as well as on other pressing environmental issues, will likely have to be made with incomplete knowledge.

Second, because of the absence of experience in the construction and operation of a geologic repository for HLWs, and given the possibility that such efforts are likely to encompass several generations (current plans call for keeping the repository open for more than a century), it appears prudent to construct and operate a proposed repository in stages, initially as a pilot plant, and with experience from each operational stage providing feedback to that which follows. The use of such an adaptive management approach was recently proposed in great detail by the National Research Council (*21*).

Last, the importance of monitoring during the construction and operation of each stage cannot be overstated, as has been argued for civil engineering endeavors in general (*22*). Only monitoring over a time frame of decades to perhaps a century can provide the data needed to begin to calibrate, test, and, as necessary, modify, current conceptual models that assess the ability of a proposed repository to isolate HLWs for even 10,000 years.

In summary, quantification of the fate of HLWs, whether emplaced underground or left at the surface is problematic. Should geologic isolation of the HLWs be opted for—as recommended repeatedly by national and international panels (*9, 16, 17, 21*)—a pilot plant approach to repository development (*21*) would be prudent. The physical setting of the proposed YM repository (i.e., in consolidated rocks ~300 meters above the water table) lends itself to such an approach by permitting ready access to and monitoring of the wastes (the major assets of surface storage), while isolating them at depth at a single location (the chief asset of geologic disposal) on remote federal land.

References and Notes

1. I. J. Winograd, *Eos* **55**, 884 (1974).
2. I. J. Winograd, *Science* **212**, 1457 (1981).
3. E. H. Roseboom Jr., *U.S. Geol. Surv. Circ.* 903 (1983).
4. H. A. Wollenberg, J. S. Y. Yang, G. E. Korbin, *An Appraisal of Nuclear Waste Isolation in the Vadose Zone in Arid and Semi-Arid Regions* (Lawrence Berkeley Laboratory Report LBL-15010, Univ. of California at Berkeley, Berkeley, CA, 1983).
5. U.S. Nuclear Regulatory Commission, 10 Code of Federal Regulations (CFR) Part 60, *Fed. Regist.* **50**, 29641 (22 July 1985).
6. A. M. Macfarlane, R. C. Ewing, *Uncertainty Underground* (MIT Press, Cambridge, MA, 2006).
7. G. S. Bodvarsson, C. K. Ho, B. A. Robinson, *Yucca Mountain Project* (Elsevier Science, Amsterdam, 2003).
8. We use the term *storage* to signify the ability to monitor and retrieve buried HLWs, whereas the term *disposal* signifies burial in a manner precluding retrieval. The term *isolation* includes either storage or disposal.
9. National Research Council (NRC), *Technical Bases for Yucca Mountain Standards* (National Academy Press, Washington, DC, 1995).
10. M. Scriven, *Science* **130**, 477 (1959).
11. E. Mayr, *Science* **134**, 1501 (1961).
12. A. M. Weinberg, *Issues Sci. Technol.* **2**, 59 (1985).
13. I. J. Winograd, *U.S. Geol. Surv. Circ.* 990 (1986).
14. L. F. Konikow, J. D. Bredehoeft, *Adv. Water Resour.* **15**, 75 (1992).
15. N. Oreskes, in *Prediction*, D. Sarewitz, R. A. Pielke Jr., and R. Byerly Jr., Eds. (Island Press, Washington, DC, 2000), pp. 23–40.
16. NRC, *The Disposal of Radioactive Waste on Land* (National Academy Press, Washington, DC, 1957).
17. NRC, *Disposition of High-Level Waste and Spent Nuclear Fuel: The Continuing Societal and Technical Challenges* (National Academy Press, Washington, DC, 2001).
18. E. A. Rosa, R. E. Dunlap, M. E. Kraft, in *Public Reactions to Nuclear Waste*, R. E. Dunlap, M. E. Kraft, and E. A. Rosa, Eds. (Duke Univ. Press, Durham, NC, 1993), pp. 291–324.
19. M. E. Raymo, P. Huybers, *Nature* **451**, 284 (2008).
20. A. L. Kafka, J. E. Ebel, *Eos* **88**, 1 and 8 (2007).
21. NRC, *One Step at a Time: The Staged Development of Geologic Repositories for High-Level Radioactive Waste* (National Academies Press, Washington, DC, 2003).
22. E. D'Appolonia, *J. Geotech. Eng.* **116**, 4 (1990).

23. The views herein are those of the authors and not of the U.S. Geological Survey. We thank L. F. Konikow, J. M. Landwehr, D. B. Stewart, and J. S. Stuckless for review comments.

10.1126/science.1156399

BIOCHEMISTRY

How Enzymes Work

Fifty years of research have led to a detailed understanding of the mechanisms of enzymatic catalysis.

Dagmar Ringe and Gregory A. Petsko

Gazing at the three-dimensional structures of enzymes that regularly grace the covers of scientific publications, it is hard to imagine that there are still people alive who remember when many biochemists thought that enzymes had no ordered structure. But that was the case until James Sumner crystallized urease in 1926 (*1*)—a development so revolutionary that he was taken into custody as a dangerous lunatic when he tried to explain what he had done to a famous European scientist. When biochemists realized that enzymes had persistent structure and that destruction of that structure could abolish enzyme activity, they rapidly adopted the view that enzymes were rigid scaffolds whose specificity and catalytic power came from the inflexible fit of the right substrate onto the preformed enzyme surface, the way a key fits a lock. Fifty years ago, Daniel Koshland challenged this view, proposing that the enzyme surface was flexible and that only the specific substrate would induce the proper interactions that led to catalysis (*2*).

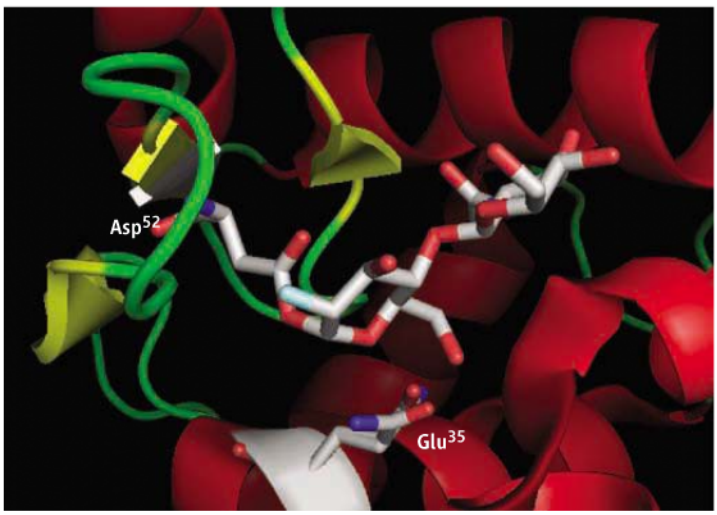

Elucidating the active site. In the crystal structure of a lysozyme mutant bound to a synthetic sugar substrate, the sugar ring in the active site is distorted, and the scissile bond is close to the acid-base residues Asp^{52} (left) and Glu^{35} (lower right; mutated to Gln in this structure) (*5*). All these features were deduced by Phillips and co-workers more than 40 years ago (*4*). Unexpectedly, the structure also shows that lysozyme can form a covalent intermediate with its substrates (*5*).

Studies of enzyme mechanisms were driven by a wish to understand the ability of enzymes to accelerate the rate of a chemical reaction by staggering amounts—up to 10^{20} times the rate of the uncatalyzed reaction in water (*3*)—while displaying a specificity so tight that some enzymes can discriminate between sulfate and phosphate. As we celebrate not only the 50th anniversary of Koshland's "induced fit" hypothesis but also ~50 years of high-resolution protein structure determination by x-ray crystallography, it is instructive to look back on the history of attempts to explain enzymatic catalysis and to summarize what we understand today about how these remarkable macromolecules function.

Before the first crystal structure of an enzyme was determined, that of lysozyme by David Phillips and his team in 1965 (*4*), speculations about how enzymes worked were based on deductions from indirect biochemical and biophysical experiments. The induced fit hypothesis was still controversial, and most models of enzyme function postulated a fairly rigid catalyst. Proximity—the holding of substrate molecules and catalytic groups on the enzyme in close approximation and in orientations favoring the appropriate bond-breaking and bond-making steps—was generally held to have an important role in catalysis, but other details were murky.

The fog lifted, brilliantly, over the course of a single weekend, when Phillips took the atomic model of his newly determined lysozyme structure, built into its active site a model of the oligosaccharide substrate, and deduced a set of structural factors that he believed could explain the ability of this enzyme to digest the peptidoglycan cell walls of many bacteria. Forty years of follow-up experiments proved his inspired reasoning correct in almost every detail, although a recent study provides a new wrinkle (see the figure) (*5*). Moreover, the factors he enumerated turned out to be applicable to almost all other enzymes.

What are the lessons from lysozyme? First, proximity and orientation are critical. Much of what an enzyme does is to bring the reacting species together in a geometry that favors reaction. This is so important that in some cases, even if almost every other factor were eliminated by mutating the enzyme, the protein would still be a respectable catalyst. Second, Koshland was right: The active-site residues usually adjust to permit the binding of the specific substrate. Induced-fit changes involving the movement of entire protein domains by several nanometers have been observed (*6*). Third, the protein structure can create specialized microenvironments that dramatically alter the reactivity of key catalytic groups, in some cases by shielding the catalytic site from contact with bulk solvent. Fourth, enzymes can distort the substrate, causing it to adopt a high-energy conformation with increased reactivity (*7*). Finally, enzymes provide extra stabilizing interactions for the transition state (or unstable intermediates) in the reaction mechanism. Specific stabilization of the transition state, particularly electrostatically, is thought to be so important that an entire industry—the development of catalytic antibodies—has been based on this single principle (*8*–*10*).

Most, if not all, enzymes derive the bulk of their catalytic power from varying combinations of these simple factors. Confirming evidence has come from a wide range of elegant experiments, notably site-directed mutagenesis, which allows specific groups on the enzyme to be changed or removed (*11*–*13*), and high-resolution x-ray crystallography, especially of enzyme-substrate and enzyme-intermediate complexes (*14*).

What was missing in this picture? Three relatively recent discoveries stand out. One is the contribution of quantum mechanical tunneling to the rates of enzyme-catalyzed reactions whose mechanisms involve the transfer of hydrogen ions (*15*). Another is the precise matching of the pK_a's (a logarithmic measure of the proton affinity of a weak acid) of the donor and acceptor atoms in hydrogen bonds that stabilize the transition state. Such matching can lead to short, symmetrical hydrogen bonds of greater-than-normal strength (*16*, *17*). But perhaps the most active area of current

Department of Biochemistry, Brandeis University, Waltham, MA 02454, USA. E-mail: petsko@brandeis.edu

research is the possible role of protein dynamics in aiding the reacting species in crossing the transition-state barrier to the reaction. As originally formulated, the structure of the enzyme was proposed to favor atomic vibrations along the reaction coordinate while disfavoring those that would not lead to productive bond-making or bond-breaking steps (*18*). Recent evidence from different enzyme systems suggests that this factor may indeed contribute to catalytic efficiency (*19*, *20*).

Given that we now have a good understanding of the principles underlying enzyme catalytic proficiency and specificity, it seems appropriate to ask where the field is likely to go next. Practical applications, such as the creation of enzymes catalyzing novel reactions, are under way. Further investigations into the role of protein dynamics in enzymatic catalysis are still needed. But we believe that a crucial next step will be to go beyond the milieu of dilute aqueous solution and individual purified enzymes that has defined enzymology for the past 100 years. Most enzymes function in the interior of the cell, where the substrate concentration is typically very low and the protein concentration may exceed 100 mM. How do enzymes function in a crowded medium of low water activity, where there may be no such thing as a freely diffusing, isolated protein molecule? In vivo enzymology is the logical next step along the road that Phillips, Koshland, and their predecessors and successors have traveled so brilliantly so far.

References and Notes

1. J. B. Sumner, *J. Biol. Chem.* **69**, 435 (1926).
2. D. E. Koshland Jr., *Nature* **432**, 447 (2004).
3. C. Lad, N. H. Williams, R. V. Wolfenden, *Proc. Natl. Acad. Sci. U.S.A.* **100**, 5607 (2003).
4. C. C. Blake *et al.*, *Proc. R. Soc. London B* **167**, 378 (1967).
5. D. J. Vocadlo, G. J. Davies, R. Laine, S. G. Withers, *Nature* **412**, 835 (2001).
6. T. A. Steitz, R. Harrison, I. T. Weber, M. Leahy, *Ciba Found. Symp.* **93**, 25 (1983).
7. D. L. Pompliano, A. Peyman, J. R. Knowles, *Biochemistry* **29**, 3186 (1990).
8. S. D. Lahiri, G. Zhang, D. Dunaway-Mariano, K. N. Allen, *Science* **299**, 2067 (2003).
9. A. Warshel *et al.*, *Chem. Rev.* **106**, 3210 (2006).
10. R. A. Lerner, C. F. Barbas III, K. D. Janda, *Harvey Lect.* **92**, 1 (1996–1997).
11. J. R. Knowles, *Nature* **350**, 121 (1991).
12. T. C. Bruice, S. J. Benkovic, *Biochemistry* **39**, 6267 (2000);
13. D. A. Kraut, K. S. Carroll, D. Herschlag, *Annu. Rev. Biochem.* **72**, 517 (2003).
14. I. Schlichting *et al.*, *Science* **287**, 1615 (2000).
15. Z. D. Nagel, J. P. Klinman, *Chem. Rev.* **106**, 3095 (2006).
16. W. W. Cleland, P. A. Frey, J. A. Gerlt, *J. Biol. Chem.* **273**, 25529 (1998).
17. D. A. Kraut *et al.*, *PLoS Biol.* **4**, e99, (2006).
18. T. Alber *et al.*, *CIBA Found. Symp.* **93**, 4 (1982).
19. S. Hammes-Schiffer, S. J. Benkovic, *Annu. Rev. Biochem.* **75**, 519 (2006).
20. K. A. Henzler-Wildman *et al.*, *Nature* **450**, 838 (2008).

21. We dedicate this paper to the memory of our good friend and long-time collaborator Jeremy R. Knowles.

10.1126/science.1159747

BIOCHEMISTRY

How Do Proteins Interact?

New results provide support for the hypothesis that interactions between proteins involve selection from an ensemble of different conformations.

David D. Boehr and Peter E. Wright

Interactions between proteins are central to biology and are becoming increasingly important targets for drug design. Upon forming complexes, protein conformations usually change substantially compared to the unbound protein. Two main hypotheses have been advanced to explain these changes (see the figure). According to the "induced fit" hypothesis, the initial interaction between a protein and a binding partner induces a conformational change in the protein through a stepwise process (*1*). In the "conformational selection" model, it is assumed that, prior to the binding interaction, the unliganded protein exists as an ensemble of conformations in dynamic equilibrium. The binding partner interacts preferentially with a weakly populated, higher-energy conformation-causing the equilibrium to shift in favor of the selected conformation. This conformation then becomes the major conformation in the complex (*2*). Although biochemistry textbooks have championed the induced fit mechanism for more than 50 years, there is now growing support for the additional binding mechanism, including the seminal work by Lange, Lakomek, and co-workers on page 1471 of this issue (*3*).

A major stumbling block for the conformational selection hypothesis has been the inability to characterize the structures of the predicted multiple conformations (or conformational substates) of a protein. The structural models resulting from x-ray crystallography tend to identify only a single dominant conformation, although different crystal forms of the same protein can provide insights into the range of conformations accessible to the protein (*4*). Help comes from nuclear magnetic resonance (NMR), a powerful method for characterizing protein dynamics and the protein conformational ensemble at the atomic level. Various NMR observables (*5*, *6*) give structural information about lowly populated, higher-energy conformations that are invisible to other techniques.

In a previous report, Vendruscolo and coworkers (*7*) combined data from NMR relaxation experiments with molecular dynamics simulations to characterize a structural ensemble of the protein ubiquitin. However, the experimental data only covered nanosecond time-scale dynamics and thus failed to capture the slower time scales that are important for molecular recognition.

Lange *et al.* have now extended the methodology to slower time scales by using residual dipolar couplings (RDCs) (*3*), which serve as restraints for structural determination by NMR and also provide dynamic information over a wide range of time scales (*8*). By analyzing RDCs measured for a large range of solution conditions, Lange *et al.* construct a structural ensemble for ubiquitin that describes its dynamic behavior up to the microsecond time scale.

The most striking feature of the ensemble is the presence of conformations that are nearly identical to the 46 known bound forms of ubiquitin observed in x-ray crystal structures. The results provide very strong evidence that complex formation by ubiquitin involves conformational selection processes. Gsponer *et al.* recently reported a similar result for calmodulin. Using the methodology of Vendruscolo and co-workers, they showed that the nanosecond ensemble for apocalmodulin contains conformations similar to calmodulin bound to myosin light chain kinase (*9*).

The structural ensemble reported by Lange *et al.* is consistent with the energy landscape theory of protein folding and function (*2*, *10*, *11*). This theory posits that there are multiple protein conformations in dynamic equilib-

Department of Molecular Biology and Skaggs Institute for Chemical Biology, The Scripps Research Institute, La Jolla, CA 92037, USA. E-mail: boehr@scripps.edu; wright@scripps.edu

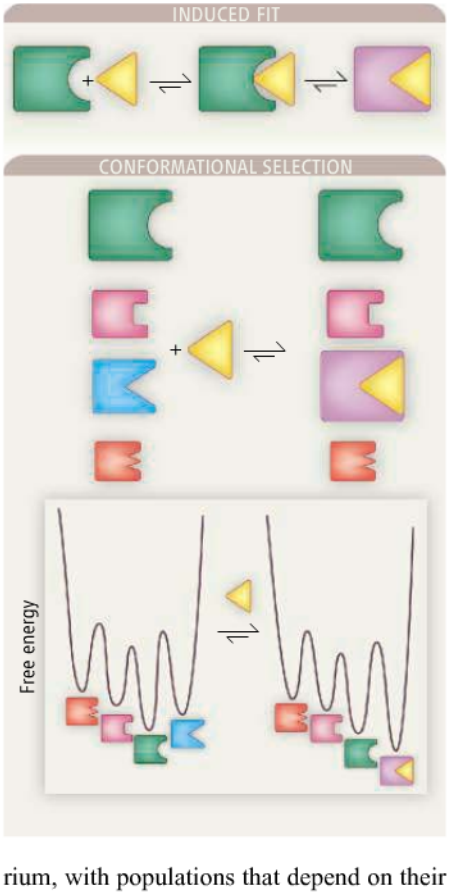

Molecular recognition mechanisms in proteins. Induced fit (**top**) assumes an initial interaction between a protein and its binding partner, followed by conformational changes that act to optimize the interaction. In conformational selection (**bottom**), a weakly populated, higher-energy conformation interacts with the binding partner, stabilizing the complex. Relative populations of conformations are indicated by size. In the structural ensemble presented by Lange *et al.*, different conformations may interact with distinct protein-binding partners. The energy diagram depicted is the simplest case; binding partners may have affinity for a number of protein substates that would further modify the structural energy landscape.

rium, with populations that depend on their relative free energies. Changes in the protein environment—such as a binding event—will alter the relative populations of the substates in the conformational ensemble (see the figure). In this context, induced fit and conformational selection are two extremes of a spectrum of possible protein binding mechanisms that can be categorized based on the initial binding interaction and the resulting structural changes in the energy landscape.

Indeed, a large body of structural work supports induced fit mechanisms (*12*), and kinetic signatures for both induced fit and conformational selection have been observed, sometimes in the same system (*13*–*15*). In a model that combines both mechanisms, the interaction proceeds through three steps: a diffusional encounter, recognition of complementary structures contained within the conformational ensembles of the free proteins, and conformational relaxation into the final bound state (*16*). As noted by Lange *et al.*, their results only characterize protein backbone structure and dynamics, and it is possible that minor backbone conformational changes or rotameric rearrangements of side chains may be induced after the initial interaction with a protein binding partner.

The analysis by Lange *et al.* provides much structural insight into the conformational ensemble of ubiquitin, but a more complete picture of the energy landscape would require more detailed kinetic and thermodynamic information. What are the relative populations of the individual structures and the rate constants of exchange among the substates in the conformational ensemble? What is the nature of the thermodynamic barriers between conformations? The information gained about the conformational ensemble can be compared with a careful kinetic analysis of ubiquitin binding interactions to provide us with a richer understanding of the diversity of protein-protein binding mechanisms.

The findings by Lange *et al.* (*3*) also pose intriguing questions about the role of dynamics in protein evolution (*17*). Either the structural fluctuations of ubiquitin evolved to interact with various protein binding partners, or new binding interactions took advantage of the intrinsic protein dynamics. The second case would help facilitate new binding interactions without compromising the structural integrity and original function of the protein. Analysis of structural ensembles populated on time scales slower than molecular tumbling, as begun by Lange *et al.*, will lead to a better understanding of evolution at the molecular level and may provide new approaches to protein engineering and drug design.

References

1. D. E. Koshland, *Proc. Natl. Acad. Sci. U.S.A.* **44**, 98 (1958).
2. B. Ma, S. Kumar, C. J. Tsai, R. Nussinov, *Protein Eng. Des. Sel.* **12**, 713 (1999).
3. O. F. Lange *et al.*, *Science* **320**, 1471 (2008).
4. H. R. Faber, B. W. Matthews, *Nature* **348**, 263 (1990).
5. C. Tang, C. D. Schwieters, G. M. Clore, *Nature* **449**, 1078 (2007).
6. A. Mittermaier, L. E. Kay, *Science* **312**, 224 (2006).
7. K. Lindorff-Larsen, R. B. Best, M. A. DePristo, C. M. Dobson, M. Vendruscolo, *Nature* **433**, 128 (2005).
8. A. Bax, A. Grishaev, *Curr. Opin. Struct. Biol.* **15**, 563 (2005).
9. J. Gsponer *et al.*, *Structure* **16**, 736 (2008).
10. H. Frauenfelder, S. G. Sligar, P. G. Wolynes, *Science* **254**, 1598 (1991).
11. T. Lazaridis, M. Karplus, *Science* **278**, 1928 (1997).
12. E. Buck, R. Iyengar, *Sci. STKE* 2003, re14 (2003).
13. C. Berger *et al.*, *FEBS Lett.* **450**, 149 (1999).
14. J. Foote, C. Milstein, *Proc. Natl. Acad. Sci. U.S.A.* **91**, 10370 (1994).
15. L. C. James, P. Roversi, D. S. Tawfik, *Science* **299**, 1362 (2003).
16. R. Grunberg, J. Leckner, M. Nilges, *Structure* **12**, 2125 (2004).
17. L. C. James, D. S. Tawfik, *Trends Biochem. Sci.* **28**, 361 (2003).

10.1126/science.1158818

DEVELOPMENTAL BIOLOGY

Sex and Poison in the Dark

Reinhard Fischer

A protein complex moves in and out of the nucleus in response to light, associating with proteins that control fungal development and metabolism.

Filamentous fungi are very successful organisms on our planet because of their metabolic versatility and potential to adapt to and survive extreme conditions. In this context, one important feature is their ability to produce different types of spores, for their dissemination in the environment and for resisting harsh conditions (*1*, *2*). Another factor is their success in chemical warfare—fungi produce molecules that help them to compete with other microorganisms (*2*). The best-known of these compounds are antibiotics, which can benefit one microorganism by inhibiting the growth of others. On the other hand, several other fungal metabolites, such as mycotoxins, cause millions of dollars in losses every year due to contaminated food and animal feed. If ingested by humans, mycotoxins, such as aflatoxin, may cause cancer or even death. Most interestingly, the phenomena of spore development and secondary metabolism are genetically linked (*3*). On page 1504 of this issue, Bayram *et al.* (*4*) unravel this association at a molecular level in the model fungus *Aspergillus nidulans* and show how this connection is controlled by light.

Most research with the filamentous fungus *A. nidulans* involves a strain in which the

Applied Microbiology, University of Karlsruhe, 76228 Karlsruhe, Germany. E-mail: reinhard.fischer@kit.edu

gene encoding the light-responsive protein VeA is mutated (*5*). *A. nidulans* develops asexually in light and sexually in the dark, and a *veA* mutation causes a shift from sexual to asexual spore formation and renders asexual sporulation independent of light. Genetic data thus suggested that VeA regulates light-dependent development. In addition to this role, VeA controls secondary metabolism—the production of molecules that are not absolutely required for the survival of the organism (such as antibiotics and mycotoxins) (*3*, *6*). For example, in the presence of light, *A. nidulans* produces less of the aflatoxin-related compound sterigmatocystin.

Orthologs of VeA have been characterized in several fungi, where the dual function in morphological and chemical differentiation appears to be conserved (*7*–*9*). Cloning of the *veA* gene reveals no indication that it encodes a transcriptional regulator or a light sensor (*6*, *10*). However, VeA contains sequences for nuclear targeting and for fast protein turnover. VeA is found in both the cytoplasm and the nucleus, where it accumulates especially in the dark (*11*). Defects in the control of protein degradation impair the coordination of development and secondary metabolism in the presence or absence of light (*12*).

The genetic regulation of secondary metabolism is well studied in *A. nidulans*. Unlike most primary metabolism genes, genes encoding secondary metabolites are clustered in the genome (*13*). Expression of several of those gene clusters is coordinately regulated by a single protein, LaeA (*14*, *15*). This global regulator is constitutively present in the nucleus and is presumably a methyltransferase, which modifies the chromatin structure of target gene clusters and activates their expression. The open question concerned how development and secondary metabolism are coupled and which role VeA and LaeA may play.

Bayram *et al.* have now solved this puzzle, showing that VeA forms a protein complex with VelB (a VeA-like protein) and LaeA. VeA and VelB appear to interact already in the cytoplasm and travel together into the nucleus to associate with LaeA. The trimeric protein complex was identified when *A. nidulans* was grown in the dark. Under light conditions, the VeA concentration in the cell was lower compared to that in the dark, and VeA interacted only with VelB (see the figure). Thus, the concentration of VeA in the nucleus appears to be one crucial parameter for secondary metabolite production and induction of the sexual developmental cycle. Because LaeA does not control sexual development, it is likely that other proteins are interacting with VeA and/or VelB to trigger this pathway.

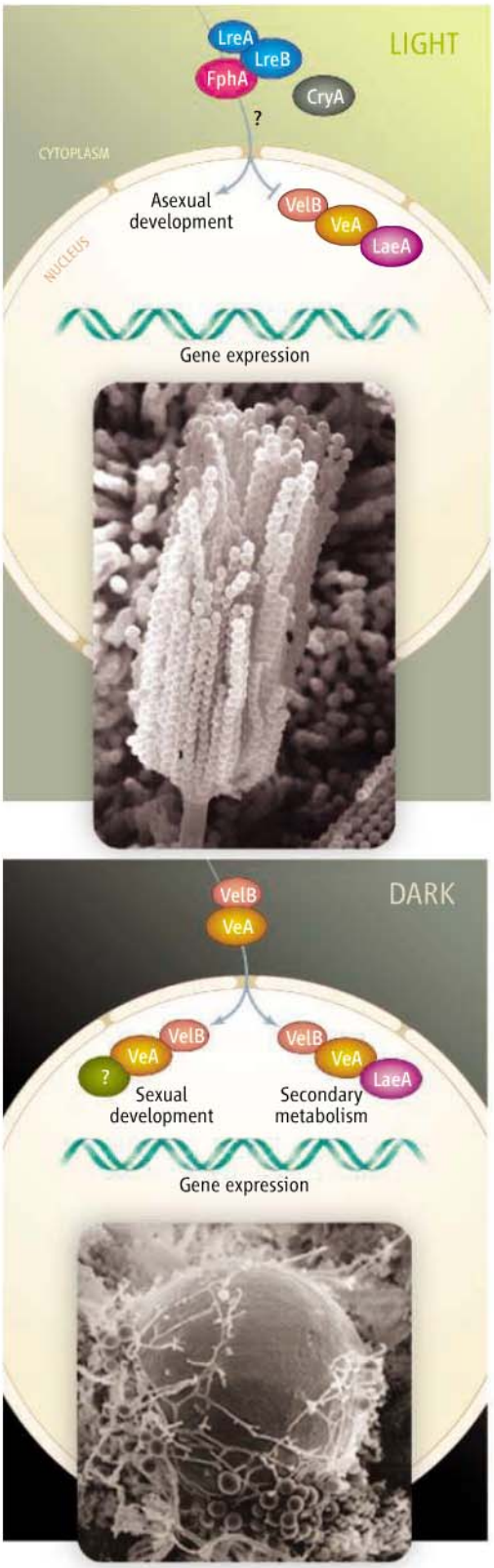

Shifts in the light. Whereas asexual development of the fungus *A. nidulans* is stimulated by light, sexual development and secondary metabolite (mycotoxin) formation are repressed. The VeA-VelB protein complex plays a central role in transmitting the light signal to signaling pathways that control gene expression.

This raises the question of how a light signal is transmitted to VeA. There are three possible upstream factors: a phytochrome, FphA; two blue-light receptor systems, LreA and LreB; and the cryptochrome, CryA (*16*–*18*). Although FphA interacts with VeA in the nucleus (*16*), a direct connection between any of the light regulators and LaeA has not been discovered through the biochemical approach of Bayram *et al.* This may indicate that interactions of VeA with light regulators are of a transient nature or that different protein interactions or protein complexes occur at different times in the cell. Whether and how the light regulators control the concentration or the activity of VeA is not yet known.

The challenge for future research will be to define specific functions for VeA and VelB in the discovered protein complex and to determine whether and how the light regulators are interlinked with the LaeA function. Insights into light signaling in *A. nidulans* may help to control mycotoxin formation or increase penicillin production.

References

1. S. Busch, G. H. Braus, *Mol. Microbiol.* **64**, 873 (2007).
2. J. J. Yu, N. Keller, *Annu. Rev. Phytopathol.* **43**, 437 (2005).
3. N. Kato, W. Brooks, A. M. Calvo, *Eukaryot. Cell* **2**, 1178 (2003).
4. Ö. Bayram *et al.*, *Science* **320**, 1504 (2008).
5. E. Käfer, *Genetics* **52**, 217 (1965).
6. A. M. Calvo, *Fungal Genet. Biol.*, 10.1016/j.fgb.2008.03.014 (2008).
7. Ö. Bayram, S. Krappmann, S. Seiler, N. Vogt, G. H. Braus, *Fungal Genet. Biol.* **45**, 127 (2007).
8. J. Dreyer, H. Eichhorn, E. Friedlin, H. Kürnsteiner, U. Kück, *Appl. Environ. Microbiol.* **73**, 3412 (2007).
9. S. Li *et al.*, *Mol. Microbiol.* **62**, 1418 (2006).
10. H.-S. Kim *et al.*, *Fungal Genet. Biol.* **37**, 72 (2002).
11. S. M. Stinnett *et al.*, *Mol. Microbiol.* **63**, 242 (2007).
12. S. Busch, S. E. Eckert, S. Krappmann, G. H. Braus, *Mol. Microbiol.* **49**, 717 (2003).
13. D. W. Brown *et al.*, *Proc. Natl. Acad. Sci. U.S.A.* **93**, 1418 (1996).
14. J. W. Bok, N. P. Keller, *Eukaryot. Cell* **3**, 527 (2004).
15. J. W. Bok, D. Norrdermeer, S. P. Kale, N. P. Keller, *Mol. Microbiol.* **61**, 1636 (2006).
16. J. Purschwitz *et al.*, *Curr. Biol.* **18**, 255 (2008).
17. A. Blumenstein *et al.*, *Curr. Biol.* **15**, 1833 (2005).
18. Ö. Bayram, C. Biesemann, S. Krappmann, P. Galland, G. H. Braus, *Mol. Biol. Cell*, 10.1091/mbc.E08-01-0061 (2008).

10.1126/science.1160123

PLANETARY SCIENCE

Enceladus—Oasis or Ice Ball?

The case has not yet been made that Saturn's satellite Enceladus meets the environmental conditions needed to support life.

Susan W. Kieffer[1] and Bruce M. Jakosky[2]

Is it possible for life to exist on Enceladus, the tiny (500 km diameter) icy satellite of Saturn? The Cassini mission found giant gaseous plumes erupting from a tectonically active and warm south polar region. One highly publicized interpretation is that liquid water is present, possibly within tens of meters of the surface (*1*), or possibly only at depths of tens of kilometers [for example, see (*2*)]. An antithetical interpretation is that Enceladus is frigid, stiff, thoroughly solid and composed of ice with interstitial gases to great depths (*3*, *4*). However, liquid water is just one of the three environmental conditions that are generally thought to be prerequisites for life (*5*). There must also be access to the elements out of which complex molecular structures can be constructed—mainly C, H, O, N, S, and—as well as an energy source that can drive metabolism. We examine the range of possible environments on Enceladus that are consistent with the observations in terms of their implications for harboring life.

Polar plume. Jets of water vapor, ice particles, gas, and trace organic compounds erupting from the surface at the south pole of Enceladus.

The instruments on Cassini provide data on gas and surface composition (*6*–*8*), thermal emission and radiated power (*9*), and optical images (*1*). These data can also provide clues to interior chemistry and conditions as well as surface temperatures and near-surface processes, but are subject to interpretation.

For example, there are competing views as to the physical state of water on Enceladus. One model holds that liquid water is present near the surface and has been dubbed "Cold Faithful" (*1*) in deference to the plume's apparent similarities to the Old Faithful geyser in Yellowstone National Park. The plume is formed from a reservoir of boiling water. The radiated energy is assumed to be transported to the surface by thermal conduction through the crust. Temperature gradients are high, and liquid water is encountered at shallow depths. In this interpretation, there is a high potential for near-surface extraterrestrial life (*10*).

In the other model, dubbed "Frigid Faithful" (*3*), the crust is a frigid mixture of ice and clathrates, a form of ice that stores foreign gas molecules in lattice cages. Fracturing of this solid crust during tectonic activity releases the gases and allows sublimation of cold water vapor. The radiated energy is transported to the surface by advection of gases in cracks in the crust, with condensation onto the walls of fractures. Temperature gradients are low; substantial warming may not occur even to 35 to 100 km (*4*). No liquid water is present, and there is little potential for life.

Given these two competing models, can a strong argument be made for the presence of liquid water? Water is certainly present in Enceladus, at least as solid and vapor, but the presence of vapor does not necessarily imply that liquid water is present

Even the warmest surface temperatures measured to date are below ~180 K (*10*). At the moment, the size of the warmest regions can be constrained to be less than a few kilometers, but they are likely to be much smaller (*11*). Kieffer *et al.* (*3*) noted that the entire discharge of a few hundred kilograms per second in the south polar plumes is similar to the discharge of Old Faithful geyser; the vent of Old Faithful is less than 1 m^2 in area. Thus, the warmest spots are likely to be very small relative to large adjacent areas that are at 80 K, and so it is difficult to envision liquid water coexisting with such large areas of cold ice. These arguments suggest that any liquid water is "deep," but this depth is not well constrained.

If liquid water is present, does it come into contact with the chemical building blocks needed for life? The elements C, H, O, and possibly N, as well as simple and complex organic molecules, have been observed in gases in the south polar plume or in ices on the surface (*12*). However, the concept of a liquid-water reservoir runs into problems in terms of the compounds observed in the plume—CO_2, CH_4, and CO or N_2. In the measured abundances, CO_2 can exist in solution in liquid water only at depths greater than 20 km, and CO, N_2, and CH_4 could not be in solution even at the center of this tiny satellite (*3*). However, in the frigid model, these molecules are readily stored in cages in the clathrates and are released during fracturing associated with the tectonic activity.

It is likely, but by no means certain, that Enceladus has most of the heavier biogenic elements. The elements that are less volatile, including S, P, and Fe, are likely to be present in any rock-containing environment [nitrogen presents a special case (*13*)]. Although rocky material is not observed on the surface, the bulk density of Enceladus exceeds that of ice by about 60%. It is generally believed that Enceladus is differentiated and has a rocky core. Near-surface liquid could be separated from access to rock by as much as 100 km of ice and clathrate.

Is there a source of energy to drive metabolism? The warm regions at the south pole radiate 3 to 7 GW of power, but organisms cannot use this enormous amount of thermal energy directly. Usable energy may

[1]Department of Geology, University of Illinois, Urbana, IL 61802, USA. E-mail: skieffer@uiuc.edu [2]Laboratory for Atmospheric and Space Physics and Department of Geological Sciences, University of Colorado, Boulder, CO 80309, USA. E-mail: bruce.jakosky@lasp.colorado.edu

be available in geological environments that bring together the biogenic elements and liquid water in the presence of rock (*14*), as is seen on Earth and postulated for Mars and Europa (*15*).

In summary, it has not been conclusively demonstrated that Enceladus meets any of the three key environmental conditions necessary to support life. The range of possible models that can explain the observations—both those invoking liquid water and those excluding it—is still being defined. An important next step will be to create a unified model of conditions and processes at the surface and in the interior that could better constrain the geologic conditions on the "regional" scale of the south polar terrain.

What would it take to resolve this controversy and get a more definitive answer? Even the strongest constraint—measurement of the temperature and size of the warm spots—must be put into context. If the temperatures remain low, then it is likely that the heat advection machine described by the frigid model is at work, although this concept needs further refinement to quantify the relation between the process and the radiated power. However, even if measured temperatures reach 273 K, which would be spectacular and tantalizing for liquid-water models, the challenge remains to explain where the compounds CO_2, CH_4, CO, or N_2 that contain some of the building blocks for life come from, and where the remaining elements are likely to be found.

Future planning of explorations should be guided by the full range of possible models and the uncertainties associated with them. A definitive answer about the potential for life may have to await a follow-on spacecraft mission that can make specific high-resolution observations that could distinguish between the competing models.

References and Notes

1. C. C. Porco *et al.*, *Science* **311**, 1393 (2006).
2. F. Nimmo *et al.*, *Nature* **447**, 289 (2007).
3. S. W. Kieffer *et al.*, *Science* **314**, 1764 (2006).
4. G. Gioia *et al.*, *Proc. Natl. Acad. Sci. U.S.A.* **104**, 13578 (2007).
5. W. Sullivan, J. Baross, Eds., *Planets and Life—The Emerging Science of Astrobiology* (Cambridge Univ. Press, Cambridge, 2007), pp. 357–387.
6. J. H. Waite Jr. *et al.*, *Science* **311**, 1419 (2006).
7. C. J. Hansen *et al.*, *Science* **311**, 1422 (2006).
8. R. H. Brown *et al.*, *Science* **311**, 1425 (2006).
9. J. R. Spencer *et al.*, *Science* **311**, 1401 (2006).
10. www.jpl.nasa.gov/videos/cassini/Enceladus_Briefing_March_26.mov
11. J. N. Spitale, C. C. Porco, *Nature* **449**, 695 (2007).
12. Initial conclusions were that N_2 was present as the molecular weight 28 compound (*6*); the presence of CO is now the favored interpretation (*10*), but this ambiguity is still not resolved.
13. Nitrogen poses a potential problem in that, if it is not identified at the surface, it may not be present in appreciable amounts.
14. E. L. Shock, *Evol. Biosphere* **20**, 331 (1990).
15. B. M. Jakosky, E. L. Shock, *J. Geophys. Res.* **103**, 19359 (1998).

10.1126/science.1159702

PHYSIOLOGY

Unfolding Lipid Metabolism

A transcription factor exhibits dual roles, regulating genes that respond to improperly folded proteins and genes that control lipid synthesis.

Jay D. Horton

Cells respond to unfolded and misfolded proteins in the endoplasmic reticulum by activating the unfolded protein response, which arrests protein synthesis and removes the accumulated, aberrant protein load, so that normal function of the organelle can be restored as soon as possible. This response has been linked to a variety of diseases, including neurodegenerative conditions, immune response disorders, cancer, diabetes, and fatty liver disease (*1*). The transcription factor X-box binding protein 1 (XBP1) controls the expression of genes required for the unfolded protein response, but on page 1492 in this issue, Lee *et al.* (*2*) establish an unexpected, independent role of XBP1 in regulating lipid synthesis in the liver. The finding provides new opportunities to develop treatments for conditions such as hyperlipidemia and fatty liver disease in humans.

XBP1 binds to promoter elements of genes that encode chaperone proteins that assist with protein folding in the endoplasmic reticulum. Global deletion of the *Xbp1* gene in mice results in the deaths of embryos from anemia, secondary to reduced numbers of hematopoietic progenitor cells and hypoplastic fetal livers (*3*). XBP1 is also required for plasma cell differentiation and the development of cardiac muscle and secretory tissues.

To study the function of XBP1 in adult mice, Lee *et al.* deleted the *Xbp1* gene exclusively in the adult mouse liver. This unexpectedly reduced liver fatty acid and cholesterol synthesis by ~85 to 90%, thus lowering concentrations of plasma cholesterol and triglycerides. Much of the cholesterol and triglycerides transported in the blood are in apolipoprotein B (apoB)–containing particles secreted by the liver, so a block in apoB secretion would result in low plasma concentrations of these lipids. Given the established role of XBP1 in promoting protein folding and secretion from cells, the observed low blood cholesterol and triglyceride concentrations could be secondary to impaired secretion of apoB and its associated lipids from liver. Surprisingly, apoB secretion from liver was unaffected by the loss of XBP1; rather, the underlying mechanism of the hypolipidemia is the regulated expression of select genes involved in lipogenesis by XBP1.

Sterol regulatory element–binding protein-1c (SREBP-1c) and carbohydrate response element–binding protein (ChREBP) are transcription factors that stimulate fatty acid synthesis in response to insulin and high glucose concentrations in plasma, respectively. Action of SREBP-1c is enhanced by the transcription factor liver X receptor (LXR). SREBP-2 stimulates the expression of genes involved in cholesterol synthesis (*4*). SREBPs are generated as inactive precursors in the membrane of the endoplasmic reticulum (see the figure). To be active, the amino-terminal domain of an SREBP (nSREBP) must be released from the membrane to enter the nucleus and activate target genes. This process requires SREBP cleavage–activating protein (SCAP), which escorts SREBPs from the endoplasmic reticulum to the Golgi. There, two proteases (S1P and S2P) cleave SREBPs to release the amino terminus from the membrane (*5*).

In mice that lack the *Scap* gene in liver, expression of nSREBPs and the expression of genes involved in fatty acid and cholesterol synthesis decrease (*6*), resulting in lower plasma triglyceride and cholesterol concentrations, similar to that observed in XBP1-deficient mice. Whereas SREBPs coordinately regulate all cholesterol and fatty acid biosynthetic genes, regulation of lipid synthesis by XBP1 appears to be more complex because the expression of nSREBP-1c or

Departments of Molecular Genetics and Internal Medicine, University of Texas Southwestern Medical Center at Dallas, 5323 Harry Hines Boulevard, Dallas, TX 75390–9046, USA. E-mail: jay.horton@utsouthwestern.edu

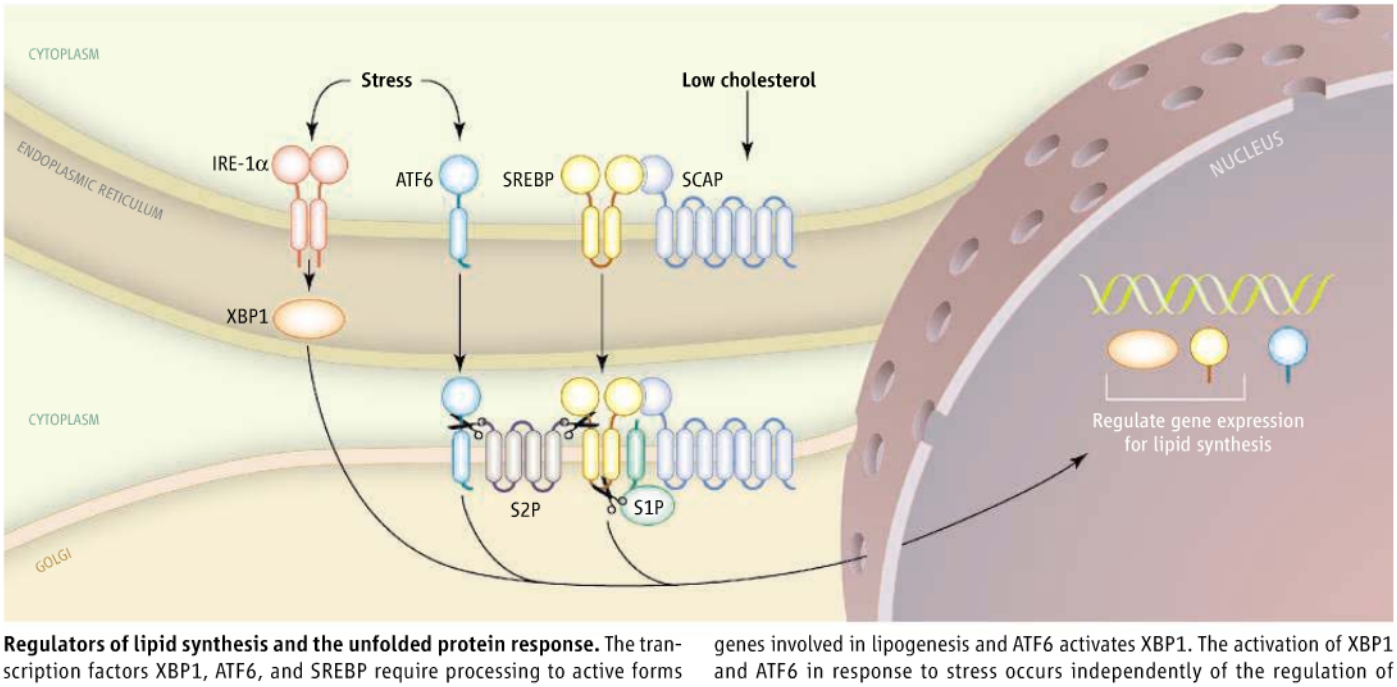

Regulators of lipid synthesis and the unfolded protein response. The transcription factors XBP1, ATF6, and SREBP require processing to active forms before entering the nucleus, where SERBPs and XBP1 control the expression of genes involved in lipogenesis and ATF6 activates XBP1. The activation of XBP1 and ATF6 in response to stress occurs independently of the regulation of SREBPs by cholesterol.

nSREBP-2 in XBP1-deficient livers was not reduced. This suggests that the decreased lipid synthesis rate is independent of SREBP-mediated transcriptional regulation.

Consistent with the normal concentration of nSREBPs in XBP1-deficent livers, expression of only three genes involved in fatty acid and triglyceride synthesis decreased—acetyl–coenzyme A (CoA) carboxylase 2 (ACC2), stearoyl–CoA desaturase 1, and acyl–CoA:diacylglycerol acyltransferase 1. By contrast, the expression of genes encoding enzymes (ACC1 and fatty acid synthase) that synthesize long-chain fatty acids was not reduced. Similarly, the expression of genes encoding 3-hydroxy-3-methylglutaryl coenzyme A (HMG-CoA) reductase and HMG-CoA synthase, key cholesterol biosynthetic enzymes, was unchanged in the absence of XBP1. Nevertheless, the rates of hepatic fatty acid and sterol synthesis were markedly reduced. These observations raise the possibility that in addition to the transcriptional changes observed in the XBP1-deficient livers, posttranscriptional regulatory mechanisms may contribute to the phenotype. One such modification that alters both cholesterol and fatty acid synthesis is phosphorylation and inactivation of HMG–CoA reductase (*7*) and ACCs (*8*) by adenosine 5′-monophosphate (AMP)–activated protein kinase (AMPK). AMPK is activated by stress that raises the cellular ratio of AMP to ATP (adenosine 5′-triphosphate), and it modulates many processes involved in cellular energetics. Whether such stress is present in XBP1-deficient livers is not yet known.

Although the fields of lipid metabolism and the unfolded protein response have developed largely in parallel, indirect links between the disciplines have emerged. For example, activating transcription factor 6 (ATF6) is activated through transport from the endoplasmic reticulum to the Golgi, where it is cleaved by S2P, the same protease that cleaves SREBPs (*9*). ATF6 activates *Xbp1* (among other targets), which in turn increases phospholipid synthesis, a process that may support the creation of new membrane in endoplasmic reticulum, allowing it to handle the stress of accumulated, improperly folded proteins (*10*). Another link between the two fields was revealed through studies of mice deficient in leptin, a hormone that controls appetite and fat metabolism. These mice are obese, insulin-resistant, and have high concentrations of triglycerides in their livers. These fatty livers also show molecular evidence of endoplasmic reticulum stress, which includes activation of RNA-activated protein kinase–like eukaryotic initiation factor 2α kinase (PERK) and inositol-requiring enzyme-1α (IRE-1α), resident membrane proteins of the organelle (*11*). PERK phosphorylates eukaryotic translational initiation factor 2α, which attenuates protein translation. Activated IRE-1α excises a portion of the messenger RNA encoding XBP1, which then is translated into the XBP1 protein that translocates to the nucleus to activate target genes (*12*, *13*). IRE-1α also triggers a signaling pathway (the c-Jun amino-terminal kinase cascade) that blocks insulin signaling (*14*), thus establishing a causal link between endoplasmic reticulum stress, cellular insulin resistance, and excess triglyceride accumulation in liver.

Even though XBP1 is well known as a transcriptional regulator of the unfolded protein response, its role in regulating lipid synthesis in liver appears to be independent of stress in the endoplasmic reticulum. XBP1 is present in the nucleus of normal mouse liver and its expression is induced after fructose feeding, suggesting that an alternative mechanism for regulating XBP1 exists in hepatocytes. Further studies are required to reveal this mechanism and to determine whether the regulation of lipid synthesis by XBP1 and SREBPs occur independently or in concert.

References

1. L. Zhao, S. L. Ackerman, *Curr. Opin. Cell. Biol.* **18**, 444 (2006).
2. A.-H. Lee, E. F. Scapa, D. E. Cohen, L. H. Glimcher, *Science* **320**, 1492 (2008).
3. A. M. Reimold *et al.*, *Genes Dev.* **14**, 152 (2000).
4. J. D. Horton, J. L. Goldstein, M. S. Brown, *J. Clin. Invest.* **109**, 1125 (2002).
5. J. L. Goldstein, R. B. Rawson, M. S. Brown, *Arch. Biochem. Biophys.* **397**, 139 (2002).
6. M. Matsuda *et al.*, *Genes Dev.* **15**, 1206 (2001).
7. R. Sato, J. L. Goldstein, M. S. Brown, *Proc. Nat. Acad. Sci. U.S.A.* **90**, 9261 (1993).
8. D. Carling, V. A. Zammita, D. G. Hardie, *FEBS Lett.* **223**, 217 (1987).
9. J. Ye *et al.*, *Mol. Cell* **6**, 1355 (2000).
10. R. Sriburi *et al.*, *J. Biol. Chem.* **282**, 7024 (2007).
11. U. Özcan *et al.*, *Science* **306**, 457 (2004).
12. M. Calfon *et al.*, *Nature* **415**, 92 (2002).
13. K. Lee *et al.*, *Genes Dev.* **16**, 452 (2002).
14. F. Urano *et al.*, *Science* **287**, 664 (2000).

10.1126/science.1159651

CREDIT: DLILLC/CORBIS

Forests in Flux

FORESTS HAVE HAD A PERVASIVE INFLUENCE ON THE EVOLUTION OF terrestrial life and continue to provide important feedbacks to the physical environment, notably climate. Today, studies of the world's forests are taking place against a backdrop of unprecedented change, largely resulting either directly or indirectly from human activity. In this special issue, we focus particularly on the future of forests in light of these changes.

Current research on the relationships of forests and climate are considered in a Review by Bonan (p. 1444), which provides an overview of how climate and forests are connected through physical, chemical, and biological processes that affect the carbon cycle, the hydrologic cycle, atmospheric composition, and the flow of solar energy and heat through the Earth system.

For scientists interested in forest dynamics (the turnover of individual trees and species over time), long-term forest plots are yielding field data on processes that take place over time scales longer than a research career. Until recently, though, the development of predictive models of forest dynamics lagged behind observation. In a Perspective, Purves and Pacala (p. 1452) explain how advances in the mathematics of forest modeling and the ecological understanding of forest communities are generating exciting new possibilities for mapping future trajectories of forests over times from decades to centuries. At longer time scales, pollen and macrofossil records, along with genetic data, have revealed past movements of species as climates changed, which in turn provide pointers to the direction of future change, as discussed by Petit *et al.* in a Perspective (p. 1450).

Three further Perspectives deal with aspects of sustainable forest management. Miles and Kapos (p. 1454) consider the question of incentives for "avoided deforestation" in the context of the recent Bali conference on climate change; Canadell and Raupach (p. 1456) discuss how carbon sequestration can protect against the effects of climate change; and Chazdon (p. 1458) considers how forests and their ecosystem services can be restored on degraded lands. In another Perspective, Agrawal *et al.* (p. 1460) spotlight some recent trends in forest governance and ownership, which in effect define the limits and opportunities for sustainability.

The three News reports take a look at how humans have reshaped wooded landscapes across the globe. Stokstad (p. 1436) takes stock of a large-scale assessment of Amazonian biodiversity in regenerating forests and tree farms. Koenig (p. 1439) examines the precariousness of the extensive rainforests in the Democratic Republic of the Congo. Morell (p. 1442) reports on the success of preservation efforts in China's Hengduan Mountain Region, one of the richest temperate forest ecosystems.

Forests and trees have been intimately bound up with the emergence and cultural development of our own species. Their future, and that of human society, depends ever more on how humans treat them in the coming decades.

–ANDREW SUGDEN, JESSE SMITH, ELIZABETH PENNISI

CONTENTS

News

1436 A Second Chance for Rainforest Biodiversity

1439 Critical Time for African Rainforests

1442 Letting 1000 Forests Bloom

Reviews

1444 Forests and Climate Change: Forcings, Feedbacks, and the Climate Benefits of Forests
G. B. Bonan

Perspectives

1450 Forests of the Past: A Window to Future Changes
R. J. Petit, F. S. Hu, C. W. Dick

1452 Predictive Models of Forest Dynamics
D. Purves and S. Pacala

1454 Reducing Greenhouse Gas Emissions from Deforestation and Forest Degradation: Global Land-Use Implications
L. Miles and V. Kapos

1456 Managing Forests for Climate Change Mitigation
J. G. Canadell and M. R. Raupach

1458 Beyond Deforestation: Restoring Forests and Ecosystem Services on Degraded Lands
R. L. Chazdon

1460 Changing Governance of the World's Forests
A. Agrawal, A. Chhatre, R. Hardin

See also related Editorial page 1395; Science *Careers article page 1514; video and podcast at www.sciencemag.org/forests/.*

Science

NEWS

A Second Chance for Rainforest Biodiversity

As ever more of the Amazon falls under the ax, a large-scale project is helping to clarify how well various tropical species survive in recovering forests

In 1967, an American billionaire named Daniel Ludwig purchased 16,000 square kilometers of rainforest in Brazil—an area half the size of Belgium. Ludwig, who had made his fortune building supertankers, was betting on a paper shortage and hoped to boost his wealth by growing *Eucalyptus* trees for pulp.

Thinking big, Ludwig shipped a preassembled paper mill from Japan and floated it up the Jari River. He built a new town, and his workers chopped down about 1300 square kilometers of rainforest to make way for the plantations. The rest remained untouched. After a little more than a decade, however, the scheme failed. Stymied by rising energy costs and business setbacks, Ludwig pulled out. Logging continues in the area, but many of the clearcuts have been returning to the wild.

Ludwig's losses have been science's gain. Given the rate at which rainforests are being cleared, some ecologists say there is a growing need to turn more attention to the woods that sprout up in their place. Whether the land is left to its own devices or managed by humans as tree farms, these second-generation ecosystems are coming to dominate the wooded landscape. Attracted by the Jari property's combination of intact rainforest, vast tree plantations, and regenerating forest, Carlos Peres recognized it was a perfect place to figure out which species persist where. "If you're trying to predict the future, this is what you need to do," says Peres. A wildlife biologist at the University of East Anglia in Norwich, U.K., he and his team have now published their follow-up of Ludwig's folly in a series of recent papers.

This research is by no means the first to look at the biodiversity of so-called secondary forests—those allowed to regrow on their own—and plantations, but it is one of the largest and most rigorous assessments in the tropics. "It's comprehensive enough that the results are convincing," says ecologist Robert Dunn of North Carolina State University in Raleigh. Whether those results are good news or bad news, however, is a matter of debate.

"The big take-home message is that there are a lot of species missing" from secondary forests and plantations, Dunn says. And for Peres's team, the findings reinforce the need to conserve the remaining old-growth tropical forests. "Primary forest is even harder to replace than many researchers expect," says Toby Gardner of the Federal University of Lavras in Brazil. "For many species, once these virgin forests have gone there is nowhere else to go."

Drawing on these and other findings, other ecologists

Different fates. The harlequin toad is one of many species that require old-growth forest, whereas the black-spotted barbet can survive in regenerating forest.

CREDIT (TOP): TOBY GARDNER; (BOTTOM LEFT TO RIGHT) JOS BARLOW; JOE HAWES

Rich habitat. Uncut rainforest near the Jari River in northeastern Brazil.

accentuate the positive. They point to the species that can cope, even thrive, in secondary forests and plantations. "There is a huge opportunity for conserving forest ecosystem functions and biodiversity," says tropical ecologist Daniel Nepstad of the Woods Hole Research Center in Falmouth, Massachusetts. Ultimately, the amount of diversity that persists in the Amazon will be determined by how much land is set aside—and by how hard humans work the rest.

Return of the forests

The statistics are grim for old-growth forests. The United Nations Food and Agriculture Organization estimated in 2005 that just 36% of the world's forests remain relatively untouched by humans. That fraction is disappearing quickly in the tropics, by as much as 12% per year, much of it destroyed by slashing and burning for fields or pasture for cattle.

Yet tropical trees are making something of a comeback. Clear-cut areas and abandoned farms are being turned into timber plantations or being reforested as part of government programs (*Science*, 23 February 2007, p. 1070). In parts of Latin America and elsewhere, trees are planted for side benefits to agriculture, such as shade and the "live fencing" they can provide.

And when the land is left alone, new saplings take hold, blossoming into secondary forests. "The amounts of land involved are absolutely staggering," says S. Joseph Wright of the Smithsonian Tropical Research Institute in Balboa, Panama. According to one global analysis, for every six or seven hectares of tropical forest cut during the 1990s, one hectare regrew (*Science*, 9 August 2002, p. 999). Costa Rica and Puerto Rico now have more secondary forest than primary. Because these new landscapes will eventually dwarf the intact forests preserved in national parks and other reserves, ecologists say these reborn places will be critical for the future of tropical biodiversity.

But relatively little is known about the potential of this habitat to serve as a refuge for the same species that depend on old-growth forest. Scientists have tended to focus on tropical forests that show no obvious sign of direct interference, in part because they are storehouses of diversity and are disappearing quickly. "Most secondary forests have been seen as trammeled and uninteresting," says geographer Susanna Hecht of the University of California, Los Angeles (UCLA). In fact, "they're much more diverse than people think."

Most of the research on secondary forests has been done in Costa Rica and other Mesoamerican countries, where original forests were mostly converted to agriculture decades ago. Patches of that land have slowly reverted to forests, whereas the remainder remains in cultivation. Such studies have tended to be small-scale, so the results don't readily apply to the Amazon's immense swaths of deforestation. "From the perspective of conserving rare species, the whole literature missed the effect of scale and disturbance," says Dunn, who published a meta-analysis in *Conservation Biology* in 2004.

New growth. When cleared land is left alone, secondary forests like this one in Mato Grosso, Brazil, can take hold.

Testing for biodiversity

The Jari landholdings have no shortage of large-scale disturbance. Peres, who grew up in the Brazilian Amazon, had visited the plantations as a teenager. Looking for a new research project in 2002, he recalled their vast size and set up shop there to assess the local biodiversity. Working primarily with his Ph.D. students Gardner and Jos Barlow, Peres initially surveyed a half-dozen major kinds of animals. But as collaborations flourished with Brazilian taxonomists from the Goeldi Natural History Museum in Belém, Brazil, that number swelled to 16 groups of vertebrates, invertebrates, and plants.

Half the battle was logistical: It was a struggle to keep the team's cars running given the daily 200 kilometers of off-road driving between field sites. Another strain was cutting transects through dense thickets of regrowth—hot, humid forests dominated by 10-meter-tall palms. "It was a crazy few years in the field," recalls Barlow, now at Lancaster University in the U.K.

Unlike many other tropical researchers, the team was able to set up multiple field sites, five each of primary forest, secondary forest, and *Eucalyptus* plantations. The sites were also extremely large—averaging 26 square kilometers for the secondary forest plots, up to 1000 times larger than field plots in previous studies.

Large plots allowed the team to minimize so-called edge effects. If animals spotted by observers are simply visiting the secondary forest from nearby primary forest, they will inflate the estimate of biodiversity that would exist, say, in a forest tract that is isolated in "a sea of soy," Gardner explains. "We maximized our ability to understand what lives in the landscape." And because the primary forest study sites are both large and surrounded by many more hectares of intact forest, they could get an accurate baseline of prelogging biodiversity.

The study's good news was that the secondary forests restored some of the ecosystem functions of the primary forests. The rate of decomposition of fallen leaves, which replenishes the soil, was about the same in primary and secondary forests (it was much lower in the plantations), the team reported with Leandro Ferreira of the Goeldi Museum in the August 2007 issue of *Forest Ecology and Management*.

But for many creatures, the news was bad (see chart, p. 1438). Secondary forests had

CREDIT: ALEX LEES

less than 40% of the bird species found in the Jari primary forest, and those present were those that prefer disturbed areas. The 14- to 19-year-old secondary forests "clearly failed to compensate for the loss of primary habitats and the habitat specialists they contain," the team concluded in the April 2007 issue of *Biological Conservation*. Amphibians, trees, and woody vines called liana that are common in tropical rainforests were also particularly depauperate.

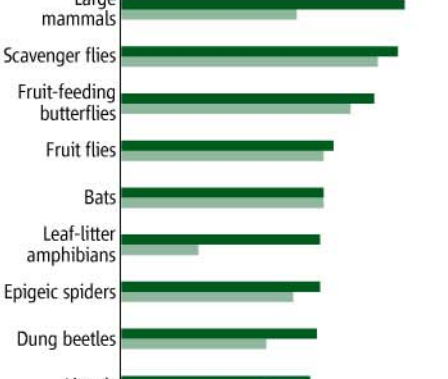

Biodiversity index. The percentage of old-growth forest species that survive in *Eucalyptus* plantations (*above*) and secondary forests varies from group to group, habitat to habitat.

Plantations were even less suitable refuges for most old-growth taxa. The rows of 4- to 6-year-old *Eucalytpus* trees had just 20% of bird species in primary forest. Yet bats and fruit flies did just as well in plantations as in secondary forests, and grasshoppers did better. A summary paper published in the 20 November 2007 *Proceedings of the National Academy of Sciences* charted all the trends.

Decreased animal diversity is cause for concern about the health of secondary forests, the team says. In a paper published in the May *Journal of Applied Ecology*, Malva Hernández of the Universidade Federal da Paraíba, Brazil, and others reported that the "exceptionally impoverished" dung beetle communities in secondary forests could have ecological repercussions, as the beetles bury many kinds of seeds, helping to repopulate the flora. Studies of dung beetles elsewhere have not seen such a stark difference in their diversity among habitats, but the team says the larger study plots make the new findings more reliable.

For some groups, total diversity—not just old-growth species—didn't change much. Species richness of scavenger flies and mammals, for example, was not measurably different between the three habitats studied by Peres and his colleagues. However, the species were not the same from one forest type to another. In the November issue of the *Journal of Tropical Ecology*, undergraduate Luke Parry of the University of East Anglia and the Jari team reported that secondary forests had more ungulate browsers but fewer fruit-eating monkeys and particularly lacked vertebrates that disperse large seeds.

The fieldwork has wrapped up, and now the team is refining its estimates of how much diversity is lost when forests are cut down and then regrow. Overall, Barlow says, the latest work is showing that widespread conversion of primary habitats to secondary forests results in species losses worse than they reported in November: Tree diversity dropped by as much as 86%, for example. "These results highlight the overwhelming importance of primary forest," he notes.

A bright side

In some ways, the results from the Jari landholdings foretell a dire future for forest biodiversity in the rest of the Amazon. Clear-cutting and burning of primary forests, such as what this area endured in the 1970s, are particularly damaging to any next generation of forest because those practices compact soil and alter its chemistry. The loss of tree canopy also makes the land reflect less sunlight; over large areas this change influences weather, reducing rainfall and drying the soil. The altered environs drive away animals. Once they vanish, plants that rely on those species to disperse their seeds have trouble reproducing and may not get reestablished. These severe impacts continue across the Amazon today.

Moreover, secondary forests throughout the Amazon aren't given enough time to recover the biodiversity of primary forests. "For some [taxonomic] groups, it may take 200 to 300 years to get a pale shadow of what a primary forest contains," Peres says. In Jari and elsewhere, regrowing forests are logged within 2 decades, and the plantations are cut even more frequently.

But that hardly makes them worthless. Secondary forests can have their own conservation benefits, says David Lindenmayer of Australian National University in Canberra. In some places, they provide a buffer around protected forests, dampening the impact of development and other human activities. And secondary forests usually benefit species that do best in disturbed areas, Lindenmayer notes.

Furthermore, other species can often do just fine with just a semblance of old-growth forest structure—an understory and a canopy with trees and gaps of various sizes, for example. "It's not actually the whole forest that needs to be [old-growth]," he says.

As has been shown in temperate and tropical forests, foresters can salvage biodiversity by retaining some of the largest trees. A few giants can have "a big effect on plantations," Lindenmayer points out. Within secondary forests, an approach called selective logging—where most of the forest is left in place—can make a huge difference, says UCLA ecologist Stephen Hubbell. If this practice is widely adopted, secondary forest "biodiversity will be okay," he says.

Peres's team hopes to continue working in the Jari area, identifying other ways that the biodiversity can be enhanced in the plantations. And even though the loss of biodiversity in the plantations is sobering, Barlow says the overall situation in Jari may be positive. The Brazilian company that owns the land behind Ludwig's grand scheme is now making a profit selling pulp from the plantations and is only selectively logging the primary forest.

–ERIK STOKSTAD

CREDIT: JOS BARLOW, GOUVEIA, BARLOW ET AL., PNAS 104 (47), 18555

NEWS

Critical Time for African Rainforests

As threats to the Congo Basin's vast forests grow, scientists race to sharpen assessments and stem destruction

KINSHASA, DEMOCRATIC REPUBLIC OF THE CONGO (DRC)—From a workshop behind her house, botanist Terese Hart can glimpse log-filled barges churning down the Congo River toward a nearby sawmill. Such traffic had come to a virtual standstill during the nation's civil conflicts, but now, she says, the "lights are blazing at night" as massive logs from the forests of Bandundu and Équateur provinces are fed, around the clock, into the jaws of giant saws.

At nearly 2 million square kilometers, the Congo River Basin's dense tropical rainforest is second in size only to the Amazon's. In *Heart of Darkness*, novelist Joseph Conrad—who piloted a steamboat on the Congo a century ago—described this as "impenetrable" territory, where "the big trees were kings."

Although deforestation is a severe problem in parts of the continent, central Africa's rainforests have so far avoided that fate. A recent analysis estimated that Africa accounted for less than 6% of the total loss of humid forest cover during the 1990s, whereas Brazil's loss represented nearly half of the total. The DRC's remoteness, political instability, bad roads, and unnavigable river rapids had helped save large tracts of its forests from exploitation. But forest degradation has been worsening in other Congo Basin countries, and a combination of factors over the past few years—including a sharp population spike in the eastern DRC and the mounting Asian interest in African timber—have raised the ax over Conrad's "kings."

The DRC contains more than 60% of the basin's remaining forests, and "the new scramble for central African resources, exerting massive pressures to open up frontier areas, has the potential to culminate in a 'perfect storm,' " says William Laurance of the Smithsonian Tropical Research Institute (STRI) in Panama, who has studied the impact of logging on wildlife in several rainforests.

Wood sale. Local needs for lumber take a toll on Congo forests.

Congo rapids. Rough water near Kinshasa impedes the transport of logs.

At issue are "the loss of biodiversity, a massive waste of forest resources, the decline of rainforest people, and—in the long run—possible climate change," warns University of Kinshasa botanist Constantin Lubini, whose garden is an oasis of flowering trees amid the dusty chaos of Kinshasa's *Debonhomme* quarter, where vendors sell charcoal along with bread and meat. In the region's fast-growing cities, the widespread use of charcoal and wood for cooking has taken a heavy toll on nearby forests.

Hart, Lubini, and other scientists—from big-picture geographers who scrutinize satellite images to on-site botanists who measure every sapling on 40-hectare rainforest plots—believe the next few years will be critical in determining the future of what is probably the least exploited yet most scantily studied of the world's humid forest regions. In conjunction with the 6-year-old Congo Basin Forest Partnership (CBFP)—an international association of government officials, nongovernmental organizations, and conservation experts—these researchers are now applying satellite maps, in-depth forest studies, and other tools

CREDITS (TOP TO BOTTOM): R. KOENIG/*SCIENCE*; R. KOENIG/*SCIENCE*

to help policymakers limit the sort of large-scale deforestation that is now decimating rainforests in the Amazon and Far East.

Eyes in the sky

Earth-observation satellites have become the watchdogs for deforestation in remote areas, helping document regions in trouble. At the cluttered Kinshasa office of the OCEAN (Organisation Concertée des Ecologistes et Amis de la Nature) ecology group, director René Ngongo negotiates through the crowd—from shouting pygmies to low-key forest analysts—toward a map taped to the wall. "These red spots show what's been destroyed," he says, tapping the satellite-generated map of Congo Basin forest change, "but there is still more green forest, and we want to keep it that way." The problem is that the map (above) shows the forests as of 2000, and the next update won't be available until later this year.

Deforestation hot spots. Based on satellite images, this map shows that forest loss occurred mainly along the Congo River and near the Uganda and Rwanda borders (far right), areas of rapid population growth.

For many technical reasons, remote sensing of Congo forests has lagged behind studies of the Amazon, which "is a much easier place to monitor," says geographer Matthew C. Hansen of South Dakota State University's Geographic Information Science Center of Excellence in Brookings. Persistent cloud cover prevents clear images of some Congo Basin areas, requiring far more images to be processed. Also, central Africa has no dish to receive data; thus, researchers get relatively few images from the Landsat satellites. And because of a glitch in Landsat 7, its images have been flawed since 2003. To make matters worse, it is far more difficult to detect the "selective" logging of just a few trees per hectare that is standard in the Congo than it is to identify clear-cut areas, typical in the Amazon. Forest change "is huge in the Amazon," Hansen says, making it simpler to map deforestation.

To tackle those challenges, North American and European groups are bringing new analyses to bear on impoverished Congo data sets. In 2003, the U.S.-funded Central African Regional Program for the Environment commissioned Hansen and Christopher Justice of the University of Maryland, College Park, to produce a decadal deforestation map. It took Hansen, Justice, and their team 3 years to automate the calibration of the infrequent but higher resolution Landsat images with data from a lower resolution NASA instrument (MODIS) that measures tree cover. This map, released last year, shows that much of the forest loss during the 1990s occurred near densely populated areas in the eastern DRC, along principal rivers, and at the basin's periphery. Even though the map is already 8 years out of date, Ngongo and other Congolese activists and officials regard it as a useful baseline for further research.

Meanwhile, a group led by Belgian forester Philippe Mayaux of the Joint Research Centre's Institute for Environment and Sustainability in Ispra, Italy, used a less comprehensive "grid sampling" technique to parse Congo forest trends across the whole basin from the satellite data. In a paper in the 15 May issue of *Remote Sensing of Environment*, they concluded that the basin's deforestation rate for the decade ending in 2000 was nearly 0.2% per year. In addition, the rate of forest degradation (thinning of forested areas) was 0.1%. The deforestation was low compared with the Amazon's annual rate of about 0.5%, but it is still of concern because on-the-ground reports indicate that logging in the Congo region is escalating.

Some new data sets also show promise. Nadine Laporte, whose teams at the Woods Hole Research Center in Falmouth, Massachusetts, have been studying logging roads and biomass in the Congo Basin, says the Chinese-Brazilian CBERS satellites may offer cost-free data to African institutions. Microwave radar imagery from Japanese and Canadian satellites is now helping some scientists better assess forest trends in persistently cloud-covered coastal areas. And Laporte's group is searching for ways to use data from NASA's LIDAR laser-pulse sensor to calibrate optical imagery and improve estimates of forest biomass.

Perhaps more importantly, French and British officials are separately considering plans to help build a receiving dish in central Africa to acquire and store up-to-date data from satellites as they fly over. Without such additional data, Hansen says, "you can only do accurate update maps for the entire basin every 3 to 5 years." Looking forward to such data, the University of Maryland's Paya de Marcken is now training central African scientists at a new remote-sensing lab at the University of Kinshasa to handle incoming images.

On the ground

Although the Congo satellite maps are outdated, they drive home the vulnerability of the forests. At his office laptop in Kinshasa, Belgian geographer Benoit Mertens opens a satellite map, defines a forest area, and enlarges the pinpointed section to reveal that it is crisscrossed by what he calls "a wishbone pattern" of roads. They are a clear indication that the tract is being logged, says Mertens, who works for the World Resources Institute's Global Forest Watch project. Laporte of Woods Hole says her group's analysis of Landsat images for evidence of forest roads showed considerable logging road construction (about 460 kilometers per year) in the north-central DRC (*Science*, 8 June 2007, p. 1451). And, says Laporte, "you can make a pretty good assessment of the extent and intensity of logging from the road maps."

What's harder to assess is the relative impact of industrial versus "informal" (sometimes illegal) logging. Mertens coordinates a five-country project to monitor the basin's timber industry. The DRC's 156 logging con-

CREDIT: CARPE/USAID/SOUTH DAKOTA STATE UNIVERSITY/UNIVERSITY OF MARYLAND/NASA

cessions control about 21 million hectares and take out about 500,000 cubic meters of timber a year. But Mertens and other experts say that chainsaw-wielding freelance loggers or farmers who practice "slash-and-burn" agriculture now account for more DRC forest degradation than industrial timber operations.

Informal logging takes place along many roads and in the forest fringes, with most of the timber used for local fuel or exported from the northeastern DRC to nearby Uganda, where population increases are driving up demand for wood. French forest scientist Robert Nasi of the Center for International Forestry Research in Bogor, Indonesia, estimates that Kinshasa alone (with a population of 8 million) consumes about 4.5 million cubic meters of wood equivalent per year for charcoal. "If you consider that all of the major cities are using fuel wood or charcoal, it dwarfs the selective logging harvest by more than an order of magnitude."

But Susanne Breitkopf, who monitors Congo Basin forests for Greenpeace, contends that industrial logging "is now the main threat to the forest" in some major provinces, "not only because of the direct impact of logging on wildlife and ecosystems but also because it acts as a catalyst for further destruction, opening once-remote areas to increased levels of hunting, settlement, and agriculture."

Tracking forest fauna and flora

Remote-sensing data can provide important mapping information, but it takes researchers on the ground—in the midst of the forests—to shed light on exactly how the Congo Basin's forests are changing and what their contribution to the global carbon cycle is. Numerous groups are now studying the impacts of civil wars, forest degradation, mining, and other factors on the region's flora and fauna.

Some scientists have been tracking the fate of animals that live and breed in the DRC, from giraffelike okapi to great apes. Those species may be at greater risk than the trees around them. The sharp increase in forest hunting and the bush-meat trade, which was exacerbated by the civil conflicts and the incursion of logging roads into the deep forests, have emptied some landscapes. "Mammals are no longer seen along the roads in many forests," observes ecologist Julien Punga-Kumanenge, who says that the DRC's bush-meat trade—the world's most extensive—has become so widespread that "even big snakes are sold in the markets."

Logging itself can lead to wildlife hazards as well. In a coastal study that directly links logging to endangered marine species, a team led by the Smithsonian's Laurance reported this year that many sea turtles that are climbing onto Gabon beaches to nest "are being tangled, impeded, and killed" by thousands of lost logs that block the way to traditional nesting sites. "This is highly relevant because the region contains some of the most important nesting areas in the world for sea turtles, including the critically endangered leatherback turtle," says Laurance.

Perhaps the longest running research survey in the DRC is the Ituri Forest project, part of STRI's Center for Tropical Forest Science (CTFS) initiative. Since 1993, Congolese forest scientist Jean-Remy Makana and colleagues have been measuring and assessing all the trees and woody vines in a 40-hectare plot, part of the 21-site CTFS network that monitors more than 3 million tropical trees across the globe. The Ituri studies have found about 470 species of trees and shrubs, along with 240 species of liana (woody vines). "Most of the diversity is not in the big-tree category but in the 'treelet' subcanopy category and in the lianas," says botanist Hart.

Recent studies of biomass across the CTFS sites have indicated that the Congo Basin forest has among the highest carbon content per hectare of any rainforest, perhaps because of the density of its flora. If the Ituri site is typical, then preservation of the Congo Basin would do relatively more to prevent carbon release than preserving forests elsewhere, Makana says.

Such carbon accumulation could provide incentives to preserve the DRC's forests if the government allowed local forest inhabitants, such as the region's half-million pygmies, to engage in carbon trading. Local groups could lease forest tracts from the government and then sell "carbon units" valued according to the amount of deforestation circumvented. These earnings would serve as an alternative to logging income.

Even if the carbon scheme proves unfeasible, an ongoing effort to preserve vast tracts of the Congo Basin's rainforests—focusing on a dozen large-scale "landscapes" with a total area larger than Texas—is showing potential. The Mayaux and Hansen studies both indicate that the "landscapes" selected by CBFP were less affected by deforestation and logging exploitation, at least through 2000. Scientists are now studying on-the-ground conservation in those landscapes. And activists such as Hart—who wants a new "landscape" designated in the central DRC—are calling for more stringent protection of biodiversity within them.

All of these efforts would be better off with more science behind them, says engineer Somnath Baidya Roy of the University of Illinois, Urbana-Champaign, who has developed a mathematical model to project how deforestation might influence climate in key central African parks and reserves. He and others are calling for more extensive land- and sky-based data and more intense research to improve methods of predicting the impacts of deforestation. Says Roy: "We need to do the same sort of work in the Congo Basin that has been done in the Amazon and elsewhere."

–ROBERT KOENIG

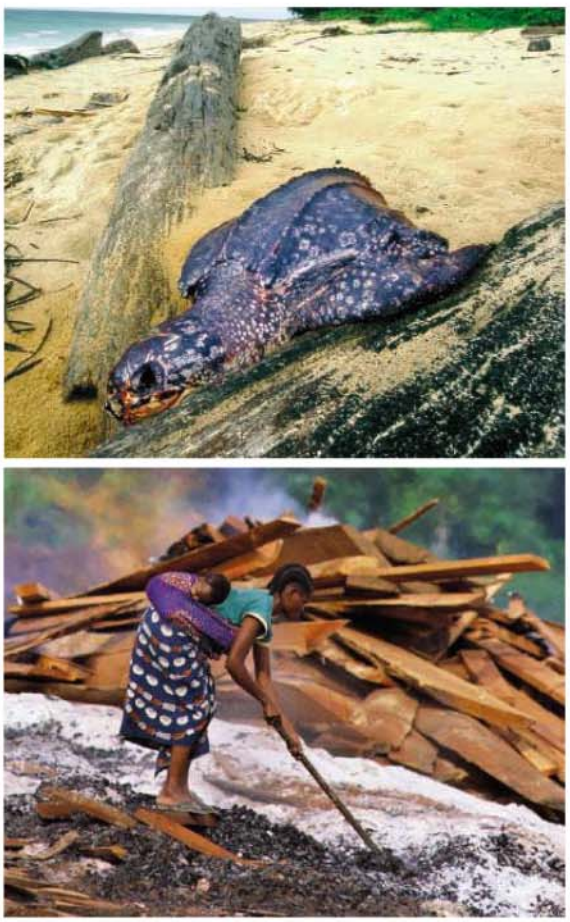

Logged in; burnt out. Stray logs keep a sea turtle from its nesting site. Elsewhere, a woman makes charcoal from felled timber.

CREDITS (TOP TO BOTTOM): DAVID LIGGETT; GEORGE STEINMETZ/CORBIS

Recovering. Now protected, the forested home of the giant panda has been coming back.

NEWS

Letting 1000 Forests Bloom

A logging ban has allowed a hot spot of China's biodiversity to recover from decades of clear-cutting, but threats still loom

In 1972, Yin Kaipu, then a young ecologist, hitched a ride aboard a loaded logging truck to a village at the base of the spectacular Qionglai Mountain Range in China's Sichuan Province. To keep from falling off, Yin and his professor, Liu Zhaoguang of the Chinese Academy of Sciences' Chengdu Institute of Biology (CIB) in Sichuan, wrapped their arms around the logs as the truck lurched down the winding dirt roads to the headquarters of the government-run logging company. What they saw was disheartening: The mountains along the road and close to the village were "shaved like a monk's head," Yin said, recalling his professor's dismay at the extensive clear-cutting.

"He knew that many special plants were being lost," along with the "habitat of many species," says Yin. The logging also posed a threat to a Chinese icon, the giant panda (*Ailuropoda melanoleuca*), which lived in small, isolated parts of the mountains' dense bamboo forests. Decades later, Premier Zhu Rongji echoed Liu's concern, decrying the Sichuan loggers as "tigers eating the whole sheep" when he toured these and other ranges in westernmost Sichuan in 1997.

Together, the ranges make up the 700,000-square-kilometer Hengduan Mountain Region, home to the world's most biologically diverse temperate forest, hosting 40% of all of China's plant species. Today, thanks in part to efforts by Yin and many others, the "logging tigers" have been tamed. After two devastating floods, the Sichuan government imposed a logging ban in 1998. Much of the region is being preserved in parks and reserves. And under a national program, local farmers are being rewarded for planting trees on fragile slopes.

But Hengduan's natural forests are not yet out of the woods. The logging ban is due to expire in 2010, and economic and population pressures still loom as threats to the recovery of the region's forests. What happens to this unique ecosystem could be an indicator of the prospects for other parts of China that have been ravaged by rapid industrialization and population growth. "The end of the logging was the first step," says Yin. "The challenge is finding a balance between people's needs and protecting the forest."

Logging legacy

China's Hengduan Mountain Region lies more than 1500 kilometers southwest of Beijing. (It is at the epicenter of the devastating earthquake that struck Sichuan last month; see *Science*, 23 May, p. 996.) "The Hengduans are like islands," says botanist John Simmons, the retired curator of Britain's Royal Botanic Gardens, Kew, who has collected extensively in the region with Yin. "They're isolated, with a range of ecological niches, from lower [600 meters] to higher elevations [more than 6000 meters]," spurring plants "to speciate like mad." They house 3500 endemic species of plants, birds, reptiles, amphibians, and mammals, including giant pandas. That's made this part of China a prime target of plant collectors and botanists since the late 19th century. "Nearly every garden today" has a plant from there, says Simmons, most likely a rhododendron, primrose, or lily.

But beginning in the 1950s and intensifying in the 1970s, loggers devoured the dense forests—part of the country's spurt to become an industrialized nation. The clear-cutting, which Yin and Liu witnessed throughout the Hengduans as they mapped and collected the region's flora, inflicted huge damage on the ecosystem. "Without a forest to protect the soil, we knew a flood would come," says Yin.

Ultimately, two catastrophic floods came, in 1981 and 1998, on the upper and lower portions of the Yangtze River. The second flood—a disaster that killed more than 1500 people, left millions homeless, and cost some $20 billion—finally spurred the Sichuan government to ban logging in its natural forests. The next

Hengduan rarities. Ecologist Yin Kaipu fought to preserve the Hengduan's local plant diversity, including the regal lily (*right*), which has become a prime garden plant.

CREDITS (TOP): PHILIP CORRIS; (BOTTOM LEFT TO RIGHT): DIANE YA-HUI PEDIA

year, China started to replant and preserve forest lands nationwide. These moves were "a major milestone," says ecologist Jianguo "Jack" Liu of Michigan State University in East Lansing, whose analysis of the recovery will soon appear in the *Proceedings of the National Academy of Sciences*.

However, the damage done before the ban was extensive. Some 20% of the region's plant species are now endangered, and much of the panda, takin, and golden monkey habitat was lost to logging. When the clear-cutting finally stopped, "roughly 35% to 40% of Sichuan's natural forests were gone," says forest ecologist Mu Changlong, deputy director of the Sichuan Academy of Forestry in Chengdu. And in some parts of the province, more than 85% of the forest was cut, even in places that the government had identified as important for soil and water conservation. "The timber companies worked in areas that were the most accessible, with the largest trees and most biodiversity," says Mu. "In some places, they logged everything up to 3000 meters [in elevation]."

Theoretically, the loggers were supposed to be followed close behind by planters. "But the loggers were faster, so in many places the clear-cuts weren't reforested, and now there are just bushes and sword bamboo," which inhibit the growth of the original conifer forest, says Mu.

Worse, in some areas, such as along the Upper Min River in the Hengduan's Min Mountain Range, the vertical terrain was so completely deforested and eroded that getting anything to grow now is "impossible," says ecologist Wu Ning, CIB's executive director. "We're simply trying to stop the expansion of what has become a desert" by building fences to keep the soil from sliding into the river, says Wu. Sichuan has now reduced its soil erosion by 1.5 billion tons, but eroded sediments in the Upper Yangtze still clog so much of the river that only ships between 5000 and 8000 tons can navigate this far upstream.

Efforts continue, as well, to bring back forests. Overall, 143,000 hectares have been replanted along the damaged Min River gorge, primarily with exotic red pine (*Pinus tabuliformis*), a fast-growing species from northern China. But 13,300 hectares of this total have been reforested with a CIB-recommended mix of native broadleaf and coniferous species, as well as exotics, in an effort to avoid the health and fire-prone problems associated with single-species stands, says Yin. And to further relieve the pressure on native forests, the government plans to plant 2.5 billion trees in plantations this year throughout the country. It wants to become self-sufficient in timber by 2050.

China has also provided economic incentives to farmers. In 1999, it initiated the Grain for Green Program, paying farmers to plant trees and shrubs on agricultural land with more than a 25-degree slope, with the goal of increasing plant cover by 32 million hectares by 2010 (*Science*, 7 December 2007, p. 1556). "That helped the people, especially those who lost jobs because of the [logging] ban," says conservation ecologist Ling Lin of the World Wide Fund for Nature in Chengdu. And under the 2002 Rural Contract Law, farmers now own the rights to what they grow, which "should help them better manage the land in a sustainable manner," says Xu Jintao, an economist at Beijing's Peking University. They can use the rights as collateral, pass them on to their children, and even sell them.

China's treasured forest. The Hengduan Mountain Region contains the world's most diverse temperate forest.

Moreover, in Sichuan, 75,000 square kilometers—about 15.5% of the province—of the natural forests are now safe in approximately 150 reserves or provincial and national parks, such as Siguniang (Four Sisters Mountain) National Park in the Qionglai Mountain Range. Two, Wolong Nature Reserve and Jiuzhaigou, where dense stands of native conifers edge more than 100 turquoise-colored lakes, are now World Heritage Sites.

Fragile progress

But concerns remain. China is now the world's largest manufacturer and exporter of wood products and has an enormous demand for the raw material. "The price of timber in China has increased two to three times over the last 5 years," says Xu. Should the Grain for Green Program subsidies end, the temptation to cut the trees will be huge, warns Jack Liu. That's why, he and others say, China has recently extended the program and may do the same for the logging ban, at least for the natural forests. In the more remote regions of the Hengduans, people continue to cut trees for fuel and home construction, notes Harvard University botanist David Bouffard.

The preserves themselves are facing another threat. "From the first day, these parks have been very popular," says Yin, adding that they now draw millions of visitors annually. "It is too many." More than 30,000 tourists can wander through Jiuzhaigou on a single day, despite requests from Yin and other ecologists to limit that number. "It's just a sea of people at the entry gate some mornings," adds Jack Liu, noting that in Jiuzhaigou the only panda "sightings" are occasional scat. "There are just too many people and too much noise," he complains.

With a government grant in hand, Yin is now looking for ways to relieve the pressure. One solution may come from his team's 2006 proposal to connect two of the largest panda reserves in the Min Mountain Range by restoring some 30 to 40 square kilometers of panda habitat.

Yin and others are also helping the State Forestry Administration set zoning limits, denoting some park areas for mass tourism and others for more individual experiences such as wilderness backpacking, and even closing a few altogether. One morning at Siguniang, where a zoning system now exists, Yin walked contentedly along a boardwalk trail through a wetland meadow, pointing out the endemic flowers and shrubs he and his professor had collected more than 30 years ago. On either side of the meadow rose snow-capped peaks, their flanks thick with the classic mixed forest of western Sichuan. "The logging tigers didn't get this far up the valley because there was no road," says Yin. There is a paved road now. But with luck, the zoning system will help Siguniang's forests survive the growing number of China's tourist tigers.

–VIRGINIA MORELL

REVIEW

Forests and Climate Change: Forcings, Feedbacks, and the Climate Benefits of Forests

Gordon B. Bonan

The world's forests influence climate through physical, chemical, and biological processes that affect planetary energetics, the hydrologic cycle, and atmospheric composition. These complex and nonlinear forest-atmosphere interactions can dampen or amplify anthropogenic climate change. Tropical, temperate, and boreal reforestation and afforestation attenuate global warming through carbon sequestration. Biogeophysical feedbacks can enhance or diminish this negative climate forcing. Tropical forests mitigate warming through evaporative cooling, but the low albedo of boreal forests is a positive climate forcing. The evaporative effect of temperate forests is unclear. The net climate forcing from these and other processes is not known. Forests are under tremendous pressure from global change. Interdisciplinary science that integrates knowledge of the many interacting climate services of forests with the impacts of global change is necessary to identify and understand as yet unexplored feedbacks in the Earth system and the potential of forests to mitigate climate change.

Forests cover ~42 million km^2 in tropical, temperate, and boreal lands, ~30% of the land surface (Fig. 1A). These forests provide ecological, economic, social, and aesthetic services to natural systems and humankind (*1*), including refuges for biodiversity, provision of food, medicinal, and forest products, regulation of the hydrologic cycle, protection of soil resources, recreational uses, spiritual needs, and aesthetic values. Additionally, forests influence climate through exchanges of energy, water, carbon dioxide, and other chemical species with the atmosphere.

Forests store ~45% of terrestrial carbon (Fig. 1B), contribute ~50% of terrestrial net primary production (*2*), and can sequester large amounts of carbon annually (Fig. 1C). Carbon uptake by forests contributed to a "residual" 2.6 Pg C year^{-1} terrestrial carbon sink in the 1990s, ~33% of anthropogenic carbon emission from fossil fuel and land-use change (*3*). Forests have low surface albedo and can mask the high albedo of snow (Fig. 1D), which contributes to planetary warming through increased solar heating of land. Forests sustain the hydrologic cycle through evapotranspiration, which cools climate through feedbacks with clouds and precipitation. The ratio of evapotranspiration to available energy is generally low in forest compared with some crops and lower in conifer forest than in deciduous broadleaf forest (Fig. 1E).

That forests influence climate has long been postulated. From the onset of European settlement of North America, it was believed that clearing of forests for cultivation, wood products, and settlement altered climate (*4*). Today, scientists have a diverse array of methodologies, including eddy covariance flux towers, free-air CO_2 enrichment systems, satellite sensors, and mathematical models to investigate the coupling between forests and the atmosphere. It is now understood that forests and human uses of forests provide important climate forcings and feedbacks (*3*), that climate change may adversely affect ecosystem functions (*5*), and that forests can be managed to mitigate climate change (*6*). What is lacking, however, is science that integrates the many interacting climate services of forests with the impacts of global change to inform climate change mitigation policy.

Accordingly, this article reviews biosphere-atmosphere interactions in tropical, temperate, and boreal forests. Emphasis is placed on biogeophysical processes (albedo and evapotranspiration) (*7*), their comparison with biogeochemical processes (carbon cycle) (*8*), and alteration of forest-atmosphere coupling through biogeographical processes (land use and vegetation dynamics) (*9*).

The Ecology of Climate Models

The influence of forests on large-scale climate is difficult to establish directly through observations. Careful examination of climatic data can sometimes reveal an ecological influence, such as the effect of leaf emergence on spring-time evapotranspiration and air temperature. Eddy covariance flux towers and field experiments provide local-scale insight to forest-atmosphere interactions, and advances in remote sensing science can aid extrapolation of this knowledge to larger spatial scales. More often, however, our understanding of how forests affect climate comes from atmospheric models and their numerical parameterizations of Earth's land surface (*10*). Paired climate simulations, one serving as a control to compare against another simulation with altered vegetation, demonstrate an ecological influence on climate.

Atmospheric models require fluxes of energy, moisture, and momentum at the land surface as boundary conditions to solve numerical equations of atmospheric physics and dynamics. The first generation of land surface parameterizations developed in the late 1960s and 1970s used bulk aerodynamic formulations of energy exchange without explicitly representing vegetation [supporting online material (SOM)]. Soil water availability regulates latent heat flux, and the hydrologic cycle, when included, was simplified to a "bucket" model of soil water. In this approach, precipitation fills the soil column up to a specified water-holding capacity, beyond which rainfall runs off.

By the mid-1980s, the second generation of land surface parameterizations, included the hydrologic cycle and the effects of vegetation on energy and water fluxes. These models explicitly represent plant canopies, including radiative transfer, turbulent processes above and within the canopy, and the physical and biological controls of evapotranspiration (Fig. 2A). Snow cover, the soil water profile, and vegetation influences on the hydrologic cycle are also included (Fig. 2B). In the mid-1990s, plant physiological theory further advanced the incorporation of biological control of evapotranspiration in the third generation of models. Models now routinely link the biochemistry of photosynthesis with the biophysics of stomatal conductance. Leaf photosynthesis and conductance are scaled to the plant canopy based on the optimal allocation of nitrogen and photosynthetic capacity in relation to light availability. Simulations with these models have routinely demonstrated biogeophysical regulation of climate by vegetation through albedo, turbulent fluxes, and the hydrologic cycle (*10*).

The current generation of models has capability beyond hydrometeorology and incorporates ecological advances in biogeochemical and biogeographical modeling (*10*). Many models simulate the carbon cycle (Fig. 2C) and vegetation dynamics (Fig. 2D). In these models, the biosphere and atmosphere form a coupled system whereby climate influences ecosystem functions and biogeography, which feed back to affect climate. Much of the natural vegetation of the world has been cleared for agriculture (Fig. 3D), and some models also include land-use change.

Tropical Forests

Climate model simulations show that tropical forests maintain high rates of evapotranspiration, decrease surface air temperature, and increase precipitation compared with pastureland (SOM). The most studied region is Amazonia, where large-scale conversion of forest to pasture creates a warmer, drier climate. Surface warming arising from the low albedo of forests is offset by strong evapo-

National Center for Atmospheric Research, P.O. Box 3000, Boulder, Colorado 80307, USA. E-mail: bonan@ucar.edu

rative cooling. Similar results are seen in tropical Africa and Asia, and the climatic influence of tropical forests may extend to the extratropics through atmospheric teleconnections. However, forest-atmosphere interactions are complex, and small-scale, heterogeneous deforestation may produce mesoscale circulations that enhance clouds and precipitation.

Flux tower measurements in the Brazilian Amazon confirm that forests have lower albedo compared with pasture, greater net radiation, and greater evapotranspiration, particularly during the dry season (*11*, *12*), producing a shallow, cool, and moist boundary layer. Observations show that forest transpiration is sustained during the dry season (*11*); this is seen also in CO_2 fluxes (*12*) and satellite monitoring of vegetation (*13*, *14*), to a greater extent than represented in many models.

Tropical forests contain ~25% of the carbon in the terrestrial biosphere (Fig. 1B), account for ~33% of terrestrial net primary production (NPP) (*2*), and can sequester large amounts of carbon annually (Fig. 1C). Deforestation released 1.6 Pg C $year^{-1}$ during the 1990s, chiefly in the tropics (*3*). Atmospheric analyses suggest that tropical forests are carbon neutral or carbon sinks, which implies offsetting of carbon uptake by undisturbed tropical ecosystems (*3*, *15*).

The net balance among these processes is likely a positive benefit that mitigates global warming through evaporative cooling and carbon sequestration (*8*). Yet a more complete analysis of forest-atmosphere interactions is required. The biogeochemistry of tropical forests and biomass burning affects atmospheric chemistry and aerosols, which can alter clouds and rainfall (*16*). Interannual climate variability modulates forest-atmosphere coupling. There is net release of carbon from the biosphere to the atmosphere during warm, dry El Niño years, seen in high atmospheric CO_2 growth rates (*3*), especially in the tropics (*17*). Drought makes tropical forests more susceptible to burning during land clearing (*18*). However, tropical forest productivity may be more resilient to drought than expected (*14*).

The future of tropical forests is at risk in a warmer, more populous 21st-century world. Tropical forests are vulnerable to a warmer, drier climate (*19*), which may exacerbate global warming through a positive feedback that decreases evaporative cooling, releases CO_2, and initiates forest dieback (*20*). Loss of natural forests worldwide in the tropics during the 1990s was as high as 152,000 km^2 $year^{-1}$ (*1*), and Amazonian forests were cleared at a rate of ~25,000 km^2 $year^{-1}$ (*19*). Such land-use pressures are expected to continue in the future and may shift the Amazonian region to a permanently drier climate once a critical threshold of clearing is reached.

Boreal Forests

Climate model simulations show that the low surface albedo during the snow season, evident in local flux measurements (*21*) and satellite-derived surface albedo (Fig. 1D), warms climate compared to when there is an absence of trees (SOM). Consequently, the boreal forest has the greatest biogeophysical effect of all biomes on annual mean global temperature (*7*). Loss of boreal forest provides a positive feedback for glaciation (*22*), whereas forest expansion during the mid-Holocene 6000 years ago amplified warming (*23*).

Boreal forests differ in their partitioning of net radiation into sensible and latent heat fluxes. Conifer forests have low summertime evaporative fraction (defined as the ratio of latent heat flux to available energy) compared with deciduous broadleaf forests, producing high rates of sensible heat exchange and deep atmospheric boundary layers (*21*). Flux tower measurements illustrate the potential for changes in species composition, arising from change in the fire regime, to affect climate (*24*). Along an 80-year fire chronosequence in Alaska, annual net radiation declined by 31% at a 3-year-old postburn

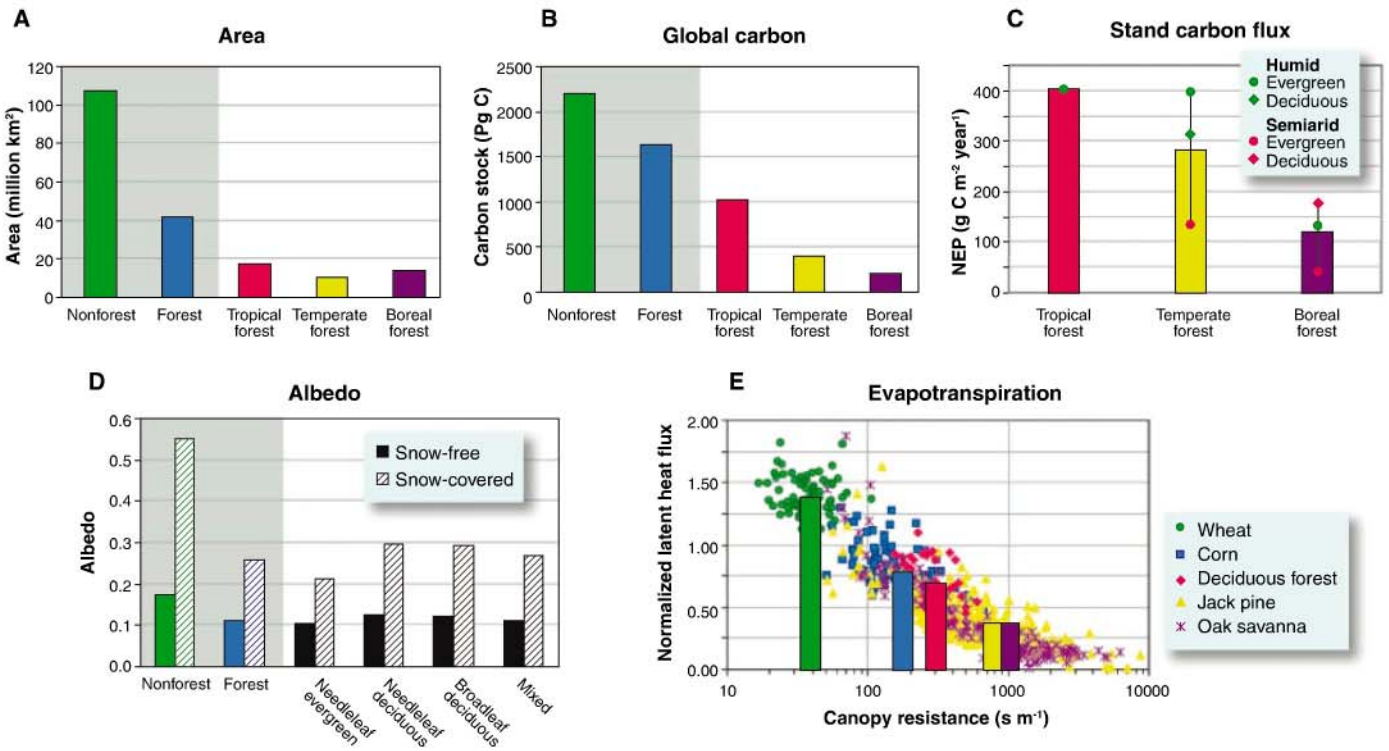

Fig. 1. Biogeochemical (carbon) and biogeophysical (albedo and evapotranspiration) processes by which terrestrial ecosystems affect climate (SOM). (**A** and **B**) Geographic extent and total (plant and soil) carbon stock of nonforest (green) and forest (blue) biomes (*2*). Individual forest biomes are also shown and sum to the forest total. (**C**) Net ecosystem production (NEP) for tropical, temperate, and boreal forest (*47*). Individual symbols shown mean NEP for humid evergreen tropical forest, three types of temperate forest, and three types of boreal forest. Vertical bars show NEP averaged across forest types. (**D**) Satellite-derived direct-beam albedo for snow-covered and snow-free nonforest (green) and forest (blue) biomes (*48*). Also shown are individual forest biomes. (**E**) Evapotranspiration normalized by its equilibrium rate in relation to canopy resistance for wheat, corn, temperate deciduous forest, boreal jack pine conifer forest, and oak savanna (*49*, *50*). Shown are individual data points and the mean for each vegetation type.

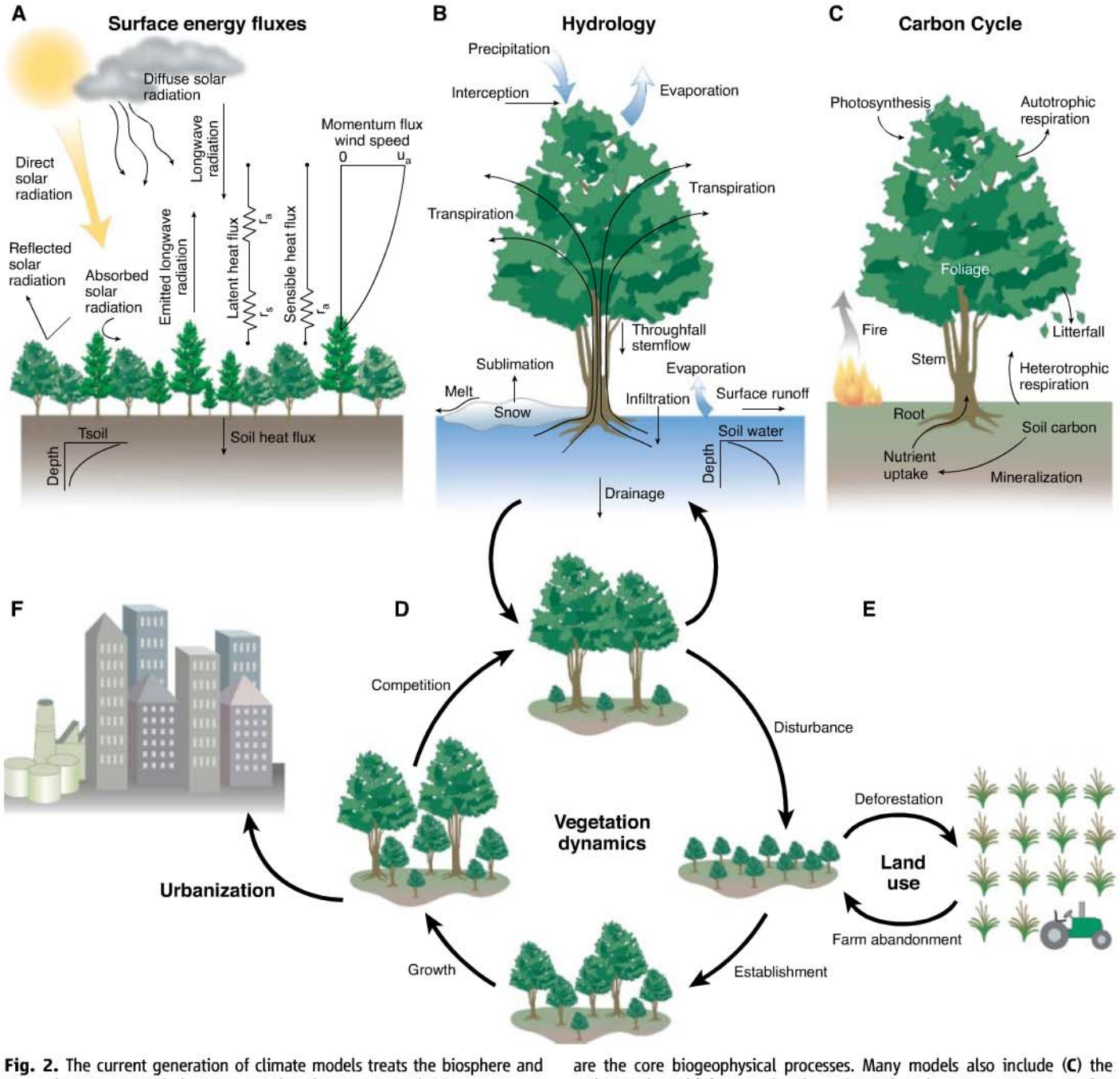

Fig. 2. The current generation of climate models treats the biosphere and atmosphere as a coupled system. Land surface parameterizations represent the biogeophysics, biogeochemistry, and biogeography of terrestrial ecosystems. (**A**) Surface energy fluxes and (**B**) the hydrologic cycle. These are the core biogeophysical processes. Many models also include (**C**) the carbon cycle and (**D**) vegetation dynamics so that plant ecosystems respond to climate change. Some models also include (**E**) land use and (**F**) urbanization to represent human alteration of the biosphere.

site dominated by grasses and a 15-year-old aspen (*Populus tremuloides*) forest compared with an 80-year-old black spruce (*Picea mariana*) forest, primarily in spring and summer. Annual sensible heat flux decreased by more than 50% compared with the 80-year site, mostly in spring and summer. During summer, the aspen forest had the highest latent heat flux, lowest sensible heat flux, and lowest midday Bowen ratio (defined as the ratio of sensible heat flux to latent heat flux).

Boreal ecosystems store a large amount of carbon in soil, permafrost, and wetland (*2*) and contribute to the Northern Hemisphere terrestrial carbon sink (*3*), although mature forests have low annual carbon gain (Fig. 1C). The climate forcing from increased albedo may offset the forcing from carbon emission so that boreal deforestation cools climate (*8*). Similar conclusions are drawn from comprehensive analysis of the climate forcing of boreal fires (*25*). The long-term forcing is a balance between postfire increase in surface albedo and the radiative forcing from greenhouse gases emitted during combustion. Averaged over an 80-year fire cycle, the negative forcing from surface albedo exceeds the smaller positive biogeochemical forcing. Yet in the first year after fire, positive annual biogeochemical forcing from greenhouse gas emission, ozone, black carbon deposited on snow and ice, and aerosols exceeds the negative albedo forcing.

Boreal forests are vulnerable to global warming (*5*). Trees may expand into tundra, but die back

CREDIT: CARIN CAIN

along southern prairie ecotones. In the main boreal forest, there may be loss of evergreen trees and a shift toward deciduous trees. Siberian forests may collapse in some areas and become more evergreen in the north. Increased disturbance from fire or insect outbreaks will shift the forest to a younger age class. Climate forcing arising from younger stand age may be comparable to that arising from biome shifts (*24*).

Temperate Forests

Much of the temperate forests of the eastern United States, Europe, and eastern China have been cleared for agriculture (Fig. 3D). Croplands have a higher albedo than forests (Fig. 1D), and many climate model simulations find that trees warm surface air temperature relative to crops (SOM). Masking of snow albedo by trees is important in cool temperate climates with snow. Studies of eastern United States forests find that trees also maintain a warmer summer climate compared with crops because of their lower albedo, augmented by evaporative cooling from crops and feedbacks with the atmosphere that affect clouds and precipitation (*26*). The influence of crops on evapotranspiration is seen in flux tower measurements. Growing season evaporative cooling is greater over watered crops compared with forests, and these plants exert less evaporative resistance (Fig. 1E).

Although global climate models find that temperate forests in the eastern United States warm summer temperature (*26*), mesoscale model simulations of the July climate of the United States find that trees increase evapotranspiration and decrease surface air temperature compared with crops (*27*, *28*). Atmospheric feedbacks that alter cloudiness affect the magnitude of the temperature response in these simulations. Flux tower analyses show that conifer and deciduous broadleaf forests in North Carolina have lower surface radiative temperature than grass fields because of greater aerodynamic conductance and evaporative cooling of trees compared with grasses (*29*), but the same may not pertain to cropland (Fig. 1E).

Interannual climate variability affects biosphere-atmosphere coupling. In western Europe, forest and agricultural land have comparable surface radiative temperature when soil is moist but respond differently to drought (*30*). Forest maintains green vegetation, as indicated by the normalized difference vegetation index, although surface temperature and sensible heat flux increase with drought. Vegetation greenness in cropland declines by ~50%, the surface warms 13°C more than in forest, and the drought enhancement in sensible heat flux is greater than for forest. The different response to drought arises from the deep roots of trees and their access to deeper reservoirs of soil water.

Temperate forests hold ~20% of the world's plant biomass and ~10% of terrestrial carbon (Fig. 1B). Carbon sequestration rates of mature forests are high (Fig. 1C), but temperate forests in the United States historically have been carbon sources because of deforestation (*31*). Socioeconomic trends in reforestation and fire suppression have shifted these forests to a carbon sink. Similar trends are seen in Europe (*3*).

The net climate forcing of temperate forests is highly uncertain. Competing biogeophysical forcings from low albedo during winter and evapotranspiration during summer influence annual mean temperature (*7*). Higher albedo with loss of forest cover could offset carbon emission so that the net climatic effect of temperate deforestation is negligible (*8*), or reduced evapotranspiration with loss of trees could amplify biogeochemical warming.

The future of temperate forests and their climate services is highly uncertain. The present carbon sink in eastern United States forests is likely to decline as recovering forests mature (*31*), and these forests face uncertain pressure from climate change, atmospheric CO_2 increase, and anthropogenic nitrogen deposition (*5*). Change in the balance between deciduous and evergreen trees is likely in the future. Temperate forests are particularly vulnerable to human land use. The trend over the past several decades has been toward farm abandonment, reforestation, and woody encroachment from fire suppression, but meeting the needs of a growing global population could place greater pressures on these forests.

Carbon Cycle Feedbacks

The carbon cycle has long been recognized as important for understanding climate change. Climate models that include the terrestrial and oceanic carbon cycle simulate a positive feedback between the carbon cycle and climate warming that increases the airborne fraction of anthropogenic CO_2 emission and amplifies warming (*3*, *32*). In a comparison of 11 models of varying degrees of complexity, carbon cycle–climate feedbacks increase atmospheric CO_2 at the end of the 21st century by 4 to 44% (multimodel mean, 18%), equivalent to an additional 20 to 224 (parts per million) (ppm) (multimodel mean, 87 ppm) (*3*). Analyses of observed atmospheric CO_2 concentrations indicate that such a decline in the efficiency of the carbon cycle to store anthropogenic CO_2 in ocean and land is occurring, and to a greater extent than estimated by models (*33*).

Much of the model uncertainty arises from the terrestrial biosphere (*3*, *32*). Plants respond to rising atmospheric CO_2 through photosynthetic enhancement, and this "CO_2 fertilization" is a negative feedback to higher atmospheric CO_2 concentration. In the multimodel comparison, land carbon storage increases with higher atmospheric CO_2 in all models, driven by a 12 to 76% increase in NPP with CO_2 doubling (multimodel mean, 48%), offset slightly by enhanced heterotrophic respiration (*3*). Free-air CO_2 enrichment studies in forests find that a ~50% increase in atmospheric CO_2 concentration sustained over several years enhances NPP by 23% (*34*), but the long-term outcome is unclear, especially when interactions with nitrogen availability are considered (*5*).

Climate change reduces carbon storage from CO_2 fertilization. Terrestrial carbon storage declines with warming in the 11 models (multimodel mean, –79 Pg C $°C^{-1}$), but this varies greatly among models (*3*). Soil carbon turnover rate increases by 2 to 10% $°C^{-1}$ in all models in a positive climate feedback (multimodel mean, 6% $°C^{-1}$). Terrestrial NPP decreases by up to –6% $°C^{-1}$ in seven models (multimodel mean, –3% $°C^{-1}$) and increases by 1 to 2% $°C^{-1}$ in four models. Climate change can enhance NPP (negative feedback) in boreal forests where temperature increases and decrease NPP (positive feedback) in tropical forests where greater evaporative demand dries soil (*35*).

Ecological responses to climate change alter the biogeophysical functioning of forests and also provide climate feedback. These "indirect" carbon cycle feedbacks include changes in stomatal conductance, leaf area index, and species composition. Decreased stomatal conductance with higher atmospheric CO_2 concentration reduces evapotranspiration and reinforces warming (SOM). More extensive tree cover may enhance warming in boreal forests by decreasing surface albedo. Reduced evapotranspiration in a drier climate may initiate a positive climate feedback leading to loss of tropical forest (*20*).

Land-Use Forcing

Although carbon emission from forest clearing has long been studied, only recently has the biogeophysical forcing of climate from land use been recognized. Vast tracts of forestland have been converted to agriculture (Fig. 3D), and climate warming over the industrial era may be smaller than that expected from rising atmospheric CO_2 alone, primarily from increased spring albedo with loss of extratropical forests (*36*).

Carbon emission from land use dampens biogeophysical cooling. The dominant competing signals from historical deforestation are an increase in surface albedo countered by carbon emission to the atmosphere. Biogeophysical cooling may outweigh biogeochemical warming at the global scale (*37*) or may only partially offset warming (*38*). The net effect of these competing processes is small globally but is large in temperate and high northern latitudes where the cooling due to an increase in surface albedo outweighs the warming due to land-use CO_2 emission.

Climate trends over the 21st century, too, should be driven by interactions among CO_2 emission, land use, and forest-atmosphere feedbacks. The biogeophysical land-use forcing of climate may in some regions be of similar magnitude to greenhouse gas climate change. The Intergovernmental Panel on Climate Change (IPCC) Special Report on Emission Scenarios (SRES) A2 narrative storyline has high CO_2 emission (SOM), and climate model simulations of Feddema *et al.* (*39*) produce 2°C warming of planetary temperature over the 21st century in the absence of land cover change. The A2 storyline describes widespread agricultural expansion with most land suitable for agriculture used for farming by 2100 to support a large global population (fig. S1). Forest loss leads to additional warming in Ama-

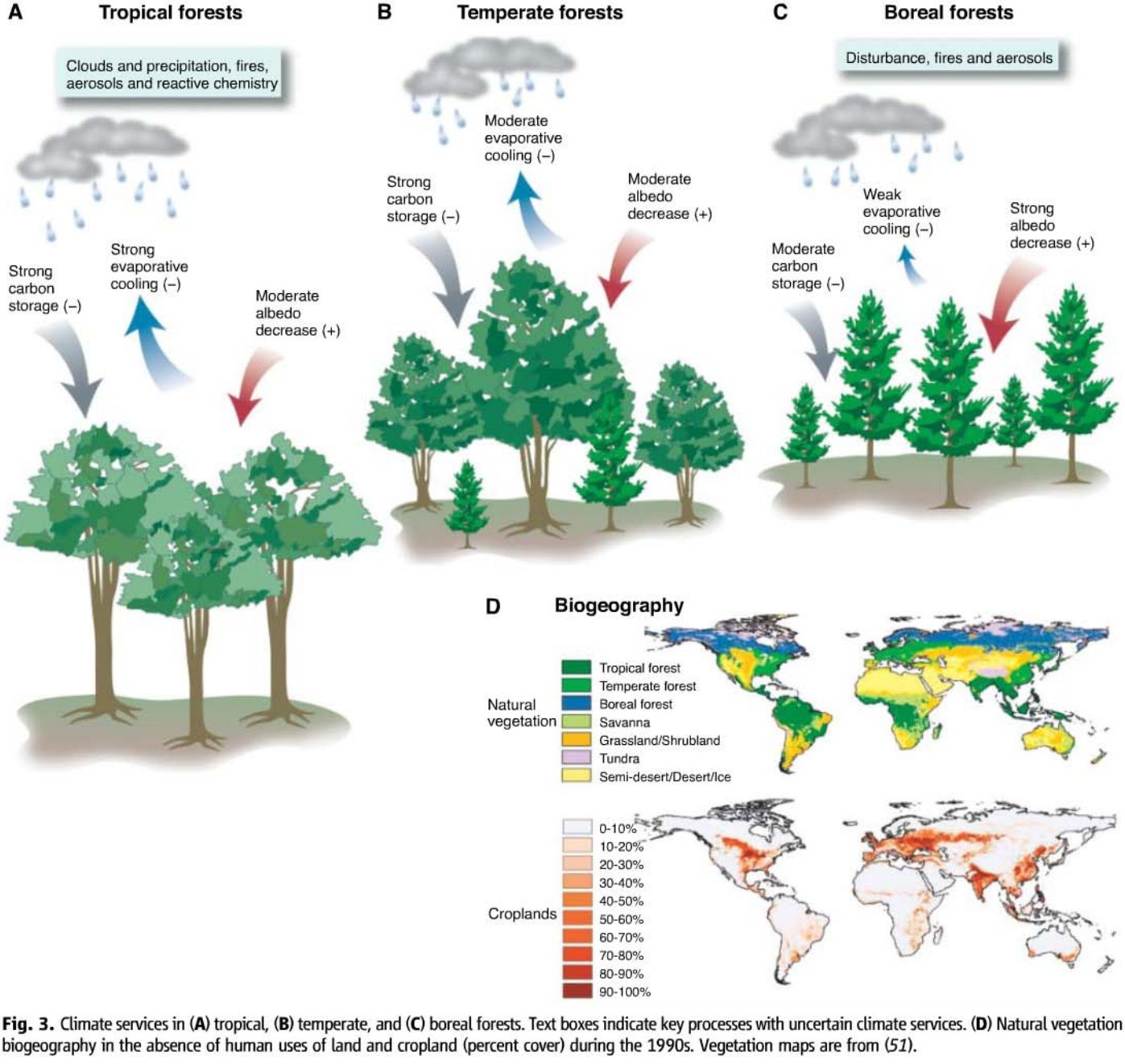

Fig. 3. Climate services in (**A**) tropical, (**B**) temperate, and (**C**) boreal forests. Text boxes indicate key processes with uncertain climate services. (**D**) Natural vegetation biogeography in the absence of human uses of land and cropland (percent cover) during the 1990s. Vegetation maps are from (*51*).

zonia, but cooling that mitigates warming in mid-latitudes (*39*). The B1 narrative storyline is a low greenhouse gas emission scenario. Farm abandonment and reforestation yield loss of farmland by 2100 because of assumed increases in agricultural efficiency and declining population (fig. S1). The model simulates 1°C warming in the absence of land cover change and weaker land-use forcing.

When the carbon cycle is included, the different SRES storylines of fossil fuel emission and land use may yield similar 21st-century climates despite vastly different socioeconomic trajectories (*9*). Widespread expansion of agriculture in A2 leads to biogeophysical cooling. Biogeophysical processes lead to warming in B1, primarily because of temperate forest regrowth. In the A2 and B1 storylines, net carbon loss from deforestation causes biogeochemical warming, greatest in A2 because of extensive deforestation and weaker in B1 because of temperate reforestation and less tropical deforestation. Biogeochemical warming offsets biogeophysical cooling in A2 to provide net global warming. The B1 net warming is similar to A2 because moderate biogeophysical warming from temperate reforestation augments weak biogeochemical warming from tropical deforestation.

Research Needs

Through albedo, evapotranspiration, the carbon cycle, and other processes, forests can amplify or dampen climate change arising from anthropogenic greenhouse gas emission. Negative climate forcing in tropical forests from high rates of carbon accumulation augments strong evaporative cooling (Fig. 3A). The combined carbon cycle and biogeophysical effect of tropical forests may cool global climate, but their resilience to drought, their status as carbon sinks, interactions of fires, aerosols, and reactive gases with climate, and the effects of small-scale deforestation on clouds and precipitation are key unknowns. The climate forcing of boreal forests is less certain (Fig. 3C). Low surface albedo may outweigh carbon sequestration so that boreal forests warm global climate, but the net forcing from fire must also be considered, as well as effects of dis-

turbance and stand age on surface fluxes. The climate benefit of temperate forests is most uncertain (Fig. 3B). Reforestation and afforestation may sequester carbon, but the albedo and evaporative forcings are moderate compared with other forests and the evaporative influence is unclear.

Much of our knowledge of forest influences on climate, and our ability to inform climate change mitigation policy, comes from models. Models of climate and the biosphere are abstractions of complex physical, chemical, and biological processes in the Earth system. Extrapolation of process-level understanding of ecosystem functioning gained from laboratory experiments or site-specific field studies to large-scale climate models remains a daunting challenge. Biosphere models must be better constrained with observational data across a range of scales from in situ experimentation, flux tower measurements of ecosystem functioning, ecological syntheses of long-term ecosystem research, satellite monitoring of vegetation, and atmospheric monitoring of CO_2. Synthesis of flux tower data from a variety of boreal, temperate, and tropical regions in various stages of ecosystem development is essential to understand the functioning of forests across wide gradients of climate, soils, disturbance history, and plant functional types (*40*). Large-scale monitoring of Northern Hemisphere "greening" (*41*) or the response of vegetation to drought (*42*) provide essential tests of model response to perturbations. Global atmospheric CO_2 analyses provide key constraints to biospheric functioning to augment process-level model validation at specific locales (*15*).

Global models of the biosphere-atmosphere system are still in their infancy, and processes not yet included in the models may initiate unforeseen feedbacks. The effect of nitrogen on carbon uptake (*43*), physiological effects of high ozone concentration (*44*), photosynthetic enhancement by diffuse radiation (*45*), and disturbance (*46*) are poorly represented, if at all. Realistic depictions of vegetation dynamics, especially the time scales of vegetation response to disturbance, long a mainstay of forest ecosystem modeling, are barely considered in the current generation of models. Nor are fires, aerosols, and reactive chemistry well represented in the models.

The carbon cycle and its response to multiple interacting drivers of global change is a key aspect of the biospheric forcing of climate. So, too, are human uses of land and the socioeconomic trends and societal responses to a changing climate that drive land use. What are the greatest uncertainties in simulating the carbon cycle of the 21st century? The prevailing paradigm of current models is that CO_2 fertilization drives terrestrial carbon sinks, weakened by global warming (*3*, *32*). This carbon cycle–climate feedback will almost certainly be refined with further studies that incorporate the nitrogen cycle. Accounting for disturbance from wildfires and insect outbreaks further weakens terrestrial carbon sequestration in Canadian forests (*46*). Trajectories of land use driven by socioeconomic needs and policy implementation will also come into play and have competing biogeophysical and biogeochemical impacts on climate (*9*).

As the climate benefits of forests become better understood, land-use policies can be crafted to mitigate climate change (*6*). It has been inferred, for example, that tropical afforestation is likely to "slow down" global warming, whereas temperate afforestation has "little to no" climate benefit and boreal afforestation is "counterproductive" (*8*). These policies must recognize the multitude of forest influences, their competing effects on climate, their different spatial and temporal scales, and their long-term effectiveness and sustainability in a changing climate.

An integrated assessment of forest influences entails an evaluation beyond albedo, evapotranspiration, and carbon to include other greenhouse gases, biogenic aerosols, and reactive gases. The geographic impact of these processes varies, as does their time scale of climate forcing. Greenhouse gases are well mixed in the atmosphere and influence global climate; biogeophysical feedbacks have a regional impact. Biogeophysical processes influence climate more immediately than does the carbon cycle. Slow rates of carbon accumulation in boreal forest may in the short-term be offset by more rapid albedo effects. How forests attenuate or amplify climate change will vary with global warming. Vegetation masking of snow albedo becomes less important in a warmer world with less extensive snow cover. The evaporative cooling of forests declines if droughts become more common. The interrelatedness of climate change science, climate impacts on ecosystems, and climate change mitigation policy requires that these be studied together in an interdisciplinary framework to craft strong science in the service of humankind.

References and Notes

1. R. Hassan, R. Scholes, N. Ash, Eds., *Ecosystems and Human Well-being: Current State and Trends, Volume 1* (Island Press, Washington, DC, 2005).
2. C. L. Sabine *et al.*, in *The Global Carbon Cycle: Integrating Humans, Climate, and the Natural World*, C. B. Field, M. R. Raupach, Eds. (Island Press, Washington, DC, 2004) pp. 17–44.
3. K. L. Denman *et al.*, in *Climate Change 2007: The Physical Science Basis. Contribution of Working Group I to the Fourth Assessment Report of the Intergovernmental Panel on Climate Change*, S. Solomon *et al.*, Eds. (Cambridge Univ. Press, Cambridge, 2007) pp. 499–587.
4. K. Thompson, *Clim. Change* **3**, 47 (1980).
5. A. Fischlin *et al.*, in *Climate Change 2007: Impacts, Adaptation and Vulnerability. Contribution of Working Group II to the Fourth Assessment Report of the Intergovernmental Panel on Climate Change*, M. L. Parry, O. F. Canziani, J. P. Palutikof, P. J. van der Linden, C. E. Hanson, Eds. (Cambridge Univ. Press, Cambridge, 2007) pp. 211–272.
6. G. J. Nabuurs *et al.*, in *Climate Change 2007: Mitigation. Contribution of Working Group III to the Fourth Assessment Report of the Intergovernmental Panel on Climate Change*, B. Metz, O. R. Davidson, P. R. Bosch, R. Dave, L. A. Meyer, Eds. (Cambridge Univ. Press, Cambridge, 2007) pp. 541–584.
7. P. K. Snyder, C. Delire, J. A. Foley, *Clim. Dyn.* **23**, 279 (2004).
8. G. Bala *et al.*, *Proc. Natl. Acad. Sci. U.S.A.* **104**, 6550 (2007).
9. S. Sitch *et al.*, *Global Biogeochem. Cycles* **19**, GB2013 10.1029/2004GB002311 (2005).
10. G. B. Bonan, *Ecological Climatology* (Cambridge Univ. Press, Cambridge, ed. 2, 2008).
11. H. R. da Rocha *et al.*, *Ecol. Appl.* **14**, S22 (2004).
12. C. von Randow *et al.*, *Theor. Appl. Climatol.* **78**, 5 (2004).
13. A. R. Huete *et al.*, *Geophys. Res. Lett.* **33**, L06405 10.1029/2005GL025583 (2006).
14. S. R. Saleska, K. Didan, A. R. Huete, H. R. da Rocha, *Science* **318**, 612 (2007).
15. B. B. Stephens *et al.*, *Science* **316**, 1732 (2007).
16. M. O. Andreae *et al.*, *Science* **303**, 1337 (2004).
17. H. Hashimoto *et al.*, *J. Geophys. Res.* **109**, D23110 10.1029/2004JD004959 (2004).
18. J. T. Randerson *et al.*, *Global Biogeochem. Cycles* **19**, GB2019 10.1029/2004GB002366 (2005).
19. Y. Malhi *et al.*, *Science* **319**, 169 (2008).
20. R. A. Betts *et al.*, *Theor. Appl. Climatol.* **78**, 157 (2004).
21. D. Baldocchi, F. M. Kelliher, T. A. Black, P. Jarvis, *Glob. Change Biol.* **6**, (s1), 69 (2000).
22. K. J. Meissner, A. J. Weaver, H. D. Matthews, P. M. Cox, *Clim. Dyn.* **21**, 515 (2003).
23. R. Gallimore, R. Jacob, J. Kutzbach, *Clim. Dyn.* **25**, 755 (2005).
24. H. Liu, J. T. Randerson, J. Lindfors, F. S. Chapin III, *J. Geophys. Res.* **110**, D13101 10.1029/2004JD005158 (2005).
25. J. T. Randerson *et al.*, *Science* **314**, 1130 (2006).
26. K. W. Oleson, G. B. Bonan, S. Levis, M. Vertenstein, *Clim. Dyn.* **23**, 117 (2004).
27. S. Baidya Roy, G. C. Hurtt, C. P. Weaver, S. W. Pacala, *J. Geophys. Res.* **108**, 4793 10.1029/2003JD003565 (2003).
28. R. B. Jackson *et al.*, *Science* **310**, 1944 (2005).
29. J.-Y. Juang, G. Katul, M. Siqueira, P. Stoy, K. Novick, *Geophys. Res. Lett.* **34**, L21408 10.1029/2007GL031296 (2007).
30. B. F. Zaitchik, A. K. Macalady, L. R. Bonneau, R. B. Smith, *Int. J. Climatol.* **26**, 743 (2006).
31. M. Albani, D. Medvigy, G. C. Hurtt, P. R. Moorcroft, *Glob. Change Biol.* **12**, 2370 (2006).
32. P. Friedlingstein *et al.*, *J. Clim.* **19**, 3337 (2006).
33. J. G. Canadell *et al.*, *Proc. Natl. Acad. Sci. U.S.A.* **104**, 18866 (2007).
34. R. J. Norby *et al.*, *Proc. Natl. Acad. Sci. U.S.A.* **102**, 18052 (2005).
35. I. Y. Fung, S. C. Doney, K. Lindsay, J. John, *Proc. Natl. Acad. Sci. U.S.A.* **102**, 11201 (2005).
36. V. Brovkin *et al.*, *Clim. Dyn.* **26**, 587 (2006).
37. V. Brovkin *et al.*, *Glob. Change Biol.* **10**, 1253 (2004).
38. H. D. Matthews, A. J. Weaver, K. J. Meissner, N. P. Gillett, M. Eby, *Clim. Dyn.* **22**, 461 (2004).
39. J. J. Feddema *et al.*, *Science* **310**, 1674 (2005).
40. M. Reichstein *et al.*, *Geophys. Res. Lett.* **34**, L01402 10.1029/2006GL027880 (2007).
41. S. Piao, P. Friedlingstein, P. Ciais, L. Zhou, A. Chen, *Geophys. Res. Lett.* **33**, L23402 10.1029/2006GL028205 (2006).
42. P. Ciais *et al.*, *Nature* **437**, 529 (2005).
43. F. Magnani *et al.*, *Nature* **447**, 848 (2007).
44. S. Sitch, P. M. Cox, W. J. Collins, C. Huntingford, *Nature* **448**, 791 (2007).
45. L. Gu *et al.*, *Science* **299**, 2035 (2003).
46. W. A. Kurz, G. Stinson, G. J. Rampley, C. C. Dymond, E. T. Neilson, *Proc. Natl. Acad. Sci. U.S.A.* **105**, 1551 (2008).
47. S. Luyssaert *et al.*, *Glob. Change Biol.* **13**, 2509 (2007).
48. Y. Jin *et al.*, *Geophys. Res. Lett.* **29**, 1374 10.1029/2001GL014132 (2002).
49. D. D. Baldocchi, C. A. Vogel, B. Hall, *J. Geophys. Res.* **102**, 28939 (1997).
50. D. D. Baldocchi, L. Xu, *Adv. Water Resour.* **30**, 2113 (2007).
51. J. A. Foley *et al.*, *Science* **309**, 570 (2005).

52. D. Lawrence, S. Levis, K. Oleson, and S. Running provided comments on this manuscript. D. Baldocchi provided data for use in Fig. 1E. The National Center for Atmospheric Research is sponsored by the National Science Foundation.

Supporting Online Material

www.sciencemag.org/cgi/content/full/320/5882/1444/DC1
SOM Text
Fig. S1
Table S1
References

10.1126/science.1155121

PERSPECTIVE

Forests of the Past: A Window to Future Changes

Rémy J. Petit,[1,2*] Feng Sheng Hu,[3] Christopher W. Dick[4,5]

The study of past forest change provides a necessary historical context for evaluating the outcome of human-induced climate change and biological invasions. Retrospective analyses based on fossil and genetic data greatly advance our understanding of tree colonization, adaptation, and extinction in response to past climatic change. For instance, these analyses reveal cryptic refugia near or north of continental ice sheets, leading to reevaluation of postglacial tree migration rates. Species extinctions appear to have occurred primarily during periods of high climatic variability. Transoceanic dispersal and colonization in the tropics were widespread at geological time scales, inconsistent with the idea that tropical forests are particularly resistant to biological invasions.

For Heraclitus, a 6th-century BCE Greek philosopher and naturalist, "change is the only constant in nature." Trees are organisms of exceptional size and longevity, and are symbols of stability and resilience in the living world. Yet, trees are no exception to Heraclitus' rule. Their ranges have been and continue to be extremely dynamic. In some parts of the world, tree species have started to shift their distributions in response to anthropogenic climatic warming (*1*, *2*). Given the long generation time of trees, and possible migrational lags, these shifts foreshadow the more pronounced future changes.

Knowledge of past forest change can inform current predictions and conservation options. Paleo-studies offer abundant evidence for climatic changes and vegetation shifts at various spatial and temporal scales. During the Quaternary period (roughly 1.8 million years ago to the present), glacial-interglacial climatic variations occurred as a result of changes in controlling factors such as Earth's orbital parameters, continental ice sheets, sea-surface temperature, and atmospheric CO_2 concentration. Abrupt climatic events at much shorter time scales have also occurred (*3*), some of which have pronounced magnitudes and rates (e.g., temperature shifts of up to ~10°C within a few decades during the last glacial-interglacial transition in some areas). Networks of fossil pollen and plant macrofossils show that in response to these climatic fluctuations, the biosphere has experienced dramatic changes, with large-scale species' range shifts, population contractions and extinctions, as well as aggregation and disassociation of forest communities. At low latitudes, forests experienced altitudinal shifts and range fragmentation, although many tropical and subtropical tree species we see today persisted in the same region through glacial and interglacial intervals (*4*). At mid-latitudes, forest development after the end of the last glaciation involved species reshuffling, changes in relative abundances, and local and permanent extinctions (*5*, *6*). Forests in high-latitude regions became established within the Holocene (past 11,600 years) as a result of population invasions from southern glacial refugia into previously ice-covered terrains and local expansions of small tree populations that survived the Last Glacial Maximum (~20,000 years ago) in "cryptic refugia" (*7*, *8*).

A key recent development in studies of past vegetation is the fusion of genetic and fossil data. Fossil records are indispensable for vegetation reconstruction and can help constrain inferences of historic events from genetic data. But fossil records rarely offer any information on population-level processes (e.g., founder events, migration of specific lineages). Geographic patterns of DNA polymorphisms are traces, albeit often somewhat fuzzy, of such processes. When fossil and genetic data are combined, much information can be acquired about the whereabouts of small populations during the last glaciation and the trajectories of postglacial population spread (Fig. 1). Recent studies that applied this integrative approach have offered new insights. For example, some temperate and boreal trees apparently survived the Last Glacial Maximum in periglacial

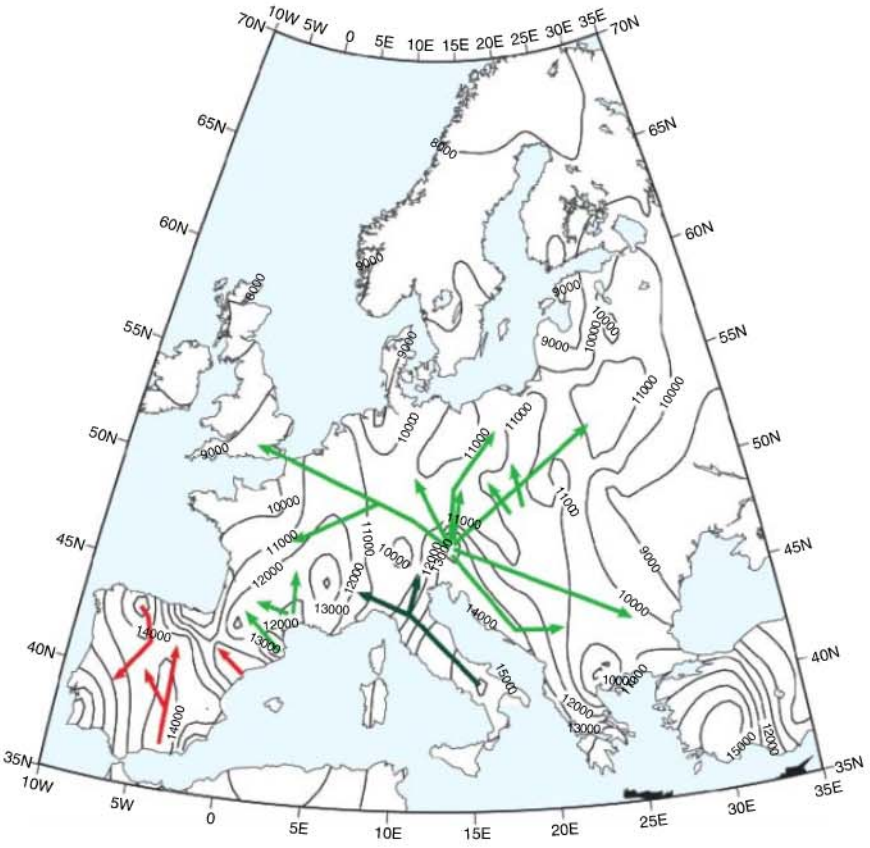

Fig. 1. Migration timing (isochrone curves) and routes (arrows) of *Pinus* in Europe inferred from paleobotanical and modern genetic data. The red, light green, and dark green arrows correspond to the migration routes for different maternal lineages of *Pinus sylvestris* (*8*).

[1]INRA, UMR1202 Biodiversity, Genes and Communities, 69 Route d'Arcachon, F-33612 Cestas, France. [2]University of Bordeaux I, UMR1202 Biodiversity, Genes and Communities, 69 Route d'Arcachon, F-33612 Cestas, France. [3]Departments of Plant Biology and Geology, and Program in Ecology, Evolution, and Conservation Biology, University of Illinois, Urbana, IL 61801, USA. [4]Department of Ecology and Evolutionary Biology and Herbarium, University of Michigan, 830 North University Avenue, Ann Arbor, MI 48103, USA. [5]Smithsonian Tropical Research Institute, Post Office Box 0843-03092, Balboa, Ancón, Republic of Panama.

*To whom correspondence should be addressed. E-mail: petit@pierroton.inra.fr

Fig. 2. Sparsely distributed spruce considered to be analogous to glacial-refuge populations. DNA and fossil pollen data suggest that such small populations survived the Last Glacial Maximum in Alaska and that they were important for boreal-forest development after the end of the last glaciation (*7*).

CREDIT: PATRICK WALSH, TOGIAK NATIONAL WILDLIFE REFUGE, ALASKA

environments probably tens of kilometers from ice sheets (*8*, *9*) and even in ice-free areas north of ice sheets (*7*). Thus, it appears that small populations of trees can endure extreme climatic conditions for tens of thousands of years (Fig. 2).

However, these studies also imply that the capacity of trees to keep up with the rate of future warming is probably more limited than suggested by previous estimates from fossil data. Extremely fast tree migrations during the early Holocene were inferred from the fossil records of certain tree species, on the assumption that northern refugia did not exist during the Last Glacial Maximum (*5*, *10*). On the basis of more recent fossil and DNA studies, it appears that the actual rates may be an order of magnitude lower, e.g., <100 m/year for two North American deciduous tree species (*11*). These estimates are far below what would be necessary for species migration to track future climatic warming (3000 to 5000 m/year), raising interest in the possibilities of "assisted migration"—the translocation of populations to areas where future climate might be favorable.

The role of adaptive responses to climatic change has rarely been considered in interpreting Quaternary paleoecological records, because of the perception that evolution occurs more slowly than climatic change (*12*). At the DNA-sequence level, evolution of trees is indeed exceptionally slow, in line with their exceptional longevity, but their high genetic diversity and large population sizes do allow rapid adaptive responses, within one or a few generations (*13*). There is therefore a growing recognition that short-term evolutionary responses of trees should be accounted for in models of forest dynamics (*12*).

Although local evolutionary responses to climate change are likely to have occurred with high frequency, there is no evidence for change in the absolute climate tolerances of species (*14*). Thus, future extinctions of tree species in response to climate change are probable, especially if their geographic distribution or climatic range is already highly restricted. Here again, the retrospective approach could be illuminating. Europe lost at least 89 tree genera during the climatic transitions of the Late Tertiary to the Quaternary (*15*). A key question is whether past extinctions took place during glacial or interglacial periods. If extinctions had taken place mostly during interglacial periods, this would support pessimistic views of the consequences of future global warming on population and species survival. However, extant Asian and American congeners of extinct European tree species are less cold-tolerant than currently widespread European trees (*16*). This suggests that most extinction events took place during glacial rather than interglacial periods. In contrast, a 320,000-year history of vegetation and climate in Hungary showed that species extinctions clustered near times of high climate variability (*17*). This interpretation is consistent with the case of a now-extinct North American spruce, *Picea critchfieldii*, which was abundant during the Last Glacial Maximum but vanished during the last deglaciation, at a time of rapid climate change (*18*).

The retrospective approach also provides a context for understanding species invasions resulting from human activities. Invasive trees (i.e., "tree weeds," such as pines escaped from plantations in the Southern Hemisphere) have caused damages to ecosystems worldwide, especially (but not only) in originally treeless areas (*19*). In contrast to the assumption that tropical forests are particularly resistant to invasions, invasions turn out to be frequent in these regions over geological times scales as a result of "sweepstakes dispersal," the dispersal of species across wide physical barriers such as oceans (*20*). For instance, sweepstake dispersal of the wind-dispersed rainforest kapok tree, *Ceiba pentandra*, was inferred on the basis of DNA-sequence phylogeography and molecular clock methods: African populations established through oceanic dispersal from Neotropical sources at least 13,000 years before the present (*21*). Many other tropical tree taxa are shared across the Atlantic. Although these forest similarities were previously attributed to Gondwana vicariance, molecular phylogenetic studies point to a predominant role of oceanic dispersal in establishing this range disjunction. In an Amazon forest inventory plot in Ecuador, at least 21% of the tree species (232 out of 1104) were derived from clades that had arrived in South America via long-distance dispersal (*20*). Thus, natural invasions of trees explain some of the similarity between tropical forests across continents, contradicting the idea that diversity could provide sufficient protection against invasions. Evaluating the frequency and consequences of sweepstakes dispersal into different communities could help predict the consequences of modern invasions into more or less "naïve" floras characterized by different levels of endemism.

Many lessons can be drawn from the study of past forest change, and our ability to acquire such knowledge is improving thanks in particular to the interactions between paleoecologists and geneticists. The integration of paleoclimate data, fossil records, and genealogical analyses within a hypothesis-testing modeling framework represents a particularly fruitful direction (*8*, *22*). However, novel climates will appear, leading to "no-analog" communities (*23*), which may limit the retrospective approach discussed here. Indeed, while no-analog communities are well documented in the paleorecord (*4*), they cannot offer a direct guide to what we may have in stock for the future because the combinations of climate and other drivers (e.g., human land use) differ drastically between the past and the future. Nonetheless, these unique paleo-communities, when coupled with paleoclimate information, provide a way to examine climate-species relationships outside the modern realm and should help validate ecological models for simulating future changes.

References and Notes

1. A. S. Jump, J. M. Hunt, J. Peñuelas, *Glob. Change Biol.* **12**, 2163 (2006).
2. A. H. Lloyd, *Ecology* **86**, 1687 (2005).
3. R. B. Alley *et al.*, *Science* **299**, 2005 (2003).
4. P. A. Colinvaux, P. E. De Oliveira, J. E. Moreno, M. C. Miller, M. B. Bush, *Science* **274**, 85 (1996).
5. B. Huntley, H. J. B. Birks, *An Atlas of Past and Present Pollen Maps for Europe: 0–13000 B.P.* (Cambridge Univ. Press, Cambridge, 1983).
6. D. Magri *et al.*, *New Phytol.* **171**, 199 (2006).
7. L. L. Anderson, F. S. Hu, D. M. Nelson, R. J. Petit, K. N. Paige, *Proc. Natl. Acad. Sci. U.S.A.* **103**, 12447 (2006).
8. R. Cheddadi *et al.*, *Glob. Ecol. Biogeogr.* **15**, 271 (2006).
9. L. D. Shepherd, L. R. Perrie, P. J. Brownsey, *Mol. Ecol.* **16**, 4536 (2007).

10. J. C. Ritchie, G. M. MacDonald, *J. Biogeogr.* **13**, 527 (1986).
11. J. S. McLachlan, J. S. Clark, P. S. Manos, *Ecology* **86**, 2088 (2005).
12. M. B. Davis, R. G. Shaw, J. R. Etterson, *Ecology* **86**, 1704 (2005).
13. R. J. Petit, A. Hampe, *Annu. Rev. Ecol. Evol. Syst.* **37**, 187 (2006).
14. C. Parmesan, *Annu. Rev. Ecol. Evol. Syst.* **37**, 637 (2006).
15. R. E. Latham, R. E. Ricklefs, *Oikos* **67**, 325 (1993).
16. J. C. Svenning, *Ecol. Lett.* **6**, 646 (2003).
17. K. J. Willis, A. Kleczkowski, M. New, R. J. Whittaker, *Ecol. Lett.* **10**, 673 (2007).
18. S. T. Jackson, C. Y. Weng, *Proc. Natl. Acad. Sci. U.S.A.* **96**, 13847 (1999).
19. R. J. Petit, R. Bialozyt, P.Garnier-Géré, A. Hampe, *For. Ecol. Manage.* **197**, 117 (2004).
20. R. T. Pennington, C. W. Dick, *Philos. Trans. R. Soc. Lond. B Biol. Sci.* **359**, 1611 (2004).
21. C. W. Dick, E. Bermingham, M. R. Lemes, R. Gribel, *Mol. Ecol.* **16**, 3039 (2007).
22. B. C. Carstens, C. L. Richards, *Evol. Int. J. Org. Evol.* **61**, 1439 (2007).
23. J. W. Williams, S. T. Jackson, *Front. Ecol. Environ* **5**, 475 (2007).
24. We thank M. Chipman and B. Clegg for constructive comments. Support for this research came from the Franco-American Fulbright Commission (F.S.H.), NSF grants (F.S.H. and C.W.D.), the European Union EVOLTREE Network of Excellence (R.J.P.), the Aquitaine Regional Government of France (F.S.H. and R.J.P.), and the Center for Tropical Forest Sciences (C.W.D.). We thank R. Cheddadi for providing Fig. 1.

10.1126/science.1155457

PERSPECTIVE

Predictive Models of Forest Dynamics

Drew Purves[1] and Stephen Pacala[2]

Dynamic global vegetation models (DGVMs) have shown that forest dynamics could dramatically alter the response of the global climate system to increased atmospheric carbon dioxide over the next century. But there is little agreement between different DGVMs, making forest dynamics one of the greatest sources of uncertainty in predicting future climate. DGVM predictions could be strengthened by integrating the ecological realities of biodiversity and height-structured competition for light, facilitated by recent advances in the mathematics of forest modeling, ecological understanding of diverse forest communities, and the availability of forest inventory data.

There are approximately a trillion canopy trees on Earth (*1*) from around 100,000 species (*2*). The trees store approximately as much carbon as is currently in the atmosphere, and forest ecosystems harbor two-thirds of terrestrial biodiversity (*3*). The challenge of predictive forest modeling is to forecast how this collection of trees will develop in the future, in response to the many perturbations to which it is being subjected, including deforestation, logging, pollution, nitrogen deposition, the loss of pollinating and seed-dispersing animals, and the effects of increased atmospheric CO_2, both direct (the job of a leaf is to convert CO_2 into plant material) and indirect (altered climate).

The most exciting recent advance in forest modeling has been the appearance of dynamic global vegetation models (DGVMs), which simulate the distribution, physiology, and biogeochemistry of forests and other vegetation at global scales, under present, historic, or simulated future climates (*4*). DGVMs have shown that future changes in global forest carbon storage could greatly affect the response of Earth's climate system to anthropogenic CO_2 emissions over the next century (*5*). However, because DGVMs were developed recently, with limited information, their predictions are currently highly uncertain (Fig. 1), making vegetation dynamics one of the largest sources of uncertainty in Earth system models. Reducing this uncertainty requires work on several fronts. For example, physiological parameters need to be better constrained with data (*6*), and we need better models of disturbances, including fire (*7*) and land-use change (*8*). But more fundamental improvements could be achieved by incorporating the ecological realities of biodiversity and competition for light. A recent explosion in forest inventory data might make this possible.

The only reason to build a trunk—to become a tree—is to overtop your neighbors and capture light before they do. This game-theoretic competition for resources is responsible for the enormous amounts of carbon stored in living trees and in undecomposed organic matter and fossil fuels, most of which began as wood. Foresters and forest ecologists have developed individual-based, height-structured models that can accurately predict productivity (*9*) and species composition (*10*). At every turn, these have revealed nonlinearities in forest dynamics caused by competition for light. For example, increased growth leads to increased overtopping, which increases mortality, which increases forest carbon loss; with the functions at each stage being nonlinear. In contrast, current DGVMs reduce whole forested regions to the total biomass in compartments (such as leaves, roots, and trunks), with simple phenomenological rules for how the carbon generated from photosynthesis is allocated to, and lost from, these compartments. Moreover, competition among species [or at least among plant functional types (PFTs)], which needs to be represented to predict biome boundaries, follows rules with weak empirical support that differ among models (*11*).

Therefore, DGVMs could be substantially improved by basing them on the height-structured models developed by foresters and forest ecologists. But because these models are individual-based, this would require simulating every tree on Earth, which would be immensely computationally demanding. A more efficient approach would be to derive so-called macroscopic equations to scale correctly from the parameters governing individual trees to the dynamics of forested regions, in the same way that the Navier Stokes equations scale correctly from molecular motion to fluid dynamics. Recent progress implies that macroscopic equations will soon form the basis of DGVMs. Moorcroft *et al.* (*12*) introduced a demographic method to scale up individual-based forest models, which has since been used to provide tractable macroscopic equations to scale from trees to stands and to scale from stands to forests (*13*).

Macroscopic equations will allow global simulations of individual-based forest models, but here arises the problem of biodiversity. The (approximately) 100,000 tree species vary hugely in properties that drive the carbon cycle, such as growth, mortality, decomposition of dead wood, and their dependency on climate. Because of a lack of appropriate data or theory, current DGVMs reduce biodiversity to a small number of PFTs, within which all parameters are constant. The PFTs represent simple morphological and biogeographical aggregations, such as broadleaf versus needleaf or tropical versus temperate. But these aggregations are unlikely to be optimal for capturing the effects of biodiversity on dynamics, because the among-species differences within PFTs dwarf the average difference between them. For example, the PFT temperate deciduous broadleaf contains the northernmost tree species (Arctic birch) along with subtropical oaks; and evergreen needleleaf contains cold-adapted spruces and firs and heat-adapted pines. Even within a forest composed of a single PFT, species parameters typically vary by an order of magnitude (*14*). Moreover, the mix of species, and hence parameters, found at a given location is strongly correlated with climate (*15*), with obvious implications for modeling the climate dependency of forest dynamics. By ignoring most biodiversity, DGVMs could be overestimating the strength of some climate responses because they fail to account for the fact that deleterious effects can be mitigated by increases in those species best

[1]Computational Ecology and Environmental Science Group, Microsoft Research, Cambridge, UK. [2]Department of Ecology and Evolutionary Biology, Princeton University, Princeton, NJ, USA.

adapted to the new conditions (*16*). But they could be underestimating other responses; for example, increased temperature could both increase the growth of extant trees and select for warm-adapted species, which have higher growth rates (*17*). Therefore, there is a need for a substantial increase in the amount of biodiversity represented in DGVMs.

However, adding biodiversity and height-structured competition into DGVMs would increase the complexity of models that are already severely underconstrained. DGVMs contain large numbers of parameters, which are hand-selected from literature values in order to qualitatively match model predictions to sparse observations of ecosystem fluxes (such as productivity) and states (such as biome boundaries). Physiological parameters are beginning to be objectively estimated with measurements from flask networks and eddy-covariance flux towers (*6*). But these data contain almost no information about the long-term dynamics of individuals, populations, or communities. Luckily, these dynamics are recorded in a kind of data that has become much more available recently. Forest inventories consist of sample plots within which trees are measured regularly (about every 5 to 10 years). The measurements are low-tech: for example, stem diameter, species, alive or dead. But the sample sizes are large, running into millions of trees in some cases (*18*, *19*). The few published biogeochemical analyses of forest inventory data have yielded results with major implications for our understanding of the global carbon cycle (*18*–*20*).

To constrain DGVMs, the tree-level measurements in forest inventories could simply be summed to provide long-term average carbon dynamics to compare with DGVM predictions. But this approach discards most of the information in the data. In contrast, if DGVMs were based around models of individual trees, the individual growth and mortality records could be used to directly estimate key tree-level parameters; although few if any inventories contain sufficient information to estimate all parameters, because they lack measurements of (for example) light, belowground carbon, nutrients, and seed dispersal. In the low-diversity boreal and temperate zones, the abundance of inventory data might be sufficient to estimate parameters for every dominant tree species. In addition to improving predictions for the carbon cycle, this might allow realistic predictions for particular species; for example, climate-induced shifts in species ranges, which to date have been predicted using only correlative methods (*21*).

In high-diversity forests, species-specific parameterization is not feasible. Instead, species need to be aggregated to reduce the number of parameters to be estimated. And although any such aggregation must result in a loss of biological information, evidence suggests that, with the correct aggregation, this loss could be minimal. This is because wherever parameters have been estimated for different tree species, they have been found to be subject to life history tradeoffs: strategic axes appearing as among-species correlations in parameters (*22*). Moreover, similar tradeoffs appear to be structuring different forest communities, such as the shade-tolerance spectrum from fast-growing, short-lived pioneers to slow-growing, long-lived species (*22*). These tradeoffs imply that most of the effects of biodiversity would be retained in models that reduced the state of a forest to the distribution of individual trees along tradeoff axes, regardless of taxonomic identity. Such models could capture the effects of biodiversity on select aspects of forest function (such as carbon dynamics), either by defining a new set of PFTs spread optimally along the axes or by treating the distribution of species as a continuum. Either approach would require fewer data than species-specific parameterization (*14*), and the continuous approach extends naturally to include parameter variation within species. These approaches correspond closely to the discrete and continuous lumping techniques used to model heterogeneous systems of chemical reactions (*23*).

All of the above add up to a major scientific challenge. We have proven individual-based, height-structured models which, using new scaling methodologies, could be implemented at global scales. We are beginning to understand the tradeoff structure of forest communities sufficiently to capture the effects of biodiversity on forest function. And for the first time, we have millions of observations of individual trees with which to constrain the structure and parameters of global models. If these pieces could be put together properly, the result could be a new generation of ecologically realistic, better-constrained DGVMs. A benchmark of success for this endeavor might be that forest dynamics are no longer one of the major sources of uncertainty in predicting the future of Earth's climate.

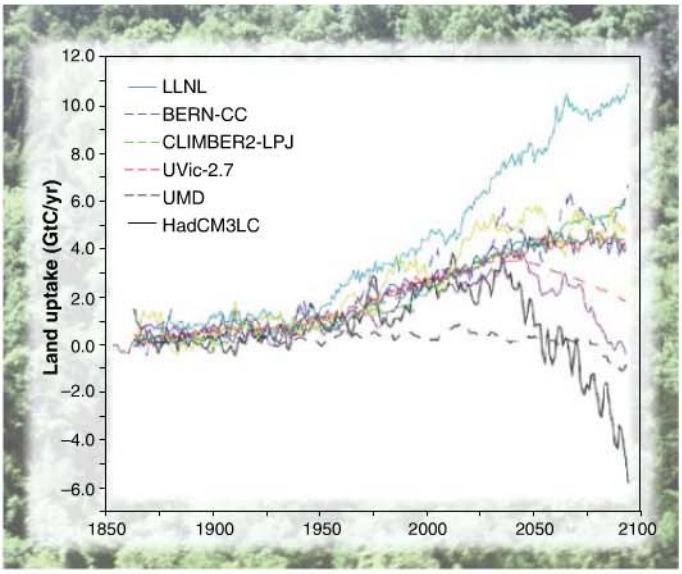

Fig. 1. DGVMs have shown that the terrestrial biosphere could be crucial in determining the future of Earth's climate. But this figure [from (*5*)] shows how divergent the predictions of DGVMs currently are. For comparison, current anthropogenic CO_2 emissions are 7.6 ± 0.6 Gt of carbon/year. True DGVMs, with a responsive global distribution of PFTs, are labeled (*5*). The remainder have a dynamic carbon cycle but a fixed distribution of PFTs. Some of the variation in Fig. 1 results from different climate models, but a large spread was also seen when different DGVMs were run uncoupled from global climate models under a common, fixed climate trajectory (*11*). LLNL, Lawrence Livermore National Laboratory climate model; BERN-CC, Bern carbon-cycle climate model; CLIMBER2-LPJ, Climate-Biosphere model, coupled to the Lund-Potsdam-Jena DGVM; UVic-2.7, University of Victoria Earth system climate model, version 2.7; UMD, University of Maryland coupled carbon-climate model; HadCM3LC, Hadley Centre coupled climate-carbon cycle model.

References and Notes

1. There are about 3 billion hectares of forest at 1000 canopy trees per hectare.
2. S. Oldfield, C. Lusty, A. MacKinven, *The World List of Threatened Trees* (World Conservation Press, Cambridge, 1998).
3. Millennium Ecosystem Assessment, *Ecosystems and Human Well-Being: Biodiversity Synthesis* (World Resources Institute, Washington, DC, 2005).
4. P. R. Moorcroft, *Proc. R. Soc. London Ser. B* **270**, 1215 (2003).
5. P. Friedlingstein *et al.*, *J. Clim.* **19**, 3337 (2006).
6. M. R. Raupach *et al.*, *Global Change Biol.* **11**, 378 (2005).
7. W. J. Bond, F. I. Woodward, G. F. Midgley, *New Phytol.* **165**, 525 (2005).
8. G. C. Hurtt *et al.*, *Global Change Biol.* **12**, 1208 (2006).
9. J. Landsberg, *Can. J. Forest Res.* **33**, 385 (2003).
10. S. W. Pacala *et al.*, *Ecol. Monogr.* **66**, 1 (1996).
11. W. Cramer *et al.*, *Global Change Biol.* **7**, 357 (2001).
12. P. R. Moorcroft, G. C. Hurtt, S. W. Pacala, *Ecol. Monogr.* **71**, 557 (2001).
13. T. Kohyama, *Ecol. Res.* **20**, 305 (2005).
14. R. Condit *et al.*, *Science* **313**, 98 (2006).
15. T. R. Baker *et al.*, *Global Change Biol.* **10**, 545 (2004).
16. D. Tilman, P. B. Reich, J. M. H. Knops, *Nature* **441**, 629 (2006).
17. C. Loehle, *J. Biogeogr.* **25**, 735 (1998).
18. J. P. Caspersen *et al.*, *Science* **290**, 1148 (2000).
19. T. R. Baker *et al.*, *Philos. Trans. R. Soc. London Ser. B* **359**, 353 (2004).
20. H. C. Keeling, O. L. Phillips, *Global Ecol. Biogeogr.* **16**, 618 (2007).
21. A. J. Davis, J. L. Jenkinson, B. Lawton, B. Shorrocks, S. Wood, *Nature* **391**, 783 (1998).
22. B. Gilbert, S. J. Wright, H. C. Muller-Landau, K. Kitajima, A. Hernandez, *Ecology* **87**, 1281 (2006).
23. M. S. Okino, M. L. Mavrovouniotis, *Chem. Rev.* **98**, 391 (1998).

24. We thank A. Brändle, D. Coomes, S. Emmott, P. Friedlingstein, A. Heil, M. Smith, and R. Williams for useful discussion.

10.1126/science.1155359

PERSPECTIVE

Reducing Greenhouse Gas Emissions from Deforestation and Forest Degradation: Global Land-Use Implications

Lera Miles[1] and Valerie Kapos[1,2]

Recent climate talks in Bali have made progress toward action on deforestation and forest degradation in developing countries, within the anticipated post-Kyoto emissions reduction agreements. As a result of such action, many forests will be better protected, but some land-use change will be displaced to other locations. The demonstration phase launched at Bali offers an opportunity to examine potential outcomes for biodiversity and ecosystem services. Research will be needed into selection of priority areas for reducing emissions from deforestation and forest degradation to deliver multiple benefits, on-the-ground methods to best ensure these benefits, and minimization of displaced land-use change into nontarget countries and ecosystems, including through revised conservation investments.

Tropical deforestation makes a major contribution to emissions of greenhouse gases, especially if the additional emissions from subsequent land use are counted (*1*). The United Nations Framework Convention on Climate Change (UNFCCC) is considering the introduction of a financial mechanism to reduce emissions from deforestation and forest degradation (REDD) in developing countries. Many environmentalists have welcomed this initiative because it may direct substantial new resources to tackling this issue (*2*–*5*). A REDD mechanism would probably credit entire nations, rather than individual projects, for their achievements in reducing deforestation. However, there is ongoing debate and hence much uncertainty about the form of the mechanism, including issues such as the deforestation baseline to be used, the role of developing countries that have a low recent rate of deforestation, and the protocols for measurement and validation of emissions reductions. The UNFCCC's Conference of Parties (CoP) in December 2007 established indicative guidance for a demonstration (pilot) phase in the period to 2012. This focuses on emissions measurement and explicitly includes forest degradation, resolving one hotly debated issue. The form of any final mechanism will affect the area and location of forests encompassed and thus the scope for cobenefits (such as biodiversity conservation, livelihoods, and watershed protection) to result. It is widely anticipated that negotiations for the next emissions reduction agreement will be completed at the fifteenth CoP in December 2009. If agreement is reached, then a major new driver for forest conservation may be born.

[1]United Nations Environmental Programme (UNEP) World Conservation Monitoring Centre (WCMC), 219 Huntingdon Road, Cambridge CB3 0DL, UK. [2]Conservation Science Group, Department of Zoology, University of Cambridge, Downing Street, Cambridge CB2 3EJ, UK. E-mail: lera.miles@unep-wcmc.org (L.M.); val.kapos@unep-wcmc.org (V.K.)

There is some controversy over how REDD should be funded. Some of the national parties to the UNFCCC wish to see the issue tackled through a traditional grant funding mechanism. Others, led by the Coalition of Rainforest Nations, seek an eventual market-based mechanism, on the basis that carbon is one of the more easily marketable ecosystem services (*4*, *6*, *7*). This may generate more funds over a longer time scale. A trading mechanism would allow developing countries to sell carbon credits on the basis of successful reductions in emissions from deforestation and forest degradation, to help developed countries achieve stringent emissions targets. Such credits would probably relate to national-scale emissions rather than being attached to individual sites, although discussions continue on the precise details.

Any such mechanism would generate significant additional funding to reduce deforestation rates in developing countries. One estimate, based on a relatively low carbon price of U.S. $10 per ton and an estimate of individual countries' ability to slow deforestation, suggests a potential market of U.S. $1.2 billion a year (*2*); a more recent estimate suggests that U.S. $10 billion may be a realistic figure (*8*). These are large sums in comparison with current investment in forest protection. For example, World Bank funding directed to forest biodiversity conservation and related activities in 2002 totaled U.S. $257 million (*9*). In the mid-1990s, total protected area expenditure in the developing world was estimated at U.S. $695 million annually; not exclusively invested in forests (*10*). In contrast, forestry exports from the developing world were worth over U.S. $39 billion in 2006 (*11*). By generating an income of the same order of magnitude, REDD could provide strong incentives for forest conservation.

These resources mean that the scale of intervention being discussed under the UNFCCC is truly huge, but few decision-makers are aware of the full breadth of its implications. It was initially assumed by many that the effects of REDD on forest-related livelihoods and conservation would only be positive, and it is certainly true that many species, ecosystems, and ecosystem services will benefit. However, it is unlikely that an international mechanism under UNFCCC will explicitly support forest ecosystem services other than carbon storage, and its implementation may generate pressures that adversely affect other ecosystems. It is crucial that decision-makers recognize and plan for potential risks as well as benefits from the resulting effects on land use.

REDD is unlikely to benefit all forests equally. For REDD to make a successful contribution to combating climate change, countries implementing it will have to target threatened forests with a total high volume of carbon in their biomass and soils (*12*, *13*). Although individual sites would not be "marketed" within most proposed REDD mechanisms, countries will still be implementing REDD actions at a site scale. Priority areas for tackling deforestation to reduce emissions will not always reflect other forest values (e.g., conservation, livelihoods support, or delivery of fresh water). Some sites may be less valuable from a carbon perspective but of high priority for other reasons. The need for additional resources to prevent deforestation at such sites will vary depending on the carbon price, the carbon content of the ecosystem, and the cost of avoiding deforestation (Fig. 1). Where the combination of the first two factors outweighs the latter, resources from REDD should be sufficient to enable forest retention. In some parts of the world, estimates of opportunity cost for REDD are very low. Lower costs and/or higher carbon prices could combine to protect more forests, including those with lower carbon content. Conversely, where the cost of action is high, a large amount of additional funding would be required for the forest to be protected.

The limited funds available for conservation will need to be carefully targeted in this context. To conserve the diversity of ecosystems and their related species and services, it may be more efficient to focus conservation funds on nonforest ecosystems and low-carbon forests rather than on forests covered by the new mechanism (Fig. 2). This would require revision of organizational and national investment strategies. The delay between planning and action means that these issues should be considered long before any mechanism comes into effect.

One obvious risk associated with REDD is the displacement of pressures, resulting from continuing demand for food, timber, and increasingly biofuels, to ecosystems perceived to contain low carbon levels. The least-productive forest ecosystems may become the most threatened simply because they are the only remaining accessible source of land and forest products. Other areas experiencing increased pressure could include nonforest ecosystems such as savannas or wetlands and forests in tropical countries not participating in REDD (Fig. 2). The demand for timber from temperate and boreal forests may also increase.

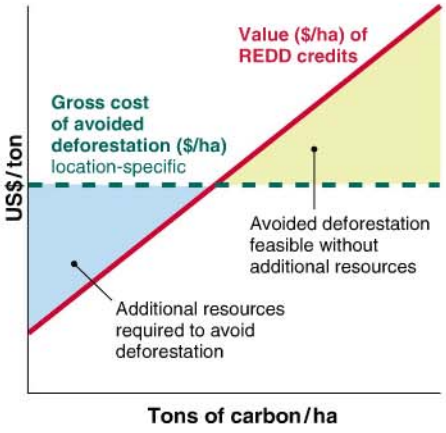

Fig. 1. Under any REDD scheme, the income generated will depend upon the total carbon stocks retained (solid line). Although the cost of avoiding deforestation (dotted line) will vary with location, it is not necessarily related to carbon stocks. Forests in the blue area of the chart contain insufficient carbon to enable avoided deforestation based on REDD funds alone. The need for additional resources to tackle deforestation within a national REDD scheme will vary depending on the carbon price, the carbon content of the ecosystem, and the cost of avoiding deforestation. As the cost of REDD and the carbon price vary, the ratio between the two shaded areas will change.

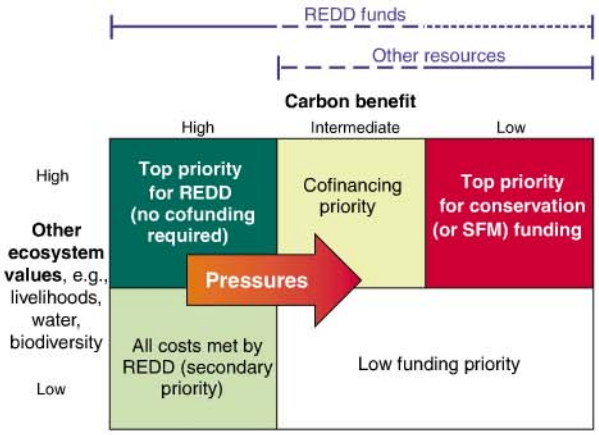

Fig. 2. Biodiversity value and carbon value are distributed differently among tropical ecosystems. Therefore funding from REDD would protect only some biodiversity values and could increase pressures on other ecosystems. Funds for other purposes such as sustainable forest management (SFM) and conservation will need to be targeted to fill the gap.

Another risk is that REDD implementation may be imperfect. Having planned for carbon savings and cobenefits from reduced deforestation, it is necessary to ensure that these are delivered. Considerable effort has been devoted to identifying the factors that influence the success of formally protected areas in limiting deforestation and in supporting and improving livelihoods, but it is often difficult to draw firm conclusions [e.g., (*14*, *15*)]. Although protected areas are typically successful in reducing deforestation, other approaches, including sustainable forest management, will sometimes be more effective in delivering a full range of benefits. Management strategies need to be designed to address local needs and deforestation drivers.

To maximize the benefits of REDD and reduce any risks, it is important to prioritize investment, both among and within countries. Various global conservation priorities have already been identified, each favoring different aspects of biodiversity (*16*). A simple approach would be to identify areas of high value for carbon and for biodiversity at either scale. However, it is also essential that deforestation pressure and the cost of preventative action are taken into account, because the primary motivation is to reduce annual greenhouse gas emissions from this sector. Multicriteria analysis is therefore required, incorporating the degree of pressure and cost as well as the forest values (*17*). Some initial analysis using a national-scale biodiversity index has been undertaken (*18*), but data specific to forest biodiversity would yield more relevant results.

A more comprehensive analysis to produce an optimized allocation of REDD and conservation funds within or even among tropical forest countries is technically feasible. Such analysis would allow the placement of each land unit within a framework like that shown in Fig. 2. Depending on the carbon price and the baseline rate of deforestation, this would help to identify those areas naturally covered by the mechanism, those requiring additional resources if they are to benefit from the mechanism, and the "losers," sites that are most at risk of loss or degradation as the result of pressures displaced by the mechanism. These may become new priorities for conservation and sustainable forest management.

It is crucial that feasibility studies and efforts to ready tropical forest countries for REDD take account of the context (resources and pressures) for biodiversity conservation and other ecosystem values. Several internationally and bilaterally funded demonstration programs are now in development. Methods for assessing their effectiveness, including the degree of displacement (leakage) of land-use change within and between countries, are urgently needed. It is vital to develop robust monitoring and reporting methods for quantifying cobenefits and assessing the impacts on them of changes in forest management and of any leakage into nontarget ecosystems. These data would help identify REDD methods that were most successful in delivering cobenefits.

There is a further need to test the agreed emissions reporting guidelines. Under current Intergovernmental Panel on Climate Change (IPCC) guidance, parties do not need to report emissions from forest areas designated as undisturbed (*13*). This leads to a risk of unrecorded anthropogenic carbon losses, such as those resulting from illegal logging or land clearance. The guidance also offers default values for accounting of soil carbon to 30 cm depth, which will certainly underestimate the effects of clearing tropical swamp forests, where peat depth can reach 20 m (*19*), and losses from drainage and fire can have substantial impacts on carbon storage.

If a REDD mechanism comes into operation, a shift in funding policies may be indicated to ensure that conservation investment is spread over the range of ecosystems not covered by REDD funding. Although many of these issues have been raised within the UNFCCC-mediated discussions, their implications for conservation investment merit attention in the world outside these carbon-focused negotiations.

References and Notes

1. N. Ramankutty *et al.*, *Glob. Change Biol.* **13**, 51 (2007).
2. J. O. Niles, S. Brown, J. Pretty, A. S. Ball, J. Fay, *Philos. Trans. R. Soc. London Ser. A* **360**, 1621 (2002).
3. L. Aukland, P. Moura-Costa, S. Brown, *Clim. Policy* **3**, 123 (2003).
4. M. Santilli *et al.*, *Clim. Change* **71**, 267 (2005).
5. R. E. Gullison *et al.*, *Science* **316**, 985 (2007).
6. W. F. Laurance, *Biotropica* **39**, 20 (2007).
7. D. Mollicone *et al.*, *Clim. Change* **83**, 477 (2007).
8. M. Dutschke, R. Wolf, *Reducing Emissions from Deforestation in Developing Countries: The Way Forward* (GTZ Climate Protection Progamme, Eschborn, Germany, 2007).
9. World Bank, *Biodiversity Conservation in Forest Ecosystems: World Bank Assistance 1992–2002* (World Bank, Washington, DC, 2002).
10. A. James, K. J. Gaston, A. Balmford, *Bioscience* **51**, 43 (2001).
11. FAO, *FAOSTAT – Production - ForesSTAT* (2008); http://faostat.fao.org/DesktopDefault.aspx?PageID=381&lang=en.
12. It is probable that carbon content will be estimated by using the IPCC Good Practice Guidance for Land Use, Land-Use Change, and Forestry, which asks that national carbon stock data are used where available but specifies default parameters for countries with none.
13. J. Penman *et al.*, Eds., *Good Practice Guidance for Land Use, Land-Use Change and Forestry and Definitions and Methodological Options to Inventory Emissions from Direct Human-Induced Degradation of Forests and Devegetation of Other Vegetation Types* [Institute for Global Environmental Strategies (IGES), for the IPCC, Hayama, Japan, 2003].
14. L. Naughton-Treves, M. B. Holland, K. Brandon, *Annu. Rev. Environ. Resour.* **30**, 219 (2005).
15. R. Defries, A. Hansen, A. C. Newton, M. C. Hansen, *Ecol. Appl.* **15**, 19 (2005).
16. T. M. Brooks *et al.*, *Science* **313**, 58 (2006).
17. K. A. Wilson, M. F. McBride, M. Bode, H. P. Possingham, *Nature* **440**, 337 (2006).
18. J. Ebeling, M. Yasué, *Philos. Trans. R. Soc. London Ser. B* **363**, 1917 (2008).
19. S. E. Page *et al.*, *Nature* **420**, 61 (2002).
20. We thank J. Hutton of UNEP-WCMC and K. Bolt of Royal Society for the Protection of Birds for their comments on this paper, as well as P. Herkenrath and J. Harrison of UNEP-WCMC, members of the Cambridge Conservation Forum and Poverty Conservation Learning Group for valuable discussions on the conservation implications of REDD, and two anonymous reviewers of this paper. Our work on REDD has been financially supported by UNEP, the Department for International Development (U.K.), the Federal Ministry for the Environment, Nature Conservation and Nuclear Safety (Germany), and WWF UK.

10.1126/science.1155358

PERSPECTIVE

Managing Forests for Climate Change Mitigation

Josep G. Canadell* and Michael R. Raupach

Forests currently absorb billions of tons of CO_2 globally every year, an economic subsidy worth hundreds of billions of dollars if an equivalent sink had to be created in other ways. Concerns about the permanency of forest carbon stocks, difficulties in quantifying stock changes, and the threat of environmental and socioeconomic impacts of large-scale reforestation programs have limited the uptake of forestry activities in climate policies. With political will and the involvement of tropical regions, forests can contribute to climate change protection through carbon sequestration as well as offering economic, environmental, and sociocultural benefits. A key opportunity in tropical regions is the reduction of carbon emissions from deforestation and degradation.

Forest ecosystems are important components of the global carbon cycle in at least two ways. First, terrestrial ecosystems remove nearly 3 billion tons of anthropogenic carbon every year (3 Pg C $year^{-1}$) through net growth, absorbing about 30% of all CO_2 emissions from fossil fuel burning and net deforestation (*1*, *2*). Forests are major contributors to this terrestrial carbon sink and its associated economic benefits (*1*). Second, 4 billion hectares of forest ecosystems (4×10^3 Mha; about 30% of the global land area) store large reservoirs of carbon, together holding more than double the amount of carbon in the atmosphere (*3*, *4*). Although the climate protection role of forests is in no doubt, it is complex to determine how much of the forest carbon sink and reservoir can be managed to mitigate atmospheric CO_2 buildup, and in what way.

A first approximation to the upper limit of carbon sequestration on land is the carbon emitted from historical land transformation, about 200 Pg C, mostly from the conversion of forests to nonforest land cover. Assuming that three-fourths of this carbon came from forest conversion and can be returned by reforestation over the next 100 years, the resulting potential sequestration of about 1.5 Pg C $year^{-1}$ would reduce the atmospheric CO_2 concentration by 40 to 70 parts per million by 2100 (*5*). However, the achievable sequestration is only a fraction of this potential because of competing land needs (agriculture, bioenergy, urbanization, and conservation) and sociocultural considerations.

Four major strategies are available to mitigate carbon emissions through forestry activities: (i) to increase forested land area through reforestation (*6*), (ii) to increase the carbon density of existing forests at both stand and landscape scales, (iii) to expand the use of forest products that sustainably replace fossil-fuel CO_2 emissions, and (iv) to reduce emissions from deforestation and degradation.

Estimates covering a range of carbon prices suggest that reforestation could average 0.16 to 1.1 Pg C $year^{-1}$ to 2100 (*7*–*9*) with land requirements up to 231 Mha. In one of the most comprehensive synthesis efforts undertaken so far, the Fourth Assessment of the Intergovernmental Panel on Climate Change estimated that an economic potential of 0.12 Pg C $year^{-1}$ could be reached by 2030 at U.S. $20 per ton of CO_2, and more than 0.24 Pg C $year^{-1}$ at U.S. $100 per ton of CO_2 (*10*, *11*). Land transformation requirements are large; for example, China has used 24 Mha of new forest plantations and natural forest regrowth to transform a century of net carbon emissions in the forest sector to net gains of 0.19 Pg C $year^{-1}$ (*3*, *12*), offsetting 21% of Chinese fossil fuel emissions in 2000.

Net carbon sequestration can also be achieved by increased forest carbon density, through both stand-scale management and landscape-scale strategies such as longer harvesting cycles or reduced disturbances. Fire suppression and harvest exclusion in U.S. forests during the 20th century, although not implemented for the purpose of carbon sequestration, led to a 15% (8.1 Pg C) increase in forest biomass between 1927 and 1990 (*13*). The overall biophysical potential of management activities to increase carbon density can be substantial and comparable to that of reforestation (*10*).

Joint use of carbon sequestration and the provision of forest-derived products (e.g., timber and biomass for energy) will optimize the contribution of forestry in climate mitigation. Such options are particularly attractive in temperate regions where land availability is limited by high prices and strong competition with other land uses (Fig. 1). Although complexities in quantifying the net carbon benefits of some of these activities may limit their role in global carbon markets, they will have a place in national mitigation strategies, particularly when used synergistically with goals and policies other than climate mitigation. For instance, fire reduction policies that require the removal of undergrowth and occasional thinning can contribute to production of bioenergy.

Finally, reducing deforestation has high potential for cost-effective contributions to climate protection. Currently, 13 Mha $year^{-1}$ are deforested, almost exclusively in tropical regions, with net emissions of 1.5 Pg C $year^{-1}$ (*2*, *3*). Reducing rates of deforestation by 50% by 2050, and stopping deforestation when countries reach 50% of their current forested area, would avoid emissions equivalent to 50 Pg C (*14*). This "50:50:50:50" estimate shows that even with continuing deforestation over the next 40 years, the mitigation potential is large, in addition to protecting the sink capacity of forest for continued removal of atmospheric CO_2.

Combining all forestry activities together, there is economic potential to achieve 0.4 Pg C $year^{-1}$ by 2030 using carbon sequestration and avoidance at U.S. $20 per ton of CO_2, and double this amount for prices under U.S. $100 per ton of CO_2 (*10*). These levels of carbon sequestration, of which one-third to one-half would be through avoided deforestation, could offset 2 to 4% of the 20 Pg C $year^{-1}$ of projected emissions by 2030 on the basis of current growth rates (*2*, *15*). Tropical regions would account for 65% of the total offset (*10*).

Climate mitigation through forestry carries the risk that carbon stores may return to the atmosphere by disturbances such as fire and insect outbreaks, exacerbated by climate extremes and climate change. A recent increase in areas affected by wildfires and insect outbreaks has driven Canadian forests from a CO_2 sink (before 2000) to a source expected to continue for at least the next two to three decades (*16*). Similarly, increased forest biomass in the western United States caused by fire suppression and reduced harvesting rates over the past century is now threatened by a factor of 4 increase in fire frequency due to longer and hotter dry seasons (*17*). These new patterns of disturbances are reshaping the view held in the past that vast forest resources anywhere would always play a major role in climate mitigation.

There is indeed uncertainty about the future size and stability of the terrestrial carbon sink and stock. Most global coupled climate-carbon models show carbon accumulation during this

Global Carbon Project, CSIRO Marine and Atmospheric Research, GPO Box 3023, Canberra, ACT 2601, Australia.

*To whom correspondence should be addressed. E-mail: pep.canadell@csiro.au

century, largely aided by the fertilization effect of increasing atmospheric CO_2 (*18*). However, there are large uncertainties in the magnitude of the CO_2 fertilization effect (*19*), and vulnerable regions with large carbon stores have been identified that could lead to the release of hundreds of Pg C by the end of this century (*20*); these include peat swamp forests in Southeast Asia where climate models uniquely agree on a future drying trend (*21*), further stressing the need for conservation and reduced human impacts.

Although sequestering carbon in forests is good for the climate, forests also affect biophysical properties of the land surface such as sunlight reflectivity (albedo) and evaporation, with further implications for radiative forcing of climate. Climate models suggest that large reforestation programs in boreal regions would have limited climate benefits because of the substitution of bright snow-dominated regions for dark forest canopies (*22*, *23*). Conversely, the climate benefits of reforestation in the tropics are enhanced by positive biophysical changes such as cloud formation, which further reflects sunlight. These patterns of full radiative forcing reinforce the large potential of tropical regions in climate mitigation, discourage major land use changes in boreal regions, and suggest avoiding large albedo changes in temperate regions to maximize the climate benefits of carbon sequestration.

Forestry, and reforestation in particular—like any large-scale transformation of land use patterns—can lead to unintended environmental and socioeconomic impacts that could jeopardize the overall value of carbon mitigation projects. Concerns include decreased food security, reduced stream flows, and loss of biodiversity and local incomes (*24*). However, well-directed carbon sequestration projects, along with the provision of sustainably produced timber, fiber, and energy, will yield numerous benefits, including additional income for rural development, prospects for conservation and other environmental services, and support for indigenous communities (*10*, *25*). Principles of sustainability must govern the resolution of trade-offs that may arise from ancillary effects in order to simultaneously maximize climate change protection and sustainable development.

The challenges facing sustainable mitigation through forestry activities, anywhere but particularly in the tropics, are surmountable but large. They include the development of appropriate governance institutions to manage the transition to new sustainable development pathways. An example of this difficulty is the lack of a sustainable tropical timber industry despite two decades of national and international efforts. Currently, only 7% of all tropical timber trade comes from sustainably managed forests (*26*).

The potential of carbon sequestration will depend on the degree to which climate protection and ancillary benefits are aligned. The magnitude of this potential will be increased by high carbon prices driven by aggressive emission reduction targets, and by the political will to include forestry activities as part of mitigation portfolios. Sustainable involvement of tropical regions is essential to take up the full global potential for climate change mitigation through forestry.

PHOTO: MICHAEL RYAN

Fig. 1. Plantations of *Pinus radiata* and *Eucalyptus nitens* in Gippsland (Victoria, Australia).

References and Notes

1. Terrestrial land sink over the period 2000–2006 was 2.8 Pg C $year^{-1}$ (*2*) or 10.3 Pg CO_2 $year^{-1}$; forests and woodlands are the dominant component of this sink. Price of a ton of CO_2 in the European Trading Scheme was €25 in April 2008, with €1 ≈ U.S. $1.56.
2. J. G. Canadell *et al.*, *Proc. Natl. Acad. Sci. U.S.A.* **104**, 18866 (2007).
3. FAO, *Global Forest Resource Assessment 2005* (Food and Agriculture Organization of the United Nations, Rome, 2006).
4. C. L. Sabine *et al.*, in *Global Carbon Cycle: Integrating Humans, Climate and the Natural World*, C. Field, M. Raupach, Eds. (Island Press, Washington, DC, 2004), pp. 17–44.
5. J. I. House, I. C. Prentice, C. Le Quere, *Glob. Change Biol.* **8**, 1047 (2002).
6. With the term reforestation we include the activities described by the IPCC as afforestation, reforestation, and natural forest regrowth in abandoned land.
7. J. Sathaye, W. Makundi, L. Dale, P. Chan, K. Andrasko, *Energy J.* (special issue), 127 (2006).
8. B. Sohngen, R. Sedjo, *Energy J.* (special issue), 109 (2006).
9. B. J. Strengers, J G. van Minnen, B. Eickhour, *Clim. Change*, 10.1007/s10584-007-9334-4 (2006).
10. G. J. Nabuurs *et al.*, in *Climate Change 2007: Mitigation*, B. Metz *et al.*, Eds. (Cambridge Univ. Press, Cambridge, 2007), pp. 541–584.
11. Calculated from regional assessment in (*9*), combining all forestry activities and using fraction of total to afforestation based on global economic model synthesis in their table 9.3.
12. S. Wang *et al.*, *J. Environ. Manage.* **85**, 524 (2007).
13. R. A. Houghton, J. L. Hackler, K. T. Lawrence, *Glob. Ecol. Biogeogr.* **9**, 145 (2000).
14. R. E. Gullison *et al.*, *Science* **316**, 985 (2007); published online 10 May 2007 (10.1126/science.1136163).
15. M. R. Raupach *et al.*, *Proc. Natl. Acad. Sci. U.S.A.* **104**, 10288 (2007).
16. W. A. Kurz, G. Stinson, G. J. Rampley, C. C. Dymond, E. T. Neilson, *Proc. Natl. Acad. Sci. U.S.A.* **105**, 1551 (2008).
17. A. L. Westerling, H. G. Hidalgo, D. R. Cayan, T. W. Swetnam, *Science* **313**, 940 (2006); published online 5 July 2006 (10.1126/science.1128834).
18. P. Friedlingstein *et al.*, *J. Clim.* **19**, 3337 (2006).
19. J. G. Canadell *et al.*, in *Terrestrial Ecosystems in a Changing World*, J. G. Canadell, D. Pataki, L. Pitelka, Eds. (Springer-Verlag, Berlin, 2007), pp. 59–78.
20. N. Gruber *et al.*, in *The Global Carbon Cycle: Integrating Humans, Climate and the Natural World*, C. B. Field, M. R. Raupach, Eds. (Island Press, Washington, DC, 2004), pp. 45–76.
21. W. Li *et al.*, *Geophys. Res. Lett.* **34**, 10.1029/2006GL028364 (2007).
22. R. A. Betts *et al.*, *Nature* **408**, 187 (2000).
23. G. Bala *et al.*, *Proc. Natl. Acad. Sci. U.S.A.* **104**, 6550 (2007).
24. R. B. Jackson *et al.*, *Science* **310**, 1944 (2005).
25. M. R. Raupach *et al.*, in *The Global Carbon Cycle: Integrating Humans, Climate and the Natural World*, C. B. Field, M. R. Raupach, Eds. (Island Press, Washington, DC, 2004), pp. 131–162.
26. International Tropical Timber Organization, *Status of Tropical Forest Management 2005*, Technical Series No. 24 (ITTO, Yokohama, 2006).

27. We thank D. Barrett, R. Jackson, S. Roxburgh, and two anonymous reviewers for their valuable feedback. This paper is a contribution to the Global Carbon Project (GCP) of the Earth System Science Partnership. We thank the Australian Climate Change Research Program for supporting the GCP office in Canberra.

10.1126/science.1155458

PERSPECTIVE

Beyond Deforestation: Restoring Forests and Ecosystem Services on Degraded Lands

Robin L. Chazdon

Despite continued forest conversion and degradation, forest cover is increasing in countries across the globe. New forests are regenerating on former agricultural land, and forest plantations are being established for commercial and restoration purposes. Plantations and restored forests can improve ecosystem services and enhance biodiversity conservation, but will not match the composition and structure of the original forest cover. Approaches to restoring forest ecosystems depend strongly on levels of forest and soil degradation, residual vegetation, and desired restoration outcomes. Opportunities abound to combine ambitious forest restoration and regeneration goals with sustainable rural livelihoods and community participation. New forests will require adaptive management as dynamic, resilient systems that can withstand stresses of climate change, habitat fragmentation, and other anthropogenic effects.

Forest succession is a stochastic process resulting from the behavior of component populations and species. Yet, restoration ecologists tend to view forest communities as tightly integrated biological systems, using metaphors for organismal health and development to describe the state of forests throughout the world. Forests are "declining," exhibit "arrested development," are "infested" with invasive species, and may require active "rehabilitation." Although many principles of restoration ecology derive from insights into successional change, guided reconstruction of forests should be clearly distinguished from the natural processes of forest succession, which are not prescribed or directed by humans and often exhibit divergent and unpredictable pathways (*1*).

Both of these processes—assisted restoration and unassisted forest regeneration—are gaining momentum across the world. As a result, global assessments show a recent decline in the net rate of forest loss from 1990 to 2000 and from 2000 to 2005 (*2*). Although the global deforestation rate remains high, 13 million ha/year, forest cover in 18 countries has begun to increase, owing to both afforestation (tree planting on previously unforested land) and natural regeneration (*2*). Natural forests expanded in Bhutan, Cuba, Gambia, Puerto Rico, St. Vincent, and Vietnam from 1990 to 2005, following earlier forest transitions in six European nations and the USA during the 19th and early 20th centuries (*3*, *4*). These increases, however, do not necessarily reflect increasing biomass or carbon sequestration (*3*). For developing countries, the Food and Agriculture Organization of the United Nations (FAO) requires a minimum of only 10% forest cover for land to be classified as forest (*4*), a criterion that would satisfy few forest-dwelling species. Moreover, forest assessment data provide no insights into the recovery of forest biodiversity or ecosystem services lost because of forest conversion or degradation. In many cases, these figures reflect the widespread establishment of plantations, which currently constitute about 4% of total forest area globally. Rates of planting of forests and trees are increasing by 2.8 million ha/year, for purposes of production, as well as for conservation and restoration (*2*). In China alone, 28 million ha of plantations were established from 2001 to 2007 (*5*). Commercial forest plantations can potentially play a role in landscape restoration and faunal conservation, if they are managed as components of a heterogeneous landscape mosaic (*6*, *7*). Unfortunately, forest cover statistics do not clearly reveal changes in the status of degraded secondary and heavily logged forests, which will not recover on their own (*8*, *9*). As classified by FAO, these forests constitute 60% of forest area globally (*2*).

Wherever actions are taken to promote forest restoration and regeneration, new forests emerging in human-impacted landscapes will not match the original old-growth forests in species composition (*10*). But forest restoration can restore many ecosystem functions and recover many components of the original biodiversity. Approaches to restoring functionality in forest ecosystems depend strongly on the initial state of forest or land degradation and the desired outcome, time frame, and financial constraints (Fig. 1). Restoration approaches should take into account the spatial distribution, abundance, and quality of residual vegetation, a strong indicator of the potential for natural regeneration (*11*). Just as forest ecosystem processes decline in a stepwise fashion with increasing human impacts (*12*), restoration approaches can "elevate" a degraded or completely altered forest ecosystem to a higher level of the restoration staircase (Fig. 1). Reclamation may be the only viable option for restoring some levels of biodiversity and ecosystem services in former coal or bauxite mining operations, where abiotic factors, such as soil removal or toxic substrata, limit establishment and growth of native vegetation (*13*). In areas with degraded soils, rehabilitation through planting of carefully selected exotic or native trees can improve soil fertility and restore productive agricultural use, while offering little enhancement of biodiversity. Where agricultural land use has been less intensive and nearby forest patches and faunal dispersal agents can ensure diverse seed rain, the most rapid and least costly path toward restoring forests is through unhindered natural regeneration (*11*, *14*). After 30 to 40 years, natural regeneration following abandonment of pasture and coffee plantations produced secondary forests in Puerto Rico with biomass, stem density, and species richness similar to the island's mature forests (*15*). Direct seeding and planting seedlings or saplings in regenerating forests can hasten recovery of species composition (*14*, *15*). In sites at intermediate levels of degradation, where soils are intact but diverse seed sources are lacking, reforestation with native species, agroforestry, and assisted natural regeneration can augment biodiversity and ecosystem services, while also providing income for rural livelihoods. Such plantings can be incorporated—along with natural regeneration—into management of buffer zones and biological corridors to enhance landscape connectivity and landscape-level biodiversity (*16*).

In both developed and developing countries, forests are being restored by local communities, as well as through state and national programs. Forest rehabilitation projects in the Philippines, Peru, Indonesia, China, North Vietnam, and the Brazilian Amazon River basin promote community organization and improvement of rural livelihoods (*17*). Local knowledge of tree characteristics, planting of diverse species of ecological and economic importance, and integration of rehabilitation programs with regional development strategies are essential elements of restoration success (*17*). Communities from 12 villages in Phuc Sen in Northwestern Vietnam organized to restore limestone forests degraded in the 1960s

Department of Ecology and Evolutionary Biology, University of Connecticut, Storrs, CT 06269–3043, USA. E-mail: chazdon@uconn.edu

and 1970s by excessive fuelwood and timber extraction. Through planting indigenous tree species and fostering natural regeneration, forests are being restored, water is again flowing to lowland rice fields, and over 30 species of rare or endemic indigenous mammals are returning to the area (*18*). In the Shinyanga region of Tanzania, large areas of dense acacia and miombo woodland were cleared by 1985, transforming the landscape into semidesert. The HASHI program helped local people from 833 villages to restore 350,000 ha of acacia and miombo woodland through traditional pastoralist practices in only 18 years (*19*).

Experimental research is required to determine the most appropriate path toward restoration. In many cases, passive methods can achieve greater success than intensive interventions and are far less costly (*13*). In the northwest Czech Republic, unassisted succession led to more successful restoration of species richness in mine spoils after 20 to 30 years than in technically reclaimed treatments, where organic amendments stimulated the growth of weeds and inhibited establishment of target species (*13*). Restoration techniques involving plowing and mechanical planting may actually slow regeneration of seasonal deciduous forests in Brazilian Cerrado (*20*). There are few rigorous, replicated studies of the effects of different restoration treatments (including unassisted natural regeneration) that account for previous land use, soils, proximity to seed sources, and age since abandonment (*20*). At what position along a forest degradation gradient does "accelerating succession" through planting trees achieve faster recovery of forest structure and composition compared with unassisted regeneration? This question is challenging to address, as the effects of management will vary with the spatial scale of restoration, as well as with synergistic effects of biotic and abiotic stresses from climate change, invasive species, and altered plant-animal relationships (*10*, *13*).

Large-scale forest restoration presents complex and poorly understood implications for the structure and composition of future forests, landscapes, and fauna. Will widespread plantations of a small number of native species—an increasingly popular form of forest restoration in tropical regions—increase biotic homogenization and decrease genetic diversity of planted species (Fig. 2)? Monoculture tree plantations may also facilitate establishment of invasive species and increase susceptibility to species-specific pathogens (*10*). Interventions to promote rapid carbon sequestration through tree plantations will increase the regional abundance of fast-growing, disturbance-tolerant species, which can impact forest dynamics in mature forest fragments (*21*). Emerging forests provide breeding grounds for invasive exotic species, which can rapidly colonize established forests in protected areas (*10*) (Fig. 2). Population explosions of the white-tailed deer (*Odocoileus virginianus*) in recovering forests of the eastern United States provide a sobering example of synergistic effects of widespread forest expansion, reduced predator populations, and spread of invasive species and human disease agents (*22*).

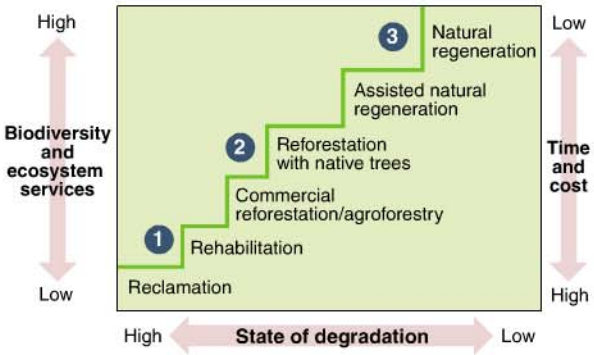

Fig. 1. The restoration staircase. Depending on the state of degradation of an initially forested ecosystem, a range of management approaches can at least partially restore levels of biodiversity and ecosystem services given adequate time (years) and financial investment (capital, infrastructure, and labor). Outcomes of particular restoration approaches are (1) restoration of soil fertility for agricultural or forestry use; (2) production of timber and nontimber forest products; or (3) recovery of biodiversity and ecosystem services.

Effects of different restoration approaches on recovery of ecosystem services are also poorly studied, despite wide recognition of the links between biodiversity, functional traits, and ecosystem services (*23*). Incentives for increasing carbon stocks in vegetation provide a major impetus for a wide range of forest restoration interventions, as well as conservation of existing forests. An aggressive global program of reforestation and natural regeneration could potentially restore forests on 700 million ha over the next 50 years (*24*). Fast-growing, short-lived species with low-density wood are favored by many reforestation projects designed to provide carbon offsets, but long-term carbon sequestration is promoted by growth of long-lived, slow-growing tree species with dense wood and slow turnover of woody tissues. These species increase in abundance and biomass throughout the course of

Fig. 2. A commercial restoration plantation in northeastern Costa Rica. In the foreground are planted individuals of *Acacia mangium*, a fast-growing tree species native to Asia and Australia, which tolerates poor soils. A fast-growing native species, *Vochysia guatemalensis* is also planted here among the *A. mangium* trees. In the background is a fragment of 25-year-old secondary forest. *Euterpe oleracea*, an exotic palm species from Brazil that was cultivated in a nearby plantation has colonized the restoration site (upper right quadrant) and is now invading secondary forests in this area. [Photograph by R. L. Chazdon]

natural forest regeneration (*23*). Short-term solutions are attractive, but forest regeneration and restoration are long-term processes that can take a century or more. Plantations have a high rate of failure if few tree species are planted and they are not well suited to site conditions. Of 98 publicly funded reforested areas in Brazil, only 2 were successful (*25*). It is essential to plan for long-term returns on restoration investments if future forests are to support the wide range of species, species interactions, and ecosystem services present in current forests.

Ambitious efforts are being mounted to restore forests, ecosystem services, and biodiversity throughout the world. The Riparian Forest Restoration Project hopes to reforest 1 million ha of riparian rainforest in the Atlantic Rainforest in São Paulo, Brazil, with up to 800 native species (*25*). Forest restoration efforts, whether at national, regional, or local scales, will take many decades, long-term financing, political will, labor, and personal commitment. In the process, these efforts will also restore new relationships between people and forests. As so clearly stated by William R. Jordan III, a founder of the field of restoration ecology, "Ultimately, the future of a natural ecosystem depends not on protection from humans but on its relationship with the people who inhabit it or share the landscape with it" (*26*).

References and Notes

1. L. R. Walker, J. Walker, R. J. Hobbs, Eds., *Linking Restoration and Ecological Succession* (Springer, New York, 2007).
2. FAO, *Global Forest Resources Assessment 2005: Progress Towards Sustainable Forest Management* (FAO, Rome, 2005).
3. P. E. Kauppi *et al.*, *Proc. Natl. Acad. Sci. U.S.A.* **103**, 17574 (2006).
4. A. Grainger, *Proc. Natl. Acad. Sci. U.S.A.* **105**, 818 (2008).
5. State Forestry Administration, *China Forestry Development Report* (China Forestry Publishing House, Beijing, 2005 to 2007).
6. D. B. Lindenmayer, R. J. Hobbs, *Biol. Conserv.* **119**, 151 (2004).
7. J. Barlow *et al.*, *Proc. Natl. Acad. Sci. U.S.A.* **104**, 18555 (2007).
8. C. Sabogal, R. Nasi, in *Forest Restoration in Landscapes: Beyond Planting Trees*, S. Mansourian, D. Vallauri, N. Dudley, Eds. (Springer, New York, 2005), pp. 361–369.
9. International Tropical Timber Organization (ITTO), *Guidelines for the Restoration, Management and Rehabilitation of Degraded and Secondary Tropical Forests* (ITTO, Yokohama, Japan, 2002)
10. R. J. Hobbs *et al.*, *Glob. Ecol. Biogeogr.* **15**, 1 (2006).
11. R. L. Chazdon, *Perspect. Plant Ecol. Evol. Syst.* **6**, 51 (2003).
12. V. A. Cramer, R. J. Hobbs, R. J. Standish, *Trends Ecol. Evol.* **23**, 104 (2008).
13. K. Prach, R. Marrs, P. Pysek, R. van Diggelen, in *Linking Restoration and Ecological Succession*, L. R. Walker, J. Walker, R. J. Hobbs, Eds. (Springer, New York, 2007), pp. 121–149.
14. D. Lamb, P. D. Erskine, J. Parrotta, *Science* **310**, 1628 (2005).
15. J. K. Zimmerman, T. M. Aide, A. E. Lugo, in *Old Fields: Dynamics and Restoration of Abandoned Farmland*, V. A. Cramer, R. J. Hobbs, Eds. (Island Press, Washington, 2007), pp. 51–74.
16. C. A. Harvey *et al.*, *Conserv. Biol.* **22**, 8 (2008).
17. U. Chokkalingam *et al.*, in *Forest Restoration in Landscapes: Beyond Planting Trees*, S. Mansourian, D. Vallauri, N. Dudley, Eds. (Springer, New York, 2005), pp. 405–414.
18. M. Poffenberger, *Int. J. Environ. Sustain. Dev.* **5**, 57 (2006).
19. G. Monela, S. Chamshama, R. Mwaipopo, D. Gamassa, *A Study on the Social, Economic and Environmental Impacts of Forest Landscape Restoration in Shinyanga Region, Tanzania* (The United Republic of Tanzania Ministry of Natural Resources and Tourism, Forestry, and Beekeeping Division, Dar es Salaam, Tanzania, and IUCN, The World Conservation Union, Eastern Africa Regional Office, Nairobi, Kenya, 2004).
20. A. B. Sampaio, K. D. Holl, A. Scariot, *Restor. Ecol.* **15**, 462 (2007).
21. W. F. Laurance *et al.*, *Ecology* **87**, 469 (2006).
22. S. D. Cote, T. P. Rooney, J.-P. Tremblay, C. Dussault, D. M. Waller, *Annu. Rev. Ecol. Evol. Syst.* **35**, 113 (2004).
23. S. Diaz *et al.*, *J. Veg. Sci.* **15**, 295 (2004).
24. L. Ciccarese, S. Brown, B. Schlamadinger, in *Restoration of Boreal and Temperate Forests*, J. A. Stanturf, P. Madsen, Eds. (CRC Press, Boca Raton, FL, 2005), pp. 111–120.
25. B. Wuethrich, *Science* **315**, 1070 (2007).
26. W. R. Jordan III, *The Sunflower Forest: Ecological Restoration and the New Communion with Nature* (Berkeley, Univ. of California Press, Berkeley, CA, 2003).

27. I thank N. Norden, V. Boukili, S. Letcher, J. P. Arroyo Mora, R. K. Colwell, and two anonymous reviewers for helpful comments on the manuscript and National Science Foundation Grant DEB-0639393 for research support.

10.1126/science.1155365

PERSPECTIVE

Changing Governance of the World's Forests

Arun Agrawal,[1]* Ashwini Chhatre,[2] Rebecca Hardin[3]

Major features of contemporary forest governance include decentralization of forest management, logging concessions in publicly owned commercially valuable forests, and timber certification, primarily in temperate forests. Although a majority of forests continue to be owned formally by governments, the effectiveness of forest governance is increasingly independent of formal ownership. Growing and competing demands for food, biofuels, timber, and environmental services will pose severe challenges to effective forest governance in the future, especially in conjunction with the direct and indirect impacts of climate change. A greater role for community and market actors in forest governance and deeper attention to the factors that lead to effective governance, beyond ownership patterns, is necessary to address future forest governance challenges.

Central governments own by far the greater proportion—about 86%—of the 5.4 billion hectares of the world's forests and wooded areas. Private and "other" (mostly communal) forms of ownership constitute just over 10% and below 4% of global forests, respectively (*1*). There are important regional variations around these averages [Fig. 1, based on (*1*)]. Official statistics on forest ownership, however, misrepresent the extent of and changes in forest cover (*2*). They also misrepresent the nature and changing forms of global forest governance.

Effective governance is central to improved forest cover and change outcomes. Changing forest governance today is for the most part a move away from centrally administered, top-down regulatory policies that characterized much of the 19th and 20th centuries. Many government-owned forests are managed as common property for multiple uses by local communities and community-based organizations (*3*). Many other forests classified under public ownership are effectively governed as private timber concessions by logging companies (*4*). Civil society organizations and market incentives increasingly play a role in forest governance through certification processes and changing consumer preferences (*5*). At the same time, the growth in the number and size of strict protected areas in the latter half of the 20th century has also meant that ~6.4 million km^2 of publicly owned forests are now under governance regimes that involve greater restrictions on human use and habitation (*6*, *7*) (fig. S1).

In the 21st century, three important forest governance trends stand out: (i) decentralization

[1]School of Natural Resources and Environment, University of Michigan, Ann Arbor, MI 48109, USA. [2]Department of Geography, University of Illinois at Urbana-Champaign, Urbana, IL 61801, USA. [3]Department of Anthropology and School of Natural Resources and Environment, University of Michigan, Ann Arbor, MI 48109, USA.

*To whom correspondence should be addressed. E-mail: arunagra@umich.edu

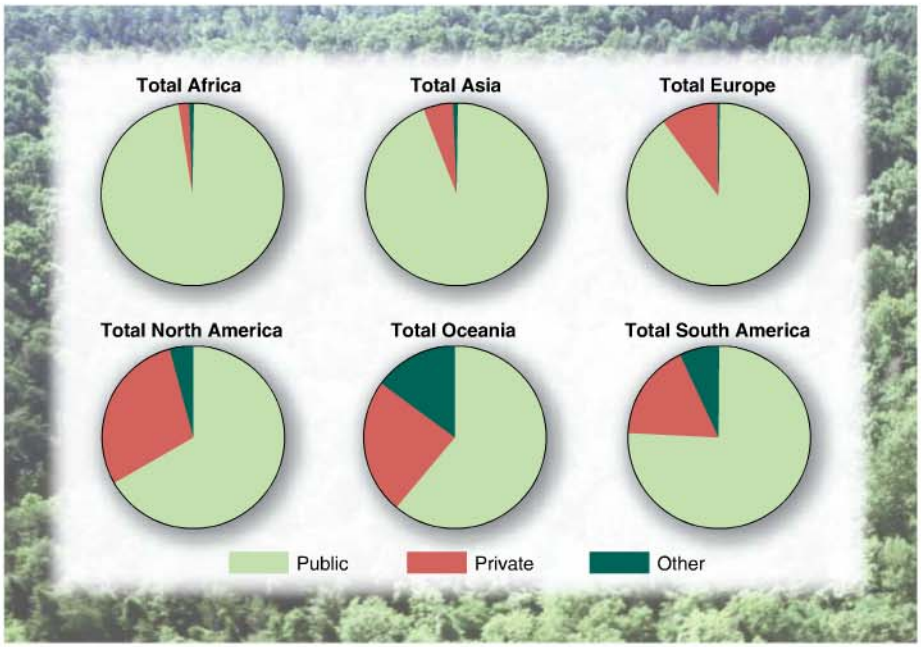

Fig. 1. Distribution of forest ownership by world regions.

of management, especially for commercially low-value forests that nonetheless play an important role in the livelihoods of hundreds of millions of rural households in developing countries; (ii) the substantial role of logging companies in forest concessions, typically for selective logging in tropical forests; and (iii) the growing importance of market-oriented certification efforts, mainly in temperate forests in the developed world.

Decentralization of forestry policies began in the mid- to late 1980s and had become a prominent feature of forest governance by the mid-1990s (*8*, *9*). It was impelled in part by infusions of material and technical support from bilateral, multilateral, and private donors who sought better forest governance from recipient countries. These external pressures coincided with domestic demands for a greater recognition of local communities' needs for forest products and their role in managing local forests for multiple purposes (*10*). They also worked in the same direction as the desire of many governments to reduce the financial burden of forest governance in an economic context characterized by substantial fiscal and budgetary pressures. An emerging body of scholarly work on local participation, resource institutions, governance, and accountability helped provide some justification for decentralization reforms (*11*, *12*). Decentralization reforms in the past two decades have often promoted local, more democratic participation in governance. In tandem with policy advocacy and social movements, such reforms have fostered new practices of forest use, sometimes provoking social tensions revolving around claims of indigenous peoples within forest zones (*10*). Overall, local communities and organizations have come to govern close to an additional 200 million hectares of forests compared to the 1980s (*13*, *14*).

The private concession model in forest governance has been in existence at least since the imperial trades of the early 1700s, enduring shifts in commodity values, political systems, and changing forest policy frameworks (*15*). Under concessionary forest governance, central governments or forest departments provide logging companies with long-term resource extraction rights in commercially valuable forests in exchange for a stream of revenues. Although a variety of logging concessions arrangements also exist in the developed world, they are a dominant form of forest governance in tropical forests in Southeast Asia, parts of the Amazon, and especially in Central and West Africa, where at least 75 million hectares of forests are under concession to logging companies (*4*). Contemporary governance through forest concessions is prompted by demand for logs and timber—often in distant markets—and governments' need for revenues. The limited enforcement of concession agreements in most countries in Southeast Asia and Africa has also meant that legal logging in concessions exists side by side with costly and unsustainable levels of illegal logging (*16*). The World Bank estimates U.S. $15 billion to be lost to developing countries every year as a result of illegal logging.

Forest certification initiatives emerged in the early 1990s as market instruments in which an independent certification body provides an assurance to consumers that forest product suppliers have conformed to some predetermined criteria of sustainable forest management (*17*). Certification efforts were launched as a way to improve the sustainability of tropical forest management. Yet they have been used far more broadly in temperate forests—

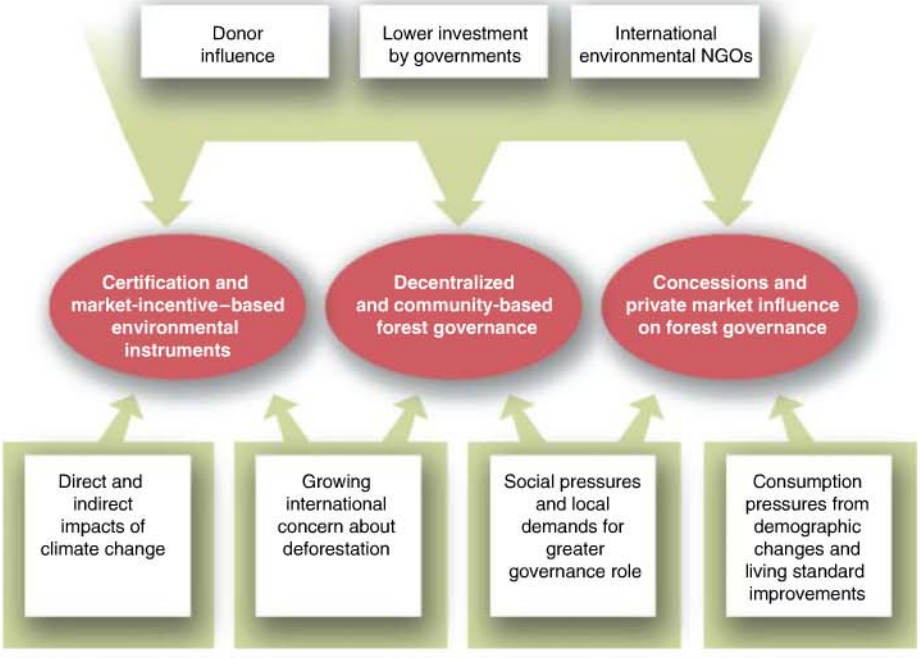

Fig. 2. Changes in forest governance and their social, economic, and political drivers.

less than 10% of 80 million hectares of certified forests in 2000 were in the humid tropics (*18*). Certification processes and performance standards are expanding into new regions and niches as a market and civil society response to public concern about deforestation, the organizational strength of international environmental nongovernmental organizations (NGOs), and continuing economic globalization (*5*).

Decentralization, concession, and certification-related trends in forest governance are the result of important social, economic, and political drivers (Fig. 2).

The role of drivers mentioned in Fig. 2 is likely to be reinforced and made more complex by climate change. Existing trends around conversion of forests to biofuel plantations, for example, are likely to affect both biodiversity and the livelihoods of the poor adversely.

In conjunction with competing demands for food and forest products from a growing, and on the average wealthier, global population, climate change impacts will strengthen governance trends (especially in the direction of concessions and certification), increase the involvement of market actors in forest governance, and create pressures toward greater formalization as governments seek to take advantage of emerging carbon funds. The intersection of production strategies for food, fuel, and forest products as competition grows for scarce land will inevitably lead to new experiments with governance arrangements at all levels, from the local to the international. It can potentially reverse contemporary trends in favor of the involvement of civil society actors and communities, instead promoting greater privatization. The need for making careful choices in this regard will become especially critical after the next two decades as the joint effects of changes in climate, demographic patterns, and living standards begin to be felt more acutely (*19*).

The effectiveness of forest governance is only partly explained by who owns forests. At the local level, existing research finds only a limited association between whether forests are under private, public, or common ownership and changes in forest cover or sustainability of forest management (*11*). National-level association between forest area under different forms of ownership and changes in forest cover is also relatively weak, especially for public ownership [Spearman's rho for proportion of forests under public ownership and forest cover change = 0.017, $P > |t| = 0.98$, based on data in (*1*)]. At the regional level, the greatest net declines in forests have occurred in tropical countries. Conversely, net increases in forest cover have occurred primarily in North America and Europe (see figs. S2 and S3 for illustration). However, the relationship between this pattern and forest ownership is limited. Moreover, there is only partial knowledge about the relationships between the condition of forests, different forms of forest ownership, and the multiple objectives of forest governance—improvements in income, livelihoods, biodiversity, carbon sequestration, and ecosystem service provision.

The need to look deeper, therefore, into how governance arrangements work is paramount if forest dwellers, users, managers, and policy-makers are to make better choices about forest governance at a variety of scales. A very large number of factors influences the effectiveness and outcomes of forest governance (*20*, *21*). Among these, careful definition of user rights and responsibilities in forests, greater participation by those who use and depend on forests, downward and horizontal accountability of decision-makers, better monitoring of forest outcomes, stronger enforcement of property rights and governance arrangements, and investments in institutional capacities at local, regional, and national levels have been identified as critically important for more effective forest governance in tropical country contexts.

Broadly speaking, the goal of forest conservation has historically not been met when in conflict with land use changes driven by the demand for food, fuel, and profit. It is necessary to recognize and advocate for better governance of forests more strongly given the importance of forests in meeting basic human needs in the future, making resources available for livelihoods and development, maintaining ecosystems and biodiversity, and addressing climate change mitigation and adaptation goals. Such advocacy must be coupled with financial incentives for governments of developing countries and a greater governance role for civil society and market actors if forests are to continue to provide benefits to humans well into the future.

Many scholars recognize the central importance of governance in influencing forest outcomes, but a review also shows major gaps in existing knowledge about the history and distribution of forest governance arrangements and in the understanding of how different features of governance affect outcomes. The challenge of understanding the coupled social and ecological systems (*22*) that all forest governance represents urgently needs more emphasis and attention than it has received until now.

References and Notes

1. Food and Agriculture Organization, *Global Forest Resources Assessment 2005* (FAO, Rome, 2005).
2. A. Grainger, *Proc. Natl. Acad. Sci. U.S.A.* **105**, 818 (2008).
3. T. M. Hayes, *World Dev.* **34**, 2064 (2006).
4. A. Karsenty, *Overview of Industrial Forest Concessions and Concession-Based Industry in Central and West Africa* (Centre de Coopération Internationale en Recherche Agronomique pour le Développement, Paris, 2007).
5. B. Cashore, F. Gale, E. Meidinger, D. Newsom, *Confronting Sustainability: Forest Certification in Developing and Transitioning Countries* (Yale University, New Haven, CT, 2006).
6. P. West, J. Igoe, D. Brockington, *Annu. Rev. Anthropol.* **35**, 251 (2006).
7. K. S. Zimmerer, R. E. Galt, M. V. Buck, *Ambio* **33**, 520 (2004).
8. K. P. Andersson, C. C. Gibson, *J. Policy Anal. Manage.* **26**, 99 (2007).
9. J. C. Ribot, A. Agrawal, A. Larson, *World Dev.* **34**, 1864 (2006).
10. P. Cronkleton, P. L. Taylor, D. Barry, S. Stone Jovicich, M. Schmink, *Environmental Governance and the Emergence of Forest-Based Social Movements* (Center for International Forestry Research, Bogor, 2008).
11. T. Dietz, E. Ostrom, P. Stern, *Science* **302**, 1907 (2003).
12. E. Ostrom, *Governing the Commons* (Cambridge Univ. Press, New York, 1990).
13. A. Molnar, S. J. Scherr, A. Khare, *Who Conserves the World's Forests?* (Forest Trends, Washington DC, 2004).
14. A. White, A. Martin, *Who Owns the World's Forests?* (Forest Trends, Washington DC, 2002).
15. R. Hardin, *Concessionary Politics in the Congo Basin* (WP #6, Institutions and Governance Program, World Resources Institute, Washington, DC, 2002).
16. M. Keller *et al.*, *Front. Ecol. Environ* **5**, 213 (2007).
17. E. E. Meidinger, *Hum. Ecol. Rev.* **4**, 52 (1997).
18. Food and Agriculture Organization, *Global Forest Resources Assessment 2000* (FAO, Rome, 2001).
19. Rights and Resources Initiative, *Transitions in Forest Tenure and Governance: Drivers, Projected Patterns and Implications* (RRI, Washington, DC, 2007).
20. A. Agrawal, A. Chhatre, *World Dev.* **34**, 149 (2006).
21. E. Ostrom, *Proc. Natl. Acad. Sci. U.S.A.* **104**, 15181 (2007).
22. J. Liu *et al.*, *Science* **317**, 1513 (2007).

23. The authors thank B. Adhikari, K. Andersson, D. Brown, C. Gibson, J. McAlpine, E. Ostrom, J. Ribot, and two anonymous reviewers for their comments on an earlier draft of the paper and R. Kornak, J. Miller, and A. Beata for help in preparing the maps. We gratefully acknowledge support from the Ford Foundation, the MacArthur Foundation, and two NSF grants numbered HSD-0527138 and CNH-0709545.

Supporting Online Material

www.sciencemag.org/cgi/content/full/320/5882/1460/DC1
Figs. S1 to S3
References

10.1126/science.1155369

Germination, Genetics, and Growth of an Ancient Date Seed

Sarah Sallon,[1] Elaine Solowey,[2] Yuval Cohen,[3] Raia Korchinsky,[3] Markus Egli,[4] Ivan Woodhatch,[4] Orit Simchoni,[5] Mordechai Kislev[5]

The ability of seeds to remain viable over prolonged periods of time is important in preserving plant genetic resources. Germination of a 1300-year-old lotus seed has been documented; however, other claims of exceptional seed longevity are controversial (*1*).

During the 1963–1965 excavations of Masada, an Herodian fortress overlooking the Dead Sea [built the second half of the first century before the common era (BCE), destroyed 70 common era (CE)], ancient seeds were discovered beneath rubble at the Northern Palace approach (*2*). Stored at room temperature for 4 decades, several seeds were obtained from this collection in 2005, all from the same archaeological area and botanically identified as dates (*Phoenix dactylifera* L.) (Fig. 1A).

Radiocarbon dating of two date seeds (controls) gave overlapping calibrated calendar ages of 102 ± 53 BCE (range from 206 BCE to 24 CE) and 13 ± 51 CE (range from 113 BCE to 128 CE) (2-σ level) (*3*).Three remaining intact seeds were planted after preparation in a quarantined site (*3*). After 8 weeks, one seed germinated. Its growth over 26 months demonstrated development similar to that of normal date seedlings propagated from modern seeds except for whitish patches on early leaves appearing to lack chlorophyll, possibly because of deficiency of essential nutrients during initial stages of germination (Fig. 1, B to D).

At 15 months, the seedling was transferred into a larger pot. Seed shell fragments clinging to rootlets were radiocarbon-dated (*3*), resulting in calibrated calendar age of 295 ± 47 CE (range 205 CE to 392 CE) (2-σ level). The difference in calendar ages between controls and germinated seed fragment appears to be due to seedling growth with incorporation of 2 to 3% modern carbon, which reduces the measured age by about 250 to 300 years (*4*) (table S1).

High summer temperatures and low precipitation at Masada may have contributed to the seed's exceptional longevity by minimizing free radical generation, an important cause of seed aging (*5*).

The date palm was domesticated over 5000 years ago, with the genotype of each cultivar highly conserved through clonal propagation of offshoots (*6*).

The Judean Dead Sea region was particularly famous for its extensive and high-quality date culture in the 1st century CE (*7*). Over the next 2 millennia, these historic cultivars were lost, and by the early twentieth century relatively few, low-quality date palms mostly propagated from seeds were recorded (*8*).

Preliminary genetic analysis of the germinated seedling and three elite date cultivars currently growing in Israel was performed with random amplified polymorphic DNA [RAPD (*3*)]. Of 399 specific DNA bands generated, over 50% were similar (monomorphic) between the seedling and Moroccan (Medjool), Egyptian (Hayani), and Iraqi (Barhee) cultivars. Polymorphic bands representing genetic differences were greatest compared with Moroccan (35.3%), with fewer differences between Iraqi (16.5%) and Egyptian (19.5%) cultivars (table S2 and fig. S1). As products of sexual reproduction, seedlings differ from their progenitors and original cultivar because each possesses a unique genotype, half paternally, half maternally derived.

On the basis of a single specimen of unknown origin, these data can therefore provide limited information on the genotype of ancient cultivars, but they are nevertheless important because they may contribute to our understanding of the contemporaneous Judean date population that flourished in the Dead Sea region 2000 years ago.

Germination of ancient seeds can provide valuable insights into the history of domestication and historic crops and has important implications for seed banking and conservation. Our case may also prove to be important to modern date palm cultivation.

References and Notes

1. J. Shen-Miller, *Am. J. Bot.* **82**, 1367 (1995).
2. Y. Yadin, *Isr. Explor. J.* **15**, 1 (1965).
3. Materials and methods are available as supporting material on *Science* Online.
4. M. Stuiver, H. A. Polach, *Radiocarbon* **19**, 355 (1977).
5. C. Bailly, *Seed Sci. Res.* **14**, 93 (2004).
6. D. Zohary, P. Spiegal-Roy, *Science* **187**, 319 (1975).
7. Pliny, *Natural History* (Harvard Univ. Press, Cambridge, MA, 1952), vol. XIII, ch. 9, pp. 44–46.
8. A. Grasovsky, J. Waitz, *Government of Palestine, Department of Agriculture and Forest Agriculture Leaflets IV: Horticulture*, vol. 29 (1932).

9. We thank E. Netzer, W. Stuppy, I. Kranner, and W. Baker for comments. Funded by the Louis L. Borick, Cammelia, Zanker, and Louise Gartner foundations.

Supporting Online Material

www.sciencemag.org/cgi/content/full/320/5882/1464/DC1
Materials and Methods
Fig. S1
Tables S1 and S2
References

30 November 2007; accepted 8 April 2008
10.1126/science.1153600

[1]Louis L. Borick Natural Medicine Research Center, Hadassah Medical Organization, Jerusalem 91120, Israel. [2]Arava Institute of the Environment, Kibbutz Ketura 88840, Israel. [3]Department of Fruit Tree Sciences, Agricultural Research Organization, Volcani Research Center 50250, Israel. [4]Radio-Carbon Laboratory, Department of Geography, University of Zurich, Winterthurerstrasse 190, 8057 Zurich, Switzerland. [5]Mina and Everard Goodman Faculty of Life Sciences, Bar-Ilan University, Ramat-Gan 52900, Israel.

Fig. 1. (**A**) Ancient date seeds from Masada. (**B**) Germinated seedling age 3 months: normal development of simple juvenile leaves. Height = 15 cm. (**C**) Age 7.5 months: some leaves showing white patches. Height = 31 cm. (**D**) Age 26 months: normal seedling development with compound leaves. Height = 121 cm. [Photo credit: G. Eisner]

An in Vivo Map of the Yeast Protein Interactome

Kirill Tarassov,[1]* Vincent Messier,[1]* Christian R. Landry,[1,2]* Stevo Radinovic,[1]* Mercedes M. Serna Molina,[1] Igor Shames,[1] Yelena Malitskaya,[1] Jackie Vogel,[3] Howard Bussey,[3] Stephen W. Michnick[1,2]†

Protein interactions regulate the systems-level behavior of cells; thus, deciphering the structure and dynamics of protein interaction networks in their cellular context is a central goal in biology. We have performed a genome-wide in vivo screen for protein-protein interactions in *Saccharomyces cerevisiae* by means of a protein-fragment complementation assay (PCA). We identified 2770 interactions among 1124 endogenously expressed proteins. Comparison with previous studies confirmed known interactions, but most were not known, revealing a previously unexplored subspace of the yeast protein interactome. The PCA detected structural and topological relationships between proteins, providing an 8-nanometer–resolution map of dynamically interacting complexes in vivo and extended networks that provide insights into fundamental cellular processes, including cell polarization and autophagy, pathways that are evolutionarily conserved and central to both development and human health.

The elucidation of protein-protein interaction networks (PINs, or interactomes) holds the promise of answering fundamental questions about how the biochemical machinery of cells organizes matter, information, and energy transformations to perform specific functions (*1*). An essential and rarely addressed question is whether protein complexes and PINs that are reconstructed or reconstituted in vitro or removed from the normal context in which they are expressed reflect their organization in living cells. For eukaryotes, the test bed for large-scale analysis of PINs is the yeast *Saccharomyces cerevisiae*, where several PIN analyses have been performed using yeast two-hybrid screens (Y2H) (*2*–*4*) or tandem affinity purification followed by mass-spectrometric analyses (TAP-MSs) (*5*–*8*). Each approach captures specific features of protein interactions; two-hybrid methods are best at measuring direct binary interactions between pairs of proteins, whereas affinity purification techniques best capture stable protein complexes. However, neither approach measures interactions between proteins in their natural cellular context, and are not easily amenable to studying protein complexes that are transiently associated or dynamic under different conditions, that do not survive in vitro purification, or that cannot be transported to the nucleus and form interactions in the absence of other

[1]Département de Biochimie, Université de Montréal Casier postal 6128, Succursale Centre-ville, Montréal, Québec H3C 3J7, Canada. [2]Centre Robert-Cedergren, Bio-Informatique et Génomique, Université de Montréal, C.P. 6128, Succursale Centre-ville, Montréal, Québec H3C 3J7, Canada. [3]Department of Biology, McGill University, 1205 Avenue Dr. Penfield, Montréal, Québec H3A 1B1, Canada.

*These authors contributed equally to this work.
†To whom correspondence should be addressed. E-mail: stephen.michnick@umontreal.ca

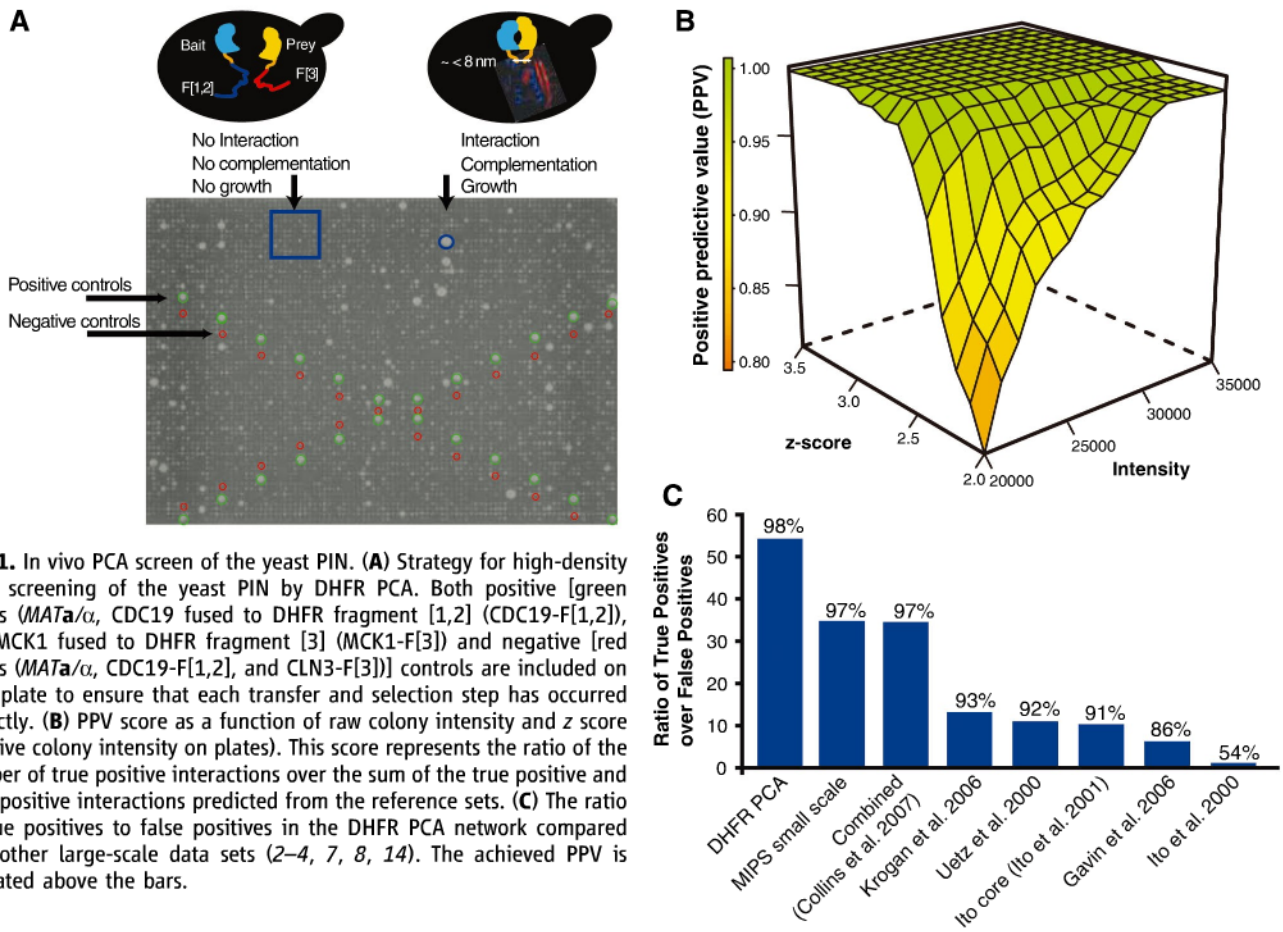

Fig. 1. In vivo PCA screen of the yeast PIN. (**A**) Strategy for high-density array screening of the yeast PIN by DHFR PCA. Both positive [green circles (*MAT***a**/α, CDC19 fused to DHFR fragment [1,2] (CDC19-F[1,2]), and MCK1 fused to DHFR fragment [3] (MCK1-F[3]) and negative [red circles (*MAT***a**/α, CDC19-F[1,2], and CLN3-F[3])] controls are included on each plate to ensure that each transfer and selection step has occurred correctly. (**B**) PPV score as a function of raw colony intensity and *z* score (relative colony intensity on plates). This score represents the ratio of the number of true positive interactions over the sum of the true positive and false positive interactions predicted from the reference sets. (**C**) The ratio of true positives to false positives in the DHFR PCA network compared with other large-scale data sets (*2*–*4*, *7*, *8*, *14*). The achieved PPV is indicated above the bars.

stabilizing interactions as necessitated in Y2H screening. Protein-fragment complementation assays (PCA) provide an alternative approach to detect protein-protein interactions (PPIs) in their natural context. In the PCA strategy, two proteins of interest are fused to complementary fragments of a reporter protein. If the proteins of interest interact physically, the reporter fragments are brought together and fold into their native structure, thus reconstituting the reporter activity of the PCA (Fig. 1A). PCA strategies provide a simple, direct means for the detection of PPIs in vivo, and do so with endogenously expressed full-length proteins in their native posttranslationally modified states and cellular locations (*9*). Further, PCAs provide spatial and topological information about PPIs. Thus, a large-scale PCA screen would provide direct insights into the global structural organization of PINs as they exist in the living cell.

Genome-wide in vivo screen. We have performed a systematic binary screen for PPIs at a genomewide scale in *S. cerevisiae* using a PCA based on the murine dihydrofolate reductase (mDHFR) assay adapted to yeast (*10*) (Fig. 1A). The DHFR PCA is a survival-selection assay based on a mutant of mDHFR that is insensitive to the DHFR inhibitor methotrexate but retains full catalytic activity and allows detection of PPIs with as few as 25 to 100 complexes per cell (*11*, *12*). We created unique homologous recombination cassettes for all 5756 consensus genes with both the F[1,2] and F[3] complementary N- and C-terminal DHFR fragment sequences (*10*). Successful cassette transformation of *S. cerevisiae* haploids was achieved for 4326 (75%) open reading frames (ORFs) with the DHFR F[1,2] fragment in *MAT***a** and 4804 (83%) ORFs with the DHFR F[3] fragment in *MAT*α strains, with a final combined coverage of 5367 (93%) of all ORFs (table S1). The entire screening process was performed on solid-phase medium (Fig. 1A and fig. S1). Briefly, *MAT***a** strains (F[1,2] fragment fusions) served as baits and were mated individually with all *MAT*α (F[3]) strains on high-density arrays. The resulting diploids were transferred to a minimal medium [synthetic complete (SC)] plate to select for methotrexate resistance (reconstituted mDHFR activity, with native *S. cerevisiae* DHFR inhibited), and colony growth was recorded using automated analysis of digital images (Fig. 1A and figs. S2 and S3). PPIs were determined based on the growth of the diploid colonies measured by the pixel intensities on the selection plates (figs. S1 to S3). In total, 3247 individual highly reproducible (fig. S4) bait screens were performed, resulting in more than 15 million individual matings.

Data filtering, quality assessment, and overlap with existing PINs. We experimentally accounted for two potential sources of false positives in a PCA screen: trapping of nonspecific complexes due to irreversible folding of the mDHFR reporter protein, and potential spontaneous complementation (folding) of the DHFR PCA fragments. First, we used the adenosine 3′,5′-monophosphate–dependent dissociation of the yeast protein kinase A complex as a test system (*13*) to show that the DHFR PCA is fully reversible, and thus the trapping of complexes is unlikely (*10*). Second, we screened all the strains against the individual F[1,2] and F[3] complementary fragments or fragment-peptide linker sequences. This allowed us to eliminate 344 promiscuous, highly expressed proteins (fig. S6 and table S2), several of which are also often observed as false-positives in affinity purifications (*10*). We next identified a threshold of colony intensity above which we could infer PPI. The Munich Information Center for Protein Sequences (MIPS) complexes were used as a standard set of true positives, along with 266,858 true negative interactions between proteins expressed in different cellular compartments or having negatively correlated expression (*14*, *15*). After several filtering steps (*10*) and benchmarking on the reference PPIs, we obtained a high-quality data set containing 2770 interactions among 1124 proteins that reach a positive predictive value (PPV) of 98.2% (Fig. 1B and tables S3 and S4). This resulted in data having precision (number of true positives relative to false positives) comparable to the MIPS small-scale experiments and all previous large-scale data sets (Fig. 1C and fig. S5). The proteins in the DHFR PCA network are highly enriched in cellular compartments [for example, organelle membranes ($P < 10^{-12}$), proteasome regulatory particles ($P < 10^{-8}$), the nucleolus ($P < 10^{-7}$), and the cell cortex ($P < 10^{-7}$)] that were less represented in comprehensive TAP-MS results (*14*) (tables S5 and S6). The high sensitivity of the DHFR PCA assay is reflected in the abundance of the proteins that populated our network, which are on average only slightly more expressed than the proteome [the median log10(protein abundance) = 2.32 versus 2.28; Wilcoxon rank sum test, $P = 0.19$] and spanning the whole distribution of protein abundance (fig. S6).

Because this study was performed in vivo, with a technique never used at this scale and in a different medium than previous experiments, we expected that many interactions would be previously undiscovered. An examination of major databases of PPIs reveals that most of the interactions (~80%) we report are among protein pairs for which no data had been previously reported (fig. S7A). However, when considering only PPIs that could be detected by both DHFR PCA and the other experiments (*10*), we confirmed between 16 and 41% of PPIs reported in previous large-scale screens, suggesting excellent concordance between the results of our and very different methods (figs. S7B and S8). Further, PPIs derived from PCA represent pairwise interactions, which contrasts with TAP-MS PINs, which identify clusters and thus complexes of interacting proteins. PPIs detected by PCA are therefore either within, between, or outside these complexes and thus complement these previous studies. For instance, 10% of the DHFR PCA PPIs map within specific complexes in the combined analyses of the two TAP-MS data sets (*7*, *15*), and 36 and 38% of the DHFR PCA PPIs are between one protein found in a complex and one protein not in the published data set, or two proteins not in the data set, respectively. We identified several inter-

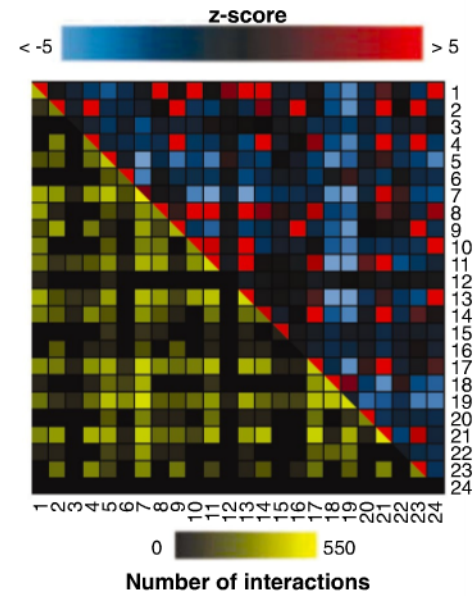

(1) Golgi apparatus; (2) cell cortex; (3) cell wall; (4) cellular bud; (5)unknown; (6) chromosome; (7) cytoplasm; (8) cytoplasmic membrane-bound vesicle; (9) cytoskeleton; (10) endomembrane system; (11) endoplasmic reticulum; (12) extracellular region; (13) membrane; (14) membrane fraction; (15) microtubule organizing center; (16) mitochondrial envelope; (17) mitochondrion; (18) nucleolus; (19) nucleus; (20) peroxisome; (21) plasma membrane; (22) ribosome; (23) site of polarized growth; (24) vacuole;

Fig. 2. Interactions are enriched within GO categories. The DHFR PCA network covers several classes of protein function, location, and biological process. The colors above the diagonal represent positive and negative deviations from the expected number of interactions between two cell compartments. A positive *z* score indicates a larger number of interactions within or between two categories as compared with a random network. A negative *z* score indicates a smaller number of interactions than expected. A *z* score of 2 or −2 corresponds to a *P* value of 0.05, and a *z* score of 5 or −5 to a *P* value of 5×10^{-7}. Values below −5 and above 5 were given these minimal and maximal values. Entries below the diagonal indicate the observed numbers of interactions on a $\log_{10}$ scale.

actions among complexes (15%), which probably mediate the integration of biological processes among PIN modules. For instance, PPIs occur among complexes that are more related in their functional annotations than would be expected to occur by chance [interacting protein pairs had a semantic similarity score of cell compartments (CCs) of 3.44 versus 1.64, $P < 10^{-100}$; of biological processes (BPs) of 3.48 versus 1.51, $P < 10^{-80}$; and of molecular functions (MFs) of 3.53 versus 2.3, $P < 10^{-10}$]. For example, we see interactions between Dhh1p and Lsm4p, both involved in the RNA metabolic process but part of the CCR4 and the RNA-splicing complex, respectively. Another example is the interaction between Reg1p and Snf1p: subunits of the serine-threonine phosphoprotein phosphatase and SNF1 complex, respectively, but both involved in the regulation of carbohydrate metabolic processes (table S7). Finally, we report 286 interactions involving one uncharacterized protein with proteins of known function ($n = 278$ interactions) or between two uncharacterized proteins ($n = 8$) (*16*), which will aid in their functional annotation.

General organization of the yeast DHFR PCA PIN. Because we detected PPIs as they occurred in intact cells, with the faithful representation of gene expression timing and protein localization, we predicted and observed stronger coregulation of interacting protein pairs (Pearson $r = 0.2$ versus $r = 0.1$, $P << 0.001$) than was expected for random networks of the same size with the same protein connectivity. This is also mirrored in the enrichment of interactions among proteins that share the same BPs, MFs, and CCs and a depletion of interactions among genes of different categories (Fig. 2 and fig. S9). PPIs among categories are somewhat more enriched in the PCA-determined network as compared with TAP-MS studies. For instance, 64, 56, and 63% of DHFR PCA interactions map to different BPs, CCs, and MFs, whereas these numbers are smaller in the TAP-MS PINs [58, 46, and 57% (*8*) and 51, 49, and 58% (*7*)]. Much of this increased enrichment of the cross-cellular components reflects interactions among proteins that the DHFR PCA method covers more of than TAP-MS; these are interactions that appear to represent the natural exchange of proteins between, for instance, the endoplasmic reticulum, Golgi, mitochondrial envelope, and vacuolar proteins, whereas others reflect the organization of complex cellular processes. For example, high enrichments in interactions between proteins localized to the bud and bud neck with those of the cell cortex, cytoskeleton, plasma membrane, and sites of polarized growth reflect the roles of these proteins in several compartments during cell division. We also saw strong compartmentalization of interactions; for example, for nuclear and nucleolar proteins, which show enrichment in interactions between proteins in these two compartments but strong depletions in interactions with those of any other compartment. Equally, patterns of cross-process and molecular function categories reflect differences in complexity and organization (fig. S9). For example, among molecular functions, RNA binding is specifically enriched in interactions between helicase and translation regulatory functions, whereas the more general transporter activity category shows links to diverse functions. The observation that PCA interactions detect links among functionally related categories is supported by a semantic analysis of the full Gene Ontology (GO) hierarchies. Proteins that show interactions with different GO Slim annotations have higher semantic similarities in their GO terms than expected by chance (CCs, 1.52 versus 0.94, $P < 10^{-231}$; BPs, 2.04 versus 1.35, $P < 10^{-122}$; and MFs, 1.89 versus 1.64, $P < 10^{-8}$), and may thus represent inter-

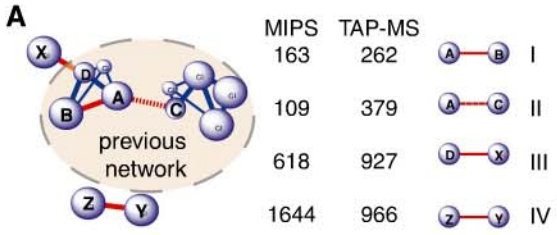

Type I. Binary, sterically accesible interaction previously inferred to be in a complex (number of proteins: MIPS = 145; Pu et al. 2007 = 270)

Type II. Binary, sterically accesible interaction not inferred to be within a complex (MIPS = 97; Pu et al. 2007 = 276)

Type III. Binary, sterically accesible interaction between one protein being in a complex and the other not in the dataset (MIPS = 173 & 317; Pu et al. 2007 = 279 & 350)

Type IV. Binary, sterically accesible interaction between two proteins not in the datasets (MIPS = 727; Pu et al. 2007 = 445)

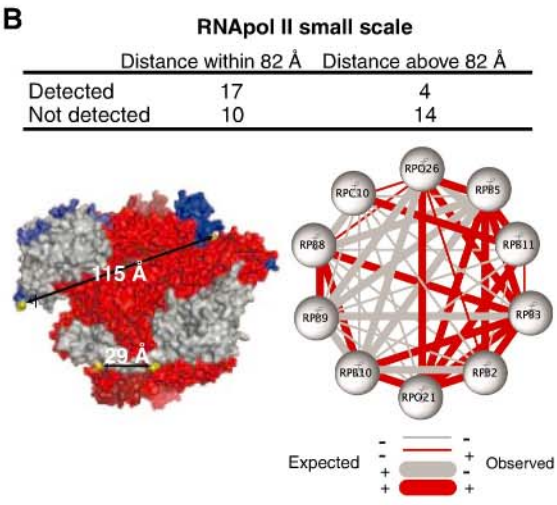

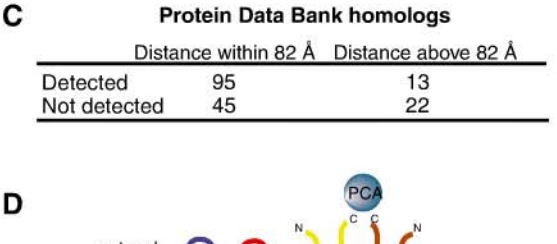

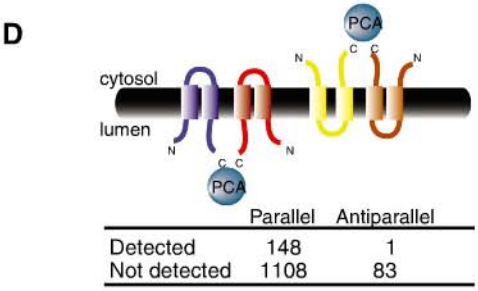

Fig. 3. The DHFR PCA results provide structural and topological insights. PCA fragments have to be in proximity to each other in order to fold into the active structure of the reporter protein. (**A**) PCA PPIs versus protein complexes. Comparison of the PCA network with databases of curated protein complexes (MIPS) and inferred from computational analysis of TAP-MS (*15*) allows classification of four types of PCA interactions: in which both proteins are found within a complex (type 1), are inferred to be in two separate complexes (type 2), one protein is in a complex and the other is not in the network (type 3), or both are absent from the network (type 4) (*15*). Columns of numbers indicate the number of PCA PPIs observed for each data set and each category. (**B**) A thorough DHFR PCA screen of the RNA polymerase II complex [Protein Data Bank (PDB) number 1I3Q] detects predicted interactions among the 10 subunits. (**C**) An interaction is 3.5 times more likely to be detected for a pair of proteins known to interact if the C termini of these proteins are within 82 Å of each other in the case of stable crystallized complexes of yeast-homologous proteins deposited in the PDB. (**D**) Membrane protein topology and PPI detection by PCA. A protein interaction is 12 times more likely to be detected if the C termini are in the same cell compartment.

actions relating information among these processes and CCs that allows their integration into higher-order networks. As we describe below, these interactions reveal specific spatial and topological relationships between known and previously unknown complexes underlying both known and previouly unknown cellular processes.

Global structure and topology of the in vivo interactome. PCA-detected interactions are interpreted differently than purified protein complexes or binary (one-to-one) interactions determined in Y2H screens, allowing us to address how protein complexes and PINs are spatially and topologically organized in living cells. Whether an interaction can be observed depends on the distance between the C termini of two proteins and the length of the polypeptide linker separating bait and prey proteins to the PCA fragments (*12*, *17*) (Fig. 1A). Given that the linkers used in this study were of 10–amino acid residues, for a given protein complex we expected to detect only binary (direct) or near-binary (indirect, C termini within 82 Å, but mediated by one or more other proteins) interactions for protein pairs separated by less than this distance. We first tested this prediction by exhaustively screening all pairwise interactions ($n = 45$ possible pairs) in the well-known RNA polymerase II complex (*10*). We found that we were 5.7 times more likely to detect an interaction if the C-termini were within 82 Å (Fisher's exact test, $P = 0.01$) (Fig. 3B). Interactions that were detected but not predicted could be due to alternative assemblies of this complex in intact cells, to changes in their configuration under different conditions, or to protein dynamics that cannot be interpreted from crystal structures. We then asked whether spatial restraint on observable interactions is reflected in the complete DHFR PCA network. An examination of homologous protein complexes with solved structures showed that we were 3.5 times more likely to detect an interaction between a pair of proteins that have C termini closer than 82 Å than for those with longer distances between C termini (Fisher's exact test, $P < 0.002$) (Fig. 3C). Further, we found that the interacting protein pairs possess domains known to mediate PPI more often than they would be expected to have possessed by chance (7.3% of protein pairs have domains known to mediate PPI versus 0.6%, $P << 0.001$). Thus, the data will be useful for predicting spatial relationships and the bases of molecular recognition among proteins, protein domains, and peptide recognition motifs. Finally, because the C termini of proteins have to be in close proximity and also oriented into the same cellular compartment, PCA provides information about membrane protein topology (Fig. 3D) (*11*, *18*–*20*). Our results demonstrate that the topology of interacting membrane proteins is also reflected in the PIN; specifically, that membrane proteins that colocalize to the same cellular compartment are 12 times more likely to show an interaction if they have a parallel rather than an antiparallel orientation (Fisher's exact test, $P < 0.0005$) (*21*). These PPIs between membrane-associated and membrane-associated and soluble proteins will serve to predict cross-compartment functional relationships, such as interactions of endoplasmic reticulum–associated membrane receptors and cytosolic or nuclear effector proteins.

Bird's-eye view of the yeast in vivo PIN. The general predictions described above led us to pose specific hypotheses for how protein complexes and networks are organized in living cells. Unsupervised hierarchical clustering of the 2770 DHFR PCA interactions provides an overview of the in vivo PIN (Fig. 4 and file S1). A number of crystallographically or biochemically well-characterized complexes are organized as clusters along the diagonal, confirming that their organization in cells reflects their predicted structures in vitro. Also, substructures of these clusters are consistent with those of previously affinity-purified subcomplexes. For instance, the nuclear pore contains a number of distinct subclusters, three of which clearly correspond to known subfractionated complexes (the Nup84 subcomplex includes Nup85, Nup120, and Nup145, which are in the network, and Nup84 and Seh1p, which are not in the network; a second subcomplex that includes Nup57, Nup49, and Nsp1, which are in the network, and Nic96, which is not in the network; the Nup82 subcomplex includes Nup159, Nup82, and Nsp1, which interacts with Nup166 for its proper localization) (*22*). These subcomplexes also represent groups of proteins that have been hypothesized to form direct contacts in a detailed architectural map of the assembly of the nuclear pore complex (*23*). Our results now suggest that such substructures exist in intact cells. Similarly, the proteasome partitions into subcomplexes that correspond to the composition of characterized fractions and of structures that can be visualized in intact cells (*24*). Complexes described in vitro can therefore accurately reflect those seen in vivo by PCA and as reported by whole-cell electron tomographic studies of protein complexes (*25*).

PPIs between complexes that reflect the cross-compartmental and cross-functional interactions described above (Fig. 2 and fig. S9) can be visualized as off-diagonal interactions on this map (Fig. 4). These represent links among several network modules that have been well described and shown to be central to eukaryotic cell biology. Our map therefore allows us to

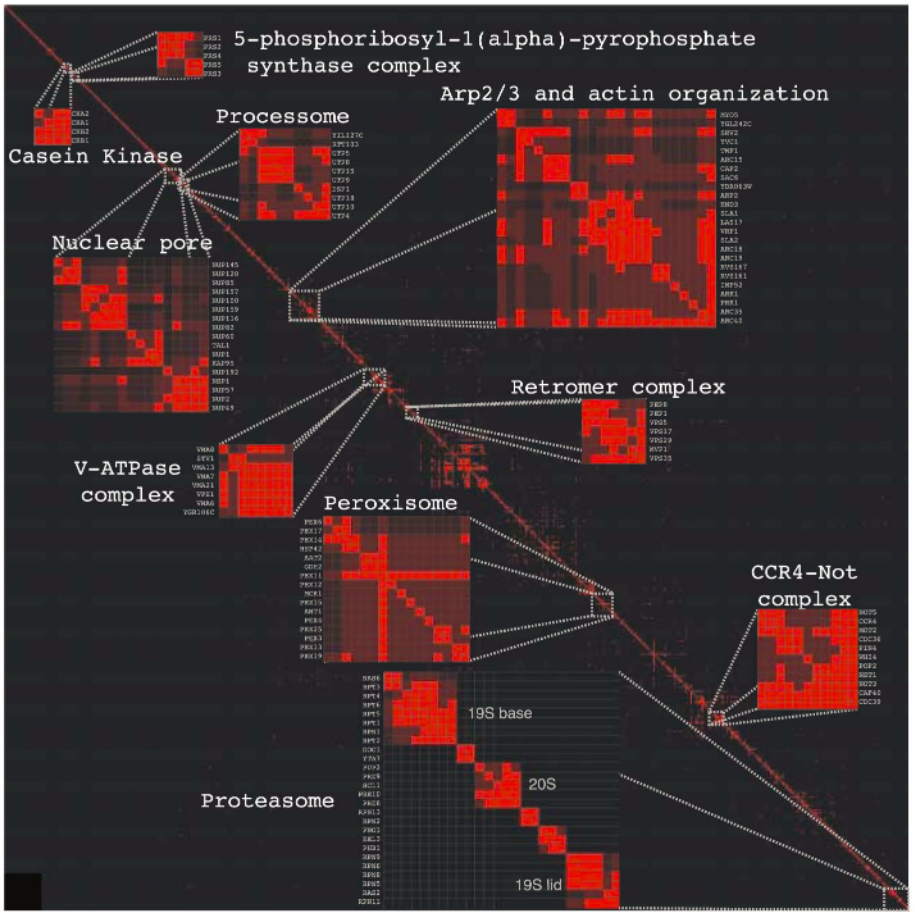

Fig. 4. The DHFR PCA network is modular and interconnected. Clustering of the DHFR PCA network reveals numerous known complexes, within which the substructure represents known subunits. Proteins that have interaction patterns similar to those of other proteins and that interact together are grouped along the diagonal.

identify previously unkown multifunctional PINs and to associate and integrate other proteins to these processes (Fig. 5). First, we showed that, starting from the Arp2-actin organization network, we are able to describe new connectivity among the complex network of interactions that integrates actin filament assembly and patch formation with secretion and cell-wall synthesis and ultimately with membrane abscission and cell separation during cell division. Second, we showed that starting from the retromer complex, we can physically integrate the protein-sorting machinery and trafficking with the synthesis of autophagosomes, links that were previously suggested from genetic and cell-biological observations.

In vivo network at the bud neck. Successful completion of a mitotic cell cycle, and the creation of a viable daughter cell, involves the tight coordination of nuclear events with mechanisms that control cell morphology. The formation of a bud is an example of this temporal and spatial coordination. The bud is the recipient of the segregated material from a mother cell, and ultimately will form the daughter cell. DNA, organelles, proteins, and mRNAs are selectively transported into the bud from the mother and after cytokinesis are enclosed within the daughter cell (*26*). After bud-site selection, recruitment and assembly of proteins that act in polarized growth and bud emergence occur at the incipient bud site. We can construct a network (Fig. 5A) that captures the dynamic assembly and localization of "polarisome" proteins and both known and previously unknown interactions to proteins that provide input signals from the cell-cycle machinery via specific cyclin–cyclin-dependent kinase 1complexes and the Rho signaling proteins that control polarity and cell integrity (*27*). These mechanisms organize and polarize the cytoskeleton and the secretory apparatus at the bud tip and bud neck during cell-cycle progression. Many polarisome proteins that localize to the bud and bud neck (Fig. 5A, blue), or predominantly to the neck (Fig. 5A, orange) are found in the PCA network. Bem1 plays a central role in bud polarization through its ability to build scaffolds, at sites of polarized growth, of an activator (Cdc24) and an effector (Ste20) of the Cdc42 Rho-like guanosine triphosphatase (GTPase) (*28*). Kel1 and Kel2 also act as scaffolds for polarity components at the bud tip and bud neck and were shown to couple to Bem1 and Spa2. Further, the exocyst complex functions in the vectoral transport of vesicles from the Golgi to the bud and promotes plasma membrane expansion, and the Arp2/3 complex, by mediating the assembly of actin patches, promotes membrane recycling through endocytosis (*29*). An extensive network of proteins containing the Arp2/3 actin-assembly complex, its activator Las17, and effectors of actin organization is represented in our network and recapitulates many known protein interactions (Fig. 5A, orange edges), but extends the level of connectivity among components (Fig. 5A, blue edges), especially for Sla2, Las17, and Arc40. However, Arc40 of the Arp2/3 complex is linked via Rvs161 to the GTPase-activating protein (GAP) Gyl1, known to function in actin-patch formation and polarized exocytosis; Gyl1 is also connected to the exocyst through the Sec4 GTPase and to Ynr065C (Fig. 5A), a large protein of previously unknown function and for which localization data are unavailable. In a further extension of this actin patch–assembly complex, we found that Las17 and Myo5, a type I myosin that associates with actin patches, interact with Syp1, a protein implicated in actin cytoskeletal organization. Further, we showed that Syp1 physically associates with multiple proteins, including the bud-neck septins Cdc11 and Shs1 and the cell-surface sensors Mid2 and Wsc2, which activate the cell-integrity pathway through Rom2. Collectively, the interactions among distinct complexes seen by PCA represent a potential regulatory network involved in bud polarization, bud-neck organization, and cytokinesis, a network that captures the dynamic transitions of polarity and exocyst components between the bud tip and the bud neck during the cell cycle.

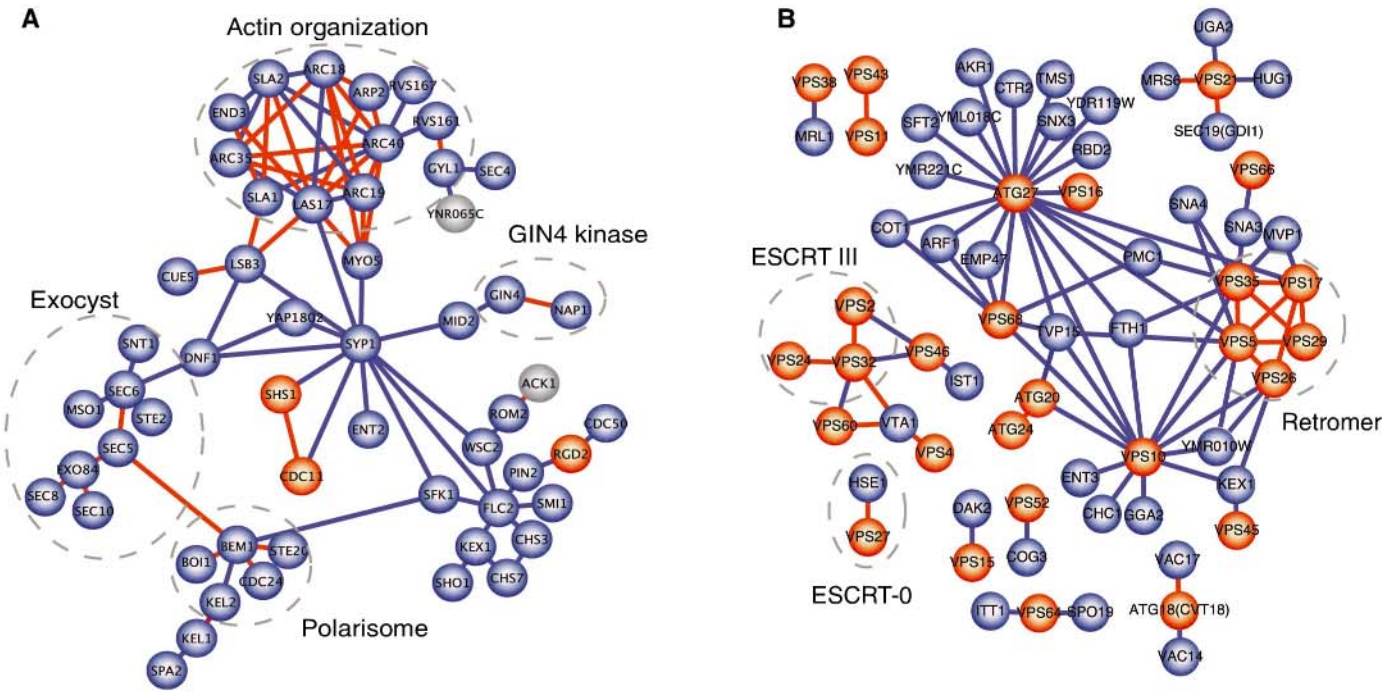

Fig. 5. The yeast DHFR PCA network provides insights into both cell polarity and autophagy. Blue edges denote previously unknown interactions (*10*) and orange edges denote interactions reported at least once in major databases. (**A**) Network at the bud neck. Physical association, detected by PCA between proteins that localize to the bud and bud neck (blue) and proteins that localize predominantly to the bud neck (orange), and proteins lacking localization data (gray), can be used to assemble the structure of a polarity PIN. This PIN shows both known interactions and previously unknown coupling between proteins involved in actin-filament organization and patch and assembly with proteins acting in secretion and cell-wall synthesis. The interactions between protein complexes in the PIN reflect the complex transition of proteins between the bud tip and the bud neck, which function in cell polarity from bud emergence to cytokinesis. (**B**) Autophagy network. Interactions directly connecting proteins involved in autophagy (ATG), vacuolar protein sorting (VPS), and cytoplasm-to-vacuole targeting (CVT) (orange) and other proteins (blue) are shown.

In vivo network of autophagy. Autophagy is the process whereby organelles and the cytosol are engulfed within membrane vesicles for delivery to the lysosome/vacuole for degradation and macromolecule recycling and is involved in development, response to stress, and pathogen resistance. Dysfunction of this conserved eukaryotic process is associated with neurodegenerative conditions, namely Huntington's, Alzheimer's, and Parkinson's diseases, and with cancer (*30*). Proteins involved in autophagy are rich in interactions in the yeast DHFR PCA network (Fig. 5B), including the endosomal sorting complexes required for transport (ESCRTs) ESCRT-0 and ESCRT-III, the retromer complex, and other known interactions (Fig. 5B, dashed gray circles). Vps32, Vps24, and Vps2 are three of the four subunits of the ESCRT-III complex that are responsible for the sorting of transmembrane proteins into the multivesicular body (MVB) pathway. Dysfunction of this complex leads to autophagosome accumulation and neurodegeneration in mammals (*31*). ESCRT-0 is required for sorting ubiquitinated membrane proteins before vacuolar degradation. Vta1 is a member of the MVB pathway and is known to bind to Vps60 and Vps4, regulating the activity of the latter (*31*). Proteins destined for secretion or for delivery to intracellular compartments follow the same route and are sorted in the trans-Golgi network. In yeast, the lysosomal/vacuolar proteins are sorted from other proteins by the carboxypeptidase Y receptor Vps10. These receptors are then returned from the prevacuolar compartments to the trans-Golgi network by the retromer complex. The role of the retromer complex in protein transport is also crucial in metazoa because, for example, it is essential to the formation of important morphogen gradients along body axes (*32*). Some of the interactions we uncovered shed light on this functional relationship between protein sorting and trafficking by the retromer complex and Vps10. For instance, we find that Vps10 shows physical interactions with the retromer complex, which was previously hypothesized on the basis of genetic interactions with Vps35 and Vps26 (*33*, *34*). These observations also suggest a topological relationship between these two proteins that add to our understanding of the structural organization of the retromer complex recently resolved by crystallography (*35*). The interaction between Chc1 (clathrin heavy chain 1 human homolog), the clathrin heavy chain involved in protein transport and endocytosis, and Vps10 was also hypothesized based on genetic data that shows Vps10 is rerouted to the plasma membrane in a *chc1 vps1* mutant instead of its normal travel to the endosome (*36*). We confirm this functional relationship and show that it is mediated through a physical interaction. Most of the interactions we see are previously undescribed (75%) (Fig. 5, blue edges) and represent a substantial advance in describing the autophagy and cytoplasm-to-vacuole targeting pathways. For instance, Atg27 shows a particularly large number of interactions. This protein plays a critical role in the formation of sequestering vesicles, including autophagosomes. It localizes to the Golgi apparatus, the mitochondrion, and the phagophore assembly site. Despite its importance, it showed no interactions in recent large-scale TAP-MS experiments and only one in previous Y2H screens (*3*). Recent work affirms its involvement in both bulk and specific autophagy, and it is hypothesized that Atg27 (along with Atg9, not represented here) labels the membrane source for its transport to and the formation of autophagosomes (*37*). Our results suggest that Atg27 occupies a central role in autophagy because it physically interacts with the retromer complex and with many other vacuolar proteins involved in the sorting of vacuolar hydrolases; further, these results implicate uncharacterized ORFs, such as YML018C, YMR221C, and YDR119W, in this process.

Conclusions. There remain many insights to be drawn beyond the general details, overview, and examples of extended structural and functional networks reported here for the in vivo protein interactome, and other dimensions of the interactome remain to be explored: How dynamic are these interactions? What are the effects of growth conditions on PPI network architecture? The functional and integrative genomic tools developed for this study will enable analysis of protein-interaction dynamics on any scale to uncover mechanisms of biochemical network regulation. A wide variety of PCA reporter enzymes can be used to study temporal and spatial dynamics of protein interactions over a broad range of time scales (from seconds to many hours) and under the influence of natural or artificial perturbations (*9*). Further, the topological requirements of PCA generate a protein-complex topology map at 8-nm resolution that will provide reference data for studying the spatial dynamics of functional protein complexes by immunofluorescence or by monitoring the localization of proteins genetically tagged with fluorescent proteins. Finally, they will also provide reference constraints for determining the architecture of macromolecular assemblies (*23*). The integration of the results from such efforts with those of gene regulation dynamics and protein modifications will lead to a fuller understanding of how complex cellular processes are orchestrated at a molecular and structural level in the living cell.

References and Notes

1. J. Monod, paper presented at the Proceedings of the Eleventh Nobel Symposium, Sodergarn, Lidingo, County of Stockholm, 1968.
2. T. Ito *et al.*, *Proc. Natl. Acad. Sci. U.S.A.* **97**, 1143 (2000).
3. P. Uetz *et al.*, *Nature* **403**, 623 (2000).
4. T. Ito *et al.*, *Proc. Natl. Acad. Sci. U.S.A.* **98**, 4569 (2001).
5. Y. Ho *et al.*, *Nature* **415**, 180 (2002).
6. A. C. Gavin *et al.*, *Nature* **415**, 141 (2002).
7. A. C. Gavin *et al.*, *Nature* **440**, 631 (2006).
8. N. J. Krogan *et al.*, *Nature* **440**, 637 (2006).
9. S. W. Michnick, P. H. Ear, E. N. Manderson, I. Remy, E. Stefan, *Nat. Rev. Drug Discov.* **6**, 569 (2007).
10. Materials and methods are available as supporting material on *Science* Online.
11. I. Remy, S. W. Michnick, *Proc. Natl. Acad. Sci. U.S.A.* **96**, 5394 (1999).
12. J. N. Pelletier, K. M. Arndt, A. Pluckthun, S. W. Michnick, *Nat. Biotechnol.* **17**, 683 (1999).
13. E. Stefan *et al.*, *Proc. Natl. Acad. Sci. U.S.A.* **104**, 16916 (2007).
14. S. R. Collins *et al.*, *Mol. Cell. Proteomics* **6**, 439 (2007).
15. S. Pu, J. Vlasblom, A. Emili, J. Greenblatt, S. J. Wodak, *Proteomics* **7**, 944 (2007).
16. T. R. Hughes, L. Pena-Castillo, *Genetics* **176**, 7 (2007).
17. I. Remy, I. A. Wilson, S. W. Michnick, *Science* **283**, 990 (1999).
18. M. Diehn, M. B. Eisen, D. Botstein, P. O. Brown, *Nat. Genet.* **25**, 58 (2000).
19. J. P. Miller *et al.*, *Proc. Natl. Acad. Sci. U.S.A.* **102**, 12123 (2005).
20. A. A. Zamyatnin Jr. *et al.*, *Plant J.* **46**, 145 (2006).
21. H. Kim, K. Melen, M. Osterberg, G. von Heijne, *Proc. Natl. Acad. Sci. U.S.A.* **103**, 11142 (2006).
22. M. Damelin, P. Silver, *Biophys. J.* **83**, 3626 (2002).
23. F. Alber *et al.*, *Nature* **450**, 683 (2007).
24. O. Medalia *et al.*, *Science* **298**, 1209 (2002).
25. S. Nickell, C. Kofler, A. P. Leis, W. Baumeister, *Nat. Rev. Mol. Cell Biol.* **7**, 225 (2006).
26. V. J. Cid *et al.*, *Microbiology* **148**, 2647 (2002).
27. D. McCusker *et al.*, *Nat. Cell Biol.* **9**, 506 (2007).
28. H. O. Park, E. Bi, *Microbiol. Mol. Biol. Rev.* **71**, 48 (2007).
29. D. Pruyne, A. Legesse-Miller, L. Gao, Y. Dong, A. Bretscher, *Annu. Rev. Cell Dev. Biol.* **20**, 559 (2004).
30. T. Shintani, D. J. Klionsky, *Science* **306**, 990 (2004).
31. J. A. Lee, A. Beigneux, S. T. Ahmad, S. G. Young, F. B. Gao, *Curr. Biol.* **17**, 1561 (2007).
32. D. Y. Coudreuse, G. Roel, M. C. Betist, O. Destree, H. C. Korswagen, *Science* **312**, 921 (2006).
33. S. F. Nothwehr, S. A. Ha, P. Bruinsma, *J. Cell Biol.* **151**, 297 (2000).
34. J. V. Reddy, M. N. Seaman, *Mol. Biol. Cell* **12**, 3242 (2001).
35. A. Hierro *et al.*, *Nature* **449**, 1063 (2007).
36. O. Deloche, R. W. Schekman, *Mol. Biol. Cell* **13**, 4296 (2002).
37. W. L. Yen, J. E. Legakis, U. Nair, D. J. Klionsky, *Mol. Biol. Cell* **18**, 581 (2007).

38. V.M., S.R., M.S., I.S., and Y.M. performed the experiments; S.R. designed the automated robotic procedures; K.T., C.R.L., and S.W.M. analyzed the results; and H.B. helped plan the research and edited the manuscript, which C.R.L., S.W.M., V.M., and J.V. wrote. We thank N. Aubin-Horth and D. Klionsky for comments on the manuscript, J.-F. Paradis for technical and management support, J. Vlasblom for providing scripts and data files, and N. Barkai for providing the gene expression profile compendium. Supported by grants from Genome Canada, Genome Quebec, and the Canadian Institutes of Health Research (CIHR) (MOP-152556) to S.W.M. S.W.M. holds the Canada Research Chair in Integrative Genomics. C.R.L. is a Natural Sciences and Engineering Research Council of Canada and CIHR Strategic Training Program in Bioinformatics postdoctoral fellow.

Supporting Online Material

www.sciencemag.org/cgi/content/full/1153878/DC1
Material and Methods
Figs. S1 to S11
Tables S1 to S9
File S1
References

7 December 2007; accepted 23 April 2008
Published online 8 May 2008;
10.1126/science.1153878
Include this information when citing this paper.

Recognition Dynamics Up to Microseconds Revealed from an RDC-Derived Ubiquitin Ensemble in Solution

Oliver F. Lange,[1]* Nils-Alexander Lakomek,[2]* Christophe Farès,[2] Gunnar F. Schröder,[1] Korvin F. A. Walter,[2] Stefan Becker,[2] Jens Meiler,[3] Helmut Grubmüller,[1] Christian Griesinger,[2]† Bert L. de Groot[1]†

Protein dynamics are essential for protein function, and yet it has been challenging to access the underlying atomic motions in solution on nanosecond-to-microsecond time scales. We present a structural ensemble of ubiquitin, refined against residual dipolar couplings (RDCs), comprising solution dynamics up to microseconds. The ensemble covers the complete structural heterogeneity observed in 46 ubiquitin crystal structures, most of which are complexes with other proteins. Conformational selection, rather than induced-fit motion, thus suffices to explain the molecular recognition dynamics of ubiquitin. Marked correlations are seen between the flexibility of the ensemble and contacts formed in ubiquitin complexes. A large part of the solution dynamics is concentrated in one concerted mode, which accounts for most of ubiquitin's molecular recognition heterogeneity and ensures a low entropic complex formation cost.

Protein function relies on structural protein dynamics, with time scales ranging from picoseconds to beyond seconds. For molecular recognition, for example, proteins adapt their structure to different binding partners, often exhibiting large structural heterogeneity. In the past 30 years, atomic information on many dynamical processes has been accumulated from a broad variety of techniques (*1*, *2*). Nuclear magnetic resonance (NMR) relaxation has been used to quantitatively probe protein dynamics at the fast end (picoseconds to nanoseconds) as well as in a much slower range (microseconds to milliseconds) of this broad spectrum of time scales (*3*–*6*). Relaxation of nuclear magnetization is caused by fluctuations of magnetic interactions between nuclei resulting from the nanosecond rotational tumbling of the molecule and internal dynamics. The amplitudes of these motions are expressed as so-called Lipari-Szabo order parameters S^2_{LS} (*7*). Internal dynamics slower than the rotational tumbling time τ_c have no impact on the overall fluctuation of the magnetic interactions. Therefore, S^2_{LS} order parameters reflect only sub-τ_c motions, at the fast end of time scales.

The slow range of time scales is accessible by relaxation dispersion measurements, based on the stochastic fluctuations of isotropic chemical shifts, which are independent of rotational tumbling (*3*, *5*). Conformational heterogeneity slower than 10 ms can be directly observed as peak splitting in NMR spectra. For backbone amides, motions faster than 50 μs do not result in sufficient line broadening to be detectable for relaxation dispersion measurements. These measurements therefore probe motions slower than about 50 μs up to about 10 ms and have been used to characterize major structural changes and enzymatic reactions (*6*, *8*). Except for certain favorable cases (*9*), it is, however, difficult to translate these fluctuations into ensembles of structures. Therefore, relaxation-based ensembles of solution structures take only motions faster than τ_c into account: They are limited to sub-τ_c dynamics (*10*, *11*). These sub-τ_c motions are typically much smaller than the structural changes involved in molecular recognition and are likely to contribute mainly to the entropy of proteins (*12*–*14*). As a consequence, the structural heterogeneity observed in protein complexes has frequently been assumed to be inaccessible to equilibrium fluctuations in solution, thus favoring induced-fit models (*15*, *16*).

RDCs probe supra-τ_c dynamics. RDCs are sensitive to motion from picoseconds to milliseconds, which includes the previously invisible time window between τ_c and 50 μs, which we will call supra-τ_c. Indeed, RDCs recorded for ubiquitin, as well as for the B1 domain of protein G, hint at substantial dynamics between nanoseconds and microseconds (*17*–*25*). Here, we present a structural ensemble of ubiquitin based on an extensive

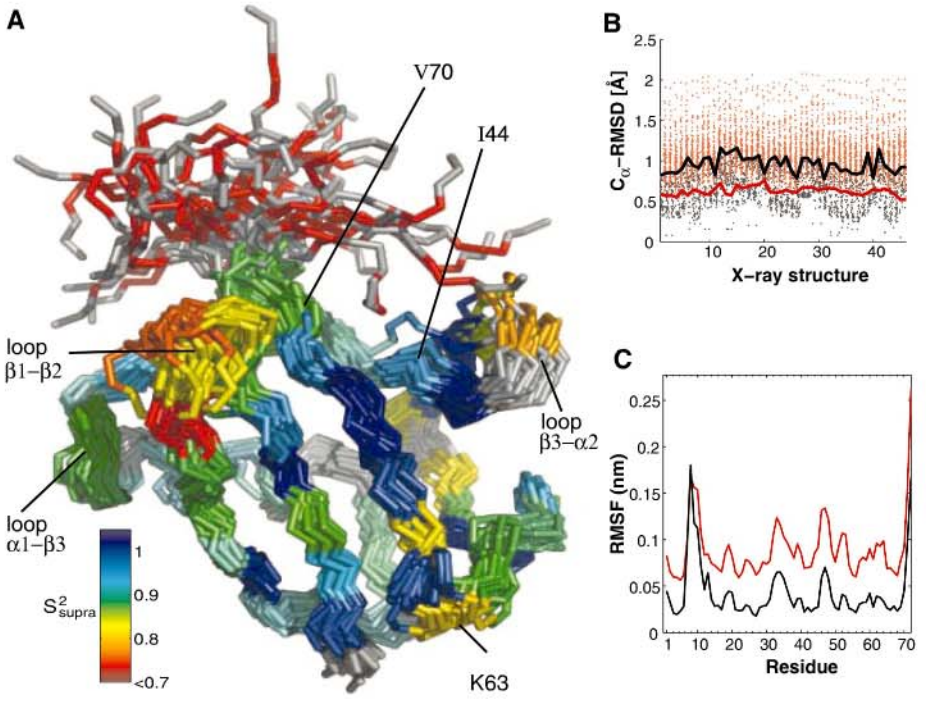

Fig. 1. Structure ensemble of ubiquitin. (**A**) Backbone trace of 40 randomly chosen structures from the EROS ensemble. Residues are colored by the amount of additional (supra-τ_c) mobility as compared with the Lipari-Szabo order parameters (Fig. 3C) $S^2_{supra} = S^2_{EROS}/S^2_{LS}$. (**B**) For each x-ray structure (for numbering on the *x* axis, see table S3), the backbone RMSDs of residues 1 to 70 are shown for superpositions with each EROS structure (red dots) and each x-ray structure (black dots). The minimal RMSD for EROS structures (red line) and the maximal RMSD for x-ray structures (black line) are highlighted to guide the eye. (**C**) Cα root mean square fluctuations (RMSF) of EROS structures (red line) and of 46 known ubiquitin x-ray structures (black line).

[1]Department of Theoretical and Computational Biophysics, Max Planck Institute for Biophysical Chemistry, Am Fassberg 11, 37077 Göttingen, Germany. [2]Department of NMR Based Structural Biology, Max Planck Institute for Biophysical Chemistry, Am Fassberg 11, 37077 Göttingen, Germany. [3]Vanderbilt University Center for Structural Biology, Nashville, TN 37212, USA.

*These authors contributed equally to this work.
†To whom correspondence should be addressed. E-mail: cigr@nmr.mpibpc.mpg.de (C.G.); bgroot@gwdg.de (B.L.dG.)

RDC data set (Fig. 1). Ubiquitin is a key to many cellular signaling networks (*26*, *27*) (as in protein degradation, for example) and is recognized by a broad variety of proteins with high specificity (*28*). Accordingly, ubiquitin crystal structures of 46 different complexes show a particularly pronounced structural heterogeneity (Fig. 2), which cannot be explained from the available sub-τ_c ensembles refined against NMR relaxation data (*10*, *11*) (Fig. 2, C and E).

RDCs are observed in an anisotropic solution, induced (for example) by a highly diluted liquid crystalline medium (*29*) or a polyacryl amide gel. In such an anisotropic solution, the protein does not adopt all orientations with the same probability. Therefore, the rotational tumbling no longer averages the dipolar coupling to zero but to a measurable RDC. The anisotropic orientation distribution is represented by an alignment tensor, which is fixed to the molecular frame. For directly bonded nuclei, the RDC D depends only on the direction (θ,ϕ) of the internuclear vector in the alignment frame

$$D(\theta,\varphi) = D_a\left[(3\cos^2\theta - 1) + \frac{3}{2}R(\sin^2\theta\cos 2\varphi)\right] \quad (1)$$

where D_a is the axial component of the alignment tensor and R describes its rhombicity (*17*, *29*). Internal dynamics lead to orientational fluctuations of the internuclear vector (θ,ϕ) in the alignment frame (and therefore also in the molecular frame) and affect the size of the RDC according to Eq. 1. This variation of the RDC is usually in the range of less than 10 Hz, and therefore the RDC D is averaged to the measured $\langle D\rangle$ for motions faster than the upper limit of relaxation dispersion (10 ms), thus sampling the previously inaccessible supra-τ_c time window.

Because the alignment tensor includes five parameters, the extraction of these fluctuations requires the measurement of RDCs in at least five independent alignment media. To assess the supra-τ_c time scale for ubiquitin, we measured RDCs for the backbone amide NH couplings in 18 different alignment conditions, as well as backbone H^NC' (amide proton to carbonyl carbon in the same peptide bond) and NC′ (amide nitrogen to carbonyl carbon in the same peptide bond) RDCs from 4 different alignment media. Together with data from the literature (*30*–*32*), 36 NH RDC data sets and 6 H^NC' and NC′ RDC data sets were available. To probe side-chain dynamics as well, we included side-chain methyl group RDCs measured for 11 alignment media in the analysis (*33*).

Supra-τ_c ubiquitin ensemble reveals conformational selection. To extract a structural ensemble from these data, we carried out cross-validated ensemble refinement from unfolded structures in explicit solvent subjected simultaneously to restraints from NMR nuclear Overhauser enhancement (NOE) and RDC data (henceforth referred to as EROS for ensemble refinement with orientational restraints). The unperturbed protein exhibits considerable flexibility, with a substantial fraction (color coded, Fig. 1A) attributed to supra-τ_c. Slower motions, at the microsecond-to-millisecond time scale, have previously been observed for only a very limited number of residues (*34*), thus confining the additional motion to the time range between the correlation time and about 50 μs. As a cross-validation, the ensemble was also calculated without NOEs. The resulting ensemble was found to be virtually unchanged [(*33*), EROS4], indicating that the ensemble is predominantly defined by the RDC data.

Unexpectedly, this supra-τ_c ensemble comprises the complete range of crystallographically observed structural changes during interface engagement (Figs. 1B and 2A), in contrast to the known fast dynamics (Fig. 2, C and E) (*10*, *11*). Indeed, each of the x-ray structures is similar to members of the solution ensemble within less than 0.8 Å backbone root mean square deviation (RMSD) (Fig. 1B), although no crystallographic data have been used during refinement. Conformational selection, rather than induced fit, thus suffices to explain all known structural adaptations that the ubiquitin backbone undergoes upon complex formation with different binding partners. Remaining induced-fit motions are restricted to rotameric side-chain rearrangements and minor backbone changes.

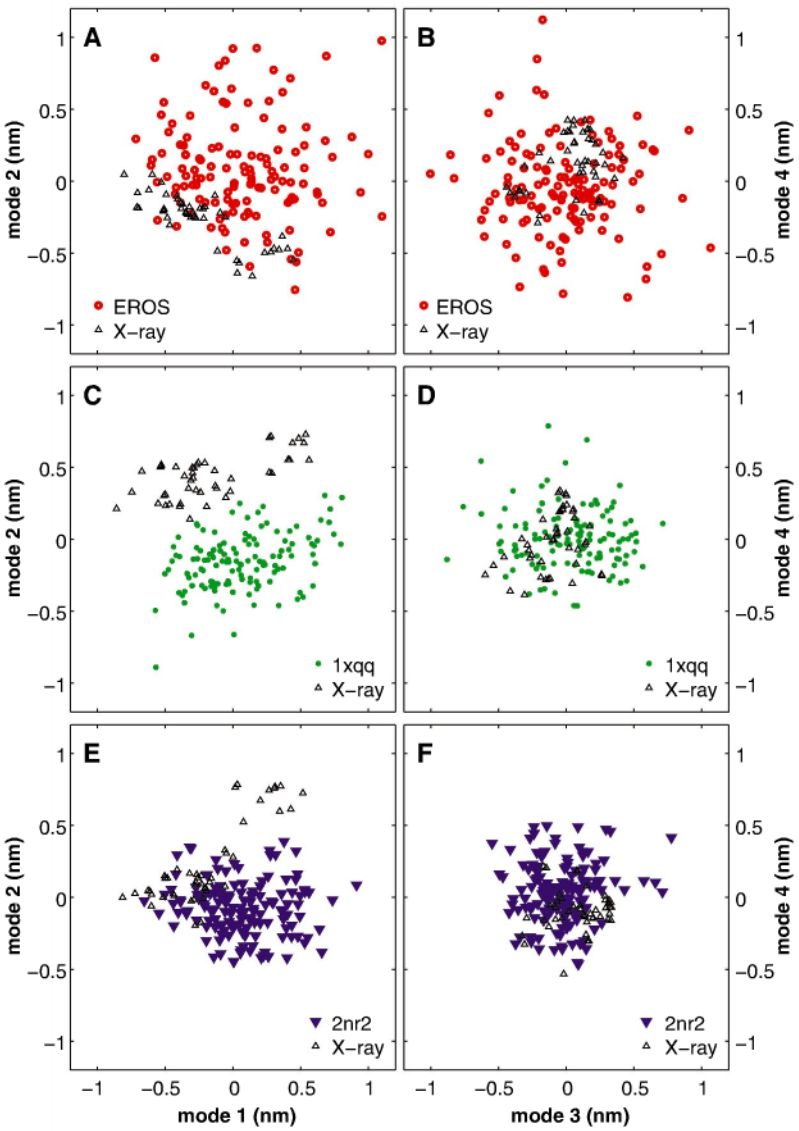

Fig. 2. Comparison of supra-τ_c and sub-τ_c solution ensembles (colors) with the collection of 46 x-ray structures (black) of ubiquitin by PCA: EROS (**A** and **B**), 1xqq (**C** and **D**), and 2nr2 (**E** and **F**). The PCA was carried out over the merged two ensembles that are displayed (in each case, the x-ray ensemble and one NMR ensemble: EROS, 1xqq, and 2nr2). Panels (A), (C), and (E) show projections onto the principal modes 1 and 2, whereas panels (B), (D), and (F) show projections onto modes 3 and 4. Systematic deviations are observed along the principal modes for both sub-τ_c ensembles but not for the supra-τ_c EROS ensemble.

As an independent validation of our ensemble, we have also applied a self-consistent RDC-based model-free (SCRM) analysis (*33*) to the set of 36 NH RDC experiments. This method is an enhanced implementation of the previously published model-free method (*21*, *24*, *25*) that largely alleviates structural bias (*33*). The SCRM analysis quantifies dynamics as the degree of orientational restriction of the amide NH bond in the molecular frame in terms of a generalized order parameter S^2(NH), which is zero for complete isotropic disorder and one for a fixed orientation of the respective NH bond. For comparison, generalized order parameters were also computed from the EROS ensemble. A correlation coefficient $r = 0.74$ between S^2_{SCRM} and S^2_{EROS} is found (Fig. 3A). This agreement between two independent approaches shows that the dynamics observed in the EROS ensemble are indeed strongly determined by the experimental RDC data. This conclusion is supported by rigorous cross-validation implemented in EROS by systematically leaving out all RDCs between backbone amide N and carbonyl C, as well as all scalar couplings, from refinement. The ensemble-averaged free RDC *R*-factor of 18.5% is considerably lower than for other solution ensembles (>24%; table S2). Combining all x-ray structures into an "ensemble" (*35*), we obtained a similarly low *R*-factor of 18.3%. As compared with the *R*-factor of 25 ± 4% for individual x-ray conformers, this result confirms that the conformational heterogeneity (as found in the EROS ensemble and in the x-ray data) considerably improves the description of the experimental solution NMR data. In addition, the correlation between order parameters derived from the x-ray "ensemble," particularly when relaxed in short (10-ps) molecular dynamics simulations at 300 K [Fig. 3B; (*33*)], and the RDC-derived order parameters S^2_{EROS} and S^2_{SCRM} suggests that the interconversion between the different ubiquitin conformations in the x-ray ensemble strongly contributes to the solution dynamics.

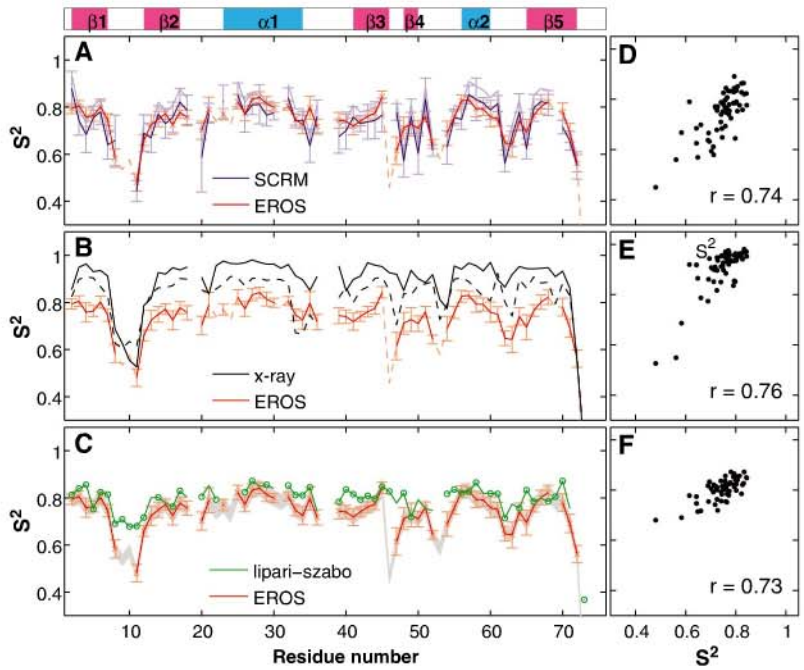

Fig. 3. Comparison of NH order parameters of ubiquitin. (**A** and **D**) The order parameters of the presented EROS ensemble (red) are compared with SCRM order parameters (blue) derived from the NH part of the RDC data used for EROS. The SCRM order parameters shown in dark blue reflect the most probable overall scaling with respect to the Lipari-Szabo–derived order parameters S^2_{LS}. The most conservative scaling of SCRM order parameters to S^2_{LS} is shown in light blue. (**B** and **E**) Order parameters intrinsic to the ensemble of 46 crystallographic structures (black). The dashed curve is obtained when the 46 structures are relaxed at 300 K by short molecular dynamics simulations of 10 ps. (**C** and **F**) Generalized order parameters obtained from NMR relaxation data (green) for the sub-τ_c dynamics of ubiquitin via Lipari-Szabo model-free analysis (*36*). Green circles mark the data points taken from the most recent and accurate measurement (*36*), whereas remaining data points are taken from previously published data (*46*). The latter (*46*) were rescaled such that they align with the newer results (*36*). The EROS order parameters were scaled by 0.93 to account for limited ensemble size and underestimation of the librational contribution (SOM text S4). Error bars (1σ) for the EROS ensemble (light-red) comprise intrinsic sampling and force-field errors as well as propagated experimental errors. The uncertainty in the libration correction was estimated as ±4% and is represented in gray. A solid line is shown for residues where sufficient RDC data were available to determine a robust value with SCRM analysis; for the other positions, EROS order parameters are shown as a dashed line. [(D) to (F)] Scatterplots for a direct comparison of the two sets of order parameters shown to the left of the respective plot.

To assess how much of the solution dynamics is slower than τ_c, we compare S^2_{EROS} and S^2_{SCRM} with order parameters derived from NMR relaxation measurements. The picosecond-to-nanosecond time scale dynamics of the ubiquitin backbone were probed previously by NMR relaxation techniques, yielding a set of S^2_{LS} order parameters as derived from a Lipari-Szabo analysis (*7*, *36*). Figure 3C compares order parameters S^2_{EROS} from the ensemble presented in Fig. 1A with S^2_{LS} order parameters. For most residues, additional mobility is seen, thus quantifying the supra-τ_c motion in the EROS ensemble, shown as color code in Fig. 1A. For EROS, absolute order parameters were derived from the RDC-refined ensemble and corrected for limited ensemble size and libration effects. For SCRM analysis, the absolute scale was determined relative to S^2_{LS} order parameters, with S^2_{LS} as an upper bound for S^2_{SCRM}, within the error bars [see supporting online material (SOM) text S1, section 1.2, and SOM text S4 for details]. Although the RDCs do not provide the absolute amplitude of the dynamics, the overall scale of the independently determined S^2_{EROS} and S^2_{SCRM} is nearly identical.

Solution fluctuations allow for interface contact formation. As noted above, the supra-τ_c motion accesses all the conformations that are observed in complex structures. To rationalize this unexpected result, we overlaid all interface-contacts (gray spheres) of the different binding partners found in the x-ray structures with a single structure of ubiquitin whose coloring represents the solution dynamics as given by S^2_{EROS}(NH) (Fig. 4A). Notably, helix α1, for which no contacts are observed, shows only little motion in solution (blue), whereas high flexibility (orange-red) is observed in regions that form many different protein-protein interfaces. A quantitative analysis of the number of interface contacts per residue (Fig. 4C) shows an unexpectedly high similarity to the conceptually unrelated order parameters S^2_{EROS}(NH), which corroborates this initial observation.

Two prominent exceptions from the observed high flexibility in the binding regions are residues Ile^{44} and His^{68} [I44 and H68 (*37*)] (two of the three "x" symbols in Fig. 4C). Both are known from mutation studies to be central hotspot (*38*) residues of a binding motif (Fig. 4B) that is involved in recognition of many different binding partners (*26*, *39*). Recently, the first crystal structure with a new recognition motif centered at hotspot D58 (one of the three "x" symbols in Fig. 4C) has been found (*40*). Our results show that, in solution, this residue is as rigid as I44/F45 and H68.

At first sight, the observed fluctuations appear incompatible with the proposed conformational

selection scenario. In particular, it seems combinatorially highly unlikely to find all involved residues simultaneously in the proper configuration required for binding, thus imposing a high entropic barrier. Only concerted fluctuations, implying reduced entropic cost, would explain the observed high physiological on-rates and affinities (*39*).

Collective molecular recognition dynamics. To check whether such concerted fluctuations are actually observed in the ubiquitin ensemble, we have carried out a principal component analysis (PCA). The conformational changes observed in x-ray structures are well described within the first five principal components. Although the number of degrees of freedom is reduced from 1839 to only 5, all x-ray structures can be described up to a backbone RMSD of 0.45 ± 0.04 Å. From linear combinations of these five principal components, we found a single collective mode that corresponds to a pincer-like motion of predominantly those residues that are frequently involved in interfaces and accounts for 25% (RMSD) of all backbone fluctuations in the solution ensemble (Fig. 5B).

Whether this mode indeed describes the molecular recognition dynamics can be tested stringently by predicting the bound ubiquitin conformations with the use of information only from the binding partner. To this end, we systematically varied the ubiquitin structure along this mode for each of altogether 41 interfaces, until the highest number of contacting interface atoms (i.e., atoms within 3 to 8 Å of the binding partner) was reached. A correlation of 0.94 between the projection of the thus predicted and the actual x-ray structure was found for the pincer-like mode (Fig. 5A). Analogously, correlations of 0.90 and 0.84 were obtained for the linearly combined first three principal components and for the third principal component, respectively. These consistently high correlations for collective modes indicate that the interface adaptation dynamics of ubiquitin are indeed well described within a few collective degrees of freedom that dominate the solution ensemble. Moreover, this analysis indicates that the ability to optimize contacts with binding partners via backbone interface adaptation is important for ubiquitin to reach sufficient affinity with many different binding partners. As illustrated in Fig. 5B, for the ubiquitin interfaces with hepatocyte growth factor–regulated tyrosine kinase substrate (HRS) and the zinc finger ubiquitin-binding domain of isopeptidase T [Protein Data Bank (PDB) accession codes 2D3G and 2G45], the collective solution mode allows molecular recognition by enabling ubiquitin to adapt to different protein interfaces.

The slow supra-τ_c time scale of ubiquitin's interface adaptation dynamics is corroborated by the observation that collective solution modes obtained from the first five principal components of nanosecond ensembles 1xqq and 2nr2 (*10*, *11*) were less adept in describing the interface adaptation. For these modes, the correlation between predicted and crystallized position dropped from 0.94 to 0.68 and to 0.55, respectively. The supra-τ_c time scale has previously been speculated to be important in the context of signal propagation of the immunoglobulin-binding domain of protein G (*20*) as well as for aggregation dynamics (*41*).

Summary. Taken together, we have determined a solution ensemble of a globular protein from experimental data that comprises all solution dynamics up to the microsecond time scale at atomic resolution. A large part of this solution dynamics is concentrated in a collective pincer-like motional mode that strongly contributes to the interface adaptation dynamics during molecular recognition events. All available crystallographic structures of ubiquitin complexed to different binding proteins were shown to be accessible in solution. Conformational selection, rather than induced fit, is thus the main contributor to the observed interface adaptations. The observed conformational selection dynamics lower entropic barriers, thereby explaining physiologically observed high affinity and fast on-rates which otherwise would need to be explained by induced-fit motions.

These findings suggest how ubiquitin recognizes many different partner proteins with a high degree of specificity and sufficient affinity. In order to reach sufficient affinity, a certain degree of structural plasticity is required that is thermally accessible in solution. In order to maintain high specificity despite the inherent flexibility, the binding interfaces are centered around the rigid hotspot (*38*) residues H68/I44 and D58. The rigidity of these mutational hotspots (*26*, *39*, *40*) might prevent promiscuous binding, because only precisely aligned

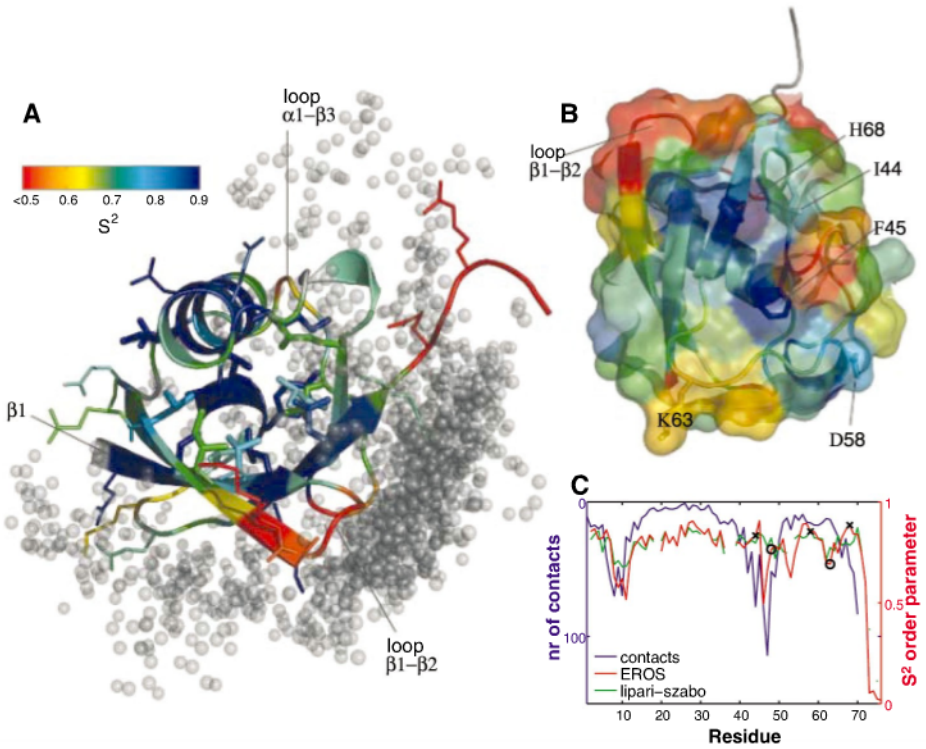

Fig. 4. Solution dynamics correlate with molecular recognition sites. (**A** and **B**) The apo structure of ubiquitin (1UBI) is colored by backbone flexibility in solution as given by S^2_{EROS}. (A) Positions of contacting atoms of complexing proteins (<5 Å distance) are shown as gray spheres. (B) View toward the surface at the most prominent recognition site around residues I44/H68. H68 (sticks) lies within a rigid crevice that connects via F45 to the other known recognition site centered at D58. The walls of this crevice are formed by regions with high flexibility. Around H68, rigidity is provided by packing of core residues L67 and L69 (not shown) against the central helix; at D58, packing of L55 and a long-range hydrogen bond from Y59 to E51 provide stability. (**C**) Number (nr) of ubiquitin-binding protein contacts per residue (blue line) and the flexibility in solution for the sub-τ_c time regime (green line) and the supra-τ_c time range, as extracted from the EROS ensemble (red line). A marked correlation between contacts and solution fluctuations is observed, particularly for the EROS ensemble. Exceptions from the observed correlation are found for known molecular recognition hotspots (marked with "x" symbols: I44/H68, D58), which may act as rigid anchors, allowing flexibility for neighboring residues. Lysines responsible for polyubiquitination are marked with circles (K48, K63).

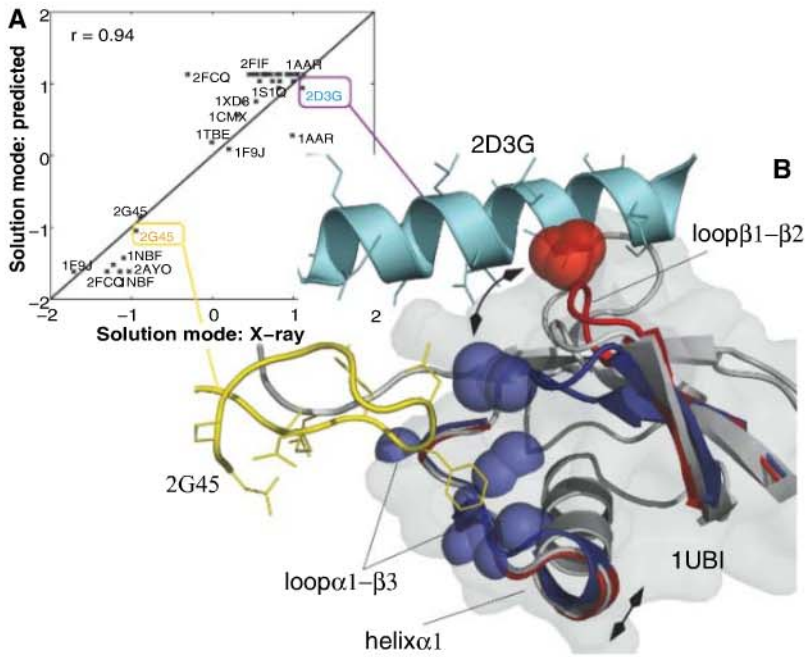

Fig. 5. Equilibrium supra-τ_c dynamics are dominated by conformational selection dynamics. A large amplitude collective solution mode entails a pincer-like motion of loop β1-β2 and loop α1-β3 including the C-terminal tip of helix α1. For each of altogether 41 binding partners, this collective solution mode was systematically varied to find a predicted position that maximized contacts. **(A)** The position on the mode of the thus predicted selected structures is plotted on the *y* axis, whereas the projected position onto this mode for the actual crystal structures is plotted on the *x* axis. **(B)** In order to illustrate the conformational selection along the collective solution mode, two of the selected snapshots (dark blue and red) are shown together with relevant parts of their respective binding partners: the zinc finger ubiquitin-binding domain of isopeptidase T (2G45, yellow) and HRS (2D3G, cyan). Contacts affected by the motion along the collective mode are shown as spheres. The crystal structure of 1UBI is shown at relevant regions as a gray cartoon. The full protein is shown as a semitransparent surface.

partner interfaces benefit from the high hotspot energy contribution. Structurally, the observed rigidity is maintained for H68 by packing with its neighbors L67 and L69 tightly into the protein core, whose rigidity is reinforced by helix 1. Similarly, I44 is anchored via F45 and decoupled from the adjacent flexible loop via an alanine-glycine linker (A46/G47). At D58, packing of L55 and a long-range hydrogen bond from Y59 to E51 provide stability. Because the solution dynamics are dominated by the collective pincer-like interface adaptation, it seems that only functionally essential flexibility is present. Apparently, ubiquitin has evolved to be as rigid as possible while remaining as flexible as necessary to engage in different interfaces.

Our finding that conformational selection is responsible for protein-protein binding of ubiquitin is in line with recent findings of conformational selection occurring for antibodies and enzymes (*42*–*44*). For the latter, relaxation dispersion experiments that are sensitive to microsecond-to-millisecond time scales (i.e., 1000 times slower than the processes we described here) show conformational selection for all steps in enzymatic reactions of dihydrofolate reductase (*9*). It should be noted that our findings differ from the stepwise model proposed for the binding of unfolded proteins to folded ones (*45*) and thus open up a whole range of possible molecular recognition mechanisms.

References and Notes

1. C. Kolano, J. Helbing, M. Kozinski, W. Sander, P. Hamm, *Nature* **444**, 469 (2006).
2. H. Frauenfelder, P. G. Wolynes, *Science* **229**, 337 (1985).
3. A. Mittermaier, L. E. Kay, *Science* **312**, 224 (2006).
4. L. E. Kay, D. A. Torchia, A. Bax, *Biochemistry* **28**, 8972 (1989).
5. M. Akke, A. Palmer, *J. Am. Chem. Soc.* **118**, 911 (1996).
6. L. Wang *et al.*, *Proc. Natl. Acad. Sci. U.S.A.* **98**, 7684 (2001).
7. G. Lipari, A. Szabo, *J. Am. Chem. Soc.* **104**, 4546 (1982).
8. K. A. Henzler-Wildman *et al.*, *Nature* **450**, 913 (2007).
9. D. D. Boehr, D. McElheny, H. J. Dyson, P. E. Wright, *Science* **313**, 1638 (2006).
10. K. Lindorff-Larsen, R. B. Best, M. A. DePristo, C. M. Dobson, M. Vendruscolo, *Nature* **433**, 128 (2005).
11. B. Richter, J. Gsponer, P. Varnai, X. Salvatella, M. Vendruscolo, *J. Biomol. NMR* **37**, 117 (2007).
12. M. Akke, R. Bruschweiler, A. G. Palmer, *J. Am. Chem. Soc.* **115**, 9832 (1993).
13. D. Yang, Y.-K. Mok, J. D. Forman-Kay, N. A. Farrow, L. E. Kay, *J. Mol. Biol.* **272**, 790 (1997).
14. K. K. Frederick, M. S. Marlow, K. G. Valentine, A. J. Wand, *Nature* **448**, 325 (2007).
15. C. S. Goh, D. Milburn, M. Gerstein, *Curr. Opin. Struct. Biol.* **14**, 104 (2004).
16. R. Grunberg, J. Leckner, M. Nilges, *Structure* **12**, 2125 (2004).
17. J. R. Tolman, J. M. Flanagan, M. A. Kennedy, J. H. Prestegard, *Proc. Natl. Acad. Sci. U.S.A.* **92**, 9279 (1995).
18. J. R. Tolman, *J. Am. Chem. Soc.* **124**, 12020 (2002).
19. N. A. Lakomek *et al.*, *Angew. Chem. Int. Ed.* **44**, 7776 (2005).
20. G. Bouvignies *et al.*, *Proc. Natl. Acad. Sci. U.S.A.* **102**, 13885 (2005).
21. N. A. Lakomek, T. Carlomagno, S. Becker, C. Griesinger, J. Meiler, *J. Biomol. NMR* **34**, 101 (2006).
22. G. Bouvignies, P. Markwick, R. Bruscheweiler, M. Blackledge, *J. Am. Chem. Soc.* **128**, 15100 (2006).
23. P. R. L. Markwick, G. Bouvignies, M. Blackledge, *J. Am. Chem. Soc.* **129**, 4724 (2007).
24. J. Meiler, J. J. Prompers, W. Peti, C. Griesinger, R. Bruschweiler, *J. Am. Chem. Soc.* **123**, 6098 (2001).
25. W. Peti, J. Meiler, R. Bruschweiler, C. Griesinger, *J. Am. Chem. Soc.* **124**, 5822 (2002).
26. L. Hicke, H. L. Schubert, C. P. Hill, *Nat. Rev. Mol. Cell Biol.* **6**, 610 (2005).
27. J. W. Harper, B. A. Schulman, *Cell* **124**, 1133 (2006).
28. P. S. Brzovic, R. E. Klevit, *Cell Cycle* **5**, 2867 (2006).
29. N. Tjandra, A. Bax, *Science* **278**, 1111 (1997).
30. K. B. Briggman, J. R. Tolman, *J. Am. Chem. Soc.* **125**, 10164 (2003).
31. K. Ruan, J. R. Tolman, *J. Am. Chem. Soc.* **127**, 15032 (2005).
32. M. Ottiger, A. Bax, *J. Am. Chem. Soc.* **120**, 12334 (1998).
33. See supporting material on *Science* Online.
34. F. Massi, M. J. Grey, A. G. Palmer, *Protein Sci.* **14**, 735 (2005).
35. R. B. Best, K. Lindorff-Larsen, M. A. DePristo, M. Vendruscolo, *Proc. Natl. Acad. Sci. U.S.A.* **103**, 10901 (2006).
36. S. L. Chang, N. Tjandra, *J. Magn. Reson.* **174**, 43 (2005).
37. Single-letter abbreviations for the amino acid residues are as follows: A, Ala; C, Cys; D, Asp; E, Glu; F, Phe; G, Gly; H, His; I, Ile; K, Lys; L, Leu; M, Met; N, Asn; P, Pro; Q, Gln; R, Arg; S, Ser; T, Thr; V, Val; W, Trp; and Y, Tyr.
38. T. Clackson, J. A. Wells, *Science* **267**, 383 (1995).
39. C. Kiel, L. Serrano, *J. Mol. Biol.* **355**, 821 (2006).
40. L. Penengo *et al.*, *Cell* **124**, 1183 (2006).
41. C. W. Bertoncini *et al.*, *Proc. Natl. Acad. Sci. U.S.A.* **102**, 1430 (2005).
42. E. Z. Eisenmesser *et al.*, *Nature* **438**, 117 (2005).
43. C. Tang, C. D. Schwieters, G. M. Clore, *Nature* **449**, 1078 (2007).
44. L. C. James, P. Roversi, D. S. Tawfik, *Science* **299**, 1362 (2003).
45. K. Sugase, H. J. Dyson, P. E. Wright, *Nature* **447**, 1021 (2007).
46. N. Tjandra, S. E. Feller, R. W. Pastor, A. Bax, *J. Am. Chem. Soc.* **117**, 12562 (1995).

47. We thank A. Munk for suggesting a scaling method for the SCRM order parameters; F. Mulder, A. Bonvin, and N. Tjandra for discussion of the overall scaling of Lipari-Szabo order parameters; K. Giller for the preparation of numerous labeled ubiquitin samples; and A. Mark, K. Riebeseel, E. d'Auvergne, L. Joachimiak, and M. Tyka for carefully reading the manuscript and fruitful discussions. This work was supported by the Max Planck Society (to H.G., C.G., and B.L.dG.), the Fonds der Chemischen Industrie (to C.G.), the German Israel Foundation (to C.G.), the Human Frontier Science Program (to O.F.L.), and the Volkswagen Foundation (to O.F.L.). Coordinates and RDCs have been deposited in the PDB (www.rcsb.org) with the accession number 2k39.

Supporting Online Material

www.sciencemag.org/cgi/content/full/320/5882/1471/DC1
SOM Text S1 to S7
Figs. S1 to S9
Tables S1 to S8
References

28 February 2008; accepted 2 May 2008
10.1126/science.1157092

Probing Cold Dense Nuclear Matter

R. Subedi,[1] R. Shneor,[2] P. Monaghan,[3] B. D. Anderson,[1] K. Aniol,[4] J. Annand,[5] J. Arrington,[6] H. Benaoum,[7,8] F. Benmokhtar,[9] W. Boeglin,[10] J.-P. Chen,[11] Seonho Choi,[12] E. Cisbani,[13] B. Craver,[14] S. Frullani,[13] F. Garibaldi,[13] S. Gilad,[3] R. Gilman,[11,15] O. Glamazdin,[16] J.-O. Hansen,[11] D. W. Higinbotham,[11]* T. Holmstrom,[17] H. Ibrahim,[18] R. Igarashi,[19] C. W. de Jager,[11] E. Jans,[20] X. Jiang,[15] L. J. Kaufman,[9,21] A. Kelleher,[17] A. Kolarkar,[22] G. Kumbartzki,[15] J. J. LeRose,[11] R. Lindgren,[14] N. Liyanage,[14] D. J. Margaziotis,[4] P. Markowitz,[10] S. Marrone,[23] M. Mazouz,[24] D. Meekins,[11] R. Michaels,[11] B. Moffit,[17] C. F. Perdrisat,[17] E. Piasetzky,[2] M. Potokar,[25] V. Punjabi,[26] Y. Qiang,[3] J. Reinhold,[10] G. Ron,[2] G. Rosner,[27] A. Saha,[11] B. Sawatzky,[14,28] A. Shahinyan,[29] S. Širca,[25,30] K. Slifer,[14] P. Solvignon,[28] V. Sulkosky,[17] G. M. Urciuoli,[13] E. Voutier,[24] J. W. Watson,[1] L. B. Weinstein,[18] B. Wojtsekhowski,[11] S. Wood,[11] X.-C. Zheng,[3,6,14] L. Zhu[31]

The protons and neutrons in a nucleus can form strongly correlated nucleon pairs. Scattering experiments, in which a proton is knocked out of the nucleus with high-momentum transfer and high missing momentum, show that in carbon-12 the neutron-proton pairs are nearly 20 times as prevalent as proton-proton pairs and, by inference, neutron-neutron pairs. This difference between the types of pairs is due to the nature of the strong force and has implications for understanding cold dense nuclear systems such as neutron stars.

Nuclei are composed of bound protons (p) and neutrons (n), referred to collectively as nucleons (N). A standard model of the nucleus since the 1950s has been the nuclear shell model, in which neutrons and protons move independently in well-defined quantum orbits in the average nuclear field created by their mutually attractive interactions. In the 1980s and 1990s, proton-removal experiments using electron beams with energies of several hundred megaelectron volts showed that only 60 to 70% of the protons participate in this type of independent particle motion in nuclear valence states (*1*, *2*). At the time, it was assumed that this low occupancy was caused by correlated pairs of nucleons within the nucleus. The existence of nucleon pairs that are correlated at distances of several femtometers, known as long-range correlations, has been established (*3*), but these accounted for less than half of the predicted correlated nucleon pairs. Recent high-momentum transfer measurements (*4*–*12*) have shown that nucleons in nuclear ground states can form pairs with large relative momentum and small center-of-mass (CM) momentum due to the short-range (scalar and tensor) components of the nucleon-nucleon interaction. These pairs are referred to as short-range correlated (SRC) pairs. The study of these SRC pairs allows access to cold dense nuclear matter, such as that found in a neutron star.

Experimentally, a high-momentum probe can knock a proton out of a nucleus, leaving the rest of the system nearly unaffected. If, on the other hand, the proton being struck is part of an SRC pair, the high relative momentum in the pair would cause the correlated nucleon to recoil and be ejected as well (Fig. 1). High-momentum knockout by both high-energy protons (*8*–*10*) and high-energy electrons (*12*) has shown, for kinematics far from particle-production resonances, that when a proton with high missing momentum is removed from the ^{12}C nucleus, the momentum is predominantly balanced by a single recoiling nucleon. This is consistent with the theoretical description that large nucleon momenta in the nucleus are predominantly caused by SRC pairing (*13*). This effect has also been shown when inclusive incident electron, scattered electron (e,e') data were used (*4*, *5*, *14*), although that type of measurement is not sensitive to the type of SRC pair. Here we identify the relative abundance of p-n and p-p SRC pairs in ^{12}C nuclei.

We performed our experiment in Hall A of the Thomas Jefferson National Accelerator Facility (JLab), using an incident electron beam of 4.627 GeV with a beam current between 5 and 40 μA. The beam was incident on a 0.25-mm-thick pure ^{12}C sheet rotated 70° to the beam line to minimize the material through which the recoiling protons passed. We used two high-resolution spectrometers (HRS) (*15*) to define proton-knockout events for ^{12}C(e,e'p). The left HRS detected scattered electrons at a central scattering angle (momentum) of 19.5° (3.724 GeV/c). These values correspond to the quasi-free knockout of a single proton with transferred three-momentum q = 1.65 GeV/c, transferred energy ω = 0.865 GeV, $Q^2 = q^2 - (\omega/c)^2 = 2(\mathrm{GeV}/c)^2$ (where Q^2 is the four-momentum, squared), and Bjorken scaling parameter $x_B = Q^2/2m\omega = 1.2$, where m is the mass of the proton. The right HRS detected knocked-out protons at three different values for the central angle (momentum): 40.1° (1.45 GeV/c), 35.8° (1.42 GeV/c), and 32.0° (1.36 GeV/c).

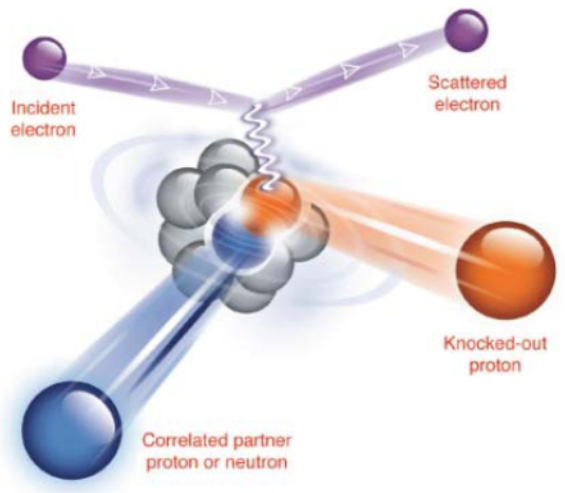

Fig. 1. Illustration of the ^{12}C(e,e'pN) reaction. The incident electron beam couples to a nucleon-nucleon pair via a virtual photon. In the final state, the scattered electron is detected along with the two nucleons that are ejected from the nucleus. Typical nuclear density is about 0.16 nucleons/fm^3, whereas for pairs the local density is approximately five times larger.

[1]Kent State University, Kent State, OH 44242, USA. [2]Tel Aviv University, Tel Aviv 69978, Israel. [3]Massachusetts Institute of Technology, Cambridge, MA 02139, USA. [4]California State University Los Angeles, Los Angeles, CA 90032, USA. [5]University of Glasgow, Glasgow G12 8QQ, Scotland, UK. [6]Argonne National Laboratory, Argonne, IL 60439, USA. [7]Syracuse University, Syracuse, NY 13244, USA. [8]Prince Mohammad University, Al-Khobar 31952, Saudi Arabia. [9]University of Maryland, College Park, MD 20742, USA. [10]Florida International University, Miami, FL 33199, USA. [11]Thomas Jefferson National Accelerator Facility, Newport News, VA 23606, USA. [12]Seoul National University, Seoul 151-747, Korea. [13]Istituto Nazionale de Fisica Nucleare (INFN), Sezione di Roma, I-00185 Rome, Italy. [14]University of Virginia, Charlottesville, VA 22904, USA. [15]Rutgers, The State University of New Jersey, Piscataway, NJ 08855, USA. [16]Kharkov Institute of Physics and Technology, Kharkov 310108, Ukraine. [17]College of William and Mary, Williamsburg, VA 23187, USA. [18]Old Dominion University, Norfolk, VA 23508, USA. [19]University of Saskatchewan, Saskatoon, Saskatchewan, S7N 5E2 Canada. [20]Nationaal Instituut voor Subatomaire Fysica, Amsterdam, Netherlands. [21]University of Massachusetts Amherst, Amherst, MA 01003, USA. [22]University of Kentucky, Lexington, KY 40506, USA. [23]Dipartimento di Fisica and INFN sezione Bari, Bari, Italy. [24]Laboratoire de Physique Subatomique et de Cosmologie, F-38026 Grenoble, France. [25]Institute "Jožef Stefan," 1000 Ljubljana, Slovenia. [26]Norfolk State University, Norfolk, VA 23504, USA. [27]University of Glasgow, Glasgow G12 8QQ, Scotland, UK. [28]Temple University, Philadelphia, PA 19122, USA. [29]Yerevan Physics Institute, Yerevan 375036, Armenia. [30]Department of Physics, University of Ljubljana, 1000 Ljubljana, Slovenia. [31]University of Illinois at Urbana–Champaign, Urbana, IL 61801, USA.

*To whom correspondence should be addressed. E-mail: doug@jlab.org

These kinematic settings covered (e,e'p) missing momenta, which is the momentum of the undetected particles, in the range from 300 to 600 MeV/c, with overlap between the different settings. For highly correlated pairs, the missing momentum of the (e,e'p) reaction is balanced almost entirely by a single recoiling nucleon, whereas for a typical uncorrelated (e,e'p) event, the missing momentum is balanced by the sum of many recoiling nucleons. In a partonic picture, x_B is the fraction of the nucleon momentum carried by the struck quark. Hence, when $x_B > 1$, the struck quark has more momentum than the entire nucleon, which points to nucleon correlation. To detect correlated recoiling protons, a large acceptance spectrometer ("BigBite") was placed at an angle of 99° to the beam direction and 1.1 m from the target. To detect correlated recoiling neutrons, a neutron array was placed directly behind the BigBite spectrometer at a distance of 6 m from the target. Details of these custom proton and neutron detectors can be found in the supporting online material (*16*).

The electronics for the experiment were set up so that for every ^{12}C(e,e'p) event in the HRS spectrometers, we read out the BigBite and neutron-detector electronics; thus, we could determine the ^{12}C(e,e'pp)/^{12}C(e,e'p) and the ^{12}C(e,e'pn)/^{12}C(e,e'p) ratios. For the ^{12}C(e,e'pp)/^{12}C(e,e'p) ratio, we found that 9.5 ± 2% of the (e,e'p) events had an associated recoiling proton, as reported in (*12*). Taking into account the finite acceptance of the neutron detector [using the same procedure as with the proton detector (*12*)] and the neutron detection efficency, we found that 96 ± 22% of the (e,e'p) events with a missing momentum above 300 MeV/c had a recoiling neutron. This result agrees with a hadron beam measurement of (p,2pn)/(p,2p), in which 92 ± 18% of the (p,2p) events with a missing momentum above the Fermi momentum of 275 MeV/c were found to have a single recoiling neutron carrying the momentum (*11*).

Because we collected the recoiling proton ^{12}C(e,e'pp) and neutron ^{12}C(e,e'pn) data simultaneously with detection systems covering nearly identical solid angles, we could also directly determine the ratio of ^{12}C(e,e'pn)/^{12}C(e,e'pp). In this scheme, many of the systematic factors needed to compare the rates of the ^{12}C(e,e'pn) and ^{12}C(e,e'pp) reactions canceled out. Correcting only for detector efficiencies, we determined that this ratio was 8.1 ± 2.2. To estimate the effect of final-state interactions (that is, reactions that happen after the initial scattering), we assumed that the attenuations of the recoiling protons and neutrons were almost equal. In this case, the only correction related to final-state interactions of the measured ^{12}C(e,e'pn)/^{12}C(e,e'pp) ratio is due to a single-charge exchange. Because the measured (e,e'pn) rate is about an order of magnitude larger than the (e,e'pp) rate, (e,e'pn) reactions followed by a single-charge exchange [and hence detected as (e,e'pp)] dominated and reduced the measured ^{12}C(e,e'pn)/^{12}C(e,e'pp) ratio. Using the Glauber approximation (*17*), we estimated that this effect was 11%. Taking this into account, the corrected experimental ratio for ^{12}C(e,e'pn)/^{12}C(e,e'pp) was 9.0 ± 2.5.

To deduce the ratio of p-n to p-p SRC pairs in the ground state of ^{12}C, we used the measured ^{12}C(e,e'pn)/^{12}C(e,e'pp) ratio. Because we used (e,e'p) events to search for SRC nucleon pairs, the probability of detecting p-p pairs was twice that of p-n pairs; thus, we conclude that the ratio of p-n/p-p pairs in the ^{12}C ground state is 18 ± 5 (Fig. 2). To get a comprehensive picture of the structure of ^{12}C, we combined the pair faction results with the inclusive ^{12}C(e,e') measurements (*4*, *5*, *14*) and found that approximately 20% of the nucleons in ^{12}C form SRC pairs, consistent with the depletion seen in the spectroscopy experiments (*1*, *2*). As shown in Fig. 3, the combined results indicate that 80% of the nucleons in the ^{12}C nucleus acted independently or as described within the shell model, whereas for the 20% of correlated pairs, 90 ± 10% were in the form of p-n SRC pairs; 5 ± 1.5% were in the form of p-p SRC pairs; and, by isospin symmetry, we inferred that 5 ± 1.5% were in the form of SRC n-n pairs. The dominance of the p-n over p-p SRC pairs is a clear consequence of the nucleon-nucleon tensor force. Calculations of this effect (*18*, *19*) indicate that it is robust and does not depend on the exact parameterization of the nucleon-nucleon force, the type of the nucleus, or the exact ground-state wave function used to describe the nucleons.

If neutron stars consisted only of neutrons, the relatively weak n-n short-range interaction would mean that they could be reasonably well approximated as an ideal Fermi gas, with only perturbative corrections. However, theoretical analysis of neutrino cooling data indicates that neutron stars contain about 5 to 10% protons and electrons in the first central layers (*20*–*22*). The strong p-n short-range interaction reported here suggests that momentum distribution for the protons and neutrons in neutron stars will be substantially different from that characteristic of an ideal Fermi gas. A theoretical calculation that takes into account the p-n correlation effect at relevant neutron star densities and realistic proton concentration shows the correlation effect on the momentum distribution of the protons and the neutrons (*23*). We therefore speculate that the small concentration of protons inside neutron stars might have a disproportionately large effect that needs to be addressed in realistic descriptions of neutron stars.

References and Notes

1. L. Lapikas, *Nucl. Phys. A.* **553**, 297 (1993).
2. J. Kelly, *Adv. Nucl. Phys.* **23**, 75 (1996).
3. W. H. Dickhoff, C. Barbieri, *Prog. Part. Nucl. Phys.* **52**, 377 (2004).
4. K. S. Egiyan *et al.*, *Phys. Rev. C Nucl. Phys.* **68**, 014313 (2003).

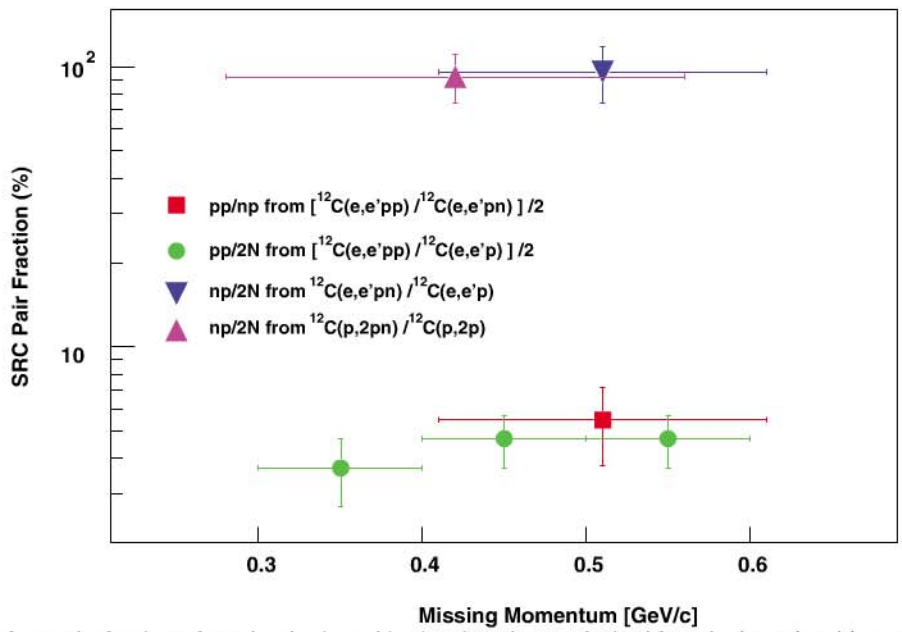

Fig. 2. The fractions of correlated pair combinations in carbon as obtained from the (e,e'pp) and (e,e'pn) reactions, as well as from previous (p,2pn) data. The results and references are listed in table S1.

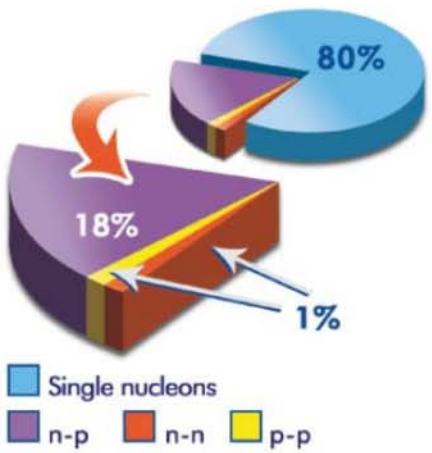

Fig. 3. The average fraction of nucleons in the various initial-state configurations of ^{12}C.

5. K. S. Egiyan *et al.*, *Phys. Rev. Lett.* **96**, 082501 (2006).
6. R. A. Niyazov *et al.*, *Phys. Rev. Lett.* **92**, 052303 (2004).
7. F. Benmokhtar *et al.*, *Phys. Rev. Lett.* **94**, 082305 (2005).
8. J. L. S. Aclander *et al.*, *Phys. Lett. B* **453**, 211 (1999).
9. A. Tang *et al.*, *Phys. Rev. Lett.* **90**, 042301 (2003).
10. A. Malki *et al.*, *Phys. Rev. C Nucl. Phys.* **65**, 015207 (2002).
11. E. Piasetzky, M. Sargsian, L. Frankfurt, M. Strikman, J. W. Watson, *Phys. Rev. Lett.* **97**, 162504 (2006).
12. R. Shneor *et al.*, *Phys. Rev. Lett.* **99**, 072501 (2007).
13. L. L. Frankfurt, M. I. Strikman, *Phys. Rep.* **76**, 215 (1981).
14. L. L. Frankfurt, M. I. Strikman, D. B. Day, M. Sargsian, *Phys. Rev. C Nucl. Phys.* **48**, 2451 (1993).
15. J. Alcorn *et al.*, *Nucl. Instrum. Methods* **A522**, 294 (2004).
16. Materials and methods are available as supporting material on *Science* Online.
17. I. Mardor, Y. Mardor, E. Piasetzky, J. Alster, M. M. Sargsian, *Phys. Rev. C Nucl. Phys.* **46**, 761 (1992).
18. R. Schiavilla, R. B. Wiringa, S. C. Pieper, J. Carlson, *Phys. Rev. Lett.* **98**, 132501 (2007).
19. M. M. Sargsian, T. V. Abrahamyan, M. I. Strikman, L. L. Frankfurt, *Phys. Rev. C Nucl. Phys.* **71**, 044615 (2005).
20. J. M. Lattimer, M. Prakash, *Science* **304**, 536 (2004).
21. G. Baym, *Nucl. Phys. A.* **590**, 233 (1995).
22. G. Baym, *Nucl. Phys. A.* **702**, 3 (2002).
23. T. Frick, H. Muther, A. Rios, A. Polls, A. Ramos, *Phys. Rev. C Nucl. Phys.* **71**, 014313 (2005).
24. This work was supported by the Israel Science Foundation, the U.S.-Israeli Binational Scientific Foundation, the UK Engineering and Physical Sciences Research Council and Science and Technology Facilities Council, NSF, and the U.S. Department of Energy (DOE) (grants DE-AC02-06CH11357 and DE-FG02-94ER40818 and U.S. DOE contract no. DE-AC05-84150, modification no. M175, under which the Southeastern Universities Research Association, Inc. operates the Thomas Jefferson National Accelerator Facility). The raw data from this experiment are archived in Jefferson Lab's mass storage silo.

Supporting Online Material

www.sciencemag.org/cgi/content/full/320/5882/1476/DC1
Materials and Methods
Figs. S1 and S2
Table S1
References

19 February 2008; accepted 8 May 2008
10.1126/science.1156675

Laser-Induced Electron Tunneling and Diffraction

M. Meckel,[1,2] D. Comtois,[3] D. Zeidler,[1,4] A. Staudte,[1,2] D. Pavičić,[1] H. C. Bandulet,[3] H. Pépin,[3] J. C. Kieffer,[3] R. Dörner,[2] D. M. Villeneuve,[1] P. B. Corkum[1]*

Molecular structure is usually determined by measuring the diffraction pattern the molecule impresses on x-rays or electrons. We used a laser field to extract electrons from the molecule itself, accelerate them, and in some cases force them to recollide with and diffract from the parent ion, all within a fraction of a laser period. Here, we show that the momentum distribution of the extracted electron carries the fingerprint of the highest occupied molecular orbital, whereas the elastically scattered electrons reveal the position of the nuclear components of the molecule. Thus, in one comprehensive technology, the photoelectrons give detailed information about the electronic orbital and the position of the nuclei.

Molecular multiphoton ionization in the tunneling limit (sketched in the upper frame of Fig. 1) is similar to tunneling in a scanning tunneling microscope (STM) (*1*). In both cases, electrons escape from the outer regions of the orbital to the continuum; that is, to the vacuum for multiphoton ionization of gas phase molecules or to the conduction band of the metal tip in a STM. In a STM, the sample is fixed and the tip is moved. Rotating the molecule with respect to the field direction is the analog of moving the tip. The resulting angle-dependent ionization probability (*2*–*5*) provides information for a molecule analogous to the position dependence of the tunneling current in a STM. However, whereas the total tunneling current is one observable, the electron wave packet that emerges into the vacuum from the tunnel retains more information about the orbital.

In contrast to the static field of a STM, the electric field in a laser pulse oscillates and forces a fraction of the tunneled electron wave packet back to the parent ion. There, the wave packet can diffract from the molecule (lower frame in Fig. 1). This phenomenon has been called laser-induced electron diffraction (LIED) (*6*) and relates to recent research on ultrafast electron diffraction, where a femtosecond electron bunch is created at a photocathode and accelerated in an electrostatic field onto a molecular (*7*) or solid state (*8*) target. In our case, the molecule serves as its own photocathode, whereas the laser provides the accelerating field. This situation produces extremely high current densities and attosecond timing (*9*).

We report the observation of molecular tunneling spectroscopy and LIED. We measured electrons produced from aligned O_2 and N_2, resolving their three-dimensional (3D) momentum distribution. Comparing experiment and theory, we show that, in the two dimensions perpendicular to the field direction, the momentum distribution for these direct electrons is determined by the highest occupied molecular orbital (HOMO), observed through the filter of the suppressed binding potential (Fig. 1) through which the electron tunnels. We also demonstrate LIED (*6*) and confirm its origin with a simulation. Selecting the wavelength of the recollision electron modifies the diffraction pattern. Thus, one set of measurements simultaneously identifies the orbital wave function of the molecule and the position of the atoms in the molecule.

Laser-induced tunneling and diffraction exploit different parts of the ionizing electron wave packet. The fraction of the electron wave packet that is created while the field strength increases within an optical half-cycle departs directly and irrevocably from its parent ion. Only tunneling stands between the orbital and the electron detector. The wave packet that is born while the field decreases returns to the ion where it can elastically scatter (diffract), inelastically scatter, or recombine to (interfere with) the orbital from which it was extracted (*10*). These three scattering processes offer different perspectives on the molecule.

Tunneling, the process underlying all, probes the electronic structure of the neutral molecule. The recombination radiation, known as high-harmonic radiation, also measures the orbital structure of the neutral molecule (*11*). However, because high-harmonic generation starts with tunneling and ends with interference, these processes must be disentangled before the techniques can be generalized to complex orbitals. In contrast, elastic and inelastic scattering occur at the molecular ion. Inelastic rescattering is closely related to field-free collision physics (*12*, *13*). It can cause multiple ionization and subsequently lead to Coulomb explosion of small molecules. The molecular structure can then be inferred from the momentum vectors of the correlated ionic fragments. Elastic scattering is also sensitive to the potential structure of the molecular ion. However, here the molecular structure is encoded in the diffracting electron wave packet, making this imaging technique scaleable to more complex molecules.

For electron diffraction to be observable, the de Broglie wavelength of the electron needs to be on the order of the dimensions of the molecule. Small diatomic molecules have a bond length of ≈1 Å [1.9 atomic units (au)]. To obtain this wavelength, an electron would need a kinetic energy of 150 eV, corresponding to a momentum of 3.3 au. Electrons that are accelerated in the laser field and recollide with the parent molecule can easily reach this range of kinetic energies (*10*).

We recorded the momentum of electrons arising from tunneling ionization of aligned O_2 and N_2, employing a Cold Target Recoil Ion Mo-

[1]National Research Council of Canada, 100 Sussex Drive, Ottawa, Ontario, Canada, K1A 0R6. [2]Institut für Kernphysik, Johann Wolfgang Goethe Universität, Max-von-Laue Straße 1, D-60438 Frankfurt, Germany. [3]Institut National de la Recherche Scientifique–Énergie, Matériaux et Télécommunication, 1650 boulevard Lionel-Boulet, Varennes, Québec, Canada, J3X 1S2. [4]Carl Zeiss SMT AG, Rudolf-Eber-Straße 2, 73447 Oberkochen, Germany.

*To whom correspondence should be addressed. E-mail: paul.corkum@nrc.ca

mentum Spectroscopy (COLTRIMS) system (*14*). COLTRIMS allows us to measure the 3D momentum vectors of single electrons and ions in coincidence. This coincidence capability is used to measure both O_2 and N_2 simultaneously under identical conditions by means of a gas mixture. It also allows us to eliminate any contribution to the electron spectra from inelastic scattering resulting in fragmentation or multiple ionization of the molecules. However, with monomolecular targets, we achieve very similar results even without the ion-electron coincidence requirement. Finally, the coincidence measurement permits us to pick up weak fragmentation channels that provide information about the quality of our alignment [see supporting online material (SOM) text B].

Our laser pulse (800 nm) had a total energy of 5 μJ (split and used for both alignment and probing) and a repetition rate of 30 kHz. We align the molecules (*15*) using a slightly stretched (60 fs), moderately intense ($\lesssim 8 \times 10^{13}$ W/cm^2) laser pulse. The intense (2.5×10^{14} W/cm^2), short (40 fs), ionizing pulse, which is applied after a delay, catches the molecule at any alignment that can be achieved with polarized light. Experimentally, aligning (pump) and ionizing (probe) pulses are perpendicularly polarized (*y* axis and *z* axis in the inset of Fig. 2A, respectively). The pump pulse creates a rotational wave packet (*15*) that results in molecules aligned primarily along the *y* axis at a well-defined time delay (sketch in Fig. 2A). At a different time delay, the alignment distribution will be confined in the *xz* plane (sketch in Fig. 2B). We refer to this complementary case as anti-alignment. A computerized delay stage moved between the respective pump-probe delays every 10 s (details in SOM text A and B).

The electron momentum distributions (Fig. 2) obtained for aligned (A) and anti-aligned (B) O_2 molecules have been correlated with singly charged O_2^+ ions. For display purposes, the distribution is projected onto three planes. Most prominent in the figure is the large dynamic range in the distribution. The color code covers five orders of magnitude. The rapid fall-off of the signal is so prominent that it is hard to discern anything else from the figure. The spectra for N_2 (fig. S1) are qualitatively indistinguishable from those of O_2.

Molecular specific structure arising from tunneling and diffraction is revealed when we employ normalized differences. The anti-aligned projections are subtracted from the aligned projections and then divided by their sum. The normalized differences for O_2 and N_2 are plotted in Fig. 2, C and D. Because the data are not symmetrized, the quadrant-to-quadrant reproducibility is a measure of the quality of the image.

The low lateral-momentum electrons ($p_\perp = \sqrt{p_x^2 + p_y^2} < 0.5$ au, where p is momentum) exhibit clear patterns in the projection perpendicular to the ionizing laser field. The vast majority of these electrons drift directly to the detector without further interaction with the parent ion. They provide information on the ionizing orbital, filtered by the tunnel. These electrons are equally evident in the other two projections. They are spread along the *z* direction between $|p_z| < 1.5$ au, reflecting the fact that ionization can occur over a range of times within a field cycle.

Figure 3 presents an expanded view of the p_x-p_y projections of the electron momenta from N_2 and O_2 and focuses on the central part of the distribution. The very different distributions created by tunneling from O_2 and N_2 reflect the very different structures of the respective ionizing orbitals. In tunneling theory, the tunnel serves as a filter for the perpendicular component $p_\perp$ of the orbital wave function. The tunneled wave packet then can be expressed as (in atomic units) (*16*–*18*)

$$\Psi(p_\perp) \propto \langle p_\perp | \Psi_i \rangle \exp\left(-\frac{\sqrt{I_p}}{\sqrt{2}E} p_\perp^2\right) \quad (1)$$

where the exponential factor is the filter function. It contains the ionization potential I_p and the electric field E of the ionizing laser pulse at the moment of tunneling. The exponential factor depends only weakly on the alignment of the molecule (through a weakly angular-dependent Stark-shift). Therefore, it is approximately cancelled in any ratio of two different alignments. However, the electronic wave function $|\Psi_i\rangle$ is locked to the molecular frame, whereas $p_\perp$ is defined with respect to the laser-field direction. Therefore, the alignment dependence of the projected wave function $\langle p_\perp | \Psi_i \rangle$ is accentuated by taking ratios. We now show that this basic tunneling concept agrees with our experimental measurements.

Using the wave function for the HOMOs of N_2 and O_2, we calculated the lateral electron momentum distributions (both shape and amplitude) that emerge from the molecules for each molecular alignment. The electrons are given initial conditions determined by tunneling and then classically propagated in the field of a pulse identical to the experiment, taking into account the parent ion's Coulomb potential (*19*, *20*). Finally, each molecular alignment contributes to the predicted spectrum, according to its weight in the measured alignment or anti-alignment distribution. There are no free parameters in this model (described more fully in SOM text C). The results are shown in the bottom row of Fig. 3. The simulation reproduces the symmetry seen in the experiment. The model also shows that imperfect alignment causes the orbital's footprint to disappear in the unnormalized spectra (Fig. 2, A and B). That is, the node is filled by the alignment distribution of ionizing molecules.

We now turn to the structures at higher electron momenta ($p_\perp > 0.5$ au) and ($|p_z| > 1.5$ au) in Fig. 2, C and D. This region is dominated by electrons that have rescattered. In Fig. 2, C and D, the relative probability of finding an electron in

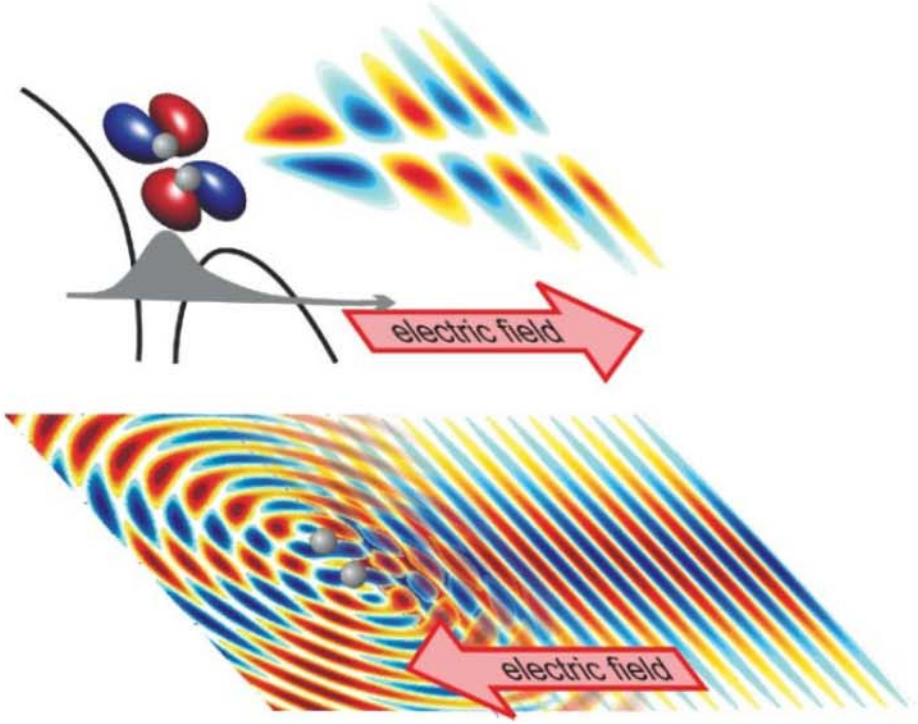

Fig. 1. (**Top**) Tunneling creates a filtered projection of the molecular orbital. Approximately half of the electron wave packet escapes directly to the detector. (**Bottom**) Remaining portion is driven back to the parent ion. Here, the central portion of the recolliding wave packet is shown diffracting from the molecule. The outer portions of the wave packet (not shown) weakly interact with the ion potential. The relative strength of each component depends on the filtered projection of the molecular orbital and therefore on molecular alignment.

the momentum region $p_z = 2$ au, $p_y = 1.5$ au in all quadrants and at $p_z = 0$ au, $p_x = 1$ au passes through rather broad local maxima. There are corresponding minima at $p_z = 2$ au, $p_x = 1.5$ au and at $p_z = 0$ au, $p_y = 1$ au. This structure contains information on the scattering potential. That is, we experimentally observed LIED.

Interpreting an electron distribution such as this is different from interpreting conventional electron diffraction because of the presence of the laser field (*17*). We analyzed our data in analogy to the attosecond streak camera (*21*) to remove the influence of the laser field on the electron momentum after the scattering has occurred. The final, observed momentum of a scattered electron is $\vec{p}_{fin} = \vec{p}_{rec} + \vec{A}_{rec}$ (*17*), where $\vec{A}_{rec} = (\vec{E}_0/\omega)\sin \omega t_{rec}$ is the vector potential defined by the electric field $\vec{E}(t) = \vec{E}_0 \cos(\omega t)$ of the probe pulse (here, ω is the frequency of the light), and $\vec{p}_{rec}$ is the electron momentum at the time t_{rec} of recollision. This analysis yields a manifold of momentum spheres centered at $p_z = \pm A_{rec}$ with radii p_{rec}. The maximum radius $p_{rec,max}$ corresponds to a recollision energy of $3.17U_p$ [where $U_p = (E_0/2\omega)^2$ is the ponderomotive potential]. Slicing the momentum spheres at perpendicular planes defined by $p_x \approx 0$ and $p_y \approx 0$ yields diffraction circles such as those illustrated in Fig. 4 (at left). Within each diffraction circle, we can relate our results to conventional electron diffraction: φ is the scattering angle, and the radius of each circle is the electron momentum or wavelength, $\lambda = h/p_{rec}$ (where h is Planck's constant), at which scattering occurs.

The four panels at right in Fig. 4 show the value of the measured electron distributions along diffraction circles of radius 1.4 au (blue), 1.2 au (red), and 1.0 au (black). Each curve is offset for clarity. Electrons in the range $0° < \varphi < 30°$ or $330° < \varphi < 360°$ are direct electrons and are not plotted in the figure (details in SOM text D).

Because the molecules were aligned along the y axis, the p_y-p_z projection is the most intuitive plane in which to analyze diffraction. At a recollision momentum p_{rec} of 1 au, the electron wavelength $\lambda = 6.3$ au is larger than twice the equilibrium bond length of O_2 ($d = 2.3$ au). However, numerical simulations (*22*, *23*) and experiments (*24*) have shown that the appropriate electron wavelength for diffraction is the wavelength at the core of the ion. That is, the recollision energy (corresponding to the radius of the diffraction circle) plus the ionization potential of the HOMO yield the appropriate diffraction wavelength. With this assumption ($\lambda = 4.57$ au), the first minimum at around 60° (and then at 300°) thus corresponds to a bond length of 2.6 au.

To help extend this interpretation, we turned to simulation (SOM text E). We used the probability of recollision as a function of the angle between the molecule and the laser electric field and averaged over the alignment distributions. The electron recollision momentum is chosen by selecting a diffraction circle for analysis. We made three final assumptions: (i) We assumed that the electron wavelength corresponds to the sum of recollision energy and the field free ionization energy. (ii) We assumed two-center diffraction. (iii) Because long trajectory electrons dominate, we concentrated on them. The resulting distributions are shown in the solid curves in Fig. 4. Comparing the calculated and measured distributions, we see that the modulation in the regions $\varphi \approx 50° - 150°$ and $\varphi \approx 210° - 310°$ arises from diffraction. The dashed lines highlight the shift of the diffraction maxima and minima with the electron wavelength. Electrons that backscatter through $\varphi \approx 180°$ are not properly described. They appear in the figure in the range $\varphi \approx 150° - 210°$. The overall agreement in the positions of the diffraction minima and maxima between simulations and experiment is good, except for N_2 in the p_x-p_z plane, where the simulated diffraction peaks appear shifted. This peak shift probably comes from an overestimation of the recollision probability for N_2 molecules oriented parallel to the laser field in the model.

There are three reasons why we obtain agreement for most angles. First, using normalized differences makes the two-center scattering contribution highly visible while making our results somewhat insensitive to details of the atomic contribution (*25*). Second, by concentrating on relatively high-energy electrons, we only need to consider the first recollision (*9*), keeping the electron trajectories relatively simple. Third, al-

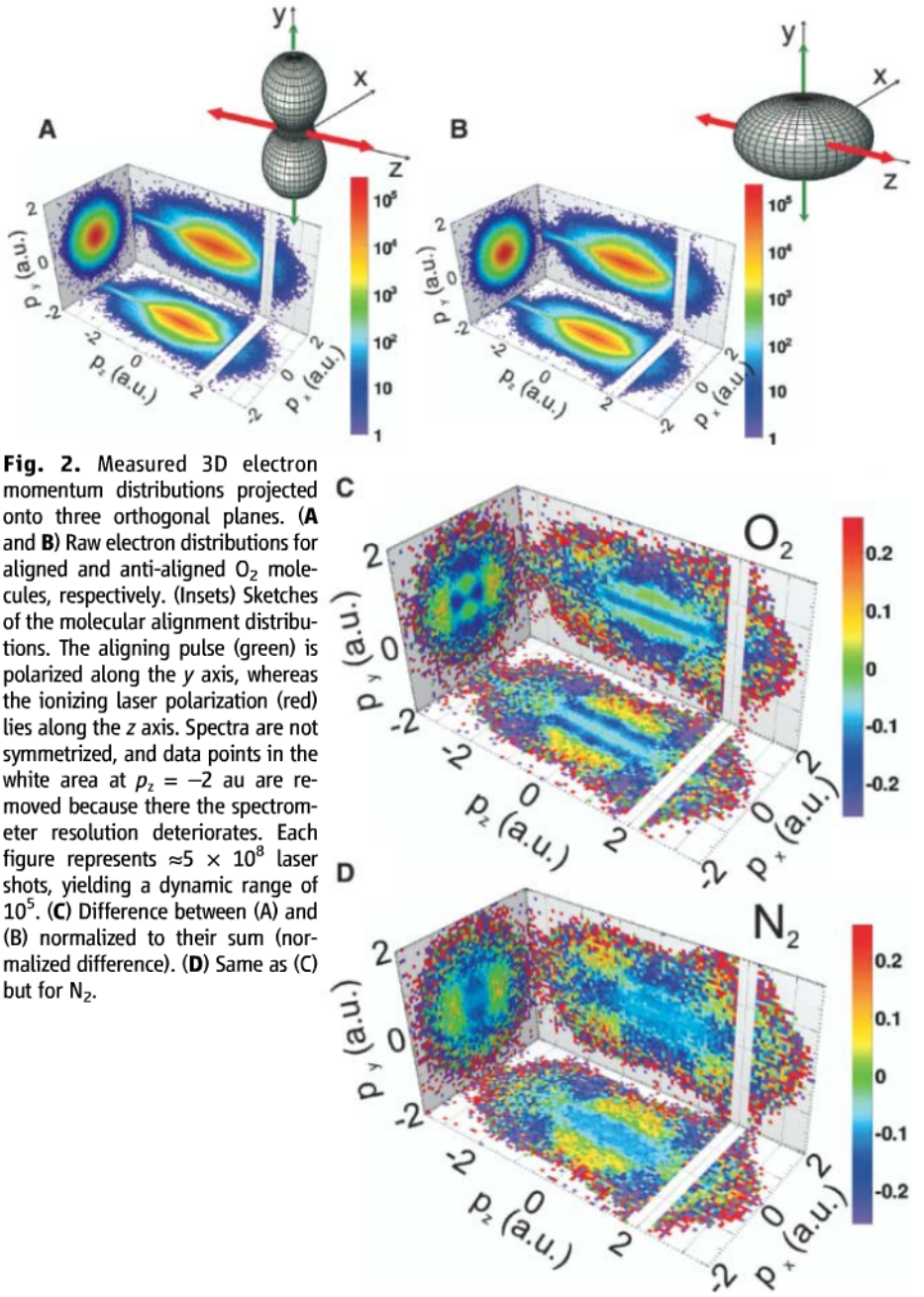

Fig. 2. Measured 3D electron momentum distributions projected onto three orthogonal planes. (**A** and **B**) Raw electron distributions for aligned and anti-aligned O_2 molecules, respectively. (Insets) Sketches of the molecular alignment distributions. The aligning pulse (green) is polarized along the y axis, whereas the ionizing laser polarization (red) lies along the z axis. Spectra are not symmetrized, and data points in the white area at $p_z = -2$ au are removed because there the spectrometer resolution deteriorates. Each figure represents $\approx 5 \times 10^8$ laser shots, yielding a dynamic range of 10^5. (**C**) Difference between (A) and (B) normalized to their sum (normalized difference). (**D**) Same as (C) but for N_2.

though the screened Coulomb potential is not fully treated in our diffraction analysis, we add the most important aspect by augmenting the electron energy measured from the scattering circles by I_p (*17*, *22*, *23*).

We have demonstrated that multiphoton ionization in the tunneling limit gives extensive information on the ionizing electronic orbital. If we rotate the molecule in small steps, all momenta from the wave function are sampled. We only need to select one angle for diffraction. This diffraction pattern reveals the interatomic dimensions of a molecule. Interestingly, the angle could be selected to favor recollision only from particular electronic configurations, allowing us to determine the structure of selected isomers or of excited states.

In a diffraction experiment, selecting a different electron wavelength λ changes the diffraction pattern in the same way as a change in the internuclear separation d ($\sin\varphi = n\lambda/d$, where n is the order of the diffraction peak). By showing that a 20% change in electron wavelength makes a measurable difference in the diffraction pattern, we indirectly demonstrate that vibrational or photochemical dynamics can be combined with LIED. Coincidence imaging allows us to use the characteristics of the correlated ion to select those events that we wish to analyze. Thus, LIED provides a method to isolate structural changes of any excited state that impresses a distinct signature on the ion.

In studies where coincidence imaging is unnecessary, employing a technology such as velocity map imaging (*26*, *27*) would allow electron spectra to be recorded using lasers with repetition rates as high as 136 MHz (*28*). Data of the same quality that we show could be obtained in milliseconds or less. Such a measurement is practical for any molecule that can be placed in the gas phase, provided that the strong field does not dislodge other electrons in an uncontrolled manner (*29*) and provided that the molecule can be aligned with sufficient precision.

Finally, we stand back and survey the emerging strong-field technology for molecular imaging. Tunneling, one of the most fundamental of the quantum mechanical processes, initiates all of the methods. Information about the ionizing orbital of the neutral molecule is imprinted on the tunneled electron. A second perspective on the molecular orbital is contained in the high-harmonic radiation that is produced upon recollision. High-harmonic radiation has two major advantages over tunneling. First, by measuring photons rather than electrons the problem of space-charge is avoided. Second, if the tunneled wave packet is independent of the angle between laser-field and molecular axis, tomography provides a well-developed algorithm for inverting the image (*11*, *30*). However, there is one major disadvantage: Tunneling and recombination are entwined in the angle-dependent harmonic spectrum (*31*). This problem has so far limited the application of orbital tomography.

A complementary insight is achieved by laser Coulomb explosion imaging (*32*–*34*) We become sensitive to the position of the nuclei in a molecular ion. LIED supplies us with the means to overcome the limitations of Coulomb explosion imaging and

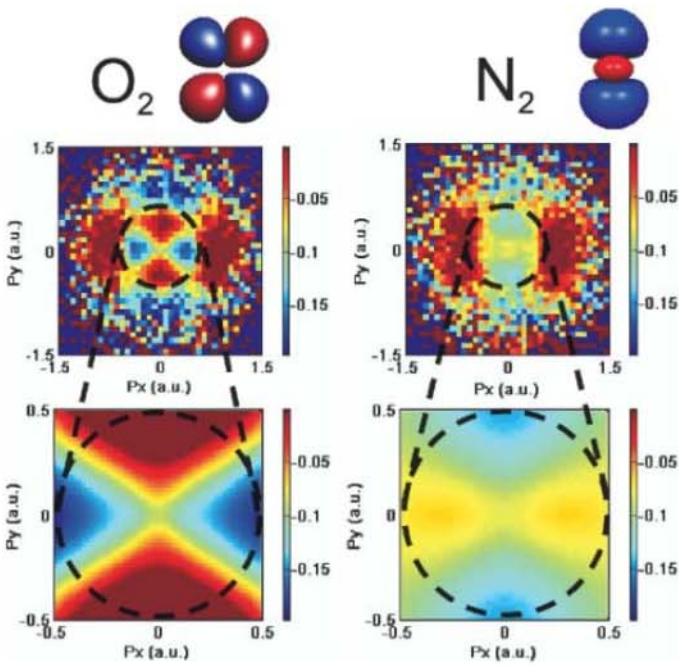

Fig. 3. p_x versus p_y projections of the normalized differences for O_2 and N_2. (**Top**) Experimental data (from Fig. 2). The color scale has been changed to emphasize the low lateral-momentum structure near the center of each figure enclosed in the dashed circle. The low lateral momentum retains the symmetry of the HOMO (shown above). (**Bottom**) Magnified results of our simulation (see text).

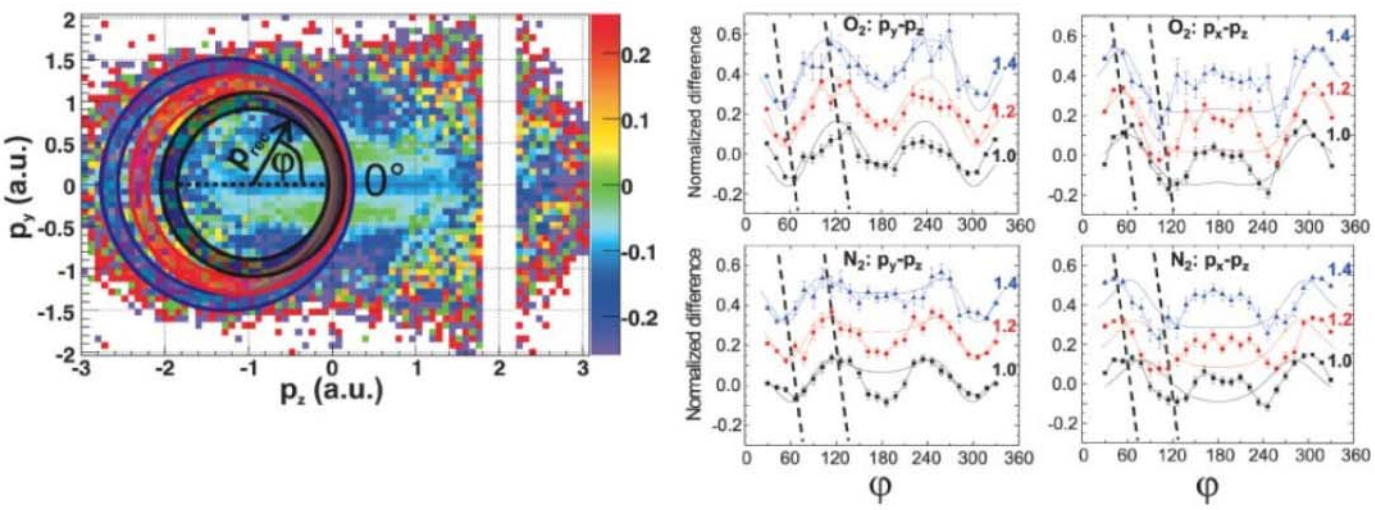

Fig. 4. Left panel is reproduced from Fig. 2C. Three color-coded diffraction circles are superimposed. The radius of the circle defines the recollision momentum p_{rec} (scattering wavelength); their width defines the range of momenta that are analyzed; and φ is the scattering angle. The four plots at right show the angular distributions within the indicated diffraction circles (see SOM text D for details). The color coding is preserved. Results of the simulations are superimposed as solid lines. The curves for recollision momentum of 1.0 au have no offset. For clarity, other curves are offset in units of 0.2. The data are shown with statistical error bars (1σ).

opens the pathway toward the imaging of larger molecules. Taken together, we can obtain a full picture of molecules. With the extension of these tools to pump-probe techniques, we will be able to simultaneously trace the temporal changes in the nuclear and electronic structure of molecules.

References and Notes

1. G. Binning, H. Rohrer, C. Gerber, E. Weibel, *Phys. Rev. Lett.* **49**, 57 (1982).
2. J. Muth-Böhm, A. Becker, F. Faisal, *Phys. Rev. Lett.* **85**, 2280 (2000).
3. X. Tong, Z. Zhao, C. Lin, *Phys. Rev. A* **66**, 033402 (2002).
4. A. Alnaser *et al.*, *Phys. Rev. A* **71**, 031403 (2005).
5. D. Pavičić, K. Lee, D. Rayner, P. B. Corkum, D. M. Villeneuve, *Phys. Rev. Lett.* **98**, 243001 (2007).
6. T. Zuo, A. Bandrauk, P. B. Corkum, *Chem. Phys. Lett.* **259**, 313 (1996).
7. H. Ihee *et al.*, *Science* **291**, 458 (2001).
8. B. J. Siwick, J. R. Dwyer, R. E. Jordan, R. J. D. Miller, *Science* **302**, 1382 (2003).
9. H. Niikura *et al.*, *Nature* **417**, 917 (2002).
10. P. B. Corkum, *Phys. Rev. Lett.* **71**, 1994 (1993).
11. J. Itatani *et al.*, *Nature* **432**, 867 (2004).
12. A. Staudte *et al.*, *Phys. Rev. Lett.* **99**, 263002 (2007).
13. A. Rudenko *et al.*, *Phys. Rev. Lett.* **99**, 263003 (2007).
14. J. Ullrich *et al.*, *Rep. Prog. Phys.* **66**, 1463 (2003).
15. H. Stapelfeldt, T. Seideman, *Rev. Mod. Phys.* **75**, 543 (2003).
16. N. B. Delone, V. P. Krainov, *J. Opt. Soc. Am. B* **8**, 1207 (1991).
17. M. Spanner, O. Smirnova, P. B. Corkum, M. Ivanov, *J. Phys. B* **37**, L243 (2004).
18. M. Ivanov, M. Spanner, O. Smirnova, *J. Mod. Opt.* **52**, 165 (2005).
19. T. Brabec, M. Ivanov, P. B. Corkum, *Phys. Rev. A* **54**, R2551 (1996).
20. D. Comtois *et al.*, *J. Phys. B* **38**, 1923 (2005).
21. J. Itatani *et al.*, *Phys. Rev. Lett.* **88**, 173903 (2002).
22. M. Lein, J. Marangos, P. Knight, *Phys. Rev. A* **66**, 051404 (2002).
23. S. Yurchenko, S. Patchkovskii, I. Litvinyuk, P. B. Corkum, G. Yudin, *Phys. Rev. Lett.* **93**, 223003 (2004).
24. D. Akoury *et al.*, *Science* **318**, 949 (2007).
25. M. Okunishi *et al.*, *Phys. Rev. Lett.* **100**, 143001 (2008).
26. C. Bordas, F. Paulig, H. Helm, D. Huestis, *Rev. Sci. Instrum.* **67**, 2257 (1996).
27. A. Eppink, D. Parker, *Rev. Sci. Instrum.* **68**, 3477 (1997).
28. I. Hartl *et al.*, *Opt. Lett.* **32**, 2870 (2007).
29. M. Lezius *et al.*, *Phys. Rev. Lett.* **86**, 51 (2001).
30. T. Kanai, S. Minemoto, H. Sakai, *Nature* **435**, 470 (2005).
31. S. Baker *et al.*, *Science* **312**, 424 (2006), published online 1 March 2006; 10.1126/science.1123904.
32. F. Légaré *et al.*, *Phys. Rev. A* **72**, 052717 (2005).
33. T. Ergler *et al.*, *Phys. Rev. Lett.* **97**, 193001 (2006).
34. A. Alnaser *et al.*, *Phys. Rev. A* **72**, 030702 (2005).

35. We gratefully acknowledge financial support from the Canadian Institute for Photonics Innovation, Natural Sciences and Engineering Research Council of Canada, Canadian Foundation for Innovation, Alexander-von-Humboldt Foundation, Deutsche Forschungsgemeinschaft, and the German Academic Exchange Service. P.B.C. acknowledges financial support from the Air Force Office of Scientific Research. M.M. thanks the German National Academic Foundation.

Supporting Online Material

www.sciencemag.org/cgi/content/full/320/5882/1478/DC1
SOM Text
Figs. S1 to S3
References

18 March 2008; accepted 16 May 2008
10.1126/science.1157980

Electrical Resistance of Long Conjugated Molecular Wires

Seong Ho Choi, BongSoo Kim, C. Daniel Frisbie*

The charge transport mechanism of a wire can be revealed by how its electrical resistance varies with length. We have measured the resistance and current-voltage characteristics of conjugated molecular wires ranging in length from 1 to 7 nanometers, connected between metal electrodes. We observe the theoretically predicted change in direct-current transport from tunneling to hopping as a function of systematically controlled wire length. We also demonstrate that site-specific disruption of conjugation in the wires greatly increases resistance in the hopping regime but has only a small effect in the tunneling regime. These nanoscale transport measurements elucidate the role of molecular length and bond architecture on molecular conductivity and open opportunities for greater understanding of electrical transport in conjugated polymer films.

Charge transport can occur through long, π-conjugated molecules (*1*–*3*), and the term "molecular wire" is often used to describe conjugated molecules in which charge transport is efficient over long distances (*4*, *5*). For example, the β-carotene molecule can transfer electrons over tens of Angstroms (*6*). In the context of molecular electronics, where the ultimate goal is the fabrication of circuitry based on the prescribed electronic function of individual molecules (*4*, *7*), it is desirable to have a quantitative definition of what constitutes a molecular wire.

A fundamental property of a wire is the scaling of its resistance (or conductance) with length. The length dependence of resistance is a direct consequence of the charge transport mechanism. In the macroscopic world, the resistance of a metallic wire increases linearly with length as a result of the diffusive nature of carrier transport in the metal. However, this particular scaling need not hold for conduction in molecules over nanometer-length scales, as has been pointed out theoretically (*8*–*10*) and observed experimentally (*2*, *3*, *11*, *12*). For short molecules (<3 nm) connected between metallic contacts, it is well-accepted that resistance scales exponentially with length according to Eq. 1.

$$R = R_0 \exp(\beta L) \quad (1)$$

where R is the junction resistance, R_0 is an effective contact resistance, L is molecular length, and β is the exponential prefactor that depends on the nature of bonding in the molecular backbone. The exponential length dependence in Eq. 1 results directly from the transport mechanism in metal/molecule/metal junctions based on short molecules, namely, direct (nonresonant) tunneling.

For longer molecules connected between metal electrodes, the scaling of resistance with length can be anticipated by comparison to fundamental studies of electron transfer in solution. Both theory and experiment on soluble donor-bridge-acceptor (D-B-A) systems (*2*, *3*, *8*, *11*, *12*) indicate that for long molecular bridges, the charge transport mechanism changes from direct tunneling to hopping, as evidenced by a change in the length dependence of the electron transfer rate constant. Specifically, for short bridges, the length dependence is exponential, corresponding to the tunneling regime, and for long bridges, the scaling is linear, as expected for hopping transport; in the experiments reported by Wasielewski and colleagues (*2*), the transition occurs when the conjugated bridge becomes longer than ~2.5 nm. The weaker length dependence associated with the hopping regime facilitates the transport of charge over greater distances, and it is this regime that might be considered most "wirelike," although tunneling through saturated peptide bonds, for example, has also been shown to provide enhanced transport over relatively large distances in redox proteins (*13*, *14*).

In the context of molecular electronics, it has been difficult to systematically examine the hopping regime in conjugated molecular wires connected to metallic contacts because of the relatively large range of molecular lengths required (spanning many nanometers) and the complexities of adsorbing long molecules to metal surfaces while controlling orientation. Electrical transport measurements on molecules up to 18 nm in length have been reported (*15*), and charge hopping in molecular junctions has been observed (*16*–*18*), but the systematic length dependence of conduction has not been a principal focus.

Here, we provide direct evidence for a change in transport mechanism from tunneling to hopping in molecular junctions based on conjugated oligophenyleneimine (OPI) wires ranging in length from 1.5 to 7.3 nm. We contacted OPI

Department of Chemistry and Department of Chemical Engineering and Materials Science, University of Minnesota, Minneapolis, MN 55455, USA.

*To whom correspondence should be addressed: frisbie@cems.umn.edu

wires grown from one electrode using controlled aryl imine addition chemistry; a metal-coated atomic force microscope (AFM) tip was used to make the second contact. We show that near 4 nm in length, the mechanism of transport in the wires changes abruptly, as evidenced by striking changes in the length, temperature, and electric field dependence of the current-voltage (*I-V*) characteristics. For longer wires, an analysis of the bias dependence established at least three different regimes of transport and provided an estimate of the single-wire conductivity. Overall, these experiments open considerable opportunities to probe the physical organic chemistry of molecular conduction, e.g., the roles of specific functional groups and bonding architectures on hopping transport in molecular wires.

OPI wires on gold substrates were prepared by a slight modification of a previously reported method (*19*). Figure 1A shows the molecular structure of OPI wire precursors (OPI-p) and OPI wires, as well as synthetic routes. The growth of OPI wires begins with OPI 1-p, prepared by immersing gold substrates into 1 mM 4-aminobenzenethiol in absolute ethanol for 24 hours. OPI-p wires were then grown by step-wise imination, with alternate addition of benzene-1,4-dicarboxaldehyde and benzene-1,4-diamine, as shown in Fig. 1A. Each OPI-p wire terminated with $-NH_2$ or –CHO groups was end-capped with benzaldehyde or aniline, respectively. The end-capping provided a consistent terminal group throughout the OPI series that facilitated reproducible electrical characterization. After each growth, both OPI-p and OPI monolayers were thoroughly rinsed with absolute ethanol and then dried in a stream of N_2.

Both OPI-p and OPI monolayers were characterized extensively by ellipsometry, x-ray photoelectron spectroscopy (XPS), reflection-absorption Fourier transform infrared spectroscopy (RAIRS), and cyclic voltammetry (CV). Key results are summarized in Table 1 as well as in the supporting online material (*20*). Monolayer thickness from ellipsometry and XPS measurements increased gradually, as expected, upon repeated imination. From the difference between estimated wire length and the measured monolayer thickness, we conclude that the OPI wires are tilted with an angle increasing from 20° to 45° with respect to the surface normal as wire length increases.

The RAIRS data, shown in Fig. 1B (left), reveal the alternate appearance and disappearance of carbonyl stretches (1710 cm^{-1}) and symmetric amine stretches (3350 cm^{-1}) in OPI-p molecules, which verified the imination mechanism and indicated near quantitative reaction of all exposed reactive end groups. The intensity of imine stretching (1620 cm^{-1}) and the benzene ring vibrational mode (1500 cm^{-1}) increased with the number of repeat units, as expected. Complete end-capping was confirmed by the disappearance of the terminal group vibrational modes in Fig. 1B (right).

Cyclic voltammograms (CV) of OPI wires are displayed in fig. S5 (*20*), and oxidation potentials and the estimated surface coverages for each OPI wire are compiled in Table 1 and table S2 (*20*). The CV sweeps of the OPI wires show nearly identical surface coverage (2.5×10^{-10} to 5.5×10^{-10} mol/cm^2) over the entire set of wires. Evidently, packing density is not greatly affected by molecular length. Collectively, the surface characterization data indicate that high-quality monolayers of OPI wires were prepared.

We investigated the transport characteristics of OPI wires using a conducting probe (CP) AFM (fig. S1), which has been used to measure conduction in a variety of molecular systems (*21–23*). In the semilog plot of resistance (*R*) versus molecular length (*L*) (Fig. 2A), each data point represents the average of 10 *I-V* traces. A clear transition of the length dependence of resistance is observed near 4 nm (OPI 5), indicating that the conduction mechanism is different in short (OPI 1 to 4) and long (OPI 6 to 10) OPI wires. In short wires, the linear fit in Fig. 2A indicates that the data are well described by Eq. 1 for nonresonant tunneling. The β value is found to be 3 nm^{-1}, which is within the range of β values of typical conjugated molecules (*24*, *25*).

For long OPI wires, there is a much flatter resistance versus molecular length relation ($\beta \sim 0.9$ nm^{-1}). The extremely small β suggests that the principal transport mechanism is hopping, as has been concluded in solution electron transfer studies of D-B-A systems (*2*, *11*, *26*). A plot of *R* versus *L* (Fig. 2A, inset) for long wires is linear, which is consistent with hopping and indicates that Eq. 1 does not apply for long wires. The change in transport mechanism apparent in the length-dependent measurements was verified by the temperature dependence. Figure 2B shows that resistance for OPI 4 is independent of temperature from 246 to 333 K, as expected for tunneling. However, both OPI 6 and OPI 10 display the strongly thermally activated transport that is characteristic of hopping. The activation energies determined from the slopes of the data are identical at 0.28 eV (6.5 kcal/mol) for both OPI 6 and

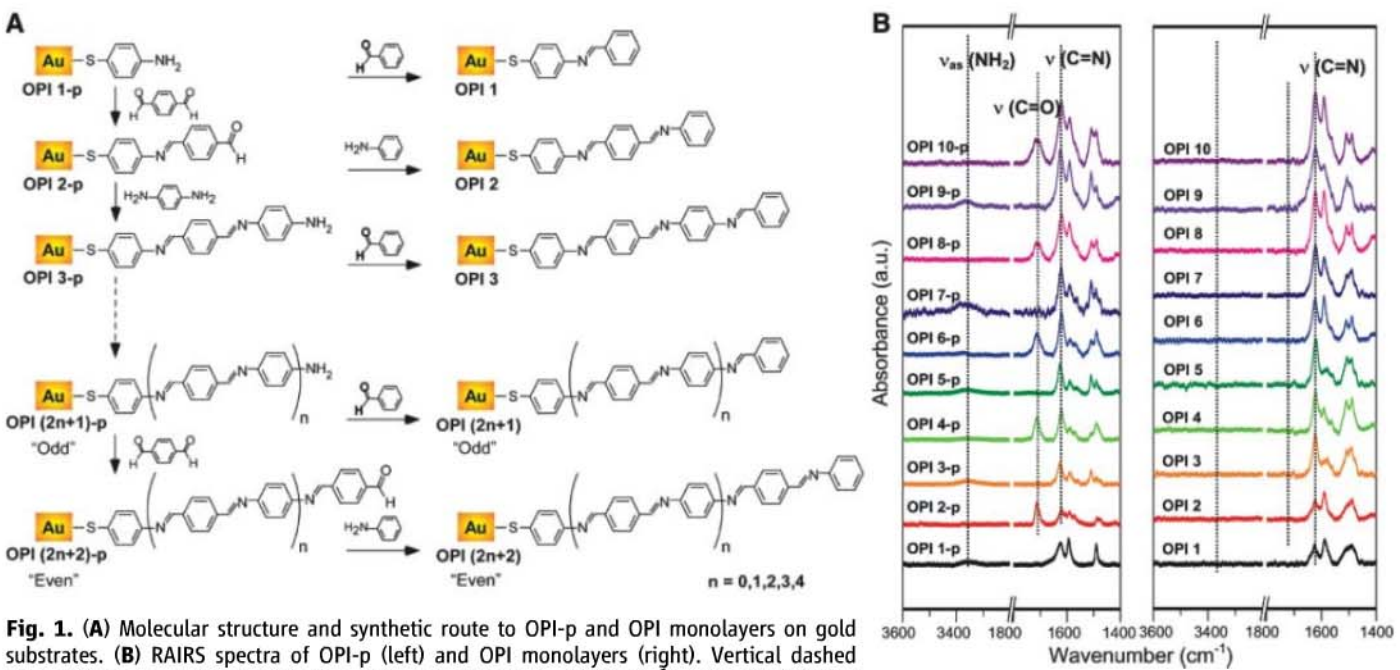

Fig. 1. (**A**) Molecular structure and synthetic route to OPI-p and OPI monolayers on gold substrates. (**B**) RAIRS spectra of OPI-p (left) and OPI monolayers (right). Vertical dashed lines indicate positions of symmetric amine stretches (NH_2, 3350 cm^{-1}), carbonyl stretches (C=O, 1710 cm^{-1}), and imine stretches (C=N, 1620 cm^{-1}). Peaks for NH_2 and C=O appear in the uncapped OPI-p wires with odd and even numbers of repeat units, respectively.

OPI 10. Contact effects are not responsible for the activated transport, because straightforward calculation shows that the injection efficiency is >99% (*27*). Collectively, the data in Fig. 2 indicate that the conduction mechanism transitions from tunneling to hopping near 4 nm.

Questions remain concerning the nature of the hopping sites in the long wires and the origin of the 0.28 eV activation energy. Electronic delocalization is limited in aromatic oligoimines because of the nonzero dihedral angle between the benzene ring and the imine bonds (*28*), that is, the wire molecules are not flat and the π-conjugation is broken. We have confirmed by ultraviolet-visible absorption spectroscopy that the conjugation does not extend over the entire wire (*20*). The optical gap (E_g) reduces with molecular length up to OPI 3 and then remains constant at 2.6 eV for longer OPI wires (Table 1). This result indicates that the π-conjugation extends over three repeating units by means of the imine linkage and that longer wires contain weakly linked conjugated subunits.

We propose that the short, three-repeat conjugated subunits are the charge-hopping sites in the wires and that the hopping activation energy corresponds to the barrier for rotation of the aromatic rings, which transiently couples the conjugated subunits. Charges are driven down the wires as the conjugation fluctuations permit. Torsional vibrations of the rings in analogous aromatic oligoimines are accompanied by coupled alterations of the C=N bond length, and this concerted motion is likely responsible for transiently coupling the conjugated subunits (*29*). The energy associated with these collective motions is indeed ~0.3 eV (*29*, *30*), which is comparable to the observed hopping barrier. From the slope of R versus L in Fig. 2 and the estimated number of wires in the junction (~100), we calculated a single-wire conductivity of 1×10^{-6} S/cm. This low value must reflect the low density of carriers in the wires and the significant hopping activation energy (*31*–*33*).

To examine the sensitivity of conduction to the wire architecture, we designed conjugation-broken OPI wires (CB-OPIs) in which an aliphatic cyclohexyl group was inserted into the molecular backbone. To incorporate the cyclohexyl moiety, we performed the imination with 1,4-diaminocyclohexane at elevated temperature (40°C) in pure ethanol for 24 hours. The structure of CB-OPI wires and their low voltage resistances are shown in Fig. 3. For CB-OPI 3 and CB-OPI 4, the resistance is increased compared with OPI 3 and OPI 4, as expected, because the aliphatic cyclohexyl links raise the average tunneling barrier. However, for the longer CB-OPI 8 and CB-OPI 10 molecules, the resistance change from the corresponding OPI 8 and OPI 10 wires is considerably greater, nearly two orders of magnitude.

Evidently, conduction in the long wires is much more sensitive to the presence of the cyclohexyl group than in the short wires, which also supports a difference in the charge transport mechanism. For hopping transport in the long wires, a large change in resistance is expected upon interrupting the conjugation. Ratner and colleagues (*34*, *35*) have calculated the site-to-site hopping probabilities for molecular wires and, indeed, a disruption in conjugation has a dramatic impact on electron transfer rates. However, tunneling is relatively insensitive to small perturbations in the conjugation of molecular bridges, because the tunneling rate reflects the average potential barrier of the bridge, not the barrier of the discrete cyclohexyl group alone. Thus, the conjugation blocking experiments confirm that conduction depends on the bond architecture, and they also support the conclusion that tunneling occurs in the short wires and hopping transport prevails in the long wires.

We have also carefully examined the voltage and electric field dependence of the *I-V* characteristics (Fig. 4). The semilog plot of I versus V for OPI wires in Fig. 4A demonstrates that current decreases as wire length increases, in keeping with the resistance results shown in Fig. 2. For the short wires (OPI 1 to 4), increasing molecular length yields large decreases in the current at all potentials. However, for the long wires (OPI 6 to 10), the log *I-V* curves show smaller decreases in current with increasing length. A plot of log I versus electric field E (Fig. 4A, inset) reveals that the traces for the long wires collapse nearly on top of one another. This result indicates that for

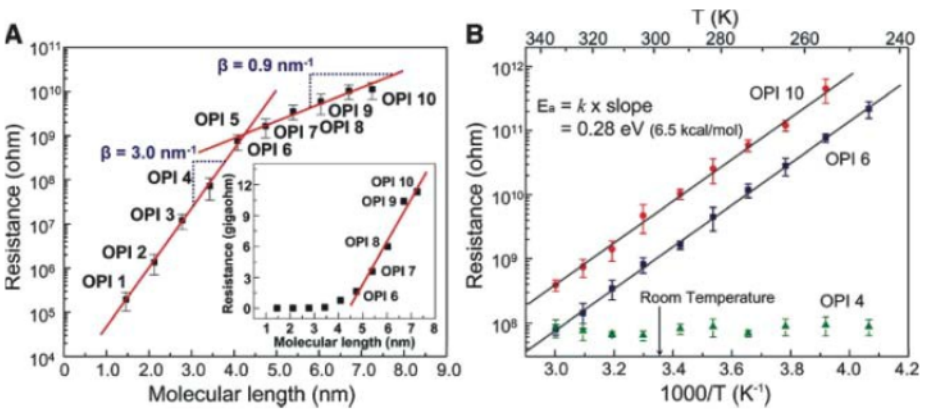

Fig. 2. Measurements of molecular wire resistance with CP-AFM. A gold-coated tip was brought into contact with an OPI monolayer on a gold substrate. The *I-V* traces were obtained over ±1.5 V for OPI 3 to 10 and ±1.0 V for OPI 1 and 2 at a load of 2 nN on the tip contact. (**A**) Semilog plot of R versus L for the gold/wire/gold junctions. Each data point is the average differential resistance obtained from 10 *I-V* traces in the range −0.3 to +0.3 V. Error bars, 1 SD. Straight lines are linear fits to the data according to Eq. 1. (Inset) A linear plot of R versus L, demonstrating linear scaling of resistance with length for the long OPI wires. (**B**) Arrhenius plot for OPI 4, OPI 6, and OPI 10. Each data point is the average differential resistance obtained at six different locations on samples in the range −0.2 to +0.2 V. Error bars, 1 SD. Straight lines are linear fits to the data.

Table 1. Selected experimental and calculated data for OPI wires. Molecular length was estimated with the Cambridge Scientific Chem3D software. Molecular length is the terminal H to S distance plus the Au-S bond length. It was assumed that Au-S bond length is 2.36 Å (*41*). Film thickness is from ellipsometry and XPS; the XPS data are underestimated because the intensity of photoelectrons from N atoms is not considered in the calculation of film thickness. The oxidation potentials were determined from the lower edge of the oxidation peak of OPI wires referenced to ferrocenium/ferrocene (Fc^+/Fc).

Monolayer	Estimated molecular length (nm)	Film thickness (by ellipsometry/XPS) (nm)	E_g (eV)	Oxidation potential (V)	n in I, I' $I \propto V^n$	n in II' $I \propto V^n$	V_{trans} (V) [E_{trans} (MV/cm)]	$V_{II'}$ (V) [$E_{II'}$ (MV/cm)]	ϕ_{FE} (eV)
OPI 2	2.1	1.8 / 1.6	3.1	0.22	1.1	–	0.85 [4.0]	–	–
OPI 3	2.8	2.5 / 1.9	2.6	0.14	1.1	–	0.75 [2.7]	–	–
OPI 4	3.4	3.0 / 2.1	2.6	0.06	1.3	–	0.75 [2.2]	–	–
OPI 6	4.7	4.1 / 2.7	2.6	0.05	1.2	2.6	1.00 [2.1]	0.5 [1.0]	0.3–0.5
OPI 10	7.3	5.3 / 4.0	2.6	0.00	0.9	2.6	0.95 [1.3]	0.40 [0.6]	0.3–0.5

the long wires, transport is field driven, as expected for a hopping mechanism in which the electric field pushes the carriers along the molecules. However, for the short wires, the *I-E* curves do not collapse on top of one another because tunneling is a voltage-driven process.

A log-log plot of the *I-V* characteristics facilitates more detailed analysis. Figure 4B displays log *I*–log *V* characteristics for OPI 4 and OPI 10, representative of the short and long wires. For OPI 4, there are two different transport regimes, labeled I and II; the transition occurs at 0.75 V. For OPI 10, the dependence is more complex, with three identifiable transport regimes (I′, II′, and III′) and transitions at 0.40 V and 0.95 V.

The data for OPI 4 in Fig. 4B demonstrate that, in regime I, the current scales linearly with voltage. Linear *I-V* behavior is expected for tunneling in the low-bias regime. To a first approximation, the metal/wire/metal junction can be modeled as a simple trapezoidal tunneling barrier. In this case, the tunneling current at low bias is given by Eq. 2.

$$I \propto V \exp\left(-\frac{2d\sqrt{2m_e\phi}}{\hbar}\right) \quad (2)$$

where d is the barrier width (wire length), m_e is the electron effective mass, and ϕ is the effective barrier height. At higher bias, the electric field changes the shape of the tunneling barrier from trapezoidal to triangular (*36*). In this case, the *I-V* behavior can be described by the Fowler-Nordheim relation:

$$\ln\left(\frac{I}{V^2}\right) \propto \frac{-4d\sqrt{2m_e\phi^3}}{3\hbar q}\left(\frac{1}{V}\right) \quad (3)$$

where q is the elementary charge.

The Fowler-Nordheim plot in Fig. 4C reveals a striking change in conduction behavior. For low voltages (Regime I), the current scales logarithmically with $1/V$, as expected from Eq. 2, indicative of direct tunneling. Above the transition voltage V_{trans} = 0.75 V (Regime II), the current scales linearly with $1/V$, with a negative slope characteristic of field emission (Eq. 3). The transition point, V_{trans}, is an estimate of the low voltage barrier height and corresponds to the voltage where the slope of the OPI 4 data changes in Fig. 4B. The V_{trans} values for the other short OPI wires are listed in table S1. The decrease of V_{trans} with length in short wires indicates that the estimated barrier height decreases as expected from the trend in oxidation potentials of OPI wires determined by cyclic voltammetry (Table 1) (*20*). Collectively, the data in Figs. 2 to 4 allow us to conclude that the transport mechanism in the short wires at low bias is direct (nonresonant) tunneling and transitions to field emission at higher bias.

We have carried out a similar analysis of the *I-V* behavior for long wires, OPI 6 to 10. The Fowler-Nordheim plot for OPI 10 in Fig. 4D reveals three distinct regimes corresponding with regimes I′, II′, and III′ in Fig. 4B. In the low-bias regime I′, the current scales linearly with voltage, which is consistent with ohmic hopping conduction. Linear scaling with V was taken as support for nonresonant tunneling in short wires in the discussion above (Eq. 2), but it is already clear that the low-bias mechanisms are different for the long and short wires, and direct tunneling is not consistent with the dependences of resistance on length or temperature evident in Fig. 2B. Ohmic (field-driven) conduction is also linear in V and requires that carriers be present in the wires. We propose that carriers are introduced in the long wires from the gold contacts and that these carriers result in ohmic hopping conduction at low biases up to $V_{II'}$, the transition voltage from regime I′ to II′. The presence of carriers (most likely positively charged holes) in the wires

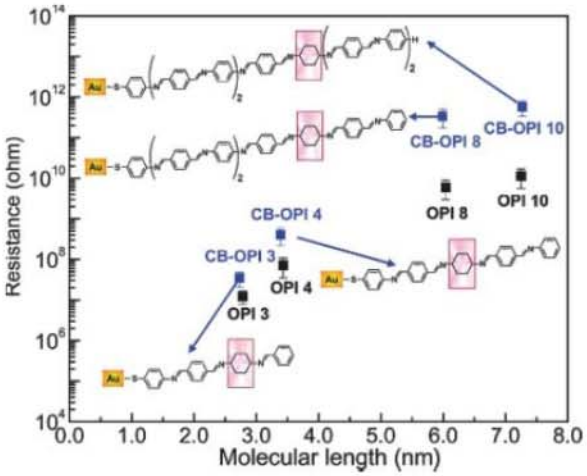

Fig. 3. Semilog plot of *R* versus *L* for gold/OPI/gold junctions and CB gold/CB-OPI/gold junctions. Each data point is the average differential resistance from 10 *I-V* traces in the interval −0.3 V to 0.3 V. Error bars, 1 SD. The blue squares are the resistances of CB-OPI wires. Pink boxes indicate the position where conjugation is broken.

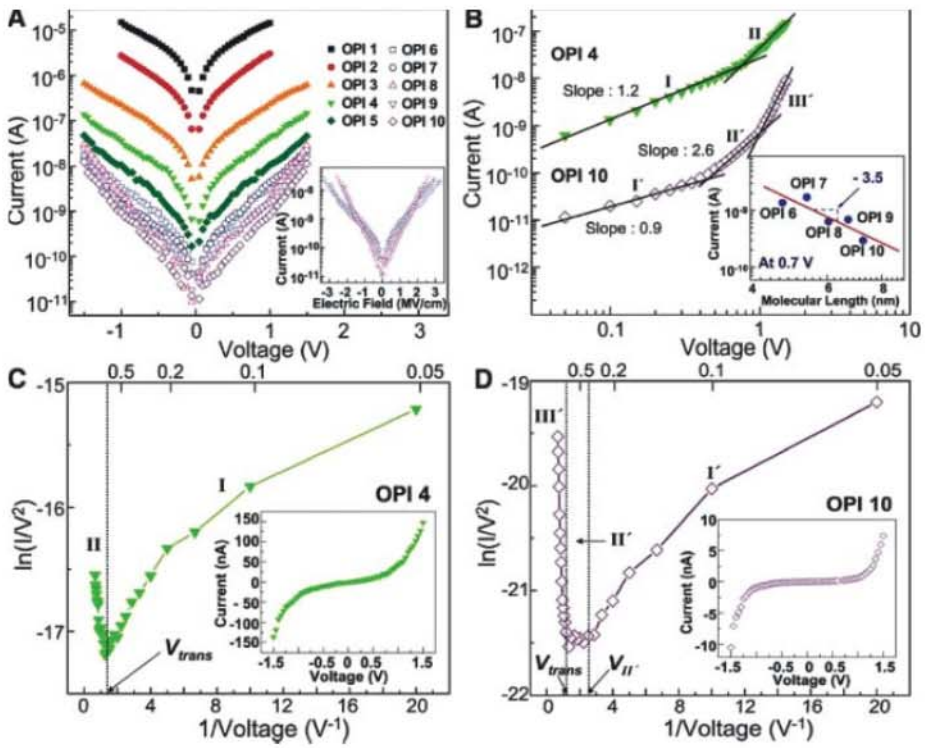

Fig. 4. (**A**) Semilog plot of the average current of 10 *I-V* traces for gold/wire/gold junctions. The inset is a semilog plot of *I* versus *E* for long OPI wires. (**B**) Log-log plot of the average of 10 *I-V* traces for the gold/OPI 4/gold and gold/OPI 10/gold junctions. Fits are shown in the different transport regimes. (Inset) A log-log plot of *I* versus *L* obtained at 0.7 V for all long OPI wires, displaying the linear fit with a slope of −3.5 (0.7 V is the bias at which all long OPI wires are within regime II′). (**C**) Fowler-Nordheim plot for the OPI 4 data in (B). Two distinct regimes (I and II) are clearly observable, with an inflection point at V_{trans}, indicating the switch from tunneling to field emission. The inset displays the sigmoidal current-voltage curve on a linear scale. (**D**) Fowler-Nordheim plot for the OPI 10 data in (B). Three distinct regimes (I′, II′, and III′) are evident. The inset shows the sigmoidal current-voltage curve.

means that the energy barrier to charge injection from the gold contacts must be smaller than the 0.7 eV E_F-E_{HOMO} offset measured by ultraviolet photoelectron spectroscopy (UPS) (*20*). Indeed, the offset will be reduced considerably by both the image potential associated with the metal contacts and the polaron shift (*16*), both of which are not accounted for in UPS measurements (*37*).

The negative slope in the high-voltage regime III′ of Fig. 4D suggests that field emission may also occur in OPI 10 (similar results were obtained for OPI 6 to 9). From the slope in regime III′, we calculated the emission barrier height (ϕ_{FE}) to be in the range of 0.3 to 0.5 eV, assuming carrier effective mass ratios in the range 0.1 to 1.0, which are typical for molecular junctions (*24*). We also considered other possible transport mechanisms in the metal/wire/metal junction, such as Schottky emission at the contact, Poole-Frenkel emission in the wires, and space-charge-limited transport in the presence of traps (*38*, *39*). However, we did not obtain reasonable values for extracted physical parameters with these other mechanisms (*20*). The estimated emission barrier heights for the other long OPI wires are also listed in Table 1 and table S1. Regime II′ is a transitional regime between ohmic conduction and field emission for OPI 10, and it may correspond to space-charge-limited conduction (SCLC), based on the slope of 2.6 in the log I versus log V plot (Fig. 4B) and the slope of –3.5 in the log I versus log L plot at 0.7 V (inset in Fig. 4B) (*39*, *40*). Further work is necessary to conclusively establish the transport mechanism in this regime.

References and Notes

1. A. Nitzan, M. A. Ratner, *Science* **300**, 1384 (2003).
2. W. B. Davis, W. A. Svec, M. A. Ratner, M. R. Wasielewski, *Nature* **396**, 60 (1998).
3. B. Giese, J. Amaudrut, A. K. Kohler, M. Spormann, S. Wessely, *Nature* **412**, 318 (2001).
4. R. L. Carroll, C. B. Gorman, *Angew. Chem. Int. Ed.* **41**, 4378 (2002).
5. H. D. Sikes *et al.*, *Science* **291**, 1519 (2001).
6. J. He *et al.*, *J. Am. Chem. Soc.* **127**, 1384 (2005).
7. K. S. Kwok, J. C. Ellenbogen, *Mater. Today* **5**, 28 (2002).
8. D. Segal, A. Nitzan, W. B. Davis, M. R. Wasielewski, M. A. Ratner, *J. Phys. Chem. B* **104**, 3817 (2000).
9. D. Segal, A. Nitzan, M. Ratner, W. B. Davis, *J. Phys. Chem. B* **104**, 2790 (2000).
10. Y. A. Berlin, A. L. Burin, M. A. Ratner, *Chem. Phys.* **275**, 61 (2002).
11. B. Giese, *Acc. Chem. Res.* **33**, 631 (2000).
12. E. M. Conwell, *Proc. Natl. Acad. Sci. U.S.A.* **102**, 8795 (2005).
13. D. N. Beratan, J. N. Onuchic, J. R. Winkler, H. B. Gray, *Science* **258**, 1740 (1992).
14. H. B. Gray, J. R. Winkler, *Proc. Natl. Acad. Sci. U.S.A.* **102**, 3534 (2005).
15. W. P. Hu *et al.*, *Phys. Rev. Lett.* **96**, 027801 (2006).
16. S. Kubatkin *et al.*, *Nature* **425**, 698 (2003).
17. Y. Selzer, M. A. Cabassi, T. S. Mayer, D. L. Allara, *J. Am. Chem. Soc.* **126**, 4052 (2004).
18. Y. Selzer *et al.*, *Nano Lett.* **5**, 61 (2005).
19. J. J. W. M. Rosink *et al.*, *Langmuir* **16**, 4547 (2000).
20. Materials and methods are available as supporting material on *Science* Online.
21. D. J. Wold, C. D. Frisbie, *J. Am. Chem. Soc.* **123**, 5549 (2001).
22. V. B. Engelkes, J. M. Beebe, C. D. Frisbie, *J. Am. Chem. Soc.* **126**, 14287 (2004).
23. X. D. Cui *et al.*, *Science* **294**, 571 (2001).
24. A. Salomon *et al.*, *Adv. Mater.* **15**, 1881 (2003).
25. M. D. Newton, *Chem. Rev.* **91**, 767 (1991).
26. F. C. Grozema, Y. A. Berlin, L. D. A. Siebbeles, *J. Am. Chem. Soc.* **122**, 10903 (2000).
27. Y. L. Shen, A. R. Hosseini, M. H. Wong, G. G. Malliaras, *Chem. Phys. Chem.* **5**, 16 (2004).
28. R. Akaba, K. Tokumaru, T. Kobayashi, *Bull. Chem. Soc. Jpn.* **53**, 1993 (1980).
29. J. Harada, M. Harakawa, K. Ogawa, *Acta Crystallogr. B* **60**, 578 (2004).
30. T. Tsuji, H. Takeuchi, T. Egawa, S. Konaka, *J. Am. Chem. Soc.* **123**, 6381 (2001).
31. F. C. Grozema *et al.*, *Adv. Mater.* **14**, 228 (2002).
32. F. C. Grozema, P. T. van Duijnen, Y. A. Berlin, M. A. Ratner, L. D. A. Siebbeles, *J. Phys. Chem. B* **106**, 7791 (2002).
33. P. Prins *et al.*, *Phys. Rev. Lett.* **96**, 146601 (2006).
34. Y. A. Berlin, G. R. Hutchison, P. Rempala, M. A. Ratner, J. Michl, *J. Phys. Chem. A* **107**, 3970 (2003).
35. Y. A. Berlin, M. A. Ratner, *Radiat. Phys. Chem.* **74**, 124 (2005).
36. J. M. Beebe, B.-S. Kim, J. W. Gadzuk, C. D. Frisbie, J. G. Kushmerick, *Phys. Rev. Lett.* **97**, 026801 (2006).
37. X.-Y. Zhu, *Surf. Sci. Rep.* **56**, 1 (2004).
38. S. M. Sze, *Physics of Semiconductor Devices* (Wiley, New York, 1981).
39. M. A. Lampert, *Phys. Rev.* **103**, 1648 (1956).
40. A. Rose, *Phys. Rev.* **97**, 1538 (1955).
41. J. M. Tour *et al.*, *J. Am. Chem. Soc.* **117**, 9529 (1995).

42. The authors thank G. Haugstad for support in the temperature-dependent measurements and X.-Y. Zhu for help with photoelectron spectroscopy. This work was supported primarily by the National Science Foundation under CHE-0616427. Partial support for facilities was provided by the NSF Materials Research Science and Engineering Centers program under DMR-0212302. Parts of this work were carried out in the Institute of Technology Characterization Facility, University of Minnesota, which receives partial support from NSF through the National Nanotechnology Infrastructure Network program.

Supporting Online Material

www.sciencemag.org/cgi/content/full/320/5882/1482/DC1
Materials and Methods
SOM Text
Figs. S1 to S8
Tables S1 and S2
References

15 February 2008; accepted 9 May 2008
10.1126/science.1156538

The Impact of Stratospheric Ozone Recovery on the Southern Hemisphere Westerly Jet

S.-W. Son,[1]* L. M. Polvani,[1,2] D. W. Waugh,[3] H. Akiyoshi,[4] R. Garcia,[5] D. Kinnison,[5] S. Pawson,[6] E. Rozanov,[7,8] T. G. Shepherd,[9] K. Shibata[10]

In the past several decades, the tropospheric westerly winds in the Southern Hemisphere have been observed to accelerate on the poleward side of the surface wind maximum. This has been attributed to the combined anthropogenic effects of increasing greenhouse gases and decreasing stratospheric ozone and is predicted to continue by the Intergovernmental Panel on Climate Change/Fourth Assessment Report (IPCC/AR4) models. In this paper, the predictions of the Chemistry-Climate Model Validation (CCMVal) models are examined: Unlike the AR4 models, the CCMVal models have a fully interactive stratospheric chemistry. Owing to the expected disappearance of the ozone hole in the first half of the 21st century, the CCMVal models predict that the tropospheric westerlies in Southern Hemisphere summer will be decelerated, on the poleward side, in contrast with the prediction of most IPCC/AR4 models.

Recent observations (*1*–*4*) indicate that the westerly jet in the Southern Hemisphere (SH) troposphere is accelerating on the poleward side; this is usually described as a positive trend of the Southern annular mode index (*1*). This acceleration has important consequences for SH climate: It directly affects the surface temperatures (*2*), the extent of sea ice (*2*), the variability of storm tracks (*5*), the location of arid regions (*6*), the strength of the wind-driven oceanic circulation (*7*), and the exchange of CO_2 and heat between atmosphere and ocean (*7*, *8*). Understanding and predicting changes in the SH westerlies are therefore of the utmost importance.

Climate models have shown that the recent wind changes likely result from an increase in greenhouse gases and the depletion of stratospheric ozone (*9*–*11*), but the relative contribution of these two effects remains an open question, especially for the 21st century when stratospheric ozone is expected to recover as a result of the implementation of the Montreal Protocol (*12*). The multimodel mean of the IPCC/AR4 atmosphere-ocean–coupled model integrations indicates that the acceleration of the SH westerlies on the

[1]Department of Applied Physics & Applied Mathematics, Columbia University, New York, NY 10027, USA. [2]Department of Earth and Environmental Sciences, Columbia University, New York, NY 10027, USA. [3]Department of Earth and Planetary Sciences, Johns Hopkins University, Baltimore, MD 21218, USA. [4]National Institute for Environmental Studies, Tsukuba, Japan. [5]National Center for Atmospheric Research (NCAR), Boulder, CO 80325, USA. [6]NASA/Goddard Space Flight Center, Greenbelt, MD 20771, USA. [7]Institute for Atmospheric and Climate Sciences/Eidgenössische Technische Hochschule (ETH), Zurich, Switzerland. [8]Physical Meteorological Observatory, World Radiation Center, Davos, Switzerland. [9]Department of Physics, University of Toronto, Toronto, Canada. [10]Meteorological Research Institute, Tsukuba, Japan.

*To whom correspondence should be addressed. E-mail: sws2112@columbia.edu

poleward side will continue in the 21st century (*5*, *13*, *14*), albeit at a weaker rate (*13*). However, because ozone recovery is not uniformly specified among the AR4 models, it is unclear at present what role, if any, ozone recovery plays in the acceleration of the SH westerlies.

To explore this issue, we examine the predictions of the CCMVal activity of the "stratospheric processes and their role in climate" (SPARC) project (*15*). These models faithfully reproduce past climate change in the SH (see the supporting online material). In this study, we analyze the output of all seven CCMVal models, which performed integrations up to the year 2050 (*16*). In contrast to AR4 models described below, the CCMVal models have a high vertical resolution in the stratosphere, a model top located above the stratopause (~ 50 km), and fully interactive stratospheric chemistry. All CCMVal models are forced with the IPCC A1B scenario for greenhouse gases and Ab scenario for halogen concentrations. The sea surface temperature is prescribed from either the coupled AR4 model on which a given CCMVal model is based or the UK Meteorological Office Hadley Centre model output (*15*).

The CCMVal model integrations are contrasted with those of AR4 models forced by A1B scenario greenhouse gases (*17*). Although the two sets of model integrations are comparable in the troposphere, they are substantially different in the stratosphere. Most AR4 models have the model top well below the stratopause (*17*, *18*). More importantly, time changes in stratospheric ozone concentration are ignored by nearly half the models. We examine the output of all 19 AR4 models, which is available at the IPCC/AR4 data archive: Of these models, 10 prescribe stratospheric ozone recovery, and the other 9 do not (*19*). The ozone recovery in the former group is specified either as simple linear function of time or from the output of two-dimensional models, which are driven by halogen loading consistent with the Montreal Protocol (*17*). The detailed spatial and temporal structures of the prescribed ozone recovery, however, have not been documented.

Because stratospheric ozone is predicted to increase approximately linearly from 2001 to 2050 in almost all CCMVal model integrations (*15*, *20*), we compute linear trends of all quantities using monthly or seasonally averaged zonal fields, from 2001 to 2050. Trends are first calculated for the individual model realizations with a least-square fit and then averaged among all available ensemble members for the same model. The multimodel mean trend in the spatial domain is produced by interpolating each model's trend linearly to the latitudes and log-linearly to the pressure levels.

We start by considering how ozone recovery affects the temperature in the upper troposphere and lower stratosphere. Figure 1A shows the SH polar-cap ozone trend predicted by multimodel mean of CCMVal models. The strongest ozone recovery is found at 50 hPa in October and at lower altitudes in the following months. This pattern is largely reminiscent of ozone depletion in the recent past (*21*, *22*), except for the reversal in sign and slightly higher location of maximum

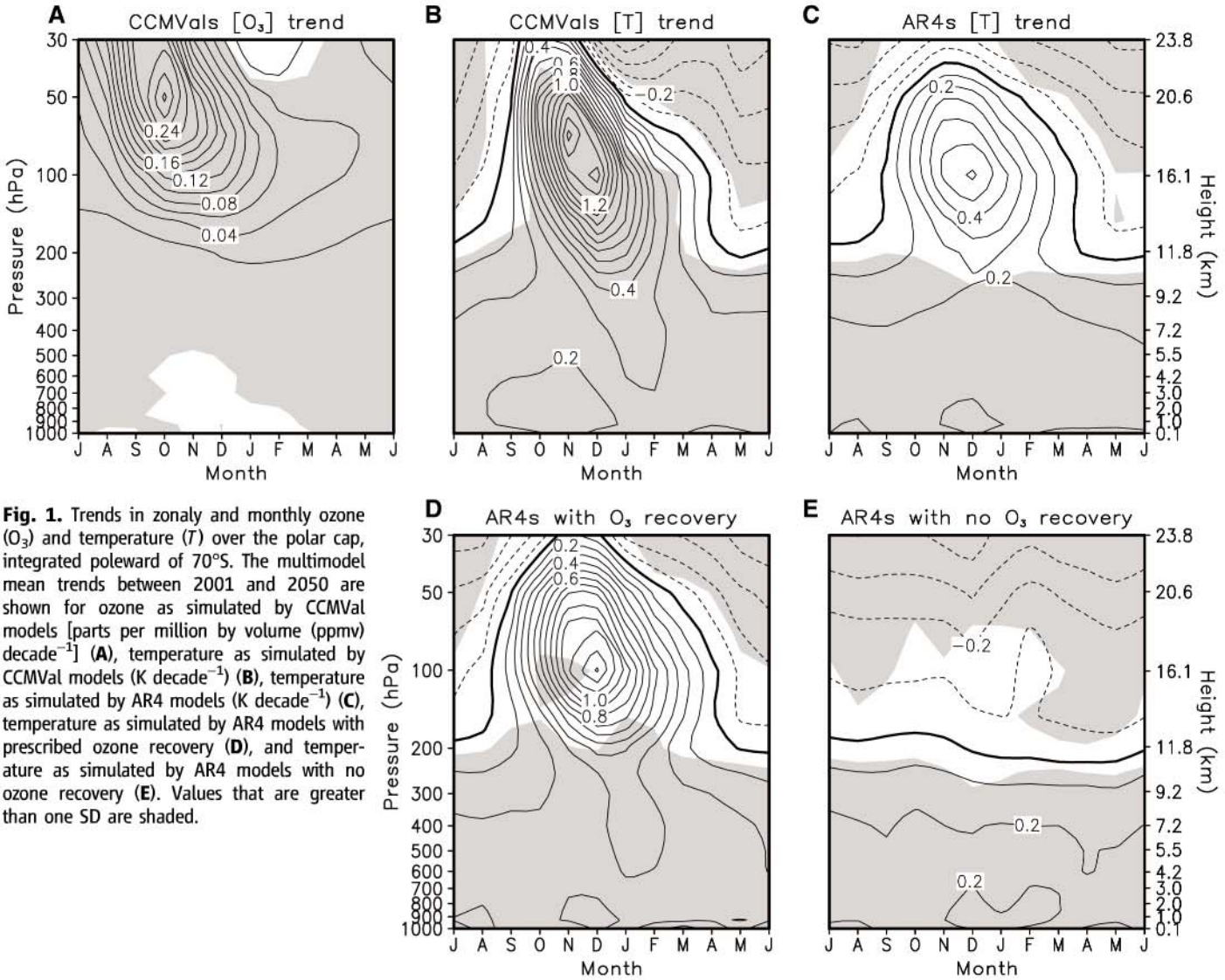

Fig. 1. Trends in zonaly and monthly ozone (O_3) and temperature (T) over the polar cap, integrated poleward of 70°S. The multimodel mean trends between 2001 and 2050 are shown for ozone as simulated by CCMVal models [parts per million by volume (ppmv) decade^{-1}] (**A**), temperature as simulated by CCMVal models (K decade^{-1}) (**B**), temperature as simulated by AR4 models (K decade^{-1}) (**C**), temperature as simulated by AR4 models with prescribed ozone recovery (**D**), and temperature as simulated by AR4 models with no ozone recovery (**E**). Values that are greater than one SD are shaded.

trend. Associated with such ozone recovery, lower-stratospheric temperatures over the polar cap increase substantially, as seen in Fig. 1B. This warming reaches down into the upper troposphere, as has been noted in stratospheric-resolving general circulation model experiments with prescribed ozone depletion (*9*) and chemistry-climate model integrations for the recent past (*22*).

Figure 1C shows corresponding polar-cap temperature trends, as predicted by all AR4 models. This multimodel mean trend shows a much weaker warming and is not statistically significant in the upper troposphere and lower stratosphere. This is due to the way in which ozone is prescribed in the AR4 models. In nearly half of those models, there is no ozone recovery, and this results in the absence of warming in the lower stratosphere for those models (Fig. 1E). Even when ozone recovery is prescribed (Fig. 1D), the AR4 models produce less robust polar-cap warming than the CCMVal models because of the large intermodel difference in temperature trends.

The ozone-induced temperature change in the lower-stratospheric polar cap has a substantial impact on the pressure and wind fields in the troposphere below (*2*, *10*, *11*). Figure 2A shows the multimodel mean trend in December-to-February mean SH westerlies simulated by CCMVal models. The tropospheric westerlies are found to be decelerated on the poleward side of the jet, implying a negative trend in Southern annular mode index in the future. This result is opposite to the one predicted by the multimodel mean of AR4 models, which shows acceleration on the poleward side of the jet (Fig. 2B). The importance of ozone-related warming is even clearer if one compares AR4 models with and without a prescribed ozone recovery. As seen in Fig. 2C, the multimodel mean trend for the subset of AR4 integrations with ozone recovery exhibits features qualitatively similar to those in CCMVal models, although the dipolar pattern is weaker and does not reach to the surface. When the ozone recovery is neglected (Fig. 2D), the AR4 models predict the opposite trend in the extratropics. This result indicates that the effect of ozone-induced warming overwhelms that of greenhouse gas–induced cooling in the lower-stratospheric polar cap and plays an important role in the acceleration of the tropospheric westerlies during the SH summer. Note that, owing to its strong seasonality (Fig. 1A), ozone recovery plays a minimal role during other seasons (*22*).

The impact of stratospheric ozone recovery on the SH westerlies is further clarified in Fig. 3, where the relationships among trends in lower-stratospheric polar-cap ozone and temperature, as well as lower-tropospheric westerlies, are shown for all model integrations. For the westerlies, trends are quantified by Δ[u]: the difference in the 850-hPa zonal wind at ±10° from the latitude of maximum wind. This is very similar to computing the Southern annular mode index (*1*) but is much simpler in practice.

First, note that the polar-cap warming in the lower stratosphere is linearly correlated with ozone recovery in the CCMVal models (Fig. 3A). A linear correlation is also found between trends in polar-cap temperature and in Δ[u] (Fig. 3B). This suggests that stronger polar-cap warming, associated with ozone recovery, results in a larger negative Δ[u] trend. This is equivalent to the larger negative trend of the Southern annular mode index (i.e., an equatorward intensification of the jet).

Second, consider the corresponding plot for AR4 models (Fig. 3C). Although essentially no relationship is found between trends in polar-cap temperature and in Δ[u] for those AR4 models with no ozone recovery (open circles), a significant negative correlation appears for those AR4 models with prescribed ozone recovery (filled circles). Moreover, the negative correlation for the latter AR4 models (dashed gray line) is similar to the one obtained from the CCMVal models (solid gray line). This shows that the response of tropospheric westerlies to polar-cap temperature trends is very robust, because it is found in two sets of substantially different climate models.

Third, observe that most CCMVal models show negative Δ[u] trends (Fig. 3B), whereas most AR4 models show positive Δ[u] trends (Fig. 3C), even when ozone recovery is prescribed. This difference is consistent with weaker polar-cap warming in AR4 models as compared with CCMVal models. Most AR4 models predict a polar-cap temperature trend smaller than ~ 1 K decade^{-1}, and such values result in a positive Δ[u] trend, even for the CCMVal models. At present, it is unclear why AR4 models underestimate the low-stratospheric polar-cap warming. On the one hand, it could result from an incorrect specification of the ozone recovery either in amplitude or spatial distribution (*23*); however, this cannot be ascertained, because the precise ozone fields used in each AR4 model have not been archived. On the other hand, it might result from the poorly resolved stratospheric circulation, the lack of vertical resolution, or artificial damping near the low model tops in AR4 models. Further work is needed to clarify this underestimate.

The detailed mechanisms through which stratospheric ozone affects the tropospheric westerly jet remain unclear at present. Several hypothe-

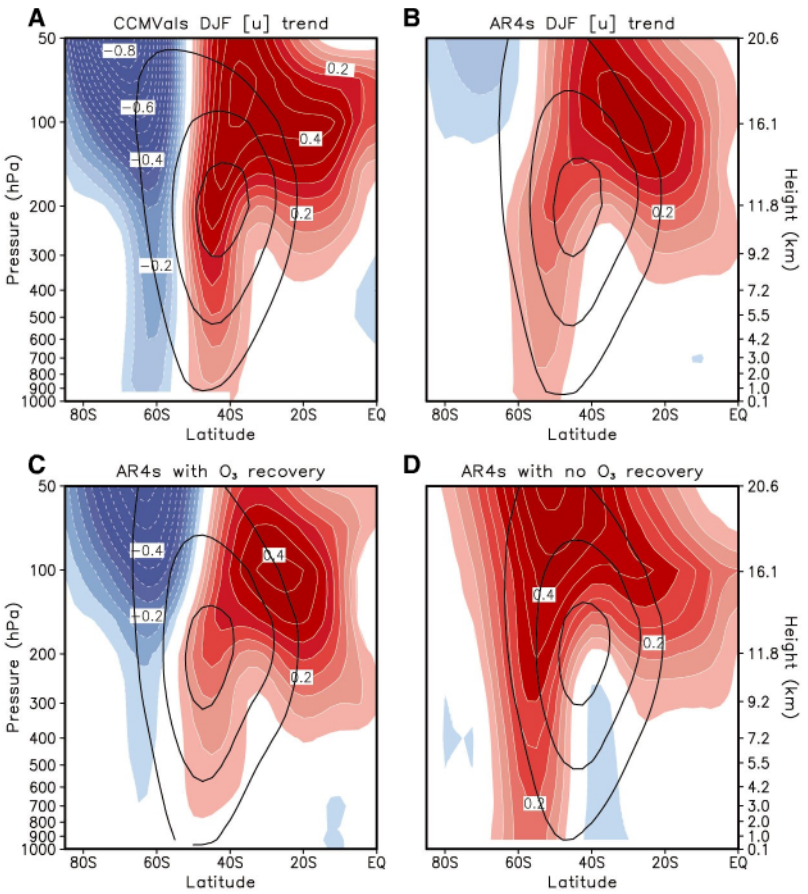

Fig. 2. Trends in December-to-February (DJF) zonal-mean zonal wind. The multimodel mean trends between 2001 and 2050 are shown for the CCMVal models (**A**), the AR4 models (**B**), the AR4 models with prescribed ozone recovery (**C**), and the AR4 models with no ozone recovery (**D**). Shading and contour intervals are 0.05 ms^{-1} decade^{-1}. Deceleration and acceleration are indicated with blue and red colors, respectively, and trends weaker than 0.05 ms^{-1} decade^{-1} are omitted. Superimposed black solid lines are DJF zonal-mean zonal wind averaged from 2001 to 2010, with a contour interval of 10 ms^{-1}, starting at 10 ms^{-1}. EQ, equator.

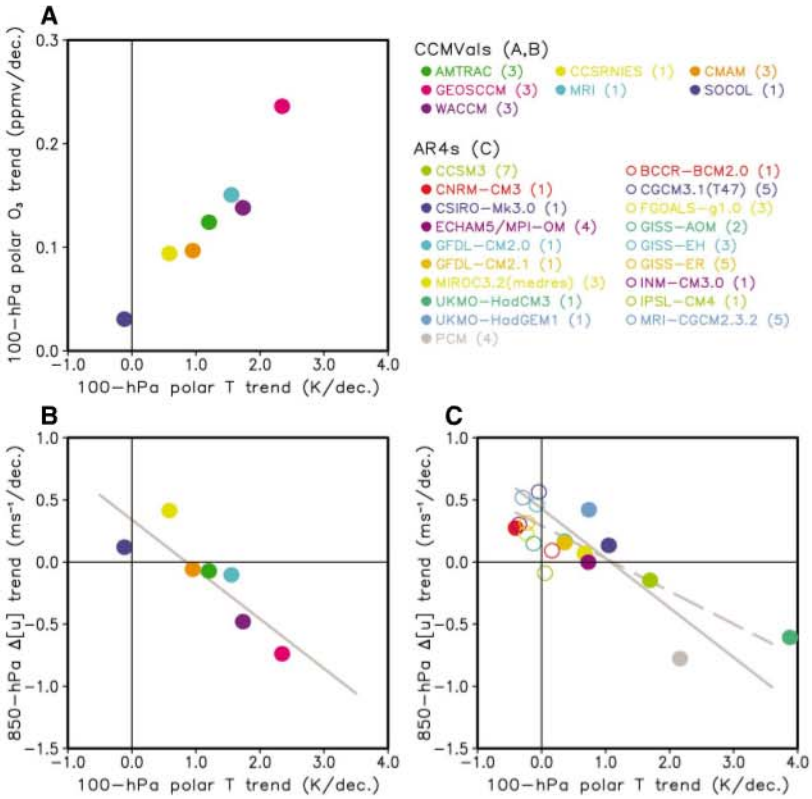

Fig. 3. Relationships among SH polar-cap ozone trend at 100 hPa, polar-cap temperature trend at 100 hPa, and extratropical zonal wind trend at 850 hPa: for ozone and temperature trends as simulated by CCMVal models (**A**), for zonal wind and temperature trends as simulated by CCMVal models (**B**), and for zonal wind and temperature trends as simulated by AR4 models (**C**). Here, ozone and temperature trends are calculated for September-to-December and November-to-January mean quantities, respectively. The averaging months are chosen to reflect the largest trends at 100 hPa, as seen in Fig. 1. The zonal wind trends at 850 hPa are quantified by Δ[u]: the difference in DJF-averaged zonal wind at ±10° from the latitude of maximum wind. Negative values denote the deceleration (acceleration) of westerlies on the poleward (equatorward) side of the maximum wind. The filled and open circles in (C) correspond to the AR4 models with and without prescribed ozone recovery. Solid and dashed gray lines in (B) and (C) indicate linear fit for CCMVal models and AR4 models with prescribed ozone recovery, respectively. Numbers within parentheses in the key denote the number of ensemble members used for each model. dec., decade.

ses have been proposed (*4*, *24*–*27*), but none have been validated or falsified. Nonetheless, our analyses suggest that stratospheric processes, and ozone recovery in particular, may be able to affect SH climate in major ways and thus should be included in predictions of SH climate in the 21st century.

References and Notes

1. D. W. J. Thompson, J. M. Wallace, G. C. Hegerl, *J. Clim.* **13**, 1018 (2000).
2. D. W. J. Thompson, S. Solomon, *Science* **296**, 895 (2002).
3. G. J. Marshall, *J. Clim.* **16**, 4134 (2003).
4. G. Chen, I. Held, *Geophys. Res. Lett.* **34**, L21805 (2007).
5. J. H. Yin, *Geophys. Res. Lett.* **32**, L18701 (2005).
6. J. Lu, G. A. Vecchi, T. Reichler, *Geophys. Res. Lett.* **34**, L06805 (2007).
7. J. Russell, K. W. Dixon, A. Gnanadesikan, R. J. Stouffer, J. R. Toggweiler, *J. Clim.* **19**, 6382 (2006).
8. B. K. Mignone, A. Gnanadesikan, J. L. Sarmiento, R. D. Slater, *Geophys. Res. Lett.* **33**, L01604 (2006).
9. N. P. Gillett, D. W. J. Thompson, *Science* **302**, 273 (2003).
10. D. T. Shindell, G. A. Schmidt, *Geophys. Res. Lett.* **31**, L18209 (2004).
11. J. M. Arblaster, G. A. Meehl, *J. Clim.* **19**, 2896 (2006).
12. A first hint of ozone recovery is already present in the most recent observations (*15*, *28*). The sharp decrease in stratospheric ozone concentration has ceased around the year 2000, and ozone levels have started to increase since then. Although weak, this increasing trend is found in almost all ground-based and satellite observations (*28*). In addition, the chemistry-climate models, discussed in the text, predict that the increase in stratospheric ozone concentration will continue in the 21st century (*15*).
13. R. L. Miller, G. A. Schmidt, D. T. Shindell, *J. Geophys. Res.* **111**, D18101 (2006).
14. D. J. Lorenz, E. T. DeWeaver, *J. Geophys. Res.* **112**, D10119 (2007).
15. V. Eyring *et al.*, *J. Geophys. Res.* **112**, D16303 (2007).
16. The CCMVal models used in this study are AMTRAC, CCSRNIES, CMAM, GEOSCCM, MRI, SOCOL, and WACCM [see table 1 of (*15*) for the detailed model configuration]. All available ensemble members are used for each model.
17. G. A. Meehl *et al.*, in *Climate Change 2007: The Physical Science Basis. Contribution of Working Group I to the Fourth Assessment Report of the Intergovernmental Panel on Climate Change* (Cambridge Univ. Press, Cambridge, 2007), pp. 747–845.
18. E. C. Cordero, P. M. de F. Forster, *Atmos. Chem. Phys.* **6**, 5369 (2006).
19. The AR4 models used in this study are BCCR-BCM2.0, CCSM3, CGCM3.1(T47), CNRM-CM3, CSIRO-Mk3.0, ECHAM5/MPI-OM, FGOALS-g1.0, GFDL-CM2.0, GFDL-CM2.1, GISS-AOM, GISS-EH, GISS-ER, INM-CM3.0, IPSL-CM4, MIROC3.2(medres), MRI-CGCM2.3.2, UKMO-HadCM3, UKMO-HadGEM1, and PCM. Among these 19 models, 10 models—CCSM3, CNRM-CM3, CSIRO-Mk3.0, ECHAM5/MPI-OM, GFDL-CM2.0, GFDL-CM2.1, MIROC3.2(medres), UKMO-HadCM3, UKMO-HadGEM1, and PCM—prescribe ozone recovery. All available ensemble members are used for each model.
20. Changes in stratospheric ozone concentration in CCMVal model integrations are not perfectly linear. Almost all CCMVal models predict a slow increase until 2010 and a relatively faster increase thereafter until about 2060 [see figure 7 in (*15*)].
21. W. Randel, F. Wu, *Geophys. Res. Lett.* **26**, 3089 (1999).
22. J. Perlwitz, S. Pawson, R. L. Fogt, J. E. Nielsen, W. D. Neff, *Geophys. Res. Lett.* **35**, L08714 (2008).
23. J. A. Crook, N. P. Gillett, S. P. E. Keeley, *Geophys. Res. Lett.* **35**, L07806 (2008).
24. D. T. Shindell, G. A. Schmidt, R. L. Miller, D. Rind, *J. Geophys. Res.* **106**, 7193 (2001).
25. J. Perlwitz, N. Harnik, *J. Clim.* **16**, 3011 (2003).
26. P. J. Kushner, L. M. Polvani, *J. Clim.* **17**, 629 (2004).
27. D. W. J. Thompson, J. C. Furtado, T. G. Shepherd, *J. Atmos. Sci.* **63**, 2616 (2006).
28. E.-S. Yang, D. M. Cunnold, M. J. Newchurch, R. J. Salawitch, *Geophys. Res. Lett.* **32**, L12812 (2005).

29. The authors thank J. Austin and J. Perlwitz for helpful discussions and suggestions on the manuscript, the National Oceanic and Atmospheric Administration Climate Diagnostics Center for providing the National Centers for Environmental Prediction–NCAR reanalysis data, the European Centre for Medium-Range Weather Forecasts for providing the ERA40 data, the World Climate Research Programme SPARC CCMVal project for organizing the chemistry-climate model (CCM) data analysis activity, the British Atmospheric Data Center for collecting and archiving the CCM output, the Program for Climate Model Diagnosis and Intercomparison for collecting and archiving the IPCC/AR4 model data, the Joint Scientific Committee of the Climate Variability Working Groups on Coupled Modeling and their Coupled Model Intercomparison Project and Climate Simulation Panel for organizing the model data analysis activity, and the IPCC Working Group I Technical Support Unit for technical support. The IPCC Data Archive at the Lawrence Livermore National Laboratory is supported by the Office of Sciences, U.S. Department of Energy. The work of S.W.S. and L.M.P. is supported, in part, by a grant from the NSF. Contributions of D.W.W. and S.P. are supported by NASA's modeling and analysis program, and GEOSCCM was run on Columbia with resources allocated by NASA's high-performance computing program. WACCM simulations were carried out at NCAR, at NASA's Ames Research Center, and at the Barcelona Supercomputing Center, Spain. The CCSRNIES's research is supported by the Global Environmental Research Fund of the Ministry of the Environment of Japan (A 071) and a grant in aid for scientific research from the Ministry of Education, Culture, Sports, Science and Technology of Japan (no. 19340138). The development and maintenance of SOCOL are supported by ETH Zurich (grant PP 1/04 1) and the Swiss National Science Foundation (grant SCOPES IB7320 110884). Contributions of the CMAM group and T.G.S. are supported by the Canadian Foundation for Climate and Atmospheric Sciences, the Natural Sciences and Engineering Research Council of Canada, and Environment Canada. NCAR is sponsored by the NSF.

Supporting Online Material

www.sciencemag.org/cgi/content/full/320/5882/1486/DC1
SOM Text
Figs. S1 to S3

31 January 2008; accepted 14 May 2008
10.1126/science.1155939

Evidence for Upwelling of Corrosive "Acidified" Water onto the Continental Shelf

Richard A. Feely,[1]* Christopher L. Sabine,[1] J. Martin Hernandez-Ayon,[2] Debby Ianson,[3] Burke Hales[4]

The absorption of atmospheric carbon dioxide (CO_2) into the ocean lowers the pH of the waters. This so-called ocean acidification could have important consequences for marine ecosystems. To better understand the extent of this ocean acidification in coastal waters, we conducted hydrographic surveys along the continental shelf of western North America from central Canada to northern Mexico. We observed seawater that is undersaturated with respect to aragonite upwelling onto large portions of the continental shelf, reaching depths of ~40 to 120 meters along most transect lines and all the way to the surface on one transect off northern California. Although seasonal upwelling of the undersaturated waters onto the shelf is a natural phenomenon in this region, the ocean uptake of anthropogenic CO_2 has increased the areal extent of the affected area.

Over the past 250 years, the release of carbon dioxide (CO_2) from industrial and agricultural activities has resulted in atmospheric CO_2 concentrations that have increased by about 100 parts per million (ppm). The atmospheric concentration of CO_2 is now higher than it has been for at least the past 650,000 years, and is expected to continue to rise at an increasing rate, leading to pronounced changes in our climate by the end of this century (*1*). Since the beginning of the industrial era, the oceans have absorbed ~127 ± 18 billion metric tons of carbon as CO_2 from the atmosphere, or about one-third of the anthropogenic carbon emissions released (*2*). This process of absorption of anthropogenic CO_2 has benefited humankind by substantially reducing the greenhouse gas concentrations in the atmosphere and minimizing some of the impacts of global warming. However, the ocean's daily uptake of 22 million metric tons of CO_2 has a sizable impact on its chemistry and biology. Recent hydrographic surveys and modeling studies have confirmed that the uptake of anthropogenic CO_2 by the oceans has resulted in a lowering of seawater pH by about 0.1 since the beginning of the industrial revolution (*3*–*7*). In the coming decades, this phenomenon, called "ocean acidification," could affect some of the most fundamental biological and geochemical processes of the sea and seriously alter the fundamental structure of pelagic and benthic ecosystems (*8*).

Estimates of future atmospheric and oceanic CO_2 concentrations, based on the Intergovernmental Panel on Climate Change (IPCC) CO_2 emission scenarios and general circulation models, indicate that atmospheric CO_2 concentrations could exceed 500 ppm by the middle of this century, and 800 ppm near the end of the century. This increase would result in a decrease in surface-water pH of ~0.4 by the end of the century, and a corresponding 50% decrease in carbonate ion concentration (*5*, *9*). Such rapid changes are likely to negatively affect marine ecosystems, seriously jeopardizing the multifaceted economies that currently depend on them (*10*).

The reaction of CO_2 with seawater reduces the availability of carbonate ions that are necessary for calcium carbonate ($CaCO_3$) skeleton and shell formation for marine organisms such as corals, marine plankton, and shellfish. The extent to which the organisms are affected depends largely on the $CaCO_3$ saturation state (Ω), which is the product of the concentrations of Ca^{2+} and CO_3^{2-} divided by the apparent stoichiometric solubility product for either aragonite or calcite:

$$\Omega_{arag} = [Ca^{2+}][CO_3^{2-}]/K'_{sp_{arag}} \quad (1)$$

$$\Omega_{cal} = [Ca^{2+}][CO_3^{2-}]/K'_{sp_{cal}} \quad (2)$$

where the calcium concentration is estimated from the salinity, and the carbonate ion con-

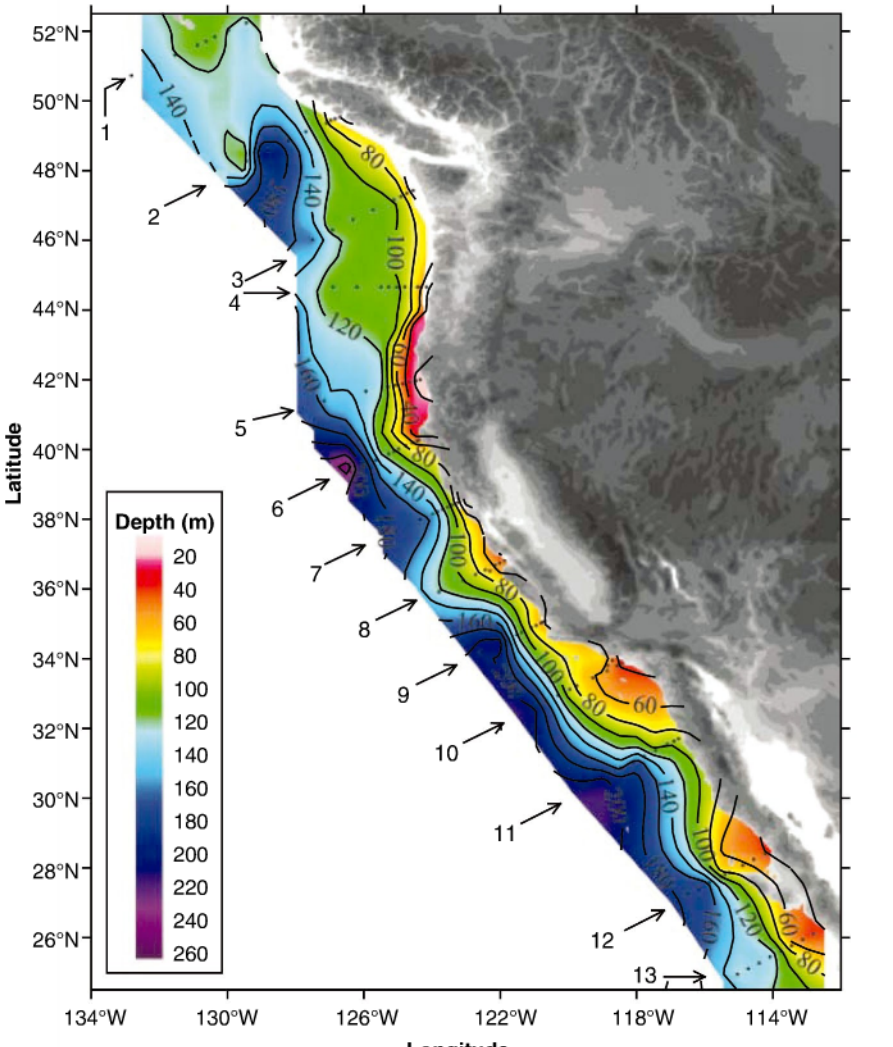

Fig. 1. Distribution of the depths of the undersaturated water (aragonite saturation < 1.0; pH < 7.75) on the continental shelf of western North America from Queen Charlotte Sound, Canada, to San Gregorio Baja California Sur, Mexico. On transect line 5, the corrosive water reaches all the way to the surface in the inshore waters near the coast. The black dots represent station locations.

[1]Pacific Marine Environmental Laboratory/National Oceanic and Atmospheric Administration, 7600 Sand Point Way NE, Seattle, WA 98115–6349, USA. [2]Instituto de Investigaciones Oceanologicas, Universidad Autonoma de Baja California, Km. 103 Carr. Tijuana-Ensenada, Ensenada, Baja California, Mexico. [3]Fisheries and Oceans Canada, Institute of Ocean Science, Post Office Box 6000, Sidney, BC V8L 4B2, Canada. [4]College of Oceanic and Atmospheric Sciences, Oregon State University, 104 Ocean Administration Building, Corvallis, OR 97331–5503, USA.

*To whom correspondence should be addressed. E-mail: richard.a.feely@noaa.gov

centration is calculated from the dissolved inorganic carbon (DIC) and total alkalinity (TA) measurements (*11*). In regions where Ω_{arag} or Ω_{cal} is > 1.0, the formation of shells and skeletons is favored. Below a value of 1.0, the water is corrosive and dissolution of pure aragonite and unprotected aragonite shells will begin to occur (*12*). Recent studies have shown that in many regions of the ocean, the aragonite saturation horizon shoaled as much as 40 to 200 m as a direct consequence of the uptake of anthropogenic CO_2 (*3*, *5*, *6*). It is shallowest in the northeastern Pacific Ocean, only 100 to 300 m from the ocean surface, allowing for the transport of undersaturated waters onto the continental shelf during periods of upwelling.

In May and June 2007, we conducted the North American Carbon Program (NACP) West Coast Cruise on the Research Ship *Wecoma* along the continental shelf of western North America, completing a series of 13 cross-shelf transects from Queen Charlotte Sound, Canada, to San Gregorio Baja California Sur, Mexico (Fig. 1). Full water column conductivity-temperature-depth rosette stations were occupied at specified locations along each transect (Fig. 1). Water samples were collected in modified Niskin-type bottles and analyzed for DIC, TA, oxygen, nutrients, and dissolved and particulate organic carbon. Aragonite and calcite saturation, seawater pH (pH_{SW}), and partial pressure of CO_2 (pCO_2) were calculated from the DIC and TA data (*11*).

The central and southern coastal region off western North America is strongly influenced by seasonal upwelling, which typically begins in early spring when the Aleutian low-pressure system moves to the northwest and the Pacific High moves northward, resulting in a strengthening of the northwesterly winds (*13*, *14*). These winds drive net surface-water Ekman transport offshore, which induces the upwelling of CO_2-rich, intermediate-depth (100 to 200 m) offshore waters onto the continental shelf. The upwelling lasts until late summer or fall, when winter storms return.

During the cruise, various stages and strengths of upwelling were observed from line 2 off central Vancouver Island to line 11 off Baja California, Mexico. We observed recent upwelling on lines 5 and 6 near the Oregon-California border. Coincident with the upwelled waters, we found evidence for undersaturated, low-pH seawater in the bottom waters as depicted by Ω_{arag} values < 1.0 and pH values < 7.75. The corrosive waters reached mid-shelf depths of ~40 to 120 m along lines 2 to 4 and lines 7 to 13 (Fig. 1). In the region of the strongest upwelling (line 5), the isolines of Ω_{arag} = 1.0, DIC = 2190, and pH = 7.75 closely followed the 26.2 potential density surface (Fig. 2). This density surface shoaled from a depth of ~150 m in the offshore waters and breached the surface over the shelf near the 100-m bottom contour, ~40 km from the coast. This shoaling of the density surfaces and CO_2-rich waters as one approaches land is typical of strong coastal upwelling conditions (*15*–*18*). The surface-water pCO_2 on the 26.2 potential density surface was about 850 µatm near the shelfbreak and higher inshore (Fig. 2), possibly enhanced by respiration processes on the shelf (*17*). These results indicate that the upwelling process caused the entire water column shoreward of the 50-m bottom contour to become undersaturated with respect to aragonite, a condition that was not predicted to occur in open-ocean surface waters until 2050 (*5*). On line 6, the next transect south, the undersaturated water was close to the surface at ~22 km from the coast. The lowest Ω_{arag} values (<0.60) observed in the near-bottom waters of the continental shelf corresponded with pH values close to 7.6. Because the calcite saturation horizon is located between 225 and 400 m in this part of the northeastern Pacific (*19*), it is still too deep to shoal onto the continental shelf. Nevertheless, the calcite saturations values drop in the core of the upwelled water (Ω_{cal} < 1.3).

As noted, the North Pacific aragonite saturation horizons are among the shallowest in the global ocean (*3*). The uptake of anthropogenic CO_2 has caused these horizons to shoal by 50 to 100 m since preindustrial times so that they are within the density layers that are currently being upwelled along the west coast of North America.

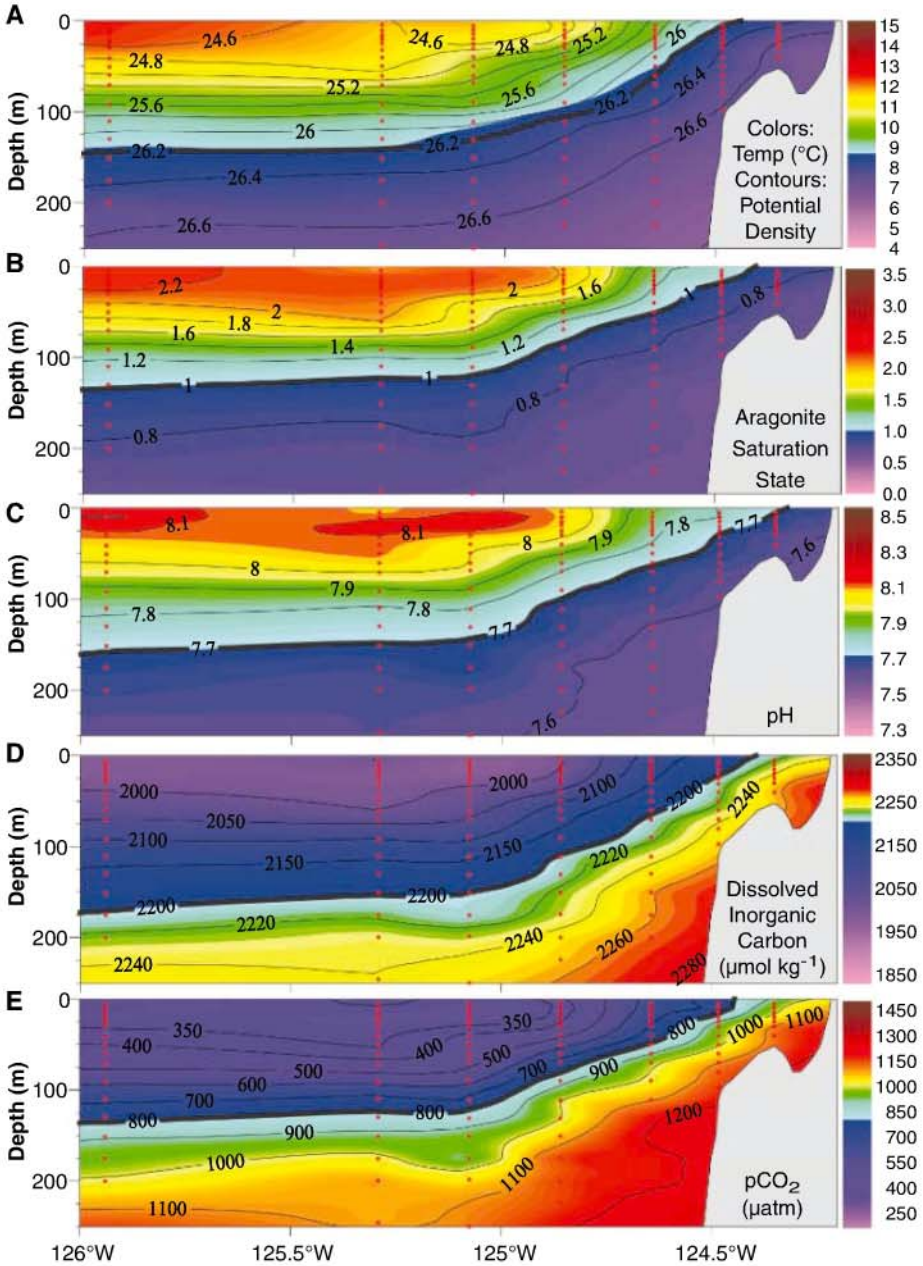

Fig. 2. Vertical sections of (**A**) temperature, (**B**) aragonite saturation, (**C**) pH, (**D**) DIC, and (**E**) pCO_2 on transect line 5 off Pt. St. George, California. The potential density surfaces are superimposed on the temperature section. The 26.2 potential density surface delineates the location of the first instance in which the undersaturated water is upwelled from depths of 150 to 200 m onto the shelf and outcropping at the surface near the coast. The red dots represent sample locations.

Although much of the corrosive character of these waters is the natural result of respiration processes at intermediate depths below the euphotic zone, this region continues to accumulate more anthropogenic CO_2 and, therefore, the upwelling processes will expose coastal organisms living in the water column or at the sea floor to less saturated waters, exacerbating the biological impacts of ocean acidification.

On the basis of our observed O_2 values and estimated O_2 consumption rates on the same density surfaces (*18*–*20*), the upwelled water off northern California (line 5) was last at the surface about 50 years ago, when atmospheric CO_2 was about 65 ppm lower than it is today. The open-ocean anthropogenic CO_2 distributions in the Pacific have been estimated previously (*4*, *19*, *21*). By determining the density dependence of anthropogenic CO_2 distributions in the eastern-most North Pacific stations of the Sabine *et al.* (*21*) data set, we estimate that these upwelled waters contain ~31 ± 4 μmol kg^{-1} anthropogenic CO_2 (fig. S2). Removing this signal from the DIC increases the aragonite saturation state of the waters by about 0.2 units. Thus, without the anthropogenic signal, the equilibrium aragonite saturation level ($\Omega_{arag} = 1$) would be deeper by about 50 m across the shelf, and no undersaturated waters would reach the surface. Water already in transit to upwelling centers carries increasing anthropogenic CO_2 and more corrosive conditions to the coastal oceans of the future. Thus, the undersaturated waters, which were mostly a problem for benthic communities in the deeper waters near the shelf break in the preindustrial era, have shoaled closer to the surface and near the coast because of the additional inputs of anthropogenic CO_2.

These observations clearly show that seasonal upwelling processes enhance the advancement of the corrosive deep water into broad regions of the North American western continental shelf. Because the region experiences seasonal periods of enhanced aragonite undersaturation, it is important to understand how the indigenous organisms deal with this exposure and whether future increases in the range and intensity of the corrosiveness will affect their survivorship. Presently, little is known about how this intermittent exposure to corrosive water might affect the development of larval, juvenile, and adult stages of aragonitic calcifying organisms or finfish that populate the neritic and benthic environments in this region and fuel a thriving economy. Laboratory and mesocosm experiments show that these changes in saturation state may cause substantial changes in overall calcification rates for many species of marine calcifiers including corals, coccolithophores, foraminifera, and pteropods, which are a major food source for local juvenile salmon (*8*, *22*–*30*). Similar decreases in calcification rates would be expected for edible mussels, clams, and oysters (*22*, *31*). Other research indicates that many species of juvenile fish and shellfish of economic importance to coastal regions are highly sensitive to higher-than-normal CO_2 concentrations such that high rates of mortality are directly correlated with the higher CO_2 concentrations (*31*, *32*). Although comprehensive field studies of organisms and their response to sporadic increases in CO_2 along the western North American coast are lacking, current studies suggest that further research under field conditions is warranted. Our results show that a large section of the North American continental shelf is affected by ocean acidification. Other continental shelf regions may also be affected where anthropogenic CO_2-enriched water is being upwelled onto the shelf.

References and Notes

1. U. Siegenthaler *et al.*, *Science* **310**, 1313 (2005).
2. C. L. Sabine, R. A. Feely, in *Greenhouse Gas Sinks*, D. Reay, N. Hewitt, J. Grace, K. Smith, Eds. (CABI, Oxfordshire, UK, 2007).
3. R. A. Feely *et al.*, *Science* **305**, 362 (2004).
4. C. L. Sabine *et al.*, *Science* **305**, 367 (2004).
5. J. C. Orr *et al.*, *Nature* **437**, 681 (2005).
6. K. Caldeira, M. E. Wickett, *J. Geophys. Res. Oceans* **110**, 365 (2005).
7. R. A. Feely *et al.*, *PICES Press* **16**, 22 (2008).
8. J. A. Kleypas *et al.*, "Impacts of Increasing Ocean Acidification on Coral Reefs and Other Marine Calcifiers: A Guide for Future Research," report of a workshop held 18 to 20 April 2005, St. Petersburg, FL, sponsored by NSF, NOAA, and the U.S. Geological Survey (2006).
9. S. Solomon *et al.*, Eds, in *Contribution of Working Group I to the Fourth Assessment Report of the Intergovernmental Panel on Climate Change* (Cambridge Univ. Press, Cambridge and New York, 2007).
10. J. Raven *et al.*, "Ocean acidification due to increasing atmospheric carbon dioxide," policy document 12/05 (The Royal Society, London, 2005).
11. The details of the analytical methods and calculations for the carbonate system and anthropogenic CO_2 are given in the supporting online material.
12. R. A. Feely *et al.*, *Mar. Chem.* **25**, 227 (1988).
13. B. Hickey, in *The Sea*, A. R. Robinson, K. H. Brink, Eds. (Wiley, New York, 1998), vol. 2.
14. J. Timothy Pennington, F. P. Chavez, *Deep Sea Res. Part II Top. Stud. Oceanogr.* **47**, 947 (2000).
15. A. van Geen *et al.*, *Deep Sea Res. Part II Top. Stud. Oceanogr.* **47**, 975 (2000).
16. G. E. Friederich, P. M. Walz, M. G. Burczynski, F. P. Chavez, *Prog. Oceanogr.* **54**, 185 (2002).
17. D. Ianson *et al.*, *Deep Sea Res. Part I Oceanogr. Res. Pap.* **50**, 1023 (2003).
18. B. Hales *et al.*, *Global Biogeochem. Cycles* **19**, 10.1029/2004GB002295 (2005).
19. R. A. Feely *et al.*, *Global Biogeochem. Cycles* **16**, 1144 (2002).
20. R. A. Feely *et al.*, *J. Oceanogr.* **60**, 45 (2004).
21. C. L. Sabine *et al.*, *Global Biogeochem. Cycles* **16**, 1083 (2002).
22. M. A. Green, M. E. Jones, C. L. Boudreau, R. L. Moore, B. A. Westman, *Limnol. Oceanogr.* **49**, 727 (2004).
23. J. M. Guinotte *et al.*, *Coral Reefs* **22**, 551 (2003).
24. C. Langdon, M. J. Atkinson, *J. Geophys. Res. Oceans* **110**, C09S07 (2005).
25. H. J. Spero *et al.*, *Nature* **390**, 497 (1997).
26. U. Riebesell *et al.*, *Nature* **407**, 364 (2000).
27. I. Zondervan *et al.*, *Global Biogeochem. Cycles* **15**, 507 (2001).
28. B. A. Seibel, V. J. Fabry, *Adv. Appl. Biodivers. Sci.* **4**, 59 (2003).
29. B. Delille *et al.*, *Global Biogeochem. Cycles* **19**, GB2023 (2005).
30. A. Engel *et al.*, *Limnol. Oceanogr.* **50**, 493 (2005).
31. F. Gazeau *et al.*, *Geophys. Res. Lett.* **34**, L07603 (2007).
32. A. Ishimatsu *et al.*, *J. Oceanogr.* **60**, 731 (2004).

33. We thank Captain Richard Verlini and the crew of the *R/V Wecoma* for logistics support. We also thank D. Greeley, D. Wisegarver, P. Covert, and S. Barry for the DIC and TA measurements. Financial support for this work was provided by the National Oceanic and Atmospheric Administration's Global Carbon Cycle Program and the National Aeronautical and Space Administration Ocean Biology and Biogeochemistry Program.

Supporting Online Material

www.sciencemag.org/cgi/content/full/1155676/DC1
Materials and Methods
Figs. S1 and S2
References

25 January 2008; accepted 13 May 2008
Published online 22 May 2008;
10.1126/science.1155676
Include this information when citing this paper.

Regulation of Hepatic Lipogenesis by the Transcription Factor XBP1

Ann-Hwee Lee,[1]* Erez F. Scapa,[2,3] David E. Cohen,[2,3] Laurie H. Glimcher[1,2]*

Dietary carbohydrates regulate hepatic lipogenesis by controlling the expression of critical enzymes in glycolytic and lipogenic pathways. We found that the transcription factor XBP1, a key regulator of the unfolded protein response, is required for the unrelated function of normal fatty acid synthesis in the liver. XBP1 protein expression in mice was elevated after feeding carbohydrates and corresponded with the induction of critical genes involved in fatty acid synthesis. Inducible, selective deletion of XBP1 in the liver resulted in marked hypocholesterolemia and hypotriglyceridemia, secondary to a decreased production of lipids from the liver. This phenotype was not accompanied by hepatic steatosis or compromise in protein secretory function. The identification of XBP1 as a regulator of lipogenesis has important implications for human dyslipidemias.

Hepatic lipid synthesis increases upon ingestion of excess carbohydrates, which are converted into triglyceride (TG) in the liver and transported to adipose tissue for energy storage. Dysregulation of hepatic lipid metabolism is closely related to the development of metabolic syndrome, a condition characterized by central obesity, dyslipidemia, elevated blood glucose, and hypertension (*1*). In mammals, hepatic lipid metabolism is controlled by transcription factors, such as liver X receptor (LXR), sterol regulatory element–binding proteins (SREBPs), and carbohydrate response element–binding protein (ChREBP), that regulate the expression of

[1]Department of Immunology and Infectious Diseases, Harvard School of Public Health, Boston, MA 02115, USA. [2]Department of Medicine, Harvard Medical School, Boston, MA 02115, USA. [3]Division of Gastroenterology, Brigham and Women's Hospital, Boston, MA 02115, USA.

*To whom correspondence should be addressed. E-mail: lglimche@hsph.harvard.edu (L.H.G.); ahlee@hsph.harvard.edu (A.-H.L.)

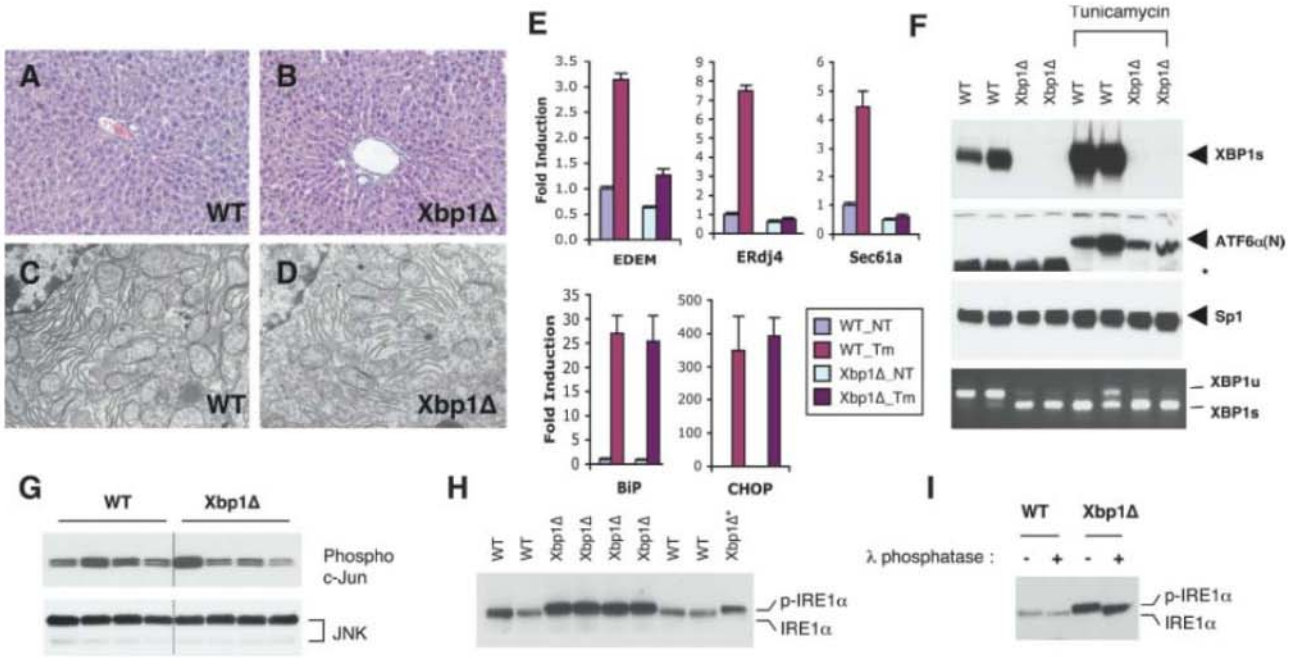

Fig. 1. ER stress response in XBP1-deficient mouse liver. (**A** and **B**) Hematoxylin and eosin staining of sections of wild-type (WT) and *Xbp1*Δ liver (magnification, 40×). (**C** and **D**) Transmission electron micrographs of WT and *Xbp1*Δ liver. (**E**) Total RNAs were prepared from the liver of WT and *Xbp1*Δ mice 8 hours after tunicamycin injection. Expression of representative UPR target genes was tested by quantitative real-time polymerase chain reaction (PCR) analysis. Fold induction represents relative expression level ± SEM compared to that of untreated WT mice; $N = 4$ per group. (**F**) Western blot of nuclear XBP1s and the processed ATF6α(N) proteins. Sp1 expression is a loading control. Levels of IRE1α-mediated XBP1 mRNA (both WT and mutant) splicing were measured by reverse transcription PCR. Asterisk denotes nonspecific band. (**G**) Total and active JNK protein levels were determined by Western blot and c-Jun kinase assay, respectively. (**H**) IRE1α was detected by immunoprecipitation followed by Western blot with IRE1α antibody. One-third of the *Xbp1*Δ immunoprecipitation product was loaded on the last lane for a better comparison of band migration. Phosphorylated IRE1α displayed slowed migration on the gel. (**I**) IRE1α immunoprecipitation products were treated with λ phosphatase. Western blot analysis shows a band shift upon phosphatase treatment.

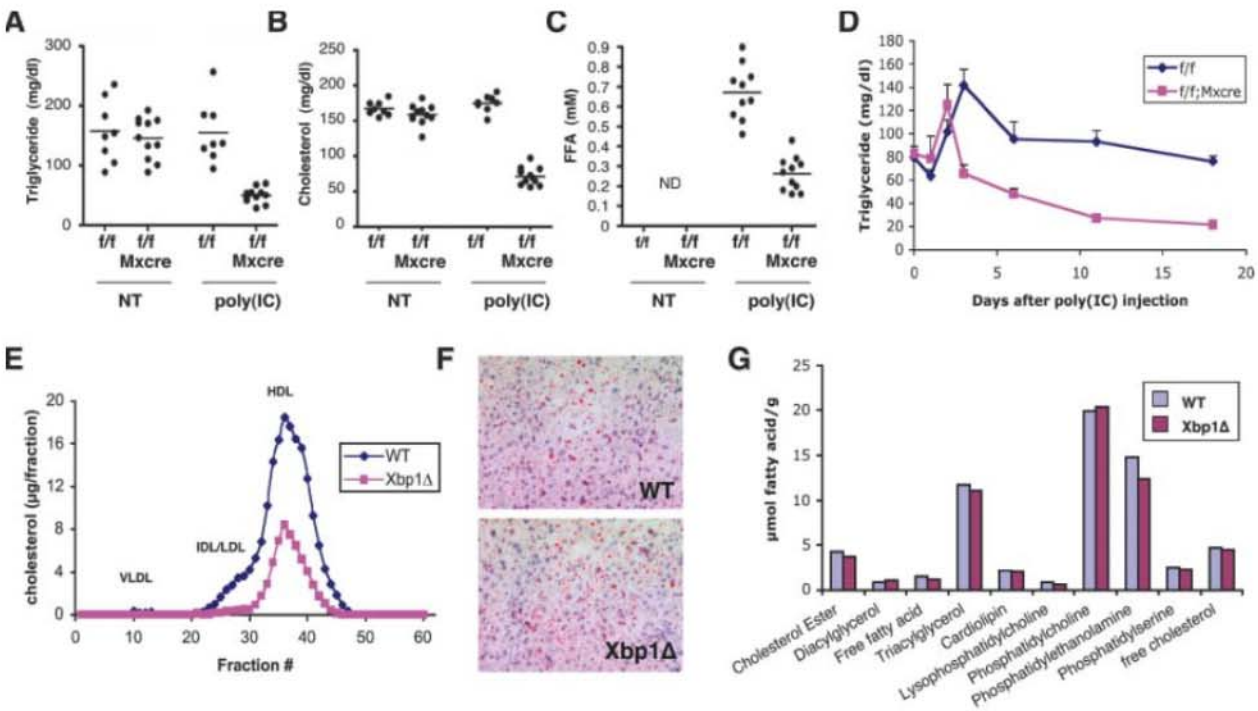

Fig. 2. Plasma and hepatic lipid profiles of XBP1-deficient mice. *Xbp1*$^{f/f}$ and *Xbp1*$^{f/f}$*;Mx1-cre* mice were injected three times with poly(I:C). (**A** to **D**) Three weeks after the last injection, plasma TG (A), cholesterol (B), and serum free fatty acid levels (C) were measured. (D) Plasma TG levels were measured over time in mice that received a single injection of 250 μg of poly(I:C). Error bars represent SEM. $N = 6$ or 7. (**E**) Distribution of plasma cholesterol was determined by FPLC separation of lipoprotein particles. (**F**) Fat content in the liver was determined by Oil Red O staining (magnification, 60×). (**G**) Lipid composition in the liver was determined by Lipomics analysis (Lipomics Technologies); $N = 4$ per group.

critical enzymes involved in glycolytic and lipogenic pathways (*2*).

XBP1 is a key regulator of the mammalian unfolded protein response (UPR) or endoplasmic reticulum (ER) stress response (*3*). Upon ER stress, the proximal sensor and endoribonuclease IRE1α induces unconventional splicing of XBP1 mRNA to generate a mature mRNA encoding an active transcription factor, XBP1s, which directly binds to the promoter region of ER chaperone genes (*4*–*6*). Mice lacking XBP1 display severe abnormalities in the development and function of professional secretory cells such as plasma B cells and pancreatic acinar cells, resulting in greatly reduced secretion of immunoglobulin and zymogens (*7*, *8*). XBP1 is also required for embryonic liver development (*9*). To investigate the role of XBP1 in postnatal hepatic function, we examined *Xbp1*Δ mice bearing an inducible, conditional disruption of the *Xbp1* gene in the liver (fig. S1).

*Xbp1*Δ mice that lacked XBP1 in the liver postnatally did not show any noticeable gross abnormalities, had normal body weight and liver mass (table S1), and presented no evidence of liver damage as determined by serum alanine aminotransferase levels and histological analysis (Fig. 1, A and B, and table S1). *XBP1*Δ hepatocytes had normal ER ultrastructure, although the ER was less abundant (Fig. 1, C and D). Serum albumin and total protein levels were slightly decreased in *Xbp1*Δ mice, suggesting minor compromise in hepatic protein secretory function (table S1). The XBP1-dependent UPR target genes *EDEM*, *ERdj4*, and *Sec61α* were only modestly down-regulated in *Xbp1*Δ liver in the basal state (Fig. 1E). Further, deletion of XBP1 in the liver did not itself evoke ER stress, as evidenced by the lack of ATF6α processing, c-Jun N-terminal kinase (JNK) activation, and induction of the pancreatic ER kinase (PERK)–regulated *BiP* and *CHOP* mRNAs (Fig. 1, E to G). Microarray analysis also confirmed normal expression of XBP1-independent stress markers in *Xbp1*Δ liver (table S2). The pharmacological ER stress inducer tunicamycin normally activated ATF6α processing and PERK-dependent gene expression in *Xbp1*Δ liver, excluding the possibility that the hepatocytes had adapted to a putative stress milieu. As expected, XBP1-dependent UPR target genes such as *EDEM*, *ERdj4*, and *Sec61α* were not induced by tunicamycin in *Xbp1*Δ liver (Fig. 1, E and F). However, XBP1 deficiency did lead to constitutive activation of its upstream activator IRE1α, made evident by robust splicing of the mutant XBP1 mRNA and induction of both IRE1α protein and its phosphorylation, as measured by a band shift sensitive to phosphatase treatment (Fig. 1, F, H, and I). Hence, IRE1α, but not PERK or ATF6, is activated in XBP1-deficient liver, which suggests feedback regulation of IRE1α by its downstream target XBP1 in an ER stress–independent manner.

Because XBP1 plays an important role in membrane lipid synthesis in the ER (*10*), we asked whether it regulates fatty acid synthesis in the liver. Injection of polyinosinic-polycytidylic acid [poly(I:C)] into *Xbp1*$^{f/f}$*;Mx1cre* mice resulted in marked decreases of plasma TG, cholesterol, and free fatty acids (Fig. 2, A to C). In a time-course experiment, the plasma TG level was lower than in wild-type mice as early as 3 days after a single injection of poly(I:C) into *Xbp1*$^{f/f}$*;Mx1cre* mice (Fig. 2D) and further decreased over time. XBP1 deletion also caused remarkable changes in the distribution of cholesterol, resulting in an almost complete absence of low-density lipoprotein (LDL)–associated cholesterol (Fig. 2E). In contrast, the content and composition of hepatic lipids were not changed in *Xbp1*Δ mice (Fig. 2, F and G), indicating that lipid retention in the liver was not responsible for low plasma lipid levels.

The liver secretes very-low-density lipoprotein (VLDL) particles that transport fatty acids in the form of TGs together with cholesterol to peripheral tissues (*11*, *12*). To test whether VLDL-associated TG secretion was impaired in XBP1's absence, we injected mice with tyloxapol (*13*), a compound that inhibits the breakdown of VLDL lipids (Fig. 3A). *Xbp1*Δ mice displayed a decreased rate of plasma TG accumulation, indicating impaired TG secretion from the liver. We next examined

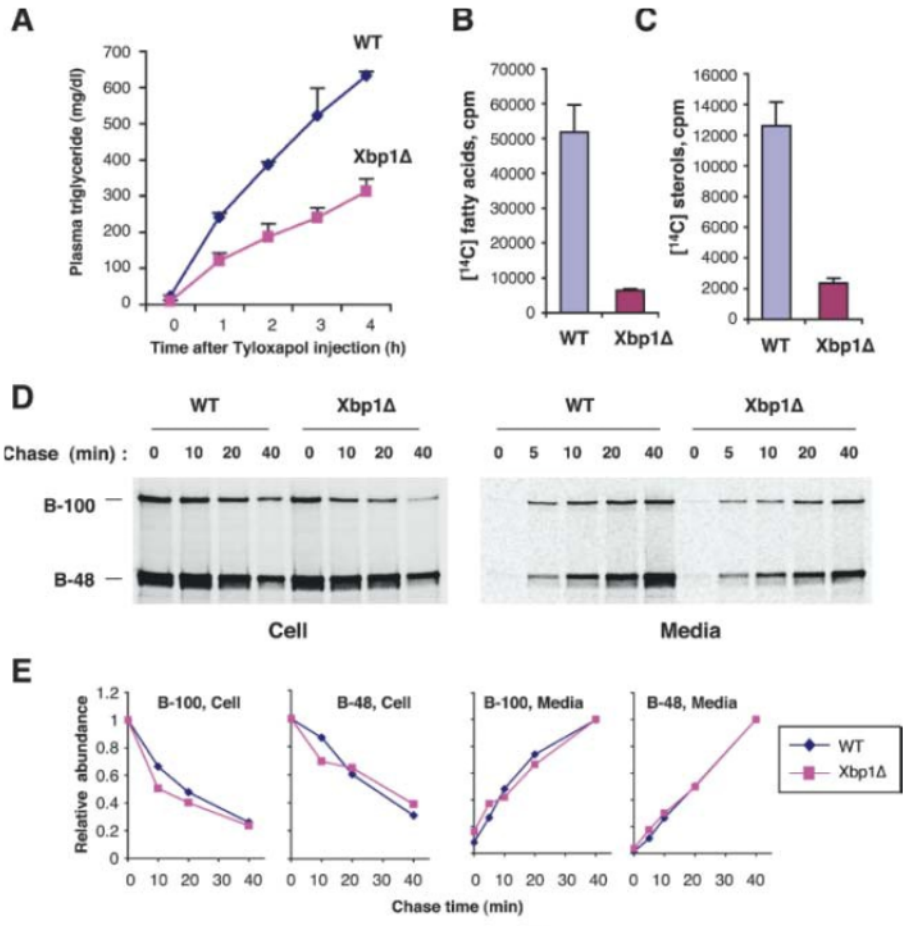

Fig. 3. Diminished hepatic TG secretion and lipid synthesis, but normal turnover of apoB, in the absence of XBP1. (**A**) Mice were injected with tyloxapol after a 4-hour fast, and plasma TG levels were measured over time (N = 4 per group). Primary hepatocytes were labeled with [^{14}C]acetate. (**B** and **C**) Radiolabeled fatty acids (B) and sterols (C) extracted from equal numbers of cells were measured by scintillation counting. (**D**) Primary hepatocytes from WT and *Xbp1*Δ mice were labeled with [^{35}S]methionine/cysteine for 30 min and then chased for the indicated times. Radiolabeled apoB protein species were immunoprecipitated from cells and media and revealed by SDS–polyacrylamide gel electrophoresis followed by fluorography. (**E**) The disappearance from cells and the accumulation in media of radiolabeled apoB protein species were determined by plotting relative radioactivity of each band (normalized to initial level in cells or final level in media) versus chase time. (**F**) Western blot analysis of plasma apoB protein.

whether the impaired TG secretion was due to compromised lipid synthesis. Incorporation of [^{14}C]acetate into fatty acids and sterols was drastically decreased in primary hepatocytes lacking XBP1 (Fig. 3, B and C), indicating that XBP1 is required for de novo lipid synthesis in the liver.

Neither the steady-state level of plasma apolipoprotein B (apoB) proteins, a major protein component of VLDL, nor the stability and secretion from primary hepatocytes of newly synthesized apoB proteins were altered by loss of XBP1 (Fig. 3, D to F). Therefore, VLDL particles produced from XBP1-deficient liver displayed low lipid but normal apoB protein content, as demonstrated by fast protein liquid chromatography (FPLC) analysis (fig. S2).

Given the compromised de novo lipid synthesis in *Xbp1*Δ liver, we asked whether XBP1 regulates the expression of genes involved in glycolysis and lipid synthesis pathways. Critical lipogenic genes such as those encoding stearyl coenzyme A (CoA) desaturase 1 (Scd1), diacylglycerol acetyltransferase 2 (Dgat2), and acetyl CoA carboxylase 2 (Acc2) were significantly down-regulated in *Xbp1*Δ liver (Fig. 4A and fig. S3). Genetic ablation or inhibition using antisense oligonucleotides of these genes has profound effects on hepatic lipid metabolism (*14*–*18*). In contrast, expression of SREBP family–regulated genes encoding fatty acid synthase (Fasn), HMG-CoA synthase (Hmgcs), and HMG-CoA reductase (Hmgcr) (*19*) was not altered in *Xbp1*Δ mice, consistent with normal SREBP-1 and SREBP-2 transcripts and processed nuclear protein species (Fig. 4A and fig. S3). ChREBP expression was also normal in *Xbp1*Δ liver. Hence, XBP1 regulates the expression of a subset of lipogenic genes in a SREBP- and ChREBP-independent manner.

Prolonged feeding of high-carbohydrate diets such as fructose increases de novo lipid synthesis in the liver through induction of genes encoding lipogenic enzymes (*20*–*22*). Hepatic XBP1s protein was markedly induced in mice fed a 60% fructose diet, along with a modest increase of its mRNA reflecting increased splicing by IRE1α (fig. S4). The ER stress markers BiP and CHOP were not induced under the same conditions, indicating an absence of ER stress. XBP1s was also induced in primary hepatocytes cultured in medium containing high glucose (Fig. 4B), which suggests that increased glucose availability upon carbohydrate ingestion induces XBP1s in the liver. As expected, the high-fructose diet markedly increased mRNA levels of lipogenic genes such as *Fasn*, *Scd1*, *Acc1*, and *Acc2* in wild-type but not *Xbp1*Δ liver (fig. S4), which suggests that XBP1 is required for the expression of a subset of critical lipogenic genes in the setting of high carbohydrate intake. Interestingly, SREBP-1c expression was modestly reduced in *Xbp1*Δ compared to wild-type liver upon high-fructose diet, perhaps contributing to the decreased expression of lipogenic genes such as *Fasn* in *Xbp1*Δ liver. The relationship of XBP1 to high-fructose feeding remains to be clarified, because fructose-induced lipogenesis leads to complex metabolic changes in the liver (*22*).

We asked whether the compromised expression of lipogenic genes was due directly to the lack of XBP1 or indirectly to constitutively active IRE1α by overexpressing a recombinant XBP1s adenovirus in primary mouse hepatocytes. Forced XBP1s expression increased mRNAs encoding Dgat2 and Acc2, as well as the known XBP1 target gene *ERdj4*, both in wild-type and *XBP1*Δ hepatocytes (Fig. 4C). XBP1s did not increase *Scd1* transcripts, suggesting the requirement for additional transcription factor(s). Further, chromatin immunoprecipitation (ChIP) assays using liver nuclear extracts from mice fed a high-fructose diet demonstrated direct XBP1 binding to promoter regions of the *Dgat2*, *Scd1*, and *Acc2* genes that was further increased by tunicamycin treatment, which increased levels of nuclear XBP1s (Fig. 4D).

Our results establish XBP1 as a novel transcription factor governing hepatic lipogenesis. XBP1 deficiency resulted in profound compromise of de novo hepatic lipid synthesis, leading to concomitant decreases in serum TG, cholesterol, and free fatty acids without causing hepatic steatosis. XBP1 was induced upon high-carbohydrate diet feeding and directly activated the transcription of key lipogenic genes in the liver. Our data reveal an unexpected and biologically critical function of XBP1 in hepatic lipogenesis, quite separate from its function as a mediator of the ER stress response (*3*). Hence, XBP1 has at least two distinct roles: In some organs and cells, it is required for protein secretion (plasma cells, pancreatic exocrine cells);

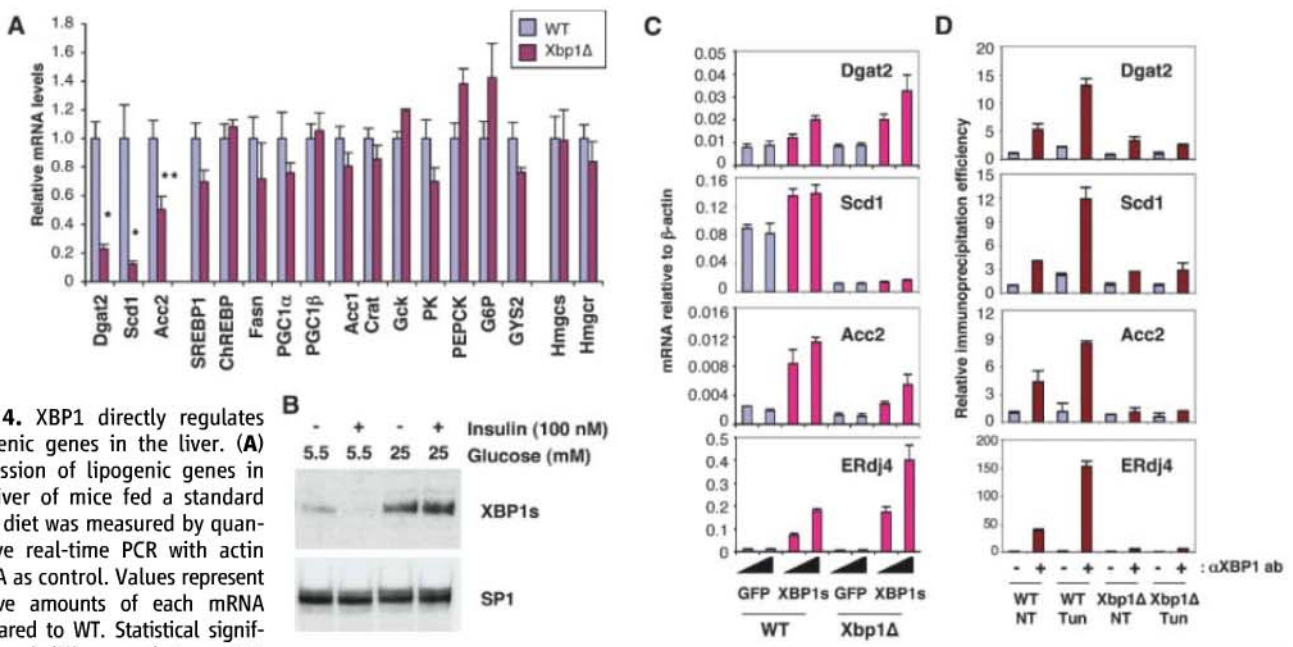

Fig. 4. XBP1 directly regulates lipogenic genes in the liver. (**A**) Expression of lipogenic genes in the liver of mice fed a standard chow diet was measured by quantitative real-time PCR with actin mRNA as control. Values represent relative amounts of each mRNA compared to WT. Statistical significance of differences between WT and *Xbp1*Δ mice was determined (*$P < 0.005$, **$P < 0.0001$). (**B**) Primary hepatocytes were cultured in media containing indicated concentrations of glucose and insulin for 24 hours. Nuclear extracts were subjected to Western blot analysis. (**C**) Primary hepatocytes were infected with adenoviruses expressing XBP1s or green fluorescent protein control at 2 or 10 plaque-forming units per cell. mRNA levels were measured 24 hours after infection by real-time PCR. (**D**) ChIP assays were performed with liver nuclei of mice untreated or injected with tunicamycin (Tun) 6 hours before killing. Values represent relative increase of real-time PCR signals compared to the signal for the untreated WT CHIP with control serum.

in others, such as adult liver, it does not substantially affect protein secretory function but rather controls select transcriptional programs such as lipogenesis. Preservation of the normal hepatic lipid profile suggests that compounds that inhibit XBP1 activation in the liver may reduce serum lipids without causing hepatic steatosis in patients with dyslipidemias.

Given XBP1's known function as a key mediator of the UPR, it was surprising that its function in regulating lipogenesis was unrelated to the ER stress response. Indeed, apoB-100 folding and secretion, as well as the overall hepatocyte protein secretory function, were minimally compromised by loss of XBP1, likely because XBP1 independent basal chaperone gene expression is sufficient to accommodate moderate secretory loads. Interestingly, IRE1α, the upstream activator of XBP1, was constitutively active in the *Xbp1*Δ liver, suggesting the presence of a negative feedback loop that precisely maintains XBP1s protein levels even in the absence of ER stress. The nature of this signal, and its relationship to the ER stress response and to the activation of XBP1 in the liver by carbohydrate feeding, require further investigation.

References and Notes

1. H. N. Ginsberg, Y. L. Zhang, A. Hernandez-Ono, *Obesity* **14** (suppl. 1), 41S (2006).
2. F. Foufelle, P. Ferre, *Biochem. J.* **366**, 377 (2002).
3. D. Ron, P. Walter, *Nat. Rev. Mol. Cell Biol.* **8**, 519 (2007).
4. A. L. Shaffer *et al.*, *Immunity* **21**, 81 (2004).
5. A. H. Lee, N. N. Iwakoshi, L. H. Glimcher, *Mol. Cell. Biol.* **23**, 7448 (2003).
6. D. Acosta-Alvear *et al.*, *Mol. Cell* **27**, 53 (2007).
7. A. M. Reimold *et al.*, *Nature* **412**, 300 (2001).
8. A. H. Lee, G. C. Chu, N. N. Iwakoshi, L. H. Glimcher, *EMBO J.* **24**, 4368 (2005).
9. A. M. Reimold *et al.*, *Genes Dev.* **14**, 152 (2000).
10. R. Sriburi, S. Jackowski, K. Mori, J. W. Brewer, *J. Cell Biol.* **167**, 35 (2004).
11. N. O. Davidson, G. S. Shelness, *Annu. Rev. Nutr.* **20**, 169 (2000).
12. M. M. Hussain, J. Iqbal, K. Anwar, P. Rava, K. Dai, *Front. Biosci.* **8**, s500 (2003).
13. M. C. Schotz, A. Scanu, I. H. Page, *Am. J. Physiol.* **188**, 399 (1957).
14. S. J. Stone *et al.*, *J. Biol. Chem.* **279**, 11767 (2004).
15. X. X. Yu *et al.*, *Hepatology* **42**, 362 (2005).
16. J. M. Ntambi *et al.*, *Proc. Natl. Acad. Sci. U.S.A.* **99**, 11482 (2002).
17. P. Cohen *et al.*, *Science* **297**, 240 (2002).
18. L. Abu-Elheiga, W. Oh, P. Kordari, S. J. Wakil, *Proc. Natl. Acad. Sci. U.S.A.* **100**, 10207 (2003).
19. J. D. Horton, J. L. Goldstein, M. S. Brown, *J. Clin. Invest.* **109**, 1125 (2002).
20. H. C. Towle, E. N. Kaytor, H. M. Shih, *Annu. Rev. Nutr.* **17**, 405 (1997).
21. M. Miyazaki *et al.*, *J. Biol. Chem.* **279**, 25164 (2004).
22. H. Basciano, L. Federico, K. Adeli, *Nutr. Metab.* **2**, 5 (2005).

23. Supported by NIH grants AI32412 and P01 AI56296 (L.H.G.), NIH grants DK48873 and DK56626 (D.E.C.), and the Ellison Medical Foundation (L.H.G.). We thank K. Rajewsky for providing *Mx1-cre* mice, J. Goldstein and M. Brown for SREBP antibodies, R. Milne for apoB antibody, K. Mori for ATF6α antibody, E. Fisher for advice on pulse-chase experiments, M. Wu and J. Wei for help with FPLC analyses, D. Hu for histologic analyses, K. Heidtman for excellent technical assistance, and M. Wein and W. Garrett for critical reading of the manuscript. L.H.G. has equity in Bristol-Myers Squibb and has filed a patent regarding methods for regulating hepatic lipogenesis with XBP1.

Supporting Online Material

www.sciencemag.org/cgi/content/full/320/5882/1492/DC1
Materials and Methods
Figs. S1 to S5
Tables S1 to S4
References

19 March 2008; accepted 17 April 2008
10.1126/science.1158042

The Rag GTPases Bind Raptor and Mediate Amino Acid Signaling to mTORC1

Yasemin Sancak,[1,2] Timothy R. Peterson,[1,2] Yoav D. Shaul,[1,2] Robert A. Lindquist,[1,2] Carson C. Thoreen,[1,2] Liron Bar-Peled,[1] David M. Sabatini[1,2,3]*

The multiprotein mTORC1 protein kinase complex is the central component of a pathway that promotes growth in response to insulin, energy levels, and amino acids and is deregulated in common cancers. We find that the Rag proteins—a family of four related small guanosine triphosphatases (GTPases)—interact with mTORC1 in an amino acid–sensitive manner and are necessary for the activation of the mTORC1 pathway by amino acids. A Rag mutant that is constitutively bound to guanosine triphosphate interacted strongly with mTORC1, and its expression within cells made the mTORC1 pathway resistant to amino acid deprivation. Conversely, expression of a guanosine diphosphate–bound Rag mutant prevented stimulation of mTORC1 by amino acids. The Rag proteins do not directly stimulate the kinase activity of mTORC1, but, like amino acids, promote the intracellular localization of mTOR to a compartment that also contains its activator Rheb.

The mTOR complex 1 (mTORC1) branch of the mammalian target of rapamycin (mTOR) pathway is a major driver of cell growth in mammals and is deregulated in many common tumors (*1*). It is also the target of the drug rapamycin, which has generated considerable interest as an anticancer therapy. Diverse signals regulate the mTORC1 pathway, including insulin, hypoxia, mitochondrial function, and glucose and amino acid availability. Many of these are integrated upstream of mTORC1 by the tuberous sclerosis complex (TSC1-TSC2) tumor suppressor, which acts as an important negative regulator of mTORC1 through its role as a guanosine triphosphatase (GTPase)–activating protein (GAP) for Rheb, a small guanosine triphosphate (GTP)–binding protein that potently activates the protein kinase activity of mTORC1 (*2*). Loss of either TSC protein causes hyperactivation of mTORC1 signaling, even in the absence of many of the upstream signals that are normally required to maintain pathway activity. A notable exception is the amino acid supply, as the mTORC1 pathway remains sensitive to amino acid starvation in cells lacking either TSC1 or TSC2 (*3*–*5*).

The mechanisms through which amino acids signal to mTORC1 remain mysterious. It is a reasonable expectation that proteins that signal the availability of amino acids to mTORC1 are also likely to interact with it, but, so far, no good candidates have been identified. Because most mTORC1 purifications rely on antibodies to isolate mTORC1, we wondered if in previous work antibody heavy chains obscured, during SDS–polyacrylamide electrophoresis (SDS-PAGE) analysis of purified material, mTORC1-interacting proteins of 45 to 55 kD. Indeed, using a purification strategy that avoids this complication (*6*), we identified the 44-kD RagC protein as copurifying with overexpressed raptor, the defining component of mTORC1 (*7*–*10*).

RagC is a Ras-related small GTP-binding protein and one of four Rag proteins in mammals (RagA, RagB, RagC, and RagD). RagA and RagB are very similar to each other and are orthologs of budding yeast Gtr1p, whereas RagC and RagD are similar and are orthologs of yeast Gtr2p (*11*–*13*). In yeast and in human cells, the Rag and Gtr proteins function as heterodimers consisting of one Gtr1p-like (RagA or RagB) and one Gtr2p-like (RagC or RagD) component (*14*, *15*). The finding that RagC copurifies with raptor was intriguing to us because, in yeast, Gtr1p and Gtr2p regulate the intracellular sorting of the Gap1p amino acid permease (*16*) and microautophagy (*17*), processes modulated by amino acid levels and

[1]Whitehead Institute for Biomedical Research and Department of Biology, Massachusetts Institute of Technology (MIT), Nine Cambridge Center, Cambridge, MA 02142, USA. [2]MIT Center for Cancer Research, 77 Massachusetts Avenue, Cambridge, MA 02139, USA. [3]Broad Institute, Seven Cambridge Center, Cambridge, MA 02142, USA.

*To whom correspondence should be addressed. E-mail: sabatini@wi.mit.edu

the TOR pathway (*18*–*20*). The Gtr proteins have been proposed to act downstream or in parallel to TORC1 in yeast because their overexpression induces microautophagy even in the presence of rapamycin, which normally suppresses it (*17*).

To verify our identification of RagC as an mTORC1-interacting protein, we expressed raptor with different pairs of Rag proteins in human embryonic kidney (HEK)-293T cells. Consistent with the Rags functioning as heterodimers, raptor copurified with RagA-C or RagB-C, but not with RagA-B or the Rap2A control protein (Fig. 1A). Because the nucleotide loading state of most GTP-binding proteins regulates their functions, we generated RagB, RagC, and RagD mutants predicted (*14*, *16*, *17*) to be restricted to the GTP- or guanosine diphosphate (GDP)–bound conformations (for simplicity, we call these mutants $RagB^{GTP}$, $RagB^{GDP}$, etc.) (*6*). When expressed with mTORC1 components, Rag heterodimers containing $RagB^{GTP}$ immunoprecipitated with more raptor and mTOR than did complexes containing wild-type RagB or $RagB^{GDP}$ (Fig. 1B). The GDP-bound form of RagC increased the amount of copurifying mTORC1, so that $RagB^{GTP}$-C^{GDP} recovered the highest amount of endogenous mTORC1 of any heterodimer tested (Fig. 1C). Giving an indication of the strength of the mTORC1-$RagB^{GTP}$-C^{GDP} association, in this same assay, we could not detect coimmunoprecipitation of mTORC1 with Rheb1 (Fig. 1C), an established interactor and activator of mTORC1 (*1*). When expressed alone, raptor, but not mTOR, associated with $RagB^{GTP}$-D^{GDP}, which suggests that raptor is the key mediator of the Rag-mTORC1 interaction (Fig. 1D). Consistent with this, rictor, an mTOR-interacting protein that is only part of mTORC2 (*1*), did not copurify with any Rag heterodimer (Fig. 1C and fig. S1). Last, highly purified raptor interacted in vitro with RagB-D and, to a larger extent, with $RagB^{GTP}$-D^{GDP}, which indicates that the Rag-raptor interaction is most likely direct (Fig. 1E).

We tested whether various Rag heterodimers affected the regulation of the mTORC1 pathway within human cells. In HEK-293T cells, expression of the $RagB^{GTP}$-D^{GDP} heterodimer, which interacted strongly with mTORC1, not only activated the pathway, but also made it insensitive to deprivation for leucine or total amino acids, as judged by the phosphorylation state of the mTORC1 substrate T389 of S6K1 (Fig. 2, A and B). The wild-type RagB-C heterodimer had milder effects than $RagB^{GTP}$-C^{GDP}, making the mTORC1 pathway insensitive to leucine deprivation, but not to the stronger inhibition caused by total amino acid starvation (Fig. 2, A and B). Expression of $RagB^{GDP}$-D^{GTP}, a heterodimer that did not interact with mTORC1 (Fig. 1, C and D), had dominant-negative effects, as it eliminated S6K1 phosphorylation in the presence, as well as absence, of leucine or amino acids (Fig. 2, A and B). Expression of $RagB^{GDP}$ alone also suppressed S6K1 phosphorylation (fig. S2). These results suggest that the activity of the mTORC1 pathway

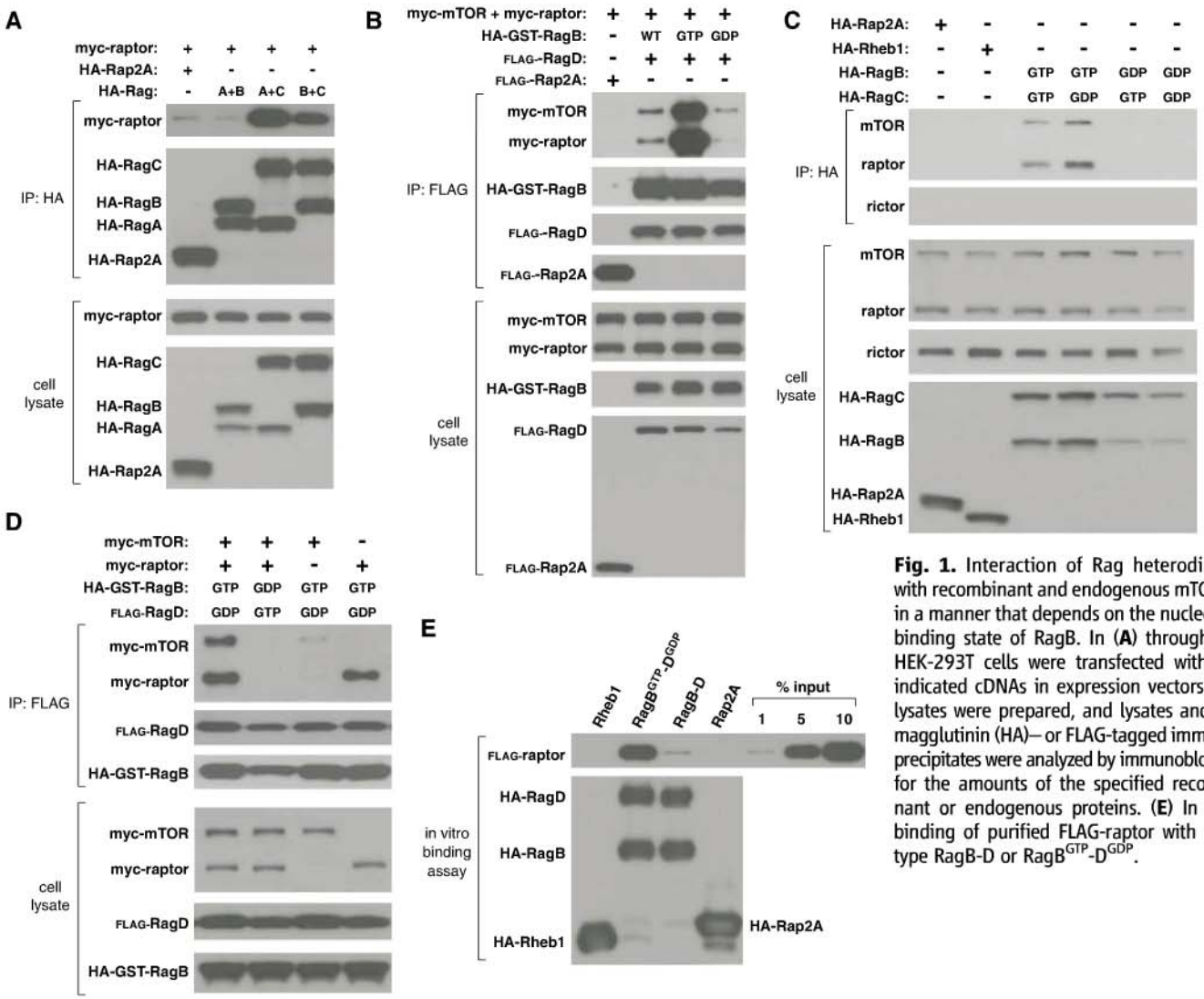

Fig. 1. Interaction of Rag heterodimers with recombinant and endogenous mTORC1 in a manner that depends on the nucleotide binding state of RagB. In (**A**) through (**D**) HEK-293T cells were transfected with the indicated cDNAs in expression vectors, cell lysates were prepared, and lysates and hemagglutinin (HA)– or FLAG-tagged immunoprecipitates were analyzed by immunoblotting for the amounts of the specified recombinant or endogenous proteins. (**E**) In vitro binding of purified FLAG-raptor with wild-type RagB-D or $RagB^{GTP}$-D^{GDP}.

under normal growth conditions depends on endogenous Rag function.

To verify the actions of the Rags in a more physiological setting than that achieved by transient cDNA transfection, we generated HEK-293T cell lines stably expressing Rheb1, RagB, or $RagB^{GTP}$ (attempts to generate lines stably expressing $RagB^{GDP}$ failed). Under normal growth conditions, these cells were larger than control cells and had higher levels of mTORC1 pathway activity (Fig. 3A). Unlike transient Rheb1 overexpression (Fig. 2, A and B), stable expression did not make the mTORC1 pathway insensitive to leucine or amino acid starvation (Fig. 3, B and C), consistent with evidence that transiently overexpressed Rheb may have nonphysiological consequences on amino acid signaling to mTORC1 (*4*, *5*). Stable expression of a $Rheb1^{GTP}$ mutant was also unable to make the mTORC1 pathway resistant to amino acid deprivation (fig. S3). In contrast, stable expression of $RagB^{GTP}$ eliminated the sensitivity of the mTORC1 pathway to leucine or total amino acid withdrawal, whereas that of wild-type RagB overcame sensitivity to leucine but not to amino acid starvation (Fig. 3, B and C). Thus, transient or stable expression of the appropriate Rag mutants is sufficient to put the mTORC1 pathway into states that mimic the presence or absence of amino acids.

To determine if the Rag mutants affect signaling to mTORC1 from inputs besides amino acids, we tested whether in $RagB^{GTP}$-expressing cells the mTORC1 pathway was resistant to other perturbations known to inhibit it. This was not the case, as oxidative stress, mitochondrial inhibition, or energy deprivation still reduced S6K1 phosphorylation in these cells (fig. S4). Moreover, in HEK-293E cells, expression of $RagB^{GTP}$-D^{GDP} did not maintain mTORC1 pathway activity in the absence of insulin (Fig. 2C). Expression of the dominant-negative $RagB^{GDP}$-D^{GTP} heterodimer did, however, block insulin-stimulated phosphorylation of S6K1 (Fig. 2C), as did amino acid starvation (Fig. 2D). Thus, although $RagB^{GTP}$ expression mimics amino acid sufficiency, it cannot substitute for other inputs that mTORC1 normally monitors.

This evidence for a primary role of the Rag proteins in amino acid signaling to mTORC1 raised the question of where, within the pathway that links amino acids to mTORC1, the Rag proteins might function. The existence of the Rag-mTORC1 interaction (Fig. 1), the effects on amino acid signaling of the Rag mutants (Figs. 2 and 3), and the sensitivity to rapamycin of the S6K1 phosphorylation induced by $RagB^{GTP}$ (fig. S4), strongly suggested that the Rag proteins function downstream of amino acids and upstream of mTORC1. To verify this, we took advantage of the established finding that cycloheximide reactivates mTORC1 signaling in cells starved for amino acids by blocking protein synthesis and thus boosting the levels of the intracellular amino acids sensed by mTORC1 (*21*–*23*). Thus, if the Rag proteins act upstream of amino acids, cycloheximide should overcome the inhibitory effects of the $RagB^{GDP}$-C^{GTP} heterodimer on mTORC1 signaling, but if they are downstream, cycloheximide should not reactivate the pathway. The results were clear: cycloheximide treatment of cells reversed the inhibition of mTORC1 signaling caused by leucine deprivation, but not that caused by expression of $RagB^{GDP}$-C^{GTP} (fig. S5). Given the place-

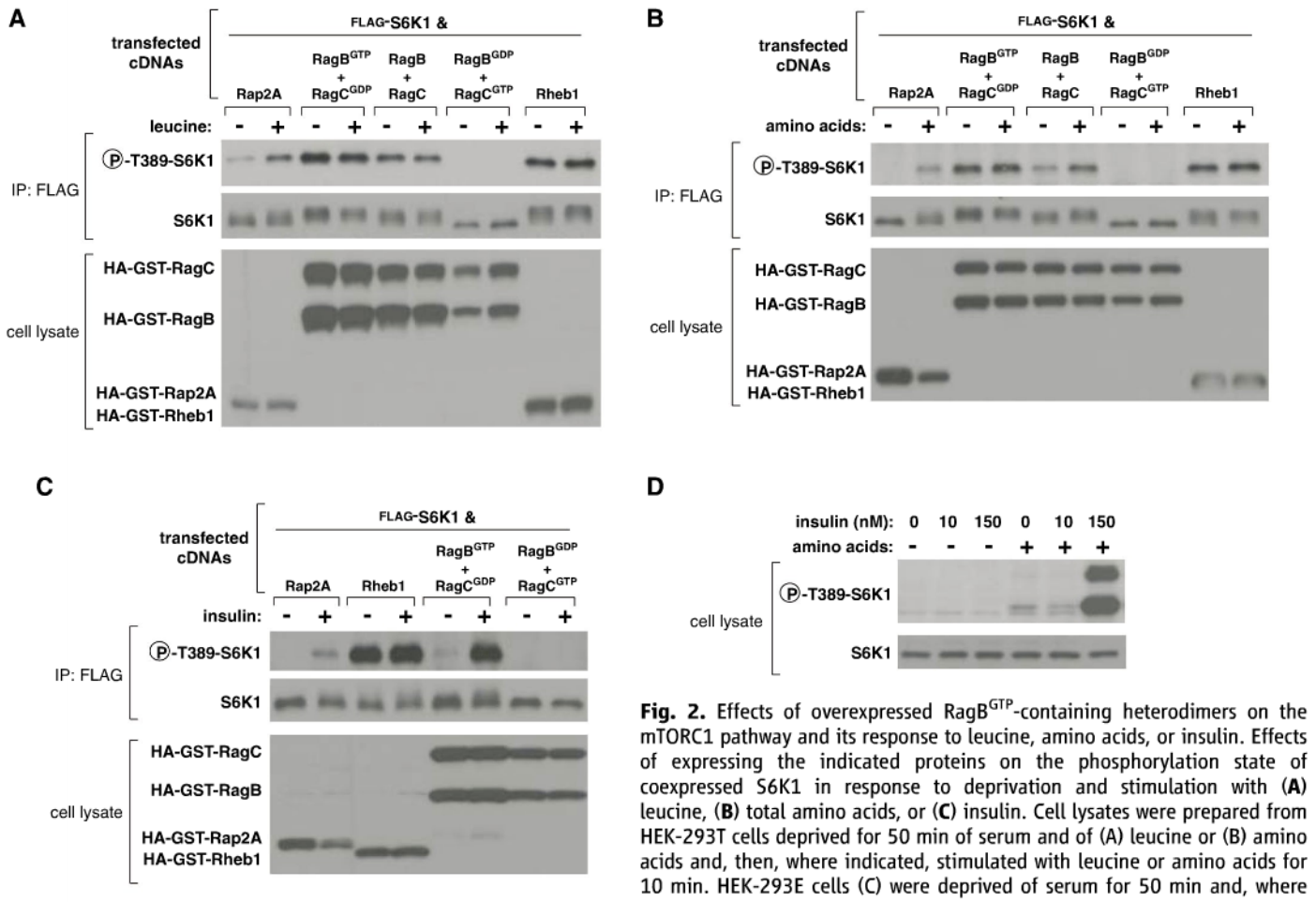

Fig. 2. Effects of overexpressed $RagB^{GTP}$-containing heterodimers on the mTORC1 pathway and its response to leucine, amino acids, or insulin. Effects of expressing the indicated proteins on the phosphorylation state of coexpressed S6K1 in response to deprivation and stimulation with (**A**) leucine, (**B**) total amino acids, or (**C**) insulin. Cell lysates were prepared from HEK-293T cells deprived for 50 min of serum and of (A) leucine or (B) amino acids and, then, where indicated, stimulated with leucine or amino acids for 10 min. HEK-293E cells (C) were deprived of serum for 50 min and, where indicated, stimulated with 150 nM insulin for 10 min. Lysates and FLAG-immunoprecipitates were analyzed for the levels of the specified proteins and the phosphorylation state of S6K1. (**D**) Effects of amino acid deprivation on insulin-mediated activation of mTORC1. HEK-293E cells were starved for serum and amino acids or just serum for 50 min, and where specified, stimulated with 10 or 150 nM insulin. Cell lysates were analyzed for the level and phosphorylation state of S6K1.

ment of the Rag proteins downstream of amino acids and upstream of mTORC1, we determined whether amino acids regulate the Rag-mTORC1 interaction within cells. Initial tests using transiently coexpressed Rag proteins and mTORC1 components did not reveal any regulation of the interaction. Because we reasoned that pronounced overexpression might overcome the normal regulatory mechanisms that operate within the cell, we developed an assay (*6*), based on a reversible chemical cross-linker, that allows us to detect the interaction of stably expressed FLAG-tagged Rag proteins with endogenous mTORC1. With this approach, we readily found that amino acids, but not insulin, promote the Rag-mTORC1 interaction when we used either FLAG-tagged RagB or RagD to isolate mTORC1 from cells (Fig. 3D and fig. S6A). As the GTP-loading state of the Rag proteins also regulates the Rag-mTORC1 interaction (Fig. 1), we determined whether amino acids modulate the amount of GTP bound to RagB. Indeed, amino acid stimulation of cells increased the GTP loading of RagB (Fig. 3E). Consistent with this, amino acids did not further augment the already high level of interaction between mTORC1 and the $RagB^{GTP}$ mutant (Fig. 3D).

To determine whether the Rag proteins are necessary for amino acids to activate the mTORC1 pathway, we used combinations of lentivirally delivered short hairpin RNAs (shRNAs) to suppress RagA and RagB or RagC and RagD at the same time. Loss of RagA and RagB also led to the loss of RagC and RagD and vice versa, which suggests that, within cells, the Rag proteins are unstable when not in heterodimers (Fig. 3F). In cells with a reduction in the expression of all the Rag proteins, leucine-stimulated phosphorylation of S6K1 was strongly reduced (Fig. 3G). The role of the Rag proteins appears to be conserved in *Drosophila* cells as double-stranded RNA–mediated suppression of the *Drosophila* orthologs of RagB or RagC eliminated amino acid–induced phosphorylation of dS6K (Fig. 3H). Consistent with amino acids being necessary for activation of mTORC1 by insulin, a reduction in Rag expression also suppressed insulin-stimulated phosphorylation of S6K1 (fig. S6B). Thus, the Rag proteins appear to be both necessary and

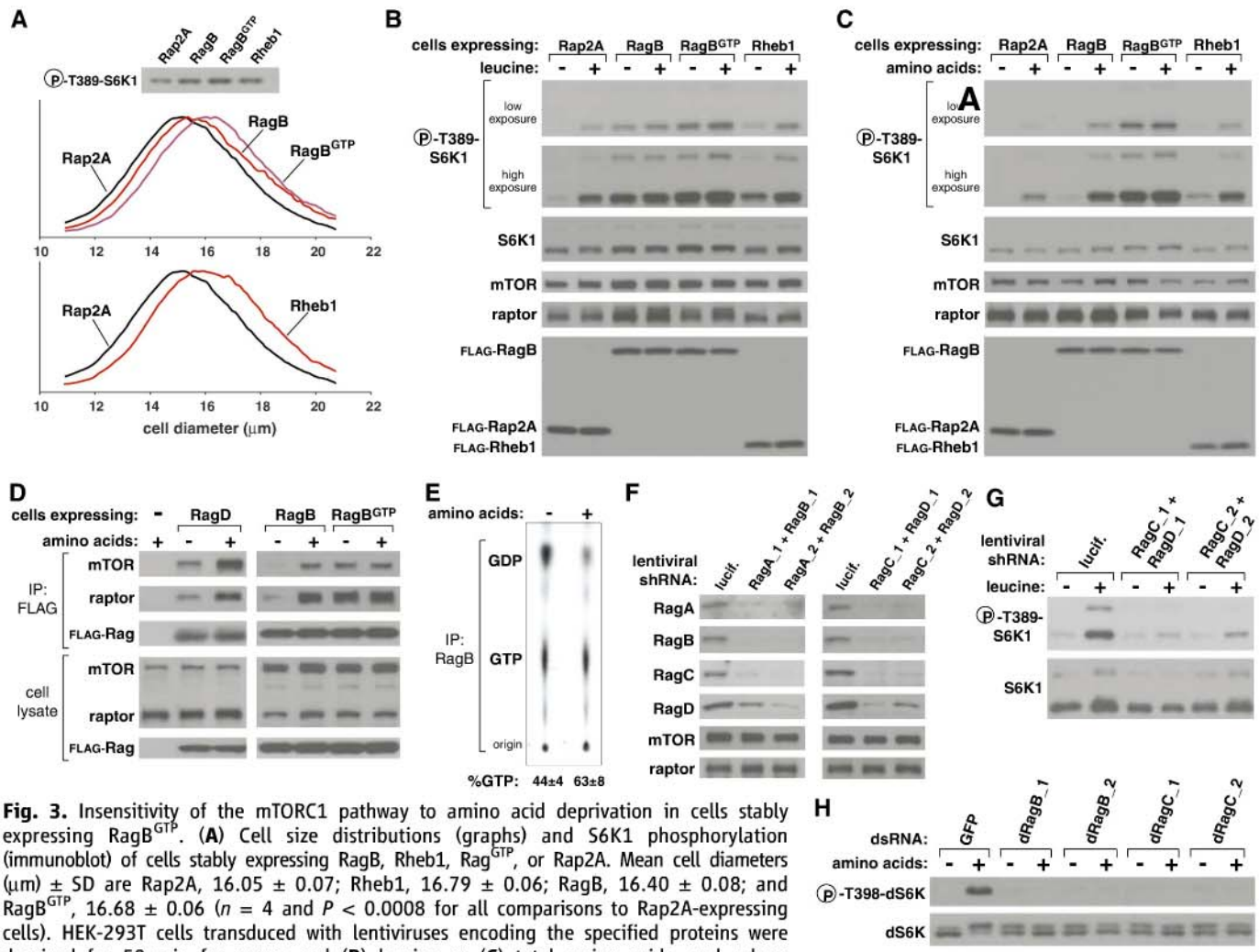

Fig. 3. Insensitivity of the mTORC1 pathway to amino acid deprivation in cells stably expressing $RagB^{GTP}$. (**A**) Cell size distributions (graphs) and S6K1 phosphorylation (immunoblot) of cells stably expressing RagB, Rheb1, Rag^{GTP}, or Rap2A. Mean cell diameters (μm) ± SD are Rap2A, 16.05 ± 0.07; Rheb1, 16.79 ± 0.06; RagB, 16.40 ± 0.08; and $RagB^{GTP}$, 16.68 ± 0.06 ($n = 4$ and $P < 0.0008$ for all comparisons to Rap2A-expressing cells). HEK-293T cells transduced with lentiviruses encoding the specified proteins were deprived for 50 min for serum and (**B**) leucine or (**C**) total amino acids, and, where indicated, restimulated with leucine or amino acids for 10 min. Cell lysates were analyzed for the levels of the specified proteins and the phosphorylation state of S6K1. (**D**) Amino acid–stimulated interaction of the Rag proteins with mTORC1. HEK-293T cells stably expressing FLAG-tagged RagB, RagD, or $RagB^{GTP}$ were starved for amino acids and serum for 50 min and, where indicated, restimulated with amino acids for 10 min. Cells were then processed with a chemical cross-linking assay, and cell lysates and FLAG immunoprecipitates were analyzed for the amounts of the indicated proteins. (**E**) Effects of amino acid stimulation on GTP loading of RagB. Values are means ± SD for $n = 3$ ($P < 0.02$ for increase in GTP loading caused by amino acid stimulation). (**F**) Abundance of RagA, RagB, RagC, and RagD in HeLa cells expressing the indicated shRNAs. (**G**) S6K1 phosphorylation in HeLa cells expressing shRNAs targeting RagC and RagD. Cells were deprived of serum and leucine for 50 min, and, where indicated, were restimulated with leucine for 10 min. (**H**) Effects of double-stranded RNA (dsRNA)–mediated knockdowns of *Drosophila* orthologs of RagB or RagC on amino acid–induced phosphorylation of dS6K.

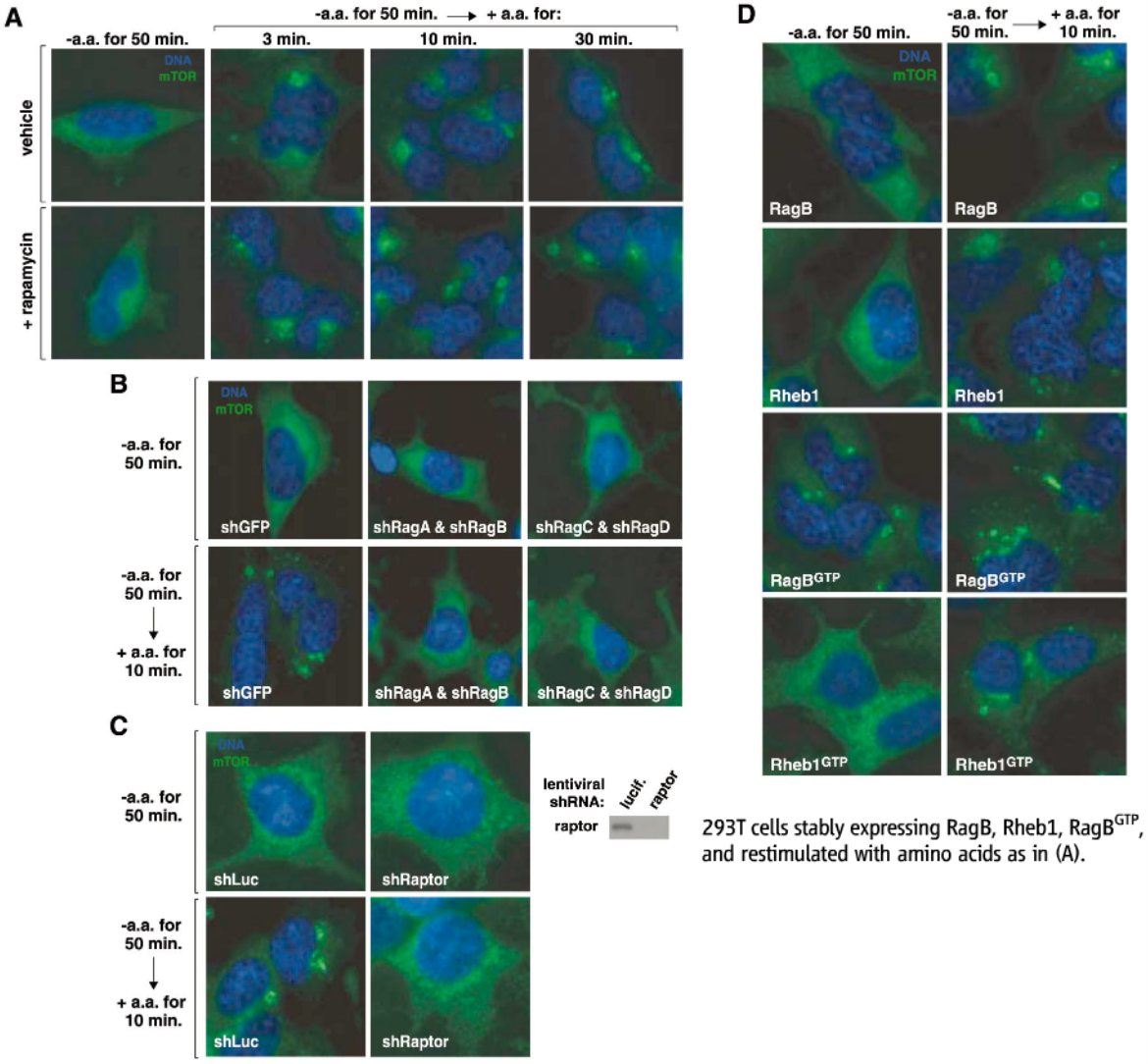

Fig. 4. Rag-dependent regulation by amino acids of the intracellular localization of mTOR. (**A**) HEK-293T cells were starved for serum and amino acids for 50 min or starved and then restimulated with amino acids for the indicated times in the presence or absence of rapamycin. Cells were then processed in an immunofluorescence assay to detect mTOR (green), costained with 4′,6′-diamidino-2-phenylindole (DAPI) for DNA content (blue), and imaged. Of these cells, 80 to 90% exhibited the mTOR localization pattern shown. (**B**) and (**C**) mTOR localization in HEK-293T cells expressing the indicated shRNAs and deprived and restimulated with amino acids as in (A). Immunoblot of raptor expression levels. (**D**) mTOR localization in HEK-293T cells stably expressing RagB, Rheb1, RagB^{GTP}, or Rheb1^{GTP} and deprived and restimulated with amino acids as in (A).

sufficient for mediating amino acid signaling to mTORC1.

Unlike Rheb (*24*, *25*), the Rag heterodimers did not directly stimulate the kinase activity of mTORC1 in vitro (fig. S7), so we considered the possibility that the Rag proteins regulate the intracellular localization of mTOR. mTOR is found on the endomembrane system of the cell, including the endoplasmic reticulum, Golgi apparatus, and endosomes (*26*, *27*). The intracellular localization of endogenous mTOR, as revealed with an antibody that we validated recognizes mTOR in immunofluorescence assays (fig. S8), was strikingly different in cells deprived of amino acids than in cells starved and briefly restimulated with amino acids (Fig. 4A and fig. S11) or growing in fresh complete media (fig. S9). In starved cells, mTOR was in tiny puncta throughout the cytoplasm, whereas in cells stimulated with amino acids for as little as 3 min, mTOR localized to the perinuclear region of the cell, to large vesicular structures, or to both (Fig. 4A). Rapamycin did not block the change in mTOR localization induced by amino acids (Fig. 4A), which indicated that it is not a consequence of mTORC1 activity but rather may be one of the mechanisms that underlies mTORC1 activation. The amino acid–induced change in mTOR localization required expression of the Rag proteins and of raptor (Fig. 4, B and C), and amino acids also regulated the localization of raptor (fig. S10).

In cells overexpressing RagB, Rheb1, or Rheb1^{GTP}, mTOR behaved as in control cells, its localization changing upon amino acid stimulation from small puncta to the perinuclear region and vesicular structures (Fig. 4D). In contrast, in cells overexpressing the RagB^{GTP} mutant that eliminates the amino acid sensitivity of the mTORC1 pathway, mTOR was already present on the perinuclear and vesicular structures in the absence of amino acids, and became even more localized to them upon the addition of amino acids (Fig. 4D). Thus, there is a correlation, under amino acid–starvation conditions, between the activity of the mTORC1 pathway and the subcellular localization of mTOR, which implies a role for Rag-mediated mTOR translocation in the activation of mTORC1 in response to amino acids.

We failed to find an established marker of the endomembrane system that colocalized with mTOR in amino acid–starved cells. However, in cells stimulated with amino acids, mTOR in the perinuclear region and on the large vesicular structures overlapped with Rab7 (Fig. 5A), which indicated that a substantial fraction of mTOR translocated to the late endosomal and lysosomal compartments in amino acid–replete cells. In cells expressing RagB^{GTP}, mTOR was present on the Rab7-positive structures even in the absence of amino acids (Fig. 5B).

The perinuclear region and vesicular structures on which mTOR appears after amino acid stimulation are similar to the Rab7-positive structures where green fluorescent protein (GFP)–tagged Rheb localizes in human cells (*28*, *29*). Unlike mTOR, however, amino acids did not appreciably affect the localization of Rheb, as GFP-Rheb1 colocalized with *Discosoma* red fluorescent protein (DsRed)–labeled Rab7 (DsRed-

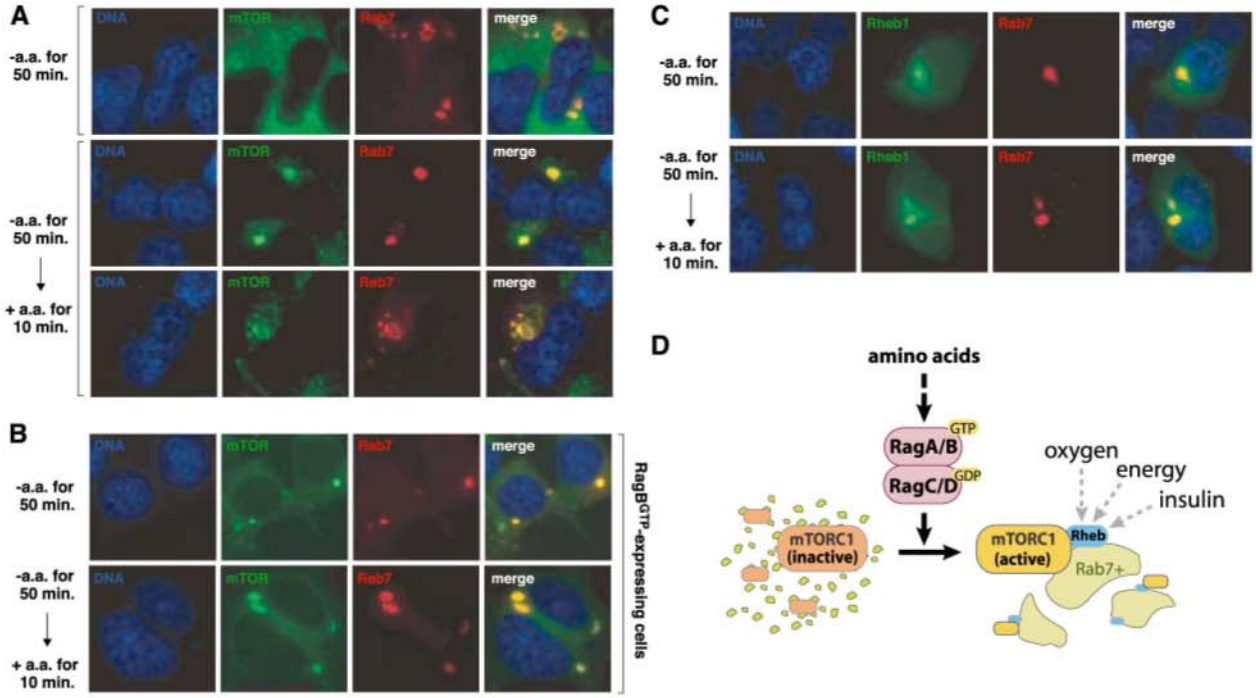

Fig. 5. Amino acids promote the localization of mTOR to a Rab7-positive compartment that also contains Rheb. (**A**) mTOR and Rab7 localization in cells deprived or stimulated with amino acids. HEK-293T cells transiently transfected with a cDNA for DsRed-Rab7 were starved for serum and amino acids for 50 min and, where indicated, stimulated with amino acids for 10 min. Cells were then processed to detect mTOR (green), Rab7 (red), and DNA content (blue), and imaged. Two examples are shown of mTOR localization in the presence of amino acids. (**B**) HEK-293T cells stably expressing $RagB^{GTP}$ and transiently transfected with a cDNA for DsRed-Rab7 were treated and processed as in (A). (**C**) Rheb1 and Rab7 localization in cells deprived or stimulated with amino acids. HEK-293T cells transiently transfected with 1 to 2 ng of cDNAs for GFP-Rheb1 and DsRed-Rab7 were treated as in (A), processed to detect Rheb1 (green), Rab7 (red), and DNA content (blue), and imaged. (**D**) Model for role of Rag GTPases in signaling amino acid availability to mTORC1.

Rab7) in the presence or absence of amino acids (Fig. 5C). Unfortunately, it is currently not possible to compare, in the same cells, the localization of endogenous mTOR with that of Rheb, because the signal for GFP-Rheb or endogenous Rheb is lost after fixed cells are permeabilized to allow access to intracellular antigens (*28*, *29*). Nevertheless, given that both mTOR and Rheb are present in Rab7-positive structures after amino acid stimulation, we propose that amino acids might control the activity of the mTORC1 pathway by regulating, through the Rag proteins, the movement of mTORC1 to the same intracellular compartment that contains its activator Rheb (see model in Fig. 5D). This would explain why activators of Rheb, like insulin, do not stimulate the mTORC1 pathway when cells are deprived of amino acids and why Rheb is necessary for amino acid–dependent mTORC1 activation (*4*) (fig. S12). When Rheb is highly overexpressed, some might become mislocalized and inappropriately encounter and activate mTORC1, which could explain why Rheb overexpression, but not loss of TSC1 or TSC2, makes the mTORC1 pathway insensitive to amino acids (*4*, *5*).

In conclusion, the Rag GTPases bind raptor, are necessary and sufficient to mediate amino acid signaling to mTORC1, and mediate the amino acid–induced relocalization of mTOR within the endomembrane system of the cell. Given the prevalence of cancer-linked mutations in the pathways that control mTORC1 (*1*), it is possible that Rag function is also deregulated in human tumors.

References and Notes

1. D. A. Guertin, D. M. Sabatini, *Cancer Cell* **12**, 9 (2007).
2. D. D. Sarbassov, S. M. Ali, D. M. Sabatini, *Curr. Opin. Cell Biol.* **17**, 596 (2005).
3. M. P. Byfield, J. T. Murray, J. M. Backer, *J. Biol. Chem.* **280**, 33076 (2005).
4. T. Nobukuni *et al.*, *Proc. Natl. Acad. Sci. U.S.A.* **102**, 14238 (2005).
5. E. M. Smith, S. G. Finn, A. R. Tee, G. J. Browne, C. G. Proud, *J. Biol. Chem.* **280**, 18717 (2005).
6. Materials and methods are available as supporting material on *Science* Online.
7. D.-H. Kim *et al.*, *Cell* **110**, 163 (2002).
8. R. Loewith *et al.*, *Mol. Cell* **10**, 457 (2002).
9. K. P. Wedaman *et al.*, *Mol. Biol. Cell* **14**, 1204 (2003).
10. K. Hara *et al.*, *Cell* **110**, 177 (2002).
11. M. Bun-Ya, S. Harashima, Y. Oshima, *Mol. Cell. Biol.* **12**, 2958 (1992).
12. A. Schurmann, A. Brauers, S. Massmann, W. Becker, H. G. Joost, *J. Biol. Chem.* **270**, 28982 (1995).
13. E. Hirose, N. Nakashima, T. Sekiguchi, T. Nishimoto, *J. Cell Sci.* **111**, 11 (1998).
14. N. Nakashima, E. Noguchi, T. Nishimoto, *Genetics* **152**, 853 (1999).
15. T. Sekiguchi, E. Hirose, N. Nakashima, M. Ii, T. Nishimoto, *J. Biol. Chem.* **276**, 7246 (2001).
16. M. Gao, C. A. Kaiser, *Nat. Cell Biol.* **8**, 657 (2006).
17. F. Dubouloz, O. Deloche, V. Wanke, E. Cameroni, C. De Virgilio, *Mol. Cell* **19**, 15 (2005).
18. J. B. Kunz, H. Schwarz, A. Mayer, *J. Biol. Chem.* **279**, 9987 (2004).
19. K. J. Roberg, N. Rowley, C. A. Kaiser, *J. Cell Biol.* **137**, 1469 (1997).
20. E. J. Chen, C. A. Kaiser, *J. Cell Biol.* **161**, 333 (2003).
21. A. Beugnet, A. R. Tee, P. M. Taylor, C. G. Proud, *Biochem. J.* **372**, 555 (2003).
22. G. R. Christie, E. Hajduch, H. S. Hundal, C. G. Proud, P. M. Taylor, *J. Biol. Chem.* **277**, 9952 (2002).
23. D. J. Price, R. A. Nemenoff, J. Avruch, *J. Biol. Chem.* **264**, 13825 (1989).
24. Y. Sancak *et al.*, *Mol. Cell* **25**, 903 (2007).
25. X. Long, Y. Lin, S. Ortiz-Vega, K. Yonezawa, J. Avruch, *Curr. Biol.* **15**, 702 (2005).
26. R. M. Drenan, X. Liu, P. G. Bertram, X. F. Zheng, *J. Biol. Chem.* **279**, 772 (2004).
27. M. Mavrakis, J. Lippincott-Schwartz, C. A. Stratakis, I. Bossis, *Autophagy* **3**, 151 (2007).
28. K. Saito, Y. Araki, K. Kontani, H. Nishina, T. Katada, *J. Biochem.* **137**, 423 (2005).
29. C. Buerger, B. DeVries, V. Stambolic, *Biochem. Biophys. Res. Commun.* **344**, 869 (2006).

30. Supported by grants from the NIH (R01 CA103866 and AI47389), Department of Defense (W81XWH-07-0448), and W.M. Keck Foundation to D.M.S. as well as an EMBO fellowship to Y.D.S. We thank T. Kang for the preparation of FLAG-raptor and members of the Sabatini lab for helpful suggestions.

Supporting Online Material

www.sciencemag.org/cgi/content/full/1157535/DC1
Materials and Methods
Figs. S1 to S12
References

10 March 2008; accepted 13 May 2008
Published online 22 May 2008;
10.1126/science.1157535
Include this information when citing this paper.

Animal Versus Wind Dispersal and the Robustness of Tree Species to Deforestation

Daniel Montoya,[1]* Miguel A. Zavala,[1,2] Miguel A. Rodríguez,[1] Drew W. Purves[3]

Studies suggest that populations of different species do not decline equally after habitat loss. However, empirical tests have been confined to fine spatiotemporal scales and have rarely included plants. Using data from 89,365 forest survey plots covering peninsular Spain, we explored, for each of 34 common tree species, the relationship between probability of occurrence and the local cover of remaining forest. Twenty-four species showed a significant negative response to forest loss, so that decreased forest cover had a negative effect on tree diversity, but the responses of individual species were highly variable. Animal-dispersed species were less vulnerable to forest loss, with six showing positive responses to decreased forest cover. The results imply that plant-animal interactions help prevent the collapse of forest communities that suffer habitat destruction.

Habitat destruction is often cited as the single greatest cause of global biodiversity loss (*1*). These anthropogenic changes trigger biological responses that sometimes end in a biotic collapse, a problem that has led ecologists to face the question of how much habitat is enough for species to persist (*2*). The dominant theoretical framework for understanding the effects of habitat loss is metapopulation theory, which focuses on the dynamic balance of local extinctions and colonizations that characterize fragmented populations at regional scales (*3*). According to this theory, regional habitat loss not only removes biodiversity held in the lost habitat but also reduces the occurrence of species within the remaining habitat (*4*). This idea has become a central tenet of conservation practice, causing a shift in focus from the local to the landscape scale. For example, it is the source of the current emphasis on the maintenance and creation of habitat corridors to foster dispersal among patches (*5*, *6*). However, empirical tests of this prediction have been restricted to short-lived animal species [especially butterflies and birds (*7*, *8*)], short spatial scales (*9*), and short time scales, over which observations are likely to be dominated by short-term responses that may or may not be indicative of the long-term impacts of habitat loss.

We analyzed the relationship between local forest cover and the occurrence of 34 canopy-dominant tree species [28 native to the study region and 6 exotic (table S1)] in 89,365 survey sites distributed across peninsular Spain (*10*) (Fig. 1). The data set was extracted from the Spanish Second National Forest Inventory (IFN2), which placed a 25-m-radius circular sample plot in each 1 × 1 km grid cell that it classified as being forested [occupied by woody vegetation (*11*)]. For each plot q, we calculated a local forest cover H_q, defined as the fraction of the nearest eight grid cells to q that were also classified as forested in IFN2 (using a larger neighborhood degraded the statistical significance of some effects documented here but had no qualitative effect on conclusions). Because the Iberian Peninsula has chronically suffered from forest destruction and conversion into agricultural and degraded states (*12*), H_q is a measure of net forest loss from prehistory to the present. Thus, we interpret the species responses to H_q observed in the IFN2 survey as responses to forest loss.

We used logistic regression to quantify, for each species j, the probability of occurrence of j in plot q as a function of H_q. For comparison among species we used the fitted logistic curves to calculate, for each species j, a scalar Ω_j, defined as the natural log of the ratio of the probability of occurrence at 0% local forest cover to the probability of occurrence at 75% cover. Negative Ω_j implies that species j shows a negative response to decreased forest cover and vice versa. We used error propagation to calculate a conservative (upper) estimate of the confidence interval for Ω_j. The results presented below are robust considering either native and exotic species combined or native species only [supporting online material (SOM)].

Of the 34 species, 24 showed a statistically significant negative response to decreased forest cover [negative Ω_j value with confidence intervals not including zero (Fig. 2A)]. This is consistent with the decrease in average tree species richness with decreased forest cover observed in the IFN2 data (Fig. 3) and in previous studies (*13*). The observed relationship between species richness in this case was approximately linear over most of the range in H_q, which was captured well by the logistic regressions (Fig. 3). However, richness was lower than expected for $H_q \geq 80\%$ and $H_q = 0$. Such abrupt changes could reflect the effects of spatial configuration (that is, fragmentation) when habitat cover goes from nearly continuous to fragmented (with the first appearance of edges) and falls to very low levels (*14*), although threshold responses can also result from some forms of animal-mediated dispersal (*15*).

Among species there was large and statistically significant variation in Ω_j. For species with statistically significant negative Ω_j (those with confidence intervals not including zero), Ω_j ranged from –0.03 to –1.53, which corresponds to a proportional reduction in probability of occurrence, for the 75 to 0% scenario, of 3 to 78%. Moreover, there were six species with statistically significant positive responses to reductions in forest cover (Fig. 2A). These species were more likely to be found in plots surrounded by nonforested land.

If this magnitude of interspecific variation in response to forest loss proves to be typical, it will be critical to identify measurable species traits that predict it. Although we did not attempt an exhaustive search of such traits, we did examine the importance of two traits related to dispersal (seed size and animal- versus wind-mediated seed dis-

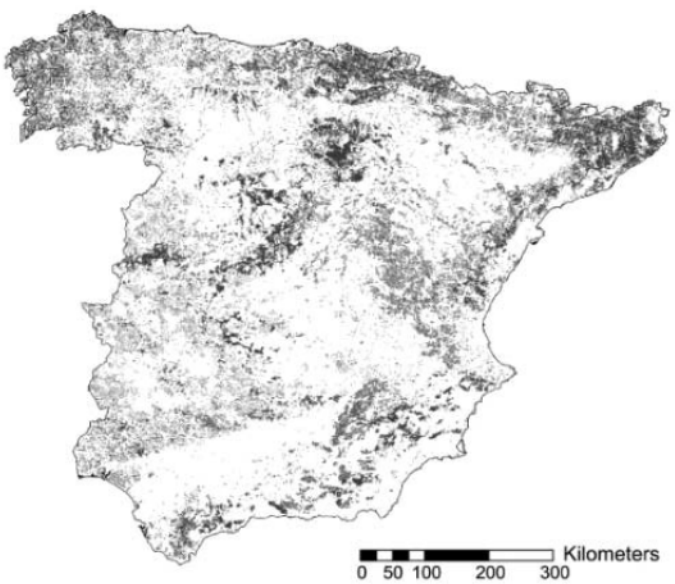

Fig. 1. Distribution of survey sites in peninsular Spain. IFN2 consisted of 89,365 circular sampling sites (radius = 25 m) distributed across peninsular Spain (average density approximately one per square kilometer). Survey sites were placed in continuous forest locations, so their distribution matches that of the remaining forest.

[1]Departamento de Ecología, Universidad de Alcalá, 28871 Alcalá de Henares, Madrid, Spain. [2]Centro de Investigación Forestal, Instituto Nacional de Investigación y Tecnología Agraria y Alimentaria, Carretera de la Coruña km 7, 5, 28040 Madrid, Spain. [3]Microsoft Research Cambridge, 7 J. J. Thomson Avenue, Cambridge CB3 0FB, UK.

*To whom correspondence should be addressed. E-mail: daniel.montoya@alu.uah.es

persal). Metapopulation theory has identified dispersal as crucial in determining species responses to habitat loss (*16*), and recent modifications of the Levins metapopulation model predict that animal-mediated seed dispersal will confer increased species robustness to habitat loss (*17*). This is because, unlike wind, animals actively deliver seeds toward suitable patches (directed dispersal), and because some forms of animal dispersal increase the average dispersal distance (*18*). Both of these behaviors help keep physically isolated habitat patches demographically connected. Directed dispersal and long dispersal distances have been observed in our study region (*19*). Seed size affects dispersal distance (*20*) and is correlated with fecundity (*21*) and establishment probability (*22*), which are also highlighted as important by metapopulation theory.

We found that animal-dispersed species are, on average, less vulnerable to decreased forest cover than are wind-dispersed species (Fig. 2). The six species showing positive responses to deforestation were all animal-dispersed, and the two species with the largest negative response were wind-dispersed. To assess the possibility that the observed difference between the two groups (animal- and wind-dispersed) could have arisen by chance, we conducted a permutation test on the difference in the position of the groups in the list of species ranked by Ω_j: The probability of finding the observed difference was less than 0.005 (SOM).

The contrasted phylogenetic composition of wind- versus animal-dispersed species raises the possibility that phylogenetically conserved traits other than dispersal mode that are shared by closely related species caused the difference in response between animal- and wind-dispersed species (*23*). To examine this possibility, we used phylogenetic eigenvector regression [PVR (*11*)]. The proportion of variation of Ω_j that can be attributed to phylogenetic relationships is low ($R^2 = 0.11$). Moreover, an analysis of covariance (ANCOVA) including Ω_j as the response variable, dispersal mode as the explanatory variable, and the three main phylogenetic eigenvectors generated by PVR (which describe 92.5% of the phylogenentic structure in the data) as covariables still found significant differences in Ω_j between wind- and animal-dispersed species ($F = 7.75890$, $P < 0.05$).

In addition to the effects of forest cover, each tree species is likely to be affected by the pronounced gradients in climate, soil, and fire frequency observed in this region, and the interactions between all of these will need to be understood before any future species responses to changes in forest cover or climate can be predicted accurately. However, PCA showed no multicolinearity between forest cover and a set of 18 environmental variables that might be critical to plant growth, reproduction, and survival in Mediterranean and Atlantic systems (table S4). This shows that at the scale of peninsular Spain, local forest cover varies independently of climate, topography, soil, and major perturbation events, so that the simple logistic regression employed here would be expected to extract the correct average response to forest loss for each species. We also estimated Ω_j controlled for these environmental factors, using multiple logistic regression. The results support the conclusions of an overall negative, yet highly variable response to decreased forest cover among tree species, with some positive responses; and greater robustness of animal-dispersed species (fig. S3, $P < 0.005$).

Significant unexplained variation remains in the response of species within each dispersal group, but this is not surprising given the biological variation among species in either group. Just in terms of dispersal itself, both groups contain a large variation in seed size [although within either group we found no effect of seed weight on Ω_j (fig. S1)]; different animal-dispersed species are dispersed by different combinations of birds and mammals [foraging behavior and body size differences among frugivores may affect seed dispersal distances (*24*, *25*)]; and many of the species are likely to benefit from occasional long-distance dispersal events by agents other than the dominant disperser (*26*). These species are also likely to differ in the other traits that metapopulation theory has predicted to be crucial in determining response to habitat loss (such as fecundity and local extinction rates). Nonetheless, our analysis suggests that the differences in species responses to local forest cover are to a large extent driven by the dispersal vector used by trees. This is consistent with predictions from metapopulation theory about the effects of animal-mediated directed dispersal. However, additional detailed field observations would be needed to rule out alternative explanations based on the interaction between dispersal and habitat loss. For example, lower amounts of habitat cover may be correlated with increased edge habitat, which has been observed in some cases to be preferred by seed-dispersing animals (*27*).

Whatever the mechanisms involved, the finding that animal-dispersed tree species are more robust to the effects of deforestation has an obvious implication for conservation policy: In the absence of detailed data (such as was available here), it might be expected that deforestation in other regions is more likely to threaten a given wind-dispersed, than a given animal-dispersed, plant species. However, the weight attached to this prediction should reflect the substantial within-group variation in response documented here (Fig. 2) and the degree of extrapolation outside

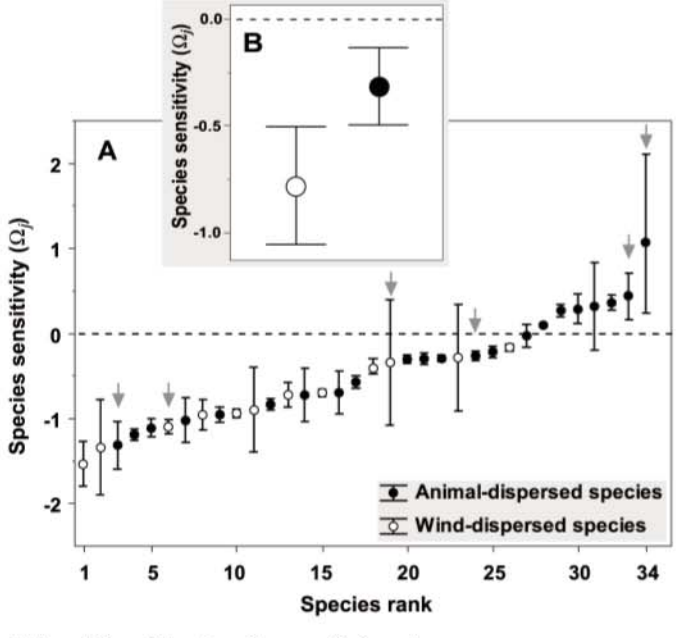

Fig. 2. (**A**) Sensitivity of 34 Spanish tree species to reduction in local forest cover (Ω_j), estimated using the maximum likelihood estimate of the parameters of a logistic regression relating the probability of occurrence of species j to local forest cover. Gray arrows indicate non-native species. Ω_j is defined as the natural logarithm of the ratio of occurrence probabilities at 0 and 75% cover. Negative Ω_j implies a negative response to habitat loss. Species are ranked by Ω_j. Error bars are 95% confidence intervals on Ω_j, calculated conservatively (*16*). (**B**) Average Ω_j of wind-dispersed species (n = 12) and animal-dispersed species (n = 22). Error bars are 95% confidence intervals on the mean Ω_j for each group.

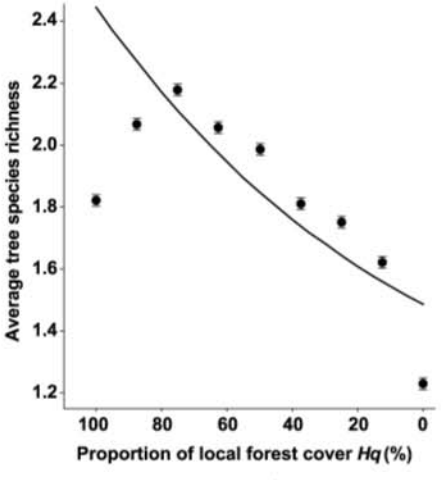

Fig. 3. Tree species richness (average number of species occurring in a 25-m-radius circular plot) versus local forest cover H_q: observed (points) and from the logistic regression (line, calculated by summing the predicted probability of occurrence over the 34 species). Error bars are standard errors on the observed average for each level of H_q. The observed richness is positively correlated with H_q; that is, negatively correlated with forest loss (Spearman rank test, $\rho_s = 0.73$, $P = 0.038$). Species richness was calculated by referring to data for the 34 study species only.

European temperate forests (such as to tropical forests or to plant species other than trees). Moreover, if seed-dispersing animals are as crucial to the persistence of plants as this and other studies suggest (*28*, *29*), then the combination of habitat loss with direct and indirect removal of animals, to which many of the world's most diverse forests are subject, is likely to have more drastic effects than either perturbation alone. In these circumstances, animal-dispersed species might be more, not less, sensitive to habitat loss. This points to the maintenance of the network of plant-animal interactions as a cornerstone of conservation policy and to the need for more studies of species responses to habitat loss.

References and Notes

1. R. V. Solé, J. Bascompte, *Self Organization in Complex Ecosystems* (Princeton Univ. Press, Princeton, NJ, 2007).
2. L. Fahrig, *Biol. Conserv.* **100**, 65 (2001).
3. I. Hanski, *Metapopulation Ecology* (Oxford Univ. Press, Oxford, 1999).
4. M. Rees, R. Condit, M. Crawley, S. Pacala, S. Tilman, *Science* **293**, 650 (2001).
5. E. I. Damschen, N. M. Haddad, J. L. Orrock, J. J. Tewksbury, D. J. Levey, *Science* **313**, 1284 (2006).
6. B. C.-L. Chetkiewicz, C. C. St. Clair, M. S. Boyce, *Annu. Rev. Ecol. Syst.* **37**, 317 (2006).
7. L. Conradt, T. J. Roper, C. D. Thomas, *Oikos* **95**, 416 (2001).
8. G. Ferraz *et al.*, *Science* **315**, 238 (2007).
9. I. Hanski, M. Kuussaari, M. Nieminen, *Ecology* **75**, 747 (1994).
10. *Segundo Inventario Forestal Nacional* (Ministerio de Agricultura, Pesca y Alimentación, Madrid, 1995).
11. Information on materials and methods is available as supporting material on *Science* Online.
12. F. González Manzaneque, *Bosques Ibéricos: Una Interpretación Geobotánica* (Planeta, Barcelona, 2005).
13. J. Bascompte, M. A. Rodríguez, *Ecol. Lett.* **4**, 417 (2001).
14. L. Fahrig, *Annu. Rev. Ecol. Syst.* **34**, 487 (2003).
15. D. W. Purves, J. Dushoff, *J. Ecol.* **93**, 658 (2005).
16. I. Hanski, *Nature* **396**, 41 (1998).
17. D. W. Purves, M. A. Zavala, K. Ogle, F. Prieto, J. M. Rey-Benayas, *Ecol. Monogr.* **77**, 77 (2007).
18. K. Johst, R. Brandl, S. Eber, *Oikos* **98**, 263 (2002).
19. J. M. Gómez, *Ecography* **26**, 573 (2003).
20. B. McEuen, L. M. Curran, *Ecology* **85**, 507 (2004).
21. C. C. Smith, S. D. Fretwell, *Am. Nat.* **108**, 499 (1974).
22. D. Sánchez-Gomez, F. Valladares, M. A. Zavala, *New Phytol.* **170**, 795 (2006).
23. A. Purvis, P.-M. Agapow, J. L. Gittleman, G. M. Mace, *Science* **288**, 328 (2000).
24. O. Spiegel, R. Nathan, *Ecol. Lett.* **10**, 718 (2007).
25. P. Jordano, C. García, J. A. Godoy, J. L. García-Castaño, *Proc. Natl. Acad. Sci. U.S.A.* **104**, 3278 (2007).
26. S. I. Higgins, R. Nathan, M. L. Cain, *Ecology* **84**, 1945 (2003).
27. C. Restrepo, N. Gómez, S. Heredia, *Ecology* **80**, 668 (1999).
28. J. M. Montoya, S. L. Pimm, R. V. Solé, *Nature* **442**, 259 (2006).
29. J. Bascompte, P. Jordano, *Annu. Rev. Ecol. Syst.* **38**, 567 (2007).

30. We thank the Ministerio de Medio Ambiente, Spain; R. Vallejo and J. A. Villanueva for help with IFN2 data; S. Pacala for hospitality during data preparation; J. A. F. Diniz-Filho, L. M. Bini, and M. A. Olalla-Tárraga for help with phylogenetic analyses; and B. A. Hawkins, J. M. Montoya, D. Coomes, and J.-C. Svenning for comments on manuscripts. D.M. was supported by the Spanish Ministry for Education and Science (fellowship AP2004-0075). M.A.R. and M.A.Z. were supported by the Spanish Ministry for Education and Science (grants CGL2006-03000/BOS and CGL2005-05830-C03-01/BOS, respectively).

Supporting Online Material

www.sciencemag.org/cgi/content/full/1158404/DC1
Materials and Methods
Figs. S1 to S3
Tables. S1 to S4
References

28 March 2008; accepted 15 May 2008
Published online 5 June 2008;
10.1126/science.1158404
Include this information when citing this paper.

VelB/VeA/LaeA Complex Coordinates Light Signal with Fungal Development and Secondary Metabolism

Özgür Bayram,[1] Sven Krappmann,[1]* Min Ni,[2] Jin Woo Bok,[3] Kerstin Helmstaedt,[1,4] Oliver Valerius,[1] Susanna Braus-Stromeyer,[1] Nak-Jung Kwon,[2] Nancy P. Keller,[3] Jae-Hyuk Yu,[2] Gerhard H. Braus[1]†

Differentiation and secondary metabolism are correlated processes in fungi that respond to light. In *Aspergillus nidulans*, light inhibits sexual reproduction as well as secondary metabolism. We identified the heterotrimeric *velvet* complex VelB/VeA/LaeA connecting light-responding developmental regulation and control of secondary metabolism. VeA, which is primarily expressed in the dark, physically interacts with VelB, which is expressed during sexual development. VeA bridges VelB to the nuclear master regulator of secondary metabolism, LaeA. Deletion of either *velB* or *veA* results in defects in both sexual fruiting-body formation and the production of secondary metabolites.

Secondary metabolites of fungi include "friends and foes" of human health, such as Aspergillis' production of penicillin (*1*) and the carcinogenic aflatoxin precursor sterigmatocystin (ST), respectively (*2*). Secondary metabolic pathways are often tightly correlated with the fungal developmental program and response to external cues including light. The mold *Aspergillus nidulans* forms airborne asexual spores in light but preferentially undergoes sexual reproduction in the dark (*3*, *4*). The latter results in the formation of sexual fruit bodies called cleistothecia, which consist of different cell types, and an increase in secondary metabolism (*5*). Mutations resulting in defects in fungal development often also impair secondary metabolism (*6*). There is genetic evidence for a connection between fruit-body formation, secondary metabolism, and light in *A. nidulans*, but the molecular mechanism is not known (*7*–*9*). One candidate for such a bridge is the conserved *velvet* protein encoded by the *veA* gene (*10*–*12*), whose expression increases during sexual development (*7*). VeA transport into the nucleus is inhibited by light (*13*). It acts as a negative regulator of asexual development (*14*) and antibiotic biosynthesis (*15*).

Biosynthetic genes for fungal secondary metabolite are often clustered and regulated by pathway-specific transcription factors (*16*, *17*). Secondary metabolism is also regulated at an upper hierarchic level by a global epigenetic control mechanism. The nuclear LaeA protein is present in numerous fungi and is a master regulator of secondary metabolism in Aspergilli (*18*).

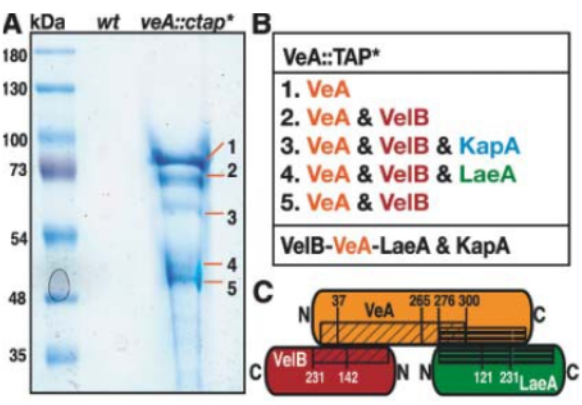

Fig. 1. Identification of VeA-associated proteins in *A. nidulans*. (**A**) Brilliant blue G-stained 10% SDS–polyacrylamide gel electrophoresis of TAP procedure for VeA. kD, kilodaltons. (**B**) The polypeptides identified from the bands of affinity purification belong to corresponding proteins (details in table S4). (**C**) Domain mapping of the interactions based on Y2H data (fig. S2). N, N terminus; C, C terminus.

[1]Institute of Microbiology and Genetics, Georg August University, D-37077 Göttingen, Germany. [2]Department of Bacteriology and Department of Genetics, University of Wisconsin-Madison, Madison, WI 53706, USA. [3]Department of Plant Pathology and Medical Microbiology and Immunology, University of Wisconsin-Madison, Madison, WI 53706, USA. [4]Deutsche Forschungsgemeinschaft (DFG) Research Center for Molecular Physiology of the Brain (CMPB), D-37077 Göttingen, Germany.

*Present address: Zentrum für Infektionsforschung, University of Würzburg, D-97070 Würzburg, Germany.
†To whom correspondence should be addressed. E-mail: gbraus@gwdg.de

The deletion of *laeA*, although not reported to affect morphological and developmental processes, results in silencing of numerous secondary metabolite gene clusters, including those responsible for the syntheses of the antibiotic penicillin as well as for toxins such as ST or gliotoxin (*17*, *19*). It has been suggested that LaeA might control accessibility of binding factors to chromatin regions of secondary metabolite clusters because the S-adenosyl methionine binding site of LaeA (*19*) prevents heterochromatin maintenance of some clusters (*20*).

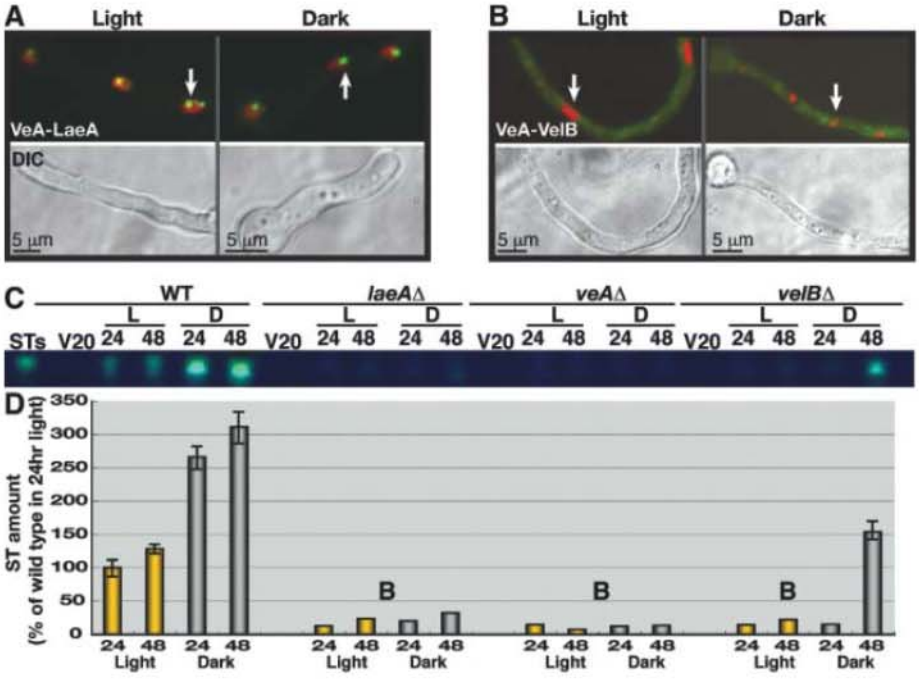

Fig. 2. BiFC studies of *velvet* complex components and their effect on ST production. (**A**) Enhanced yellow fluorescent protein fused to the N terminus of *veA* gene (N-EYFP::VeA) interacts with C-EYFP::LaeA in vivo, which is indicated as yellowish green specks in the nucleus. [Histone 2A red fluorescent protein (H2A::mRFP) fusion visualizes the entire nucleus.] Interaction does not take place in the whole nucleus but in certain points (gene clusters) that LaeA probably acts on (indicated by arrows). Differential interference contrast (DIC) shows hyphal cells. (**B**) N-EYFP::VeA fusion protein interacts with C-EYFP::VelB in the cytoplasm and nucleus. (**C**) ST production in respective mutant backgrounds and WT at different time points. STs, ST standard; V20, 20 hours vegetative growth; L, light; D, dark. 24 and 48 hour time points are shown. (**D**) Quantification of ST production using thin layer chromatography: In the dark, more ST is produced in the WT. Deletion of either *laeA* or *veA* results in no ST above background (denoted by B) fluctuations. Loss of *velB* results in basal ST production in dark.

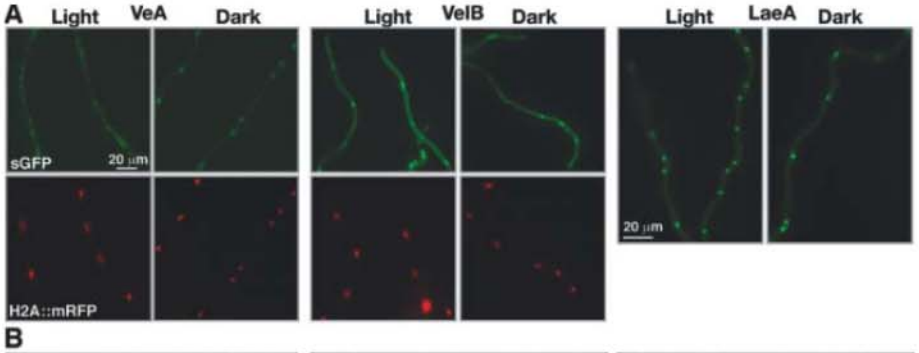

B

Nuclear / Cytoplasmic ratio for VeA		Nuclear / Cytoplasmic ratio for VelB		Nuclear / Cytoplasmic ratio for LaeA	
Light	Dark	Light	Dark	Light	Dark
0.3 ± 0.17	8.34 ± 2.7	1.80 ± 0.44	2.90 ± 0.89	3.99 ± 1.27	4.20 ± 1.25

Fig. 3. Subcellular localization of the subunits of the *velvet* complex. (**A**) VeA-, LaeA-, and VelB-sGFP localizations in the presence or absence of light. VeA-sGFP shows light-dependent nuclear enrichment (counterstained with H2A::mRFP for visualization of the entire nucleus). (**B**) Nuclear/cytoplasmic GFP signal ratio of 100 hyphal cells each (Openlab software 5.0.1) (*28*). Growth in the dark results in increased nuclear and decreased cytoplasmic fluorescence for VeA. VelB and LaeA distribution is hardly affected by illumination.

We used tandem affinity purification (TAP) (*21*–*23*) to identify VeA-interacting proteins (Fig. 1A and fig. S1A) (*24*). Final eluates of dark- and light-grown *A. nidulans* carrying the functional *veA* gene tagged at its C terminus by TAP tag (*veA::ctap**) were analyzed by mass spectrometry. We identified the *velvet*-like protein B (VelB) (fig. S3, A and B), the regulator LaeA, and the α importin KapA as proteins that interact with VeA in the dark (Fig. 1B and table S4). In the light, tagged VeA is hardly expressed (fig. S1B) and only copurifies with VelB. Reciprocal affinity purifications of tagged VelB and LaeA in the dark confirmed the interaction partners, except for the α importin KapA (fig. S1, C and D). Only tagged VelB can additionally recruit the regulator of sporogenesis VosA in the dark (*25*), which seems to be an alternative binding partner for this protein.

Yeast two-hybrid (Y2H) analysis (*26*) confirmed the VeA-VelB and VeA-LaeA interactions, where VelB and LaeA do not interact in this assay, suggesting that VeA acts as a bridge between VelB and LaeA (Fig. 1C). The Y2H VosA-LaeA interaction supports a role of LaeA in development (fig. S2). The C-terminal part of VeA interacts with LaeA, whereas the N-terminal part of VeA, which includes the nuclear localization signal (NLS), is required for interaction with VelB (Fig. 1C and fig. S2). VelB, which is conserved in the fungal kingdom, shares 18% amino acid identity with VeA but has no typical NLS (fig. S3B). Transcript analysis reveals that *velB* expression increases like that of *veA* (*7*) at late developmental stages (fig. S3C). The VeA-LaeA and VeA-VelB interactions were visualized by bimolecular fluorescence complementation (BiFC) in living cells (*27*). Distinct fluorescent specks show that the VeA-LaeA interaction occurs in the nucleus, whereas VeA and VelB interact in the cytoplasm and within the nucleus (Fig. 2, A and B).

The physical interaction of VeA with VelB, as well as with LaeA, leads to the prediction that VeA and VelB are functionally interdependent. Similar to *veA*Δ, the *velB*Δ mutant (fig. S5A) no longer displays a light-dependent developmental pattern and is unable to form sexual fruit bodies, even in the dark. Asexual sporulation in *velB*Δ is impaired but not as strongly as in a *veA* deletion strain. Reintroduction of the *velB* locus fully rescued all of the defects (fig. S5A). The *veA*Δ/*velB*Δ double mutant exhibited a near-identical phenotype to that of the *veA*Δ single mutant. Neither *velB* overexpression in a *veA*Δ background nor *veA* overexpression in a *velB*Δ background rescued the defects of the individual mutants; likewise, *laeA* overexpression could not rescue secondary metabolite defects of *veA*Δ (fig. S6). Unlike overproduction of VeA, overexpression of *velB* in a *veA*+ background does not cause excessive production of cleistothecia, but it induces a twofold increase in asexual sporulation in comparison to the wild type (WT). This suggests that VeA

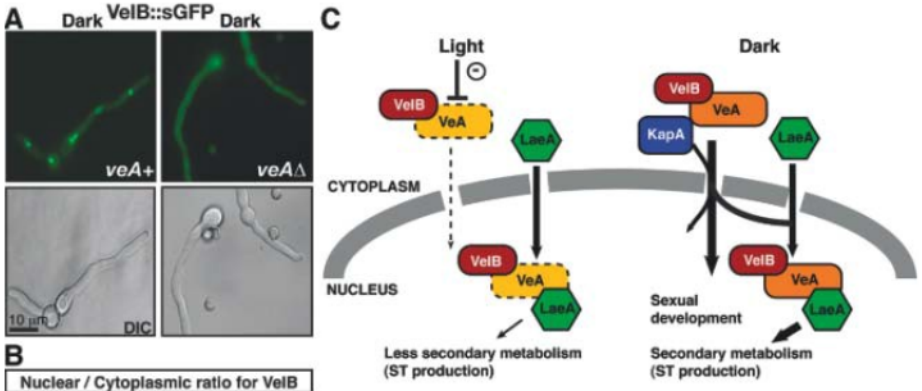

Fig. 4. VeA supports nuclear localization of VelB and formation of the *velvet* complex. (**A**) Fluorescence patterns in strains expressing *velB::sgfp* in the dark in *veA*+ and *veA*Δ backgrounds. (**B**) Nuclear/cytoplasmic GFP signal ratio of 100 hyphal cells each. Nuclear signal intensity is higher in the *veA*+ strain background than in *veA*Δ. (**C**) Model: (Light) VeA is mostly retained in the cytoplasm, VelB supports asexual spore formation, and LaeA shows low activity. (Dark) An increased amount of VeA is imported into the nucleus by KapA and, in addition, supports the nuclear transport of VelB. Dotted lines indicate the decreased amount of VeA that is present in the cell in the light and the impairment of VeA nuclear transport in the light. VelB/VeA control development and LaeA activity by formation of the *velvet* complex that affects secondary metabolite clusters expression.

controls the number of sexual structures, whereas VelB has additional developmental functions.

Secondary metabolism is impaired in *veA*Δ, resulting in a similar brownish pigment (*8*) as is produced by the *velB*Δ strain. Changes in gene expression and in LaeA activity were monitored in the *veA*Δ and *velB*Δ strains (Fig. 2, C and D, and figs. S5, B and C, and S7). ST production is abolished in *veA*Δ and *laeA*Δ strains. In contrast, reduced and delayed but significant ST production in *velB*Δ suggests residual activity of a VeA/LaeA complex in the dark

VeA is enriched in the nucleus in the dark (*13*), whereas VelB was found in both the nucleus and the cytoplasm and is hardly affected by illumination (Fig. 3, A and B). Because LaeA is constitutively nuclear (Fig. 3, A and B) (*18*) and the interaction of VeA and LaeA occurs in the nucleus (Fig. 2A), VelB has to enter the nucleus, despite the lack of an obvious NLS to fully control LaeA. Localization of the VelB-sGFP fusion protein (where GFP is green fluorescent protein) in a *veA*Δ background is shifted toward the cytoplasm, whereas the presence of VeA increases the nuclear localization of VelB (Fig. 4, A and B). This suggests that VeA can assist VelB to allow an enhanced transport into the nucleus.

Our data suggest that the mechanism underlying the coordinated regulation of sexual development and secondary metabolism in *A. nidulans* might be the interaction between the key developmental regulatory complex VelB/VeA and LaeA. We propose that in the dark the VelB/VeA/LaeA *velvet* complex interaction controls and presumably supports the epigenetic activity of LaeA, which subsequently controls the expression of secondary metabolite gene clusters. In the light, this interaction is diminished because we find less VeA protein, and the entrance of the bridging factor VeA to the nucleus is decreased. Because the absence of LaeA has a minor impact on development, VeA and VelB have presumably additional functions in fungal differentiation. This is also supported by the identification of VosA, a recently identified regulator of fungal sporogenesis (*25*), as an additional binding partner of VelB (fig. S1, C and D, and table S4).

A. nidulans produces many compounds relevant to biotechnology and human health and is a well-suited model for the analysis of the interplay between secondary metabolism, light, and differentiation. *A. nidulans* grows vegetatively in the soil by hyphal tip extension until competent for development and secondary metabolism (*3*). Light triggers asexual development, corresponding to the release of high numbers of asexual spores (conidia) into the environment. These phenotypes correlate with the light-dependent cytoplasmic localization of VeA, the constitutive nuclear function of LaeA, and the partial nuclear localization of VelB, respectively. Under light conditions, when low amounts of VeA and VelB are present in the nucleus, the secondary metabolism regulator LaeA seems to be primarily active in those hyphae that are not exposed to light. Accordingly, the deletion of *laeA* results in a loss of mycelial pigmentation at the bottom of the colony (*18*).

The newly described fungal protein VelB, in conjunction with VeA, connects light-dependent development to LaeA-controlled secondary metabolism in *A. nidulans*. We present evidence that the formation of this complex is the molecular basis that synchronizes developmental and metabolic changes to the disappearance of light. We propose to designate this trimeric complex the *velvet* complex. We suggest that VelB/VeA is part of the epigenetic control of chromatin remodeling by modulating LaeA methyltransferase activity (*16*–*18*). We propose a scenario (Fig. 4C) in which VeA is functionally active in the dark, forms a complex with increased amounts of VelB, and enhances the transport of VelB to the nucleus. Because VeA and VelB are both partially nuclear, even in the light, we presume a certain threshold is probably necessary to initiate sexual development and control LaeA.

Fungal morphogenesis and secondary metabolism have traditionally been viewed as separate fields. Our studies on the VelB/VeA/LaeA *velvet* complex elucidate the molecular mechanisms underlying the intimate relation between fungal development and secondary metabolism.

References and Notes

1. A. A. Brakhage, *FEMS Microbiol. Lett.* **148**, 1 (1997).
2. J. Hicks, K. Shimizu, N. P. Keller, in *The Mycota*, vol. 11, F. Kempken, Ed. (Springer, Berlin, 2002), pp. 55–69.
3. T. H. Adams, J. K. Wieser, J.-H. Yu, *Microbiol. Mol. Biol. Rev.* **62**, 35 (1998).
4. J. Purschwitz *et al.*, *Curr. Biol.* **18**, 255 (2008).
5. G. H. Braus, S. Krappmann, S. Eckert, in *Molecular Biology of Fungal Development*, H. D. Osiewacz, Ed. (Marcel Dekker, New York, 2002), pp. 215–244.
6. A. M. Calvo, R. A. Wilson, J. W. Bok, N. P. Keller, *Microbiol. Mol. Biol. Rev.* **66**, 447 (2002).
7. H. Kim *et al.*, *Fungal Genet. Biol.* **37**, 72 (2002).
8. N. Kato, W. Brooks, A. M. Calvo, *Eukaryot. Cell* **2**, 1178 (2003).
9. S. Busch, S. E. Eckert, S. Krappmann, G. H. Braus, *Mol. Microbiol.* **49**, 717 (2003).
10. S. Krappmann, Ö. Bayram, G. H. Braus, *Eukaryot. Cell* **4**, 1298 (2005).
11. S. Li *et al.*, *Mol. Microbiol.* **62**, 1418 (2006).
12. J. Dreyer, H. Eichhorn, E. Friedlin, H. Kürnsteiner, U. Kück, *Appl. Environ. Microbiol.* **73**, 3412 (2007).
13. S. M. Stinnett, E. A. Espeso, L. Cobeño, L. Araújo-Bazán, A. M. Calvo, *Mol. Microbiol.* **63**, 242 (2007).
14. J. L. Mooney, L. N. Yager, *Genes Dev.* **4**, 1473 (1990).
15. P. Spröte, A. A. Brakhage, *Arch. Microbiol.* **188**, 69 (2007).
16. C. P. Woloshuk *et al.*, *Appl. Environ. Microbiol.* **60**, 2408 (1994).
17. N. P. Keller, G. Turner, J. W. Bennett, *Nat. Rev. Microbiol.* **3**, 937 (2005).
18. J. W. Bok, N. P. Keller, *Eukaryot. Cell* **3**, 527 (2004).
19. J. W. Bok, D. Noordermeer, S. P. Kale, N. P. Keller, *Mol. Microbiol.* **61**, 1636 (2006).
20. E. K. Shwab *et al.*, *Eukaryot. Cell* **6**, 1656 (2007).
21. O. Puig *et al.*, *Methods* **24**, 218 (2001).
22. J. S. Rohila, M. Chen, R. Cerny, M. E. Fromm, *Plant J.* **38**, 172 (2004).
23. S. Busch *et al.*, *Proc. Natl. Acad. Sci. U.S.A.* **104**, 8089 (2007).
24. Materials and methods are available as supporting material on *Science* Online.
25. M. Ni, J. H. Yu, *PLoS One* **2**, e970 (2007).
26. J. Gyuris, E. Golemis, H. Chertkov, R. Brent, *Cell* **75**, 791 (1993).
27. C. D. Hu, Y. Chinenov, T. K. Kerppola, *Mol. Cell* **9**, 789 (2002).
28. Openlab software 5.0.1, www.improvision.com/.

29. We thank V. Pretz, G. Heinrich, V. Große, and Ö. S. Bayram for technical assistance. This project was supported by the DFG, CMPB, Volkswagen Vorab, and Fonds der Chemischen Industrie to G.H.B; Hatch (WIS04667) and NSF (MCB-0421863) grants to J.-H.Y.; and an NSF grant (MCB-0236393) to N.P.K. The GeneID for *velB* is 2876142.

Supporting Online Material

www.sciencemag.org/cgi/content/full/320/5882/1504/DC1
Materials and Methods
Figs. S1 to S7
Tables S1 to S4
References

30 January 2008; accepted 29 April 2008
10.1126/science.1155888

Activation of the Cellular DNA Damage Response in the Absence of DNA Lesions

Evi Soutoglou and Tom Misteli

The cellular DNA damage response (DDR) is initiated by the rapid recruitment of repair factors to the site of DNA damage to form a multiprotein repair complex. How the repair complex senses damaged DNA and then activates the DDR is not well understood. We show that prolonged binding of DNA repair factors to chromatin can elicit the DDR in an ATM (ataxia telangiectasia mutated)– and DNAPK (DNA-dependent protein kinase)–dependent manner in the absence of DNA damage. Targeting of single repair factors to chromatin revealed a hierarchy of protein interactions within the repair complex and suggests amplification of the damage signal. We conclude that activation of the DDR does not require DNA damage and stable association of repair factors with chromatin is likely a critical step in triggering, amplifying, and maintaining the DDR signal.

The DNA damage response (DDR) cascade senses genome damage and activates several downstream pathways, including cell cycle checkpoints and apoptotic programs (*1*–*3*). The earliest step in the response is the rapid targeting and accumulation of DNA repair factors near the damage site, giving rise to nuclear repair foci (*4*). The repair cascade consists of the early DNA damage sensor complex MRN (MRE11/Rad50/NBS1), the transducer proteins MDC1 and 53BP1, followed by the phosphatidylinositol 3-kinases (PI 3-kinases) ATM/DNAPK/ATR (ataxia telangiectasia mutated/DNA-dependent protein kinase/ataxia telangiectasia and Rad3-related), which in turn phosphorylate the histone variant H2AX and downstream effectors, including the Chk1 and Chk2 cell cycle kinases (*5*). The functional relevance of the increased local concentration of DNA repair factors at sites of DNA damage has not been clear, nor is it known precisely how the DDR is activated on chromatin.

To address these questions, we stably targeted individual DNA repair components to chromatin in living cells and assessed their contribution to the DDR. DNA repair factors were fused to the *Escherichia coli* lac-repressor (lacR) and tagged with Cherry-red fluorescent protein. The fusion

National Cancer Institute, National Institutes of Health, Bethesda, MD 20892, USA. E-mail: mistelit@mail.nih.gov (T.M.); soutogle@mail.nih.gov (E.S.)

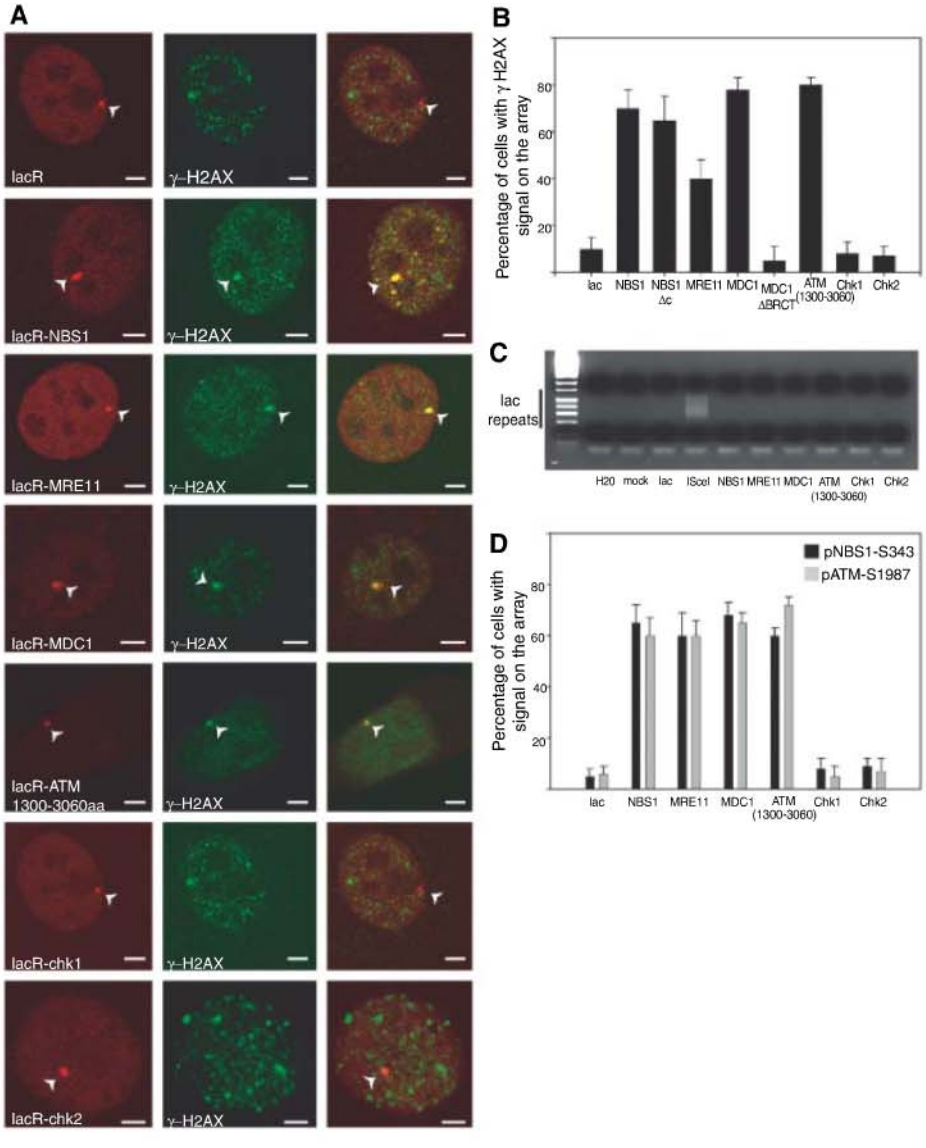

Fig. 1. Immobilization of single repair factors on chromatin leads to DDR activation. **(A)** Immunofluorescence microscopy on NIH 2/4 cells transiently transfected for 16 hours with the indicated repair factor fused to Cherry-lacR (red). DDR activation is indicated by phosphorylation of H2AX (green). Bar, 2 μm. **(B)** Quantitative analysis of H2AX phosphorylation on the lacO array after transfection of the indicated repair factors for 16 hours. Values represent the means ± SD (n = 40 cells) from four independent experiments. **(C)** Absence of DNA lesions upon tethering. Ligation-mediated PCR on NIH 2/4 cells transfected for 16 hours with the indicated repair factor fused to Cherry-lacR. The PCR product is a ladder due to the repetitive nature of the lac operator. Transfection of ISceI alone is used as a control. **(D)** Quantitative analysis of NBS1 (S343) or ATM (S1987) phosphorylation on the array after transfection of the indicated repair factor for 24 hours. Values represent the means ± SD (n = 60 cells) from two independent experiments.

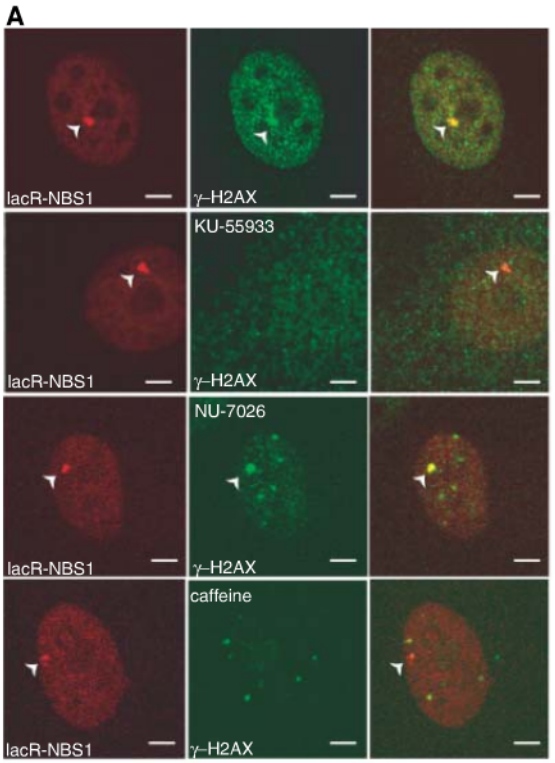

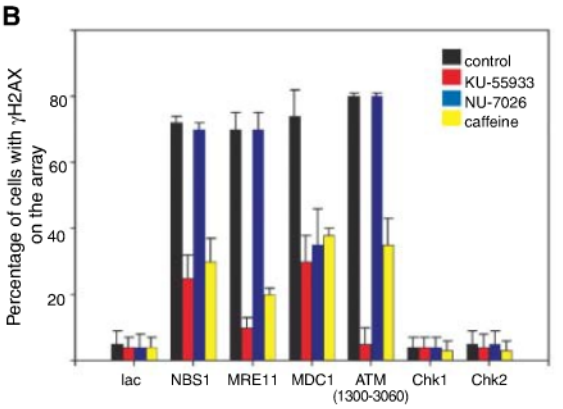

Fig. 2. Activation of the DDR depends on ATM and DNAPK. (**A**) Detection of γH2AX by indirect immunofluorescence in NIH 2/4 cells transiently transfected for 24 hours with lacR–NBS1–Cherry-red (red) and treated with the indicated kinase inhibitor for 24 hours. γH2AX (green). Bar, 2 μm. (**B**) Quantitative analysis of H2AX phosphorylation on the lacO array after immobilization of the indicated repair factors in the presence of signaling inhibitors. Values represent the means ± SD (n = 50 cells) from four independent experiments.

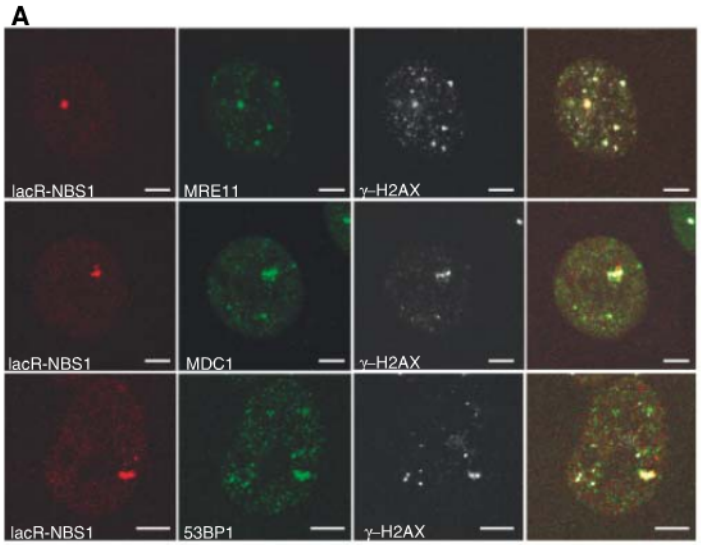

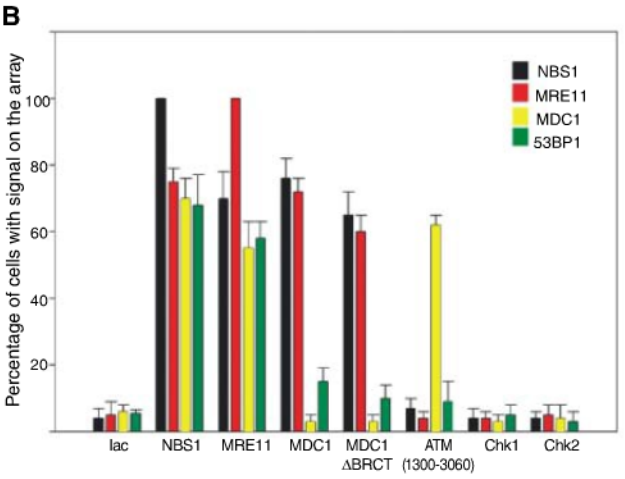

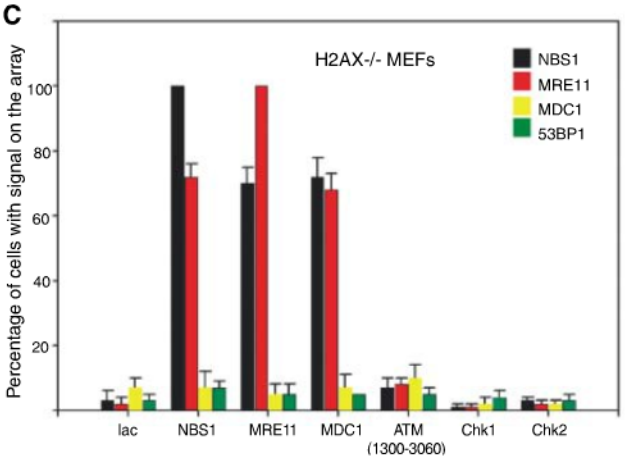

Fig. 3. Cross-recruitment of repair factors. (**A**) Immunofluorescence microscopy on NIH 2/4 cells transiently transfected for 24 hours with lacR-NBS1 (red) with the indicated antibodies (green). Bar, 2 μm. (**B**) Quantitation of repair factor accumulation on the array in NIH 2/4 cells after immobilization of the indicated repair factors. Values represent the means ± SD (n = 40 cells) from three independent experiments. The antibody used to detect MDC1 recognizes only the mouse isoform and not human MDC1 present in the LacR fusion protein. (**C**) Quantitation of repair factor accumulation on the array on H2AX$^{-/-}$ MEFs containing the lacO array after immobilization of the indicated repair factors. Values represent the means ± SD (n = 50 cells) from three independent experiments.

proteins were introduced into an NIH-3T3 cell line that contains 256 repeats of the lac operator sequence (lacO) stably integrated on chromosome 3 (*6*). The fusion proteins were effectively recruited and retained at sites of DNA damage upon ultraviolet laser damage (fig. S1A). As expected, fusion proteins accumulated at the lacO array as distinct nuclear foci (Fig. 1A). When assessing the effect of bound fusion proteins, we found that immobilization of NBS1 or MRE11 alone activated the DDR, as indicated by phosphorylation of H2AX at the lacO site in 60 to 70% of cells (Fig. 1B and fig. S1B). Notably, activation of the DDR upon immobilization of NBS1 or MRE11 occurred in the absence of DNA damage. The presence of DNA lesions was excluded by ligation-mediated polymerase chain reaction (PCR) (Fig. 1C), the absence of bromodeoxyuridine incorporation at the lac array, and lack of staining for the single strand–binding protein RPA (fig. S2, A and B). Activation of the DDR was not due to overexpression of fusion proteins because no γH2AX was detected in the presence of isopropyl-β-D-thiogalactopyranoside (IPTG), which interferes with binding of fusion proteins to lacO (fig. S3A). Induction of γH2AX phosphorylation was rapid and replication-independent (fig. S3, B and C). The response to immobilizing single repair factors to chromatin was not limited to H2AX because immobilization also efficiently induced phosphorylation of Ser^{343} (S343) in NBS1 and Ser^{1987} (S1987) in ATM, two key hallmarks of general DDR activation (Fig. 1D). These observations suggest that stable binding of individual early components of the DNA repair machinery is sufficient to induce the cellular DDR even in the absence of DNA lesions.

To extend these observations, we tested the ability of downstream factors to induce the DDR. Stable immobilization of MDC1 to chromatin led to activation of the DDR with an efficiency similar to that of NBS1 binding (Fig. 1, A, B, and D). This observation is consistent with the notion that H2AX phosphorylation and MDC1 foci formation are mutually interdependent (*7*–*9*). MDC1 ΔBRCT, which lacks the two C-terminal BRCT domains involved in its recruitment to γH2AX (*9*), did not elicit the DDR (Fig. 1B), suggesting that downstream effects of MDC1 rely on the BRCT domain.

The downstream ATM kinase is a key player in triggering the DDR (*10*). It is thought to exist as an inactive dimer in the absence of DNA damage, which becomes activated via autophosphorylation upon genomic insult (*11*). Immobilization of a major fragment of ATM (amino acids 1300 to 3060), which includes the kinase domain, was sufficient to activate the DDR as judged by phosphorylation of H2AX, NBS1, and ATM (Fig. 1, A, B, and D), suggesting that damaged DNA is not an absolute requirement for ATM activation. Unlike ATM, immobilization of the downstream effector kinases Chk1 and Chk2, which normally do not form DNA repair foci, did not lead to phosphorylation of H2AX (Fig. 1, A, B, and D). The correlation between accumulation at sites of DNA damage and ability to induce the DDR when immobilized suggests that prolonged physical association of repair factors at sites of DNA damage might contribute to eliciting DDR in vivo.

Upon stable binding of NBS1, MRE11, or $ATM^{1300\text{-}3060}$ to chromatin, phosphorylation of H2AX was largely blocked in the presence of the ATM inhibitor KU-55933 (*12*) or the PI 3-kinase inhibitor caffeine, but not an inhibitor of DNAPK, NU-7026 (Fig. 2, A and B). H2AX phosphorylation by immobilized MDC1-lacR was dependent on both ATM and DNAPK activities (Fig. 2B), but not on the DNAPK-interacting partner Ku80 (fig. S4). Reducing the expression of ATR by RNA interference had no effect on the extent of H2AX phosphorylation after immobilization of NBS1, MRE11, or MDC1 (fig. S5, A and B). These results demonstrate that tethering-mediated DDR occurs via the ATM and DNAPK pathways, but not the ATR pathway.

We next used our experimental system to systematically determine the interdependencies of recruitment among repair factors in vivo. To this end, we probed the composition of repair foci formed upon stable binding of each individual factor. Immobilization of NBS1 led to recruitment of its direct interaction partner MRE11, but also of the downstream adaptors MDC1 and 53BP1 (Fig. 3, A and B). Similarly, immobilization of MRE11 led to accumulation of endogenous NBS1, MDC1, and 53BP1 (Fig. 3B). Although MDC1 acts downstream of the early MRN sensor complex, immobilized MDC1 was able to efficiently recruit the upstream MRN components NBS1 and MRE11 and, to a lesser extent, 53BP1 (Fig. 3B), suggesting a feedback loop between MDC1 and the MRN complex, possibly as a means to amplify the damage response (*7*, *13*, *14*). This observation is consistent with the findings that MDC1 interacts with the MRN components and that down-regulation of MDC1 in human cells fails to efficiently accumulate the MRN complex in irradiation-induced foci (*15*, *16*). MDC1ΔBRCT, which does not induce the DDR upon tethering, is still able to recruit NBS1 and MRE11. This observation is in agreement with the possibility that the BRCT domain may protect γH2AX from rapid dephosphorylation by phosphatases (*9*). LacR-$ATM^{1300\text{-}3060}$ was unable to recruit any of the upstream factors with the exception of MDC1 (Fig. 3B). This effect is likely due to the ATM-induced phosphorylation of H2AX to which MDC1 binds with high affinity (Fig. 3B) (*17*). As expected, immobilized Chk1 and Chk2 did not recruit any upstream factors, further supporting their roles as loosely associated downstream components of the DDR pathway (Fig. 3B) (*18*). The differences in recruitment ability of ATM compared to NBS1, MRE11, and MDC1 suggests that ATM belongs to a distinct level of hierarchy within the repair complex.

To discriminate whether a given factor is recruited through protein-protein interactions with the immobilized protein or via phosphorylated H2AX, we assayed the composition of repair foci after binding individual proteins to chromatin in $H2AX^{-/-}$ mouse embryo fibroblasts (MEFs) containing the lacO array (*6*). Loss of H2AX had no effect on recruitment of NBS1 and

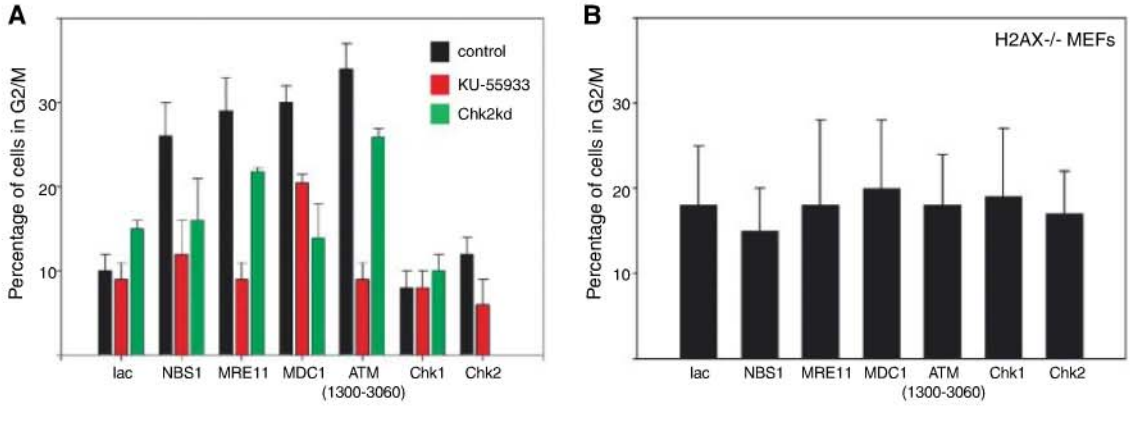

Fig. 4. Targeting of single repair factors to chromatin induces G_2 delay. (**A**) Quantitation of cells with phosphoH3 on Ser^{10} on pericentromeric chromatin in NIH 2/4 cells after immobilization of the indicated repair factors in control cells, cells treated with the ATM inhibitor KU-55933, or cells transfected with small interfering RNA (siRNA) against Chk2. The siRNA eliminated also the expression of the fusion protein (absence of green bar in lacR-Chk2). Values represent the means ± SD (n = 150 cells) from at least two independent experiments. (**B**) Quantitation of cells with phosphoH3 on Ser^{10} on pericentromeric chromatin in $H2AX^{-/-}$ MEFs after immobilization of the indicated repair factors. The baseline level of phosphoS10H3 is slightly elevated in MEFs compared to NIH 2/4 cells. Values represent the means ± SD (n = 150 cells) from at least two independent experiments.

MRE11 by either MRN component or by MDC1 (Fig. 3C). However, upon immobilization of NBS1 or MRE11, the accumulation of the downstream factors MDC1 and 53BP1 was strongly impaired in the absence of H2AX (Fig. 3C). Recruitment of MDC1 by ATM$^{1300\text{-}3060}$ was similarly decreased, suggesting that phosphorylation of H2AX is an important step in recruiting and maintaining these factors at sites of damage (*17*, *19*).

To finally test whether individual repair factors are sufficient to induce a physiological DDR, we assessed the effect of immobilization on cell cycle progression (Fig. 4). Upon targeting of NBS1, MRE11, MDC1, or ATM, but not Chk1 or Chk2, to chromatin, cells accumulated in G_2 phase as determined by staining of pericentromeric heterochromatin with an antibody to phosphoS10H3 (Fig. 4A) (*20*). Cell cycle delay was confirmed by increased phosphorylation of retinoblastoma protein at Ser^{807}/Ser^{811} (fig. S6). Furthermore, the cell cycle delay was sensitive to the presence of Chk2 and required ATM activity, suggesting involvement of the checkpoint kinase Chk2 (Fig. 4A). H2AX$^{-/-}$ cells were resistant to G_2/M delays upon immobilization of repair factors (Fig. 4B). This observation is in line with the finding that cells lacking H2AX manifest a G_2/M checkpoint defect after exposure to low doses of irradiation (*21*).

We report here that activation of cellular DNA damage response pathways does not require DNA damage but can be triggered by stable association of single repair factors with chromatin. Our observations suggest that the physical interaction of DNA repair factors with chromatin is a key step in activation of the DDR signaling cascade, and that the observed buildup at DNA damage foci probably contributes appreciably to establishing the cellular response to damaged DNA (*4*). Our observation that immobilized downstream factors can recruit upstream components indicates that activation of a full DDR involves amplification via formation of multiple repair complexes and perpetuation of γH2AX phosphorylation. A critical role for signal amplification on DNA is also suggested by the findings that in the absence of γH2AX or MDC1, several repair factors, including NBS1 and 53BP1, are recruited to sites of double-strand breaks, but do not accumulate and are not efficiently retained (*16*, *19*). Our observation of phosphorylation of several key components of the DDR, including H2AX, NBS1, and ATM, and the appearance of cell cycle delays upon tethering indicate that the observed cellular response mimics to a large extent the physiological DDR. Given the apparent importance of the physical interaction of DNA repair factors with chromatin, it will be essential to uncover the precise role of higher-order chromatin structure and chromatin-remodeling complexes in triggering the DDR.

References and Notes

1. J. Lukas, J. Bartek, *Cell* **118**, 666 (2004).
2. Y. Shiloh, *Curr. Opin. Genet. Dev.* **11**, 71 (2001).
3. S. P. Jackson, *Carcinogenesis* **23**, 687 (2002).
4. S. Bekker-Jensen *et al.*, *J. Cell Biol.* **173**, 195 (2006).
5. J. Bartek, J. Lukas, *Cancer Cell* **3**, 421 (2003).
6. E. Soutoglou *et al.*, *Nat. Cell Biol.* **9**, 675 (2007).
7. Z. Lou *et al.*, *Mol. Cell* **21**, 187 (2006).
8. A. Peng, P. L. Chen, *J. Biol. Chem.* **278**, 8873 (2003).
9. M. Stucki *et al.*, *Cell* **123**, 1213 (2005).
10. Y. Shiloh, *Cell Cycle* **2**, 116 (2003).
11. C. J. Bakkenist, M. B. Kastan, *Nature* **421**, 499 (2003).
12. I. Hickson *et al.*, *Cancer Res.* **64**, 9152 (2004).
13. S. Bekker-Jensen, C. Lukas, F. Melander, J. Bartek, J. Lukas, *J. Cell Biol.* **170**, 201 (2005).
14. G. S. Stewart, B. Wang, C. R. Bignell, A. M. Taylor, S. J. Elledge, *Nature* **421**, 961 (2003).
15. M. Goldberg *et al.*, *Nature* **421**, 952 (2003).
16. C. Lukas *et al.*, *EMBO J.* **23**, 2674 (2004).
17. M. Stucki, S. P. Jackson, *DNA Repair (Amst.)* **5**, 534 (2006).
18. C. Lukas, J. Falck, J. Bartkova, J. Bartek, J. Lukas, *Nat. Cell Biol.* **5**, 255 (2003).
19. A. Celeste *et al.*, *Nat. Cell Biol.* **5**, 675 (2003).
20. K. Monier, S. Mouradian, K. F. Sullivan, *J. Cell Sci.* **120**, 101 (2007).
21. O. Fernandez-Capetillo *et al.*, *Nat. Cell Biol.* **4**, 993 (2002).

22. We thank J. Lukas and Y. Shiloh for reagents and comments; A. Belmont, T. Paull, and M. Kastan for reagents; S. Snyder for technical assistance; and M. Kruhlak for help with microscopy. Imaging was performed at the National Cancer Institute (NCI) Fluorescence Imaging Facility. E.S. was supported by a fellowship from the Human Frontier Science Program. This research was supported by the Intramural Research Program of the NIH, NCI, and Center for Cancer Research.

Supporting Online Material

www.sciencemag.org/cgi/content/full/1159051/DC1
Materials and Methods
Figs. S1 to S7
References

14 April 2008; accepted 1 May 2008
Published online 15 May 2008;
10.1126/science.1159051
Include this information when citing this paper.

Transfer of Learning After Updating Training Mediated by the Striatum

Erika Dahlin,[1,2]* Anna Stigsdotter Neely,[3] Anne Larsson,[2,4] Lars Bäckman,[5] Lars Nyberg[1,2,4]

Process-specific training can improve performance on untrained tasks, but the magnitude of gain is variable and often there is no transfer at all. We demonstrate transfer to a 3-back test of working memory after 5 weeks of training in updating. The transfer effect was based on a joint training-related activity increase for the criterion (letter memory) and transfer tasks in a striatal region that also was recruited pretraining. No transfer was observed to a task that did not engage updating and striatal regions, and age-related striatal changes imposed constraints on transfer. These findings indicate that transfer can occur if the criterion and transfer tasks engage specific overlapping processing components and brain regions.

Task-specific performance enhancement and altered patterns of brain activity have been demonstrated after training on complex executive tasks (*1*, *2*). Training can also improve performance on untrained transfer tasks (*3*), but the magnitude of gain is considerably smaller and often there is no transfer at all (*2*). One current hypothesis is that transfer will occur if the criterion and transfer tasks involve overlapping processing components and engage, at least in part, the same brain regions (*4*). In the present study, we studied learning and transfer of a specific skill: updating. Updating is a basic executive function (*5*, *6*) related to measures of intelligence (*7*) and working memory, in particular to working-memory tasks that require manipulation of information (*6*). Updating has been associated with the striatum (*8*), and, in a recent computational model (*9*), striatal neurons serve a gating function for updating in working memory.

To map training-induced changes in brain activity, functional magnetic resonance imaging (fMRI) was used before and after 5 weeks of computer-based updating training (*10*). A test of letter memory served as the updating criterion task (*5*). It consisted of 10 lists of randomly presented letters (A to D), and the task was to recall the four last presented letters. The *n*-back task (*11*) with three levels of load (1, 2, and 3) was used as the transfer task. This task differed from letter memory in terms of memorial content (letters versus numbers), set size, presentation rate, and response format (*10*). These differences are important given that previous research has indicated that even subtle procedural variations can reduce the degree of transfer (*12*), but, critically, *n*-back requires updating and hence shares a basic process with letter memory. A Stroop test was also included. Letter memory and Stroop tap different executive processes (*5*, *6*) and activate specific neural systems (*13*), but transfer could be mediated through a common frontoparietal network (*13*, *14*). Alternatively, no transfer to Stroop should be observed if transfer specifically depends on training-induced

[1]Department of Integrative Medical Biology, Umeå University, 90187 Umeå, Sweden. [2]Department of Radiation Sciences, Umeå University, 90187 Umeå, Sweden. [3]Department of Psychology, Umeå University, 90187 Umeå, Sweden. [4]Umeå Center for Functional Brain Imaging (UFBI), Umeå University, 90187 Umeå, Sweden. [5]Aging Research Center, Karolinska Institute, 11330 Stockholm, Sweden.

*To whom correspondence should be addressed. E-mail: erika.dahlin@physiol.umu.se

changes in a striatal updating system. In a second experiment, we used the same basic procedure to investigate training effects in older adults (*10*). Task-specific training gains and altered patterns of brain activity after training on complex executive tasks have been demonstrated in older adults (*15*, *16*), but transfer to untrained tasks tend to be more difficult to demonstrate in older than in younger adults (*12*, *17*–*19*). It is well established that age-related changes are prominent in the striatum (*20*, *21*), which could impose constraints on transfer of updating training to untrained task performance.

In experiment 1, the training and control groups were comparable on relevant background characteristics (table S1), and the groups were indistinguishable on letter memory before training (table S2). The training group showed considerably larger gains in letter memory, as revealed by a significant group-by-session interaction ($F_{1,20}$ = 26.45, $P < 0.001$). Further, the effect size for the training group was significantly larger than for the control group (Fig. 1A) [$t(20) = 5.14$, $P < 0.001$]. Evaluation of performance on the Stroop task did not reveal any significant training-related changes in performance (table S2). For the *n*-back task, there was a significant group-by-session interaction ($F_{1,20}$ = 10.32, $P < 0.01$) for 3-back, and the effect size for trained participants was significantly greater than for controls (Fig. 1A) [$t(20) = 4.05$, $P < 0.001$]. No significant interaction was found for 1- and 2-back, reflecting pretraining ceiling effects (table S2). Analyses of the *n*-back imaging data were therefore restricted to 3-back.

The hypothesis that transfer will occur if the criterion and transfer tasks initially engage similar processes and brain circuits predicts overlapping activity before training. We tested this prediction with a conjunction analysis of pretraining activity ($N = 22$) for letter memory and 3-back and observed joint activation in left striatum ($x = -16$, $y = -2$, and $z = 16$; $x = -20$, $y = 4$, and $z = 14$) along with common frontoparietal activation (Fig. 2A). In addition, a direct comparison of letter memory and 3-back at pretest revealed several differences in brain activity, as expected from differences in task demands (fig. S1). A similar conjunction analysis of letter memory with the Stroop task did not reveal any overlap in striatal regions, despite overlap in frontoparietal regions (Fig. 2A). Analyses of pre- and post changes in the fMRI data for letter memory revealed relatively greater activity after training in left striatum ($x = -26$, $y = -4$, and $z = -4$; t = 4.32) (see table S3 for other areas), along with decreased frontoparietal activity (table S3). In the analyses of transfer effects, training-related increases were seen in left striatum ($x = -30$, $y = 4$, and $z = 6$; $T = 4.74$) and frontal cortex for 3-back (see table S3 for other areas), but no significant changes were found for Stroop. On the basis of these findings of posttraining activity increases in left striatum for both letter memory and 3-back, we conducted a conjunction analysis to assess commonalities in between-session activation changes for these tasks. This analysis revealed overlap in left striatum ($x = -28$, $y = 8$, and $z = -2$; $T = 3.91$). Critically, the striatal region showing training-related increases for both letter memory and 3-back overlapped with the striatal region that was jointly activated at the pretraining session for these two tasks (Fig. 3A). This overlap in activity fell within the associative striatum (*22*).

In experiment 2, the older training and control groups were comparable on relevant background characteristics (table S1), and the two groups performed at similar levels on letter memory at pretraining (table S2). Both groups improved their performance in the posttraining session,

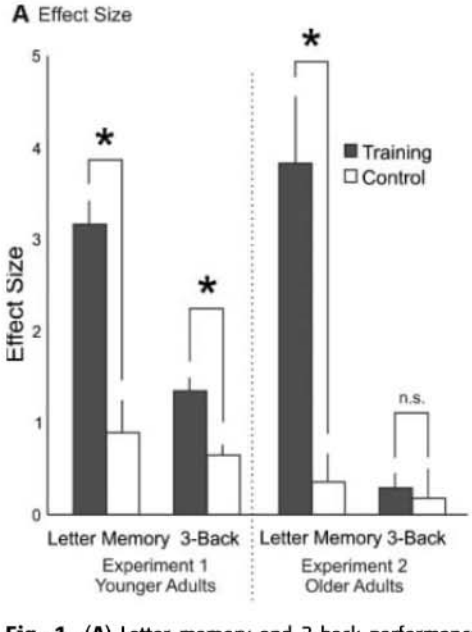

Fig. 1. (**A**) Letter memory and 3-back performance for training and control groups. The histograms denote mean effect sizes. (**B**) Training gains in younger and older adults during the 5-week intervention period. Error bars indicate SEM. Asterisks indicate statistical significance; n.s., not significant.

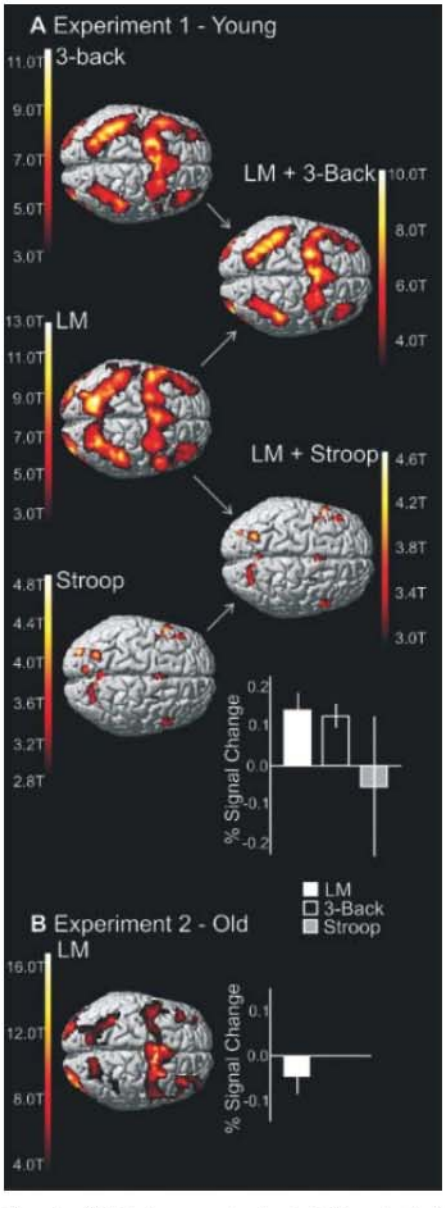

Fig. 2. (**A**) Brain maps to the left (dorsal view) show activation of bilateral parietal cortex and lateral and medial frontal cortex for all tasks at pretraining. Conjunction analyses of the letter memory (LM) task with Stroop and 3-back revealed overlapping frontoparietal activation patterns for the criterion task and both transfer tasks (cortical maps to the right). The bar graph (bottom) shows the striatal activation profile across tasks at pretraining and reveal overlapping activations in LM and 3-back (plotted at peak $x = -20$, $y = 4$, and $z = 14$). (**B**) Brain map to the left shows activation of bilateral parietal cortex and lateral and medial frontal cortex for LM pretraining. The bar graph shows no significant striatal activation in LM for older adults (plotted at peak $x = -24$, $y = 10$, and $z = -2$, where selective training-related increases were found). Error bars indicate SEM.

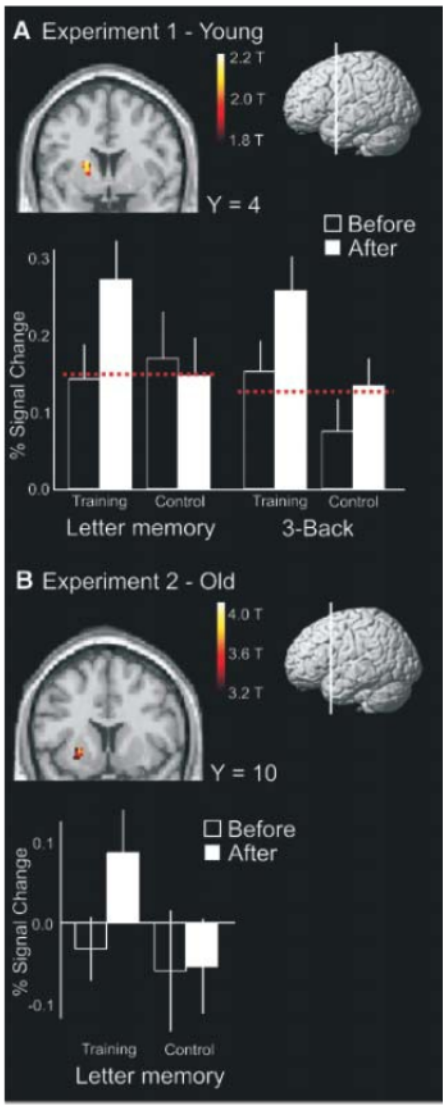

Fig. 3. (**A**) Left striatum (peak $x = -20$, $y = 4$, and $z = 14$) was activated before training and showed a training-related increase for both letter memory and 3-back in younger adults. The bar graph shows the activation profiles across tasks and sessions. The red line indicates mean baseline bold values for the striatal region (mean of trained before, controls before, and controls after). (**B**) Left striatum (peak $x = -24$, $y = 10$, and $z = -2$) showed a training-related increase for letter memory in older adults. Error bars indicate SEM.

but the increase in performance was larger for the trained group compared with controls as indicated by a significant group-by-session interaction ($F_{1,17} = 20.56$, $P < 0.001$). Further, the effect size was significantly larger for the old training group compared with controls (Fig. 1A) [$t(17) = 4.53$, $P < 0.001$]. However, the older adults showed no transfer to 3-back (Fig. 1A). This finding is in keeping with prior findings of limited transfer for older adults (*12*, *17*–*19*). Furthermore, a comparison of the learning curves from experiments 1 and 2 showed that the trained older adults had significantly lower performance at the beginning [$t(24) = 3.38$, $P < 0.005$] as well as at the end of training [$t(24) = 4.99$, $P < 0.001$] compared with the trained younger adults, and the final level of letter memory performance in the trained older group was below the level reached by younger adults after 2 weeks of training (Fig. 1B). These behavioral findings indicate age-related neural constraints on updating learning and transfer, which was supported by the fMRI analyses. Specifically, the striatum was not significantly activated during letter memory in the pretraining session for older adults, although they did activate frontoparietal regions ($N = 19$) (Fig. 2B). Analyses of prepost changes for letter memory revealed training-related activity increases in left striatum for trained older adults relative to controls ($x = -24$, $y = 10$, and $z = -2$; $T = 4.17$) (Fig. 3B; see table S3 for other areas), but no significant changes were found for the 3-back transfer task.

Our findings reveal a critical role for the striatum in mediating transfer of learning after updating training. Transfer after other forms of training, taxing different executive processes, will likely depend on other brain regions. The striatal region where a common training-related increase was seen for the letter memory and 3-back tasks was also activated at pretraining for these tasks. By contrast, no striatal activation was observed for the Stroop task, and updating training did not influence Stroop performance. Some previous research has found striatal activation during the Stroop task (*23*), but this is not a typical finding (*24*, *25*) and the Stroop task should not tax updating. Thus, although a similar frontoparietal cortical system was activated for all three tasks examined, the transfer effect apparently required that both the criterion and transfer tasks engaged a specific processing component (i.e., updating) and associated brain systems (i.e., striatum). Even though this conclusion is based on a limited regime of tasks, the observed selectivity in the neural basis of transfer is consistent with numerous behavioral findings of limited transfer. The hypothesis that a basis for transfer is that training and transfer tasks recruit overlapping neural systems (*4*) may thus be too general.

The finding of substantial performance increments on the criterion task for the older participants is consistent with previous demonstrations of enhanced performance after executive training in advanced age (*15*). However, there were pronounced age-related performance deficits on the updating criterion task and, most critically, on the magnitude of transfer to the 3-back task. Also, the older adults did not show significant striatal activation before training. These results indicate that restricted transfer of learning after updating training in older age may reflect deficient striatal functioning (*21*, *24*). Importantly, the differences in task characteristics and associated brain activity (fig. S1) and the finding of pronounced task differences in training-related frontal changes (table S3) converge with the observation of significant improvement on letter memory along with no transfer to 3-back in older adults. Although the distinction between training and transfer tasks remains to be defined precisely, collectively our findings illustrate the distinct nature of the current criterion and transfer tasks.

A key role for the striatum in learning and transfer of an updating skill is consistent with much previous work. A recent study identified striatum as being responsible for allowing only relevant information into working memory (*26*). Anterior parts of the striatum form an associative network with dorsolateral frontal regions (*22*, *27*). Neurons in the striatum may regulate updating in working memory by affecting dopaminergic modulation of the prefrontal cortex (*9*, *28*), and increased striatal dopamine release has been observed during performance of tasks requiring specific executive processes (*29*).

References and Notes

1. K. I. Erickson *et al.*, *Cereb. Cortex* **17**, 192 (2007).
2. P. J. Olesen, H. Westerberg, T. Klingberg, *Nat. Neurosci.* **7**, 75 (2004).
3. M. C. Lovett, J. R. Anderson, *J. Exp. Psychol. Learn. Mem. Cogn.* **20**, 366 (1994).
4. J. Jonides, *Nat. Neurosci.* **7**, 10 (2004).
5. A. Miyake *et al.*, *Cognit. Psychol.* **41**, 49 (2000).
6. E. E. Smith, J. Jonides, *Science* **283**, 1657 (1999).
7. N. P. Friedman *et al.*, *Psychol. Sci.* **17**, 172 (2006).
8. R. O'Reilly, M. Frank, *Neural Comput.* **18**, 283 (2006).
9. R. C. O'Reilly, *Science* **314**, 91 (2006).
10. Materials and methods are available as supporting material on *Science* Online.
11. J. D. Cohen *et al.*, *Hum. Brain Mapp.* **1**, 293 (1993).
12. A. Derwinger *et al.*, *Aging Neuropsychol. Cogn.* **10**, 202 (2003).
13. F. Collette *et al.*, *Hum. Brain Mapp.* **25**, 409 (2005).
14. T. Klingberg *et al.*, *J. Am. Acad. Child Adolesc. Psychiatry* **44**, 177 (2005).
15. K. I. Erickson *et al.*, *Neurobiol. Aging* **28**, 272 (2006).
16. H. W. Mahncke *et al.*, *Proc. Natl. Acad. Sci. U.S.A.* **103**, 12523 (2006).
17. A. Stigsdotter Neely, L. Bäckman, *J. Gerontol. B Psychol. Sci. Soc. Sci.* **48**, 233 (1993).
18. K. Ball *et al.*, *JAMA* **288**, 2271 (2002).
19. G. W. Rebok, M. C. Carlson, J. B. S. Langbaum, *J. Gerontol. B Psychol. Sci. Soc. Sci.* **62B**, 53 (2007).
20. R. L. Buckner, *Neuron* **44**, 195 (2004).
21. N. Raz *et al.*, *AJNR* **24**, 1849 (2003).
22. D. Martinez *et al.*, *J. Cereb. Blood Flow Metab.* **23**, 285 (2003).
23. B. S. Peterson *et al.*, *Cogn. Brain Res.* **13**, 427 (2002).
24. B. H. Schott *et al.*, *Brain* **130**, 2412 (2007).
25. D. E. Nee, T. D. Wager, J. Jonides, *Cogn. Affect. Behav. Neurosci.* **7**, 1 (2007).
26. F. McNab, T. Klingberg, *Nat. Neurosci.* **11**, 103 (2008).
27. R. B. Postuma, A. Dagher, *Cereb. Cortex* **16**, 1508 (2006).
28. J. D. Cohen, T. S. Braver, J. W. Brown, *Curr. Opin. Neurobiol.* **12**, 223 (2002).
29. O. Monchi, J. H. Ko, A. P. Strafella, *Neuroimage* **33**, 907 (2006).
30. The authors thank M. Andersson for support with statistical analyses, A.-K. Johansson for helping in collecting the data, and the staff at the MRI center. This work was funded by grants from the Swedish Research Council and the Joint Committee for Nordic Research Councils in the Humanities and the Social Sciences to L.N. for a Nordic Center of Excellence (NCoE) in Cognitive Control and by grants from the Swedish Research Council and Swedish Brain Power to L.B.

Supporting Online Material

www.sciencemag.org/cgi/content/full/320/5882/1510/DC1
Materials and Methods
Fig. S1
Tables S1 to S3

22 January 2008; accepted 15 May 2008
10.1126/science.1155466

Cryostat

The Leica CM1950 cryostat is designed to meet the requirements for high-quality sectioning, user safety, and improved workflow. The instrument includes two innovative features: the CryoZone cooling system and the optional vacuum waste removal system. The CryoZone system controls a zone of uniformly cool air in the critical areas of the cryometer. The cool air circulates around the specimen, knife, and antiroll guide to create the best conditions for consistent, high-quality sectioning. The optional vacuum system aids efficient workflow by keeping sections flat and wrinkle-free and enhances user safety by removing waste material. With precise microtome and object feed mechanisms, rapid freezing, and accurate temperature control, the Leica CM1950 provides full control of each tissue section. Optional extras include a dual compressor for independent temperature control of the specimen head and a hesitation-free, motor-driven cutting stroke.

Leica
For information 800-248-0123
www.leica-microsystems.com

Heat Sealer and Microplate Thawer

The Thermobond 2 is a new generation heat sealer designed to seal polypropylene collection plates, polymerase chain reaction plates, microplates, and deep-well blocks with a specially prepared pierceable film or foil. The Thermobond 2 incorporates an ergonomic design to minimize risk while creating a reproducible, high-integrity seal every time. The Microsteam microplate thawing station circulates ambient air across the base of a frozen microplate or tube rack to gently and evenly thaw samples without risk of damage. It is economical, quiet, and compact.

Porvair Sciences
For information +44-1932-240255
www.porvair.com

Perfusion Chamber

The Moist Chamber Type 834/8 is a flexible tool for perfusion of organs such as liver and kidney from rodent models. In its basic configuration, the Moist Chamber consists of a deep (110 mm by 40 mm by 35 mm) organ chamber with a tight-fitting cover. Both components are double-walled and water-jacketed to provide a stable, temperature-controlled environment. The perfusion medium is warmed by passage through a built-in heat exchanger and bubble trap immediately before contact with the organ. Inside the chamber, a flexible silicone platform acts as a rest for preparation and cannulation of the organ. Several measurement and sample ports provide easy access to the inner chamber for collecting a wide range of physiological data. The Moist Chamber can be part of a simple constant flow perfusion system for testing potential vasoactive compounds or form the core of a combined constant pressure and flow system for more complex perfusion and dose-response regimes.

Harvard Apparatus
For information 800-272-2775
www.harvardapparatus.com

Stem Cell cDNA Libraries

The SuperScript Human Stem Cell cDNA Libraries consist of complementary DNA (cDNA) isolated from commonly used, well-characterized human embryonal carcinoma and human embryonic stem cell lines. These libraries have many uses as a reference set of stem cell genes and can be used for gene discovery, polymerase chain reaction analysis, the construction of cDNA arrays, and functional screening. With these libraries, researchers can begin to characterize key genes in stem cell lines, allowing for the identification of the gene expression profile at various stages of cell development.

Invitrogen
For information 800-955-6288
www.invitrogen.com

Multimode Luminometer

The GlaxMax-Multi Detection System's multimode capability includes luminescence, fluorescence, and absorbance detection in 96-well plates. The modular design allows a user to expand into these applications as needed, which is particularly applicable for cancer research, cell biology, and drug screening. With a simple touch-screen interface, GloMax operates as an independent workstation with no need for a computer to operate it, but data can be transferred via a USB port. The GloMax is suitable for the multiplexing of assays, and an injection system is available for use with the Dual-Luciferase Reporter Assay System.

Promega
For information 608-274-4330
www.promega.com

Bead-Based Multiplex Assays

The Widescreen EpiTag ERK Pathway Assays are the first wave of bead-based, multiplex assays based on EpiTag Technology licensed from Epitome Biosystems. The new line of assays will enable researchers to make quantitative, highly multiplexed measurements of important cell targets to facilitate drug discovery efforts. The assays detect key events in the extracellular signal-regulated kinases (ERK) pathway from both human and mouse samples. ERK pathway protein levels and phosphorylation are deregulated in many types of cancer and are considered strong candidates for the development of therapeutic approaches. These assays will enable researchers to determine the effect of candidate compounds on multiple analytes to allow a better understanding of on- and off-target effects.

EMD Chemicals
For information 608-422-4006
www.emdchemicals.com

Electronically submit your new product description or product literature information! Go to **www.sciencemag.org/products/newproducts.dtl** for more information.

Newly offered instrumentation, apparatus, and laboratory materials of interest to researchers in all disciplines in academic, industrial, and governmental organizations are featured in this space. Emphasis is given to purpose, chief characteristics, and availabilty of products and materials. Endorsement by *Science* or AAAS of any products or materials mentioned is not implied. Additional information may be obtained from the manufacturer or supplier.

Sustaining Forests in a Changing World

HALF-COVERED IN TREES AND BLESSED—or cursed—with hot, dry summer days, Greece is used to wildfires. Yet the blazes that swept across Greece last summer were the worst in living memory. According to the European Commission, 64 people died and about 180,000 hectares of forest and agricultural land were burned in just the most severe of the blazes, which raged between 24 and 30 August. It was, says Andreas Drouzas, a Greek forest evolutionary geneticist at Aristotle University of Thessaloniki, "something that both professionally and personally someone cannot take out of his or her mind."

While some tree species have evolved to regenerate naturally after fire, last summer's fires destroyed fir trees in the mountainous Peloponnesus peninsula and in Mount Parnitha near Athens that are not normally affected by fire. "The fir forests need hundreds and even thousands of years to be established, and they don't have any mechanism to survive or overcome the fire," Drouzas says. "That is because the fires at high elevations were a rare event, but due to the climate change nowadays, the fires burned down even forests of high elevations."

Unfortunate events such as these may have some positive scientific consequences. Stresses on ecological systems, and the global changes and human activities that cause them, nudge the science of forests in new directions, creating professional opportunities. "As the forests have decreased and the society has become more … aware of the consequences of loss of natural ecosystems and biodiversity, and the associated decline of ecosystem services, there has been more and more interesting research in forest ecology, and this trend will continue," says Kamaljit Bawa, a tropical forest evolution and conservation ecologist at the University of Massachusetts, Boston.

An evolving field

Over the past decade or so, the focus of ecology has shifted from studies of undisturbed ecosystems to the impact of human activities, propelling some subfields—including forest ecology—into a period of renaissance. Because forest ecosystems help maintain water and air quality, regulate the local and global climates, protect soils from erosion, and host the greatest biodiversity on land, they are central to most of today's global environmental issues.

Sustaining biodiversity. Andreas Drouzas wants to create a gene bank so that forests in the Peloponnesus peninsula can be restored after fires.

In Europe, the European Commission has made environmental research one of its 10 thematic priorities in its 2007–13 funding framework program, earmarking nearly €1.9 billion for environmental research from a €50.5 billion budget—a sharp increase from the previous framework. Forest research is expected to grab a healthy chunk of Europe's spending on environmental research; the new framework offers many topics on which forest ecologists could submit proposals, Drouzas says.

In the United States, National Science Foundation (NSF) funding for environmental research and education increased by about 40% between 2000 and 2004, after which it flat-lined. But Susan Stafford, a forest statistical ecologist at the University of Minnesota, St. Paul, and chair of the NSF Advisory Committee for Environmental Research and Education, says a large-scale research program focused on the sustainability of complex environmental systems is in the pipeline. "We are very optimistic that the funding for all environmental fields" will increase after 2010. And "forestry [is] a very major component in all of environmental and ecosystem sciences," she says.

Dirty boots and other basics

Working in forest ecology requires a special set of skills: a foundation in biology, chemistry, physics, and mathematics; a deep understanding of ecological principles and forest ecosystems; and enough knowledge about botany and taxonomy to recognize known species and new ones. It also requires

an array of field techniques for measuring forest structure, soil chemistry, and climatic conditions, for example.

Forest ecologists also need "a lot of grit," says Catherine Cardelús, a tropical forest canopy ecologist at the University of Florida, Gainesville. Cardelús commonly puts on a 15-kg backpack filled with climbing gear, hikes 4 hours into the middle of the forest, then goes up trees. "You need to be able to handle that," Cardelús says, while remaining flexible—and not just literally. "We are constantly updating and revising the situation" as the work and conditions require, she says.

Getting along in forests requires survival skills, especially in the tropics. You have to know how to avoid the pervasive snakes and spiders, for example. Then there's the risk of getting lost, being stung by a swarm of bees, or being urinated on by howler monkeys. "The canopy is where they live," and monkeys will yell and throw things at you, and even urinate on you, if you don't leave their tree and let them eat in peace, Cardelús says.

In such a hazardous world, caution reigns, and remaining safe requires some technical and physical skill. "I can drop out of a tree in 15 seconds in case I am swarmed by bees," Cardelús says. "What I do is inherently dangerous, but I am very safe."

The best way to acquire the needed skills is by getting your boots muddy. "Volunteer to join a field trip expedition, just to get some experience to see what is involved rather than just being in lectures or lab work," says Yadvinder Malhi, an ecosystem scientist working on tropical and temperate forests at Oxford University in the United Kingdom.

You may also have to make some personal sacrifices. Most forest ecologists travel extensively and collect data in the wild for several months at a time. "You need to love being in the woods, without much of what we take for granted in our civilized world," says Jérôme Chave, a tropical forest ecologist at the Laboratory for Evolution and Biological Diversity in Toulouse, France. "It is tiring and … difficult to combine with a full personal life."

An interdisciplinary skill set

Forest ecologists use approaches ranging in scale and complexity from molecules and genes, through populations and communities, to whole ecosystems and the biosphere. Researchers may have to weave together aspects of the forest as diverse as population and community dynamics, plant physiology, microbiology, entomology, soil physics and chemistry, hydrology, geography, and climatic and geographical conditions. No one has the skills to do even part of this alone, so

A woman ascending. When Catherine Cardelús started out, most "people who were climbing were men."

CREDIT: JAMES E. WATKINS JR

A SELF-MADE CLIMBER

Catherine Cardelús, 36, discovered her passion for tropical forests while listening to a teacher describe the astounding diversity of rainforests. "I decided to be a rainforest [ecologist] without having seen" a rainforest, Cardelús says. The following summer, she flew to La Selva Biological Station in Costa Rica on a summer fellowship and climbed her first tree. She "got so excited about going up that I didn't think about how to get down," she says. As she reached the first branch 15 m above the ground, "I looked up into it and I saw another forest."

Cardelús has since taught herself how to move freely up and down trees, but she's still struggling to understand a key scientific question: Why is there so much plant diversity 50 m above the ground?

After obtaining her B.A. in biology from Barnard College in 1996, Cardelús did a Ph.D. on the distribution of vascular epiphytes—plants that grow on other plants—in tropical forests in the Department of Ecology and Evolutionary Biology at the University of Connecticut, Storrs. Part of her project involved looking at how microclimate affects the way plants are laid out on the branches of individual trees. She built networks of sensors to monitor light, humidity, and temperature along the branches, powering them from the ground with a motorcycle battery. She studied the distribution of epiphytes at 500-m intervals along a 2900-m elevation gradient between La Selva and the Volcán Barva in Costa Rica.

In 2003, Cardelús took a postdoc at the University of Florida, Gainesville, to study the nutrient dynamics of epiphyte communities. Together with her husband—a functional plant ecologist—and their 9-month-old son, she spent the first year of her postdoc at La Selva Biological Station comparing soil and canopy nutrient sources.

Cardelús splits her time between the United States, where she does a lot of analytical and biochemistry lab work quantifying nutrient dynamics, and field trips. Her eldest son, now 5, routinely accompanies her to Costa Rica, and her second son, age 2, will come along the next time.

Starting in July, Cardelús and her husband will each take assistant professorships at Colgate University in Hamilton, New York, where she plans to extend her research to nutrient dynamics in relation to local pollution and climate change. "It hasn't been until recently that I … and other canopy researchers … have had enough baseline data to begin addressing these questions," she says. Nowadays, "most researchers, especially forest ecologists, are incorporating climate change impacts into their research, both for funding reasons and because climate change is having a serious impact on forest ecosystems."

Of Hispanic origin, Cardelús is keen to share her passion for forest canopies with younger scientists and to nurture minority students and women in particular. "I had more barriers to overcome," she says. In her early days, most "people who were climbing trees were men. I wasn't even considered a serious player" at the time. **–E.P.P.**

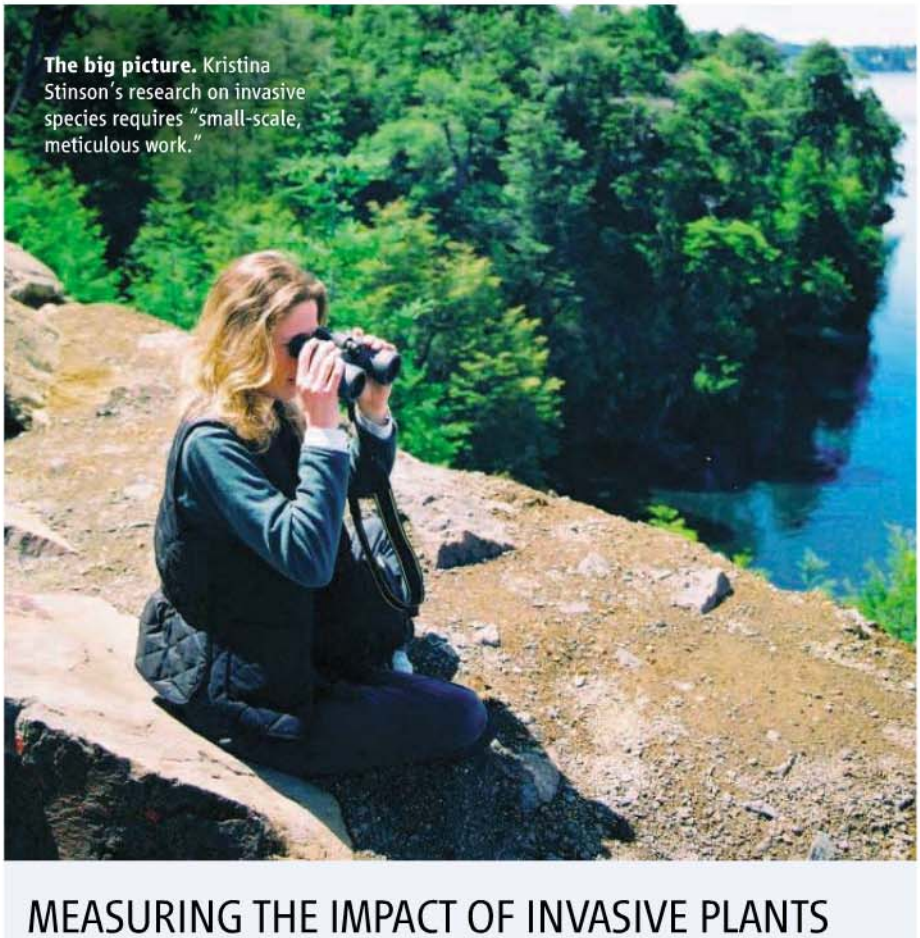

The big picture. Kristina Stinson's research on invasive species requires "small-scale, meticulous work."

MEASURING THE IMPACT OF INVASIVE PLANTS

"I have always been fascinated by the complexity of nature and the way that [organisms] interact with one another," says Kristina Stinson, 38, a plant population biologist at Harvard Forest in Petersham, Massachusetts.

After obtaining two bachelor's degrees, one in literature and languages and another in natural sciences and mathematics, Stinson did a Ph.D. at the Department of Ecology and Evolutionary Biology at Princeton University, conducting her research on how global warming influences the flowering time of alpine plants on the verge of extinction at the Rocky Mountain Biological Laboratory in Crested Butte, Colorado. After graduating in 1998, Stinson took a postdoc at Harvard University, where she studied the dynamics of ragweed populations in elevated atmospheric carbon dioxide levels as well as the physiological processes that turn plants into invasive species outside their home ranges.

Stinson's fieldwork took her to Harvard Forest, where she applied a population perspective to studying how invasive plants affect forest ecosystems. They "really change the way the forests work because they form very dense populations of single species and often replace or displace the native plant," Stinson says. After a couple of years working on this topic as a research associate at Harvard, she was offered her current staff position at Harvard Forest.

Stinson's work on garlic mustard—an invasive plant able to kill fungi essential to the growth of tree seedlings—involves "crouching down in the woods [with] a clicker counter to count individuals" at 1-by-1-meter sampling sites all around New England. It is "small-scale, meticulous work." She brings soil samples back to the lab to monitor the presence of fungi and quantify how much garlic mustard affects the growth of tree seedlings in greenhouses. "It really spans the whole spectrum of fieldwork to lab work," she says.

Stinson's work has implications for forest management. "It's very important to be able to demonstrate when an invasive plant is actually having a negative impact and what the negative impact is, because forest managers are working to manage an ecosystem that has all kinds of management problems and limited resources," she says. She has also done research and management advisory work for U.S.-based conservation charity The Nature Conservancy. It's "very gratifying to see that your research has the potential to have an impact," Stinson says.

–E.P.P.

young forest ecologists need to be "doing their homework, … building the international partnerships with colleagues that allow them to … create very realistic and vigorous scientific … projects," says Stafford.

Forest ecology depends on increasingly sophisticated technical, quantitative, statistical, and computer skills. New data-gathering platforms like the National Ecological Observatory Network and the international Global Earth Observation System of Systems are coming online, and growing quantities of data, spanning ever-larger geographical and time scales, await analysis. Researchers need a strong technical understanding of tools like geographic information systems, distributed sensor networks, and the Global Positioning System "to take most advantage of the enormous volumes of remotely sensed data," Stafford says. Advanced computer-modeling skills have also become essential as researchers try to understand the role of forests in global dynamics and to predict the impact of environmental pressures on forests. Some experts, including Malhi, believe there aren't enough scientists who can combine biological insight with competence in modeling the physics of biological systems.

Social science enters the picture as well. When looking at how local usage may drive certain forest species to extinction, for example, scientists must "not only focus on the population dynamics of that species but also on how people harvest these species, and what social and economic interactions govern the harvesting and use of these species," Bawa says. "In order to do that, you have to be aware of the methods that are used by social scientists" to study social institutions and economic determinants of human behavior, he adds.

Some institutions are now bringing diverse disciplines closer in efforts to provide such broad training. The College of Forestry at Oregon State University, Corvallis, for example, participates in a graduate program in ecosystem informatics and another in environmental sciences that spans life, physical, and social sciences. The Department of Environmental Science, Policy, and Management at the University of California, Berkeley, offers a graduate program that integrates the natural and social sciences and allows students to work on forests. Last year, the Ashoka Trust for Research in Ecology and the Environment, a research, policy analysis, and education nonprofit Bawa founded in Bangalore, India, launched a doctoral program in conservation science in collaboration with Manipal University. The program is for natural and social scientists interested in working on forests, among other ecosystems.

CREDIT: COURTESY OF KRISTINA STINSON

AN ADVENTUROUS PHYSICIST

When Jérôme Chave stepped into a tropical forest for the first time, "I was even unable to identify a weed in my backyard at home, and the idea that hundreds of plant species were coexisting peacefully in tiny areas of forest astounded me," he says. The impact prompted Chave to leave theoretical condensed matter physics to focus on tropical forests. Ten years later, Chave, 35, runs his own forest ecology group at the Laboratory for Evolution and Biological Diversity in Toulouse, France.

Chave grew up in a family of artists with no particular interest in nature, he says. After obtaining a postgraduate diploma in mathematics and physics from the École Centrale in Paris, he pursued a Ph.D. on the statistical properties of complex systems at the French Atomic Energy Commission Laboratory of Condensed Matter Physics in Saclay, near Paris. Halfway through his Ph.D., Chave's adviser met some ecologists investigating paleoenvironments in Africa and South America. "They had the sense that modelers could bring a more synthetic view in their problems. We had a sense that we would have a model to study complex systems that would be a lot more fun than particle systems," Chave says.

Before he knew it, Chave was walking in a pristine rainforest in French Guiana designing a model of tree population dynamics. "I was blown away by the tremendous complexity and amazing diversity" of forests, he says. Starting in 1999, Chave did a postdoc in the Department of Ecology and Evolutionary Biology at Princeton University. There, he used computer modeling and field data to elucidate how forest ecosystems store and recycle carbon and to compare alternative theories for species coexistence.

Since coming back to France in 2001 to take a position at the French National Center for Scientific Research, Chave has continued to cross disciplines. On his team, biologists and mathematicians work together on projects that encompass climate change, biodiversity, community phylogenetics, population genetics, and tropical-tree defenses.

Changing scales. Jérôme Chave left theoretical physics to study tropical forests.

Chave learned the ecology, molecular biology, and chemistry he needed by talking to colleagues, going to seminars, and reading papers. Botany wasn't so easy. "I spent a long time in the field trying to learn my species. … If you don't start at the age of 3, you don't know how to look at nature in the proper way."

Chave, who every year spends about 2 months in the field, learned how to live and work in tropical forests by doing. Still, doing botany in the tropics means climbing 50-m trees to collect leaves, as some of them cannot be identified from the ground. For someone who gets dizzy with height, "it was a big challenge," Chave says.

Once beyond the most adventurous aspects, "you realize how quiet it is to be in a tropical forest rather than in an urban area full of stressed people and telephones. You just enjoy the monkeys around and the birds. It's great."

–E.P.P.

But at most institutions, acquiring the necessary skills is "a question of the student taking the initiative to familiarize him[self] or herself with other areas [by] perhaps having an interdisciplinary master's or Ph.D. committee and taking … courses in disciplines other than the ones that [they] are doing," says Daniel Simberloff, a community ecologist working on forests at the University of Tennessee, Knoxville. Other proven techniques include attending seminars in other departments and joining the relevant scientific societies.

But forest ecologists must also remember to focus their work narrowly. "It's such an interesting field that it's often hard for students to narrow their focus and to do a doable project. … At any level, it's important to home in on what questions you are going to focus on," says Kristina Stinson, a plant population biologist at Harvard Forest in Petersham, Massachusetts.

Engaging the human part of the ecosystem

Many forest researchers consider feeding their results into the global political debate a part of their jobs. "Scientists, because they have certain expertise, are almost obligated to provide that information," Simberloff says. That means learning "to effectively communicate the results to a wide array of audiences, not only scientists but people in the media, citizens, and of course policy- and decision-makers," Bawa says.

Dealing with such sensitive issues is a tricky game. You have to engage in the debate, yet expressing personal opinions can be hazardous. Make sure you base this participation on well-grounded, credible, and objective science, Malhi says: "There is an important distinction between a concerned, informed scientist and a partisan lobbyist."

Opportunities

Many experts see pockets of growth in the forest ecology field. "The job market remains strong, with expanding opportunities in invasive species ecology, … rare and endangered species, fire ecology, and climate change ecology," Robert Teskey, a forest ecophysiologist who earlier this year chaired a selection committee in the Warnell School of Forestry and Natural Resources at the University of Georgia, Athens, writes in an e-mail to *Science*. In addition to "forestry and natural resources programs in the U.S., … many other programs hire ecologists who focus their research in forest ecosystems," he adds. Michigan Technological University in Houghton, for example, last year launched a multidisciplinary hiring initiative to fill 10 new tenure-track positions in sustainability science, with interactions between forests and the atmosphere among the research themes.

Despite these signs of strength, "it's really competitive at the moment," says Cardelús, who has just been awarded a position in the Department of Biology at Colgate University in Hamilton, New York. Teskey acknowledges that his university has "raised expectations for new hires at the assistant professor level and [is] expecting individuals to provide a stronger résumé with evidence of quality peer-review[ed] journal articles, success in obtaining grant funds, and experience in teaching."

Still, "it's a very interesting position and time to be a forest ecologist," Stafford says. The rewards, Bawa adds, "include the knowledge that one can potentially make fundamental contributions to the resolution of some of the most pressing issues faced by … society, the sheer joy and privilege of working at some of the most pristine places on earth, the satisfaction of enjoying natural as well as cultural diversity, and the opportunities of learning about different knowledge systems as these pertain to forests."

–ELISABETH PAIN

Elisabeth Pain is a contributing editor for *Science* Careers.

CREDIT: COURTESY OF JÉRÔME CHAVE

POSITIONS OPEN

NEUROSCIENCE FACULTY POSITION

The Department of Biomedical Sciences at Marquette University invites applications for a tenure-track faculty position at the level of **ASSISTANT PROFESSOR.** Successful candidates will be expected to develop an independent, extramurally funded research program. We are particularly interested in applicants whose research utilizes molecular techniques to investigate an area of neurobiology that complements current departmental strengths. Teaching responsibilities will include contributions at the graduate and undergraduate level. The Department of Biomedical Sciences **(website: http://www.marquette.edu/chs/bisc/)** provides a highly collaborative work environment that is experiencing rapid growth. Interested individuals with a Ph.D. in a neuroscience-related field and at least two years of postdoctoral training should apply online by submitting curriculum vitae and statement of research interests **(website: http://careers.marquette.edu/applicants/Central?quickFind=50954).** Review of applications will begin on July 16, 2008, and continue until the positions are filled. Inquiries can be addressed to: **Linda Vaughn, Ph.D., Department of Biomedical Sciences, Marquette University, P.O .Box 1881, Milwaukee, WI 53201-1881 (e-mail: linda.vaughn@mu.edu).** *Marquette University is an Affirmative Action/Equal Opportunity Employer.*

The UNIVERSITY of TEXAS SOUTHWESTERN MEDICAL CENTER at DALLAS

The Department of Internal Medicine, Division of Nephrology, seeks research-oriented faculty at the **INSTRUCTOR** level who will conduct independent research in cardiovascular and kidney biology and disease using mouse genetic approaches with special emphasis on WNK kinase models. Applicant must have an M.D. or Ph.D. degree with minimal three years of relevant postdoctoral experience. Visit our **website: http://www.utsouthwestern.edu/nephrology.** Send curriculum vitae, description of research, and three reference letters to:

Chou-Long Huang, M.D., Ph.D.
University of Texas Southwestern Medical Center
5323 Harry Hines Boulevard
Dallas, TX 75390-8856
E-mail: chou-long.huang@utsouthwestern.edu

UT Southwestern is an Equal Opportunity/Affirmative Action Employer.

ENVIRONMENTAL RESEARCH ANALYST. Conduct research and analyze commercial land for potential development with emphasis on environmental effects including physical and health hazards. Analyze data to interpret correlations between commercial property development and environmental effects. Prepare reports to present to city, state, and federal authorities for permits. Conduct feasibility studies for development of physical plants. Review plans, designs, layout and physical requirements for commercial sites and buildings. Required: Master of Science in chemical engineering, chemistry, or forestry. Equivalent of 40 hours per week. Job/interview site: Torrance, California. Send curriculum vitae to: **Person Realty Incorporated, 21641 S. Western Avenue, Suite C, Torrance, CA 90501.**

ENVIRONMENTAL SCIENTIST

Conduct environment inspections and soil and groundwater sampling. Compile and analyze derived data. Support operation of remediation system. Write risk assessments, prepare reports, and manage database. Required: B.S. in environmental engineering or environmental science, or foreign equivalent. Forty hours/week. Job/interview site: Irvine, California. Fax curriculum vitae to: **GeoTrans, Incorporated. Human Resources, fax: 240-804-8008.**

POSITIONS OPEN

POSTDOCTORAL POSITION in RICKETTSIAL PATHOGENESIS and CELL BIOLOGY

We are actively recruiting two Postdoctoral Research Fellows in the area of bacterial pathogenesis and genetics, cell biology, or host/vector/pathogen interaction. The successful candidate will drive independent research projects in Rickettsial pathogenesis and Rickettsial cell biology. Candidates should have a Ph.D. in relevant field including bacterial pathogenesis and genetics or molecular entomology. Candidates with interest in multidisciplinary laboratory should submit their curriculum vitae by e-mail to: **A.F. Azad, Ph.D., Professor of Microbiology and Immunology, University of Maryland Baltimore, School of Medicine (e-mail: aazad@umaryland.edu).**

The College of Sciences and Mathematics at Auburn University located in Auburn, Alabama **(website: http://www.auburn.edu/cosam)** is seeking candidates for the position of **POSTDOCTORAL FELLOW** in the sciences and mathematics. From time to time, Postdoctoral positions become available under a variety of research grants and projects in the College. We are seeking applications from individuals with a Ph.D. in any one area such as biology, chemistry, geology, geography, mathematics, statistics, physics, or related fields.

The candidate selected for these positions must be able to meet eligibility requirements to work in the United States at the time appointment is scheduled to begin and continue working legally for the proposed term of employment; excellent communication skills required. The positions are available for a minimum of one year as full-time 12 month, with renewal possible. Salary will be commensurate with education and experience. Review of applications will begin after July 1, 2008, and continue throughout the year as positions become available. Please send curriculum vitae and statement of research interests, along with a list of three references and contact information to: **Dr. Marie Wooten, Associate Dean for Research, College of Sciences and Mathematics, 315 Roosevelt Concourse, Auburn University, AL 36849. E-mail: adcocba@auburn.edu; fax: 334-844-5525**

Minorities and women are encouraged to apply.

Auburn University is an Affirmative Action/Equal Opportunity Employer.

The Michigan Society of Fellows invites applications to its **POSTDOCTORAL FELLOWSHIP PROGRAM** for recent Ph.D.s in the humanities, arts, sciences, and professions. These three-year positions at the University of Michigan are open to recent Ph.D.s who wish to pursue research opportunities while teaching at a major research university. Eight fellowships are available, with an annual stipend of $51,500. Four of these fellowships will be awarded in the humanities, with the support of the Andrew W. Mellon Foundation. Applications must be submitted electronically by midnight September 30, 2008. The online application is available at **website: http://www.rackham.umich.edu/sof.** Questions may be submitted to **e-mail: society.of.fellows@umich.edu.**

CAREER OPPORTUNITY

This unique program offers the candidate with an earned Doctorate in the life sciences the opportunity to obtain the Doctor of Optometry (OD) degree in 27 months (beginning in March of each year). Employment opportunities exist in research, education, industry, and private practice. Contact the **Admissions Office, telephone: 800-824-5526** at the **New England College of Optometry, 424 Beacon Street, Boston, MA 02115.** Additional information at **website: http://www.neco.edu, e-mail: admissions@neco.edu.**

INDUSTRIAL POSTDOCS:
THE ROAD LESS TRAVELED

Many scientists opt for a research career in the pharmaceutical or biotech industry, so why not kick-start the process by also doing a postdoc in industry? Industrial postdocs often provide higher salaries and greater access to resources than their academic counterparts. But how do you find out about available positions and whether they are a good fit for you? Will a position as a postdoctoral fellow provide you a foot in the door at a company? And what if you don't like it? Will an industrial postdoc cut you off from returning to academia? **By Laura Bonetta**

It can be difficult to find answers to these questions, in part because there just aren't that many industrial postdoc positions around. According to data from the 2006 National Science Foundation (NSF) Survey of Doctoral Recipients, 59 percent of individuals who received their doctorates in the life or physical sciences in the past five years had completed or were participating in postdoctoral appointments. Of these individuals only a minority—11 percent in the life sciences and 14 percent in the physical sciences—were doing their postdoc in for-profit or nonprofit companies, compared to 75 percent in educational institutions. "The number of postdocs in the for-profit sector is really small compared to that in academia," says **Nirmala Kannankutty,** a senior analyst at NSF.

In addition, industrial postdoc appointments can vary considerably in length, application process, scope, and expectations, depending on the company and, in some cases, depending on each company's site.

Looking for a Foot in the Door

Postdoc appointments typically lead to permanent positions at some companies, but not others. The chemical company Ciba employs about 60 interns, both diploma graduates and Ph.D.s, each year at its headquarters in Basel, Switzerland (for more on internships, see page 1861). They currently include nine postdoctoral fellows with one- to two-year appointments, according to **Kristina Schueller,** manager of university marketing. "Our postdocs work in projects both independently and in close cooperation with the teams, depending on the project," says Schueller. "Most of them do end up becoming permanent employees with the company. We aim at retaining them."

But this would not be the case at a place like the biotechnology company Genentech. Only about 10 percent of postdocs at the South San Francisco–based biotech company end up being hired by the company as scientists; the majority move on to become scientists at other corporations or assistant professors in academia, or they pursue other careers. "We actively encourage and help postdocs establish an academic career, for example, by funding scientific meetings organized by them," says **Vishva Dixit,** vice president for research at Genentech.

Genentech's postdoctoral program, which started in 1990, currently employs about 120 researchers. Appointments are up to four years with a starting salary of over $49,000 for the first year, compared to the $38,000 or so stipend at most universities.

Genentech postdocs are strictly kept away from any research that has to do with a potential product. This policy ensures that the postdocs are free to talk about their work, make reagents available to others, and continue to work on their projects when they leave the company. "Genentech postdocs are actively encouraged to speak about their results in open forums. If they don't, this is considered a negative in their yearly evaluation," says Dixit.

Why Opt for Industry

Many companies, even ones without a formal postdoc training program like the one at Genentech, see value in having postdocs around. "We see a lot of benefit in having postdocs involved in a project. It helps our scientists remain intellectually involved and maintain a basic research focus, and it really adds to the scientific atmosphere across the company," says **Donald Nicholson,** vice president and franchise worldwide basic research head at Merck Research Laboratories.

Nicholson, whose lab is located at the Merck facility in Rahway, New Jersey, says that he applies similar criteria as his colleagues in academia when selecting a postdoc to join his continued »

> "If I ever leave I will have a background and skills that are valued in academia."

Top: **Marc-Olivier Baradez**
Bottom: **Vikki Tsefrikas**

UPCOMING FEATURES

Focus on Europe—July 11

Careers/Graduate Programs, BS/MS—Augus

Postdoc Survey Results—August 29

EMD SERONO

The people of EMD Serono, Inc. are committed to discovering innovative products that address unmet medical needs, with a focus on specialized therapeutic areas including neurology, reproductive health and metabolic endocrinology, as well as oncology and autoimmune and inflammatory diseases.

Integrating cutting-edge science with comprehensive patient support systems, our focus is on helping people live more fully. Embracing life. Enhancing life. That is the spirit of EMD Serono.

Current Openings at EMD Serono, Inc.

Research

Research Scientist, Phage Display
Senior Research Associate, Phage Display
PI, Structural Biology, Protein Engineering
Project Manager, Discovery Research
Group Leader – In Vivo, Pharmacology
DMPK Scientist
Histologist – In Vivo Pharmacology / Oncology
PI, Protein Engineering Technology Development
Senior PI – Translational Oncology
Senior Scientist, Research Informatics
Sr. Scientist, Medicinal Chemistry
Scientist, Medicinal Chemistry
Knowledge Management Research Scientist
Scientist, Cell Sciences
Associate Scientist, Cell Sciences
Associate Scientist, Protein Sciences

Technical Operations

Quality Control Analyst
Regulatory Compliance Specialist/Technical Writer
Validation Engineer

EMD Serono recently announced a planned expansion of its research operations in Billerica, MA, with a $50M investment that will support the creation of a center of excellence in discovery. When the new facility is complete in 2010, EMD Serono will harness the combined critical mass of more than 250 scientists and employees, committed to discovering and developing new therapies for people living with serious unmet needs, like cancer and infertility.

To learn more or to apply for one of these positions, visit www.emdserono.com/careers.

EMD Serono, Inc., an affiliate of Merck KGaA, Darmstadt, Germany, is a biopharmaceutical leader with US headquarters in Rockland, MA. For a complete list of openings or to apply, please visit www.emdserono.com/careers. EMD Serono is an equal opportunity employer committed to a diverse workforce.

06/08

Johnson & Johnson
Family of Companies

small-company environment
big-company impact

You're an achiever and you're passionate about your work. You have an inquisitive nature, and want to make a difference. You understand the advantages of a small company compared to the opportunity and reach of a global organization. You wonder which environment will be best for unleashing your potential.

Who says you have to choose?

Within the Johnson & Johnson Family of Companies you can experience an entrepreneurial atmosphere that encourages teamwork and innovation—in fast-paced environments that have the feel of a small company—where people are empowered to be innovative and to drive their own careers. But you'll also find the impact of the world's most comprehensive and broadly based manufacturer of health care products.

Discover the many small-company environments behind the big-company impact of the Johnson & Johnson companies.


MEDICAL DEVICES & DIAGNOSTICS


CONSUMER


PHARMACEUTICAL

find more
jnj.com/careers

ASIA-PACIFIC
EUROPE/MIDDLE EAST/AFRICA
LATIN AMERICA
NORTH AMERICA

Johnson & Johnson Services, Inc. is a member of the Johnson & Johnson Family of Companies.

"If you go to a company without a formal postdoc program there are few safeguards. In my case my supervisor was very good and very academically oriented."
—Richard Kho

CREDIT: COURTESY OF KHO

lab. "We look for highly motivated, intellectually hungry individuals with a track record of accomplishment," he says, adding that it also pays to be a team player. "The students and Ph.D.s that thrive in this environment have the ability to collaborate both within the company and outside."

From the perspective of the applicant, one of the main advantages for doing a postdoc in industry—many agree—is the access to state-of-the-art equipment and facilities and to colleagues with a wide range of research expertise from biology to chemistry to bioinformatics. That is what attracted Nicholson to industry when he first took a postdoc position at the Merck Frost Center for Therapeutic Research in Montreal, Canada. "What I realized, for example, was the power that chemistry could bring to bear on biological questions," he recalls.

The other advantage to doing a postdoc in industry is the exposure to the business side of a company. That early experience can be particularly valuable to someone who has his or her eyes set on an industrial career path. After completing a Ph.D. in organic chemistry at Boston College, **Vikki Tsefrikas** became a postdoctoral research associate in the cancer chemistry department at the AstraZeneca Pharmaceuticals facility in Waltham, Massachusetts. "I knew I wanted to go into industry," says Tsefrikas. "This position allowed me to be in that environment and experience it firsthand."

Tsefrikas's two-year appointment at AstraZeneca allows her to work on multiple projects, some directly related to AstraZenca's company portfolio and some more investigative in nature. "I like the variety," she says. "I have an insight into what the company works on but still have the opportunity to publish."

Exploring Other Options

Would an industrial postdoc be a good fit for someone who is not set on a career in industry? Some postdoc projects and programs do provide valuable research training, not unlike that of an academic postdoc, but in an industrial setting.

That is the vision behind the Presidential Postdoctoral Fellowship Program established in late 2003 at the Novartis Institutes for BioMedical Research (NIBR), the research arm of the pharmaceutical giant Novartis. "We wanted to provide postdocs with an opportunity to do the kind of science they were excited about in this kind of an environment that is different from academia," says **Rajesh Ranganathan,** head of NIBR's education office. "We wanted to create a program that opens more doors rather than close some of them."

NIBR currently employs 85 postdocs at four sites. The majority are evenly split between the Cambridge, Massachusetts, and Basel, Switzerland, NIBR campuses, with a few postdocs at the Emeryville, California, and Horsham, UK, sites. Each postdoc has two mentors, one within NIBR and the other at a local academic institution, both providing research and career advice during the stipulated three-year period.

After completing their training at NIBR, postdocs go on to a variety of positions, including assistant professor posts in academia for about 10 percent of them. "When the program started, many people were skeptical that someone trained at a pharmaceutical company would be able to get a good job in academia," says Ranganathan. "But we have shown that this is possible."

As a rule NIBR does not place restrictions on its postdocs' publications, and the projects are designed to accommodate this. "In rare instances postdocs willfully make the decision to work on projects that cannot be published. Such postdocs see a benefit in perhaps being an inventor on a patent instead and are choosing to take their career in a different direction," says Ranganathan. "We talk to them at the outset and explain the constraints, so they embark on such efforts with eyes wide open."

How to Apply for an Industrial Postdoc

Companies like NIBR and Genentech have formal application and screening processes for their postdocs, which are managed through a centralized office. Prospective postdocs at many other companies apply to the human resources department in response to a specific position listed on the company's website or advertised elsewhere. In some cases postdocs at large pharmaceutical companies without a formal postdoc program obtained their positions by contacting individual researchers directly.

It pays to be creative. **Richard Kho** found a position as a postdoc at the San Diego–based biotech company Triad Therapeutics (which closed its doors in 2004) even when there wasn't one available. Late in 2000, when Kho was finishing his Ph.D. and had decided he did not want to stay in academia, he saw an advertisement for a research associate position at Triad on an Internet job search engine. While the position was a perfect fit for his research interests—a mix of bioinformatics and genetics—it called for someone with a Bachelor's degree who would report to a Ph.D.-level scientist. "I replied to the advert and explained that I had a Ph.D. but wanted to work in this area," says Kho. "We were able to turn it into a postdoc position."

Kho ended up with a patent and two publications during his two-year postdoc, which then led to a permanent position at Triad. Although the strategy worked well for Kho—now an employee with the UK-based software company InforSense—he admits it was a gamble. "If you go to a company without a formal postdoc program there are few safeguards. In my case my supervisor was very good and very academically oriented," says Kho. "If you seek a postdoc position where a postdoc program does not exist, you should be proactive to get the training you need."

Marc-Olivier Baradez used a recruitment agency to find a postdoc position at ReNeuron, a company formed 10 years ago as a spin-off of research conducted at Kings College London. After completing his Ph.D. in the stem cell field at Kingston University in South West London, followed by postdoctoral research at Rice University in Texas, Baradez started looking for a second postdoc position in London, in the same research area. After not finding anything that met his expectations within academia, he turned his sights to the biotech sector.

"A big advantage here at ReNeuron is that there is a lot more money to do the work. We have few constraints other than sticking to a deadline and achieving a set of goals by the deadline," he says. Baradez also enjoys the fact that his research is focused on therapeutic applications. "It is like having a justification for what you do on a daily basis." continued »

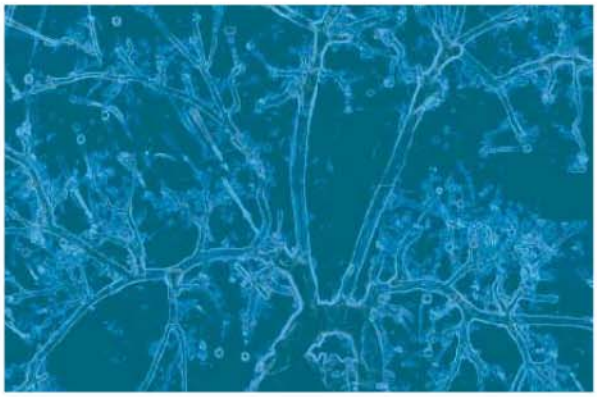

Greg, Avastin® Patient

BECAUSE

Our CAUSE is Greg and his cancer.

For more than 30 years, Genentech has been at the forefront of the biotechnology industry, using human genetic information to develop novel medicines for serious and life-threatening diseases. Today, Genentech is among the world's leading biotech companies, with multiple therapies on the market for cancer and other serious medical conditions.

Research: The Wellspring of Future Therapies
Genentech's Research department aims to strike a balance between basic biomedical research and translational research aimed at developing therapies for unmet medical needs. Genentech's Research organization combines the best of the academic and corporate worlds, allowing researchers not only to pursue important scientific questions, but also to watch an idea move from the laboratory into clinical development.

Research has opportunities at all levels in the following areas:

- Antibody/Protein Engineering
- Bioinformatics
- Immunology
- Molecular Biology
- Oncology Diagnostics
- Neurobiology
- Pathology
- Oncology/Tumor Biology and Angiogenesis
- Small Molecule Drug Discovery

Product Development: Translating Science Into Patient Benefit
Genentech's Product Development group drives the development of breakthrough therapies through innovation, decisive leadership, teamwork and effective partnerships with regulators and collaborators. The Product Development functions work together to select molecules for development, develop molecules into potential therapies and ensure that future Genentech therapies are targeted, safe and effective for patients through clinical trials.

Product Development has opportunities at all levels in the following areas:

- Early Stage - Clinical Pharmacokinetics and Pharmacodynamics
- Modeling and Simulation - Pharmacometrics
- BioAnalytical Sciences
- Oncology and Immunology Diagnostics
- Oncology Pharmacodynamic Biomarkers
- Study Management and Toxicology

Genentech is dedicated to fostering an environment that is inclusive and encourages diversity of thought, style, skills and perspective. To learn more about our current opportunities, please visit **careers.gene.com**. Use "Ad – Science" when a source is requested.

If you are not able to find any suitable positions at this time, but would like to share your expertise and interests with us for networking purposes, please visit **www.gene.com/gene/genetalent/events/randpd.html**.

Genentech is an equal opportunity employer.

In January 2008, Genentech was named to FORTUNE's list of the "100 Best Companies to Work For" for the tenth consecutive year.

Genentech
IN BUSINESS FOR LIFE

Internship Opportunities

Because industrial postdocs are not a good fit for everyone, internships can provide a good way to test the water without making long-term commitments. These positions, typically available at the undergraduate, graduate, and postgraduate levels, last anywhere from six weeks to a year. "The summer internship program at Merck gives students a flavor for what it is like to work in industry. Some are enamored and some decide it is not for them. It is a really important trial," says Donald Nicholson, vice president and franchise worldwide basic research head at the Merck Research Laboratories.

Some of the companies that provide internship opportunities to students in science and engineering fields are:

Amgen
www ext.amgen.com/careers/campus.html

Amylin Pharmaceuticals, Inc.
careers.amylin.com/intership.asp

AT&T Labs, Inc.
www.research.att.com/index.cfm?portal=18

Becton Dickinson and Company
www.bd.com/careers/internships

BioLogic Company
www.biologicco.com/employment/intern.htm

Boeing
www.boeing.com/employment/college/internshipDetails.html

Ciba
www.ciba.com/myfuture

Eli Lilly and Company
www.lilly.com/careers/

Genentech
www.gene.com/gene/careers/university/internships/

Genzyme
www.genzyme.com/corp/careers/intern_positions.asp

GlaxoSmithKline
www.us.gsk.com/html/career/career-summer.html

IBM
domino.research.ibm.com/hr/w3www_summer_watson.nsf/pages/index2.html

Johnson & Johnson
www.jnj.com/careers/global/graduate_target/internships_co-ops/index.htm

Merck & Co.
www.merck.com/careers/university/internships.html

Novartis Institutes for BioMedical Research
www.nibr.novartis.com/careers/internship/index.shtml#VI

Pfizer
www.pfizer.com/careers/working_for/summer_internships.jsp

Procter & Gamble
www.pg.com/jobs/jobs_us/recruitblue/internships.jhtml

Roche
www2.roche.com/careers/Internships.html

Making the Right Choice

Depending on the company and the project, it can be more of a challenge to get publications out as a postdoc in industry. One way to determine whether a company encourages its scientists to publish is to do a PubMed search that includes the company's name. Many companies also list publications on their website.

"There is tight control about how much we can publish, although we are encouraged to attend meetings," says Baradez, adding that he does not think this would necessarily hurt his chances of returning to academia. "If I ever leave I will have a background and skills that are valued in academia."

Because research at a company often involves proprietary information, it can be difficult to share results with other scientists. "I have been on several hiring committees for people going from one company to another and often they cannot really talk about what they have done," says **Sam John,** a staff scientist at the National Institutes of Health (NIH). "The interview process then becomes challenging in identifying candidates that fit the needs of the company."

John chose to do a postdoc at the former biotech company Tularik in San Francisco (which was acquired by Amgen in 2004) because the people who headed the company had a reputation for excellence in research. At Tularik, John had an interesting project and all the support he needed to complete it in a two-year period. Despite the resources, he quickly realized that industry was not for him. "The nature of industry projects is highly focused and I wanted something with more wiggle room," he explains. He remained at Tularik less than a year and then opted for a more traditional postdoc appointment at Penn State. After a short stint at another biotech company, he joined the National Cancer Institute at NIH.

Featured Participants

Amgen
www.amgen.com

AstraZeneca
www.astrazeneca.com

Boston College
www.bc.edu

Ciba
www.ciba.com

Genentech
www.gene.com

Merck
www.merck.com

National Institutes of Health
www.nih.gov

National Science Foundation
www.nsf.gov

Novartis
www.novartis.com

Novartis Institutes for BioMedical Research
www.nibr.novartis.com

ReNeuron
www.reneuron.com

Industrial postdocs offer a valuable experience for those wishing to pursue a career in industry—providing an early start along that chosen path. But these positions can sometimes be a good choice for those who end up staying in academia. Depending on the program, they can offer an opportunity to do high level science in a different environment and to establish connections with researchers in the industrial sector. These positions may be harder to find than the more traditional postdoctoral appointments in academia, but for some they are worth the extra effort.

Laura Bonetta is a scientist turned freelance writer based in the Washington, D.C., area.

DOI: 10.1126/science.opms.r0800055

Discover tomorrow's medicines. Apply today.

At Novartis Institutes for BioMedical Research (NIBR), the global research organization of Novartis, we are committed to discovering innovative medicines to cure disease and improve human health. This is today's frontier of science. Our culture of science is open, entrepreneurial, and collegial, unwilling to accept barriers or conventional wisdom. By hiring the best academic, biotech, and pharmaceutical trained scientists, we have fostered an atmosphere for drug discovery where innovation is rewarded. We have created a dynamic and flexible culture that values and leverages each associate's diverse background, unique style and wealth of experience.

NIBR has sites in Cambridge, Massachusetts (headquarters); Emeryville, CA; East Hanover, NJ; Basel, Switzerland; Horsham, UK; and Shanghai, China. Disease area research includes autoimmunity/transplantation/inflammatory disease, cardiovascular and metabolic diseases, gastrointestinal diseases, oncology, infectious diseases, musculoskeletal diseases, ophthalmology, neuroscience, and respiratory diseases. Platform technologies include Analytical and Imaging Sciences, Biologics, Global Discovery Chemistry, Developmental & Molecular Pathways, Proteomic Chemistry, and Epigenetics. For immediate consideration, please visit the Career section at www.novartis.com/nibr.

NOVARTIS
INSTITUTES FOR
BIOMEDICAL RESEARCH

Novartis is committed to embracing and leveraging diverse backgrounds, cultures, and talents to achieve competitive advantage. Novartis is an equal opportunity employer M/F/D/V.

MORE

Accelerate
Bioinformatics
Community
Drug discovery
Epigenetics
Fast
Gibco
Humanity
Innovative
Jump start
Knowledge
Labeling and detection
Magnetic beads
Nanotechnology
Online tools
People
Quality
Reliable
Stem cells
Talent
Unique
Validated
Worldwide
X Y
Yield
Zoom

Invitrogen is redefining the vocabulary of science. From accelerating the pace of research to groundbreaking online tools to worldwide service and support, Invitrogen is doing everything it can to make your research more reliable—in every way possible from A to Z.

Invitrogen offers challenging careers in all areas of the life science industry. To explore current opportunities, visit **www.invitrogen.com/careers.**

invitrogen™

CAREERS IN BIOTECH AND PHARMA

POSITIONS OPEN

Fondazione
Ri.MED

Ri.MED FOUNDATION

Call for applications for the award of
12 Postdoctoral Fellowships
for training and research activities
in biomedical and biotechnology research
(Ref. Ri.MED – Ric/08)

The Ri.MED Foundation was created in 2006 as an international partnership between the Italian Government, the Region of Sicily, the University of Pittsburgh, and the University of Pittsburgh Medical Center (UPMC). To develop the investigators who will later staff the planned Biomedical Research and Biotechnology Center in Sicily, the Ri.MED Foundation is calling for applications for the award of twelve (12) one-year fellowships (which may be renewed in one-year increments) based on qualifications and interviews.

The selected candidates will undertake mentored training and research activities in the laboratories of the University of Pittsburgh in the fields of Structural Biology, Computational Biology, Neuroscience, Pharmacology, Vaccine Development, Tissue Engineering/Regenerative Medicine, Biomedical Devices, Nanotechnology Development, Molecular Imaging, and other related areas.

Eligible fellowship candidates must meet the following requirements: Degree in Medicine and State certification, or PhD degree related to biomedical research already achieved or to be obtained in 2008, with no more than two years of post-PhD research. Also required: excellent (spoken/written) English proficiency, knowledge of the Italian language, and good knowledge of main software applications. Preferred: previous research experience in one of the aforementioned areas.

Candidates of both sexes (Law 903/77) are requested to submit the following documents in English, preferably via email at selezione02@fondazionerimed.com, or via regular mail, no later than July 15, 2008:

1. application request (to be downloaded at www.fondazionerimed.com)
2. CV with a list of publications, and authorization to review personal data (Law Decree 196/2003)
3. description of research interests, experience, and goals
4. two reference letters (one by degree/PhD dissertation supervisor, one by a nonsupervisor researcher/professor)
5. no more than 5 original publications.

Selection will take place over the following 6 months, with a start date in 2009. Applications will be evaluated by a Scientific Committee, which will interview and select candidates on the basis of submitted documentation. Ri.MED Foundation fellowships are not compatible with any other conferred research fellowship, grant, work activity, or other activity that may compromise the execution of the training and research period, unless otherwise authorized by the Foundation. The training and research activity performed at the University of Pittsburgh does not represent a later employment contract.

Ri.MED Foundation – Piazza Sett'Angeli 10, 90134 Palermo, Italy

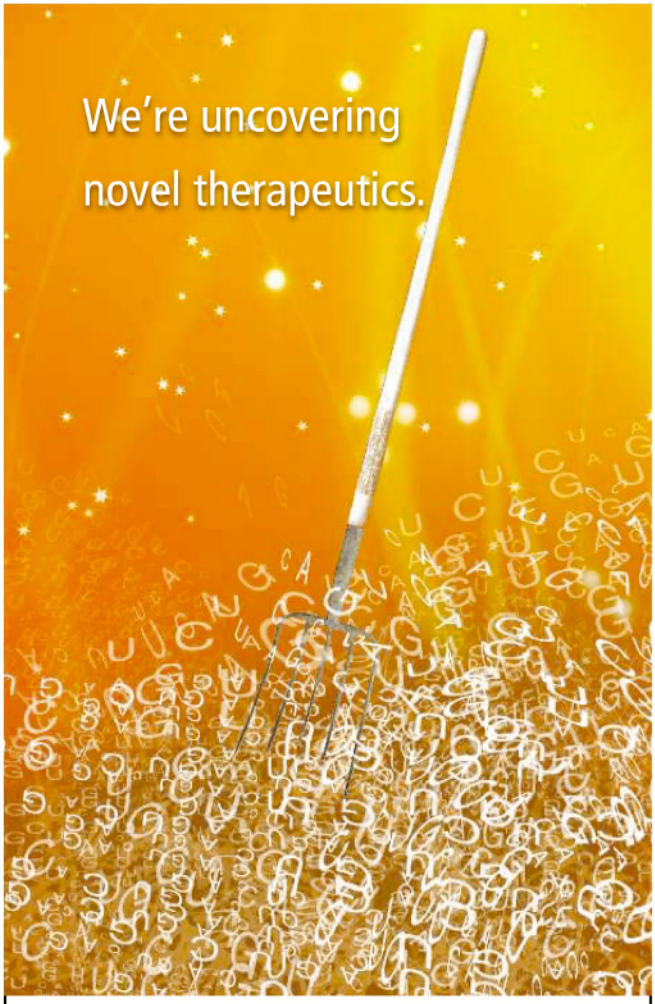

Regulus Therapeutics, formed as a joint venture of Isis Pharmaceuticals and Alnylam Pharmaceuticals, is a rapidly-growing biopharmaceutical company created to discover and develop therapeutic products targeted to microRNA pathways. This novel, exciting approach has the potential to offer a new paradigm to the field of pharmaceutical drug discovery. Regulus has assembled a seasoned team supported by a world class board of microRNA research advisors to aid in this journey. Regulus offers an environment where results-driven professionals thrive. Join us to be a part of something truly exciting and revolutionary. Please visit our website to find a listing of current opportunities in the following areas:

- Molecular Biology
- Synthetic Nucleotide Chemistry
- Analytical Chemistry
- Computational Biology

Regulus Therapeutics provides unprecedented opportunities for highly motivated people to see their efforts come to fruition. **Apply online at: www.regulusrx.com.** EEO M/F/D/V.

REGULUS
THERAPEUTICS

www.regulusrx.com

National Institute of General Medical Sciences
National Institutes of Health
Department of Health and Human Services

The National Institute of General Medical Sciences (NIGMS) in Bethesda, Maryland is seeking applications from outstanding candidates with a strong background in clinical genetics/genomics for a Medical Officer position in the Division of Genetics and Developmental Biology. The Division, which primarily supports basic research and research training, has an interest in expanding its support for research on the genetics/genomics of complex human phenotypes.

The incumbent for this position will be responsible for developing and managing a portfolio of research grants that emphasizes the application of genetic and genomic data to understand the biological basis of normal human phenotypes and genetic disorders. Candidates must have clinical genetics experience and a broad background in genetics/genomics, as well as specialized experience in one or more of the following areas: DNA replication, mutagenesis, and repair, regulation of gene expression, physiology, computational/systems biology, or related areas.

Applicants must possess an M.D. or Doctor of Osteopathy degree, clinical genetics experience, independent research experience, and knowledge of the NIH peer review and grants process.

Salary is commensurate with qualifications, and includes a full package of benefits. A detailed vacancy announcement **(NIGMS-08-266255-DH)** with the mandatory qualifications and application procedures can be obtained via the NIGMS web page at **http://www.nigms.nih.gov/about/job_vacancies.html** and the USAJobs web page at **http://www.usajobs.opm.gov**. Questions on application procedures may be addressed to **Wendy Evans at (301) 594-2386**. Applications, and supporting documentation, must be received by close of business **07/01/2008**. The NIH is an equal opportunity employer.

The National Institutes of Health inspires public confidence in our science by maintaining high ethical principles. NIH employees are subject to Federal government-wide regulations and statutes as well as agency-specific regulations described at **http://ethics.od.nih.gov**. We encourage you to review this information.

NIDDK | NATIONAL INSTITUTE OF DIABETES AND DIGESTIVE AND KIDNEY DISEASES

New Research Initiative – Fatty Liver Disease & Obesity - Tenure Track Position

The Liver Diseases Branch of the National Institute of Diabetes and Digestive and Kidney Diseases (NIDDK), National Institutes of Health (NIH) invites applications for one tenure track position from scientists interested in basic and/or clinical research involving non-alcoholic fatty liver disease and metabolic syndrome. Specific areas of research interest include pathogenesis and mechanism of metabolic derangement in non-alcoholic fatty liver disease and its pathophysiologic link to inflammation, insulin resistance, metabolic syndrome and obesity. Priority will be given to applicants at the Assistant Professor level in traditional universities or those finishing their post-doctoral/fellowship positions. The applicant must have a proven record of accomplishments and will be expected to propose and pursue an independent research program in one of these fields. The position offers unparalleled opportunities for interdisciplinary collaboration within NIDDK and throughout NIH.

The Liver Diseases Branch of NIDDK is located on the main intramural campus of the NIH in Bethesda, Maryland, a suburb of Washington, D.C.

Interested applicants should send a Curriculum Vitae and list of publications, copies of three major publications, a summary of research accomplishments, a plan for future research, and two letters of recommendation (preferred but not required) to **Ms. Michelle Whitley, Search Committee, Liver Diseases Branch, NIDDK, Building 10-9B16, NIH, Bethesda, MD, 20892-1800. Application deadline: September 15, 2008**.

WWW.NIH.GOV

National Cancer Institute

CHIEF, CHEMICAL BIOLOGY LABORATORY

CENTER FOR CANCER RESEARCH

Application Deadline: September 15, 2008

NCI is seeking an outstanding, internationally recognized scientist to serve as Chief of the Chemical Biology Laboratory (CBL) in the Center for Cancer Research (CCR). The position, which is the equivalent of an academic Department Chair, is a key component of a major initiative to build CCR's chemistry program at the Frederick campus (http://www.ncifcrf.gov/). The CBL Chief will play a leading role in developing an integrated program of chemistry, structural biology, and lead compound discovery that both promotes the application of chemical biology approaches across CCR's research portfolio and interfaces with the Division of Cancer Treatment and Diagnosis's Chemical Biology Consortium. In addition to institute-wide responsibilities, the CBL Chief will direct an extensive individual research program that will complement and augment CCR expertise in chromosome biology, immunology, HIV/AIDS, cancer biology and molecular oncology, areas in which its Centers of Excellence have been established. Supported with stable financial resources, the CBL will have access to a wide array of intellectual and technological assets, including high-quality technology cores dedicated to protein chemistry, natural products chemistry, biophysics, mass spectrometry, imaging, microscopy, proteomics and genomics, bioinformatics/biostatistics, and flow cytometry, in addition to clinical support.

The National Cancer Institute (NCI) is part of the National Institutes of Health (NIH) in the Department of Health and Human Services (DHHS), a federal government agency. CCR is the largest component of the NCI Intramural Research Program, providing an environment conducive to advancing translational research and collaborative interactions through investigator-initiated and interdisciplinary team science. Additional information on CCR research priorities can be found at: http://ccr.cancer.gov/.

In addition to a Ph.D. or M.D./Ph.D. degree in a relevant discipline, applicants should possess outstanding communication skills and documented leadership experience. Tenured faculty or industrial scientists of equivalent rank with a demonstrated commitment to chemical biology should apply. Salary will be commensurate with experience and accomplishments. Applications should include a description of research interests and leadership philosophy, career synopsis, and current curriculum vitae with complete bibliography.

Applications should be postmarked or received by email at cortnerj@mail.nih.gov by September 15, 2008.
Send applications to: **Stuart Le Grice, Ph.D., Chair, Chemical Biology Laboratory Search Committee, c/o Janelle Cortner, Ph.D., Building 428, National Cancer Institute at Frederick, Frederick MD 21702.**

DHHS, NIH and NCI are Equal Opportunity Employers

NATIONAL INSTITUTES OF HEALTH

NATIONAL CANCER INSTITUTE

NIAID

NATIONAL INSTITUTE OF ALLERGY AND INFECTIOUS DISEASES

Help Us Help Millions

RESEARCH FELLOW, Flavivirus Group, Laboratory of Infectious Diseases

The National Institute of Allergy and Infectious Diseases (NIAID), a major research component of the National Institutes of Health (NIH) and the Department of Health and Human Services, is recruiting for a Research Fellow. The position will be available in the Flavivirus group of the Laboratory of Infectious Diseases, and scientists with a M.D., Ph.D., or D.V.M. are eligible. The Research activity involves (1) the development of live attenuated dengue and Japanese encephalitis vaccine candidates and their characterization in rodents, non-human primates, and humans; (2) the development and use of reverse genetic systems for these viruses to examine basic questions of viral genetics, molecular virology, viral pathogenesis, and the molecular basis of attenuation; (3) the development and implementation of methods for the evaluation of the histopathologic basis of disease caused by Japanese encephalitis virus; (4) production of novel candidate vaccines using site-directed mutagenesis to introduce desired attenuating mutations into viral genomes; and (4) the evaluation of the immunologic determinants of resistance to infection and illness caused by these flaviviruses. This full-time research position offers a unique opportunity to work on investigations that range from basic molecular biology to applied vaccine development in a collaborative environment, and provides excellent training for scientists who plan a research career in infectious diseases.

Qualifications: Research Fellow applicants should have three or more years of relevant post-doctoral experience; the salary range is $44,180 - $108,319. A full package of benefits (including retirement, health, life and long term care insurance, Thrift Savings Plan participation, etc.) is available. Applicants with an MD degree are eligible for the NIH Loan Repayment Program.
Application Process: Applicants should send their curriculum vitae, a letter of interest, and names and addresses of three (3) references to Brian Murphy, 50 South Drive Room 6517 MSC 8007, Bethesda, MD 20892-8007, FAX: (301) 480-1268, email: bm25F@nih.gov.

Department of Health and Human Services
National Institutes of Health
National Institute of Allergy and Infectious Diseases

VENTANA MEDICAL SYSTEMS, INC.

A member of the Roche Group.

- **Senior Scientist, Applications IRC7082**

This position will play a lead role in developing new multi-parameter tissue-based applications. Strong technical expertise in the quantitation of nucleic acids and proteins in tissues, including method development, antigen recovery, and trouble-shooting, is required. Experience in fluorescence microscopy is highly desired. Duties include publication/presentation of findings, writing technical reports, data analysis, and the development of patent applications. Also expected is the development of productive relationships with external collaborators and with internal technical and marketing groups.

Education/Experience:
Ph.D. degree in Life Sciences with 2+ years or Master's degree with 5+ years relevant experience. May also include exceptional individuals without an advanced degree by approval.

- **Senior Scientist, Bioinformatician IRC7086**

This position will play a lead role in the development of multi-analyte diagnostic applications. Strong background in the Life Sciences with bioinformatics training is required. Demonstrated knowledge of classification algorithms is specifically desired. Specific responsibilities include performing correlative quantitative analyses among a variety of experimental platforms, including image data. The individual will also conduct statistical analysis to determine the validity of clinical trials. Interacts with consultants and with clinical investigators to determine protocol design. Evaluates databases and statistical analysis programs and interacts with software developers to determine hardware/software compatibility. Maintains expertise in state-of-the-art data handling and statistical analyses.

Education/Experience:
Ph.D. degree in Life Sciences, Bioinformatics or Biostatistics. 2+ years experience developing and applying quantitative methodologies in the life sciences, preferably in support of the development of diagnostic reagents and technologies, or Master's degree with 5+ years relevant experience.

- **Senior Scientist, Mass Spectrometrist IRC7102**

This position will play a lead role in the development of tissue-based mass spectrometry methods. Strong background in proteomics with mass spectrometry specialization/training is required. This position will facilitate development and application of biomarker approaches (proteomics) to investigate disease states. The applicant is an experienced and highly motivated mass spectrometry specialist with demonstrated experience in biomarker research. Requirements include excellent analytical and deductive capabilities with expertise in the application of a range of sample preparation strategies and MS (Q-ToF, MALDI-ToF and triple quadrupole) techniques. Ideally this background would be demonstrated by a track record in other proteomic techniques including bioinformatics analyses.

Collaborative work is expected with internal and external academic and industry partners. Maintains expertise in state-of-the-art expertise in methods development in mass spectrometry and data analyses.

Education/Experience:
Ph.D. degree Chemistry/Biochemistry, 2+ years experience developing and applying MS methodologies, preferably in support of the development of tissue-based assays, or Master's degree with 5+ years relevant experience.

Ventana offers a complete benefits package. Employees can select options that meet their individual needs incl medical, dental, vision, 401K and company paid life insurance. To be considered for the position you must register at **https://careers.ventanamed.com. Ventana Medical Systems, Inc., A member of the Roche Group, 1910 Innovation Park Drive, Tucson, AZ 85755**

Ventana is an Equal Opportunity Employer. M/F/D/V

The Department of Pharmacology, Toxicology, & Neuroscience at the **Louisiana State University Health Sciences Center** in Shreveport invites applications for a 12-month, tenure-track faculty position as an Assistant/Associate Professor in Pharmacology. The LSU Health Sciences Center in Shreveport is the largest medical facility in the Tri-State area and has a reputation for excellence in medical and graduate student education and research. We are seeking qualified faculty with expertise that compliments ongoing research in the department including: the neuropharmacology of addiction, behavioral pharmacology, neuropharmacology, cellular/molecular pharmacology or toxicology, and/or psychoneuroimmunology. Candidates with expertise in the neurobiology of addiction are especially encouraged to apply. Candidates must have a doctoral degree in pharmacology or a related discipline with demonstrated research ability. He/She will be involved in graduate and medical student teaching and will be expected to develop an independent research program. Excellent core facilities exist within the LSU Health Sciences Center and the adjoining Biomedical Research Institute. The position will be available in the fall of 2008. Candidates should submit a letter of application, curriculum vitae, and a detailed description of research accomplishments and future plans, and provide the names and contact information for three or more references familiar with your work.

LSU Health Sciences Center SHREVEPORT

Nicholas E. Goeders, Ph.D.
Professor and Head
Department of Pharmacology, Toxicology, & Neuroscience
LSU Health Sciences Center
P.O. Box 33932
Shreveport, LA 71130-3932
ngoede@lsuhsc.edu
www.sh.lsuhsc.edu

Louisiana State University is an Equal Opportunity/ Affirmative Action Employer.

University of Oxford

Department of Physiology, Anatomy and Genetics

Professorship of Development and Reproduction

Applications are invited for the above post, tenable from as early a date as can be arranged. A non-stipendiary fellowship at Jesus College is attached to the professorship. The new professorship will enhance and strengthen the Department's developmental biology programme and provide a bridge to scientists working on reproduction in the Division. You will be able to demonstrate evidence of international distinction in research in development/reproduction through publications and invited lectures, evidence of major long-term peer-reviewed funding, an ability to contribute to the teaching and training of pre-clinical and graduate students and demonstrable commitment to the organisation and delivery of teaching.

Further particulars, including details of how to apply, are available from http://www.admin.ox.ac.uk/fp/ or from the Registrar, University Offices, Wellington Square, Oxford OX1 2JD, tel. (01865) 270200. The closing date for applications is Monday 21 July 2008.

As an Equal Opportunity employer, we positively encourage applications from people of all backgrounds

www.ox.ac.uk/jobs

sfi
science foundation ireland
fondúireacht eolaíochta éireann

EXCELLENCE ENGAGED STRATEGIC INNOVATIVE INTEGRITY FRONTIERS

HAVE A POSITIVE IMPACT ON IRISH SCIENCE

Science Foundation Ireland (SFI), the National Foundation for Excellence in Scientific Research, was established to undertake and support strategic research of world class status in key areas of scientific endeavour which would underpin economic development, particularly in the fields of Biotechnology, Information and Communications Technologies (ICT) and Sustainable Energy and Energy Efficient Technologies.

SFI will build and strengthen scientific and engineering research and its infrastructure in the areas of greatest strategic value to Ireland's long term competitiveness and development. Through innovation, investment and the development of ideas, SFI is helping to drive forward research of globally recognised excellence and that of nationally significant economic importance.

SFI is currently seeking highly motivated individuals to fill a number of key positions as Scientific Programme Officers and Associate Scientific Programme Officers in all areas relating to:

• **Engineering** • **Information & Communications Technology** • **Lifesciences** • **Chemistry** • **Materials**

SCIENTIFIC PROGRAMME OFFICERS (SFI 526E-08)

As a Scientific Programme Officer, you will be helping Irish science to improve its international profile and to play an increasing role on the world stage. You will be a key decision maker within the Foundation and will have responsibility for managing a portfolio of investments made by SFI. In managing the peer-review process, you will be required to interact with international researchers at the highest level.

Candidates must possess a PhD in an appropriate discipline together with a minimum five years' experience beyond the PhD in academia or industry. Candidates should also possess highly developed project management and interpersonal skills.

ASSOCIATE SCIENTIFIC PROGRAMME OFFICERS (SFI 527E-08)

As an Associate Scientific Programme Officer, you will assist the Scientific Programme Officers and participate in the initiation, implementation, support and promotion of SFI programmes. You will ensure the effective conduct of SFI sponsored research and maximise the capability and opportunities arising from this research consistent with the mission, policies and goals of SFI.

Candidates must possess a PhD in an appropriate discipline together with a minimum three years' experience beyond the PhD in academia or industry. Candidates should also possess highly developed project management and interpersonal skills.

BIOTECHNOLOGY ENERGY INFORMATION & COMMUNICATIONS TECHNOLOGY

NDP
National Development Plan 2007 - 2013

www.sfi.ie

SFI – RESEARCH FOR IRELAND'S FUTURE

To apply for the above positions please email your CV quoting the relevant reference number to hr@sfi.ie or post to: Patricia Ryder, Human Resources Manager, Science Foundation Ireland, Wilton Park House, Wilton Place, Dublin 2, Ireland.
For complete job descriptions visit www.sfi.ie

The closing date for receipt of applications is Friday 27th June 2008.

An attractive remuneration package and employment arrangements are available to the successful candidates. SFI is an equal opportunities employer.

GRANTS

Scientific Leadership Opportunities

Animal, Plant, Environmental and Food Biosciences

Teagasc 2030
creating knowledge for the bioeconomy

Teagasc, the leading agriculture and food research organisation in Ireland, is seeking to appoint 14 permanent research scientists at Principal Investigator or Senior Researcher level to provide leadership on its new bioscience research Vision programme.

As part of the Government's investment of €8.2bn in Science, Technology and Innovation under the National Development Plan, the Teagasc Research Vision programme will help place the agriculture and food industries central to Ireland's economic prosperity in the future. The exploitation of the natural bioscience technologies in the agricultural and food areas is a central pillar of the Irish knowledge-based bioeconomy.

This ambitious research programme requires forward-thinking scientists with ability to create, innovate and collaborate nationally and on a world stage. The essential requirements for each post are outlined in the individual Job Specifications (available at www.teagasc.ie/careers/vision/vacancies.htm) and applicants can apply at the level at which they feel qualified.

Animal Bioscience Centre, Grange, Co. Meath

- **Animal Health Bioscientist -** immune function, markers for resistance to diseases / parasites
- **Nutritional Physiologist -** impact of absorbed nutrients on key biological processes
- **Molecular Biologist -** improving animal production efficiency
- **Computational Biologist -** developing tools to mine genomic and proteomic data
- **Growth Biologist -** genetic regulation of growth and function of adipose and skeletal muscle tissue

Johnstown Castle Environment Research Centre, Wexford

- **Bio-Geochemist** - nutrient and carbon transformations, utilisation / loss pathways in soils

Crops Research Centre, Oak Park, Carlow

- **Scientist - Industrial Crop Uses -** lignocellulose / biomass conversion, biorefining
- **Agronomist - Production Systems** - sustainable crop production systems

Moorepark Food Research Centre, Fermoy, Co Cork

- **Scientist - Microbial Genomics -** complexity of the human gut microbiota, targeted nutrition
- **Cell Biologist/Endocrinologist -** satiety in the human gut, nutrient-induced endocrine response
- **Cell Biologist - Obesity -** lipid metabolism and fat storage
- **Scientist - Food Structure -** health and sensory attributes from an obesity-related perspective

Ashtown Food Research Centre, Dublin

- **Systems Analytical Chemist -** isolation / characterisation of organic species from natural products
- **Natural Products/Organic Chemist -** functional foods , nutraceuticals

An attractive remuneration package will be available for these vacancies. Full details, Job Specifications, qualification requirements and the application procedure can be accessed on our website at www.teagasc.ie/careers/vision/vacancies.htm. The closing date for receipt of completed applications is **5.00pm on Monday 28 July 2008.**

NDP
NATIONAL DEVELOPMENT PLAN

Smithsonian Tropical Research Institute

IS SEARCHING FOR A DEPUTY DIRECTOR

The Smithsonian Tropical Research Institute (STRI), headquartered in the Republic of Panama, seeks an excellent scientist with extensive administrative and research experience to serve as Deputy Director. The Deputy will assist the Director in fostering and evaluating staff research programs, and administrative and outreach support activities, by providing leadership and guidance to staff, fellows, students and visiting scientists. The Deputy also has significant liaison roles with Panamanian government authorities, national education institutions and civil society.

STRI is a unit of the Smithsonian Institution that is primarily devoted to fundamental research in tropical sciences, including animal behavior, anthropology, archaeology, botany, ecology, evolution, geology, molecular biology, paleontology, plant physiology, and soils science; additional programs center on conservation biology and applied ecology **(see http://www.stri.org).**

STRI maintains modern research laboratories, a library, administrative and support centers in Panama City, several major facilities for marine and terrestrial field research in Panama, a 100' research vessel, and canopy access cranes. STRI coordinates a global network of forest-dynamics plots through its Center for Tropical Forest Sciences/SI Global Earth Observatories. In collaboration with other institutions, STRI also participates in the operation of large research facilities in Brazil and Kenya. STRI employs approximately 40 scientists and 300 technical and support personnel, and annually hosts more than 1000 scientific visitors. STRI is committed to advanced scientific training through rigorous Fellowship and Internship Programs, and via cooperative programs with leading educational institutions.

Applicants should have a Ph.D and research experience in a relevant field of science, and a record of excellence in scientific administration. Fluency in Spanish, and familiarity with Latin America, is desirable.

Interested candidates should submit a curriculum vitae; a summary of administrative experience and accomplishments; a summary of scientific research interests; a vision statement on the future of tropical biology and related fields; and the names and contact information of five potential referees. Annual salary and benefits are commensurate with experience.

Review of applications will begin in August 2008 and continue until the position is filled. Please send applications electronically to the **Director of STRI, c/o Ms. Luz Latorraca, Office of Human Resources at: LatorraL@si.edu.** Address inquiries concerning the position to **Dr. William Wcislo, Acting Deputy Director, at: WcisloW@si.edu**

STRI is an Equal Opportunity Employer and appointments are made regardless of nationality.

The Humboldt-Universität zu Berlin and the Leibniz-Institut für Molekulare Pharmakologie (FMP) invite applications for a

Full Professor (W3) Chemical Biology/Head of Department

(Successor of Prof. Dr. Michael Bienert)

The professorship includes the position as a head of department within the research section "Chemical Biology" at the FMP. The FMP is a research institute funded in equal parts by the federal government and the state of Berlin. It is located on the life science campus Berlin-Buch and provides an excellent research environment.

We are looking for an internationally renowned scientist to be core of the research section "Chemical Biology", which includes protein and peptide chemistry, medicinal chemistry, a screening unit for small molecules, an automated microscope as well as state-of-the-art mass spectrometry.

Successful applicants will have a record of outstanding productivity in the field of chemical biology. Preferably, they will be able to provide expertise in developing methods and techniques in chemical biology, especially in probing protein functions with small molecules or through the development of chemical tools that visualize proteins or cellular processes. The FMP will host an international symposium on these topics in summer 2008. The applicant is expected to engage in close collaborations with other research groups at the FMP, e. g. in structural biology and cell biology, and to further the scientific exchange with research institutes of Humboldt-Universität and of other institutions.

The candidate will be involved in the teaching of students (reduced teaching obligation). Applicants must meet the requirements for a university professor as stipulated in § 100 of the "Berliner Hochschulgesetz".

The Leibniz-Institut für Molekulare Pharmakologie and the Humboldt-Universität are equal opportunity employers, committed to the advancement of individuals without regard to ethnicity, religion, sex, age, disability or any other protected status.

Applications, including a statement of current and future research interests, curriculum vitae, list of publications, and the names of three references should be sent to: Dekan der Mathematisch-Naturwissenschaftlichen Fakultät I, Humboldt-Universität zu Berlin, code **PR/025/08**, Unter den Linden 6, 10099 Berlin, not later than 30.11.2008. Application materials will not be returned. Therefore, you are requested to send only copies of all documents. An electronic copy of all materials should be included.

To accelerate the process, applicants are kindly requested to send their application materials both in written form as well as electronically via https://www2.physik.hu-berlin.de/ssl/chem_biologie/

For further information visit the FMP website www.fmp-berlin.de and the website of the Humboldt-Universität www.hu.berlin.de.

Postdoctoral positions are immediately available in the Cardiovascular Research Center at Temple University to study stem cell therapy for cardiac repair, calcium mediated myocyte remodeling, the role of inflammation and inflammatory proteases in cardiac remodeling and gene transfer therapy. Applicants should have an M.D and/or Ph.D. degree with a strong background in cell physiology, stem cell biology, cell and molecular biology, biochemistry or related disciplines. Applicants should have demonstrated scientific productivity, good interpersonal and communication skills, and be able to conduct independent research.

Please send a copy of your CV, a brief statement of research interests, and contact information for three referees to:

Steven R. Houser, Ph.D.
Professor and Chair of Physiology
Email: steven.houser@temple.edu

Abdelkarim Sabri, Ph.D.
Assistant Professor
Cardiovascular Research Center
Temple University Medical School
Philadelphia, PA 19140
E-mail: sabri@temple.edu

Temple University is an Affirmative Action/ Equal Opportunity Employer and strongly encourages applications from women and minorities.

Wellman Center for Photomedicine

Position: Assistant or Associate Professor (Photodynamic Therapy)

The Wellman Center for Photomedicine at Harvard Medical School and the Harvard University-Massachusetts Institute of Technology Division of Health Sciences and Technology (HST) are collaborating in the search for a candidate at either the Assistant or Associate Professor level who will establish new research programs in biomedical optics, focused on the application of photodynamic therapy (PDT) in areas such as (but not limited to) cancer research, infectious diseases, and imaging. The candidate will be expected to promote and foster multidisciplinary research with joint faculties within Wellman, HST, and the larger MGH and Harvard research communities (**http://www.mgh.harvard.edu/wellman**). Applicants should submit by **June 27, 2008**, a CV, a statement of research and teaching interests and potential collaborative possibilities with WCP and HST faculty (**http://hst.mit.edu**). Three letters of recommendation sent directly to the Search Committee Chair are required. All materials mailed to: **Tayyaba Hasan, Ph.D., Chair of WCP/HST PDT Faculty Search Committee, c/o Susan Weeks, Wellman Center for Photomedicine/MGH, 40 Blossom Street BAR 604, Boston, MA 02114**. Electronic versions of the application materials should also be sent to **WCPFacultySearch@partners.org**.

Massachusetts General Hospital, Harvard University and Massachusetts Institute of Technology are Equal Opportunity Employers. Women and minorities are encouraged to apply.

AWARDS

Boehringer Ingelheim (Canada) Ltd.

Canadian Young Investigator Award

The recipient of the 2008 Boehringer Ingelheim Canadian Young Investigator Award in Biological Sciences is:

Prof. Marie Kmita
Principal Investigator
Institut de recherches cliniques de Montréal (IRCM)
Research Assistant Professor
Université de Montréal

Dr. Kmita is studying the genetics underlying the morphogenesis of the skeleton during embryonic development. Utilizing chromosome engineering and mouse genetics, her research team has developed mouse models for congenital skeletal malformations. She is currently investigating the function of the Hox genes in osteo-chondrogenesis and limb patterning.

The R&D division of Boehringer Ingelheim Canada Ltd. is one of Canada's largest pharmaceutical research centres. One of our important corporate policies is to support and encourage basic research in Canadian universities. To this end, we have established the Boehringer Ingelheim Young Investigator Award in Biological Sciences. The award is made annually to a new faculty member conducting biological research in a Canadian university, and consists of an unrestricted three-year research grant.

Previous recipients

2007 **Dr. Zhong-Ping Feng**, Department of Physiology, University of Toronto
2006 **Dr. Hao Ding**, Department of Biochemistry and Medical Genetics, University of Manitoba
2005 **Dr. John H. Brumell**, University of Toronto
2004 **Dr. Shun-Cheng Li**, University of Western Ontario
2003 **Dr. Michele Barry**, University of Alberta

Boehringer Ingelheim

Fundación **BBVA**

2008 **BBVA** Foundation Frontiers of Knowledge Awards

Nominations close June 30, 2008

The **BBVA Foundation Frontiers of Knowledge Awards** seek to recognize research in the basic sciences, biomedicine, the environment, information technologies and economics, along with creative output in the arts. Awards are also granted for research and/or projects addressing two core concerns of the 21st century, climate change and development cooperation.

The **BBVA Foundation Frontiers of Knowledge Awards** will consist of 400,000 euros, a diploma and a commemorative artwork in each prize category.

For more information, visit:
www.fbbva.es/awards

The BBVA Foundation Frontiers of Knowledge Awards cover the following categories:

- Basic Sciences (Physics, Chemistry, Mathematics)
- Biomedicine
- Ecology and Conservation Biology
- Information and Communication Technologies
- Economics, Finance and Management
- Arts (Music, Painting, Sculpture, Architecture)
- Climate Change
- Development Cooperation

CSIC
CONSEJO SUPERIOR DE INVESTIGACIONES CIENTÍFICAS

POSITIONS OPEN

CARDIOVASCULAR PHYSIOLOGIST

Research opportunity is available within a research environment in a large teaching hospital for an individual whose professional career has advanced past the postdoctoral level and into the area of individual research productivity as evidenced by consistent publications and grant funding. The position will permit the individual pursuit of research interests in cardiovascular and pulmonary patho-physiology in a research laboratory well equipped for cardiovascular hemodynamic and metabolic studies. Its connection to the Thoracic Surgery Department and a private research institution within a large medical center will provide the potential for growth, development, and pursuit of new research areas and ideas. Previous research has dealt with, but was not limited to, heart preservation, control of heart metabolism, heterotopic heart transplant models, aortic valve, Marfan syndrome, and myocardial angiogenesis. Interested individuals should submit their curriculum vitae to: **Dr. Thomas Masters, e-mail: tom.masters@carolinashealthcare.org.**

POSITIONS OPEN

LECTURER POSITION

The Department of Biological Sciences at University of Illinois at Chicago (UIC) invites applications for a Lecturer position for the academic year 2008–2009. The position is for the overall coordination of the laboratory sections of genetics. Duties include responsibility for setting up and maintaining the laboratories, preparing laboratory exercises, training and supervising teaching assistants, assigning course grades, and course development. This is a nontenured position. Minimum requirements are a Master's degree in a related science field and relevant teaching experience. Minimum salary is $35,000, including a nine-month academic year and a two-month summer appointment, full time. For fullest consideration, please submit your application by June 30, 2008. Please send curriculum vitae and three reference letters to: **Stephanie Davis, Department of Biological Sciences, University of Illinois at Chicago, 845 W. Taylor Street, M/C 066, Chicago, IL 60607. E-mail: sydavis@uic.edu.** *UIC is an Affirmative Action/Equal Opportunity Employer.*

MARKETPLACE

What if staying up to date with the latest technology published in journals and patents were as easy as pushing a button?

It is.

With the "Keep Me Posted" alerting feature, SciFinder sends you automatic updates on areas you—and your competitors—are interested in.

You can monitor specific research topics, companies, authors, substances, or sequences, and choose how frequently you receive notifications: daily, monthly, or weekly.

The service isn't just convenient, it's incredibly current. Journal article records often appear in SciFinder before they're even in print. New references, substances, and sequences are added daily. Patents from all the major offices are added within two days of issuance.

As with all SciFinder features, Keep Me Posted is integrated with your workflow. At any point in a search (including the beginning), simply click on the Keep Me Posted button. SciFinder tracks your steps and will generate the appropriate alert—even for complex topics. When you receive a notification, you can follow each reference as you would in a search: find citing or cited articles (with links to the electronic full text), and follow referenced substances and reactions for further information.

Comprehensive, intuitive, seamless—SciFinder doesn't just alert you, it's part of the process. To find out more, call us at 800-753-4227 (North America) or 614-447-3700 (worldwide) or visit www.cas.org.

SciFinder®

Part of the process.™